

WL-TR-93-2126

AD-A279 144



LUBRICANT EVALUATION AND PERFORMANCE II



Costandy S. Saba, Michael A. Keller, Kenneth K. Chao,  
Douglas K. Toth, Mary F. Borchers, and Hoover A. Smith  
University of Dayton Research Institute  
Dayton, OH 45469-0166

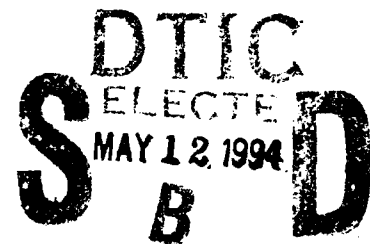
47581 94-14070



February 1994

Final Technical Report for Period 1 January 1991 - 12 July 1993

APPROVED FOR PUBLIC RELEASE; DISTRIBUTION UNLIMITED



AERO PROPULSION AND POWER DIRECTORATE  
WRIGHT LABORATORY  
AIR FORCE MATERIEL COMMAND  
WRIGHT-PATTERSON AIR FORCE BASE, OHIO 45433-7103

DTIC QUALITY INSPECTED 1

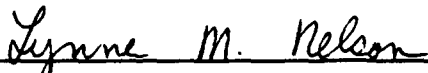
94 5 10 011

## NOTICE

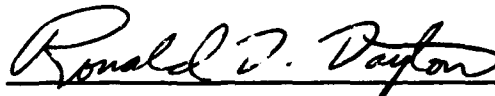
When government drawings, specifications, or other data are used for any purpose other than in connection with a definitely government-related procurement, the United States Government incurs no responsibility or any obligation whatsoever. The fact that the government may have formulated or in any way supplied the said drawings, specifications, or other data is not to be regarded by implication, or otherwise in any manner construed, as licensing the holder or any other person or corporation, or as conveying any rights or permission to manufacture, use, or sell any patented invention that may in any way be related thereto.

This report has been reviewed by the Office of Public Affairs (ASD/PA) and is releasable to the National Technical Information Service (NTIS). At NTIS, it will be available to the general public, including foreign nations.

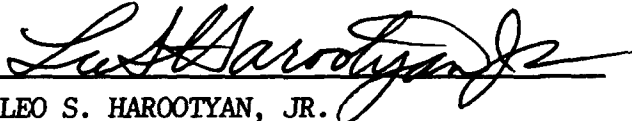
This technical report has been reviewed and is approved for publication.



LYNNE M. NELSON, Project Engineer  
Lubrication Branch  
Fuels and Lubrication Division  
Aero Propulsion and Power Directorate



RONALD D. DAYTON, Chief  
Lubrication Branch  
Fuels and Lubrication Division  
Aero Propulsion and Power Directorate



LEO S. HAROOTYAN, JR.  
Chief, Fuels & Lubrication Division  
Aero Propulsion & Power Directorate

If your address has changed, if you wish to be removed from our mailing list, or if the addressee is no longer employed by your organization, please notify WL/POSL, Wright-Patterson AFB OH 45433-7103 to help us maintain a current mailing list.

Copies of this report should not be returned unless return is required by security considerations, contractual obligations, or notice on a specific document.

REPORT DOCUMENTATION PAGE			Form Approved OMB No. 0704-0188	
<small>Public reporting burden for this collection of information is estimated to average 1 hour per response, including the time for reviewing instructions, searching existing data sources, gathering and maintaining the data needed, and completing and reviewing the collection of information. Send comments regarding this burden estimate or any other aspect of this collection of information, including suggestions for reducing this burden to Washington Headquarters Services, Directorate for Information Operations and Reports, 1215 Jefferson Davis Highway, Suite 1204, Arlington, VA 22202-4302, and to the Office of Management and Budget, Paperwork Reduction Project (0704-0188), Washington, DC 20503</small>				
1. AGENCY USE ONLY (Leave blank)		2. REPORT DATE February 1994	3. REPORT TYPE AND DATES COVERED 1 January 1991 - 12 July 1993	
4. TITLE AND SUBTITLE  Lubricant Evaluation and Performance II			5. FUNDING NUMBERS F33615-88-C-2817 PE 62203F PR 3048 TA 06 WU 48	
6. AUTHOR(S)  Costandy S. Saba, Michael A. Keller, Kenneth K. Chao, Douglas K. Toth, Mary F. Borchers, and Hoover A. Smith				
7. PERFORMING ORGANIZATION NAME(S) AND ADDRESS(ES)  University of Dayton Research Institute 300 College Park Dayton, OH 45469-0160			8. PERFORMING ORGANIZATION REPORT NUMBER  UDR-TR-93-81	
9. SPONSORING/MONITORING AGENCY NAME(S) AND ADDRESS(ES)  Aero Propulsion and Power Directorate Wright Laboratory Air Force Materiel Command Wright-Patterson AFB, OH 45433-7103			10. SPONSORING/MONITORING AGENCY REPORT NUMBER  WL-TR-93-2126	
11. SUPPLEMENTARY NOTES				
12a. DISTRIBUTION/AVAILABILITY STATEMENT  Approved for Public Release; Distribution is Unlimited.			12b. DISTRIBUTION CODE	
13. ABSTRACT (Maximum 200 words)  Thermal and oxidative stability, deposition and foaming techniques were developed for predicting the performance of candidate 4 cSt lubricants, polyphenyl ether (PPE), C-ether and other experimental fluids for use in advanced aircraft turbine engines. A novel sealed tube test was developed to study the rate of reaction in both liquid and vapor phase using only microliter quantities of the lubricants. Blending agents and/or diluents were used to improve the low temperature properties and high temperature oxidative stability of PPE. In-line magnetic wear sensors were evaluated as condition monitoring devices for oil systems with sensitivity well below 5 micrometers. Microfiltration effect on wear was investigated with the results showing effective reduction in secondary wear. HP-DSC analysis technique was limited as an oxidative stability screening device for PPE but was effective in demonstrating differences among various PPE formulations. The tribological behavior of high temperature fluids was evaluated and compared in the boundary lubrication regime using various steel and ceramic specimens. A sliding three-ball-on-disk wear test device was developed for reducing sample size, controlling scar geometry and determining lubricant consumption rate and tribochemistry. The effect of soft and hard solid particulates on the fatigue and wear lives of rolling elements was investigated using a recently developed three-ball rolling test.				
14. SUBJECT TERMS  High Temperature Lubricants, Stability, Coking, Foaming, Condition Monitoring, Spectrometric Oil Analysis, Lubricant Monitoring, Thermal Analysis, Sealed Tube Oxidation Test, Pumpability, Three-Ball-on-Disk, Fatigue and Wear Test			15. NUMBER OF PAGES 477	
			16. PRICE CODE	
17. SECURITY CLASSIFICATION OF REPORT  Unclassified	18. SECURITY CLASSIFICATION OF THIS PAGE  Unclassified	19. SECURITY CLASSIFICATION OF ABSTRACT  Unclassified	20. LIMITATION OF ABSTRACT  UL	

## FOREWORD

This report describes the research conducted by personnel of the University of Dayton Research Institute on Contract No. F33615-88-C-2817. The work was performed at the Aero Propulsion and Power Directorate, Wright Laboratory, Air Force Materiel Command, Wright-Patterson AFB, Ohio during the period January 1991 to July 1993.

The work was accomplished under Project 3048, Task, 304806, Work Unit 30480648, Lubricant Evaluation and Performance II, with Mrs. Lynne Nelson as the project monitor.

Accession For	
NTIS GRA&I	<input checked="checked" type="checkbox"/>
DTIC TAB	<input type="checkbox"/>
Unannounced	<input type="checkbox"/>
Justification	
By	
Distribution	
Availability Codes	
Dist	Avail. Codes
A-1	Special

## TABLE OF CONTENTS

<u>SECTION</u>	<u>PAGE</u>
I INTRODUCTION	1
II DEVELOPMENT OF IMPROVED METHODS FOR MEASURING LUBRICANT PERFORMANCE	3
1. OXIDATIVE STABILITY OF ESTER BASE LUBRICANTS	3
a. Introduction	3
b. Test Apparatus and Test Procedure	3
c. Test Lubricants	3
d. Results and Discussion	3
e. Summary	20
2. LUBRICANT CORROSION AND OXIDATIVE STABILITY OF HIGH TEMPERATURE FLUIDS	27
a. Introduction	27
b. Corrosion and Oxidation Stability Testing of TEL-91001	27
c. Depletion of Antioxidant from Polyphenyl Ether During Laboratory Testing	32
(1) Introduction	32
(2) Depletion of Tin Oxide During Four-Ball Testing	32
(3) Analysis of Four-Ball Test Bearing Surface by Auger Electron Spectroscopy (AES)	35
(4) Quantitation of Tin from Four-Ball Test Bearings	35
(5) Quantitation of Tin Present in Four-ball Filtrate Washings	38
(6) Antioxidant Tin Levels in Minisimulator Tested PPEs	38
(7) Tin Analysis on Minisimulator Deposits	41
(8) Conclusion	42
d. Improvement of Low Temperature Properties	42
(1) Introduction	42
(2) Diluents	43
(a) Background	43
(b) Approach	43
(c) Screening and Test Procedure	44
(d) Results	49

## TABLE OF CONTENTS (continued)

<u>SECTION</u>	<u>PAGE</u>
II	
(3) Blends	49
(4) Blends and Diluents	53
(a) Approach	53
(b) Results	53
(5) Conclusions	57
(6) Recommendations	57
e. Performance Improvement of the Polyphenyl Ether	59
(1) Introduction	59
(2) Lubricity Effect of Some Additives in Polyphenyl Ether Basestock	59
(3) Comprehensive Study of TCP for the PPE Fluids	63
(4) Comparison of TCP With TPP in the O-77-6 Fluid	69
(5) More Test Results of TPP/O-77-6 Formulations	69
(6) Addition of TPPO to the TPP/O-77-6 Formulation	83
(7) Addition of TPPP to the TPP/O-77-6 Formulation	83
(8) Summary	90
f. Sealed Tube Test	93
(1) Introduction	93
(2) Experimental Development	95
(3) Results and Discussion	97
(4) Conclusions	106
g. Stability Testing of a C-Ether (O-64-20)	109
(1) Introduction	109
(2) C&O Testing at 320, 305 and 290°C	109
(3) C&O Testing Without Metal Specimens and Condensate Return	112
(4) C&O Testing of O-64-20 Mixed with Phenyl Disulfide	112
(5) C&O Testing of O-64-20 With an Organotin Additive	112
(6) C&O Testing of O-64-20 with Phenylphosphinic Acid and Perfluoroglutaric Acid	115
(7) Silver Corrosion as a Function of C&O Stressing Time	115

## TABLE OF CONTENTS (continued)

<u>SECTION</u>	<u>PAGE</u>
II	
(8) Vapor Phase Corrosion of Metals	116
(9) C&O Testing of O-64-20 with APP and DPBA	116
(10) Conclusions	122
h. Chemical Analysis of Oxidized C-ethers	122
(1) Introduction	122
(2) Analytical Method Development	125
(3) Chromatographic Analysis and Identification of Degradation Products	125
(4) Analysis of Higher Molecular Weight Oxidation Products	130
(5) Degradation Mechanism	130
(6) Basestock Consumption Analysis of Oxidized O-64-20	132
(7) Conclusions	134
i. Stability Testing of Cyclophosphazene Based Fluids	134
(1) Introduction	134
(2) Effect of Metal Specimens	134
(3) Effect of a Teflon C&O Test Apparatus	136
(4) Effect of a Nickel C&O Test Apparatus	136
(5) Effect of Different Atmospheres and Condensate Return	136
(6) Conclusions	144
j. Chemical Analysis of Degraded Cyclophosphazenes	144
(1) Introduction	144
(2) Analytical Method Development	145
(3) Background	145
(4) Analysis of Oxidized Cyclophosphazenes	146
(5) Conclusions	150
3. LUBRICANT DEPOSITION STUDIES	150
a. AFAPL Static Coker	150
(1) Introduction	150
(2) Apparatus and Test Procedure	150
(3) Test Lubricants	150

## TABLE OF CONTENTS (continued)

<b><u>SECTION</u></b>	<b><u>PAGE</u></b>
II	
(4) General Discussion of Data	152
(5) High Temperature Ester Base Fluids	152
(6) High Temperature Polyphenyl Thioether (C-Ether)	157
(7) Summary	161
b. Micro Carbon Residue Tester (MCRT)	163
(1) Introduction	163
(2) Apparatus and Procedure	163
(3) Test Lubricants	164
(4) Results and Discussion of Data	164
(a) General	164
(b) High Temperature Ester Base Fluids	164
(c) High Temperature Polyphenyl Thioether	166
(d) Effect of Dilution on MCRT Deposits of Polyphenyl Ether Lubricant 0-67-1	166
(e) Correlation of MCRT with AFAPL Static Coker	166
(f) Summary	169
4. MINISIMULATOR	169
a. Introduction	169
b. Apparatus	172
c. Test Method	172
d. Evaluation Procedure	174
e. Results	177
f. Discussion	185
g. Conclusions	189
5. LUBRICANT FOAMING	189
a. Introduction	189
b. Test Apparatus and Procedure	190
c. Test Lubricants	190

## TABLE OF CONTENTS (continued)

<b><u>SECTION</u></b>	<b><u>PAGE</u></b>
II	
d. Results and Discussion	190
(1) High Temperature Ester Base Fluids	190
(2) High Temperature Nonester Base Fluids	193
e. Summary	193
III	
DEVELOPMENT OF IMPROVED LUBRICATION SYSTEM HEALTH MONITORING TECHNIQUES	195
1. FERROSCAN 310	195
a. Introduction	195
b. Results and Discussion	195
(1) Effect of Oil Velocity	195
(2) Effect of Temperature	197
(3) Effect of Particle Size Using 5-10, 10-20, and 20-30 Micron Fe Powder	197
(4) Effect of Wear from a Wear Metal Generator on RDN	211
(5) Effect of Particles Less than 5 Micron on RDN	215
(6) Effect of Wear Debris from TBOD on RDN	218
(7) Effect of Test Duration on RDN	221
c. Conclusions	221
d. Summary	224
2. METALSCAN MARK 3	224
a. Introduction	224
3. IMPACT OF FILTRATION ON SECONDARY WEAR	225
a. Introduction	225
b. Preliminary Testing	226
c. 20-Hour TBOD Tests	236
d. Conclusions	251
e. Future Work	251

## TABLE OF CONTENTS (continued)

<b><u>SECTION</u></b>	<b><u>PAGE</u></b>
<b>IV CANDIDATE HIGH TEMPERATURE LUBRICANT DIAGNOSTIC DEVICES</b>	<b>253</b>
1. HP-DSC FOR SCREENING OF HIGH TEMPERATURE LUBRICANTS	253
a. Background	253
b. Experimental	253
c. Limitations of GPC Analysis on HP-DSC Samples	255
d. HP-DSC Analysis of O-67-1 at Various Temperatures	255
e. HP-DSC Analysis of Prestressed O-67-1	257
f. HP-DSC Analysis of TEL-8085 and TEL-8087	257
g. Conclusions	260
<b>V TRIBOLOGICAL EVALUATION OF CANDIDATE FLUIDS</b>	<b>261</b>
1. FOUR-BALL TEST	261
a. Material Comparison with PPE	261
(1) M50, 52100, Si <sub>3</sub> N <sub>4</sub> , and Brass	261
(2) M50 versus 52100 at 50°C	263
b. Four-Ball Scarring	273
c. Wear Versus Temperature Comparison of Candidate Fluids	280
d. TCE-Diluted PPE	285
e. ASTM Four-Ball Testing	285
f. Summary	287
2. THREE-BALL-ON-DISK (TBOD) TEST	289
a. Introduction	289
b. Experimental Development	291
c. Results and Discussion	298
(1) O-77-6	298
(a) Lubricant Degradation	298
(b) Wear	302
(c) Friction	305

## TABLE OF CONTENTS (continued)

<u>SECTION</u>	<u>PAGE</u>
V	
(2) O-77-6, O-77-10, and O-90-10	305
(a) Friction and Wear	305
(b) Lubricant Consumption and Tribochemistry	311
(3) O-77-6, TEL-90102, TEL-91001, TEL-90013, and O-64-20	311
(a) Friction	311
(b) Wear	311
(c) Lubricant Thickening Due To Wear Debris	316
(d) Lubricant Tribochemistry	316
(e) Lubricant Consumption	320
d. Summary	323
(1) O-77-6	323
(2) O-77-6, O-77-10, and O-90-10	323
(3) O-77-6, TEL-90102, TEL-91001, TEL-90013, and O-64-20	324
f. Advantages	324
3. THREE-BALL ROLLING FATIGUE (TBRF) TEST	325
a. Introduction	325
b. Experimental Development	326
c. Results and Discussion	328
d. Summary	330
e. Conclusions	330
APPENDIX A - LUBRICANT PERFORMANCE TEST DATA	331
APPENDIX B - DETERMINATION OF THE BETA PARAMETER FOR THREE-BALL-ON-DISK WEAR SCARS	429
REFERENCES	441

## LIST OF ILLUSTRATIONS

<b>Figure</b>	<b>Page</b>
1. Viscosity Increases of TEL-91001 During Corrosion/Oxidation Testing at 340, 350, and 360°C.	30
2. Effective Lubricant Life as a Function of Temperature for TEL-91001 Based on (a) the 15%, 25%, and 35% Viscosity Limits at 40°C and (b) the 5%, 10%, and 15% Viscosity Limits at 100°C.	31
3. Change in Relative Tin and Additive A Levels in O-67-1 During Four-Ball Testing (150°C, 52100 Steel Balls, 145 N Load, 1 to 20 Hours).	34
4. Change in Relative Tin and Additive A Levels in O-67-1 During Four-Ball Testing at 150, 250, and 315°C (52100 Steel Balls, 145 N Load, 3 to 20 Hours).	36
5. Auger Electron Spectroscopy Depth Profile of 52100 Steel Ball From a Four-Ball Test of O-67-1 (#380, 250°C, 20 Hours).	37
6. Tin Levels in TEL-90102 During Minisimulator Test WLM003.	39
7. Tin Levels in TEL-90102 During Minisimulator Test WLM004.	40
8. The Viscosity of O-77-6 Blended with Various Levels of 3P2E (1,3-diphenoxybenzene), 4P3E (O-59-9), and C-Ether (O-64-20).	54
9. Antiwear Characteristics of Various Additives in the Polyphenyl Ether Basestock (O-77-6).	60
10. Antifriction Characteristics of Various Additives in the Polyphenyl Ether Basestock (O-77-6).	60
11. Four-Ball Wear and Friction Coefficient Curves for Tests of a Phosphate Ester (PE) Mixture in O-77-6 at 150°C (M50 Balls, 145 N Load, 1200 rpm).	62
12. Total Wear Volume as a Function of TCP Concentration in the Polyphenyl Ether Fluids. Four-Ball Test Condition: 1200 rpm, 145 N, 150°C, Three Hours, and M50 Balls.	64
13. Coefficient of Friction as a Function of TCP Concentration in the Polyphenyl Ether Fluids. Four-Ball Test Condition: 1200 rpm, 145 N, 150°C, Three Hours, and M50 Balls.	66
14. Alpha Value as a Function of TCP Concentration in the Polyphenyl Ether Fluids. Four-Ball Test Condition: 1200 rpm, 145 N, 150°C, Three Hours, and M50 Balls.	67

## LIST OF ILLUSTRATIONS (continued)

<b>Figure</b>	<b>Page</b>
15. Molecular Structures of PPE, TCP, TPP, TPPO, and TPPP.	68
16. Total Wear Volume as a Function of TCP or TPP Concentration in the O-77-6 Fluid. Four-Ball Test Condition: 1200 rpm, 145 N, 150°C, Three Hours, and M50 Balls.	71
17. Coefficient of Friction as a Function of TCP or TPP Concentration in the O-77-6 Fluid. Four-Ball Test Condition: 1200 rpm, 145 N, 150°C, Three Hours, and M50 Balls.	72
18. Alpha Value as a Function of TCP or TPP Concentration in the O-77-6 Fluid. Four-Ball Test Condition: 1200 rpm, 145 N, 150°C, Three Hours, and M50 Balls.	73
19. GPC Chromatograms of the O-77-6 Solution Containing 20% TPP, Before and After the Corrosion/Oxidation Test.	79
20. Total Wear Volume as a Function of TPP Concentration in the O-77-6 Fluid. Four-Ball Test Condition: 1200 rpm, 145 N, 150 and 315°C, Three Hours, and M50 Balls.	80
21. Coefficient of Friction as a Function of TPP Concentration in the O-77-6 Fluid. Four-Ball Test Condition: 1200 rpm, 145 N, 150 and 315°C, Three Hours, and M50 Balls.	81
22. Alpha Value as a Function of TPP Concentration in the O-77-6 Fluid. Four-Ball Test Condition: 1200 rpm, 145 N, 150 and 315°C, Three Hours, and M50 Balls.	82
23. Improvement in Viscosity, C&O Test at 320°C, Wear and Friction as a Result of Adding 20% TPP or 0.15% Additive A into O-77-6 (TEL-90102).	84
24. GPC Chromatograms of the O-77-6 Solution Containing 30% TPP and 10% TPPO, Before and After the Corrosion/Oxidation Test.	87
25. GPC Chromatograms of the O-77-6 Solution Containing 30% TPP and 10% TPPP, Before and After the Corrosion/Oxidation Test.	92
26. A Schematic Drawing of the Sealed Tube Device.	96
27. GPC Chromatograms of 1 mm <sup>3</sup> O-77-6 After Stressed in the Sealed Tube Test for 30 Minutes at 300°C, Compared with that of a Fresh Standard.	98

## LIST OF ILLUSTRATIONS (continued)

<b>Figure</b>	<b>Page</b>
28. Lubricant Remained in the Test Cup and in the Test Chamber versus Time from Testing of 1 mm <sup>3</sup> O-77-6 in the Sealed Tube Device at 300°C. (Examples of Slopes Shown is for Calculating Evaporation and Reaction Rates).	99
29. Comparison of Three Principal Rates as Functions of Test Time.	104
30. An Enlarged-Scale Plot of the Two Chemical Reaction Rates Presented in Figure 29, Showing Details of Their Functional Relationships.	105
31. Chemical Reaction Rates Based on Per Mole of Fresh O-77-6 Molecules in Their Respective Phases (Liquid or Gas).	107
32. An Extended Range of the Gas Phase Reaction Rate, Covering Both Two-Phase and One-Phase Segments of the Test.	108
33. Viscosity Increases for Corrosion and Oxidation Tested O-64-20 at 290, 305, and 320°C.	111
34. Auger Electron Spectroscopy Depth Profile of M50 Washer from the Corrosion and Oxidation Test of O-64-20 with 1.35% Diphenylborinic Anhydride.	123
35. Auger Electron Spectroscopy Depth Profile of Silver Washer from the Corrosion and Oxidation Test of O-64-20 with 1.35% Diphenylborinic Anhydride.	124
36. Gel Permeation Chromatogram of an Oxidized Polyphenyl Thioether (C-Ether).	126
37. Gas Chromatogram with Flame Ionization Detection (GC-FID) of an Oxidized Polyphenyl Thioether (C-Ether). Compound Identification is in Figure 39.	127
38. Reverse Phase Liquid Chromatogram (RPLC) of an Oxidized Polyphenyl Thioether (C-Ether). Compound Identification is in Figure 39.	128
39. Compound Identification for Figures 37 and 38.	129
40. Comparison of FTIR Spectra of the Acetonitrile Insolubles from Oxidized Polyphenyl Thioether (C-Ether) and Oxidized Polyphenyl Ether.	131
41. Basestock Consumption of O-64-20 (PPTE) During Corrosion and Oxidation Testing at 290, 305, and 320°C.	133
42. Viscosity Increase for TEL-92026 During Corrosion and Oxidation Testing in the Nickel Test Apparatus.	142

## LIST OF ILLUSTRATIONS (continued)

<b>Figure</b>	<b>Page</b>
43. Gel Permeation Chromatogram of an Oxidized Substituted Cyclophosphazene (TEL-90013, 54 Hours at 280°C).	147
44. Gas Chromatogram with Atomic Emission Detection (GC-AED) of an Oxidized Substituted Cyclophosphazene (TEL-90013, 54 Hours at 280°C).	148
45. Gas Chromatogram with Mass Spectrometry (GC-MS) of Trapped Volatiles from the Corrosion and Oxidation Test of a Substituted Cyclophosphazene (TEL-90024).	149
46. Correlation of AFAPL Static Coker Deposits with MCRT Deposits (New 4 cSt Oils).	168
47. Wright Laboratory Miniaturized High-Temperature Turbine Engine Lubrication System Simulator.	170
48. Minisimulator Test Stand.	171
49. Minisimulator Test Section Components.	175
50. Viscosity Increases for an Ester (O-87-2) and PPE Basestock (O-77-6) During Minisimulator Tests at 175°C Bulk Oil and 260°C Bearing Temperatures.	179
51. Viscosity Increases for PPE Basestock (O-77-6) and Inhibited PPE (TEL-90102) During Minisimulator Tests at 300°C Bulk Oil and 360°C Bearing Temperatures.	180
52. Viscosity Increases During Four Minisimulator Tests of PPE Basestock (O-77-6) at 300°C Bulk Oil and 360°C Bearing Temperatures.	181
53. Minisimulator Test Section.	184
54. Deposits Within the Test Head from Inhibited PPE (TEL-90102) After WLM003.	187
55. Ferrosan Output of Oil Spiked with Three 5-mg Additions of 5-10 Micron Fe Powder for Each of the Four Pumping Outputs Shown.	196
56. Ferrosan Output for Oil Circulating at 2.75 m/s with One 100-mg Addition of 5-10 Micron Fe Powder.	198
57. Ferrosan Output for Oil Circulating at 2.75 m/s with 22 30-mg Additions of 5-10 Micron Fe Powder.	200

## LIST OF ILLUSTRATIONS (continued)

<b>Figure</b>	<b>Page</b>
58. Comparison of the Relative Debris Number Increases for 5-10 Micron Fe Particles Based on the Average Values and the Minimum and Maximum Values of Adjacent "Steps" in Figure 57.	201
59. Ferrosan Output for Oil Circulating at 2.75 m/s with 21 30-mg Additions of 10-20 Micron Fe Powder.	202
60. Comparison of the Relative Debris Number Increases for 10-20 Micron Fe Particles Based on the Average Values and the Minimum and Maximum Values of Adjacent "Steps" in Figure 59.	203
61. Ferrosan Output for Oil Circulating at 2.75 m/s with 20 30-mg Additions of 20-30 Micron Fe Powder.	204
62. Comparison of the Relative Debris Number Increases for 20-30 Micron Fe Particles Based on the Average Values and the Minimum and Maximum Values of Adjacent "Steps" in Figure 61.	205
63. Ferrosan Output for Oil Circulating at 2.75 m/s with 24 30-mg Additions of 10-20 Micron Fe Powder.	207
64. Comparison of the Relative Debris Number Increases for 10-20 Micron Fe Particles Based on the Average Values and the Minimum and Maximum Values of Adjacent "Steps" in Figure 63.	209
65. Three-Ball-on-Disk Wear Test Configuration for a Circulating Oil Flow.	212
66. Wear Rate During a Three-Ball-on-Disk Test Given by the Vertical Displacement of the Ball Specimens (1018 Steel Disk, M50 Steel Balls, 250 rpm, Successive Loads of 30, 50, and 70 kg).	213
67. Ferrosan Output During the 5-Hour TBOD Test of Figure 66.	214
68. Wear Particle Size Distribution for Three TBOD Tests.	216
69. Ferrosan Output for Oil Circulating at 1.5 m/s with Four 5-mg Additions of Less Than 5 Micron Fe Particles.	217
70. Ferrosan Output for Oil Circulating at 1.5 m/s with Four 5-mg Additions of TBOD Wear Particles.	219

## LIST OF ILLUSTRATIONS (continued)

<b>Figure</b>	<b>Page</b>
71. Wear Rate During a Three-Ball-on-Disk Test Given by the Vertical Displacement of the Ball Specimens (1018 Steel Disk, M50 Steel Balls, 250 rpm, Successive Loads of 30, 40, 50, and 60 kg).	222
72. Ferrosan Output During the 90-Minute TBOD Test of Figure 71.	223
73. Oil Flow Network for TBOD Testing With Filtration.	227
74. Comparison of the Wear Rates of Three Unfiltered TBOD Tests Run at the Same Operating Conditions.	228
75. Comparison of the Friction Coefficients During the Three TBOD Tests of Figure 74.	229
76. Comparison of the Wear Rates of Two TBOD Tests Run at the Same Conditions as Those in Figure 74 but with a 10-Micron Filter.	230
77. Comparison of the Friction Coefficients During the Two TBOD Tests of Figure 76.	231
78. Comparison of the Wear Rates of Two TBOD Tests Run at the Same Conditions as Those in Figure 74 but with a 5-Micron Filter.	232
79. Comparison of the Friction Coefficients During the Two TBOD Tests of Figure 78.	233
80. Comparison of the Wear Rates of Two TBOD Tests Run at the Same Conditions as Those in Figure 74 but with a 3-Micron Filter.	234
81. Comparison of the Friction Coefficients During the Two TBOD Tests of Figure 80.	235
82. Wear Rate During a 50-Hour TBOD Test with a Confined Oil Volume of 75 mL.	237
83. Wear Rate During a 66.7-Hour TBOD Test with Oil Circulated Through a 3-Micron Filter.	238
84. Wear Rate During a 50-Hour TBOD Test with Oil Circulated without Filtration.	239
85. Constant Wear and Constant Friction Coefficient Curves for Three TBOD Tests with Filtration.	241
86. Constant Wear and Varying Friction Coefficient Curves for Five TBOD Tests with Filtration.	242

## LIST OF ILLUSTRATIONS (continued)

<b>Figure</b>	<b>Page</b>
87. Varying Wear and Varying Friction Coefficient Curves for Six TBOD Tests with Filtration.	243
88. Friction and Wear Results from TBOD Testing without Filtration.	246
89. Friction and Wear Results from TBOD Testing with a 10-Micron Filter.	247
90. Friction and Wear Results from TBOD Testing with a 5-Micron Filter.	248
91. Friction and Wear Results from TBOD Testing with a 3-Micron Filter.	249
92. Friction and Wear Results from TBOD Testing with a 3-Micron Filter and an In-Line Magnet.	250
93. Typical DSC Thermogram of a Lubrication Oil (from Reference 57).	254
94. HP-DSC Thermograms of O-67-1 at 320, 360 and 400°C.	256
95. HP-DSC Thermograms of Fresh PPE (O-67-1), Basestock (O-77-6) and C&O Tested O-67-1 at 320°C for 144 Hours and 216 Hours.	258
96. HP-DSC Thermograms at 360°C for TEL-8085, TEL-8087 and C&O Tested TEL-8040 (330°C, 24 Hours).	259
97. Total Four-Ball Wear for Various Specimen Materials Lubricated with O-67-1 at 75°C (3-Hour Tests at 1200 rpm with 145-N Loads).	262
98. Total Four-Ball Wear for Various Specimen Materials Lubricated with O-67-1 at 150°C (3-Hour Tests at 1200 rpm with 145-N Loads).	264
99. Total Four-Ball Wear for Various Specimen Materials Lubricated with O-67-1 at 250°C (3-Hour Tests at 1200 rpm with 145-N Loads).	265
100. Total Four-Ball Wear for Various Specimen Materials Lubricated with O-67-1 at 315°C (3-Hour Tests at 1200 rpm with 145-N Loads).	266
101. Total Four-Ball Wear Versus Temperature for M50/Si <sub>3</sub> N <sub>4</sub> Ball Combinations Lubricated with O-67-1 (3-Hour Tests at 1200 rpm with 145-N Loads).	267
102. Hardness as a Function of Temperature for Three Bearing Steels (from Advanced Bearing Technology).	269

## LIST OF ILLUSTRATIONS (continued)

<b>Figure</b>	<b>Page</b>
103. Total Four-Ball Wear Versus Temperature for 52100 Steel Balls.	270
104. Total Four-Ball Wear Versus Temperature for M50 Steel Balls.	270
105. Wear Scar Size Versus Temperature for Four-Ball Tests of Polyphenyl Ether (1-Hour Tests at 600 rpm in Nitrogen with M10 Balls) (from Reference 11).	271
106. Glass Transition by Isothermal Compression from Liquid (Dilatometry) (from Reference 13).	274
107. Heuristic Estimates of the Relationship Between Conditions in an EHD Contact and Glass-Liquid Phase Diagrams of Three Lubricants (Lubricant Supply Temperature about 20°C) (from Reference 13).	274
108. Surface Profiles of the Upper Ball Wear Scars from Two Four-Ball Tests of O-67-1 at 75°C (M50 Balls, 3-Hour Tests, 1200 rpm, 145-N Load, 0.1 mm per Division Horizontal Scale, 0.01 mm per Division Vertical Scale).	276
109. Surface Profiles of the Upper Ball Wear Scars from Two Four-Ball Tests of O-67-1 at 150°C (M50 Balls, 3-Hour Tests 1200 rpm, 145-N Load, 0.1 mm per Division Horizontal Scale, 0.01 mm per Division Vertical Scale).	277
110. Surface Profiles of the Upper Ball Wear Scars from Two Four-Ball Tests of O-67-1 at 250°C (M50 Balls, 3-Hour Tests, 1200 rpm, 145-N Load, 0.1 mm per Division Horizontal Scale, 0.01 mm per Division Vertical Scale).	278
111. Surface Profile of the Upper Ball Wear Scar from a Four-Ball Test of O-67-1 at 315°C (M50 Balls, 3-Hour Test, 1200 rpm, 145-N Load, 0.1 mm per Division Horizontal Scale, 0.01 mm per Division Vertical Scale).	279
112. Four-Ball Wear Versus Temperature Curves for Three 5P4E Polyphenyl Ethers (M50 Balls, 3-Hour Tests, 1200 rpm, 145-N Load).	281
113. Four-Ball Wear Versus Temperature Curves for Three Experimental Fluids (M50 Balls, 3-Hour Tests, 1200 rpm 145-N Load).	282
114. Four-Ball Wear Versus Temperature Curves for a 6P5E Polyphenyl Ether, a C-Ether, and a Perfluoropolyalkyl Ether (M50 Balls, 3-Hour Tests, 1200 rpm, 145-N Load).	283
115. Four-Ball Wear Versus Temperature Curves for Polyphenyl Ether Basestock with and without Trichloroethylene Dilution.	284

## LIST OF ILLUSTRATIONS (continued)

<b>Figure</b>	<b>Page</b>
116. Four-Ball Wear Versus Temperature Curves for Inhibited Polyphenyl Ether with and without C-Ether Dilution.	284
117. Four-Ball Wear Rates for Two Identically Tested Fluids Presented Using the Displacement of the Upper Ball Versus Test Time.	286
118. Four-Ball Wear Scar Length Versus Test Time Calculated from the Data of Figure 117.	286
119. Ranking of Fluids by the Average Scar Diameter After Four-Ball Testing at the Conditions in ASTM D 4172.	288
120. A Schematic Diagram of the Three-Ball-on-Disk (TBOD) Wear Test Device.	292
121. Components of TBOD: (a) TBOD Test Head Assembly and (b) Profile of the Indented Disk Surface.	294
122. Consumption Rates of O-77-6 at 30, 150 and 250°C. Rotating Speed: 200 rpm; Load: 22.68 kg; Lubricant Volume: 20 mm <sup>3</sup> .	299
123. GPC Chromatograms of O-77-6, Showing Build-up of the Tetrahydrofuran Soluble High Molecular Weight (HMW) Wear Products.	301
124. Photomicrographs of Ball Wear Scars: (a) From the Four-Ball Test. Lubricant: 5P4E; Test Specimen: M50 Balls; Temperature: 150°C; Rotating Speed: 1200 rpm; Load: 14.74 kg; Lubricant Volume: 30 cm <sup>3</sup> ; Test Duration: 180 min., (b) From the TBOD Test. Lubricant: 5P4E; Test Specimen: M50 Balls and Disk; Temperature: 150°C; Rotating Speed: 200 rpm; Load: 22.68 kg; Lubricant Volume: 20 mm <sup>3</sup> ; Test Duration: 60 min.	303
125. Wear Rates of M50 Specimens at 30, 150, and 250°C. Rotating Speed: 200 rpm; Load: 22.68 kg; Lubricant Volume: 20 mm <sup>3</sup> .	304
126. Beta Values Corresponding to the Wear Data Presented in Figure 6.	306
127. Wear Ratio (Wear of Three Balls/Total Wear) as a Function of the Beta Parameter for a Fixed Scar Length. The Limits of Scar Lengths Observed from the Experiment are Indicated.	307
128. Coefficient of Friction at 30, 150, and 250°C. Rotating Speed: 200 rpm; Load: 22.68 kg; Lubricant Volume: 20 mm <sup>3</sup> .	308

## LIST OF ILLUSTRATIONS (continued)

<b>Figure</b>	<b>Page</b>
129. Coefficient of Friction at 150°C. Rotating Speed: 200 rpm; Load: 22.68 kg; Lubricant Volume: 20 mm <sup>3</sup> .	309
130. Wear Rates of M50 Specimens at 150°C. Rotating Speed: 200 rpm; Load: 22.68 kg; Lubricant Volume: 20 mm <sup>3</sup> .	310
131. Lubricant Consumption Rates at 150°C. Rotating Speed: 200 rpm; Load: 22.68 kg; Lubricant Volume: 20 mm <sup>3</sup> .	312
132. GPC Chromatograms of the Three Tested Fluids, Together with Their Corresponding Fresh Standards.	313
133. Coefficient of Friction for the Five Test Fluids. Rotating Speed: 200 rpm; Load: 22.68 kg; Lubricant Volume: 20 mm <sup>3</sup> ; Temperature: 250°C.	314
134. Total Wear Volume of M50 Specimens. Rotating Speed: 200 rpm; Load: 22.68 kg; Lubricant Volume: 20 mm <sup>3</sup> ; Temperature: 250°C.	315
135. Wear Scar Diameter of M50 Balls. Rotating Speed: 200 rpm; Load: 22.68 kg; Lubricant Volume: 20 mm <sup>3</sup> ; Temperature: 250°C.	317
136. GPC Chromatograms of the Five Test Fluids, Showing Build-up of the THF Soluble HMW Wear Products.	318
137. Lubricant Consumption of the Five Test Fluids. Rotating Speed: 200 rpm; Load: 22.68 kg; Lubricant Volume: 20 mm <sup>3</sup> ; Temperature: 250°C.	321
138. A Breakdown of the Total Consumption of O-64-20 into Two Major Components. Rotating Speed: 200 rpm; Load: 22.68 kg; Lubricant Volume: 20 mm <sup>3</sup> ; Temperature: 250°C.	322
139. A Schematic Diagram of the Rolling Bearing Used in the TBRF Test, Together with a Still Photo of the Actual Bearing Components and Their Holders.	327
A-1 Squires Oxidative Stability Data Curves for O-91-13 Showing: (a) Percent Weight Loss; (b) TAN Increase; (c) Percent Viscosity Increase, 100°C, and (d) Percent Viscosity Increase, 100°C (Manually Drawn).	404
A-2 Squires Oxidative Stability Data Curves for TEL-90103 Showing: (a) Percent Weight Loss; (b) TAN Increase, and (c) Percent Viscosity Increase, 100°C.	405

## LIST OF ILLUSTRATIONS (continued)

<u>Figure</u>	<u>Page</u>
A-3 Squires Oxidative Stability Data Curves for TEL-91002 Showing: (a) Percent Weight Loss; (b) TAN Increase; (c) Percent Viscosity Increase, 40°C, and (d) Percent Viscosity Increase, 100°C.	406
A-4 Squires Oxidative Stability Data Curves for TEL-91003 Showing: (a) Percent Weight Loss; (b) TAN Increase; (c) Percent Viscosity Increase, 40°C, and (d) Percent Viscosity Increase, 100°C.	407
A-5 Squires Oxidative Stability Data Curves for TEL-91052 Showing: (a) Percent Weight Loss; (b) TAN Increase; (c) Percent Viscosity Increase, 40°C, and (d) Percent Viscosity Increase, 100°C.	408
A-6 Squires Oxidative Stability Data Curves for TEL-91053 Showing: (a) Percent Weight Loss; (b) TAN Increase, and (c) Percent Viscosity Increase, 100°C.	409
A-7 Squires Oxidative Stability Data Curves for TEL-91063 Showing: (a) Percent Weight Loss; (b) TAN Increase; (c) Percent Viscosity Increase, 40°C, and (d) Percent Viscosity Increase, 100°C.	410
A-8 Squires Oxidative Stability Data Curves for TEL-92036 Showing: (a) Percent Weight Loss; (b) TAN Increase; (c) Percent Viscosity Increase, 40°C, and (d) Percent Viscosity Increase, 100°C.	411
A-9 Squires Oxidative Stability Data Curves for TEL-92039 Showing: (a) Percent Weight Loss; (b) TAN Increase; (c) Percent Viscosity Increase, 40°C, and (d) Percent Viscosity Increase, 100°C.	412
A-10 Squires Oxidative Stability Data Curves for TEL-92040 Showing: (a) Percent Weight Loss; (b) TAN Increase; (c) Percent Viscosity Increase, 40°C, and (d) Percent Viscosity Increase, 100°C.	413
A-11 Squires Oxidative Stability Data Curves for TEL-92041 Showing: (a) Percent Weight Loss; (b) TAN Increase; (c) Percent Viscosity Increase, 40°C, and (d) Percent Viscosity Increase, 100°C.	414
A-12 Squires Oxidative Stability Data Curves for TEL-92049 Showing: (a) Percent Weight Loss; (b) TAN Increase; (c) Percent Viscosity Increase, 40°C, and (d) Percent Viscosity Increase, 100°C.	415
A-13 Squires Oxidative Stability Data Curves for TEL-92050 Showing: (a) Percent Weight Loss; (b) TAN Increase; (c) Percent Viscosity Increase, 40°C, and (d) Percent Viscosity Increase, 100°C.	416

## LIST OF ILLUSTRATIONS (continued)

<u>Figure</u>	<u>Page</u>
A-14 Effective Lubricant Life as a Function of Temperature for O-91-13 Based on: (a) Percent Weight Loss Limits; (b) TAN Increase Limits; (c) Percent Viscosity Change at 100°C, and (d) Percent Viscosity Change at 100°C (Data Points from Manually Drawn Curves of Fig. A-1)	417
A-15 Effective Lubricant Life as a Function of Temperature for O-90-6 Based on: (a) Percent Weight Loss Limits and (b) Percent Viscosity Change at 100°C.	418
A-16 Effective Lubricant Life as a Function of Temperature for TEL-90087 Based on: (a) Percent Weight Loss Limits and (b) Percent Viscosity Change at 100°C.	419
A-17 Effective Lubricant Life as a Function of Temperature for TEL-90103 Based on: (a) Percent Weight Loss Limits; (b) TAN Increase Limits; and (c) Percent Viscosity Change at 100°C.	420
A-18 Effective Lubricant Life as a Function of Temperature for TEL-91002 Based on: (a) Percent Weight Loss Limits; (b) TAN Increase Limits; (c) Percent Viscosity Change at 40°C, and (d) Percent Viscosity Change at 100°C.	421
A-19 Effective Lubricant Life as a Function of Temperature for TEL-91053 Based on: (a) Percent Weight Loss Limits; (b) TAN Increase Limits; and (c) Percent Viscosity Change at 100°C.	422
A-20 Effective Lubricant Life as a Function of Temperature for TEL-91063 Based on: (a) Percent Weight Loss Limits; (b) TAN Increase Limits; (c) Percent Viscosity Change at 40°C, and (d) Percent Viscosity Change at 100°C.	423
A-21 Effective Lubricant Life as a Function of Temperature for TEL-92039 Based on: (a) Percent Weight Loss Limits; (b) TAN Increase Limits; (c) Percent Viscosity Change at 40°C, and (d) Percent Viscosity Change at 100°C.	424
A-22 Effective Lubricant Life as a Function of Temperature for TEL-92040 Based on: (a) Percent Weight Loss Limits; (b) TAN Increase Limits; (c) Percent Viscosity Change at 40°C, and (d) Percent Viscosity Change at 100°C.	425
A-23 Effective Lubricant Life as a Function of Temperature for TEL-92041 Based on: (a) Percent Weight Loss Limits; (b) TAN Increase Limits; (c) Percent Viscosity Change at 40°C, and (d) Percent Viscosity Change at 100°C.	426
A-24 Effective Lubricant Life as a Function of Temperature for TEL-92049 Based on: (a) Percent Weight Loss Limits; (b) TAN Increase Limits; (c) Percent Viscosity Change at 40°C, and (d) Percent Viscosity Change at 100°C.	427

## LIST OF ILLUSTRATIONS (concluded)

<b>Figure</b>	<b>Page</b>
A-25 Effective Lubricant Life as a Function of Temperature for TEL-92050 Based on: (a) Percent Weight Loss Limits; (b) TAN Increase Limits; (c) Percent Viscosity Change at 40°C, and (d) Percent Viscosity Change at 100°C.	428
B-1 TBOD Configuration Showing One Ball Before and After Wear.	435
B-2 Scar Surface, $s$ , Corresponding to Wear on Both the Ball and the Disk.	436
B-3 Cross-Section of the Ball and Disk at the Deepest Part of the Disk Wear Track (Ball Slides in the + $z$ Direction).	437
B-4 Relationship Between Scar Width and Chord Length for Selected Values of Beta Ranging from 0 to 1.	438
B-5 View of Scarred Ball (Looking in - $y$ Direction) Along with Cross-Sections of the Scar Region in Different $x$ - $z$ Planes.	439
B-6 Sensitivity of Volume Calculations to the Beta Parameter.	440

## LIST OF TABLES

<u>Table</u>		<u>Page</u>
1	DESCRIPTION OF ESTER BASE LUBRICANTS USED IN OXIDATIVE STABILITY STUDY	4
2	EFFECTIVE LUBRICANT LIFE AS A FUNCTION OF TEMPERATURE FOR 0-90-6 BASED ON WEIGHT LOSS AND VISCOSITY INCREASE	6
3	EFFECTIVE LUBRICANT LIFE AS A FUNCTION OF TEMPERATURE FOR O-91-13 BASED ON TAN, WEIGHT LOSS AND VISCOSITY INCREASE	7
4	EFFECTIVE LUBRICANT LIFE AS A FUNCTION OF TEMPERATURE FOR TEL-90087 BASED ON WEIGHT LOSS AND VISCOSITY INCREASE	8
5	EFFECTIVE LUBRICANT LIFE AS A FUNCTION OF TEMPERATURE FOR TEL-90103 BASE ON TAN, WEIGHT LOSS AND VISCOSITY INCREASE	9
6	EFFECTIVE LUBRICANT LIFE AS A FUNCTION OF TEMPERATURE FOR TEL-91002 BASED ON VISCOSITY INCREASE WEIGHT LOSS AND TAN INCREASE	10
7	EFFECTIVE LUBRICANT LIFE AS A FUNCTION OF TEMPERATURE FOR TEL-91003 BASED ON TAN, WEIGHT LOSS AND VISCOSITY INCREASE	11
8	EFFECTIVE LUBRICANT LIFE AS A FUNCTION OF TEMPERATURE FOR TEL-91005 BASED ON PERCENT VISCOSITY INCREASE, PERCENT WEIGHT LOSS AND TAN	12
9	EFFECTIVE LUBRICANT LIFE AS A FUNCTION OF TEMPERATURE FOR TEL-91053 BASED ON TAN, WEIGHT LOSS AND VISCOSITY INCREASE	13
10	EFFECTIVE LUBRICANT LIFE AS A FUNCTION OF TEMPERATURE FOR TEL-91063 BASED ON TAN, WEIGHT LOSS AND VISCOSITY INCREASE	14
11	EFFECTIVE LUBRICANT LIFE AS A FUNCTION OF TEMPERATURE FOR TEL-92039 BASED ON TAN, WEIGHT LOSS AND VISCOSITY INCREASE	15
12	EFFECTIVE LUBRICANT LIFE AS A FUNCTION OF TEMPERATURE FOR TEL-92040 BASED ON TAN, WEIGHT LOSS AND VISCOSITY INCREASE	16
13	EFFECTIVE LUBRICANT LIFE AS A FUNCTION OF TEMPERATURE FOR TEL-92041 BASED ON TAN, WEIGHT LOSS AND VISCOSITY INCREASE	17

# LIST OF TABLES (continued)

<b>Table</b>		<b>Page</b>
14	EFFECTIVE LUBRICANT LIFE AS A FUNCTION OF TEMPERATURE FOR TEL-92049 BASED ON TAN, WEIGHT LOSS AND VISCOSITY INCREASE	18
15	EFFECTIVE LUBRICANT LIFE AS A FUNCTION OF TEMPERATURE FOR TEL-92050 BASED ON VISCOSITY INCREASE, WEIGHT LOSS AND TAN INCREASE	19
16	RANKING OF LUBRICANTS ACCORDING TO LIMITING VALUES OF TAN AT 210°C	21
17	RANKING OF LUBRICANTS ACCORDING TO LIMITING VALUES OF VISCOSITY CHANGE AT 210°C	22
18	RANKING OF LUBRICANTS ACCORDING TO LIMITING VALUES OF WT LOSS AT 210°C	23
19	MAXIMUM EFFECTIVE LIFE (HOURS) FOR TWO (MINIMUM AND MAXIMUM) LIMITING LIFE VALUES AT TEMPERATURES	24
20	MINIMUM EFFECTIVE LIFE (HOURS) FOR TWO (MINIMUM & MAXIMUM) LIMITING LIFE VALUES AT TEMPERATURES OF 210°C and 225°C	25
21	RANKING OF LUBRICANTS ACCORDING TO LIMITING VALUES OF 1.5 TAN, 25% VIS. CHG. @ 100°C AND 25% WEIGHT LOSS AT 210°C	26
22	IDENTIFICATION OF HIGH TEMPERATURE LUBRICANTS	28
23	CORROSION AND OXIDATION DATA FOR TEL-91001 USING SQUIRES TUBES, 10 L/H AIRFLOW, AND INTERMEDIATE SAMPLING	29
24	EFFECTIVE LUBRICANT LIFE AS A FUNCTION OF TEMPERATURE FOR TEL-91001 AT THE 15%, 25% AND 35% VISCOSITY LIMITS AT 40°C AND THE 5%, 10% AND 15% VISCOSITY LIMITS AT 100°C ALONG WITH THE CONSTANTS FROM THE LEAST SQUARES LINE EQUATION	33
25	ADM/AA ANALYSES FOR TIN IN DEPOSITS FROM MINISIMULATOR RUNS WLM003 AND WLM004 (TEL-90102)	41
26	PHYSICAL PROPERTY DATA FOR POTENTIAL PPE DILUENTS WITH FLASH POINTS ABOVE 38°C	45

# LIST OF TABLES (continued)

<u>Table</u>		<u>Page</u>
27	TOXICITY DATA FOR POTENTIAL PPE DILUENTS HAVING FLASH POINTS ABOVE 38°C	46
28	PHYSICAL PROPERTY DATA FOR POTENTIAL PPE DILUENTS HAVING FLASH POINTS BELOW 38°C	47
29	TOXICITY DATA FOR POTENTIAL PPE DILUENTS HAVING FLASH POINTS BELOW 38°C	48
30	THE EFFECT OF SOLVENTS ON THE -34.4°C VISCOSITY OF PPE AT 20% VOLUME DILUTIONS AS A FUNCTION OF MOLAR CONCENTRATION AND DILUENT MELTING POINT	50
31	COMPARISON OF C&O TEST DATA FOR UNDILUTED AND DILUTED TEL-90102 AT 320°C/48 HOURS, SQUIRES TUBES WITH INITIAL CONDENSATE RETURN (ICR)	51
32	COMPARISON OF C&O TEST DATA FOR UNDILUTED AND DILUTED TEL-90102 AT 320°C/48 HOURS, SQUIRES TUBES WITHOUT INITIAL CONDENSATE RETURN (ICR)	52
33	COMPARISON OF C&O TEST DATA FOR 50/50 O-64-20/TEL-90102 BLEND, O-64-20 AND TEL-90102 AT 320°C, 48 HOURS, SQUIRES TUBES	55
34	VISCOSITIES AT 34.4°C FOR DILUENTS IN 5P4E AND DILUENTS IN BLENDS OF 5P4E AND 4P3E, C-ETHER AND 3P2E	56
35	SUMMARY OF DILUENTS, BLENDS AND DILUENT/BLENDS OF POLYPHENYL ETHER THAT MEET THE -34.4°C (-30°F) PUMPABILITY SPECIFICATION	58
36	FOUR-BALL TEST RESULTS FOR PE/PPE SOLUTIONS AT 150°C	63
37	VISCOSITY MEASUREMENTS OF TCP AND TPP IN THE O-77-6 FLUID	70
38	OXIDATION TESTS (WITHOUT METAL COUPONS) FOR 24 HOURS AT 280, 300, AND 320°C OF BULK OIL TEMPERATURES	74
39	CORROSION/OXIDATION TEST OF TPP/O-77-6 FORMULATIONS AT 320°C FOR 24 AND 48 HOURS	76

# LIST OF TABLES (continued)

<b><u>Table</u></b>		<b><u>Page</u></b>
40	WEIGHT VARIATION OF METAL COUPONS FROM THE CORROSION/OXIDATION TESTS PRESENTED IN TABLE 39	78
41	CORROSION/OXIDATION TEST OF MORE O-77-6 FORMULATIONS WITH EITHER ADDITIVE A OR TPPO, IN ADDITION TO TPP	85
42	WEIGHT VARIATION OF METAL COUPONS FROM THE CORROSION/OXIDATION TESTS PRESENTED IN TABLE 41	86
43	VISCOSITY MEASUREMENTS OF TPPP IN THE O-77-6 FLUID	88
44	CORROSION/OXIDATION TEST OF THE O-77-6 SOLUTION CONTAINING 30% TPP AND 10% TPPP, AT 320°C FOR 24 AND 48 HOURS	89
45	WEIGHT VARIATION OF METAL COUPONS FROM THE CORROSION/OXIDATION TESTS PRESENTED IN TABLE 44	91
46	EXAMPLES OF OXIDATION TECHNIQUES FOR LIQUID LUBRICANTS	94
47	CORROSION AND OXIDATION DATA FOR O-64-20 USING SQUIRES TUBES, 10 L/H AIRFLOW, AND INTERMEDIATE SAMPLING	110
48	EFFECT OF METAL SPECIMENS AND CONDENSATE RETURN ON CORROSION AND OXIDATION TEST DATA FOR O-64-20 (320°C, 96 HOURS)	113
49	EFFECT OF VARIOUS ADDITIVES ON C&O TEST PERFORMANCE OF O-64-20 (320°C, 48 HOURS)	114
50	SILVER SPECIMEN CORROSION DATA FOR O-64-20 320°C, SQUIRES TUBE, 10 L/HOUR AIRFLOW	115
51	VAPOR PHASE CORROSION AND OXIDATION DATA RESULTS FOR O-64-20 AT 320°C, 48 HOUR, TEST DURATION, SQUIRES TUBES AND 10 L/H AIRFLOW	117
52	C&O TEST DATA FOR O-64-20 FORMULATIONS	118
53	C&O TEST DATA AT 320°C FOR O-64-20 WITH 1.35% DIPHENYLBORINIC ANHYDRIDE	119

# LIST OF TABLES (continued)

<u>Table</u>		<u>Page</u>
54	C&O TEST DATA AT 320°C FOR O-64-20 WITH 0.5% DIPHENYLBORINIC ANHYDRIDE	120
55	X-RAY PHOTOELECTRON SPECTROSCOPIC (XPS) ANALYSIS OF M50 AND SILVER WASHERS FROM THE CORROSION AND OXIDATION TEST OF O-64-20 WITH 1.35% DIPHENYLBORINIC ANHYDRIDE	121
56	CORROSION AND OXIDATION TEST DATA FOR TEL-90013 AT 280°C, SQUIRES TUBES AND 10 L/H AIRFLOW	135
57	CORROSION AND OXIDATION TEST DATA FOR TEL-90013 WITH THE TPFE APPARATUS AND 10 L/H AIRFLOW	137
58	C&O TEST DATA FOR TEL-92026 AT 240°C	138
59	C&O TEST DATA FOR TEL-92026 AT 260°C FOR 144 HOURS	139
60	C&O TEST DATA FOR TEL-92026 AT 260°C FOR 125 HOURS	140
61	C&O TEST DATA FOR TEL-92026 AT 280°C	141
62	THERMAL STRESSING DATA FOR TEL-92026 UNDER DIFFERENT TEST CONDITIONS AT 280°C FOR 48 HOURS	143
63	DESCRIPTION OF TEST FLUIDS USED IN AFAPL STATIC COKER STUDY	151
64	AFAPL STATIC COKER DATA FOR HIGH TEMPERATURE ESTER BASE LUBRICANTS (300°C, 3 H TEST TIME, SS-302 TEST SURFACE, 0.5 g SAMPLE, TPFE SEALS)	153
65	EFFECT OF TEST SURFACE ON AFAPL STATIC COKING VALUES (300°C, 3H TEST TIME, TPFE SEALS, 0.5g SAMPLE)	154
66	EFFECT OF TEST TIME ON AFAPL STATIC COKER VALUES (300°C SS-302 TEST SPECIMENS, 0.5g SAMPLE, TPFE SEALS)	155
67	COMPARISON OF AFAPL STATIC COKER DATA USING SS-302 STEEL SEALS AND TPFE SEALS (STAINLESS STEEL TEST SURFACE, 300°C TEST TEMP & 0.5g SAMPLE)	156
68	AFAPL STATIC COKER TEST DATA FOR C-ETHER O-64-20 USING SS-302 TEST SPECIMEN, 0.5g SAMPLE	158

# LIST OF TABLES (continued)

<b><u>Table</u></b>	<b><u>Page</u></b>
69 EFFECT OF C&O PRESTRESSING ON AFAPL STATIC COKER DEPOSITS OF C-ETHER O-64-20	159
70 EFFECT OF USING SILVER TEST SPECIMENS ON AFAPL STATIC COKER DEPOSITS OF C-ETHER O-64-20 (TEST TEMP. 375°C, 3 TEST HOURS, 0.5 g SAMPLE)	160
71 EFFECT OF WEAR METAL ON AFAPL STATIC COKER DEPOSITS FOR C-ETHER O-64-20	162
72 MCRT DEPOSIT VALUES FOR HIGH TEMPERATURE ESTER BASE LUBRICANTS	165
73 MCRT TEST DATA FOR C-ETHER O-64-20	167
74 DEPOSIT TYPES AND THEIR DEMERIT VALUES	176
75 DEMERIT WEIGHTING FACTORS FOR THE COMPONENTS OF THE MINISIMULATOR TEST SECTION	177
76 MINISIMULATOR TEST SUMMARY	178
77 COMPARISON OF TARGET TEMPERATURES (°C) TO AVERAGE TEMPERATURES (°C) FOR CRITICAL SECTIONS OF THE MINISIMULATOR	182
78 MAXIMUM ELEMENTAL CONCENTRATIONS IN OIL SAMPLES FROM MINISIMULATOR TESTING	183
79 DESCRIPTION OF FLUIDS USED IN FORMING STUDIES	191
80 FOAMING CHARACTERISTICS OF HIGH TEMPERATURE ESTER BASE LUBRICANTS	192
81 FOAMING CHARACTERISTICS OF HIGH TEMPERATURE NON-ESTER BASE FLUIDS	194
82 COEFFICIENTS FOR LINEAR REGRESSIONS FOR THE DATA IN FIGURES 58, 60, AND 62	206
83 COEFFICIENTS FOR LINEAR REGRESSIONS DONE ON DATA OF FIGURES 60 AND 64	208

LIST OF TABLES (concluded)

<b><u>Table</u></b>	<b><u>Page</u></b>
84 SENSITIVITY LOSS OF THE FERROSCAN 310 FOR VARIOUS FE PARTICLE SIZES	210
85 RDN INCREASES FROM FOUR ADDITIONS OF LESS THAN 5 MICRON FE PARTICLES	215
86 RDN INCREASES FROM FOUR ADDITIONS OF TBOD WEAR PARTICLES	220
87 TBOD WEAR FROM 20-HOUR TESTS OF M50 BALLS AND 1018 DISKS USING FILTERED MIL-L-7808	244
88 CHEMICAL COMPOSITION OF SELECTED STEELS	272
89 CHEMICAL COMPOSITION AND PHYSICAL PROPERTIES OF THE M50 STEEL	295
90 A LIST OF THE TEST LUBRICANTS	296
91 A SUMMARY OF THE TBRF TEST RESULTS	329
A-1 SQUIRES OXIDATIVE TEST DATA	332
A-2 CORROSION AND OXIDATION TEST DATA	347
A-3 AFAPL STATIC COKER TEST DATA	396
A-4 MCRT COKING TEST DATA	401
A-5 LUBRICANT FOAMING TEST DATA WITH VARIABLE TEST CONDITIONS	402

## **SECTION I**

### **INTRODUCTION**

**Fluid lubricants capable of superior performance in advanced aircraft turbine engine environments at temperatures from 500-750°F are required by the United States Air Force to improve their propulsion capabilities. Lubricant requirements include thermal-oxidative stability within an engine oil system environment, compatibility with various engine materials and satisfactory tribological performance.**

**This work describes the second half of research conducted for developing improved methods for measuring lubricant performance. These methods were used to predict performance of selected high temperature candidate fluids. The work also includes the development of lubrication system monitors for assessing condition of engine health, development of techniques satisfactory for monitoring lubricant condition and evaluation of candidate fluids tribological behavior. Methods developed in this work are applicable to potential high temperature turbine engine candidate fluids including polyphenyl ethers, C-ethers, cyclophosphazenes, perfluoroalkyl ethers, and other proprietary experimental fluids and additive modified versions of such fluids.**

**Sections II, III, IV and V deal with work performed as specified in Tasks I, II, III and V, respectively, of the work statement (Contract No. F33615-88-C-2817). Task IV, "Lubricant Load Carrying Test Assessment," was completed earlier in the program and reported in WL-TR-91-2111, Interim Report, January 1992.**

## SECTION II

### DEVELOPMENT OF IMPROVED METHODS FOR MEASURING LUBRICANT PERFORMANCE

#### 1. OXIDATIVE STABILITY OF ESTER BASE LUBRICANTS

##### a. Introduction

The objective of this phase of the program was to investigate the oxidative stability of 4 centistoke (cSt) turbine engine lubricants as it relates to temperature and determine the fluid stability in terms of effective lubricant life based upon limiting values of physical properties. Viscosity, acidity, volatility, electrochemical characteristics and composition were the properties determined after the oxidative stressing of the lubricant with only viscosity, acidity and volatility measurements being used for determining lubricant effective life.

##### b. Test Apparatus and Test Procedure

Both the test apparatus and test procedure have been described previously<sup>1</sup> and remained unchanged during this investigation.

##### c. Test Lubricants

A total of 16 lubricants were studied during this phase of the program and are described in Table 1. Test conditions ranged from 210°C to 225°C test temperatures and test durations to 196 hours. Testing was terminated after severe degradation or after very high lubricant loss had occurred.

##### d. Results and Discussion

The oxidative stability data obtained for the 4 cSt (100°C) ester base high temperature lubricants are given in Appendix A, Table A-1. These data include lubricant identification, sample size, test temperature and test times, visual appearance of any tube deposits and lubricant property data including total acid number (TAN), viscosity and percent change, weight loss and COBRA readings. These data were used in the development of figures and tables describing the rate of change of various lubricant properties with test temperature and time, the development of Arrhenius curves showing "Effective Lubricant Life" as a function of selected limiting lubricant properties and the comparative ranking of the lubricants based upon Squires oxidative testing.

**TABLE 1**  
**DESCRIPTION OF ESTER BASE LUBRICANTS USED IN**  
**OXIDATIVE STABILITY STUDY**

Test Fluid	Description	Viscosity, cSt	
		40°C	100°C
O-85-1 <sup>1</sup>	Candidate Lubricant	17.68	4.04
O-90-6 <sup>1</sup>	Different Lot O-85-1	17.62	4.01
O-91-13	Different Lot O-85-1	18.51	4.14
TEL-90087 <sup>1</sup>	Candidate Lubricant	17.65	4.02
TEL-90103	" "	17.09	3.97
TEL-91002	" "	17.69	4.00
TEL-91003	" "	17.60	4.02
TEL-91005	" "	17.76	4.04
TEL-91053	" "	16.70	3.99
TEL-91063	" "	17.01	4.02
TEL-92036	" "	18.38	4.10
TEL-92039	" "	18.04	4.10
TEL-92040	" "	16.63	3.99
TEL-92041	" "	17.56	4.10
TEL-92049	Different Lot TEL-92036	18.25	4.10
TEL-92050	Candidate Lubricant	17.66	4.05

<sup>1</sup>Squires oxidative test data reported or partially reported in Reference 3

Graphical representations of the relationships between test time and lubricant property changes which provided the necessary data for the development of Arrhenius curves are shown in Appendix A. With the exception of lubricant TEL-92036, all lubricants were tested at three or more temperatures depending upon the stability shown by initial testing at 205°C or 210°C. The temperature range of all testing was 195°C to 235°C. In most cases, these curves are as expected in that increasing the test temperature increased the rate of change in the measured properties. As an exception, the curve for TEL-90103 lubricant shows the weight loss to be about the same for both the 225°C and 235°C testing until about 50 test hours after which testing at 235°C shows a much greater rate of increase. Limited sample volume of TEL-92036 permitted testing at only two temperatures. However, lubricant TEL-92049 (different lot of TEL-92036) was of sufficient quantity to permit testing at three temperatures. Both lubricants showed very similar performance as shown by Figure A-8 (TEL-92036) and Figure A-12 (TEL-92049).

Tables 2 through 15 show the effective lubricant life as a function of test temperature based for limiting values of TAN, % viscosity increase and % weight loss. For example in Table 2, lubricant O-90-6 would require 76 test hours at 215°C for the % viscosity change (measured at 100°C) to reach the limit of 25% change. These tables also show the values of the constants "a" and "b" of the equation  $Y = a + bX$  where Y is the log of the effective life in hours, and X is  $1 \times 10^{-3}/T$  (where T is in °K). Arrhenius plots were developed for each lubricant using the effective life data given in Tables 2 through 15 for the various limiting life criteria and are shown in Figures A-14 to A-25. In general these plots show three distinct groups as follows.

Group A: All Arrhenius curves, regardless of "property" or "level" of limiting life criterion, converge with increasing test temperature.  
(example lubricant TEL-92049, Figure A-24)

Group B: Arrhenius curves for weight loss and viscosity change converge with increasing test temperature but Arrhenius curves for TAN change converge with decreasing test temperature.  
(example lubricant TEL-91053, Figure A-19)

Group C: All Arrhenius curves for each "limiting" life property are parallel.  
(example lubricant TEL-92040, Figure A-22)

TABLE 2

**EFFECTIVE LUBRICANT LIFE AS A FUNCTION OF  
TEMPERATURE FOR 0-90-6 BASED ON WEIGHT  
LOSS AND VISCOSITY INCREASE**

Temp.,°C	% Weight Loss Limits		
	15%	25%	35%
210	53	86	108
215	28	50	70
220	28	41	51
225	18	31	38
a <sup>1</sup>	-12.190	-12.057	12.923
b <sup>1</sup>	6.700	6.705	7.218

Temp.,°C	% Viscosity (100°C) Increase Limits		
	15%	25%	35%
210	130	182	236
215	71	76	81
220	32	38	42
225	26	27	29
a	-25.325	-27.664	-22.214
b	13.300	14.474	11.754

<sup>1</sup>a = Y intercept, b = slope,  $Y = a + b X$   
Effective life values given in hours

TABLE 3

EFFECTIVE LUBRICANT LIFE AS A FUNCTION OF TEMPERATURE FOR  
O-91-13 BASED ON TAN, WEIGHT LOSS AND VISCOSITY INCREASE

% Viscosity (100°C) Increase Limits			
Temp.°C	15%	25%	35%
205	42.3	84.9	124.8
210	38.5	53.4	61.6
210 <sup>1</sup>	34	57	71
220	20.6	34.5	47.3
220 <sup>1</sup>	22	29	34
a <sup>2</sup>	-9.1455	-10.560	-10.793
b <sup>2</sup>	5.1644	5.9579	6.1303
a	-7.7955	-13.438	-16.269
b	4.5095	7.3453	8.7712

% Weight Loss Limits			
	15%	25%	35%
205	53.0	100.2	150.2
210	48.7	64.6	90.7
220	26.5	38.4	50.5
a	-8.6983	-11.485	-13.127
b	4.9975	6.4388	7.3064

TAN Increase Limits			
	1.0	1.5	3.0
205	80.8	106.3	161.6
210	44.1	62.2	96.7
220	21.0	31.1	54.3
a	-17.0751	-15.338	-13.083
b	9.0641	8.2929	7.2994

<sup>1</sup>Values extracted manually from hand-drawn curves<sup>2</sup>a = Y intercept, b = slope, Y = a + b X

Effective life values given in hours

TABLE 4

**EFFECTIVE LUBRICANT LIFE AS A FUNCTION OF  
TEMPERATURE FOR TEL-90087 BASED ON WEIGHT  
LOSS AND VISCOSITY INCREASE**

Temp., °C	% Weight Loss limits		
	15%	25%	35%
197	44	116	220
210	29	58	97
225	18	32	51
a <sup>1</sup>	-5.238	-7.841	-8.897
b <sup>1</sup>	3.236	4.650	5.275

Temp., °C	% Viscosity (100°C) Increase Limits		
	15%	25%	35%
197	50	105	180
210	28	56	79
225	15	24	32
a	-7.568	-9.348	-11.080
b	4.356	5.350	6.251

<sup>1</sup>a = Y intercept, b = slope

Effective life values given in hours

TABLE 5

**EFFECTIVE LUBRICANT LIFE AS A FUNCTION OF TEMPERATURE  
FOR TEL-90103 BASE ON TAN, WEIGHT LOSS AND  
VISCOSITY INCREASE**

TAN Increase Limits				
Temp., °C	1.0	1.5	3.0	
210	98	168	336	
225	40	61	102	
235	22	30	48	
a <sup>1</sup>	-11.174	-12.928	-14.628	
b <sup>1</sup>	6.363	7.324	8.288	
% Weight Loss Limits				
	15%	25%	35%	
210	38	73	109	
225	15	26	46	
235	12	22	42	
a	-8.913	-9.147	-6.776	
b	5.058	5.304	4.243	
% Viscosity Increase Limit at 100°C				
	15%	25%	35%	
210	19	51	68	
225	11	19	24	
235	7	14	20	
a	-7.447	-9.983	-9.385	
b	4.219	5.638	5.404	

<sup>1</sup>a = Y Intercept, b = slope  
Effective life values given in hours

TABLE 6

**EFFECTIVE LUBRICANT LIFE AS A FUNCTION OF TEMPERATURE  
FOR TEL-91002 BASED ON VISCOSITY INCREASE  
WEIGHT LOSS AND TAN INCREASE**

Temp., °C	% Viscosity Increase at 40°C		
	15%	25%	35%
205	136	177	206
220	49	64	73
225	34	44	53
a <sup>1</sup>	-13.502	-13.437	-13.129
b <sup>1</sup>	7.481	7.505	7.388

Temp., °C	% Viscosity Increase at 100°C		
	15%	25%	35%
205	172	225	266
220	64	82	92
225	46	57	65
a	-12.706	-13.164	-13.576
b	7.149	7.425	7.656

Temp., °C	% Weight Loss Limits		
	15%	25%	35%
205	75	127	182
220	29	48	67
225	24	39	52
a	-11.241	-11.728	-12.091
b	6.271	6.616	6.865

Temp., °C	TAN Increase Limits		
	1.0	1.5	3.0
205	155	209	482
220	65	94	103
225	51	60	68
a	-10.525	-11.881	-19.792
b	6.082	6.796	10.751

<sup>1</sup>a = y Intercept; b = slope

TABLE 7

EFFECTIVE LUBRICANT LIFE AS A FUNCTION OF TEMPERATURE FOR  
TEL-91003 BASED ON TAN, WEIGHT LOSS AND VISCOSITY INCREASE

Temp., °C	TAN Increase Limits		
	1.0	1.5	3.0
210	106.4	149.8	248.2
225	54.8	75.5	120.0
235	28.4	37.2	51.8
a <sup>1</sup>	-9.3819	-9.8355	-11.0510
b <sup>1</sup>	5.5195	5.8116	6.5083

	% Weight Loss Limits		
	15%	25%	35%
210	70.1	119.0	170.2
225	31.9	61.2	93.1
235	20.1	35.7	51.7
a	-9.1776	-8.4118	-8.0680
b	5.3244	5.0704	4.9823

	% Viscosity Increase at 100°C		
	15%	25%	35%
210	101.6	156	168
225	50.6	79.9	99
235	25.1	37.6	47.3
a	-10.062	-10.030	-8.5653
b	5.8393	5.9161	5.2262

	% Viscosity Increase at 40°C		
	15%	25%	35%
210	63.5	117.3	157.8
225	31.9	52.1	70.6
235	18.6	28.5	36.5
a	-8.9077	-10.299	-10.548
b	5.1778	5.9781	6.1628

<sup>1</sup>a = Y intercept, b = slope  
Effective life values given in hours

TABLE 8

**EFFECTIVE LUBRICANT LIFE AS A FUNCTION OF TEMPERATURE FOR  
TEL-91005 BASED ON PERCENT VISCOSITY INCREASE, PERCENT  
WEIGHT LOSS AND TAN**

Temp., °C	% Viscosity Increase Limit at 100°C		
	15%	25%	35%
195	36.4	91.6	156.1
210	25.3	43.9	61.9
225	10.7	18.7	27.6
a <sup>1</sup>	-7.164	-9.434	-10.259
b <sup>1</sup>	4.102	5.340	5.831
	% Weight Loss Limit		
	15%	25%	35%
195	54.7	113.6	190.5
210	24.4	47.7	78.2
225	11.9	25.4	43.4
a	-9.229	-8.735	-8.385
b	5.133	5.045	4.984
	TAN Increase Limit		
	1.0	1.5	3.0
195	250.1	355.7	538.7
210	80.8	116.8	189.5
225	26.4	42.4	88.8
a	-13.752	-12.738	-10.256
b	7.562	7.156	6.072
	% Viscosity Increase Limit at 40°C		
	15%	25%	35%
195	20.9	46.4	78.1
210	13.7	24.4	35.5
225	6.8	11.6	16.6
a	-6.706	-8.276	-9.233
b	3.767	4.659	5.209

<sup>1</sup>a = Y intercept, b = slope; Effective Life values in hours

TABLE 9

EFFECTIVE LUBRICANT LIFE AS A FUNCTION OF TEMPERATURE FOR  
TEL-91053 BASED ON TAN, WEIGHT LOSS AND VISCOSITY INCREASE

Temp., °C	TAN Increase Limits		
	1.0	1.5	3.0
200	283.5	362.5	480.6
210	116.4	157.7	233.0
220	47.9	64.8	102.2
a <sup>1</sup>	-16.520	-15.807	-13.820
b <sup>1</sup>	8.9760	8.6914	7.8105
	% Weight Loss Limits		
	15%	25%	35%
200	39.0	93.7	165.4
210	24.5	56.7	98.2
220	16.2	25.8	32.7
a	-7.8032	-11.750	-14.999
b	4.4430	6.5016	8.1652
	% Viscosity Increase at 100°C		
	15%	25%	35%
200	58.9	130.6	207.9
210	47.8	82.8	114.8
220	24.2	40.2	54.7
a	-7.6432	-10.427	-11.906
b	4.4693	5.9433	6.7343

<sup>1</sup>a = Y intercept, b = slope  
Effective life values given in hours

TABLE 10

**EFFECTIVE LUBRICANT LIFE AS A FUNCTION OF TEMPERATURE  
FOR TEL-91063 BASED ON TAN, WEIGHT LOSS AND  
VISCOSITY INCREASE**

TAN Increase Limits			
Temp., °C	1.0	1.5	3.0
205	94.3	142.0	263.0
210	72.0	105.0	182.9
220	38.7	53.1	85.9
a <sup>1</sup>	-10.926	-12.099	-13.739
b <sup>1</sup>	6.1721	6.8178	7.7290
% Weight Loss Limits			
	15%	25%	35%
205	32.2	78.5	138.0
210	32.5	64.0	103.7
220	23.4	40.4	59.3
b	-3.4160	-7.7451	-10.017
a	2.3651	4.6118	5.8135
% Viscosity Increase at 40°C			
	15%	25%	35%
205	24.2	50.2	81.0
210	22.1	40.8	62.7
220	17.3	27.3	37.0
a	-3.4619	-7.0800	-9.4001
b	2.3187	4.1987	5.4087
% Viscosity Increase at 100°C			
	15%	25%	35%
205	50.3	98.4	148.9
210	36.0	76.0	118.0
220	25.7	45.9	65.2
a	-7.6396	-8.9793	-9.8588
b	4.4574	5.2471	5.7579

<sup>1</sup>a = Y intercept; b = slope  
Effective life values given in hours

**TABLE 11**  
**EFFECTIVE LUBRICANT LIFE AS A FUNCTION OF TEMPERATURE**  
**FOR TEL-92039 BASED ON TAN, WEIGHT LOSS AND**  
**VISCOSITY INCREASE**

Temp., °C	TAN Increase Limits		
	1.0	1.5	3.0
205	153.9	179.0	285.5
215	81.3	101.8	123.4
225	37.2	44.7	49.9
a <sup>1</sup>	-13.162	-12.733	-16.396
b <sup>1</sup>	7.346	7.167	9.018
	% Weight Loss Limits		
	15%	25%	35%
205	84.8	156.7	226.7
215	47.0	86.4	125.6
225	29.4	1.0	71.0
a	-9.513	-9.953	-10.190
b	5.467	5.807	5.999
	% Viscosity Increase at 40°C		
	15%	25%	35%
205	56.1	105.4	155.7
215	30.0	53.6	81.6
225	18.3	29.9	40.6
a	-10.362	-11.617	-12.347
b	5.787	6.520	6.955
	% Viscosity Increase at 100°C		
	15%	25%	35%
205	96.4	178.6	245.9
215	49.4	94.8	118.3
225	29.4	47.1	61.4
a	-10.880	-12.156	-12.609
b	6.147	6.893	7.171

<sup>1</sup>a = Y intercept, b = slope  
Effective life values given in values

**TABLE 12**  
**EFFECTIVE LUBRICANT LIFE AS A FUNCTION OF TEMPERATURE FOR**  
**TEL-92040 BASED ON TAN, WEIGHT LOSS AND VISCOSITY INCREASE**

Temp., °C	% Viscosity Increase at 40°C		
	15%	25%	35%
205	29.9	57.8	89.4
215	21.5 <sup>1</sup>	37.5 <sup>1</sup>	59.3
225	12.6	21.1	29.9
a <sup>2</sup>	-7.9204	-9.1298	-9.8671
b <sup>2</sup>	4.4924	5.2137	5.6616
	% Viscosity Increase at 100°C		
	15%	25%	35%
205	64.2	111.0	157.5
215	39.7	68.9	98.6
225	23.7	39.0	54.5
a	-8.9872	-9.2668	-9.2776
b	5.1637	5.4131	5.4921
	% Weight Loss Limits		
	15%	25%	35%
205	50.4	85.2	135.3
215	35.5 <sup>1</sup>	56.7	80.6
225	19.6	33.4	50.6
a	-8.4661	-8.2036	-8.5110
b	4.8712	4.8509	5.0877
	TAN Increase Limits		
	1.0	1.5	3.0
205	145.1	235.6	397.0 <sup>3</sup>
215	76.3	108.0	178.5
225	33.5	48.7	84.0
a	-13.664	-14.668	-14.198
b	7.5746	8.1498	8.0314

<sup>1</sup>lifetime in hours calculated using Arrhenius equation; <sup>2</sup>a = Y intercept; b = slope;  
<sup>3</sup>lifetime in hours read directly from Squires data plot

TABLE 13

EFFECTIVE LUBRICANT LIFE AS A FUNCTION OF TEMPERATURE FOR  
TEL-92041 BASED ON TAN, WEIGHT LOSS AND VISCOSITY INCREASE

% Viscosity Increase at 40°C				
Temp.,°C	15%	25%	35%	
205	33.3	63.7	107.4	
215	27.9	45.1	61.6	
225	11.1	25.4	36.6	
a <sup>1</sup>	-10.307	-8.1207	-9.6242	
b <sup>1</sup>	5.6831	4.7545	5.5728	
% Viscosity Increase at 100°C				
	15%	25%	35%	
205	76.2	161.5	237.3	
215	48.2	71.4	93.2	
225	27.4	41.9	50.2	
a	-9.1639	-12.403	-14.441	
b	5.2863	6.9778	8.0313	
% Weight Loss Limits				
	15%	25%	35%	
205	60.2	111.3	172.2	
215	28.0	50.6	79.3	
225	20.1	34.3	49.3	
a	-10.093	-10.715	-11.305	
b	5.6629	6.0891	6.4653	
TAN Increase Limits				
	1.0	1.5	3.0	
205	266.9	321.9	430.2	
215	57.5	127.9	188.1	
225	16.2	49.2	65.8	
a	-27.871	-17.798	-17.648	
b	14.480	9.7119	9.7071	

<sup>1</sup>a = Y intercept, b = slope

Effective life values given in hours

TABLE 13

EFFECTIVE LUBRICANT LIFE AS A FUNCTION OF TEMPERATURE FOR  
TEL-92041 BASED ON TAN, WEIGHT LOSS AND VISCOSITY INCREASE

% Viscosity Increase at 40°C				
Temp., °C	15%	25%	35%	
205	33.3	63.7	107.4	
215	27.9	45.1	61.6	
225	11.1	25.4	36.6	
a <sup>1</sup>	-10.307	-8.1207	-9.6242	
b <sup>1</sup>	5.6831	4.7545	5.5728	
% Viscosity Increase at 100°C				
	15%	25%	35%	
205	76.2	161.5	237.3	
215	48.2	71.4	93.2	
225	27.4	41.9	50.2	
a	-9.1639	-12.403	-14.441	
b	5.2863	6.9778	8.0313	
% Weight Loss Limits				
	15%	25%	35%	
205	60.2	111.3	172.2	
215	28.0	50.6	79.3	
225	20.1	34.3	49.3	
a	-10.093	-10.715	-11.305	
b	5.6629	6.0891	6.4653	
TAN Increase Limits				
	1.0	1.5	3.0	
205	266.9	321.9	430.2	
215	57.5	127.9	188.1	
225	16.2	49.2	65.8	
a	-27.871	-17.798	-17.648	
b	14.480	9.7119	9.7071	

<sup>1</sup>a = Y intercept, b = slope  
Effective life values given in hours

TABLE 15

**EFFECTIVE LUBRICANT LIFE AS A FUNCTION OF TEMPERATURE  
FOR TEL-92050 BASED ON VISCOSITY INCREASE,  
WEIGHT LOSS AND TAN INCREASE**

Temp., °C	% Viscosity Increase at 40°C		
	15%	25%	35%
205	73	133	184
215	56	81	103
220	35	74	88
a <sup>1</sup>	-8.281	-7.131	-9.163
b <sup>1</sup>	4.862	4.424	5.464

Temp., °C	% Viscosity Increase at 100°C		
	15%	25%	35%
205	137	209	264
215	85	122	156
220	74	95	110
a	-7.442	-9.566	-10.639
b	4.580	5.686	6.252

Temp., °C	% Weight Loss Limits		
	15%	25%	35%
205	76	133	196
215	40	71	106
220	37	65	100
a	-9.658	-9.344	-8.533
b	5.513	5.480	5.172

Temp., °C	TAN Increase Limits		
	1.0	1.5	3.0
205	146	244	408
220	71	89	107
225	45	54	70
a	-10.628	-14.286	-17.446
b	6.126	7.982	9.596

<sup>1</sup>a = Y Intercept; b = slope

These three groups are the result of the degradation of all lubricants being formulation and test method dependent.

Tables 16 through 18 show the "ranking of the 15 lubricants (14 for TAN) for the three "limiting life" values for each of the three measured properties. Ranking of the lubricants based upon TAN changes (Table 16) is about the same for most of the lubricants regardless of TAN level. However, changes in rankings did occur such as lubricant TEL-92039 which was fifth (16 h below first lubricant) at the limiting value of 1.0, eighth (69 h below first lubricant) at the limiting value of 1.5 and tenth (150 h below first lubricant) at the limiting value of 3.0. Table 17 shows the ranking of the 15 lubricants based on the three limiting values of viscosity change. The rankings are about the same for most lubricants for all viscosity change levels but again some changes in rankings did occur such as lubricant TEL-90087 which ranked eighth at 15% change, twelfth at 25% change and fourth at 35% change. Table 18 shows the ranking of the 15 lubricants based on percent weight loss. Like the TAN and viscosity change rankings, the weight loss rankings are about the same for all limiting weight loss values but again some lubricants showed a change in rankings such as lubricant O-91-13 which was sixth at 15% change, tenth at 25% percent change and thirteenth at 35% change.

The range of effective life values (hours) for all the 4 cSt lubricants at two test temperatures and for the minimum and maximum limiting life criteria for the three measured properties are given in Tables 19 and 20. The data in these two tables show that vast differences exist between lubricant stability regardless of the test temperature, measured property or limiting life property change.

Ranking of the lubricants are given in Table 21 for intermediate limiting life criteria of 1.5 TAN, 25% viscosity change (100°C) and 25% weight loss with testing being conducted at 210°C. These data clearly show that no specific lubricant is superior for all measured properties.

#### e. Summary

The oxidative stabilities of several 4 cSt ester base candidate lubricants have been determined using the "Squires" oxidation test. Data obtained from these oxidative stability studies were used to develop Arrhenius plots relating "effective lubricant life" as a function of test temperature using three different levels of limiting life criteria for TAN, percent viscosity change and percent weight loss. Ranking of lubricants based on these criteria was found to vary depending on test temperature, test property being measured and level of test property change being used as the limiting life criteria.

**TABLE 16**  
**RANKING OF LUBRICANTS ACCORDING TO**  
**LIMITING VALUES OF TAN AT 210°C**

Limiting TAN Values		
1.0	1.5	3.0
126 (TEL-92041) <sup>1</sup>	201 (TEL-92041)	336 (TEL-90103)
116 (TEL-91002)	172 (TEL-92050)	288 (TEL-91002)
116 (TEL-91053)	168 (TEL-90103)	278 (TEL-92041)
113 (TEL-92050)	158 (TEL-91053)	262 (TEL-92050)
110 (TEL-92039)	158 (TEL-92040)	248 (TEL-91003)
106 (TEL-91003)	153 (TEL-91002)	245 (TEL-92040)
103 (TEL-92040)	150 (TEL-91003)	233 (TEL-91053)
98 (TEL-90103)	132 (TEL-92039)	200 (TEL-90087)
81 (TEL-91005)	130 (TEL-90087)	190 (TEL-91005)
72 (TEL-90087)	117 (TEL-91005)	186 (TEL-92039)
72 (TEL-91063)	105 (TEL-91063)	183 (TEL-91063)
70 (O-85-1)	100 (O-85-1)	180 (O-85-1)
44 (O-91-13)	62 (O-91-13)	107 (TEL-92049)
41 (TEL-92049)	62 (TEL-92049)	97 (O-91-13)
Range 85 h (67% of max.)	139 h (69% of max.)	239 (71% of max.)

<sup>1</sup>Values in hours, (Test oil)

TABLE 17

RANKING OF LUBRICANTS ACCORDING TO  
LIMITING VALUES OF VISCOSITY CHANGE AT 210°C

Limiting Viscosity Change, % Measured @ 100°C

15	25	35
130 (O-90-6) <sup>1</sup>	182 (O-90-6)	236 (O-90-6)
123 (TEL-91002)	160 (TEL-91002)	200 (TEL-92050)
109 (TEL-92050)	160 (TEL-92050)	185 (TEL-91002)
102 (TEL-91003)	156 (TEL-91003)	180 (TEL-90087)
85 (O-85-1)	129 (TEL-92039)	171 (TEL-92039)
70 (TEL-92039)	124 (O-85-1)	170 (O-85-1)
60 (TEL-92041)	109 (TEL-92041)	168 (TEL-91003)
50 (TEL-90087)	86 (TEL-92040)	152 (TEL-92041)
50 (TEL-92040)	83 (TEL-91053)	123 (TEL-92040)
48 (TEL-91053)	76 (TEL-91063)	118 (TEL-91063)
43 (TEL-92049)	74 (TEL-92049)	114 (TEL-91053)
38 (O-91-13)	56 (TEL-90087)	87 (TEL-92049)
36 (TEL-91063)	53 (O-91-13)	68 (TEL-90103)
25 (TEL-91005)	51 (TEL-90103)	62 (O-91-13)
19 (TEL-90103)	44 (TEL-91005)	62 (TEL-91005)
Range: 111 h (85% of max.)	138 (76% of max.)	174 (74% of max.)

<sup>1</sup>Value in hours, (Test Oil)

TABLE 18

**RANKING OF LUBRICANTS ACCORDING TO  
LIMITING VALUES OF WT LOSS AT 210°C**

Limiting % Weight Loss Values		
15	25	35
70(TEL-91003) <sup>1</sup>	119 (TEL-91003)	170 (TEL-91003)
63 (TEL-92039)	116 (TEL-92039)	168 (TEL-92039)
57 (TEL-92050)	100 (TEL-92050)	149 (TEL-92050)
55 (TEL-91002)	92 (TEL-91002)	131 (TEL-91002)
53 (O-90-6)	86 (O-90-6)	119 (TEL-92041)
49 (O-91-13)	78 (TEL-92049)	114 (TEL-92049)
48 (TEL-92049)	77 (TEL-92041)	109 (TEL-90103)
42 (TEL-92041)	73 (TEL-90103)	108 (O-90-6)
41 (TEL-92040)	69 (TEL-92040)	104 (TEL-91063)
38 (TEL-90103)	65 (O-91-13)	104 (TEL-92040)
37 (O-85-1)	64 (TEL-91063)	98 (TEL-91053)
32 (TEL-91063)	62 (O-85-1)	97 (TEL-90087)
29 (TEL-90087)	58 (TEL-90087)	91 (O-91-13)
24 (TEL-91005)	57 (TEL-91053)	90 (O-85-1)
24 (TEL-91053)	43 (TEL-91005)	78 (TEL-91005)
Range: 46 h (66% of max.)	71 h (60% of max.)	92 (54% of max.)

<sup>1</sup>Value in hours, (Test Oil)

TABLE 19

**MAXIMUM EFFECTIVE LIFE (HOURS) FOR TWO  
(MINIMUM AND MAXIMUM)  
LIMITING LIFE VALUES AT TEMPERATURES**

**Maximum Effective Life Values**

**TAN**

Temp., °C	a <sup>1</sup>	b <sup>2</sup>
210	126 (TEL-92041) <sup>3</sup>	336 (TEL-90103)
225	55 (TEL-91003)	120 (TEL 91003)

**Visc. Chg @ 100°C**

Temp., °C	a	b
210	130 (O-90-6)	236 (O-90-6)
225	56 (TEL-92050)	99 (TEL-91003)

**Weight Loss, %**

Temp., °C	a	b
210	70 (TEL-91003)	170 (TEL-91003)
225	32 (TEL-91003)	93 (TEL-91003)

<sup>1</sup>a = Limiting values of 1.0 TAN, 15% Visc. Chg. (100°C) and 15% wt. loss

<sup>2</sup>b = Limiting values of 3.0 TAN, 35% Vis. Chg. (100°C) and 35% wt. loss

<sup>3</sup>Values in hours (Test oil)

TABLE 20

**MINIMUM EFFECTIVE LIFE (HOURS) FOR TWO  
(MINIMUM AND MAXIMUM) LIMITING LIFE VALUES  
AT TEMPERATURES OF 210°C and 225°C**

**Minimum Effective Life Values,****TAN**

Temp., °C	a <sup>1</sup>	b <sup>2</sup>
210	41 (TEL-92049) <sup>3</sup>	97 (O-91-13)
225	6 (O-85-1)	20 (O-85-1)

**Vis. Chg. @ 100°C, %**

Temp., °C	a	b
210	19 (TEL-90103)	62 (O-91-13) (TEL-91005)
225	11 (TEL-91003)	22 (O-91-13) (TEL-91005)

**Wt. Loss, %**

Temp., °C	a	b
210	24 (TEL-91005)	78 (TEL-91005) (TEL-91053)
225	12 (TEL-91005)	25 (TEL-91053)

<sup>1</sup>a = Limiting values of 1.0 TAN, 15% Vis. Chg. (100°C) and 15% wt. loss

<sup>2</sup>b = Limiting values of 3.0 TAN, 35% Vis. Chg. (100°C) and 35% wt. loss

<sup>3</sup>Values in hours (Test oil)

TABLE 21

**RANKING OF LUBRICANTS ACCORDING TO LIMITING  
VALUES OF 1.5 TAN, 25% VIS. CHG. @ 100°C AND  
25% WEIGHT LOSS AT 210°C**

<b>Ranking High to Low</b>	<b>TAN</b>	<b>Vis. Chg @ 100°C</b>	<b>Wt. Loss, %</b>
1	201 (TEL-92041) <sup>1</sup>	182 (O-90-6)	119 (TEL-91003)
2	172 (TEL-92050)	160 (TEL-92050)	116 (TEL-92039)
3	168 (TEL-90103)	160 (TEL-91002)	100 (TEL-92050)
4	158 (TEL-91053)	156 (TEL-91003)	92 (TEL-91002)
5	158 (TEL-92040)	129 (TEL-92039)	86 (O-90-6)
6	153 (TEL-91002)	124 (O-85-1)	78 (TEL-92049)
7	150 (TEL-91003)	109 (TEL-92041)	77 (TEL-92041)
8	132 (TEL-92039)	86 (TEL-92040)	73 (TEL-90103)
9	130 (TEL-90087)	83 (TEL-91053)	69 (TEL-92040)
10	117 (TEL-91005)	76 (TEL-91063)	65 (O-91-13)
11	105 (TEL-91063)	74 (TEL-92049)	64 (TEL-91063)
12	100 (O-85-1)	56 (TEL-90087)	62 (O-85-1)
13	62 (O-91-13)	53 (O-91-13)	58 (TEL-90087)
14	62 (TEL-92049)	51 (TEL-90103)	57 (TEL-91053)
15	62 (O-90-6) <sup>2</sup>	44 (TEL-91005)	48 (TEL-91005)
<b>Range</b>	<b>139 h (69% of max)</b>	<b>138 h (76% of max)</b>	<b>71 h (60% of max)</b>

<sup>1</sup>Values in hours, (Test oil)

<sup>2</sup>Inconsistent TAN Data, not ranked

## 2. LUBRICANT CORROSION AND OXIDATIVE STABILITY OF HIGH TEMPERATURE FLUIDS

### a. Introduction

Several candidate high temperature liquid lubricants were studied during this phase of the program and are listed in Table 22. TEL-91001, a new formulation of polyphenyl ether (PPE), was stressed in the corrosion and oxidation test at three different temperatures and Arrhenius plots developed from the data. The loss of tin oxide (PPE antioxidant) during laboratory stressing and field usage of polyphenyl ethers was investigated. A novel sealed tube test was developed to study the rate of evaporation and the rate of reaction in both the liquid and vapor phase using only microliter quantities of liquid lubricants. The effect of specific blending agents and/or diluents on the -34.4°C viscosity and corrosion and oxidation stability of polyphenyl ether was also investigated. The corrosion and oxidation stability of a C-ether (O-64-20) was investigated under a variety of test conditions and with various additives. Chemical analysis methods were developed and used to analyze degraded O-64-20 and a degradation mechanism proposed from these results. The corrosion and oxidation stability of a substituted cyclophosphazene basestocks (TEL-90013 and TEL-92026) was investigated in a nickel test vessel (nonreactive towards HF) under a variety of test conditions. Chemical analysis methods were developed and used to analyze degraded cyclophosphazenes in order to determine the nature of the fluid anomalous corrosion and oxidation test behavior.

### b. Corrosion and Oxidation Stability Testing of TEL-91001

Corrosion and oxidation testing of inhibited 5P4E fluid TEL-91001 was completed at three test temperatures and Arrhenius plots developed. TEL-91001 is reported to be a new version of TEL-8039/TEL-8085 having an antioxidant with improved shelf life stability. Test conditions were 10 L/h air flow, intermediate sampling, Squires tubes and test temperatures of 340, 350 and 360°C. C&O test results are presented in Table 23 and the percent viscosity increase data are plotted against time in Figure 1. C&O data for TEL-91001 indicate that this PPE has exceptional oxidative stability. No corrosion on any of the test coupons was observed. Small amounts of coke-like deposits were observed in the posttest tubes. Arrhenius plots for TEL-91001 are shown in Figure 2 with the results of the effective lubricant life calculations

TABLE 22

## IDENTIFICATION OF HIGH TEMPERATURE LUBRICANTS

Test Lubricant	Description	Viscosity, cSt	
		40°C	100°C
O-59-9	Experimental Fluid (4P3E)	64.76	6.24
O-64-20	Polyphenyl Thioether (C-ether)	21.71	4.01
O-67-1	MIL-L-87100 Oil (5P4E)	280.3	12.61
O-77-6	Basestock for MIL-L-87100 Oil	280.4	12.52
TEL-90013	Cyclophosphazene Fluid	195.4	10.66
TEL-90101	Different Lot of O-67-1	288.4	12.94
TEL-90102	Different Lot of O-67-1	283.0	12.77
TEL-91001	Modified Polyphenyl Ether	289.2	12.67
TEL-92026	Cyclophosphazene Fluid	215.3	10.91

TABLE 23

**CORROSION AND OXIDATION DATA FOR TEL-91001 USING SQUIRES  
TUBES, 10 L/H AIRFLOW, AND INTERMEDIATE SAMPLING**

**340°C Test Temperature**

Hours	40°C Visc., cSt	% Increase at 40°C	100°C Visc., cSt	% Increase at 100°C	TAN, mg KOH/g
0	289.17	-	12.67	-	0
24	300.18	3.8	12.94	2.1	-
72	319.80	10.6	13.31	5.1	-
123	344.09	19.0	13.73	8.4	-
192	390.50	35.0	14.45	14.1	-
310	497.95	72.2	17.11	35.0	0

**350°C Test Temperature**

24	305.37	5.6	13.04	2.9	-
48	334.01	15.5	13.61	7.4	-
72	379.67	31.3	14.25	12.5	-
109.5	429.80	48.6	15.11	19.3	-
130.5	464.78	60.7	15.55	22.7	-
144.5	492.56	70.3	15.92	25.7	0

**360°C Test Temperature**

24	314.42	8.7	13.33	5.2	-
48	350.11	21.1	13.94	10.0	-
98.25	469.48	62.3	15.64	23.4	-
120	527.83	82.5	16.43	29.7	0

**Specimen Corrosion data, mg/cm<sup>2</sup>**

Test Temp, °C	Al	Ag	M-St	M-50	Wasp	Ti
340	0.0	0.0	+0.22	+0.30	+0.04	+0.04
350	0.0	+0.06	+0.30	+0.14	-0.04	0.0
360	-0.02	0.0	+0.14	+0.22	-0.02	-0.04

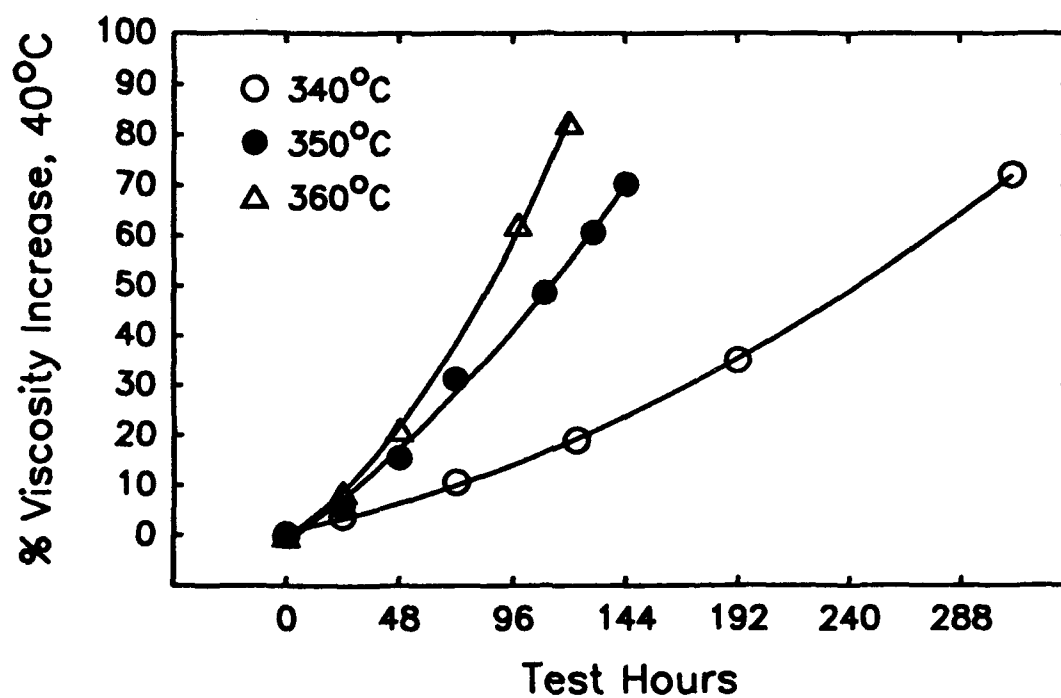
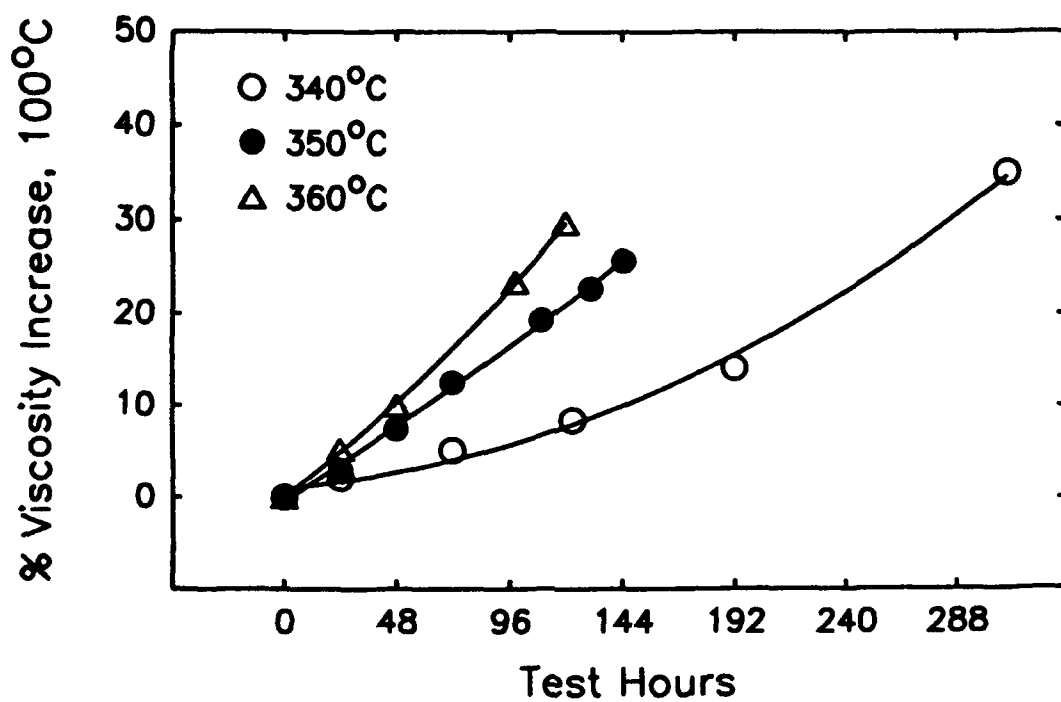


Figure 1. Viscosity Increases of TEL-91001 During Corrosion/Oxidation Testing at 340, 350, and 360°C.

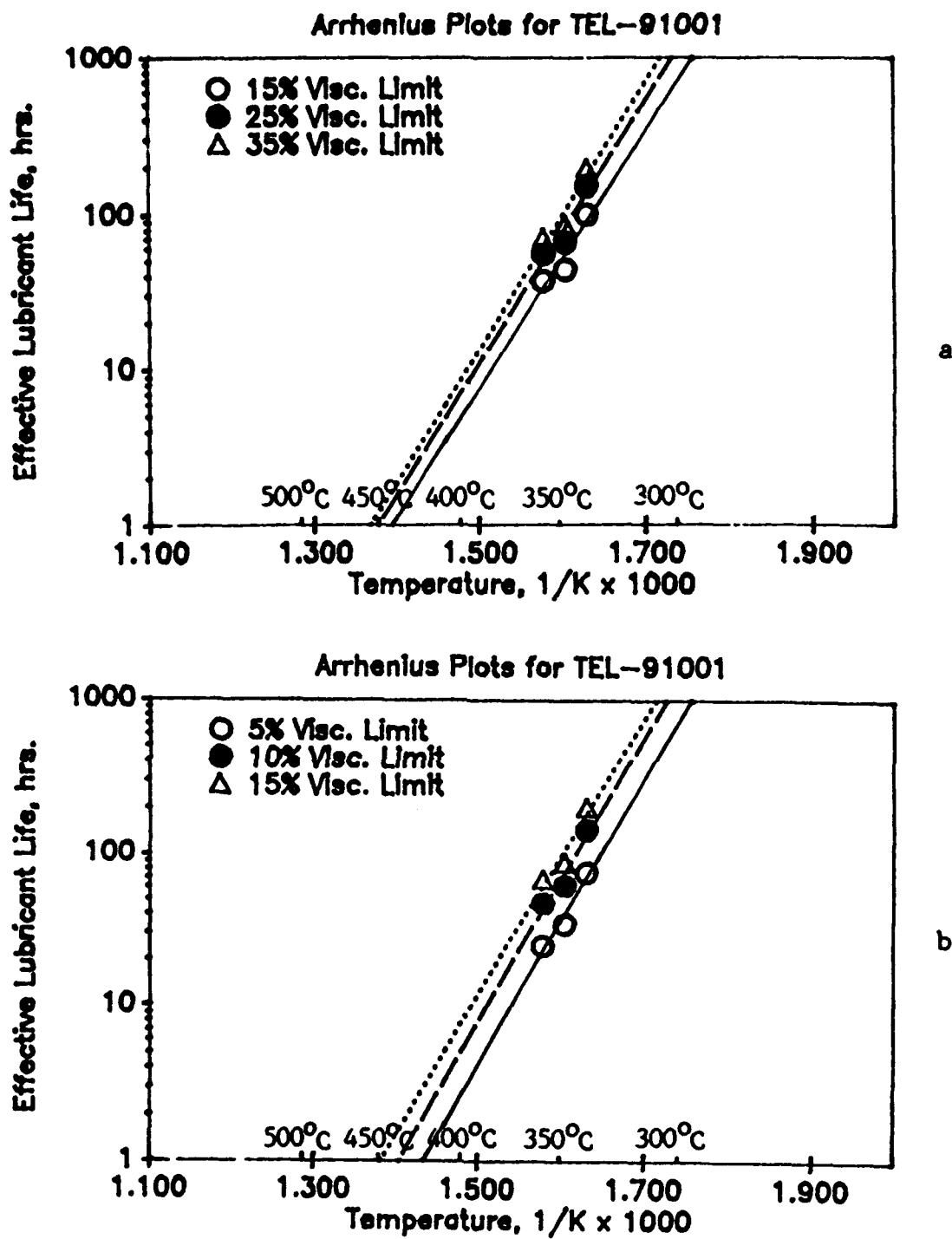


Figure 2. Effective Lubricant Life as a Function of Temperature for TEL-91001 Based on (a) the 15%, 25%, and 35% Viscosity Limits at 40°C and (b) the 5%, 10%, and 15% Viscosity Limits at 100°C.

appearing in Table 24. Arrhenius data on other PPE fluids have been reported previously.<sup>3</sup> It appears that TEL-91001 has C&O stability superior to other inhibited PPE fluids (TEL-8092, TEL-8087, TEL-8085, TEL-8040 and TEL-8039). For example, based on the 25% viscosity limit, TEL-91001 has a predicted lubricant life of about 70 hours at 350°C where TEL-8092, a 5P4E with 0.15% Additive A, has an effective lubricant life of only 11 hours.

c. Depletion of Antioxidant from Polyphenyl Ether During Laboratory Testing

(1) Introduction

The depletion of organic antioxidants in ester based lubricants during laboratory testing or actual service is an expected phenomenon and occurs as a result of the radical scavenging and/or peroxide decomposing reactions that the antioxidants undergo while protecting the lubricant basestock from oxidation. High temperature lubricants, however, generally employ dispersed metallic salt compounds as antioxidants and would not be expected to deplete by the same mechanism. For the original Skylube 600 PPE formulation (O-67-1), the organometallic tin compound that is used as an antioxidant was shown to oxidatively decompose to tin oxide at fairly moderate temperatures.<sup>3</sup> Previous research found that the tin oxide, which is the true antioxidant, does not deplete nor change chemical form during corrosion and oxidation testing. However, in sliding four-ball and minisimulator testing as well as in actual engine service of this formulation it has been found that depletion of the tin oxide antioxidant occurs. Previously, the depletion of the antioxidant in engine stressed PPE lubricants was reported.<sup>3</sup> The following section documents this phenomenon in sliding four-ball and minisimulator tests and attempts to explain the source of this depletion.

(2) Depletion of Tin Oxide During Four-Ball Testing

It had been previously shown that the organometallic tin additive in O-67-1 depleted at a faster rate during sliding four-ball testing than during simple oxidative stressing during testing.<sup>3</sup> But the physical loss of tin from the PPE lubricant during testing seems to be a separate phenomenon.

A number of four-ball tested O-67-1 lubricants (150°C, 52100 steel, 5 to 20 hours) were analyzed for total tin by atomic absorption-acid dissolution method (AA/ADM) in order to correlate the tin loss with test time and the degradation of Additive A. The results (Figure 3) show that tin loss is fairly linear with time, losing half

TABLE 24

EFFECTIVE LUBRICANT LIFE AS A FUNCTION OF TEMPERATURE  
FOR TEL-91001 AT THE 15%, 25% AND 35% VISCOSITY LIMITS  
AT 40°C AND THE 5%, 10% AND 15% VISCOSITY LIMITS AT  
100°C ALONG WITH THE CONSTANTS FROM THE LEAST SQUARES  
LINE EQUATION

Viscosity Limits Measured at 40°C

Temperature, °C	15%	25%	35%
340	99.1	150.6	192.7
350	44.1	65.7	84.5
360	37.0	55.1	69.4
a*	-11.470	-11.566	-11.672
b**	8.228	8.398	8.529

Viscosity Limits Measured at 100°C

	5%	10%	15%
340	74.5	143.0	199.8
350	34.0	61.7	87.2
360	24.3	46.9	67.5
a*	-13.421	-13.072	-12.523
b**	9.357	9.311	9.063

\*a = Intercept

\*\*b = Slope

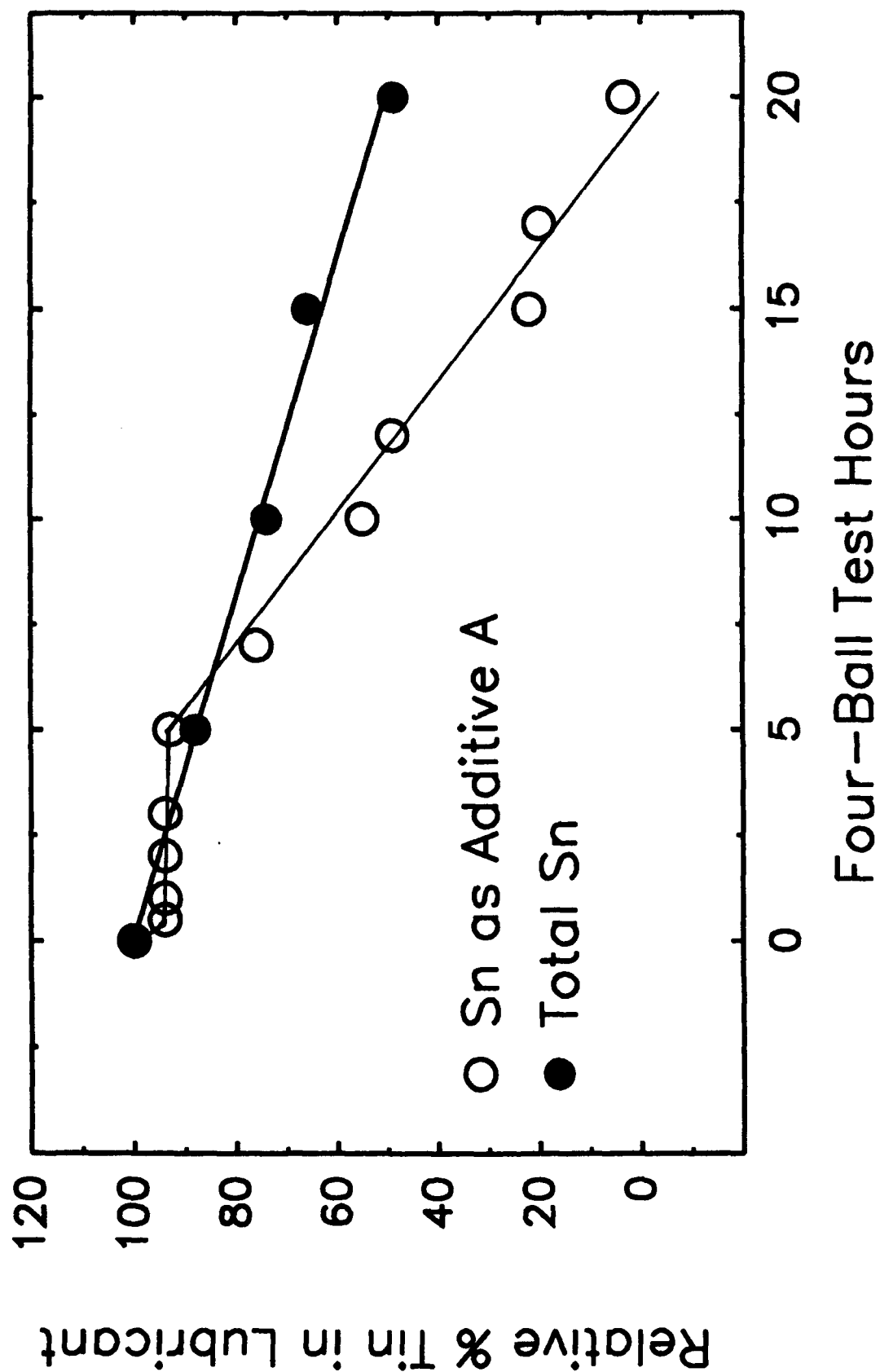


Figure 3. Change in Relative Tin and Additive A Levels in O-67-1 During Four-Ball Testing (150°C, 52100 Steel Balls, 145 N Load, 1 to 20 Hours).

of its original value, and does not correlate with Additive A degradation. A linear drop in tin concentration versus test hours was also observed for a series of engine tested lubricants (TEL-9070).<sup>3</sup> These samples had no detectable Additive A content so tin loss in this lubricant must occur with SnO<sub>2</sub>.

AA/ADM analysis of a limited number of four-ball tested lubricants from higher test temperatures (250 and 315°C) show that tin loss occurs at a much higher rate than at 150°C (Figure 4). Since Additive A degrades rapidly at these higher temperatures, being completely converted to tin oxide by 3 hours, tin loss may occur only after tin oxide conversion.

(3) Analysis of Four-Ball Test Bearing Surface by Auger Electron Spectroscopy (AES)

AES with ion beam sputtering was used to examine a posttest 52100 bearing from four-ball test # 380 (250°C, 20 hours) in order to determine if surface plating of the tin oxide could constitute a source of tin loss. AES is a very surface sensitive technique (about 30 Å depth) that can give approximate elemental composition. The ion beam sputtering removes material at a controlled rate thus allowing elemental depth profiling. The results from the bearing surface away from the wear scar (Figure 5) indicate that the bluish hue of the bearing is due to an approximately 700 Å thick layer of iron oxide of unknown stoichiometry. Note that a fairly high level of carbon exists in a thin surface layer, probably organic in nature. Also, in this same general region is a thin layer of tin (about 2 atom % maximum) that is very concentrated relative to its level in the lubricant. These data indicate that both tin and some carbonaceous material are being adsorbed onto the surface of the bearing.

(4) Quantitation of Tin from Four-Ball Test Bearings

In order to determine if the tin present on the four-ball test bearing could account for the tin loss from the lubricant, quantitative analysis of tin on bearing surfaces was determined by extracting a single bearing with 0.5 mL of aqua regia with ultrasonic agitation and analysis by atomic absorption. This method was used on 52100 bearings from four-ball tests that had considerable tin loss from the lubricants (Tests 380, 381, and 365). The results of these analyses show that the total amount of tin extracted from the surfaces of these bearings is extremely small. Whereas total tin loss from the lubricants from these four-ball tests was in milligram quantities, the total amount of tin extracted from a single bearing was in the microgram range. Thus, it must be concluded that surface absorption of tin oxide by the bearing constitutes a very minor source of loss.

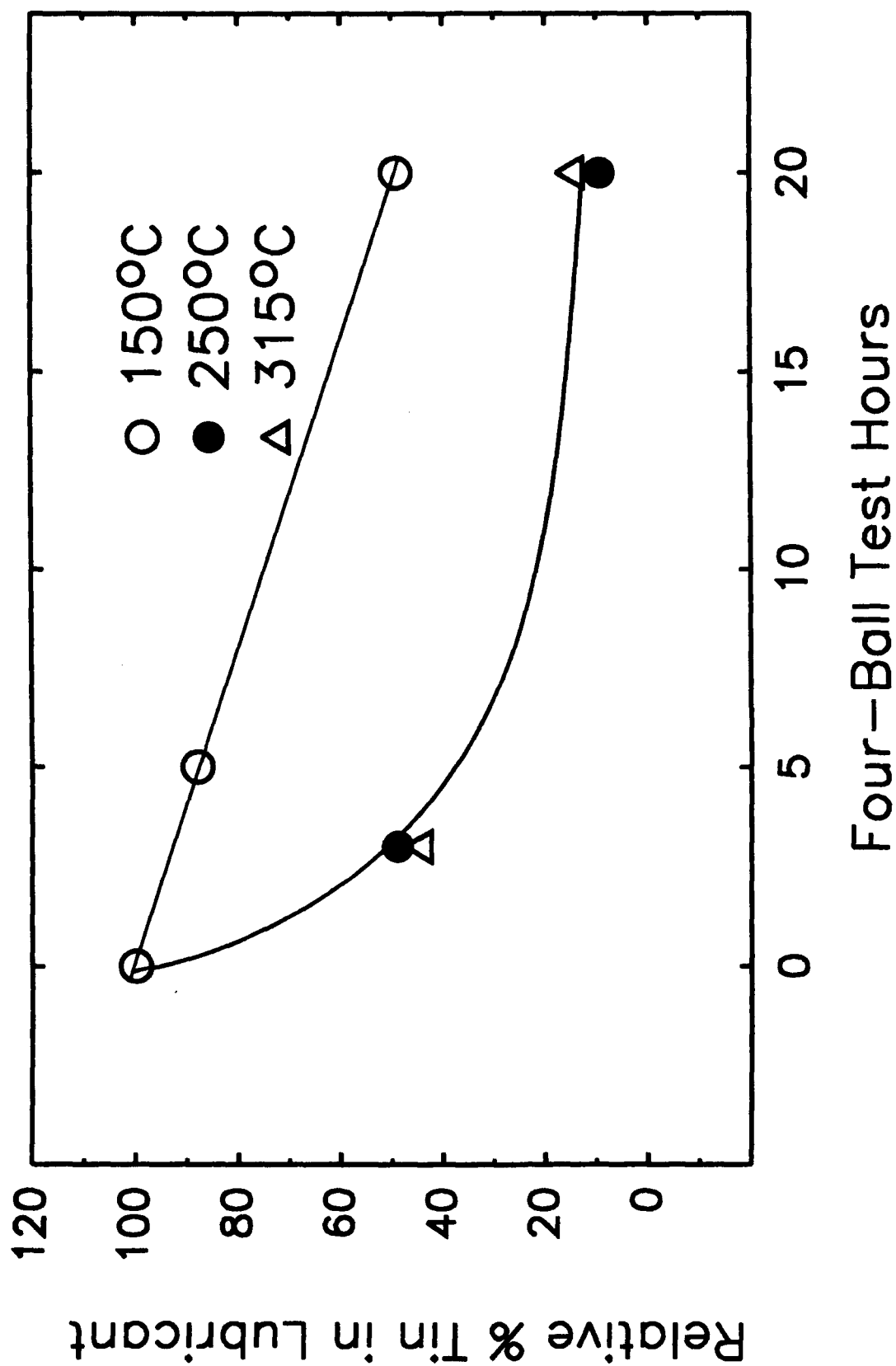


Figure 4. Change in Relative Tin and Additive A Levels in O-67-1 During Four-Ball Testing at 150, 250, and 315°C (52100 Steel Balls, 145 N Load, 3 to 20 Hours).

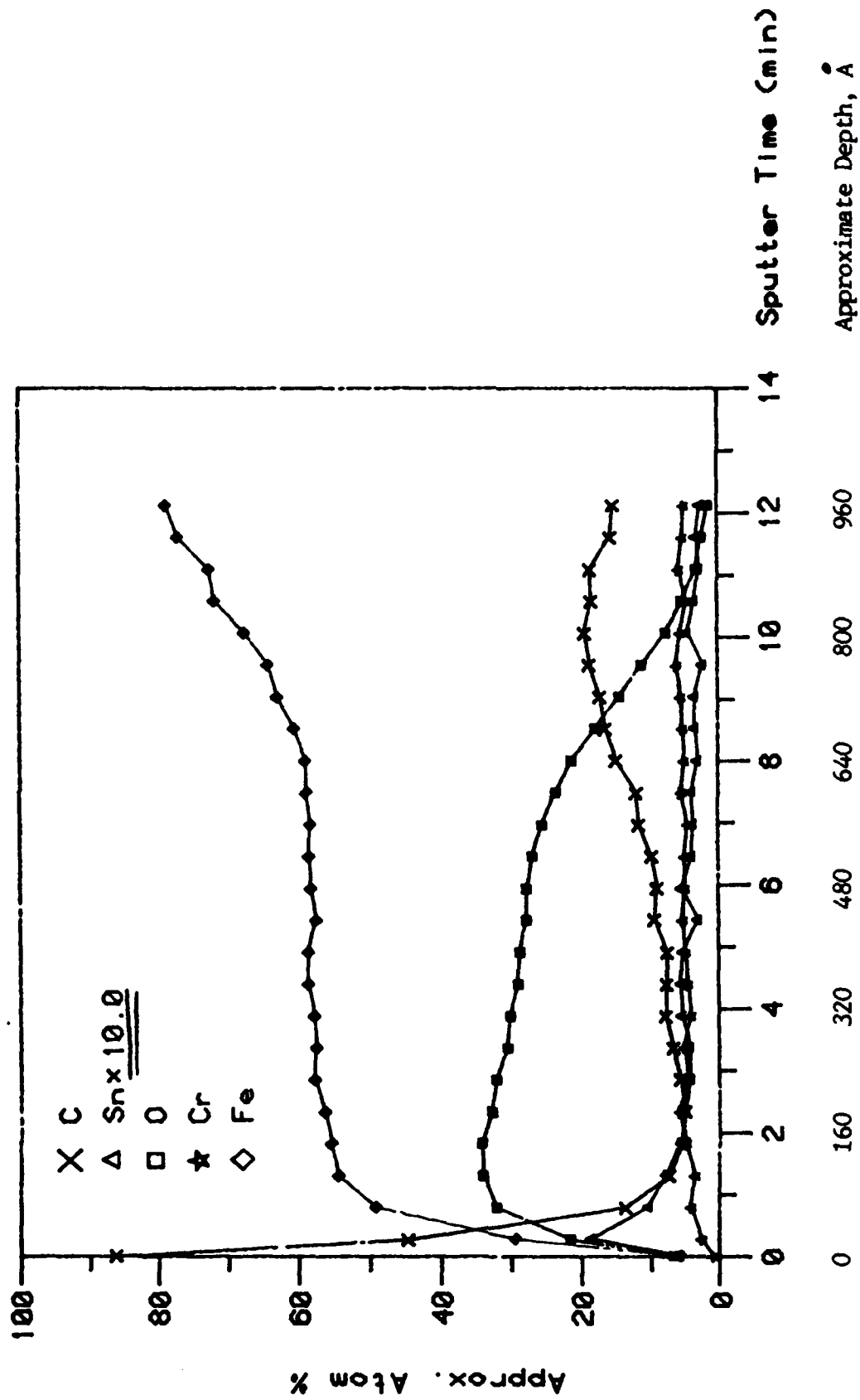


Figure 5. Auger Electron Spectroscopy Depth Profile of 52100 Steel Ball From a Four-Ball Test of O-67-1 (#380, 250°C, 20 Hours).

#### (5) Quantitation of Tin Present in Four-ball Filtrate Washings

Since some of the lubricant is left behind on the walls of the test cup, tin analyses were made on the toluene washing of the posttest four-ball test cup. This washing contained a thin layer of lubricant from the metal surfaces as well as large particulates that may have settled from the bulk of the lubricant. Thus, the 3-micron filtrate from the toluene washing of four-ball test # 409 (315°C, 20 hours, 52100 bearings) was analyzed for tin by emission spectroscopy. The bulk lubricant from this test had displayed a drop in tin concentration from 400 to 33 ppm. The results of this analysis indicate that a total of 27 mg of tin (in some form) is present on the filter. This is approximately 10 mg more tin than was lost from the lubricant during the test, the disparity is probably due to a combination of analysis and weighing errors. More importantly, these results indicate that a relatively large amount of tin (probably as an oxide) exists either in a thin lubricant film or as fairly large particles. Furthermore, the amount of tin found could easily account for the tin loss from the lubricant during four-ball testing of O-67-1.

This experiment was repeated with the toluene washing from another four-ball test (Test # 624, TEL-90102, M50, 145 N load, 315°C, 20 hours). The results indicated that of the 15.0 mg of tin originally present in the fresh lubricant, 5.6 mg is present in the posttest lubricant, which is a fairly typical decrease in this component. However, only 1.6 mg of tin was found in the toluene washing of the test cup leaving 7.7 mg of tin unaccounted. Since some deposition occurs with such tests and is not recovered, there may be a high concentration of tin in these deposits. Thus, it seems that settling out or deposition processes may be responsible for at least part of the loss of tin oxide during four-ball testing.

#### (6) Antioxidant Tin Levels in Minisimulator Tested PPEs

The tin level in intermediate samples from minisimulator tests WLM003 and WLM004 was determined by AA-ADM. The results for test WLM003 (Figure 6) show a very steady drop in tin concentration that levels out after about 32 hours. This drop is significant (85%) and is similar to drops in tin observed in four-ball tested and engine stressed PPEs. The results for minisimulator test WLM004 are very similar (Figure 7).

Analysis of the 4-hour sample from test WLM003 indicated that the organometallic tin additive (the original form of the tin additive) had been completely changed to tin oxide. This is consistent with the poor oxidative stability of this compound at the

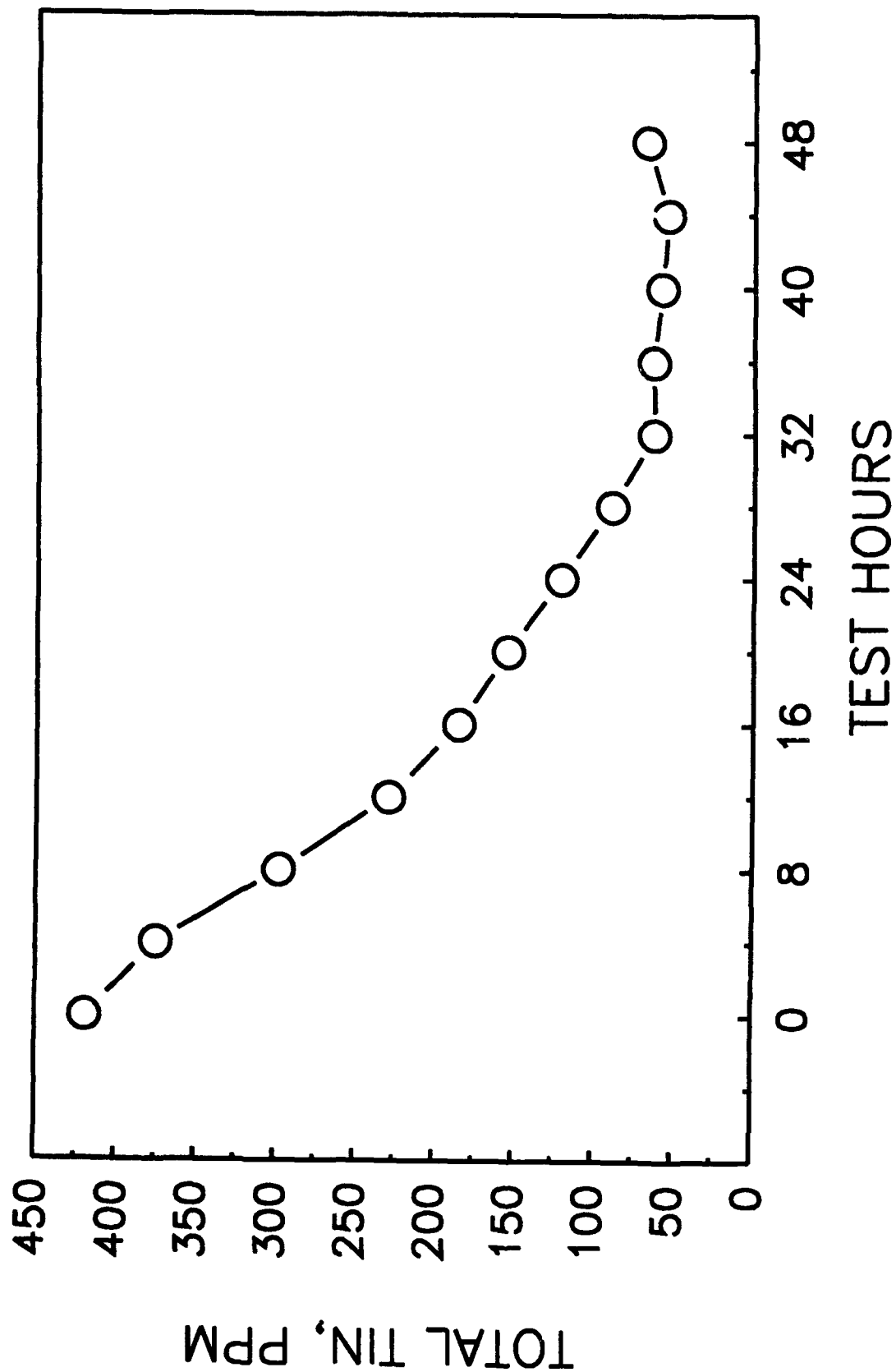


Figure 6. Tin Levels in TEL-90102 During Minisimulator Test WLM003.

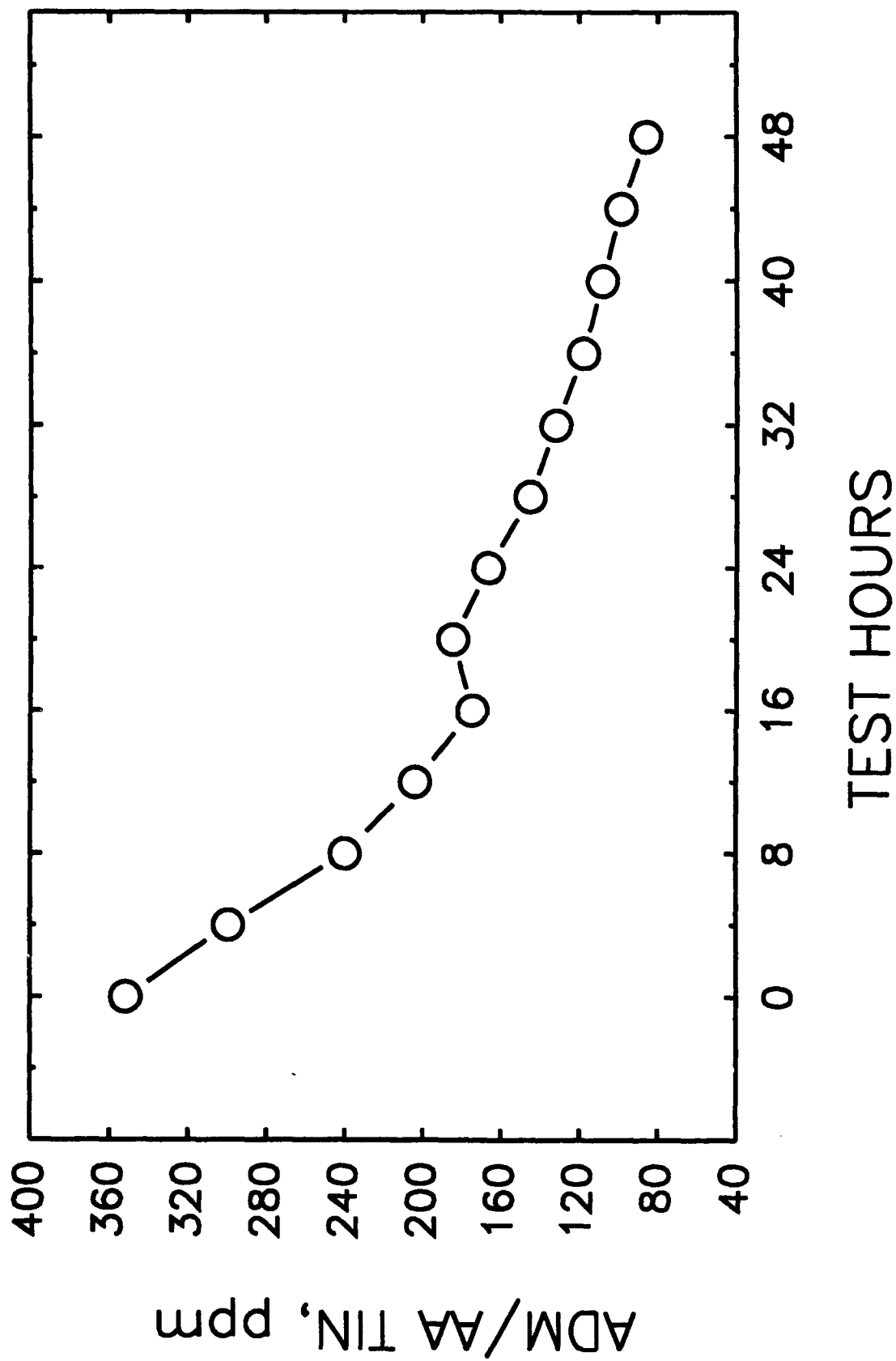


Figure 7. Tin Levels in TEL-90102 During Minisimulator Test WLM004.

temperatures experienced in the minisimulator. The drop in tin level is also consistent with this conversion which indicated that tin loss in four-ball tested and engine stressed PPEs did not occur until the Additive A had been oxidized into tin oxide. Despite the large drop in the antioxidant level, the viscosity increase of the lubricant was not excessive. Nevertheless, this agrees with previous C&O testing of PPEs with reduced tin levels (120 ppm) which showed very little differences in viscosity after 48 hours at 320°C relative to PPEs with normal antioxidant levels. But at longer test times, the lower antioxidant level PPE displayed much greater viscosity increases.

#### (7) Tin Analysis on Minisimulator Deposits

Three samples of coke were taken from different sections of the minisimulator rig after the test runs with TEL-90102 (WLM003 and WLM004). In order to determine the homogeneity of tin throughout the test rig, coke was sampled from different sections of the test head as well as the bearing cap (where deposition was minor) for WLM003 and from different sections of the test head for WLM004. The coke samples were washed with trichloroethylene, in order to remove residual lubricant, and the samples pulverized prior to AA-ADM analysis. The results (Table 25) indicate a higher level of tin in all newly sampled sections of coke relative to what was originally present in the oil (400 ppm). Although it is not possible to mass balance lubricant tin loss based on these results, it is reasonable to conclude that the deposition process is a significant if not major source of antioxidant tin loss during the minisimulator test of TEL-90102.

TABLE 25

#### ADM/AA ANALYSES FOR TIN IN DEPOSITS FROM MINISIMULATOR RUNS WLM003 AND WLM004 (TEL-90102)

Run	Tin, ppm			
	Top of Head	Middle of Head	Bottom of Head	Bearing Retainers
WLM003	4800	-	1900	8000
WLM004	1413	1162	750	-

## **(8) Conclusion**

The depletion of antioxidant tin oxide from the PPE lubricant by a nonoxidative mechanism may decrease the oxidative stability of the lubricant. Since the use of dispersed inorganic type antioxidants is common in high temperature lubricant formulations, this depletion may be a general phenomenon. The data presented here suggest the depletion of the tin oxide is related to the deposition that occurs during four-ball and minisimulator testing and engine stressing. Since no loss of the additive occurs before the oxidative transformation of the original organometallic tin additive to tin oxide, it is presumed that volatilization loss is insignificant. Likewise, no evidence can be found to support the loss of the tin by plating out on metal surfaces, such as steel balls. Although the exact process by which deposition removes tin oxide from the lubricant is not known, the abnormally high tin concentrations in deposits from the sliding four-ball and minisimulator tests suggests that incorporation of the nonvolatile tin oxide particles into the deposit is a major source of antioxidant depletion.

### **d. Improvement of Low Temperature Properties**

#### **(1) Introduction**

Renewed interest in high temperature lubricants has encouraged manufacturers to improve the high temperature oxidative stability of polyphenyl ether (PPE). However, the low temperature viscosity properties of PPEs are still quite poor. Therefore, a program was developed to produce a -34.4°C (-30°F) pumpable PPE lubricant by using diluents and/or blending agents.

Previously in actual engine use, PPEs were diluted with a chlorinated solvent (trichloroethylene, tetrachloroethylene) to facilitate engine startup. While the chlorinated solvents have been successfully used to lower the low temperature viscosity of PPE, environmental concerns have prompted the search for a replacement. Reported here are efforts to improve the low temperature properties of PPE. The specification goal is to produce a pumpable (<20,000 cSt) PPE at -34.4°C using less than 20% volume of a volatile diluent.

## (2) Diluents

### (a) Background

The current practice to lower the pour point of 5P4E lubricants is to dilute the lubricant with tetrachloroethylene (TCE). TCE is volatile and boils off during early use without affecting the lubrication capabilities of the 5P4E. Early research<sup>4</sup> also showed that diethyl oxalate and tetrahydronaphthalene in addition to TCE could be used to decrease the pour point of 5P4E with a minimum of metal attack or basestock degradation during service. The diluents were chosen because they volatilized completely before maximum engine operating temperatures are reached while possessing flash points as high as possible (TCE-nonflammable, other candidates above 155°C). A later paper<sup>5</sup> stated that trichloroethylene did not affect the fatigue life of bearings during engine tests.

### (b) Approach

As a primary property it is important that a potential diluent have excellent PPE solubility characteristics. In order to screen the large number of potential diluents for PPE solubility, solubility parameters (SP) were used. SP parameters are thermodynamically calculated numbers based on the cohesive energy of a solvent (which is a function of its heat of vaporization). When the parameters are similar, sufficient energy is gained on dispersion to allow mixing. When the parameters are dissimilar, more energy is required for dispersal than is gained by mixing, so immiscibility results. Although the SP of 5P4E is not known, the solvents in which it is most soluble are known and their SP were used to scan a range of parameters for potential diluents. From these data, it appears that SP parameters in the range of 8.5 to 10, as well as solvents with higher numbers that are poor to moderate hydrogen bonders, would be most appropriate.

Many other properties of the diluent that are probably important were not specifically defined. Ideally, a potential diluent would be noncombustible or possess a high flash point and fire point, possess a high autoignition point, and have no negative lubricant effects or environmental or toxicity problems. Unfortunately, no such solvent exists. Therefore, the following criteria were used to select solvents for screening: flash point > 38°C, autoignition temperature > 371°C, boiling point < 200°C and no severe toxicity or any carcinogenic properties.

Using these limits resulted in the selection of only four solvents. Four previously proposed solvents<sup>4</sup> were also screened. In addition to these eight solvents, the previously used chlorinated diluents were included for comparison. It is obvious from the physical property data (Table 26) that none of the alternate diluents possess the excellent properties of trichloroethylene, although there is some improvement in the toxicological properties (Table 27). Also, five of the solvents possess at least partial water solubility which is not desirable.

Later in the study, the work was expanded to include solvents with flash points below 38°C due to the poor results of the previously selected diluents (Tables 28 and 29).

### (c) Screening and Test Procedure

Screening of candidate diluents was accomplished by placing 20% (wt/wt) of the solvent in the PPE lubricant in a screw cap culture tube. This tube was placed in a -34.4°C bath for 15 minutes at which time the tube was tilted and visually checked for flow. Any candidates which exhibited some flow were subjected to -34.4°C viscosity measurements. Initial dilutions were made by weight, while later dilutions (diluents with flash points less than 38°C) were made by volume since it was felt that this would be more appropriate for field dilutions.

in order to determine if the diluent had an adverse effect on the oxidative stability of PPE, 20% dilutions were subjected to two different types of corrosion/oxidation testing. First, the solution was subjected to a normal C&O test setup with condensate return. Then the solution was tested initially without condensate return until the solvent evaporated (as indicated by the test oil temperature reaching the set temperature) at which time the condenser was returned to the test apparatus until the end of the test. All tests were conducted at 320°C for 48 hours with both immersed and vapor phase specimens.

TABLE 26

**PHYSICAL PROPERTY DATA FOR POTENTIAL  
PPE DILUENTS WITH FLASH POINTS ABOVE 38°C<sup>1</sup>**

Solvent	Solubility Parameter <sup>2</sup>	Flash Pt., °C	Autoignition Temp., °C	Boiling Pt, °C	Melting Pt, °C
Trichloroethylene	9.2	None <sup>3</sup>	410	87	-73
Tetrachloroethylene	9.3	None	None	121	-22
Decahydronaphthalene (Decalin)	8.8	58	250	195	-43
Tetrahydronaphthalene (Tetralin)	9.5	77	385	206	-31
Diethyl Oxalate	8.6	76	NDF	186	-41
2-Ethoxyethyl acetate <sup>4</sup> (cellosolve acetate)	8.7	49	379	156	-62
Diethyl formamide <sup>5</sup>	10.6	58	NDF	178	NDF
Ethyleneglycol diacetate <sup>4</sup>	10.1	96	482	191	-42
Ethyl Lactate <sup>5</sup>	10.0	46	400	154	-26
Diethylene glycol dimethyl ether <sup>5</sup> (diglyme)	NDF	67	NDF	162	-68

NDF = No Data Found

<sup>1</sup> Taken from: The Condensed Chemical Dictionary, Eighth Edition, Gessner G.,  
Van Nostrand Reinhold Company, New York (1971)  
And: Solvent Safety Handbook, D.J. DeRenzo, Noyes Publication (1988)

<sup>2</sup> Handbook of Chemistry and Physics, 65th Edition, Weast, R.C., CRC Press, Boca Raton, FL,  
1984-1985

<sup>3</sup> Some sources report a flash point of 90°F (closed cup)

<sup>4</sup> Partially soluble in water

<sup>5</sup> Miscible with water

TABLE 27

TOXICITY DATA FOR POTENTIAL PPE  
DILUENTS HAVING FLASH POINTS ABOVE 38°C<sup>1</sup>

Solvent	Toxicity
Trichloroethylene	Irritant; mildly toxic by ingestion and inhalation, carcinogen
Tetrachloroethylene	Irritant; moderately toxic by inhalation and ingestion
Tetrahydronaphthalene (Tetralin)	Irritant; moderately toxic by ingestion and skin contact
Decahydronaphthalene (Decalin)	Moderately toxic by inhalation and ingestion; mildly toxic by skin contact; irritant
Diethyl Oxalate	Toxic by ingestion
2-Ethoxyethyl acetate (cellosolve acetate)	Moderately toxic by inhalation, skin contact and ingestion
Diethyl Formamide	No Data Found
Ethyleneglycol Diacetate	Irritant; mildly toxic by ingestion and inhalation
Ethyl Lactate	Moderately toxic by ingestion
Diethyleneglycol dimethyl ether (Diglyme)	Essentially non-toxic; may form explodable peroxides upon exposure to air

<sup>1</sup> Taken From: Dangerous Properties of Industrial Materials,  
N. Irving Sax and Richard J. Lewis,  
Van Nostrand Reinhold Co., New York (1989)

TABLE 28

PHYSICAL PROPERTY DATA FOR POTENTIAL  
PPE DILUENTS HAVING FLASH POINTS BELOW 38°C<sup>1</sup>

Solvent	Solubility Parameter <sup>2</sup>	Flash Point (°C)	Autoignition Temperature (°C)	Boiling Point (°C)	Melting Point (°C)
Ethylbenzene	8.8	15	432	126	-95
n-Butyl Propionate	8.8	32	427	146	-89
2-Pentanone	8.7	7	505	100	-78
Methyl propionate	8.9	-2	469	79	-88
Propyl Acetate	8.8	14	450	102	-95
Propyl Formate	9.2	-3	455	81	-93
1-Bromopropane	8.9	26	490	71	-110

<sup>1</sup> Taken From: The Condensed Chemical Dictionary, Eighth Edition, Gessner  
G., Van Nostrand Reinhold Company, New York (1971)  
And: Solvent Safety Handbook, D.J. DeRenzo, Noyes Publication (1988)

<sup>2</sup> Handbook of Chemistry and Physics, 65th Edition, Weast, R.C., CRC Press, Boca Raton, FL,  
1984-1985

TABLE 29

TOXICITY DATA FOR POTENTIAL PPE  
DILUENTS HAVING FLASH POINTS BELOW 38°C<sup>1</sup>

SOLVENT	TOXICITY
Ethylbenzene	Moderately toxic by ingestion; mildly toxic by inhalation and skin contact
n-Butyl propionate	Skin irritant; mildly toxic by ingestion
2-Pentanone	Skin irritant; moderately toxic by ingestion; mildly toxic by inhalation and skin contact
Methyl propionate	Skin irritant; moderately toxic by ingestion; mildly toxic by inhalation
Propyl Acetate	Skin irritant; moderately toxic by ingestion and inhalation
Propyl Formate	Skin and eye irritant; moderately toxic by ingestion
1-Bromopropane	Moderately toxic by ingestion and inhalation

<sup>1</sup> Taken From: Dangerous Properties of Industrial Materials,  
N. Irving Sax and Richard J. Lewis,  
Van Nostrand Reinhold Co., New York (1989)

#### (d) Results

The results of the  $-34.4^{\circ}\text{C}$  viscosity screening show that none of the diluents with flash points of  $38.1^{\circ}\text{C}$  or above (Table 30) gave specification results except for trichloroethylene. Among the diluents having flash points below  $38^{\circ}\text{C}$  only two (propyl formate and 1-bromopropane) met the pumpability requirement, although many of the other diluents gave respectable results. The data show that there is a relationship between both molar concentration of the diluent, the melting point of the diluent and the resultant viscosity of the mixture. The best results are observed for solvents with relatively high molar volumes and low melting points.

C&O testing was conducted only on the solvents that gave measurable  $-34.4^{\circ}\text{C}$  viscosities. The results with and without condensate return (Tables 31 and 32, respectively) show that only diglyme and 1-bromopropane contributed significantly to the C&O test instability of their mixtures when tested with condensate return. Under the same test conditions, 2-pentanone and ethylbenzene showed viscosity increases somewhat higher than the other diluents. All diluent mixtures, however, gave acceptable C&O results when tested without condensate return.

#### (3) Blends

Basestock blending is quite distinct from solvent dilution in that the blending agent has volatility similar to the basestock. Thus, the blending agent will have a long residence time in the engine as opposed to a very short residence time for a diluent. As a consequence, the blending agent must meet the same stringent stability requirements of a high temperature lubricant as the polyphenyl ether.

Previously, many attempts have been made to improve the low temperature viscosity of thermally stable organic compounds by the introduction of side chains or different functional groups. Thus, various substituted terphenyls,<sup>6</sup> biphenyls,<sup>7</sup> polyphenyl ethers,<sup>7,8</sup> phosphonitriles<sup>9</sup> and pyrazines<sup>10</sup> were synthesized. Although good improvements in low temperature fluidity were observed, it was generally accompanied with large decreases in oxidative stability.

Based on the physical property data for the high temperature lubricants tested on this contract, blending will not produce a  $-34.4^{\circ}\text{C}$  pumpable PPE fluid. Cyclophosphazenes and C-ethers have pour points well above  $-34.4^{\circ}\text{C}$  and perfluoroalkylethers are not miscible with PPE. Lower molecular weight homologues of PPEs and C-ethers may give acceptable blends but are too volatile for blending use.

TABLE 30

THE EFFECT OF SOLVENTS ON THE -34.4°C VISCOSITY  
OF PPE AT 20% VOLUME DILUTIONS AS A FUNCTION OF  
MOLAR CONCENTRATION AND DILUENT MELTING POINT

Diluent Data		20% Volume in PPE Data	
Solvent	Melting Pt., °C	Molar Concentration of Diluent, M/L	-34.4°C Viscosity, cSt
trichloroethylene	-73	2.23	18,000
1-bromopropane	-110	2.20	16,505
methyl propionate	-88	2.08	29,945
propyl formate	-93	2.05	18,043
ethyl lactate	-26	1.97*	highly viscous
tetrachloroethylene	-22	1.96	highly viscous
2-pentanone	-78	1.89	35,460
diethylformamide	NDF	1.80*	highly viscous
propyl acetate	-95	1.74	68,231
tetrahydro- naphthalene	-31	1.74	highly viscous
cellosolve acetate	-62	1.73*	highly viscous
diglyme	-68	1.69*	38,669
ethylbenzene	-95	1.63	143,633
decahydronaphthalene	-43	1.63*	highly viscous
ethylene glycol diacetate	-42	1.62*	highly viscous
diethyl oxalate	-41	1.60*	highly viscous
butyl propionate	-89	1.34	204,210

\*20% by weight, molar concentration values would be lower for 20% by volume

NDF = No Data Found

TABLE 31

COMPARISON OF C&O TEST DATA FOR UNDILUTED AND  
DILUTED TEL-90102 AT 320°C  
48 HOURS, SQUIRES TUBES  
WITH INITIAL CONDENSATE RETURN (ICR)<sup>1</sup>

Diluent (20% Volume)	Visc., cSt 40°C	% Visc. Chg. <sup>2</sup> 40°C	Visc., cSt 100°C	% Visc. Chg. <sup>2</sup> 100°C
None, fresh	282.99	-	12.77	-
None, undiluted	335.56	18.6	13.72	7.4
Diglyme	oil degraded			
1-Bromopropane	oil degraded			
Propyl formate	324.85	14.8	13.41	5.0
Methyl propionate	324.66	14.7	13.53	6.0
2-Pentanone	365.28	29.1	14.29	11.9
Propyl acetate	331.94	17.3	13.55	6.1
Ethylbenzene	380.74	34.5	14.59	14.3
Butyl propionate	344.16	21.6	13.83	8.3
Trichloroethylene	326.84	15.5	13.52	5.9

<sup>1</sup> Condenser used throughout test

<sup>2</sup> Based on fresh TEL-90102

TABLE 32

COMPARISON OF C&O TEST DATA FOR UNDILUTED AND  
DILUTED TEL-90102 AT 320°C  
48 HOURS, SQUIRES TUBES  
WITHOUT INITIAL CONDENSATE RETURN (ICR)<sup>1</sup>

Diluent (20% Volume)	Visc., cSt 40°C	% Visc. Chg. <sup>2</sup> 40°C	Visc., cSt 100°C	% Visc. Chg. <sup>2</sup> 100°C
None, fresh	282.99	-	12.77	-
None, undiluted	335.56	18.6	13.72	7.4
Diglyme	343.52	21.4	13.79	8.0
1-Bromopropane	327.14	15.6	13.54	6.0
Propyl formate	326.85	15.5	13.45	5.3
Methyl propionate	329.08	16.3	13.52	5.9
2-Pentanone	331.53	17.2	13.54	6.0
Propyl acetate	330.59	16.8	13.54	6.0
Ethylbenzene	335.13	18.4	13.68	7.1
Butyl propionate	332.14	17.4	13.59	6.4

<sup>1</sup> Condenser applied after lubricant reached 320°C (i.e. after the solvent evaporated)

<sup>2</sup> Based on fresh TEL-90102

As an example, it was necessary to make 50% blends of either phenyl ether or phenyl sulfide (the lowest molecular weight homologues of PPE and C-ether, respectively) in order to reach the  $-34.4^{\circ}\text{C}$  pumpability requirement. Unfortunately, both of these compounds have boiling points well below the projected bulk oil operating temperature of the engine and therefore volatilization losses would be excessive. The effect of blending higher molecular weight homologues (3P2E, 4P3E and C-ether) on the viscosity of PPE is shown in Figure 8. These compounds will not be capable of producing a  $-34.4^{\circ}\text{C}$  pumpable fluid by themselves; however, their use in conjunction with diluents should allow this goal to be reached more easily.

Since the lower molecular weight homologues of PPEs should have similar, if not identical, oxidative stabilities and mechanisms of decomposition, it is assumed that their blends with 5P4E will have acceptable stability. Therefore, no C&O testing of these blends was conducted. However, the C-ether fluid not only has lower oxidative stability, its mechanism of degradation is quite different than that of PPE. Therefore, C&O testing at  $320^{\circ}\text{C}$  was conducted for a 50/50 weight percent blend of TEL-90102 and O-64-20. The results (Table 33) show that the blended lubricant gave oxidative stability and corrosion results approximately equal to what would be expected. The mixing of the two fluids does not result in any positive or negative synergism and the results are within specification except for silver corrosion. Based on these results, it is inferred that the diluent/C-ether/PPE blends would have acceptable C&O stability.

#### (4) Blends and Diluents

##### (a) Approach

Since neither blends nor diluents alone gave very satisfactory results, a combined approach involving both types was tried. The approach should not only allow more lubricant system candidates to meet the  $-34.4^{\circ}\text{C}$  pumpability requirement, but should likewise decrease the amount of diluents that must be added to the lubricant to meet the pumpability specification. Thus, 50% (wt/wt) solutions of PPE with 3P2E, 4P3E and C-ether were made and the volume of diluent necessary to achieve  $-34.4^{\circ}\text{C}$  pumpability was determined.

##### (b) Results

The viscosity results of these diluent/blends (Table 34) show that both the 3P2E and C-ether blends allowed seven of the diluents to meet the viscosity criteria. The 4P3E blend allowed five of the diluents to meet the specification. As expected these blends

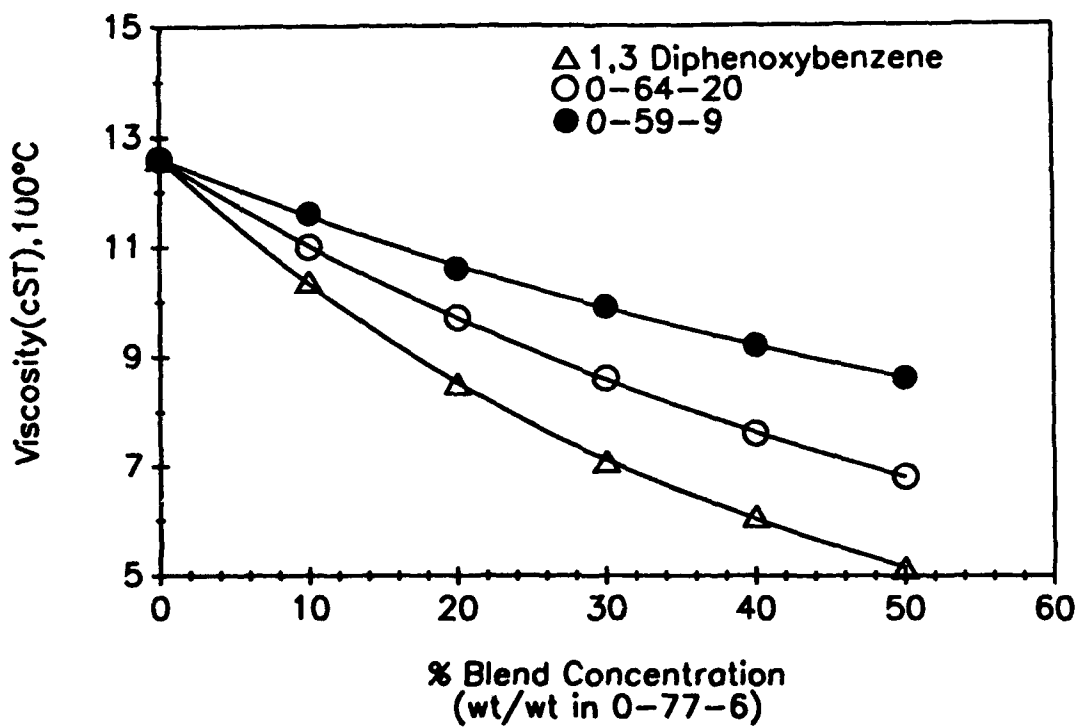
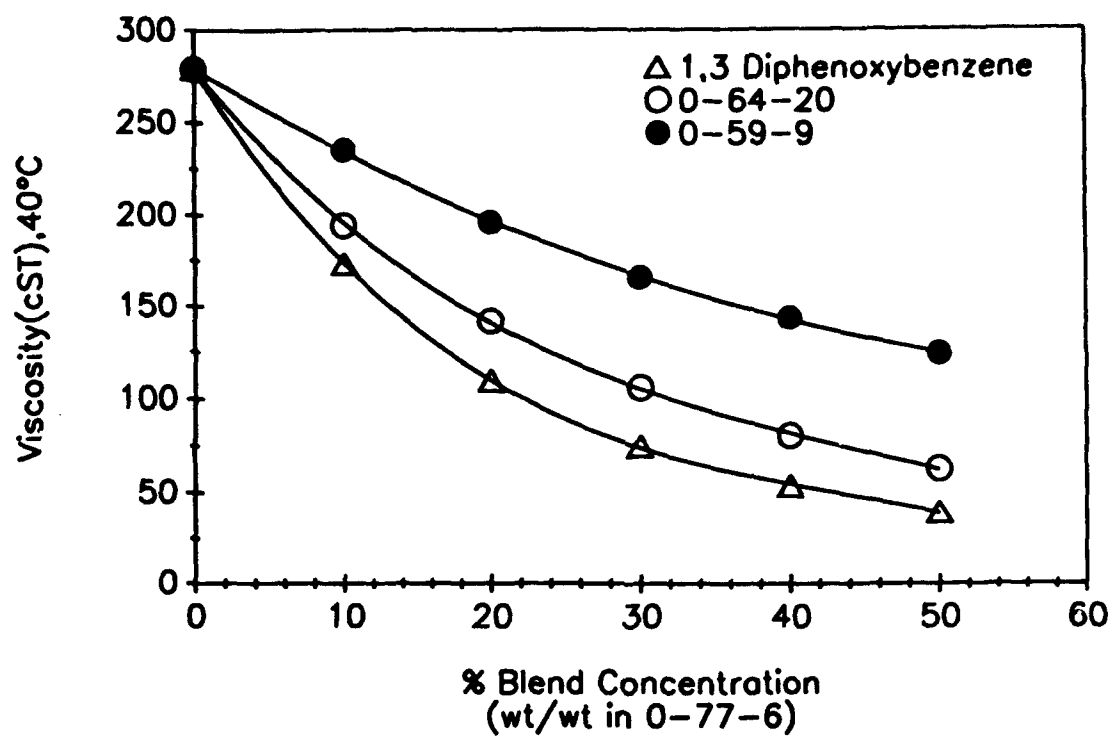


Figure 8. The Viscosity of O-77-6 Blended with Various Levels of 3P2E (1,3-diphenoxybenzene), 4P3E (O-59-9), and C-Ether (O-64-20).

TABLE 33

COMPARISON OF C&O TEST DATA FOR 50/50  
O-64-20/TEL-90102 BLEND, O-64-20 AND TEL-90102  
AT 320°C, 48 HOURS, SQUIRES TUBES

Sample	Visc., cSt 40°C	% Visc. Chg. 40°C	Visc., cSt 100°C	% Visc. Chg. 100°C
Fresh 50/50 O-64-20/TEL-90102 Blend	59.89	-	6.64	-
Stressed Blend	73.21	22.2	7.30	9.9
Fresh TEL-90102	282.99	-	12.77	-
Stressed TEL-90102	335.56	18.6	13.72	7.4
Fresh O-64-20	21.71	-	4.01	-
Stressed O-64-20	25.79	18.8	4.39	9.5

Specimen Corrosion Data  
Wt. Chg. in mg/cm<sup>2</sup>

	Al	Ag	M-St	M-50	Wasp	Ti
Stressed Blend	0	-0.28	0.02	0.02	0.04	0.06
Stressed TEL-90102	0	0	0.04	0.02	0	0
Stressed O-64-20	0.15	-0.68	0.06	0.08	0.06	0.04

TABLE 34

VISCOSITIES AT -34.4°C FOR DILUENTS IN 5P4E AND  
DILUENTS IN BLENDS OF 5P4E AND 4P3E, C-ETHER AND 3P2E<sup>1</sup>

Diluent	% Diluent Conc. Vol	Blend (50% wt/wt)			
		5P4E	4P3E/5P4E	C-ether/5P4E	3P2E/5P4E
1-Bromopropane	10	-	-	-	60756
	15	-	105858	14554	5214
	20	16505	6376	-	-
Propyl formate	10	-	-	-	49791
	15	88041	14138	6380	-
	20	18043	6867	-	-
Methyl propionate	10	-	-	-	92942
	15	151624	15292	7805	-
	20	29945	8875	3153	-
2-Pentanone	15	-	-	36347	11611
	20	35466	14377	3694	-
Propyl acetate	15	-	-	32093	19383
	20	68231	25075	8320	-
Ethylbenzene	15	-	-	88998	26045
	20	143633	58843	9757	4313
Butyl propionate	15	-	-	-	39290
	20	204210	83471	17845	8002

<sup>1</sup> Viscosity values in cSt

allowed for lower volumes of some of the diluents to be used in order to reach the -34.4°C pumpability requirement.

#### (5) Conclusions

Producing a -34.4°C (-30°F) pumpable lubricant using 5P4E polyphenyl ether as the base lubricant has proven to be a difficult task. Because of the scarcity of organic compounds with high temperature oxidative stability and good low temperature viscosity properties, blending of PPE was only able to produce small decreases in low temperature viscosity. With 20% by volume as a maximum limit, only one solvent was capable of meeting the pumpability criterion. The use of both blends and diluents allowed a much wider range of PPE mixes to meet the specification. A summary of diluent or diluent/blend PPE mixes that meet the previously established criteria is shown in Table 35.

#### (6) Recommendations

Although specific diluent and diluent/blend PPE mixes (Table 35) are listed as having acceptable -34.4°C pumpability, any recommendations for their use are dependent upon the correctness of many of the important but largely self-defined physical property criteria. These include boiling point, flash point, autoignition temperature and toxicity/environmental properties as well as the appropriateness of the corrosion/oxidation tests as conducted. Additionally, the higher volatility of the blending agents used (3P2E, 4P3E and C-ether) relative to 5P4E should be considered. Finally, the effect of blending on other tribological properties (i.e., wear) must be addressed prior to blending considerations.

TABLE 35

SUMMARY OF DILUENTS, BLENDS AND DILUENT/BLENDS OF POLYPHENYL ETHER  
THAT MEET THE -34.4°C (-30°F) PUMPABILITY SPECIFICATION

1. Diluents Only  
20% Propyl Formate
  
2. Blends Only  
None
  
3. Blends and Diluents
  - a. 50/50 (wt/wt) 3P2E/5P4E
 

20% Butyl propionate	15% Propyl formate
15% Propyl acetate	20% Ethylbenzene
15% Methyl propionate	15% 2-pentanone
  
  - b. 50/50 (wt/wt) 4P3E/5P4E
 

20% Propyl acetate	20% propyl formate
20% Methyl propionate	20% 2-pentanone
  
  - c. 50/50 (wt/wt) C-ether/5P4E
 

20% Butyl propionate	15% Propyl formate
20% Propyl acetate	20% Ethylbenzene
15% Methyl propionate	20% 2-pentanone

e. Performance Improvement of the Polyphenyl Ether Fluids.

(1) Introduction

Because of their excellent high temperature properties and outstanding radiation resistance, 5P4E polyphenyl ethers were first used as hydraulic fluids in the aviation industry during the 1950s and 1960s.<sup>11</sup> Oxidative stabilities of these liquids are generally above 295°C,<sup>3</sup> and they are thermally stable up to 430°C.<sup>12</sup> However, poor low temperature flowability and pumpability due to their high viscosity and pour point are major concerns in field applications. As mentioned in Section 2.d. above, diluting 5P4E with TCE has caused environmental concerns. Thus, a search for some nonvolatile pour point depressants is warranted.

(2) Lubricity Effect of Some Additives in Polyphenyl Ether Basestock

When polyphenyl ether (PPE) based lubricants are subjected to M50 four-ball sliding contacts, the amount of friction and wear incurred is often large. Hence, a search for effective antiwear and antifriction additives for the PPE basestock (O-77-6) has been initiated. The less favorable four-ball performance of O-77-6 may be attributed to its glass transition to form an unfavorable solid or semisolid film inside the sliding contacts.<sup>13</sup> This in situ formation of solid film is likely to increase the stress of the tribo-junction. In order to avoid this unwanted stress, an attempt has been made to modify the junction condition by introducing lubricity additives into the polyphenyl ether fluid. The additive has a dual function: (1) to alter the tribo-surface chemistry via preferential adsorption/reaction of additive species on the rubbing surfaces, and (2) to reduce the chance of in situ solid formation by effectively lowering the PPE concentration inside the sliding contacts. It should be mentioned that the concentration of polar additive species could be much higher inside the tribo-junctions than in the bulk oil.<sup>14</sup>

As a preliminary screening, the following additives have been tested: phenyldisulfide (PDS), oleic acid (OA), stearic acid (SA), and tricresyl phosphate (TCP). The antiwear and antifriction characteristics of these additives are presented in Figures 9 and 10, respectively. A ball pot temperature of 150°C was used in this study because any chemical species intended for high temperature applications should pass this level of thermal stress. Moreover, a relatively high concentration of additive was applied in the O-77-6 fluid to ensure a resulted impact. As shown by the experimental data, antiwear effect of PDS is not as good as other species. This may be due its relatively low concentration. The solubility of PDS in

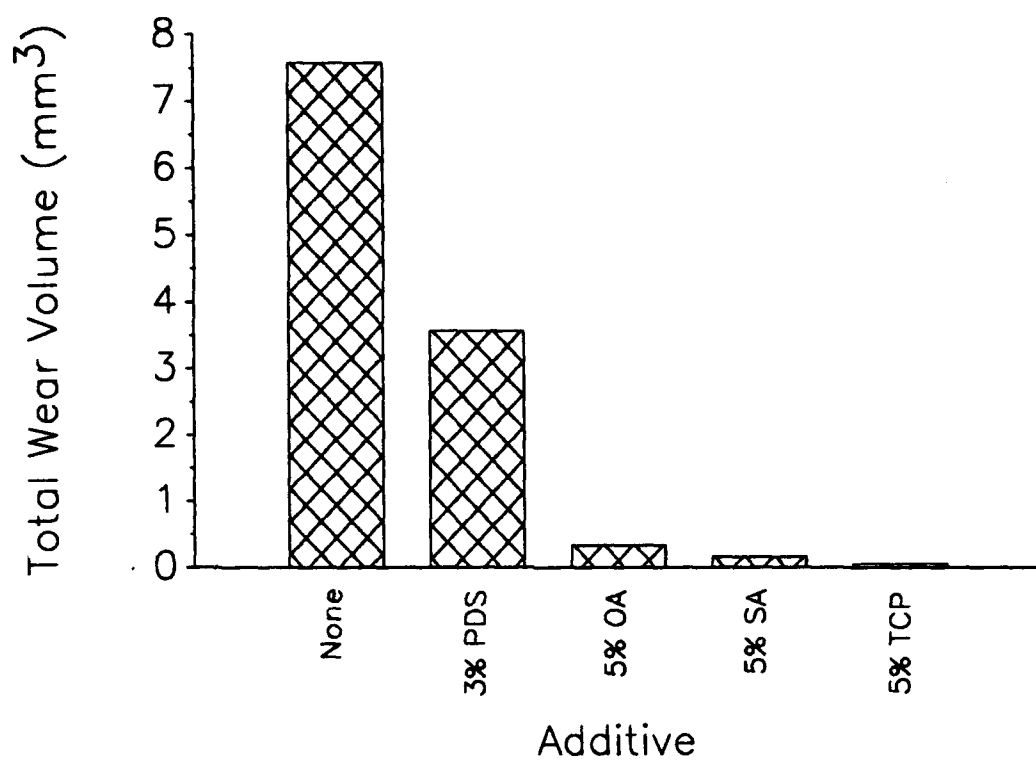


**Figure 9. Antiwear Characteristics of Various Additives in the Polyphenyl Ether Basestock (O-77-6).**

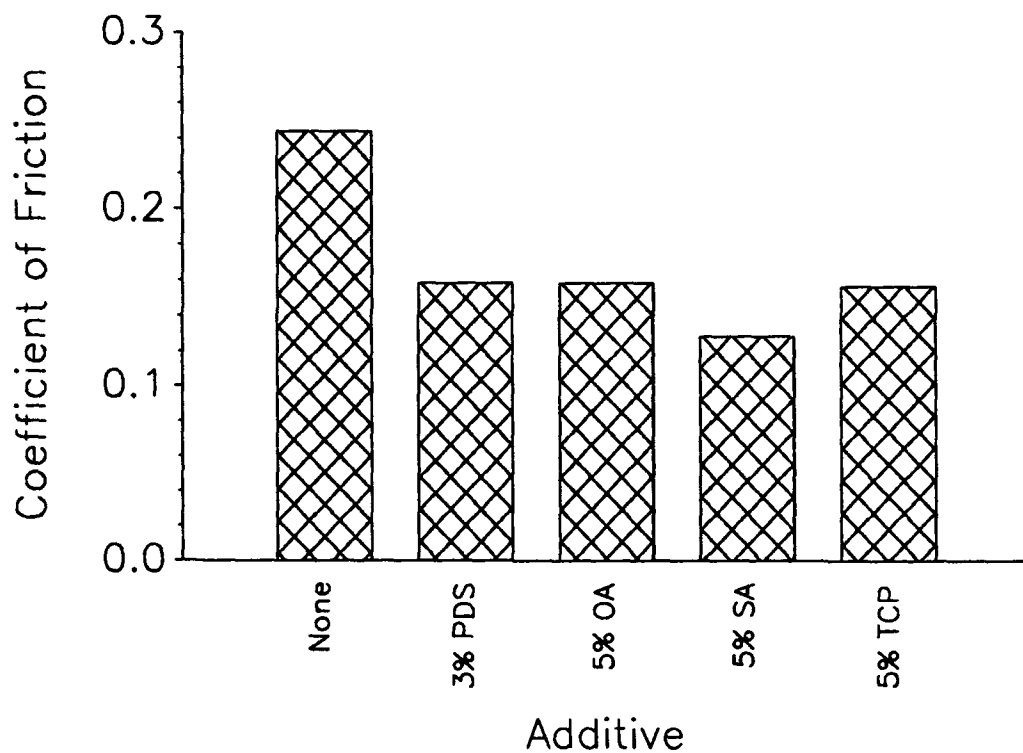


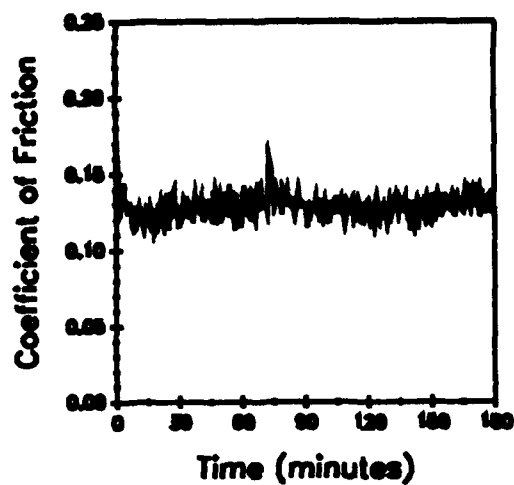
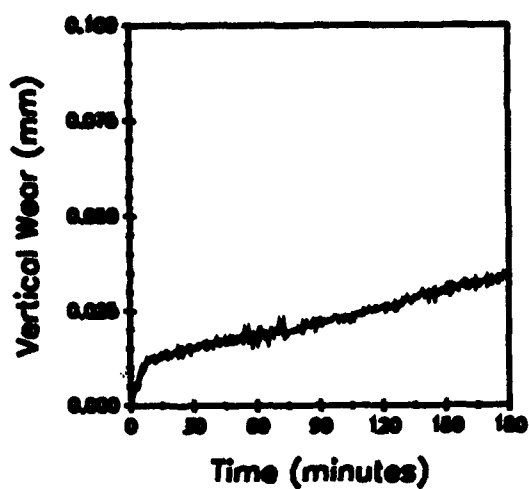
**Figure 10. Antifriction Characteristics of Various Additives in the Polyphenyl Ether Basestock (O-77-6).**

polyphenyl ether is limited to 3% instead of the usual 5%. Oleic acid achieves a wear level less than one twentieth of that for pure PPE. This could be the result of oleic acid forming a multilayer liquid crystal between the two sliding surfaces.<sup>15</sup> By a different mechanism, the effectiveness of stearic acid is believed to be due to the formation of a mono-molecular adsorbed film on the metal surface. The adsorbed molecules are oriented in such a way so that its polar carboxylic ends are attached to the solid surface and the hydrocarbon chains are extended away from the surface.<sup>16</sup> This orientation yields a tightly packed monolayer, which may be the reason for its excellent antiwear and antifriction properties as witnessed in those figures. Its wear is only about one fiftieth of that of the pure PPE, and the friction level is the lowest of all.

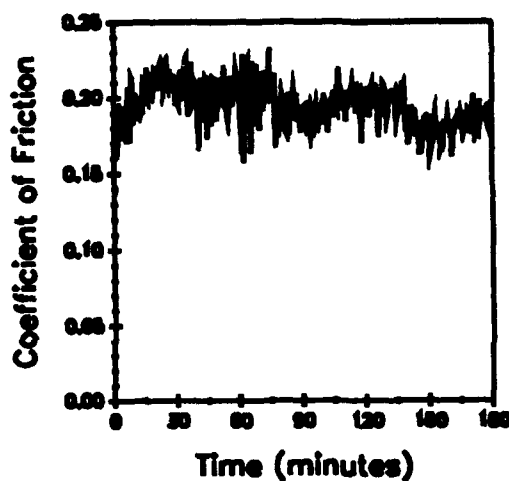
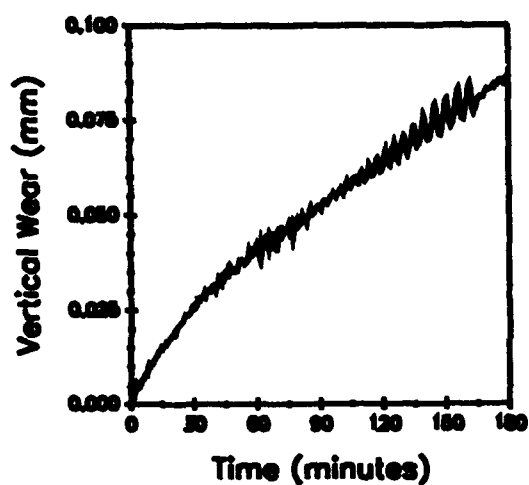
The antiwear nature of TCP is again manifested through its effectiveness in a sliding four-ball wear test when mixed as an additive in PPE. The amount of wear generated from the 5% TCP solution is less than one hundredth of that of pure PPE. This is a significant reduction of wear volume. It is well documented that TCP is able to form iron phosphate ( $\text{FePO}_4$ ) film on the rubbing steel surface, which is thought to be the predominant mechanism for its antiwear effectiveness.<sup>17,18</sup> The formation of iron phosphate film is probably due to a chemical reaction between the steel and phosphoric acid. The acid could be present either originally as an impurity or formed later in situ from TCP aging and/or heating.<sup>19,20</sup>

Four-ball testing of the PPE basestock has also been done with 5% additions of a stressed phosphate ester (PE) mixture. Two samples of the PE were prepared by first stressing them at high temperature under two different environments. An oxygen environment was used for the first sample for thermal-oxidative breakdown while nitrogen was used for the second sample for thermal breakdown only. Testing was done for friction and wear comparisons to the four-ball test of 5% fresh PE in O-77-6.

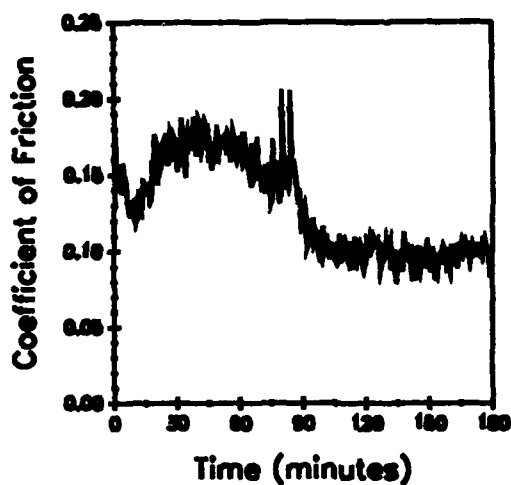
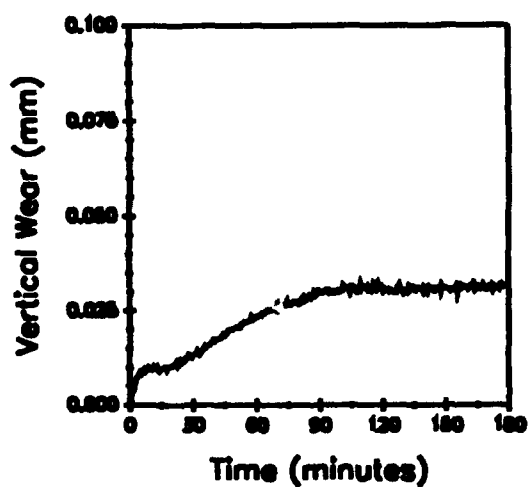
The results from the four-ball testing of the two stressed PE/O-77-6 solutions are presented in Figure 11 along with the results from the single test of fresh PE in O-77-6. Figure 11(a) shows the wear rate (vertical displacement of the top ball during testing) and friction coefficient for the 5% weight addition of fresh PE. In Figure 11(b), the wear rate and friction data of the oxidized PE are presented. Finally in Figure 11(c), the wear rate and friction plots during the test with the nitrized PE are shown. The total wear during these tests and a test of pure O-77-6 fluid is listed in Table 36 along with the average coefficient of friction during each test.



a. 5% unstressed PE



b. 5% oxidized PE



c. 5% nitrized PE

Figure 11. Four-Ball Wear and Friction Coefficient Curves for Tests of a Phosphate Ester (PE) Mixture in O-77-6 at 150°C (M50 Balls, 145 N Load, 1200 rpm).

TABLE 36

## FOUR-BALL TEST RESULTS FOR PE/PPE SOLUTIONS AT 150°C

Additive	Conc. in PPE (weight %)	Total Wear mm <sup>3</sup>	Friction Coefficient (average)
none	-	7.15	0.252
fresh PE	5	0.0820	0.129
oxidized PE	5	0.2440	0.195
nitridized PE	5	0.0351	0.128

The values listed in Table 36 show that each additive solution is effective in reducing both the four-ball wear and friction over the pure PPE. The nitridized PE reduces wear and friction most and is effective in preventing wear after about 90 minutes of the test (see the wear curve of Figure 11(c)). The leveling of the wear curve and the accompanying reduction in friction coefficient is unique to the nitridized PE test.

Another four-ball test was done at 250°C with the oxidized PE in PPE to begin a study of antiwear additives at higher temperatures. This test produced only 0.0228 mm<sup>3</sup> of total wear, but the PPE solution left severe carbon deposits on all of the oil-wetted surfaces of the four-ball test rig. In contrast, the tests of PE/PPE samples conducted at 150°C generated no excessive deposits.

### (3) Comprehensive Study of TCP for the PPE Fluids

Additional study of TCP effectiveness in both PPE basestock and inhibited PPE (TEL-90102) has been executed. Evaluation was primarily focused on three important aspects of the lubricant: (1) tribological performance, (2) thermal-oxidative stability, and (3) low temperature flowability or pumpability.

Samples containing various TCP concentrations were tested in the four-ball wear machine. A semilog plot of total wear volume versus TCP concentration is shown in Figure 12. For PPE, a sharp reduction of wear is realized for TCP concentrations between 3% and 5% TCP, with little or virtually no change of wear in any other regions. Comparatively, the transition is moderate in the case of inhibited PPE (TEL-90102), which is probably due to the presence of Additive A (a commercial antioxidant for PPE fluids). It is very likely that Additive A could interfere with TCP and alter the experiment outcome. Nevertheless, a clear wear

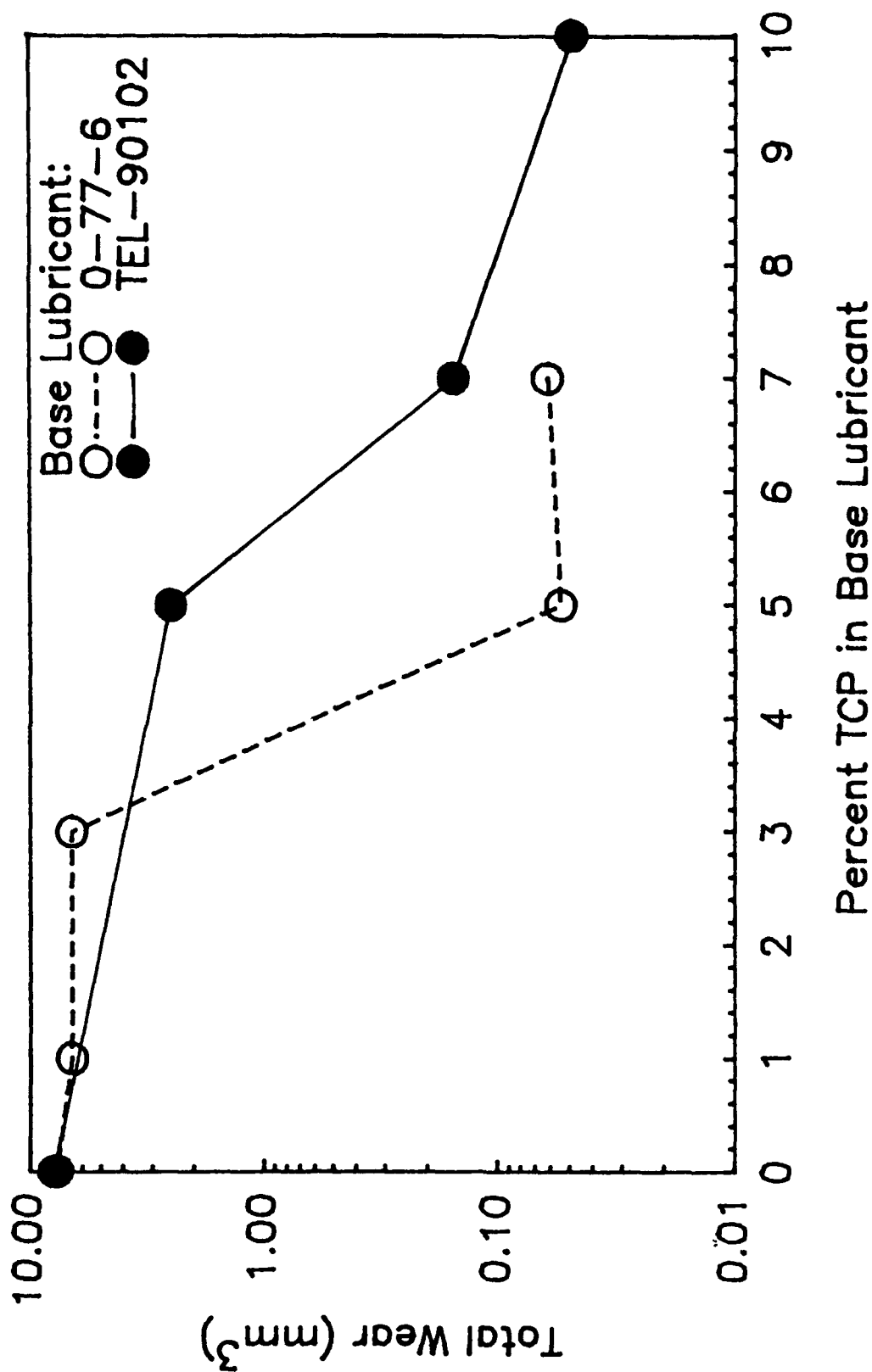


Figure 12. Total Wear Volume as a Function of TCP Concentration in the Polyphenyl Ether Fluids. Four-Ball Test Condition: 1200 rpm, 145 N, 150°C, Three Hours, and M50 Balls.

transition in either case strongly suggests a shifting of wear modes. Similar changes can also be seen from Figure 13, where the frictional coefficient tends to decrease with an increase in TCP concentration. This could be the result of TCP producing an easily sheared film within the sliding junction through its chemical interaction with the tribo-surfaces. Figure 14 demonstrates an interesting trend of alpha value with TCP concentration. In the four-ball configuration, the sliding surfaces (or wear scars) of the three stationary balls are subjected to constant frictional heating and wearing. On the contrary, the rubbing areas on the rotating top ball undergo a periodic stressing cycle. If chemical reaction is a dominant factor in the tribo-mechanism, more "corrosive" wear will be generated from the three stationary balls than from the top ball halo. Consequently, large alpha values (or circular wear scars) will be obtained through the "corrosive" wear. This speculation is consistent with the observations from Figures 12, 13, and 14.

Besides its tribo effectiveness, TCP can also reduce the viscosity of PPE fluids, so as to improve their low temperature flowability. For example, a 10% TCP in O-77-6 gives a viscosity of 215 cSt at 40°C, which is considerably below the original 280 cSt from the pure PPE basestock. Although the tribological performance of TCP is impressive and it can also enhance PPE flowability, its thermal-oxidative stability is, however, inadequate for high temperature applications. This can be seen from the corrosion-oxidation (C&O) test results obtained in this laboratory. Concentrations of 7% and 10% TCP were utilized for each PPE fluid (O-77-6 or TEL-90102), tests were conducted at temperatures of 280°C and 320°C with and without the presence of metal coupons. In all these cases, build up of heavy sludge and deposits was observed after only a 24-hour test period. Metal coupons were also severely corroded.

From its C&O test results, TCP is too reactive at temperatures of 280°C and above. Although chemical reactivity is needed for its antiwear effectiveness, the same can also cause an adverse effect on lubricant stability. A careful balance among all these factors is critical in formulating a high temperature candidate fluid. Several other chemical species of the same class have been selected and tested. Their molecular structures are displayed in Figure 15, together with those of PPE and TCP. Choice of those chemicals is based on the following rationale.

All three species (TPP, TPPO, and TPPP) can be perceived as a "closed-loop" PPE molecule, wherein the phosphorous atom is well hidden by the steric protection of three out-stretched aryl groups and one oxygen atom. These four groups can provide an adequate shelter in the three dimensional space, at the same time do not seem to create excessive

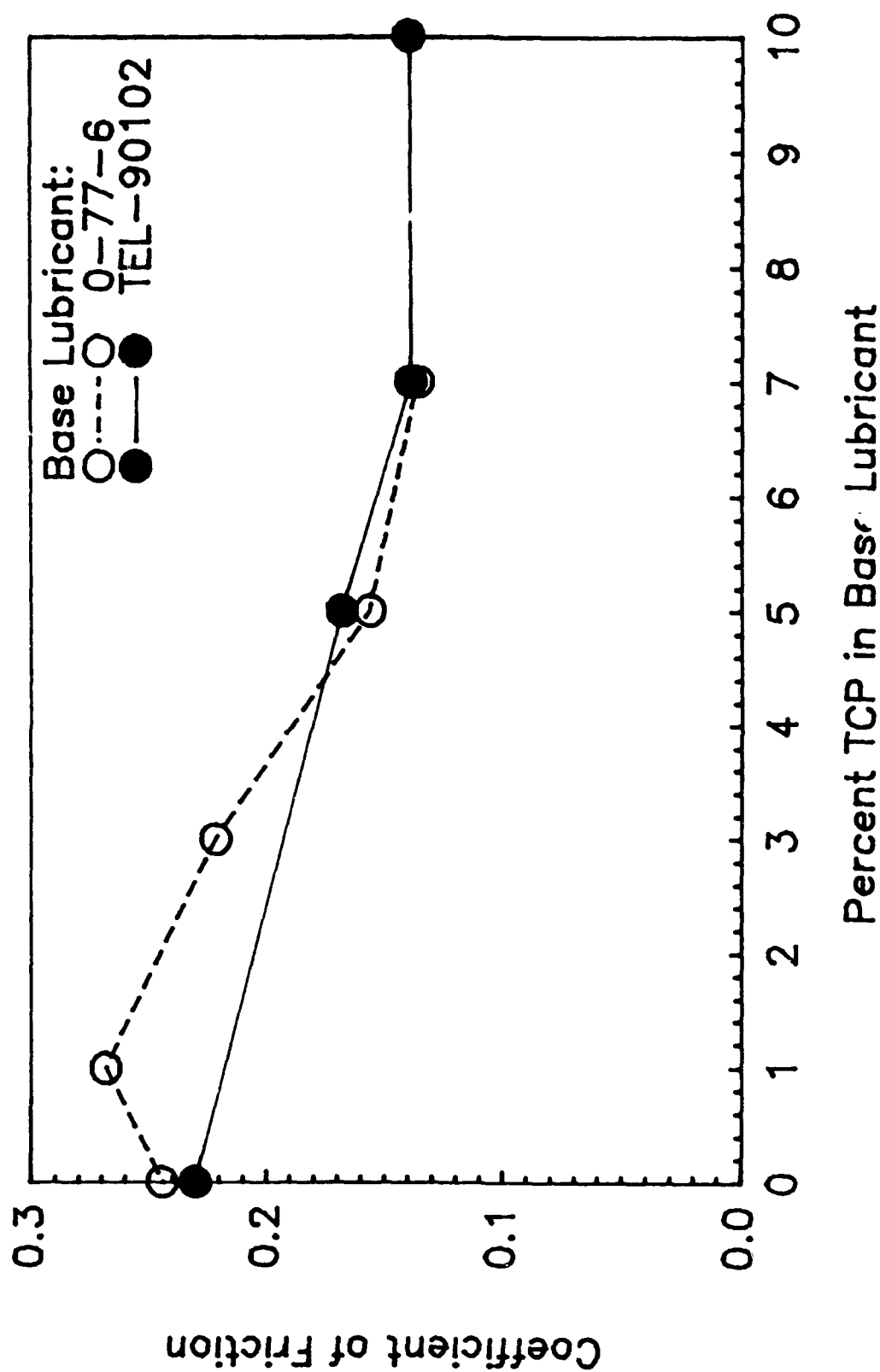


Figure 13. Coefficient of Friction as a Function of TCP Concentration in the Polyphenyl Ether Fluids. Four-Ball Test Condition: 1200 rpm, 145 N, 150°C, Three Hours, and M50 Balls.

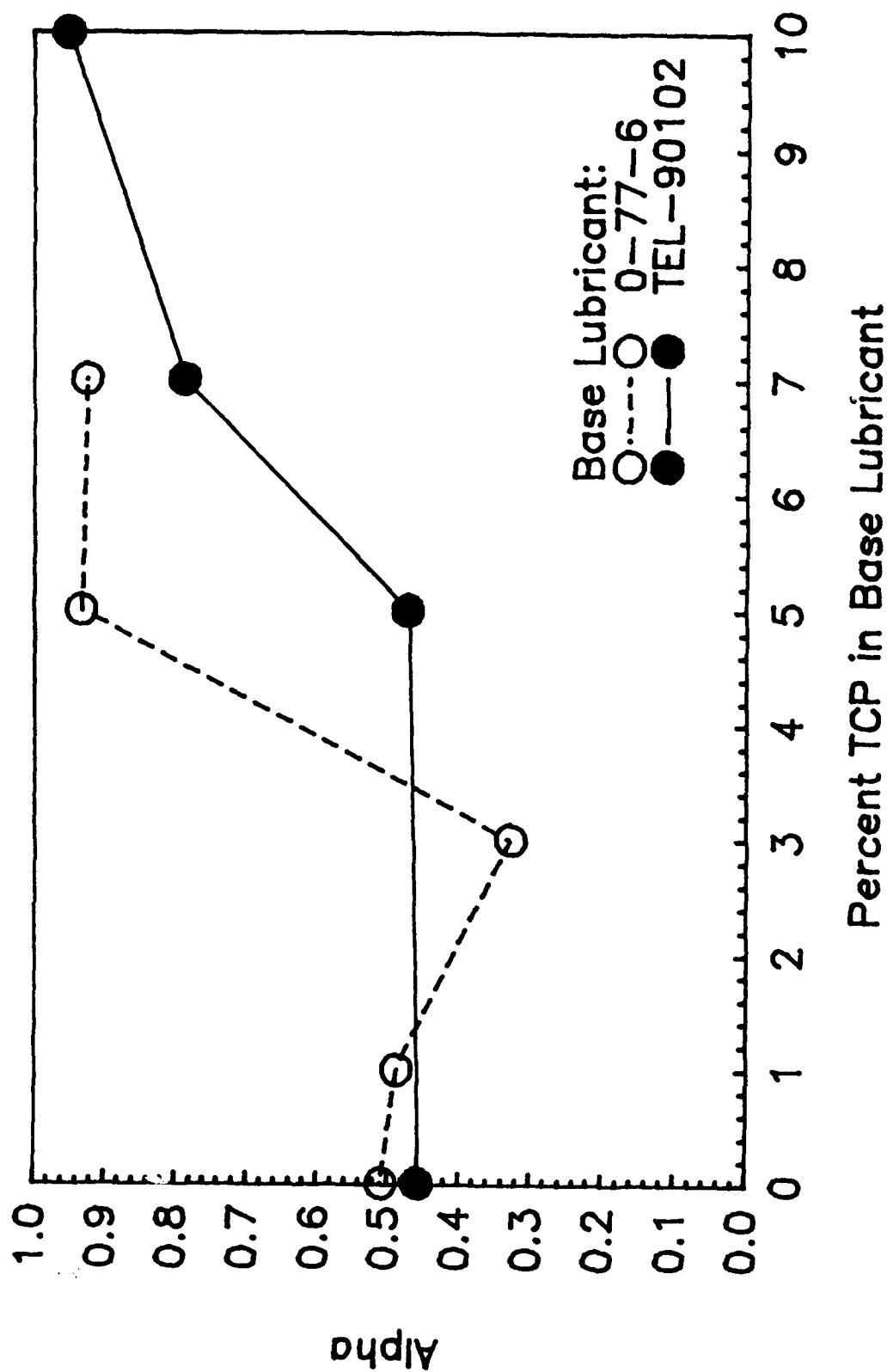
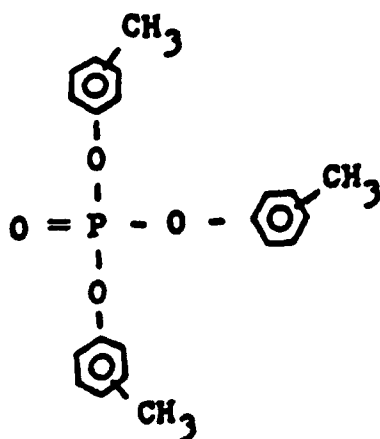


Figure 14. Alpha Value as a Function of TCP Concentration in the Polyphenyl Ether Fluids. Four-Ball Test Condition: 1200 rpm, 145 N, 150°C, Three Hours, and M50 Balls.

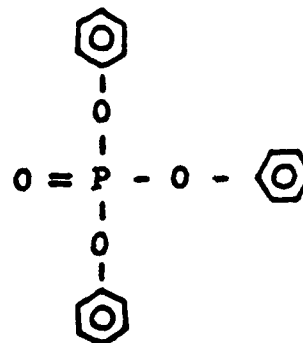
Polyphenyl Ether (PPE)



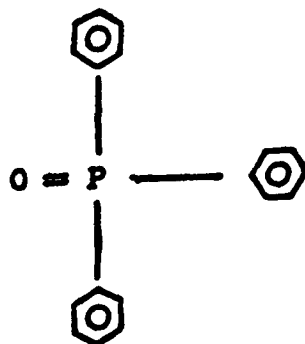
Tricresyl Phosphate (TCP)



Triphenyl Phosphate (TPP)



Triphenylphosphine Oxide (TPPO)



Tri(phenoxy phenyl) Phosphate (TPPP)

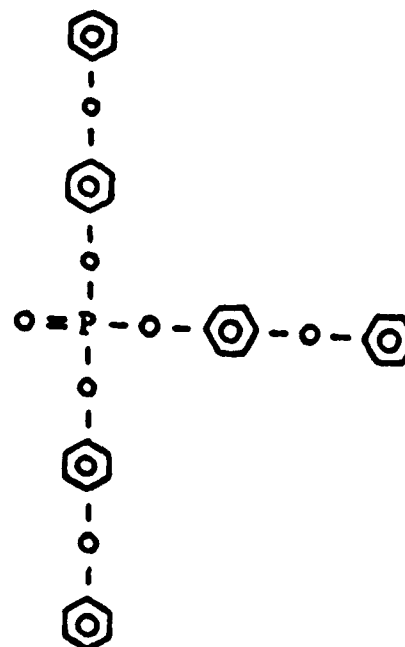


Figure 15. Molecular Structures of PPE, TCP, TPP, TPPO, and TPPP.

intramolecular stress which could lead to reduced stability. Even though TPP, TPPO and TPPP are readily soluble in PPE, the "bulky" structures of these species, on the other hand, could make them decompose easily under the shearing action of rubbing junctions, and the otherwise well hidden phosphorous atom will be exposed to the rubbing surfaces. The same kind of chemically induced  $\text{FePO}_4$  film as in the case of TCP could be produced on the steel surface.

#### (4) Comparison of TCP With TPP in the O-77-6 Fluid

After examining the molecular structure of TCP, it is suggested that the sources of instability could originate from three attached methyl groups within the molecule. If this is true, triphenyl phosphate (TPP) might be more oxidatively stable than TCP. Our experimental results have shown that TPP is indeed more stable than TCP, and it is capable of withstanding a 24-hour C&O test at  $320^\circ\text{C}$ . Table 37 provides a comparison of TCP and TPP for their viscosity reduction capabilities in the O-77-6 fluid. TPP undoubtedly outperforms TCP as a potential candidate for pour point depressant. However, solubility of TPP in O-77-6 is limited to a maximum near 30% where recrystallization occurred after several days of storage at ambient condition. For the sake of comparison the viscosity data of a ternary mixture consisting of 10% TCP and 20% TPP in O-77-6 is also included, and the measured pour point of this mixture was below  $-20.5^\circ\text{C}$ .

Because the molecular structure of TPP is inherently more stable than TCP, it is not surprising to find that TPP is somehow less effective in wear reduction relative to TCP. This can be seen from Figure 16 (note the semilog scale). In order to reach its effective antiwear capability, a large dose of TPP is required for the PPE basestock. However, the antifriction characteristic of TPP is quite similar to that of TCP as shown in Figure 17. It is believed that tribochemistry plays a predominant role in the mechanism of friction/wear reduction when aryl phosphate esters, like TCP and TPP, are used.<sup>21</sup> This is again consistent with the curves present in Figure 18, therein large  $\alpha$  values are being produced in the region of effective lubrication which is an indication of chemical wear as mentioned earlier.

#### (5) More Test Results of TPP/O-77-6 Formulations

A series of brief oxidation tests, of 24-hour period without metal coupons, were performed using the existing C&O apparatus. Bulk oil temperatures of 280, 300, and  $320^\circ\text{C}$  were used. Several formulated TPP/O-77-6 compositions were evaluated and compared and their experimental data are listed in Table 38. Additive A, a commercial antioxidant for the

TABLE 37

## VISCOSITY MEASUREMENTS OF TCP AND TPP IN THE O-77-6 FLUID

Lubricant	Viscosity (cSt)	
	@ 40°C	@ 100°C
O-77-6	280.40	12.52
7% TCP in O-77-6	235.11	11.68
10% TCP in O-77-6	216.94	11.33
1% TPP in O-77-6	260.35	12.33
5% TPP in O-77-6	215.11	11.43
10% TPP in O-77-6	169.98	10.43
15% TPP in O-77-6	136.69	9.55
20% TPP in O-77-6	110.66	8.73
25% TPP in O-77-6	90.93	8.12
30% TPP in O-77-6 *	77.28	7.42
10% TCP & 20% TPP in O-77-6	91.08	7.90

\*: TPP crystallized out (needle-like) from the solution after several days of storage.

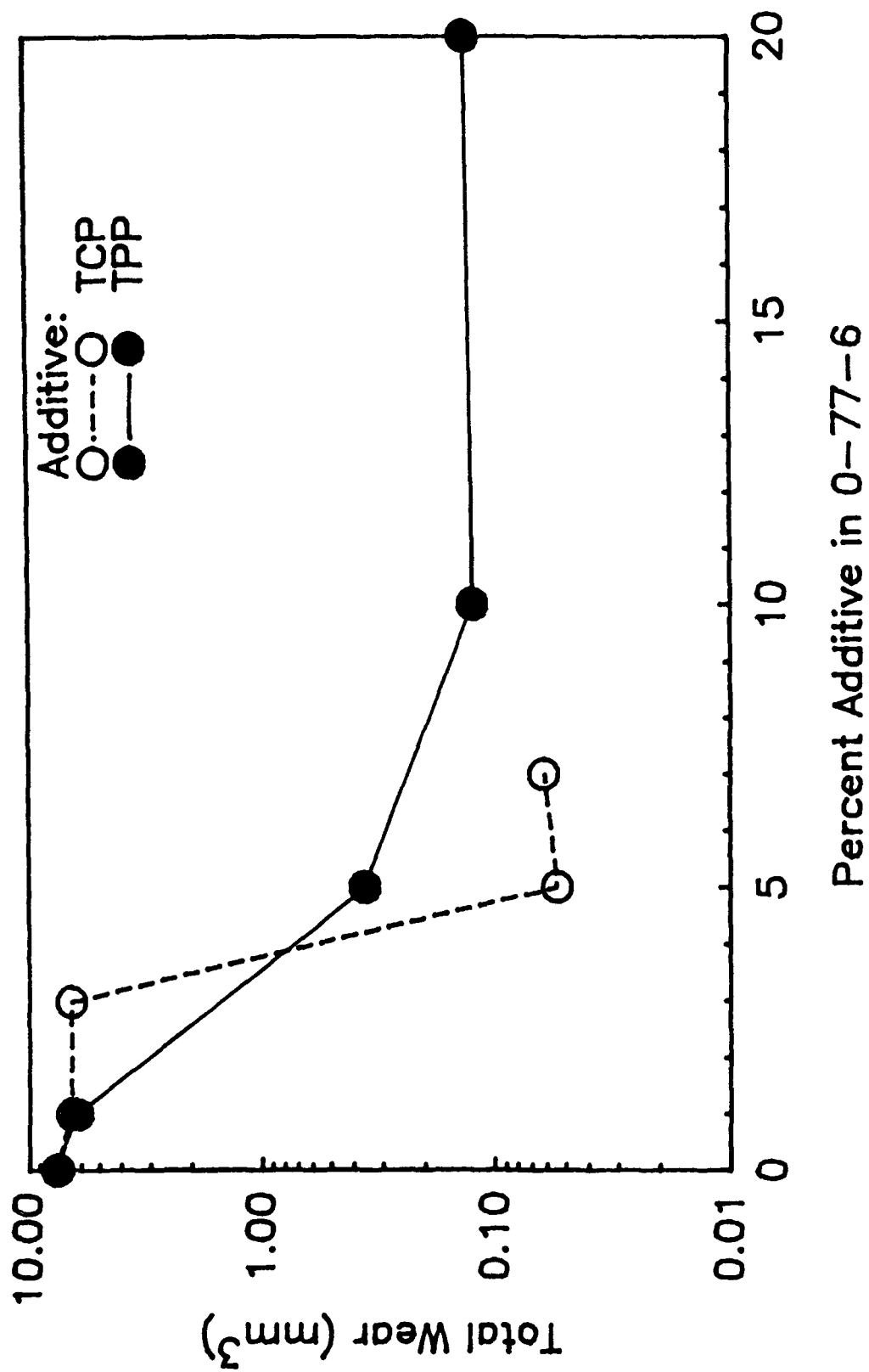


Figure 16. Total Wear Volume as a Function of TCP or TPP Concentration in the O-77-6 Fluid. Four-Ball Test Condition: 1200 rpm, 145 N, 150°C, Three Hours, and M50 Balls.

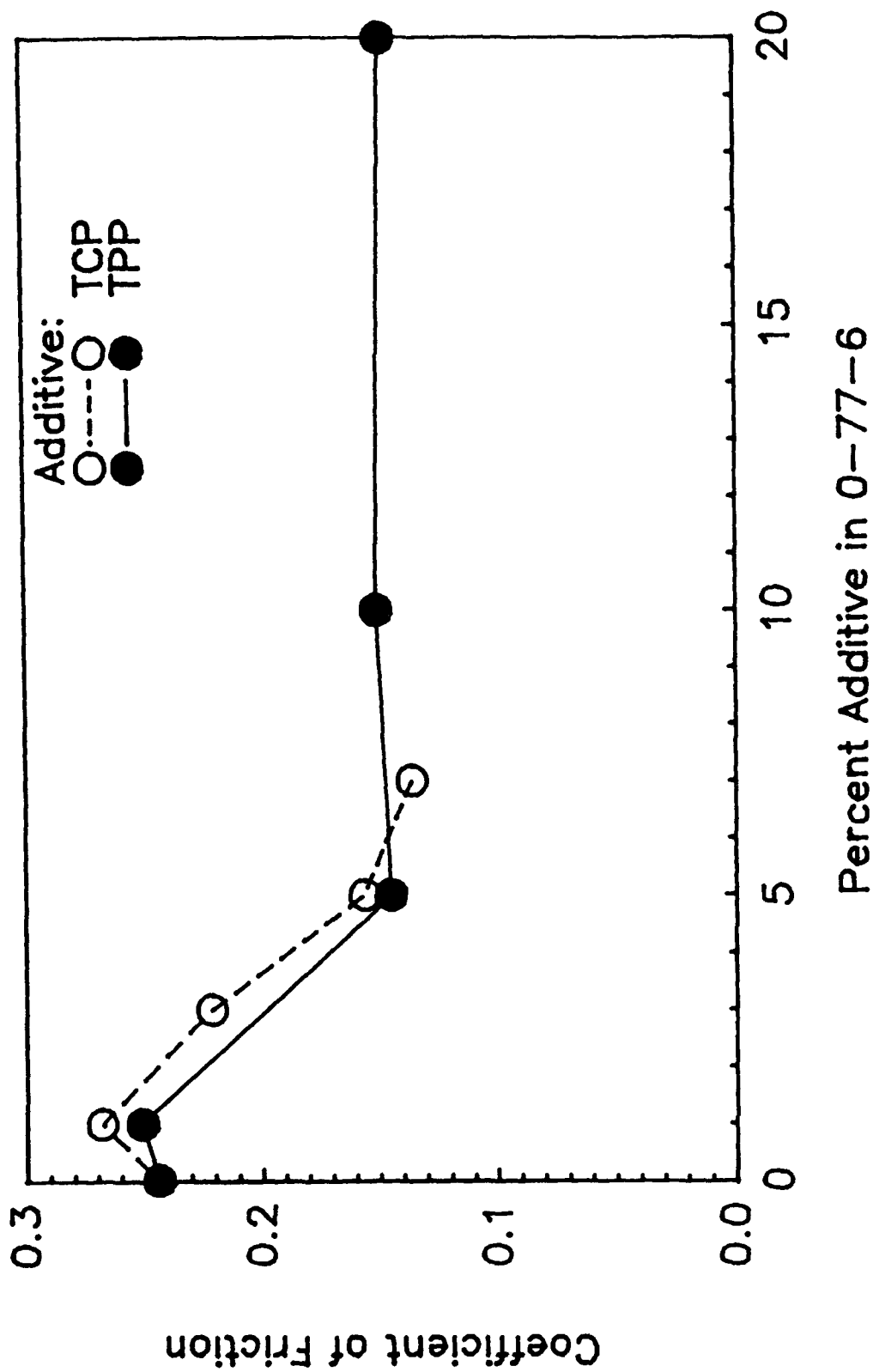


Figure 17. Coefficient of Friction as a Function of TCP or TPP Concentration in the O-77-6 Fluid. Four-Ball Test Condition: 1200 rpm, 145 N, 150°C, Three Hours, and M50 Balls.

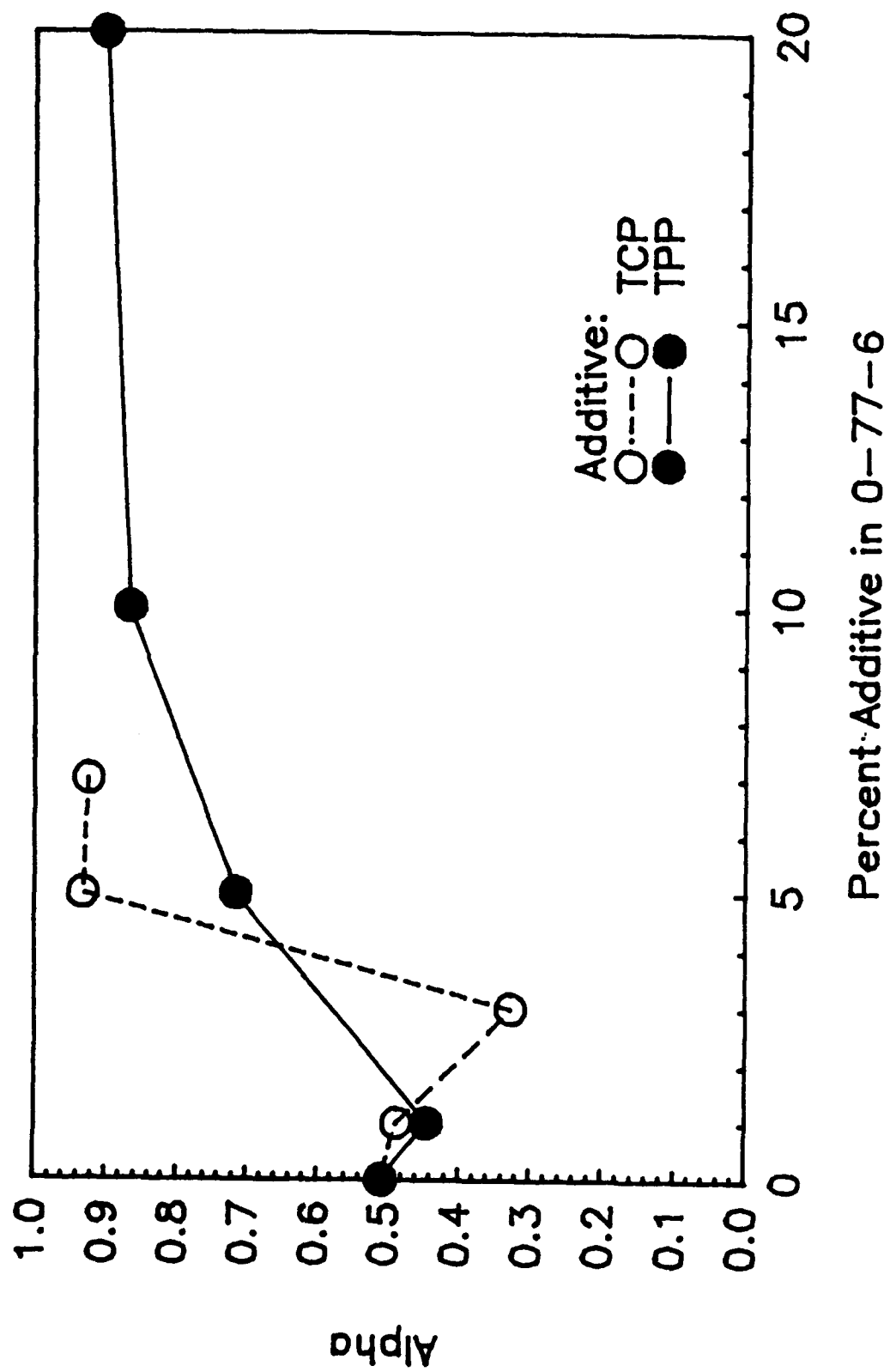


Figure 18. Alpha Value as a Function of TCP or TPP Concentration in the O-77-6 Fluid. Four-Ball Test Condition: 1200 rpm, 145 N, 150°C, Three Hours, and M50 Balls.

TABLE 38

**OXIDATION TEST (WITHOUT METAL COUPONS) FOR 24 HOURS AT 280, 300,  
AND 320°C OF BULK OIL TEMPERATURES**

(a) 24 hours at 280°C.

Lubricant	I. Visc.(cs)		% Visc.Inc.		I.TAN	TAN Inc.	% Wt.Loss
	40°C	100°C	40°C	100°C			
5% TPP, 0.15% additive A in 0-77-6	216.4	11.37	18.49	13.10	0.000	0.488	0.00
5% TPP in 0-77-6	218.2	11.42	8.415	3.327	0.000	0.009	0.00

(b) 24 hours at 300°C.

Lubricant	I. Visc.(cs)		% Visc.Inc.		I.TAN	TAN Inc.	% Wt.Loss
	40°C	100°C	40°C	100°C			
0-77-6	273.3	12.56	13.24	4.538	0.000	0.031	2.52
5% TPP in 0-77-6	211.1	11.45	39.66	12.58	0.000	0.019	6.88

(c) 24 hours at 320°C.

Lubricant	I. Visc.(cs)		% Visc.Inc.		I.TAN	TAN Inc.	% Wt.Loss
	40°C	100°C	40°C	100°C			
5% TPP in 0-77-6	215.7	11.41	148.1	55.57	0.000	0.875	1.30
10% TPP in 0-77-6	170.4	10.47	68.93	27.70	0.000	0.436	2.45

polyphenyl ether fluids, was first examined to see its possible beneficial impact on the TPP/O-77-6 formulation (Table 38(a)). Results show that Additive A is not effective in deterring the oxidative degradation of the 5% TPP in O-77-6 solution at 280°C. Secondly, the sole effect of TPP on the oxidation stability of O-77-6 at 300°C was assessed (Table 38(b)). The interpretation of the experimental data is rather complicated; the presence of 5% TPP tends to raise the percent viscosity increase while at the same time reducing the gain of total acid number (TAN). Finally, the variation of TPP concentration upon the oxidation stability of the TPP/O-77-6 formulation is also studied at a test temperature of 320°C (Table 38(c)). Improved oxidation stability is achieved at TPP concentration higher than 10%. Also as expected, the degradation of the 5% TPP solution accelerates as the temperature rises from 280°C to 320°C.

Having investigated the TPP/O-77-6 formulation in the pure oxidation test, full-scale C&O test with metal coupons was then carried out. Table 39 lists the data obtained at 320°C, for 24 and 48 hours of test periods. The data of the pure O-77-6 fluid are also included for comparison. As shown clearly, the performance of TPP/O-77-6 formulation surpasses that of pure O-77-6. In the 24-hour tests (Table 39(a)), all three TPP/O-77-6 solutions yielded small TAN values and acceptable viscosity increases with a minimum at the 20% TPP concentration. Moreover, by comparing the C&O results of the 10% TPP solution with those from the pure oxidation test (Table 38(c)), it becomes apparent that the involvement of metal coupons actually improves the stability of the solution. This is possible if reactive species generated from the bulk oxidation preferentially attack the metal surface instead of triggering new reactions in the bulk oil phase. It is also conceivable that organometallic compounds formed during the test may function as peroxy radical scavengers to terminate the chain reactions. However, as C&O tests were extended from 24 to 48 hours none of the TPP/O-77-6 solutions were able to survive (Table 39(b)).

It is not completely clear what factors were involved in the degradation process. One interesting phenomenon was observed during the 48-hour C&O test. At some point after the 24-hour test mark, significant amounts of condensed material started to build up on the condenser wall. Later on, this liquid accumulation gradually crystallized and its amount increased. Gas chromatography (GC) analysis of this condensed material reveals the presence of large quantity of phenol with traces of TPP, PPE (O-77-6) and other unknown species. It appeared that in the second half of the 48-hour test, some TPP molecules reacted with moisture (presumably produced during the early stages of the test) to form volatile phenol species. From the literature, the recorded boiling point of pure phenol is 181.7°C (lower than the C&O bulk oil

TABLE 39

**CORROSION/OXIDATION TEST OF TPP/O-77-6 FORMULATIONS AT  
320°C FOR 24 AND 48 HOURS**

(a) 24 hours at 320°C.

Lubricant	I. Visc.(cs)		% Visc.Inc.		I.TAN	TAN Inc.	% Wt.Loss
	40°C	100°C	40°C	100°C			
0-77-6	279.5	--	102.2	--	0.000	--	1.75
10% TPP in 0-77-6	169.2	10.39	30.57	13.19	0.000	0.349	0.80
20% TPP in 0-77-6	110.8	8.751	20.34	8.800	0.000	0.736	0.71
25% TPP in 0-77-6	90.93	8.119	24.59	9.729	0.000	1.183	1.17

(b) 48 hours at 320°C.

Lubricant	I. Visc.(cs)		% Visc.Inc.		I.TAN	TAN Inc.	% Wt.Loss
	40°C	100°C	40°C	100°C			
0-77-6	285.4	12.52	too thick to measure		0.000	--	2.56
15% TPP in 0-77-6	136.1	9.548	too thick to measure		0.000	--	6.59
20% TPP in 0-77-6	110.9	8.729	551.2	132.1	0.000	11.68	5.96

**Note:** At some point after the 24-hour test mark, condensed material started to build up on the condenser wall. Later, this liquid condensation turned into crystal-like solid and kept growing on the condenser wall.

temperature), and its melting point is 43°C (higher than the condenser wall temperature), which is consistent with the experimental observation.

Information about weight changes of the metal coupons from the C&O test is given in Table 40. Again, for 24-hour tests the results of the 20% TPP solution are seemingly the best. Generally speaking, metal coupons are all heavily coated after the 48-hour C&O tests.

Further study was focused on the O-77-6 solution containing 20% TPP, which demonstrated to be the best from the C&O test. Gel permeation chromatography (GPC) was used to determine the molecular weight distribution of the mixture before and after the C&O test as shown in Figure 19. Despite traces of high molecular weight (HMW) oxidation products, the chromatogram of the 24-hour C&O test is very similar to that of the original standard before the test. Very differently however, a strong appearance of the HMW peak is observed from the 48-hour tested sample. Moreover, depletion of TPP can also be seen from the 48-hour chromatogram, which is in agreement with the above GC results.

The high temperature lubricity study of the TPP/O-77-6 formulation was conducted in the four-ball machine at a bulk oil temperature of 315°C. The test results are compared with the data obtained from 150°C as shown in Figures 20, 21, and 22. As seen from the curves of 315°C, instead of lowering the friction and wear levels set by pure O-77-6, increased values of both quantities were observed for the O-77-6 solution containing 10% TPP. However, these increments in friction and wear dropped again as the TPP concentration was raised to 20%.

At 315°C, clear difference also exists between alpha values of the two TPP/O-77-6 solutions. A large alpha value (0.92), produced by the 10% TPP solution, indicates the importance of tribochemistry in the overall wearing mechanism. This is readily explainable by the high temperature (thermal activation energy) and large TPP concentration (chemical driving force) involved in the test. Unlike the case of 150°C where the dominance of chemical wear (large alpha values) always concomitant with antiwear effectiveness, the amount of wear produced by the 10% TPP solution at 315°C is large. This is probably due to the combined effect of strong chemical corrosion and weakened specimen hardness, especially at such a temperature of 315°C. The small alpha value of 0.41 obtained from the 20% TPP solution is even more puzzling. It seems like the role of tribochemistry is overshadowed by other factors.

TABLE 40

**WEIGHT VARIATION OF METAL COUPONS FROM THE CORROSION/OXIDATION  
TESTS PRESENTED IN TABLE 39**

(a) 24 hours at 320°C.

Lubricant	Weight Change of Metal Coupon (mg/cm <sup>2</sup> )					
	Al	Ag	M-St	M-50	Wasp	Ti
0-77-6	0.08	0.04	0.10	0.06	0.10	0.06
10% TPP in 0-77-6	0.06	-0.26	0.12	0.10	0.02	-0.02
20% TPP in 0-77-6	0.04	-0.02	0.22	0.18	-0.02	0.02
25% TPP in 0-77-6	0.08	0.32	0.30	0.14	0.02	0.02

(b) 48 hours at 320°C.

Lubricant	Weight Change of Metal Coupon (mg/cm <sup>2</sup> )					
	Al	Ag	M-St	M-50	Wasp	Ti
0-77-6	0.36	0.10	0.08	0.08	0.06	-0.04
15% TPP in 0-77-6 *	13.5	17.3	13.0	11.3	10.2	11.5
20% TPP in 0-77-6	0.74	1.00	0.68	0.60	0.30	0.34

\*: Thick layer of coke formed on the surface of all metal coupons.

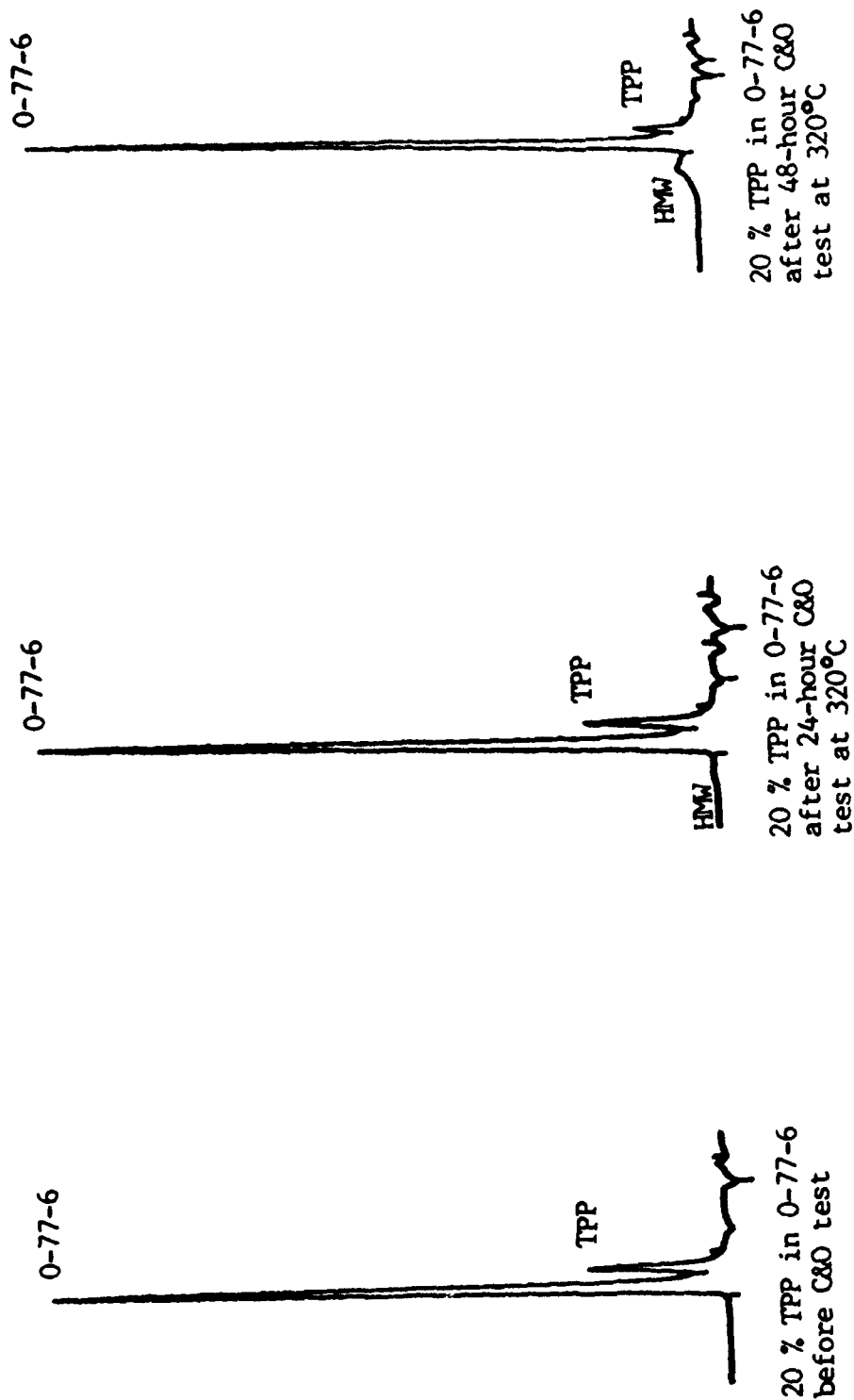


Figure 19. GPC Chromatograms of the O-77-6 Solution Containing 20% TPP, Before and After the Corrosion/Oxidation Test.

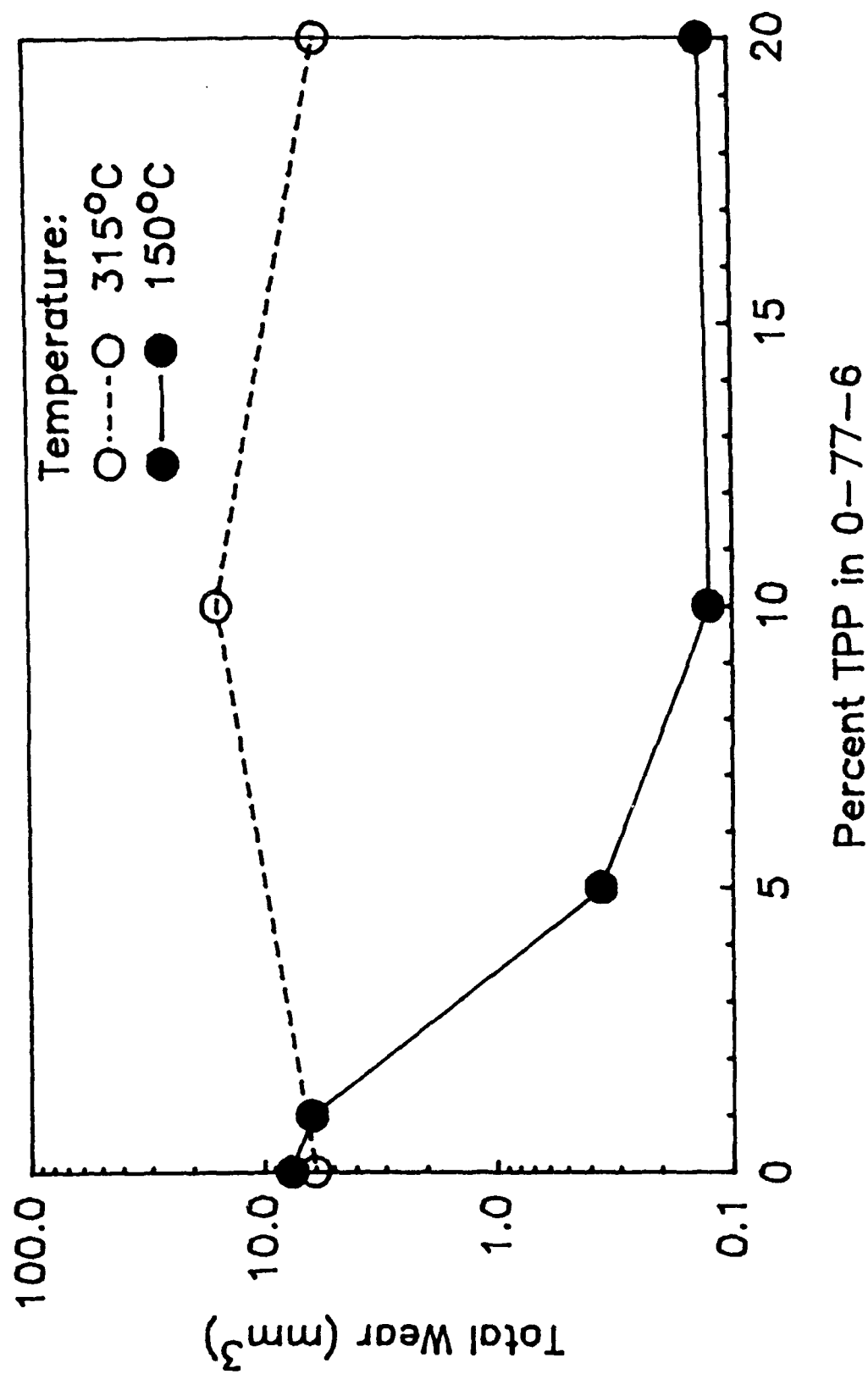


Figure 20. Total Wear Volume as a Function of TPP Concentration in the O-77-6 Fluid. Four-Ball Test Condition: 1200 rpm, 145 N, 150 and 315°C, Three Hours, and M50 Balls.

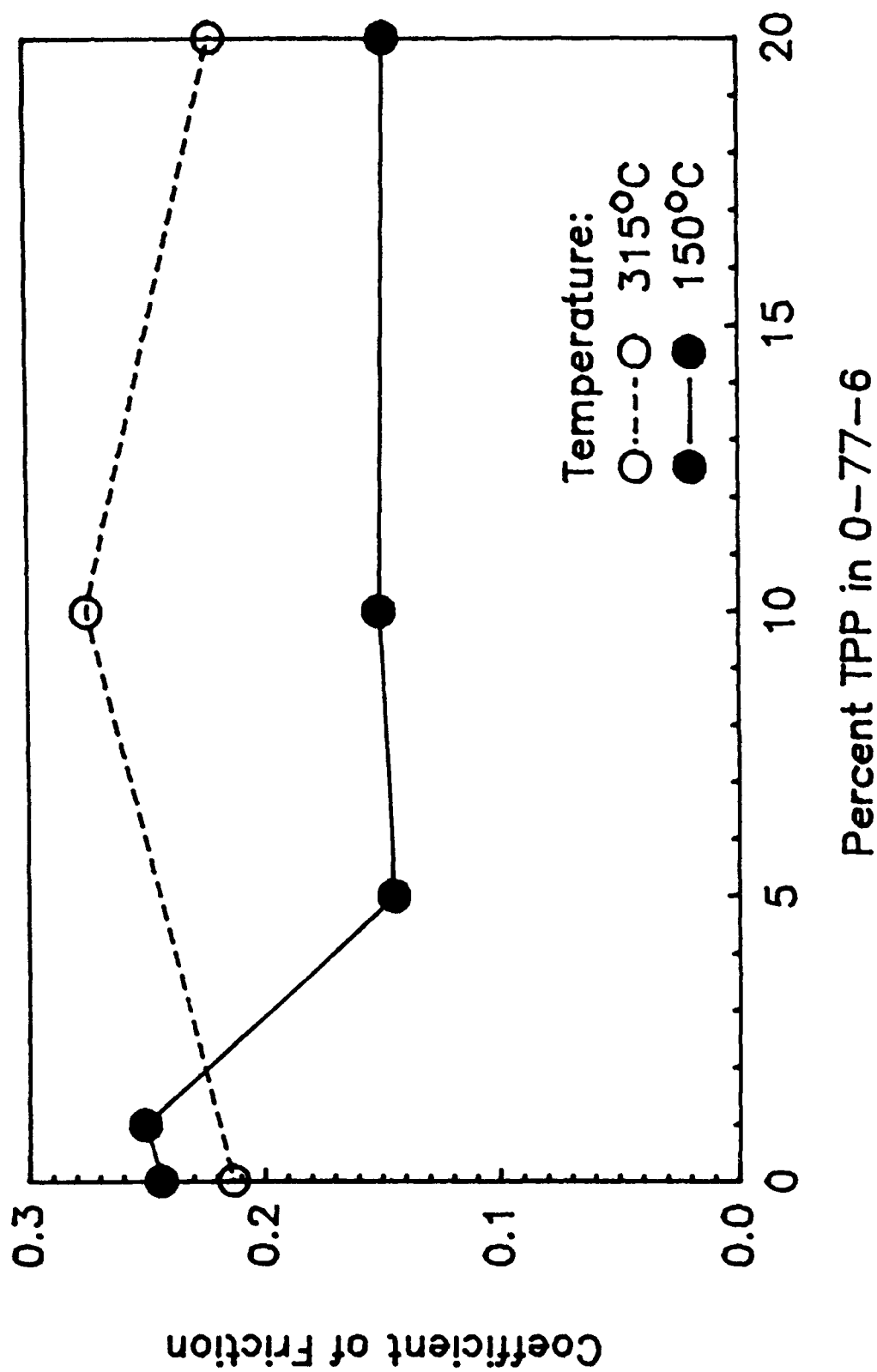


Figure 21. Coefficient of Friction as a Function of TPP Concentration in the O-77-6 Fluid. Four-Ball Test Condition: 1200 rpm, 145 N, 150 and 315°C, Three Hours, and M50 Balls.

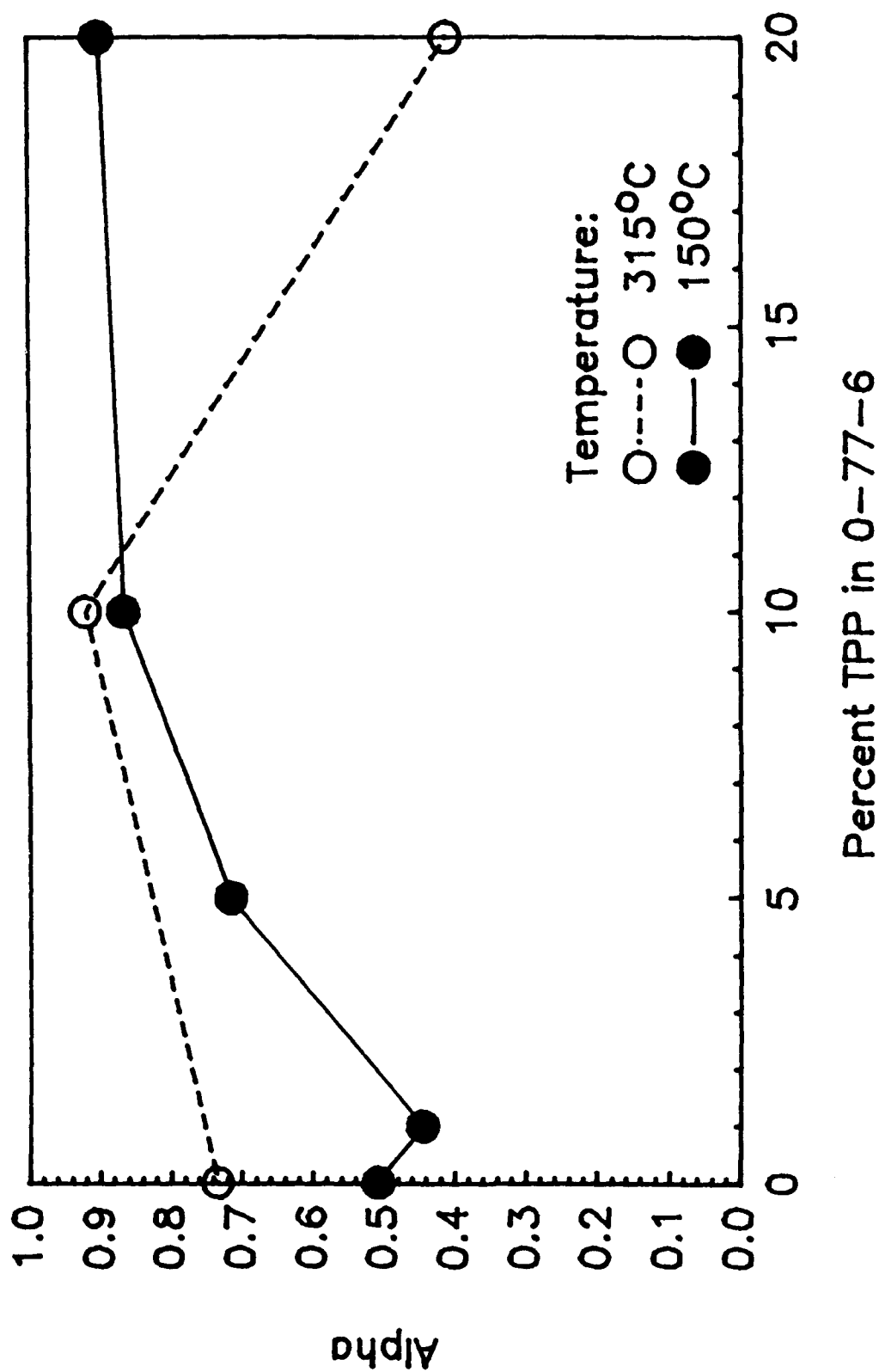


Figure 22. Alpha Value as a Function of TPP Concentration in the O-77-6 Fluid. Four-Ball Test Condition: 1200 rpm, 145 N, 150 and 315°C, Three Hours, and M50 Balls.

Overall performance of the 20% TPP in O-77-6 formulation has established this solution as a winner among other candidates. Improvements achieved through this formulation are shown by Figure 23, in comparison with those made by 0.15% Additive A in O-77-6 (namely, the TEL-90102 fluid). It is clear that the test results of this newly formulated 20% TPP / 80% O-77-6 binary mixture are very encouraging.

(6) Addition of TPPO to the TPP/O-77-6 Formulation

A third component was added to the TPP/O-77-6 mixture to improve its low temperature flowability. The new additive was added not only to lower the existing viscosity but also enhance the oxidative stability and lubricity properties. This new additive, triphenylphosphine oxide (TPPO), was first tested alone in the O-77-6 fluid. The outcome for a 10% TPPO in PPE however was not successful as a grease or semisolid structure was formed. Like Additive A, TPPO was then mixed with TPP and O-77-6 to form ternary mixtures. Viscosities of these samples and their C&O test results are presented in Tables 41 and 42. Experimental data of several binary mixtures as well the pure PPE are also included for comparison. As seen from those data, the test sample consisting of 30% TPP and 10% TPPO in PPE gives a viscosity of 87.6 cSt at 40°C. However, its C&O performance was very poor, which discouraged further research efforts. Figure 24 shows the GPC chromatograms of this ternary mixture before and after the C&O test. Note that TPP was preferentially consumed during the test, and some high molecular weight (HMW) reaction products were generated.

(7) Addition of TPPP to the TPP/O-77-6 Formulation

Another chemical compound, tri(phenoxy phenyl) phosphate (or TPPP), was also tested. A binary solution of 30% TPPP in O-77-6 gives a higher viscosity than that of the pure O-77-6 (Table 43). Moreover, some ternary solutions of TPPP, TPP and O-77-6 tend to recrystallize during their storage at ambient condition. Fortunately however, TPPP did promote the solubility of TPP in O-77-6, and a ternary solution of 30% TPP and 10% TPPP in O-77-6 demonstrated a superior viscosity of 81.1 cSt at 40°C. No recrystallization was observed in this ternary mixture at temperatures of 25°C (room condition), 5°C or even -10°C.

Thermal-oxidative stability of this ternary solution is also quite encouraging as shown in Table 44. Its 24-hour C&O results are very compatible with the data obtained from the 20% TPP in O-77-6 formulation (see Table 39). Furthermore, outcomes of its 48-hour test are considerably better than those of the binary solution. The extent of metal

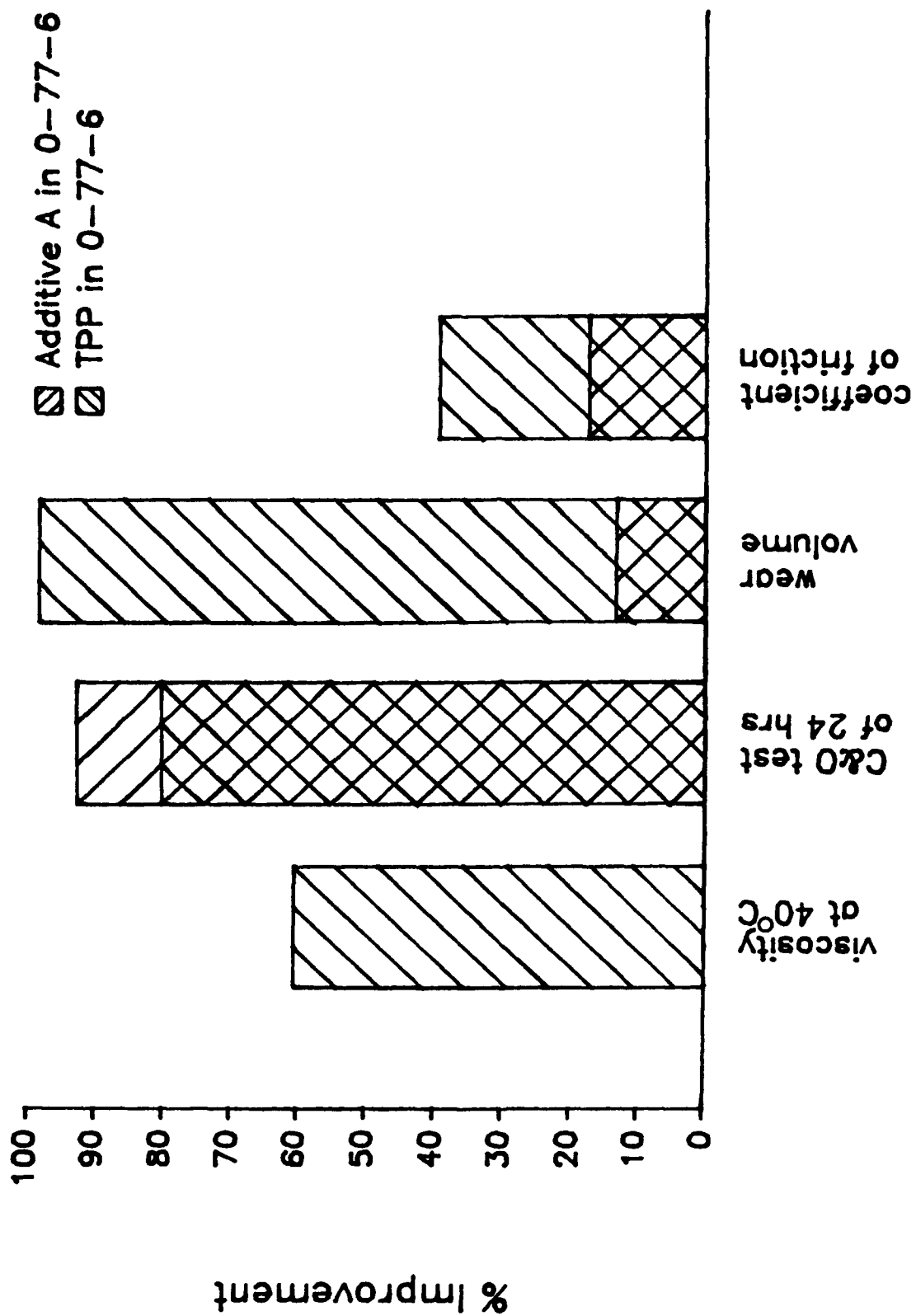


Figure 23. Improvements in Viscosity, C&O Test at 320°C, Wear and Friction as a Result of Adding 20% TPP or 0.15% Additive A into O-77-6 (TEL-90102).

TABLE 41

**CORROSION/OXIDATION TEST OF MORE O-77-6 FORMULATIONS WITH EITHER  
ADDITIVE A OR TPPO, IN ADDITION TO TPP**

24-hours at 320°C.

Lubricant	I. Visc.(cs)		% Visc.Inc.		I.TAN	TAN Inc.	% Wt.Loss
	40°C	100°C	40°C	100°C			
0-77-6	279.5	--	102.2	--	0.000	--	1.75
10% TPP in 0-77-6	169.2	10.39	30.57	13.19	0.000	0.349	0.80
10% TPP in TEL-90102	206.6	10.45	too thick to measure		0.000	2.313	1.66
20% TPP in 0-77-6	110.8	8.751	20.34	8.800	0.000	0.736	0.71
20% TPP in TEL-90102	112.5	8.826	too thick to measure		0.000	15.84	0.58
10% TPPO in 0-77-6	the fresh lubricant displays a grease-like structure at ambient condition						
10% TPP, and 10% TPPO in 0-77-6	* 204.4	10.71	too thick to measure		0.000	14.36	4.36
30% TPP, and 10% TPPO in 0-77-6	87.64	7.563	too thick to measure		0.000	29.01	5.93

\* Recrystallization inside the fresh lubricant takes place at ambient condition after several days of storage.

TABLE 42

**WEIGHT VARIATION OF METAL COUPONS FROM THE CORROSION/OXIDATION  
TESTS PRESENTED IN TABLE 41**

24-hours at 320°C.

Lubricant	Weight Change Of Metal Coupon (mg/cm <sup>2</sup> )					
	Al	Ag	M-St	M-50	Wasp	Ti
0-77-6	0.08	0.04	0.10	0.06	0.10	0.06
10% TPP in 0-77-6	0.06	-0.26	0.12	0.10	0.02	-0.02
10% TPP in TEL-90102	0.34	0.68	0.36	0.28	0.10	0.06
20% TPP in 0-77-6	0.04	-0.02	0.22	0.18	-0.02	0.02
20% TPP in TEL-90102	0.54	-2.64	0.72	0.70	0.42	0.20
10% TPPO in 0-77-6	--	--	--	--	--	--
10% TPP, and 10% TPPO in 0-77-6	0.14	-1.86	0.12	0.28	0.06	0.06
30% TPP, and 10% TPPO in 0-77-6	0.16	-2.14	0.12	0.35	0.08	0.02

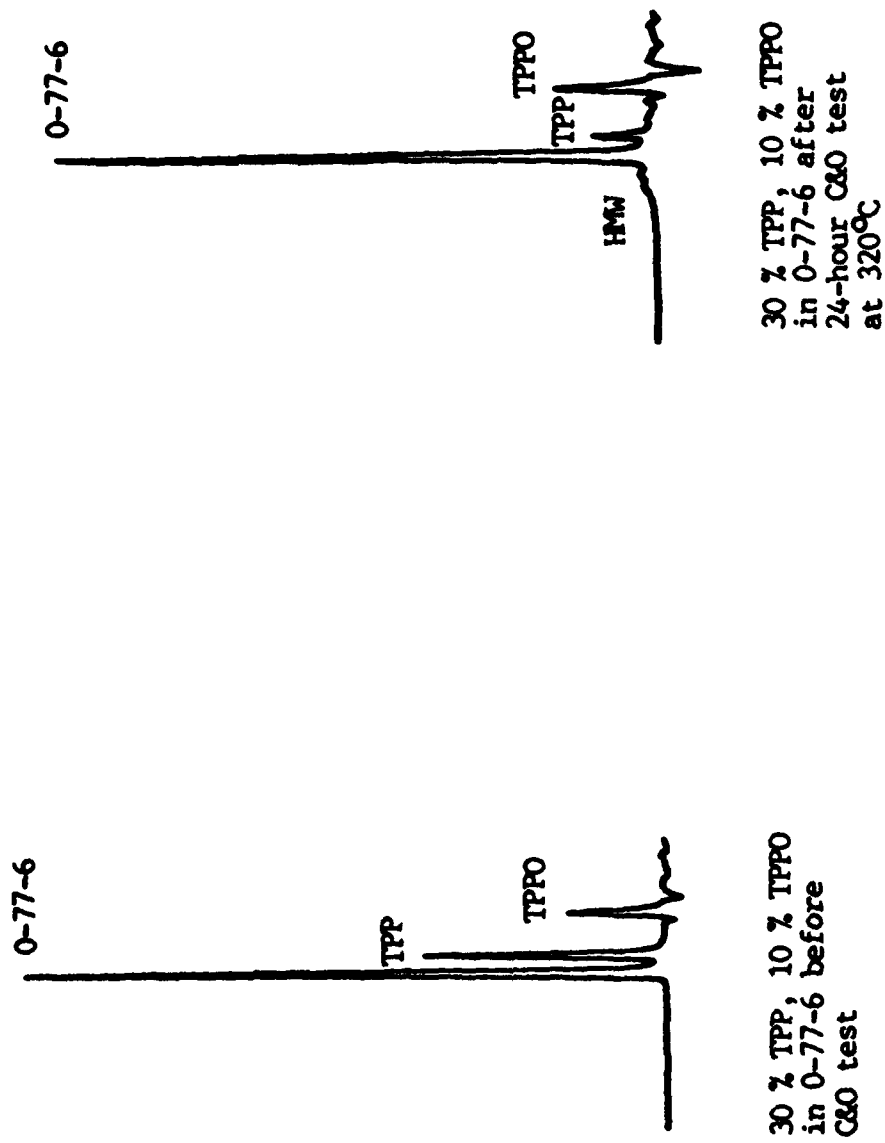


Figure 24. GPC Chromatograms of the O-77-6 Solution Containing 30% TPP and 10% TPPO, Before and After the Corrosion/Oxidation Test.

**TABLE 43**

**VISCOSITY MEASUREMENTS OF TPPP IN THE O-77-6 FLUID**

Lubricant		Viscosity at 40°C (cSt)
O-77-6		280.40
30% TPPP in O-77-6	*	355.07
10% TPP & 10% TPPP in O-77-6		181.86
10% TPP & 30% TPPP in O-77-6	*	153.23
20% TPP & 20% TPPP in O-77-6	*	127.23
30% TPP & 10% TPPP in O-77-6		81.05
40% TPP & 10% TPPP in O-77-6	#	58.97

\*: Recrystallization takes place at 25°C (room temperature).

#: Recrystallization takes place at 5°C.

TABLE 44

**CORROSION/OXIDATION TEST OF THE O-77-6 SOLUTION CONTAINING 30% TPP  
AND 10% TPPP, AT 320°C FOR 24 AND 48 HOURS**

(a) 24 hours at 320°C.

Lubricant	I. Visc.(cs)		% Visc.Inc.		I.TAN	TAN Inc.	% Wt.Loss
	40°C	100°C	40°C	100°C			
O-77-6	279.5	--	102.2	--	0.000	--	1.75
30% TPP & 10% TPPP in O-77-6	81.9	7.36	27.2	18.1	0.000	1.78	1.11

(b) 48 hours at 320°C.

Lubricant	I. Visc.(cs)		% Visc.Inc.		I.TAN	TAN Inc.	% Wt.Loss
	40°C	100°C	40°C	100°C			
O-77-6	279.5	--	102.2	--	0.000	--	1.75
O-77-6	285.4	12.52	too thick to measure		0.000	--	2.56
30% TPP & 10% TPPP in O-77-6	81.9	7.36	161.7	64.5	0.000	4.46	3.65

**Note:** At some point after the 24-hour test mark, condensed material started to build up on the condenser wall. Later, this liquid condensation turned into crystal-like solid and kept growing on the condenser wall.

corrosion after the 48-hour test can be seen from Table 45. Despite relatively heavy loss of silver, weight changes of other metal coupons are moderate in general. Figure 25 shows GPC chromatograms of the 24 and 48-hour tested samples, and the fresh standard as well. Only a very small quantity of high molecular weight (HMW) polymeric materials was found at the end of the 24-hour test. As expected, a stronger appearance of the HMW peak is seen in the 48-hour chromatogram. Large amounts of phenol was still formed as in the case of the binary TPP/O-77-6 formulation. The presence of phenol can also be detected in the 48-hour GPC chromatogram as indicated by the arrow.

Because of the short supply of TPPP, tribological evaluation of this ternary mixture was not performed.

#### (8) Summary

A search of effective additives for the 5P4E polyphenyl ether (PPE) fluids, such as O-77-6 and TEL-90102, has been carried out. Evaluation of additive species was based on three criteria: (1) tribological performance, (2) thermal-oxidative stability, and (3) low temperature flowability or pumpability. It was found that TPP outperforms TCP, and it is effective in all these categories when used in the PPE basestock (O-77-6). For instance, a 20% TPP / 80% O-77-6 binary mixture is able to make the following improvements over the pure O-77-6 fluid: 60.53% reduction in bulk viscosity, 80.1% increase in thermal-oxidative stability, 98.2% reduction in wear volume, and 39.3% reduction in friction.

The multifunctionality of TPP in O-77-6 has been further exploited through the addition of a third chemical species, namely TPPP. A ternary solution consisting of 30% TPP / 10% TPPP / 60% O-77-6 could be more effective than the binary formulation of 20% TPP / 80% O-77-6, at least in terms of its lower viscosity and higher oxidative stability.

The growing amount of phenol during the 48-hour C&O tests of both the binary and ternary mixtures should be controlled in future formulations. One potentially useful chemical compound, which we did not have time to synthesize and test, is tri(4-phenoxyphenyl) phosphine oxide. Its molecular formula is  $(C_6H_5OC_6H_4)_3PO$ . This chemical species might have better compatibility with the TPP/O-77-6 formulation than TPPO and TPPP.

TABLE 45

**WEIGHT VARIATION OF METAL COUPONS FROM THE CORROSION/OXIDATION  
TESTS PRESENTED IN TABLE 44**

**(a) 24 hours at 320°C.**

Lubricant	Weight Change Of Metal Coupon (mg/cm <sup>2</sup> )					Ti
	Al	Ag	M-St	M-50	Wasp	
0-77-6	0.08	0.04	0.10	0.06	0.10	0.06
30% TPP & 10% TPPP in 0-77-6	--	--	--	--	--	--

**(b) 48 hours at 320°C.**

Lubricant	Weight Change Of Metal Coupon (mg/cm <sup>2</sup> )					Ti
	Al	Ag	M-St	M-50	Wasp	
0-77-6	0.36	0.10	0.08	0.08	0.06	-0.04
30% TPP & 10% TPPP in 0-77-6	0.10	-1.26	0.20	0.24	0.04	0.10

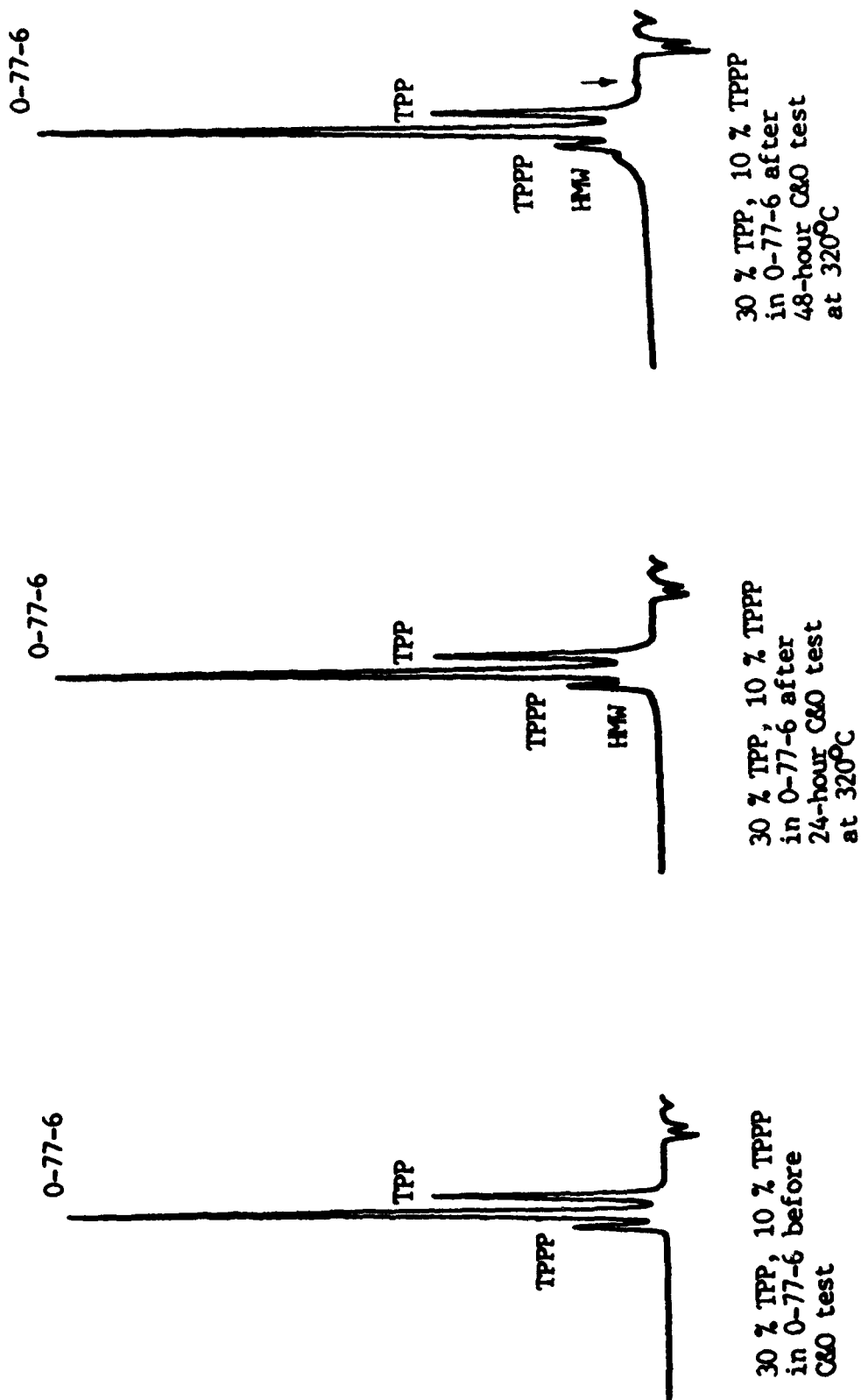


Figure 25. GPC Chromatograms of the O-77-6 Solution Containing 30% TPP and 10% TPPP, Before and After the Corrosion/Oxidation Test.

## **f. Sealed Tube Test**

### **(1) Introduction**

Thermal-oxidative stability of liquid lubricants is frequently examined in a static reaction manner, rarely through the use of dynamic tribological test whose primary function is to address lubricity merit of the fluids. All available oxidation tests of liquid lubricants can be generally divided into two categories: (1) bulk oxidation testing, and (2) thin-film oxidation testing. Both testing concepts can be carried out in either an open or a closed system. Examples of these various techniques<sup>22-27</sup> are listed in Table 46.

The bulk oxidation method is good for simulating the condition of lubricant degradation within an oil reservoir or sump. When a liquid is thermally stressed, the oxygen consumption rate due to liquid-phase chemical reaction usually exceeds the oxygen supply rate via its diffusion process in the liquid medium. As a result, the overall rate of reaction sequence will be governed by the oxygen diffusion step, better known as the state of oxygen diffusion limitation.<sup>28</sup> This shortage of oxygen supply becomes worse as the diffusion route gets longer, i.e., farther away from the liquid surface. Because the bulk oxidation method, even with a certain degree of air bubbling, is typically complicated by the factor of oxygen diffusion limitation, it is not recommended for analytical study of liquid reaction kinetics.

The concern of oxygen diffusion limitation in the liquid phase is greatly eased in the case of thin-film oxidation. However, resistance to oxygen transfer from the gas phase to the liquid phase still exists in the liquid-gas interface. Especially at high temperatures, strong evaporation current is likely to be produced on the liquid surface which could slow down the flow of incoming gaseous oxygen species.<sup>29</sup>

Another critical testing feature, which associates itself with experimental apparatus rather than the lubricant sample, is whether the test vessel is an open system or a closed one. In an open test device, lubricant consumption is totaled from both chemical reaction and evaporation. For a closed system, though, only chemical reaction is being counted; volatile loss from a sealed test chamber is unlikely. One other distinction between open and closed systems is that the physical and chemical properties of an open atmosphere are usually maintained fairly constant throughout the test, while those traits of a closed atmosphere could vary substantially as the test proceeds.

**TABLE 46**

**EXAMPLES OF OXIDATION TECHNIQUES FOR LIQUID LUBRICANTS**

III \ II \ I	I	
	Bulk Oxidation	Thin-Film Oxidation
Open System	Corrosion and Oxidation Stability Test (ASTM D4636)	Penn State Micro-oxidation Test
Closed System	Rotary Bomb Oxidation Test (ASTM D2272)	Thin-Film Oxygen Uptake Test (ASTM D4742)

- I:** Lubricant Oxidation Mode  
**II:** Test Device Character  
**III:** Examples

Obtaining a direct and precise measure of lubricant evaporation in an open system is not an easy task. On the other hand, the changing atmosphere inside a closed system, itself, could become an essential test variable and create extra intricacy in the process of data interpretation. One way to circumvent these obstacles is of combining the beneficial aspects of the two systems together as will be illustrated by a novel concept of the sealed tube test introduced in this section.

## (2) Experimental Development

Structural design of the experiment apparatus is very simple; a schematic drawing of its main constituents is shown in Figure 26. Within the sealed tube a mini test cup is placed at the bottom center. The objective of this testing scheme is to make a closed system, namely the sealed tube, operate like an open system.

A very small lubricant sample of  $1 \text{ mm}^3$  (or,  $1 \mu\text{L}$ ) was utilized for each experiment, in contrast to the much larger volume of the  $17.383 \text{ cm}^3$  test chamber. Based on an assumption that 1 mole of fresh O-77-6 molecules will react with 1 mole of oxygen molecules during its entire oxidation process, only about 1.5 % or less of the total oxygen originally present inside the sealed tube will be consumed at the end of the test, provided that the tube was initially filled with dry air at ambient condition. Because of such a minor variation in gaseous oxygen concentration, and the huge capacity of the test chamber to absorb any volatile species derived from the tiny test sample, the physical as well as chemical characteristics of the chamber atmosphere will be kept virtually unchanged during the test. Therefore, the closed test chamber could effectively act like an open atmosphere.

Both test cup and tube are fabricated from M50 tool steel. A Swagelok® cap, made from type 316 stainless steel, provides a tight seal for the test chamber. In order to minimize additional loss of oxygen during the test, the surface of the test chamber (not the cup) was preoxidized at the projected test temperature of  $300^\circ\text{C}$ . Before each experiment, the test cup and interior chamber wall were rinsed first with reagent grade hexane, followed by HPLC grade tetrahydrofuran. The rinsed parts were then air dried. The 5P4E polyphenyl ether (O-77-6), a high-temperature basestock with a well established literature data base, is chosen as the test fluid in this preliminary study. A micro syringe is used for accurate delivery of the  $1 \text{ mm}^3$  O-77-6 sample into the mini test cup. The calculated thickness of the lubricant film is around  $0.137 \text{ mm}$ , which practically fills the test cup. After the charged test cup is carefully seated inside the tube, the test tube is firmly closed.

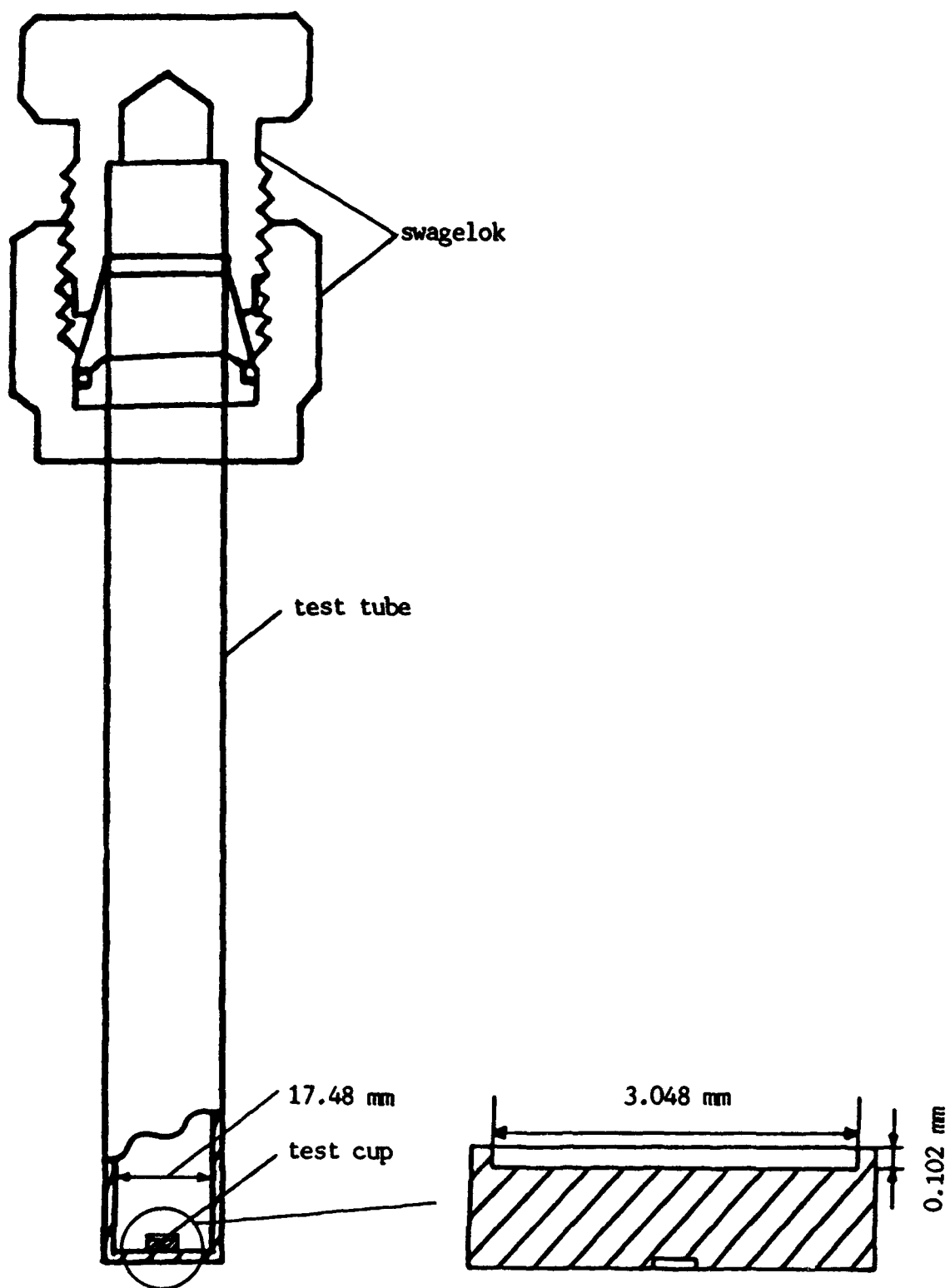


Figure 26. A Schematic Drawing of the Sealed Tube Device.

A small convection oven, with its time programmable feature and precise temperature control capability, was used for thermal stressing of the test samples. The oven can easily accommodate three test tubes at the same time, which offers excellent test efficiency. In the current test procedure, the warm-up (or ramping) period of the oven is set for 30 minutes. Selection of this ramping rate is resulted from a compromise intended to avoid both excessive temperature overshooting and lubricant degradation at the end of this warm-up period. As soon as the oven reaches the designated test temperature of 300°C timing of the test begins. Some of our early study showed that under bulk oxidation condition the 5P4E polyphenyl ether basestock is able to withstand temperatures as high as 295°C.<sup>3</sup> The present test temperature of 300°C is, thus, considered to be a reasonable choice. Also, at this level of thermal stress chemical deposition of gaseous 5P4E on the steel chamber wall seems to be negligible.<sup>30</sup> It should be noted that at 300°C the chamber pressure of the sealed tube has been approximately doubled.

Having been stressed for a certain duration one or more test tubes may be removed from the oven at a time. Immediately afterward, these tubes were rapidly cooled down and left intact overnight to make sure that all vaporized lubricant species have condensed within the chamber. The surviving lubricant residues in the test cup and those condensed on the tube wall are, separately, dissolved by 1 cm<sup>3</sup> (or, 1 mL) of tetrahydrofuran (THF). These THF solutions are then analyzed by gel permeation chromatography (GPC). Quantification of the remaining O-77-6 can be achieved by comparing the GPC chromatogram of its solution with that of a fresh standard made from 1 mm<sup>3</sup> O-77-6 and 1 cm<sup>3</sup> of THF. It is conceivable that species recovered from the wall of the test chamber were originally present in the gas phase, and THF solubles in the test cup likely remained as a liquid when the experiment was concluded.

### (3) Results and Discussion

An illustration of GPC chromatograms of a stressed O-77-6 sample retrieved from both test cup and chamber, together with the GPC chromatogram of a fresh standard, is present in Figure 27. Results of the GPC analysis are then used to produce a plot (Figure 28) showing an entire set of curves for the O-77-6 fluid. The data demonstrate that after the 2-hour test mark liquid O-77-6 in the test cup is completely consumed through either chemical reaction or evaporation, leaving only the vapor-state O-77-6 present in the test chamber. Also revealed in this plot is a formulated scheme, which makes it possible for simultaneously determining lubricant reaction rates in both liquid and gas phases, as well as its evaporation rate from the liquid phase to the gas phase.

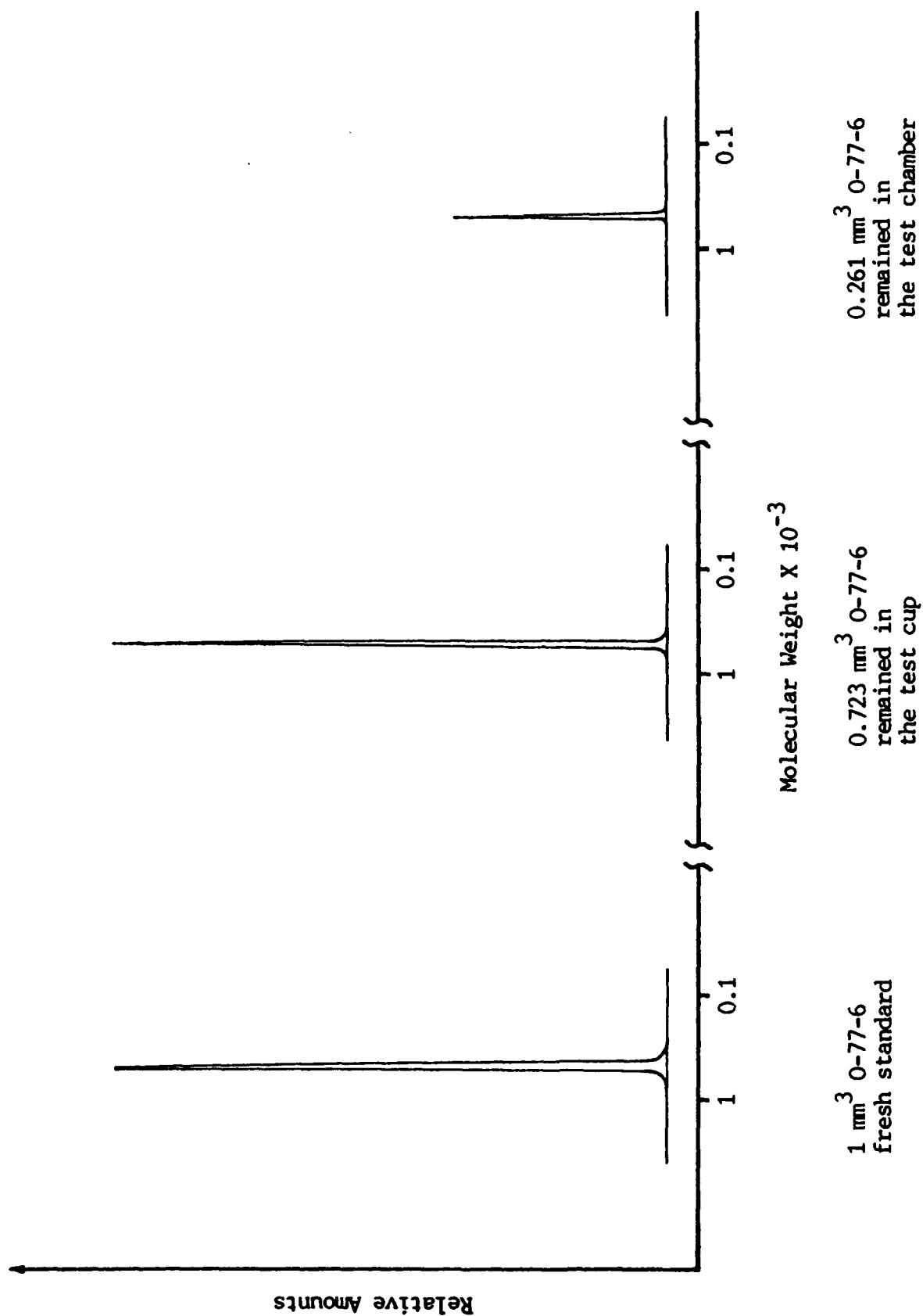


Figure 27. GPC Chromatograms of 1 mm<sup>3</sup> O-77-6 After Stressed in the Sealed Tube Test for 30 Minutes at 300°C, Compared with that of a Fresh Standard.

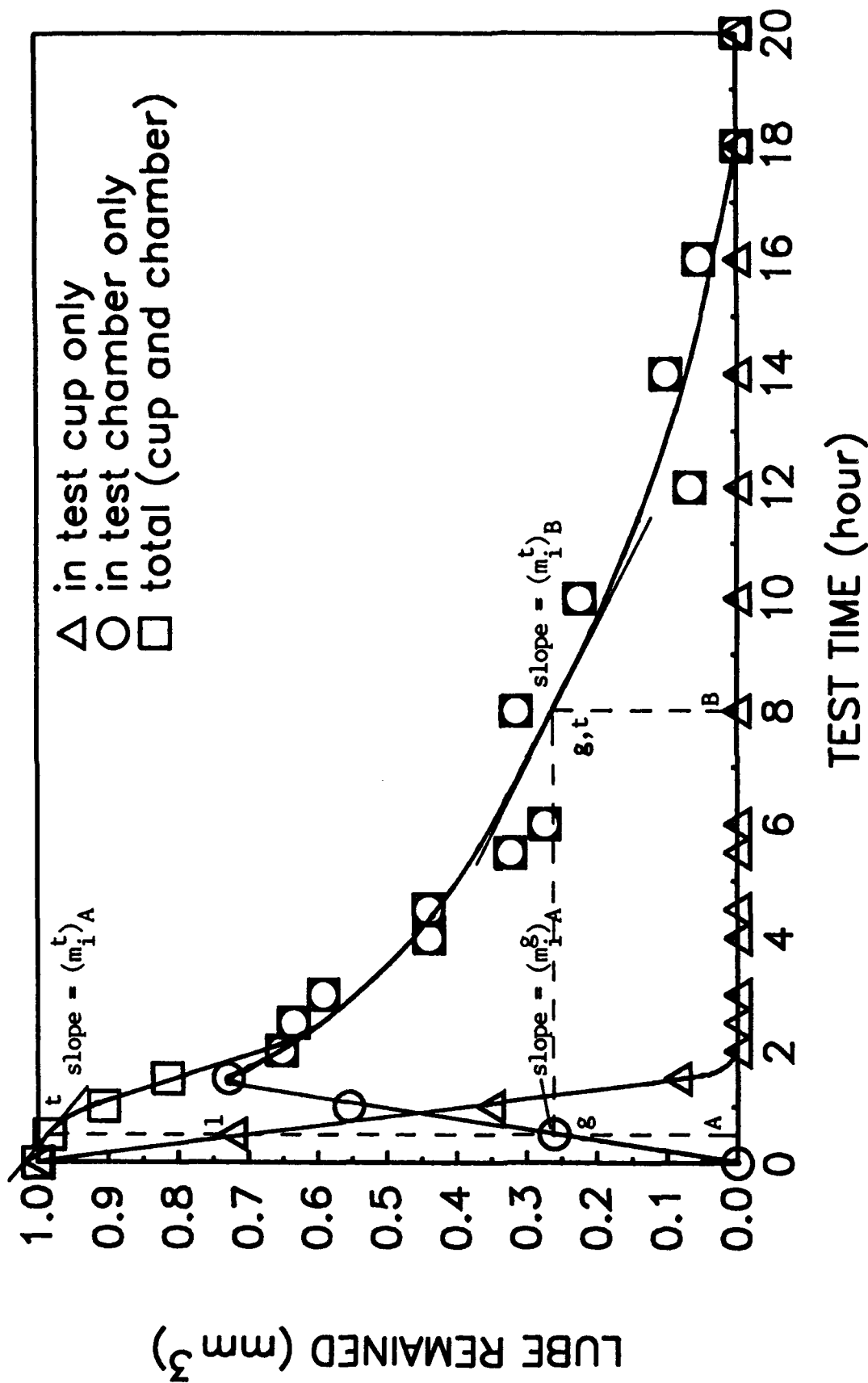


Figure 28. Lubricant Remained in the Test Cup and in the Test Chamber versus Time from Testing of 1 mm<sup>3</sup> O-77-6 in the Sealed Tube Device at 300°C. (Example of Slopes Are Shown for Calculating Evaporation and Reaction Rates).

The following derivation, with the help of that scheme outlined in Figure 28, demonstrates how these reaction and evaporation rates can be determined from the experimental results.

### Nomenclature

superscript l: liquid phase (in test cup only)  
 superscript g: gas phase (in test chamber only)  
 superscript t: total (sum of cup and chamber)  
 $r_i$ : chemical reaction rate of lubricant species i (or, PPE)  
 $R_i$ : evaporation transfer rate of species i  
 $m_i$ : measured gain or loss rate of species i  
 $T$ : reaction temperature  
 $P_i$ : partial pressure of species i in the gas phase  
 $P_O$ : partial pressure of oxygen in the gas phase  
 $P_{etc}$ : partial pressures of the rest gaseous reactants  
 subscript A: at the test time A  
 subscript B: at the test time B  
 $K( )$ ,  $F( )$ , and  $f( )$ : functionalities

### Theoretical Considerations

In the gas phase, the reaction rate of lubricant species i is:

$$(-r_i^t) = K(T) F(P_i, P_O, P_{etc})$$

For a fixed test temperature  $T$ , and nearly constant  $P_O$  and  $P_{etc}$  (because only less than 1.5 % of the chamber oxygen is consumed throughout the test), the rate equation can be reduced to:

$$(-r_i^g) = f(P_i)$$

As  $(P_i)_A = (P_i)_B$  (see Figure 28); or, the quantity of lubricant species present in the gas phase at time A and at time B is equal.

Therefore, the chemical reaction rate of i in the gas phase at time A is:

$$(-r_i^t)_A = (-r_i^t)_B = (-r_i^g)_B = (-m_i)_B$$

or:

$$(-r_i^g)_A = 0.039 \text{ mm}^3/\text{hour}$$

which is obtained from the particular scheme outlined in Figure 28.

Note, at any time during the test the following two equations are valid

$$(-r_i^t) = (-m_i^t)$$

and:

$$(-r_i^t) = (-r_i^g) + (-r_i^l)$$

The chemical reaction rate of i in the liquid phase at time A is:

$$(-r_i^l)_A = (-r_i^t)_A - (-r_i^g)_A = (-m_i^t)_A - (-m_i^t)_B$$

or:

$$(-r_i^l)_A = 0.065 - 0.039 = 0.026 \text{ mm}^3/\text{hour}$$

which is obtained from the particular scheme outlined in Figure 28.

The evaporation (gain) rate of i in the gas phase at time A is:

$$(R_i^g)_A = (m_i^g)_A + (-r_i^g)_A = (m_i^g)_A + (-m_i^t)_B$$

or:

$$(R_i^g)_A = 0.522 + 0.039 = 0.561 \text{ mm}^3/\text{hour}$$

which is obtained from the particular scheme outlined in Figure 28. This rate is also equal to the evaporation (loss) rate of lubricant species i in the liquid phase.

#### Sample Calculations (for time A = 0.5 hour)

As indicated by the scheme presented in Figure 28, the directly measured rates of O-77-6 at 0.5 hour of the sealed tube test are:

$$(-r_i^s)_A = 0.039 \text{ mm}^3 / \text{hour}$$

$$(-r_i^l)_A = 0.065 - 0.039 = 0.026 \text{ mm}^3 / \text{hour}$$

$$(R_i^s)_A = 0.522 + 0.039 = 0.561 \text{ mm}^3 / \text{hour}$$

Since the density of 5P4E (O-77-6) is  $1.125 \text{ g/cm}^3$  and its molecular weight is equal to 446 g/mole, the ratio of density to molecular weight gives:

$$\frac{1.125 \text{ g/cm}^3}{446 \text{ g/mole}} = 2.522 \times 10^{-3} \text{ mole/cm}^3$$

Also, the following are true:

$$\text{volume of the gas phase at any time} = 17.383 \text{ cm}^3;$$

$$\text{volume of the liquid phase at time A (0.5 hour)} = 7.05 \times 10^{-4} \text{ cm}^3;$$

$$\text{liquid volume of condensed gaseous i at time A} = 2.55 \times 10^{-4} \text{ cm}^3;$$

$$\text{total surface area of the gas-liquid interface} = 7.297 \times 10^{-2} \text{ cm}^2.$$

From the preceding information, the following items can be calculated:

Chemical reaction rates based on the total volume (or total moles) in each phase are:

$$(-r_i^s)_A = 9.835 \times 10^{-8} \text{ mole / hour}$$

and:

$$(-r_i^l)_A = 6.556 \times 10^{-8} \text{ mole / hour}$$

Chemical reaction rates based on one mole of O-77-6 in each phase are:

$$(-r_i^s)_A = 0.153 \text{ mole / mole - of - gaseous - i / hour}$$

and:

$$(-r_i^l)_A = 0.037 \text{ mole / mole - of - liquid - i / hour}$$

Evaporation rate based on the total liquid volume (or total area of the gas-liquid interface) is:

$$(R_i^s)_A = (-R_i^l)_A = 1.415 \times 10^{-6} \text{ mole / hour}$$

Evaporation rate based on one unit area of the gas-liquid interface is:

$$(R_1^*)_{\text{A}} = (-R_1^*)_{\text{A}} = 1.939 \times 10^{-5} \text{ mole / cm}^2 \text{ / hour}$$

It should be noted that the type of computation just performed is satisfactory and reliable only within a certain time range in Figure 28. First of all, this time range has to be in the two-phase (liquid and gas) segment of the test, basically prior to the 2-hour test mark. The scope of this usable range is then further restrained by two factors as addressed below.

On the lower side, large degree of uncertainty is imposed on slope measurement at the very early stage of each curve, and the accuracy of that early section of curve, in reality, is also influenced by minor degradation of lubricant sample (reaction and evaporation) during the warm-up period.

On the upper side, the point, where the curve of the gas phase (in test chamber only) converges with the line of total (cup and chamber), sets the limit for the measurable reaction rate in the gas phase.

### Assembled Plots

After consolidating various aspects of the current sealed tube test procedure, four points have been selected within the usable time range in the two-phase segment of the test. Their calculated results are plotted in Figure 29. It becomes apparent that the evaporation rate of O-77-6 is about an order of magnitude higher than either its liquid-phase or its gas-phase chemical reaction rate. This evaporation rate increases linearly with test time.

As both of the reaction rates (liquid and gas) are close to each other in magnitude, there are still a number of important differences that should be examined. The two chemical reaction rates are replotted through an enlarged scale as shown in Figure 30. A linear relationship, going through the origin of the coordinates, exists between the gas-phase reaction rate and test duration. In fact, when the timing of the actual test starts trace amount of O-77-6 molecules has already evaporated into the gas phase during the warm-up period, and evidently the gas-phase reaction is underway. However, because of its insignificant amount, thus negligible long-term impact, the data shown in Figure 30 can be treated equivalently as if initially there were no gaseous O-77-6. Increase of the gas-phase reaction rate coincides nicely with the growing number of gaseous O-77-6 molecules as manifested in Figure 28. Quite the contrary, the liquid-phase reaction rate accelerates as the test proceeds, regardless of the diminishing liquid phase in the test cup.

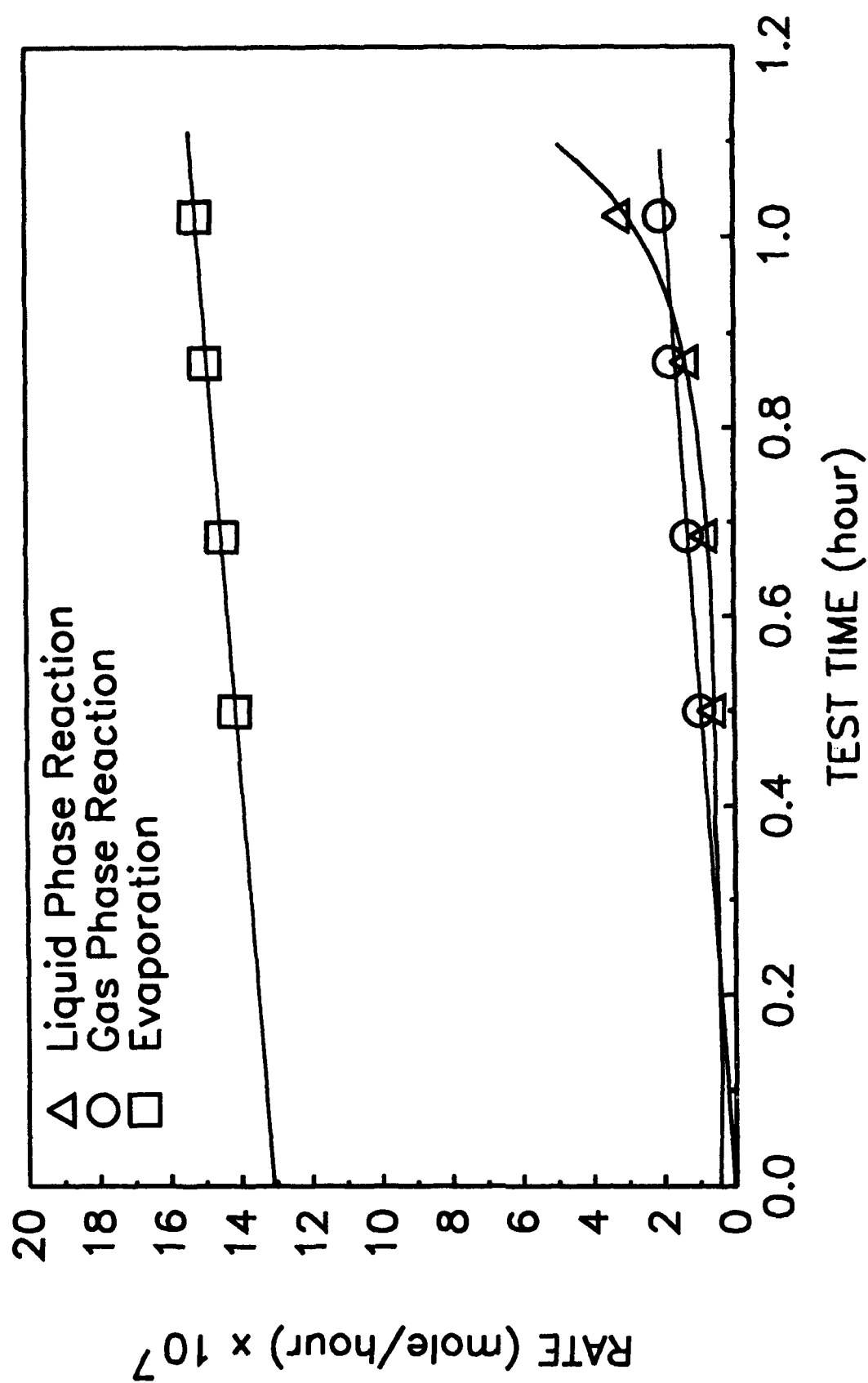


Figure 29. Comparison of Three Principal Rates as Functions of Test Time.

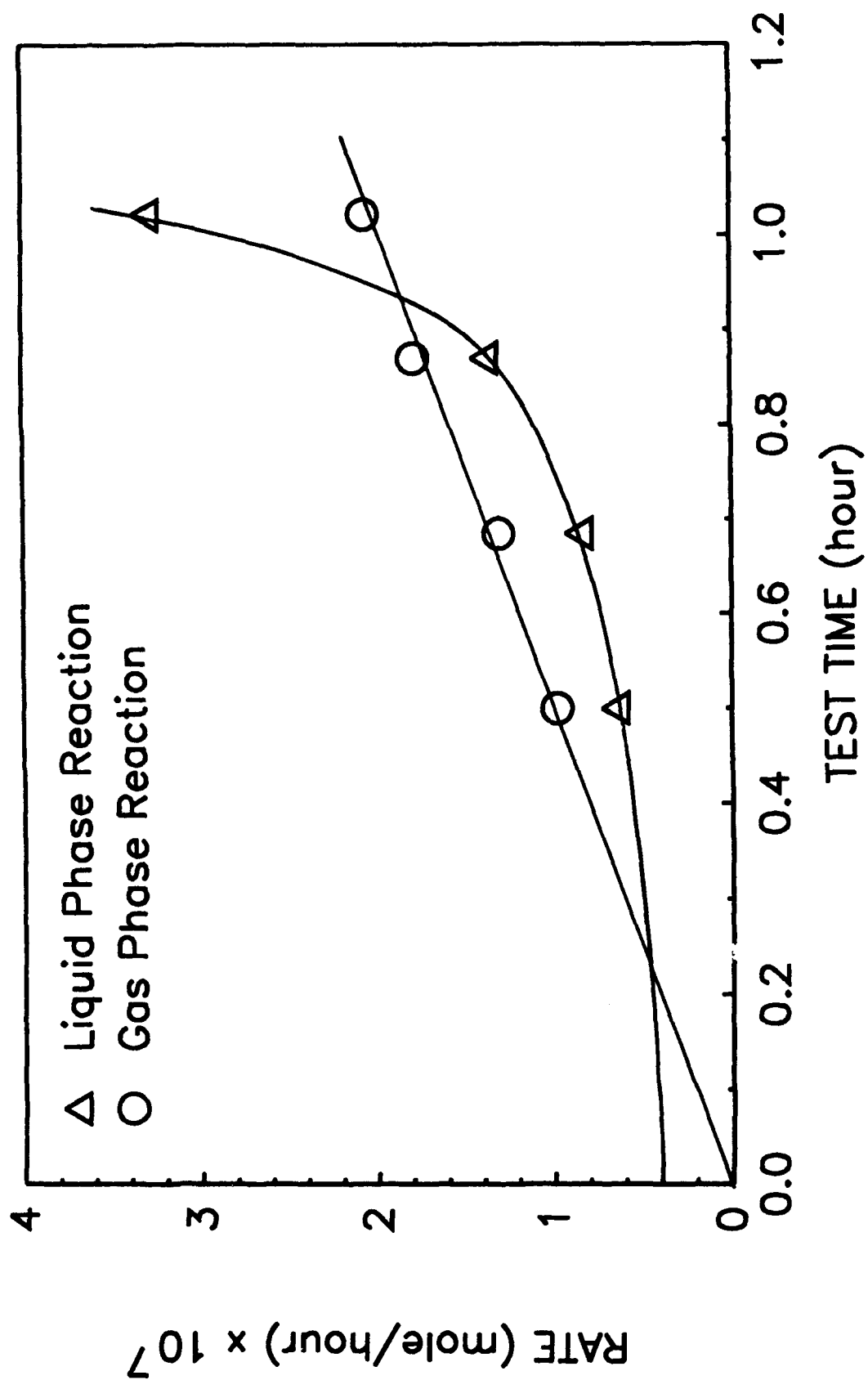


Figure 30. An Enlarged-Scale Plot of the Two Chemical Reaction Rates Presented in Figure 29, Showing Details of Their Functional Relationships.

This observation of liquid 5P4E (O-77-6) oxidation is consistent with our previous findings from a bulk oxidation test (ASTM D 4636) of the 5P4E fluids. The reaction products of 5P4E primarily consist of a dimer (labeled HMW-1) and other higher molecular weight compounds (labeled HMW-2). It is believed that HMW-2 compounds are less stable than the fresh 5P4E basestock, and would effectively catalyze further basestock degradation.<sup>31</sup>

Theoretically, integration of the area directly beneath any portion of a rate curve (shown in Figure 29 or Figure 30) will provide the knowledge about collective sum of O-77-6 depleted under that particular portion of the curve. If integration is performed from the very beginning of the test, then it will give the overall lubricant loss under a rate curve.

It is also curious to see the calculated reaction rates based on not only per unit time but also per mole of O-77-6 in their corresponding phases (liquid or gas). Figure 31 is a plot of that nature. It is clear that while the liquid-phase reaction rate behaves almost the same as in Figure 30, radical transformation of the rate curve for gas-phase reaction is obvious. The unyielding reaction rate in the gas phase implies again the immense capacity of the chamber atmosphere.

Additional calculations have been made in the single-phase (gas) segment of the test. Figure 32 contains all of the acquired data for the gas-phase reaction rate. It seems like for the 5P4E polyphenyl ether basestock its gas-phase reaction rate will eventually rise same as its liquid-phase reaction rate.

#### (4) Conclusions

By incorporating the concept of a closed system with that of an open system a novel thin-film oxidation technique, the sealed tube test, has been developed. Analytical method based on this technique makes it possible for simultaneous acquisition of the following eight principal measurements of lubricant degradation at a specified test time:

- (1) quantity of lubricant remaining in the liquid phase
- (2) quantity of lubricant remaining in the gas phase
- (3) lubricant liquid-phase reaction rate
- (4) lubricant gas-phase reaction rate
- (5) lubricant evaporation rate
- (6) collective sum of lubricant reacted in the liquid phase
- (7) collective sum of lubricant reacted in the gas phase
- (8) collective sum of lubricant evaporated

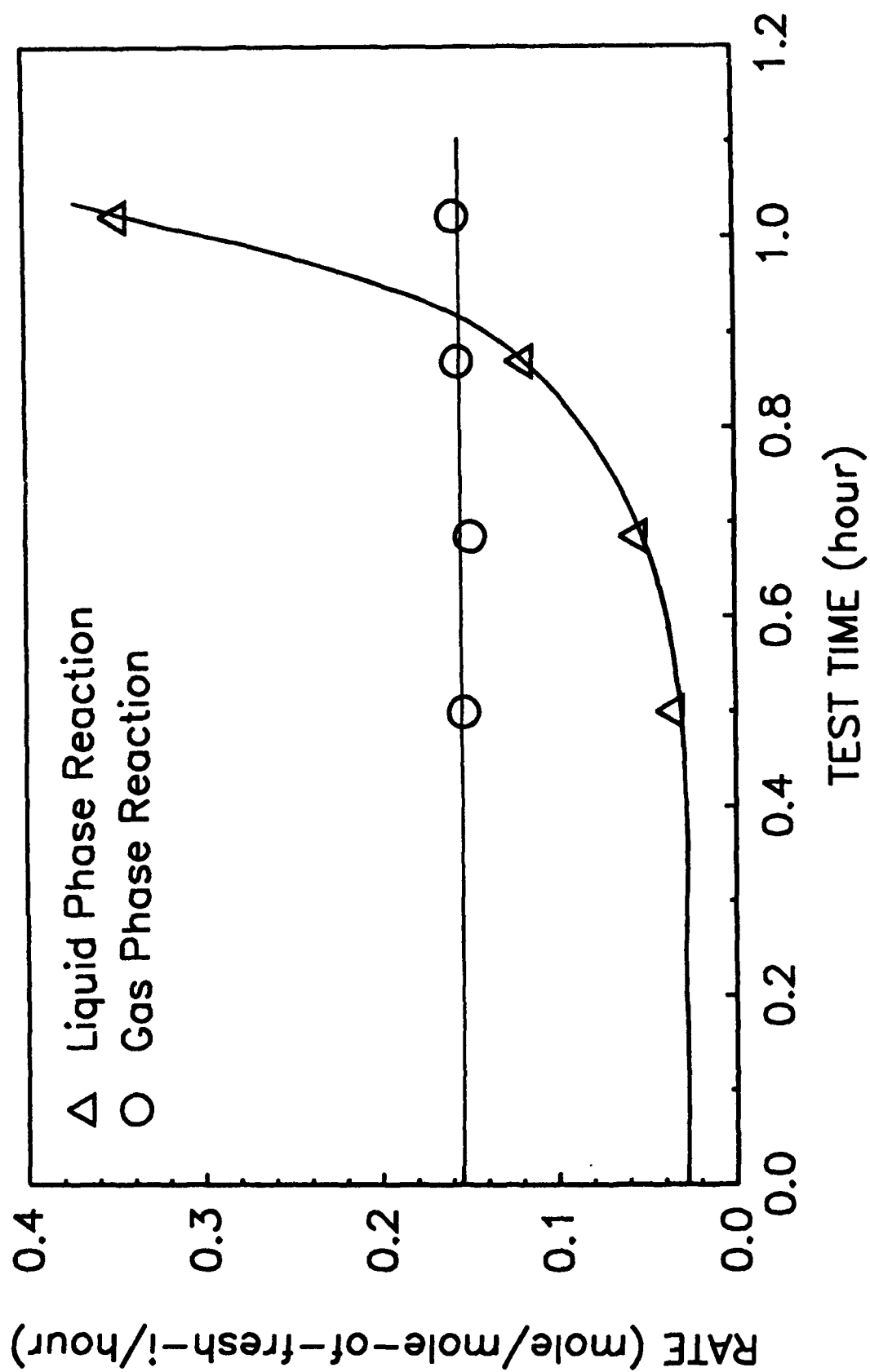


Figure 31. Chemical Reaction Rates Based on Per Mole of Fresh O-77-6 Molecules in Their Respective Phases (Liquid or Gas).

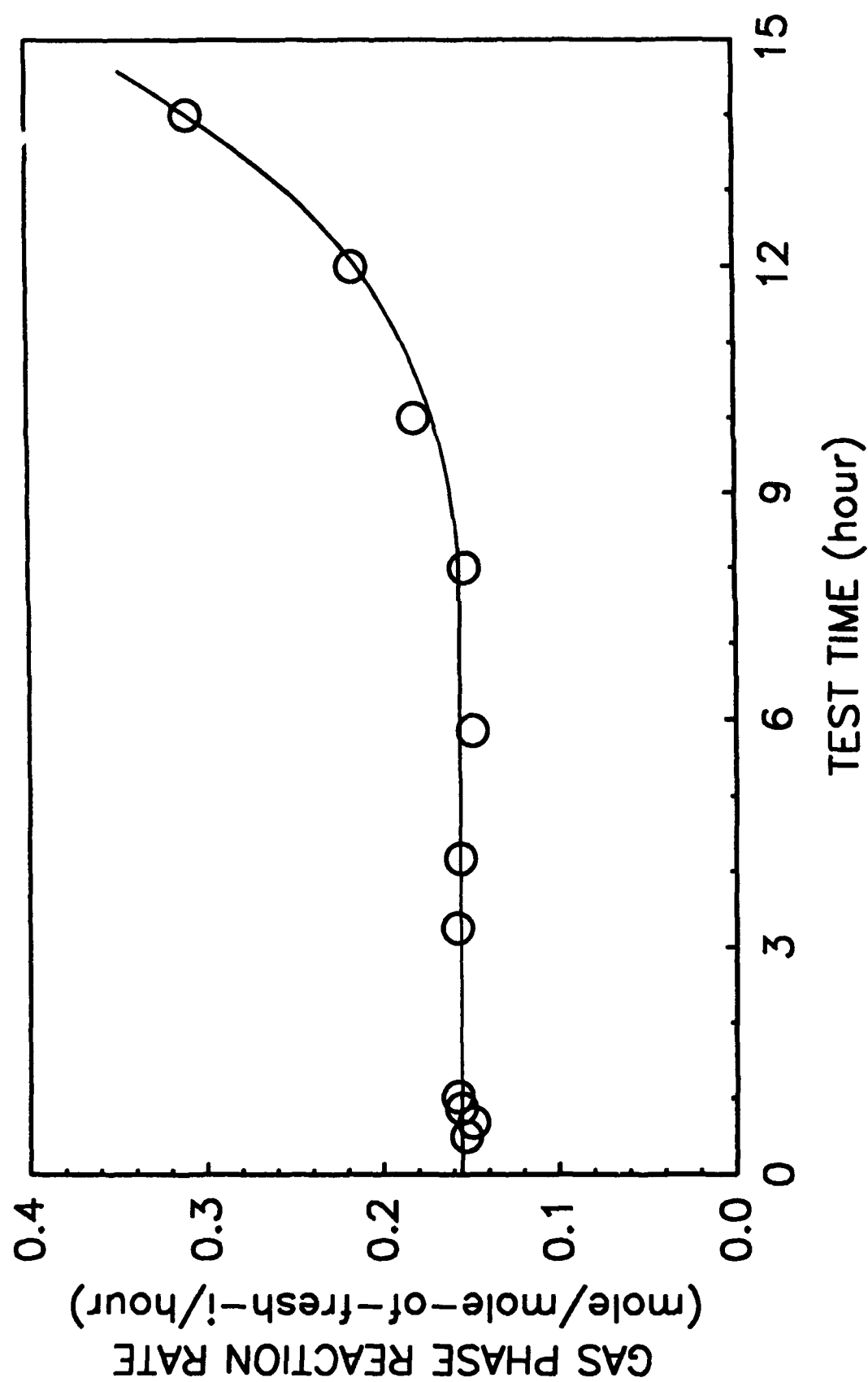


Figure 32. An Extended Range of the Gas Phase Reaction Rate, Covering Both Two-Phase and One-Phase Segments of the Test.

Because all these measurements are from a single test condition they intrinsically associate with each other, thus, providing additional clues to aid the task of data interpretation.

Under the experimental condition used in this work, the evaporation rate of a 5P4E polyphenyl ether basestock (O-77-6) is about an order of magnitude greater than either of its chemical reaction rates (liquid-phase or gas-phase). If based on not just a unit time but also per mole of fresh O-77-6 in each phase, the corresponding reaction rate shows a relatively flat early period then rises rapidly, thereafter. The high molecular weight reaction products of 5P4E seems to have a catalytic effect on the basestock degradation in either liquid or gas phase.

Besides its effective test results, both initial and operating costs of this sealed tube test are very low. The 1 mm<sup>3</sup> sample provides an easy way for rapid stressing of the test fluid. It also allows an extremely large body of tests being performed out of a small vial of lubricant, which alleviates much of the anxiety caused by short supply of experimental lubricant. The mini test cup and the tube are easy to make, and require very small amounts of cleaning solvent.

g. Stability Testing of a C-Ether (O-64-20)

(1) Introduction

C-ethers are high temperature lubricant candidates that are a mixture of polyphenyl thioethers having a combination of ether and thioether linkages. These compounds were first examined in the 1960s<sup>32</sup> and were shown to possess excellent thermal and oxidative stability, but induced silver and copper corrosion.<sup>32,33</sup> They also were shown to have produced lower wear and friction coefficients than esters or polyphenyl ethers,<sup>34,35</sup> but were plagued by excessive wear and deposition in bearing rig tests.<sup>33</sup> Reported here are the results of corrosion and oxidation (C&O) testing of O-64-20 (unformulated C-ether) under various test conditions and with various additives.

(2) C&O Testing at 320, 305, and 290°C

C&O testing was conducted at three different temperatures in order to develop Arrhenius plots. The results (Table 47, Figure 33) show nonstandard behavior in two ways. First, the viscosity increase accelerates initially (24 hours) and then decelerates. Second,

TABLE 47

CORROSION AND OXIDATION DATA FOR O-64-20 USING  
SQUIRES TUBES, 10 L/H AIRFLOW, AND INTERMEDIATE SAMPLING

320°C Test Temperature				
Hours	40°C Visc. cSt	% Increase at 40°C	100°C Visc., cSt	% Increase at 100°C
0	21.71	-	4.01	-
24	24.76	14.1	4.33	8.0
48	26.37	21.5	4.43	10.5
72	28.29	30.3	4.60	14.7
96	28.75	32.4	4.65	16.0

305°C Test Temperature				
24	24.01	10.6	4.20	4.7
72	25.50	17.5	4.37	9.0
144	28.30	30.4	4.62	15.2
192	29.39	35.4	4.69	17.0

290°C Test Temperature				
72	26.06	20.0	4.36	8.7
144	27.64	27.3	4.53	13.0
240	29.87	37.6	4.71	17.5
312	30.93	42.5	4.83	20.5

Specimen Corrosion Data, mg/cm <sup>2</sup>						
	Al	Ag	M-St	M-50	Wasp	Ti
320	+0.02	-1.96	+0.04	+0.08	-0.02	+0.02
305	+0.20	-1.58	+0.04	+0.08	0	+0.02
290	0	-1.76	+0.02	+0.06	+0.06	-0.02

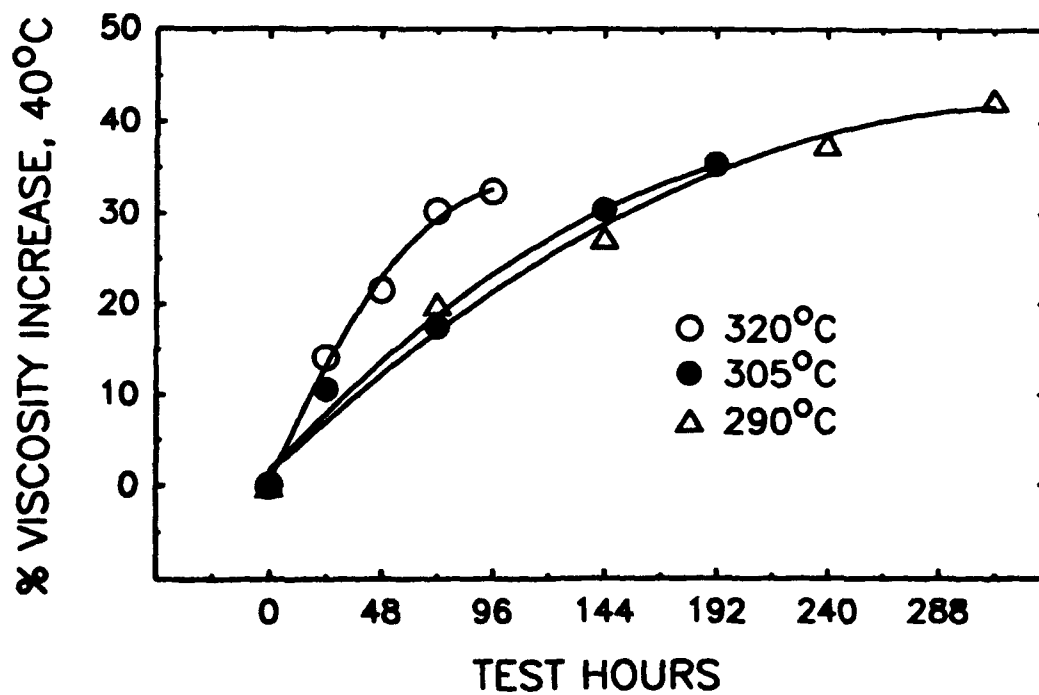
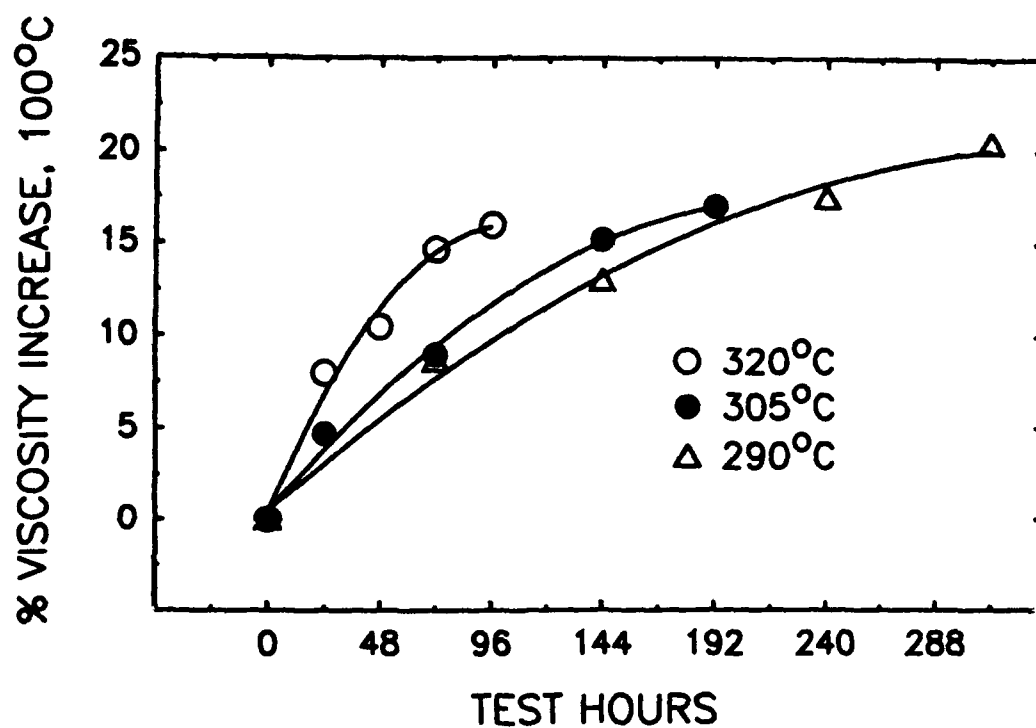


Figure 33. Viscosity Increases for Corrosion and Oxidation Tested O-64-20 at 290, 305, and 320°C.

there is no difference between the 305 and 290°C test data. The latter point precludes the development of meaningful Arrhenius data for the above temperatures (a minimum of three temperatures are needed). The cause of this nonstandard behavior was investigated and is reported in Section II.2.h.

### (3) C&O Testing Without Metal Specimens and Condensate Return

The effects of metal specimens and returned condensate on the oxidative stability of O-64-20 were investigated. A 96-hour C&O test at 320°C was run without metal specimens and another test was run without condensate return and the results compared to a 96 hour test using the normal setup. The results (Table 48) show that the absence of metal specimens did not significantly alter the oxidative stability of O-64-20, an expected and previously shown result.<sup>32</sup> The lack of condensate return significantly increased the rate of viscosity increase. Generally, this type of behavior is indicative of a significant loss of volatiles. Since C-ethers are composed mainly of 3P2E and 4P3E with thioether/ether linkages, it is expected that the lower molecular weight components volatilize first leaving the more viscous components behind. Such behavior, for example, is not observed for polyphenyl ethers<sup>3</sup> since PPE (5P4E) is higher molecular weight than C-ether. Alternatively, it is possible that returned volatiles may have a stabilizing effect upon the C-ether lubricant.

### (4) C&O Testing of O-64-20 Mixed with Phenyl Disulfide

Since a small amount of phenyl disulfide (PDS) was found by GC-MS to exist in the fresh O-64-20 fluid, a comparable amount (0.15%) of PDS was added to O-64-20 to determine its effect upon its oxidative stability (320°C, 48 hours). PDS would be expected to be thermally unstable and would cleave homolytically to produce thiophenoxy radicals that could act as radical initiators. Gas chromatographic analysis of a stressed sample (24 hours, 290°C) indicates that PDS is absent. The results (Table 49) show that the added PDS had a marginal effect upon the test results relative to the fresh fluid. These results indicate that PDS may be partially responsible for the very large initial rise in viscosity during C&O testing of O-64-20.

### (5) C&O Testing of O-64-20 With an Organotin Additive

Since C-ethers are chemically related to PPEs, the PPE organotin antioxidant (Additive A) was formulated in O-64-20 (0.15%) and a 48 hour 320°C C&O test was run in order to determine the effectiveness of this antioxidant. The results (Table 49) show that this additive had a positive but marginal effect upon C&O stability.

TABLE 48

**EFFECT OF METAL SPECIMENS AND CONDENSATE RETURN  
ON CORROSION AND OXIDATION TEST DATA FOR O-64-20  
(320°C, 96 HOURS)**

	Condensate Return & Metal Specimen	No Cond. Return	No Metal Specimens
Initial 40°C Viscosity, cSt	21.71	21.71	21.71
Final 40°C Viscosity, cSt	28.75	36.41	31.18
40°C Viscosity Increase, %	32.4	67.7	43.6
Initial 100°C Viscosity, cSt	4.01	4.01	4.01
Final 100°C Viscosity, cSt	4.65	5.24	4.89
100°C Viscosity Increase, %	16.0	30.7	21.9
<b>Specimen Corrosion Data</b>			
<b>Weight Change, mg/cm<sup>2</sup></b>			
Al	+0.02	+0.04	-
Ag	-1.96	-0.84	-
M-St	+0.04	0.00	-
M-50	+0.08	+0.06	-
Wasp	-0.02	+0.08	-
Ti	+0.02	0.00	-

TABLE 49

**EFFECT OF VARIOUS ADDITIVES ON C&O TEST PERFORMANCE  
OF O-64-20 (320°C, 48 HOURS)**

	No Additives	0.15% PDS <sup>1</sup>	0.15% Additives A	NASA Additives <sup>2</sup>
Final 40°C Viscosity, cSt <sup>3</sup>	25.79	26.81	25.12	26.44
40°C Viscosity Increase, %	18.8	23.5	15.7	21.8
Final 100°C Viscosity, cSt <sup>3</sup>	4.39	4.56	4.36	4.46
100°C Viscosity Increase, %	9.5	13.7	8.7	11.2
<b>Specimen Corrosion Data</b>				
mg/cm <sup>2</sup>				
Al	+0.15	+0.18	0	0
Ag	-0.68	-0.38	-0.30	-1.44
M-St	+0.06	+0.02	0	+0.12
M-50	+0.08	+0.16	-0.04	+0.14
Wasp	+0.06	+0.02	0	+0.10
Ti	+0.04	+0.04	-0.04	+0.08

<sup>1</sup> PDS = phenyl disulfide

<sup>2</sup> 0.05% phenylphosphinic acid, 0.07 % perfluoroglutaric acid

<sup>3</sup> Initial viscosity: 21.71 at 40°C, 4.01 at 100°C

(6) C&O Testing of O-64-20 with Phenylphosphinic Acid and Perfluoroglutaric Acid

The additive combination of 0.05% phenylphosphinic acid and 0.07% perfluoroglutaric acid in C-ether was reported to be effective in reducing deposits and extending run times in bearing tests.<sup>34</sup> A C&O test of this formulation was conducted at 320°C for 48 hours in order to determine the effect of these antiwear additives on corrosion and oxidative stability. The results (Table 49) show that these additives did not significantly affect the oxidative stability of the lubricant while having a negative effect on metal corrosion.

(7) Silver Corrosion as a Function of C&O Stressing Time

Since the rate of viscosity increase decelerates as a function of C&O stressing time for O-64-20, the effect of this apparent degradation rate decrease on the amount of silver corrosion was investigated. A 48 hour 320°C C&O test was run with a silver coupon. A fresh silver coupon was added and the test run for another 48 hours. The results (Table 50) show that the amount of corrosion was actually larger in the second 48 hours than the first 48 hours, exactly the opposite of the rate of viscosity increase. Thus, the results show that silver corrosion is independent of the oxidation rate of O-64-20.

TABLE 50

SILVER SPECIMEN CORROSION DATA FOR O-64-20 320°C,  
SQUIRES TUBE, 10 L/HOUR AIRFLOW

Specimen No.	Wt Change (mg/cm <sup>2</sup> )
1	-0.28
2	-0.62

#### (8) Vapor Phase Corrosion of Metals

In order to determine the effect of volatile degradation products on metal corrosion, a 48 hour C&O test was run on O-64-20 with both immersed and vapor phase metal specimens. The results (Table 51) show that the vapor phase specimens have reduced corrosion relative to the liquid phase. These data indicate that the volatile degradation products of O-64-20 are not particularly corrosive.

#### (9) C&O Testing of O-64-20 with APP and DPBA

Two additives, 4-aminopyrozolo[3,4-d]pyrimidine (APP) and diphenylborinic anhydride (DPBA) were reported to be effective in reducing copper and silver corrosion in C-ethers.<sup>36,37</sup> Thus, formulations containing 1% APP or 1.35% DPBA were C&O tested at 320°C for hours (silver coupon only) to determine their effectiveness as corrosion inhibitors and their effect on the lubricant oxidative stability. The results (Table 52) show that the 1% APP formulation was an ineffective corrosion inhibitor while destabilizing the lubricant. A true solution of APP in O-64-20 was never achieved and the 100°C viscosity could not be measured due to plugging of the viscometer capillary. The DPBA additive was very effective in reducing silver corrosion while resulting in slight viscosity increases. However, a repeat of this work with two different levels of DPBA (1.35 and 0.5%) with the full set of metal coupons yielded disappointing results (Tables 53 and 54). Not only was the additive ineffective in preventing silver corrosion, but M-50 and M-St steel corrosion had become a significant problem. It appears that the other metals interfere with the efficacy of this additive despite the fact that boron analysis of the posttest lubricant indicated no significant loss of the additive.

XPS and Auger spectra were obtained on silver and M50 specimens from the 96 hour 320°C C&O test of O-64-20 with 1.35% DPBA. The XPS results (Table 55) show that the surface composition of both specimens consist largely of organic matter. Relatively little boron exists on the M50 surface and virtually none on the silver surface, indicating that the boron compound is not forming a protective layer on the surface of the silver. Interestingly, the surfaces of both specimens contain a small amount of phosphorous, apparently as a surface contaminant. It may be that these specimens were previously used in a PPE/triphenyl phosphate C&O test and that normal polishing did not remove all of the extensive corrosion that occurred during this test.

TABLE 51

VAPOR PHASE CORROSION AND OXIDATION DATA RESULTS FOR O-64-20 AT  
320°C, 48 HOUR, TEST DURATION, SQUIRES TUBES AND 10 L/H AIRFLOW

Time h	Visc. at 40°C, cSt	% Visc. Chg at 40°C	Visc. at 100°C, cSt	% Visc. Chg at 100°C	Total Acid No. mg KOH/g
0	21.71	-	4.01	-	0
48	25.76	18.7	4.42	10.2	0

Specimen Corrosion Data, mg/cm<sup>2</sup>

	A1	Ag	M-ST	M50	Wasp	Ti
Liquid Phase	0.06	-0.30	0.14	0.10	0.0	0.02
Vapor Phase	0.02	-0.06	0.06	0.06	0.02	0.02

TABLE 52

## C&amp;O TEST DATA FOR O-64-20 FORMULATIONS

Formulation	Visc., 40°C cSt	% Visc. Chg. 40°C	Visc., 100°C cSt	% Visc., Chg. 100°C	Ag Corrosion Wt.(mg/cm <sup>2</sup> )
Fresh (no C&O Testing)	21.74	-	4.01	-	-
No Additive	28.57	31.4	4.62	15.2	-0.26
1% APP <sup>1</sup>	41.86	92.6	-	-	-0.30
1.35% DPBA <sup>2</sup>	32.72	50.5	4.97	23.9	-0.04

<sup>1</sup> 4-aminopyrozolo[3,4-d]pyrimidine

<sup>2</sup> diphenylborinic anhydride

TABLE 53

**C&O TEST DATA AT 320°C FOR O-64-20 WITH 1.35%  
DIPHENYLBORINIC ANHYDRIDE**

**Viscosity Data, cSt**

Test Hours	40°C	% Increase	100°C	% Increase	Ag ppm	Fe ppm
0	21.96	-	3.99	-	-	-
24	25.71	17.1	4.41	10.5	7.8	2.5
48	26.77	21.9	4.64	16.3	5.9	3.3
72	28.01	27.6	4.55	14.0	5.2	4.1
96	28.81	31.2	4.67	17.0	5.1	5.2

**Specimen Corrosion Data, mg/cm<sup>2</sup> (96 hours)**

Al	Ag	M-St	M50	Wasp	Ti
0	-0.48	-0.28	0	-0.02	0

TABLE 54

**C&O TEST DATA AT 320°C FOR O-64-20 WITH 0.5%  
DIPHENYLBORINIC ANHYDRIDE**

**Viscosity Data, cSt**

Test Hours	40°C	% Increase	100°C	% Increase	Ag ppm	Fe ppm
0	21.82	-	3.99	-	-	-
24	25.07	14.9	4.34	8.8	10.7	4.3
48	26.39	20.9	4.48	12.3	9.1	8.3
72	27.11	24.2	4.53	13.5	8.3	11.2
96	28.35	29.9	4.64	16.3	8.1	13.0

**Specimen corrosion Data, mg/cm<sup>2</sup> (96 hours)**

Al	Ag	M-St	M50	Wasp	Ti
0	-0.28	-0.36	-0.50	-0.02	0

TABLE 55

X-RAY PHOTOELECTRON SPECTROSCOPIC (XPS) ANALYSIS OF M50 AND SILVER WASHERS FROM THE CORROSION AND OXIDATION TEST OF O-64-20 WITH 1.35% DIPHENYLBORINIC ANHYDRIDE

Surface Compositions of Washers Exposed to 0-64-20 + 1.3% Diphenylborinic Anhydride as Determined by XPS

Washer	C					O			Fe	Ag	B	S	P
	O-C=O	C=O	C-O	C-C=O	CH, C	C-O, OH	C=O, OH	Fe-O					
M-50	2.4	3.5	9.2	6.6	34.0	13.0	10.3	3.5	11.0	-	2.5	2.7	1.1
Silver	2.1	3.8	10.5	8.0	36.2	17.7	8.3	-	-	7.2	-	2.3	3.8

Auger analysis using depth profiling (ion beam sputtering) of the M50 specimen (Figure 34) revealed an iron oxide layer approximately 200 nm thick that showed an enrichment of sulfur at the metal/oxide interface and a similar enrichment of boron approximately half way into the oxide layer. The Auger depth profile of the silver specimen (Figure 35) was unremarkable, with the sulfur and carbonaceous components decreasing with depth. Boron levels were below detection limits (2.3%) for this specimen.

#### (10) Conclusions

Corrosion and oxidation testing of a C-ether (O-64-20) yielded results similar to those previously published. That is, this lubricant basestock has good thermal and oxidative stability but a significant silver corrosion problem. The C&O test behavior was unusual in that the viscosity increase decelerates until nearly leveling off. Also, the near overlap of the 290 and 305°C data precluded the development of Arrhenius plots. Variation of test conditions revealed that the metal specimens did not significantly affect lubricant oxidative stability and that the rate of silver corrosion did not correlate with the rate of oxidative degradation. It was also found that the lack of condensate return accelerated the rate of viscosity increase and that the volatile products were not especially corrosive to metal specimens.

The addition of a PPE organotin additive (Additive A) resulted in a slight stabilization effect. Two previously tested antiwear additives increased the level of metal corrosion but did not affect oxidative stability. Two patented anticorrosion additives did not yield the expected results.

#### h. Chemical Analysis of Oxidized C-ethers

##### (1) Introduction

Because of the unusual behavior of C-ethers in corrosion and oxidation tests, an investigation was made into its degradation chemistry. Analytical techniques were developed for analyzing the degraded lubricant and for measuring basestock consumption rates. These techniques were used to identify degradation products and the data used to explain the anomalies in the C-ether oxidation behavior through a proposed degradation mechanism.

M-50 Washer 0-64-20 + 1.3% Diph.  
bor. Anh. AES Depth Profile

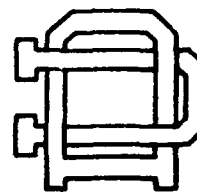
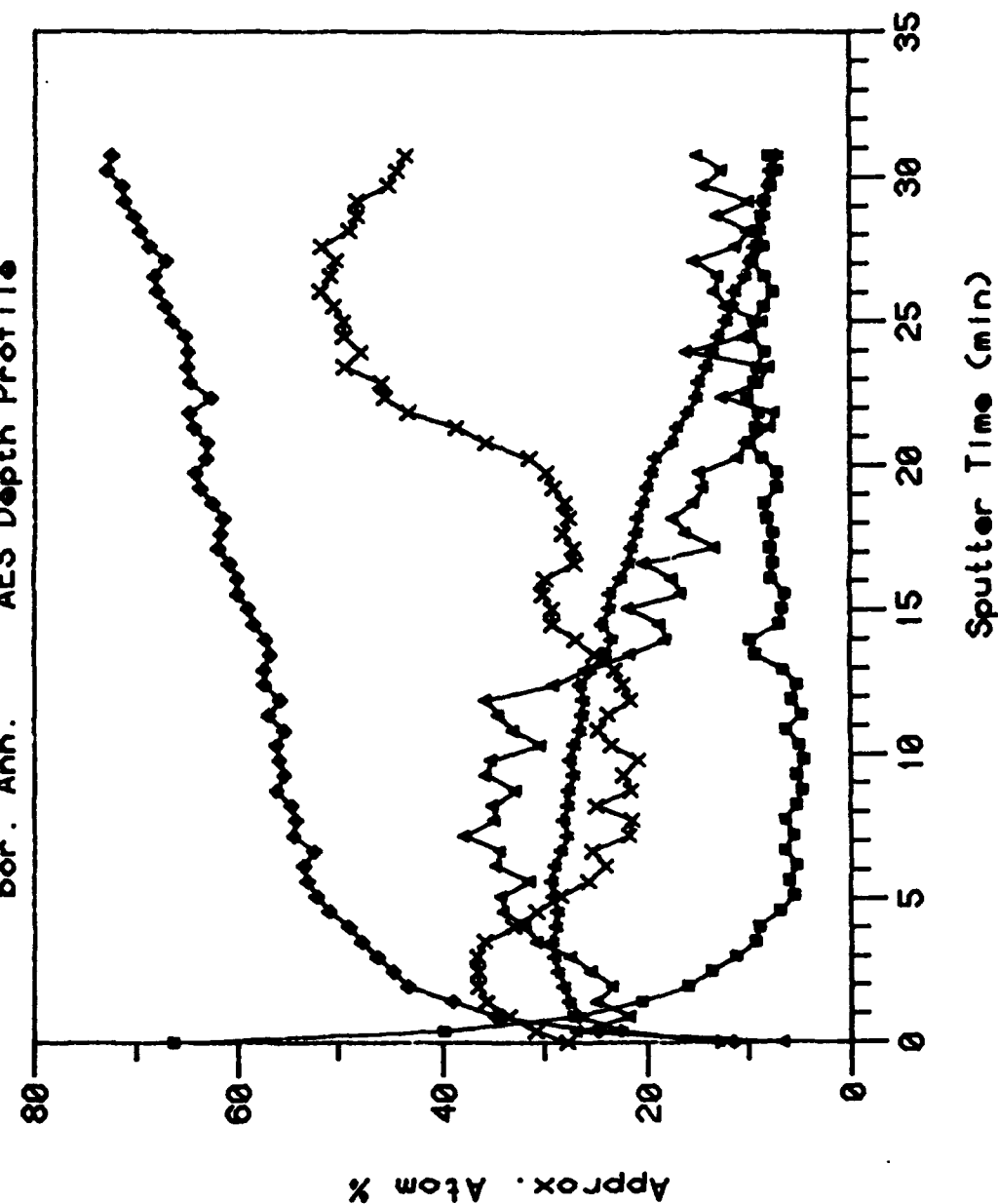


Figure 34. Auger Electron Spectroscopy Depth Profile of M50 Washer from the Corrosion and Oxidation Test of O-64-20 with 1.35% Diphenylborinic Anhydride.

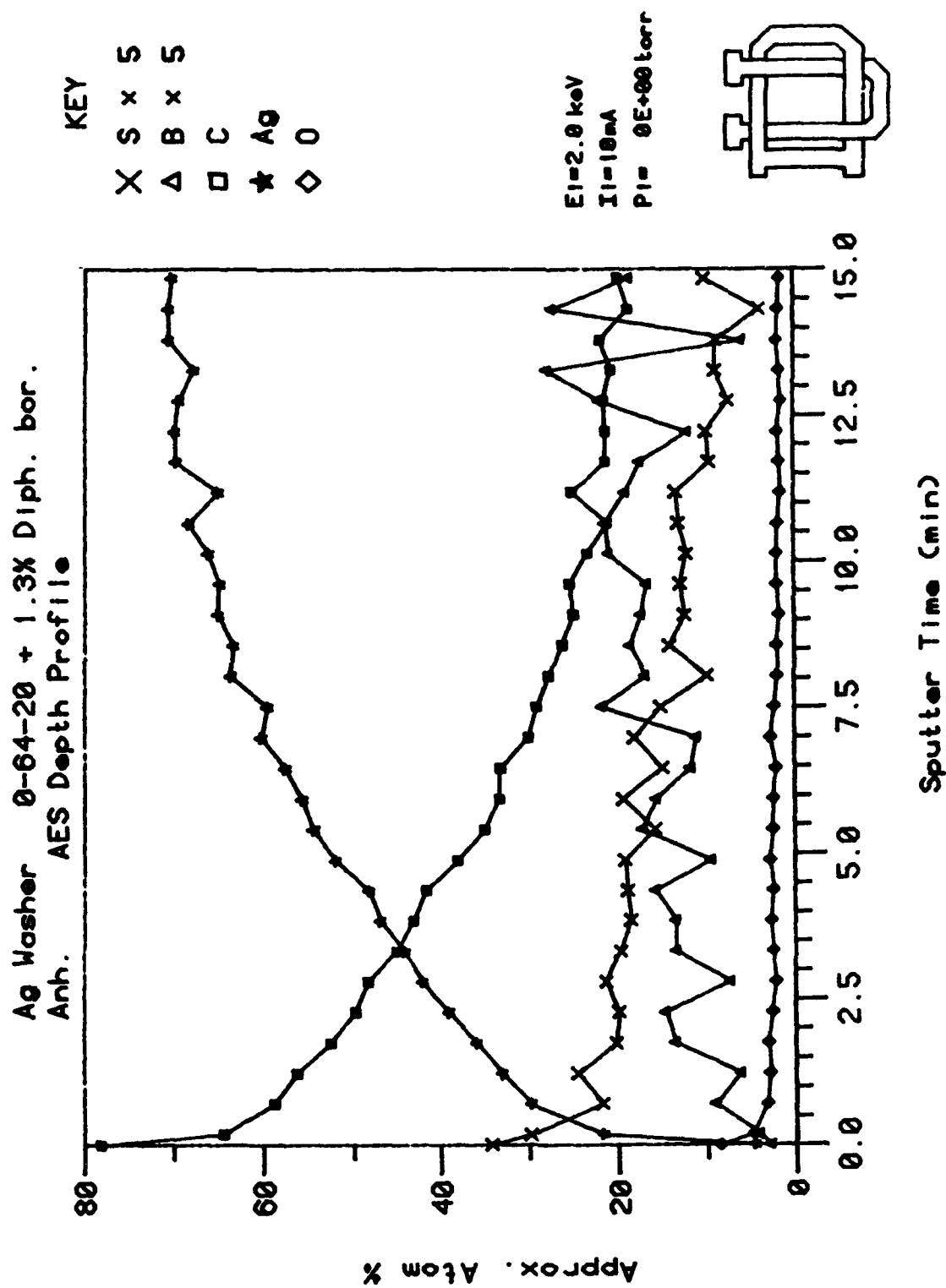


Figure 35. Auger Electron Spectroscopy Depth Profile of Silver Washer from the Corrosion and Oxidation Test of O-64-20 with 1.35% Diphenylborinic Anhydride.

## (2) Analytical Method Development

The following chromatographic techniques and conditions were used to characterize the degradation products. Gel Permeation Chromatography (GPC): 500, 100 and 50 Angstrom columns; tetrahydrofuran at 1.0 mL/min; UV detection at 254 nm. Reverse Phase Liquid Chromatography (RPLC): Octadecyl column; 85/15 acetonitrile/water for 0 to 10 minutes, ramp to 100/0 from 10 to 12 minutes, hold to 25 minutes; UV detection at 254 nm. Gas Chromatography (GC): 25 M X 0.52 mm ID X 0.17  $\mu$ m film thickness of HT-5, fused silica capillary column; direct column injection at 300°C; FID detector at 325°C, oven program, 100 to 325°C at 8°C/minute, 5 minutes final hold.

Gas chromatography - mass spectroscopy was used to identify lower boiling degradation products, including entrapped volatiles. Higher boiling compounds (those greater than the basestock) were identified by isolation of submilligram quantities by reverse phase liquid chromatography and analysis by direct probe-mass spectroscopy.

Higher molecular weight oxidation products were isolated by acetonitrile extraction in a manner similar to that used to isolate oxidation products from polyphenyl ether.<sup>31</sup> These compounds were analyzed by FTIR as a 2% KBr pellet and also by GPC. Basestock composition quantitation of degraded samples were measured by reverse phase liquid chromatography via an external standard method calibrated with fresh basestock.

## (3) Chromatographic Analysis and Identification of Degradation Products

The GPC chromatograms (Figure 36) of an oxidized polyphenyl thioether (PPTE) show a range of compounds similar to that seen by Jones and Morales.<sup>38</sup> A plot of retention times versus log of anticipated number of phenyl groups shows the expected linearity, indicating a progressive chain length increase. The GC-FID and RPLC chromatograms (Figures 37 and 38) show the compounds that form during high temperature stressing. Since oxidative processes normally produce a large number of compounds, the neatness and simplicity of the chromatogram is rather unusual. GC-MS and direct probe MS analyses of these compounds identify them as both higher and lower molecular weight homologues of the original basestock components (Figure 39). The MS data are not necessarily capable of determining the exact positional isomeric form of these compounds. However, capillary gas chromatography has adequate resolution to separate different isomeric forms of these compounds, so it is assumed that the lack of multiple peaks with the same mass means that only single isomeric forms are present. The same compounds are observed when the PPTE is stressed under a nitrogen

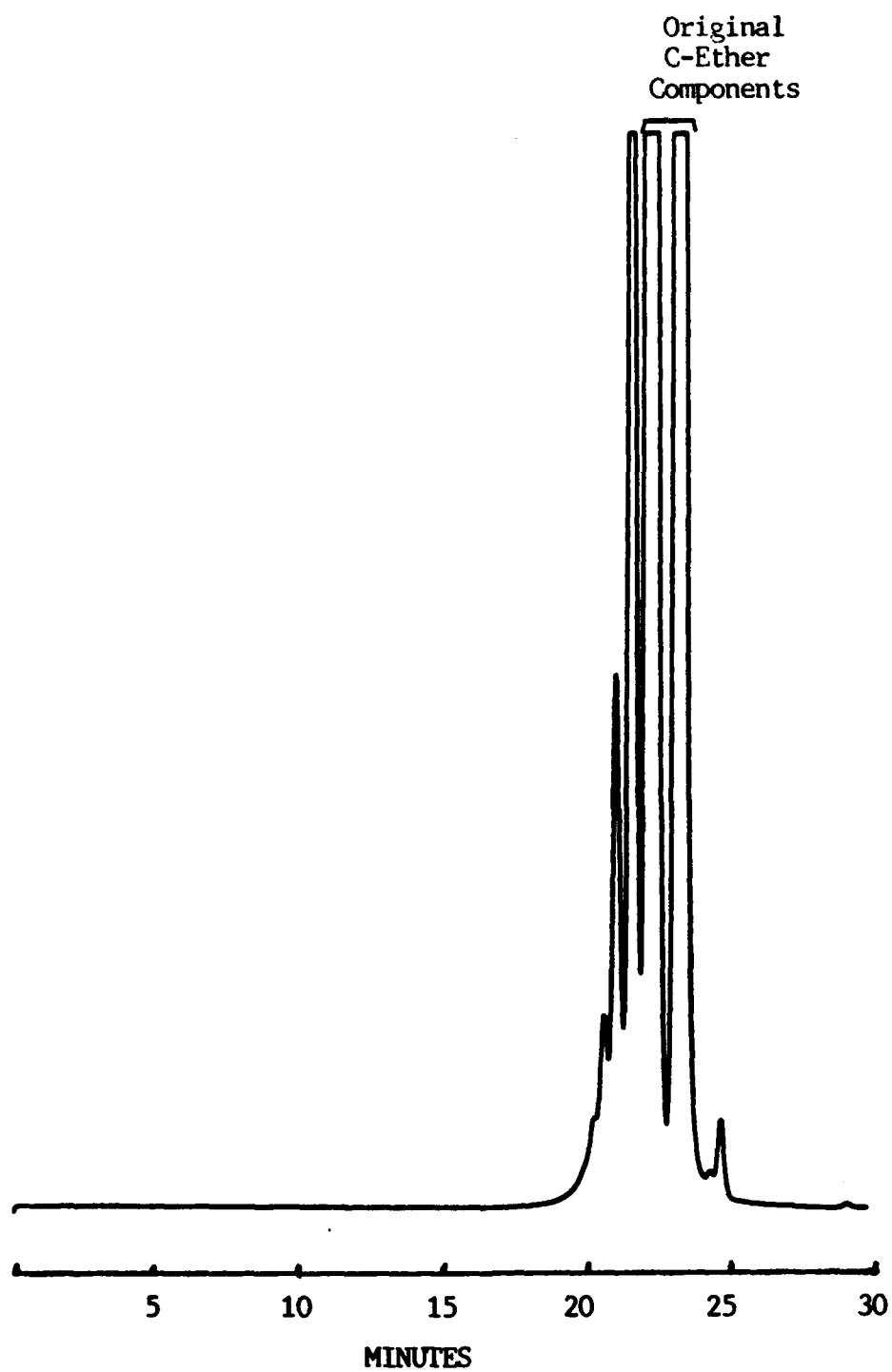


**Figure 36.** Gel Permeation Chromatogram of an Oxidized Polyphenyl Thioether (C-Ether).

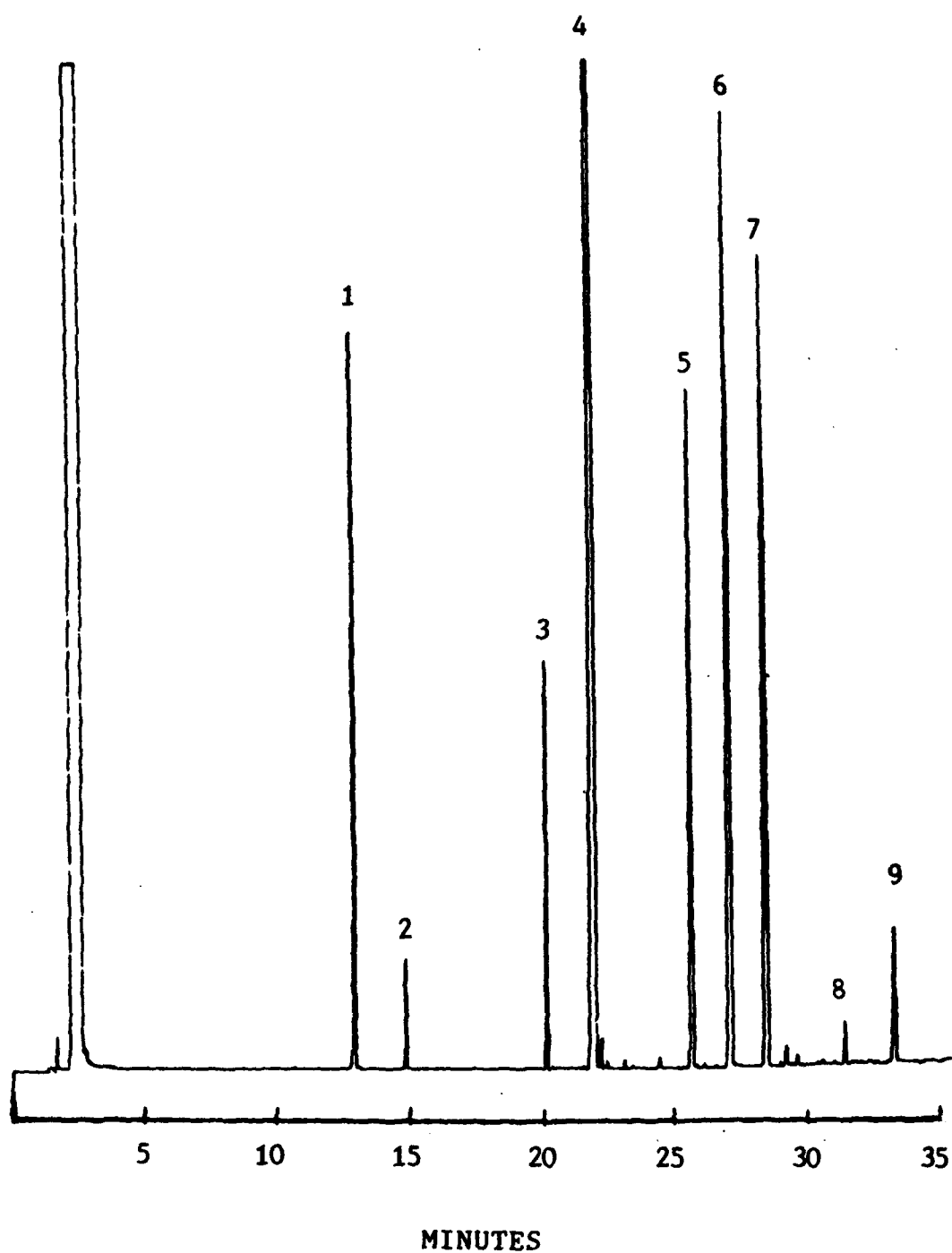


**Figure 37.** Gas Chromatogram with Flame Ionization Detection (GC-FID) of an Oxidized Polyphenyl Thioether (C-Ether). Compound Identification is in Figure 39.

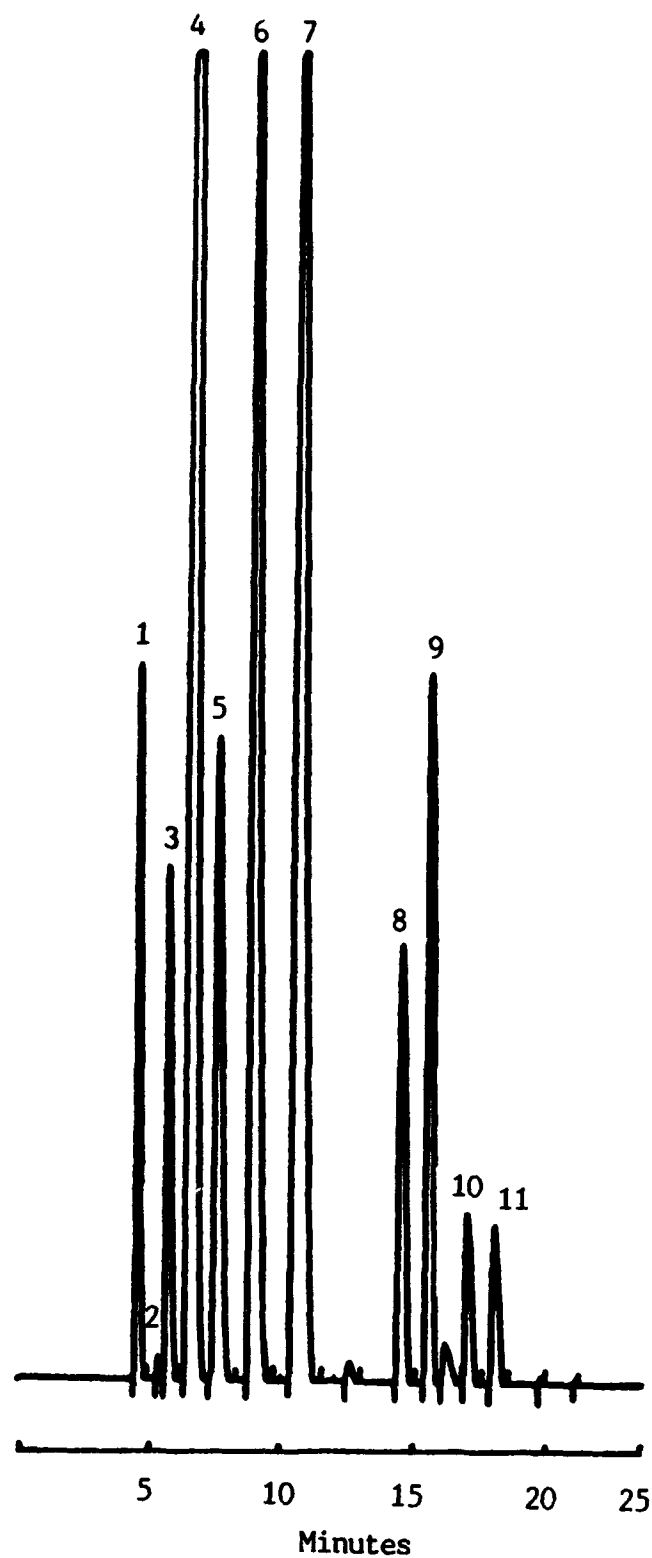


Figure 38. Reverse Phase Liquid Chromatogram (RPLC) of an Oxidized Polyphenyl Thioether (C-Ether). Compound Identification is in Figure 39.

PEAK NUMBER

STRUCTURE

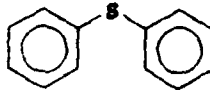
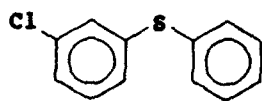
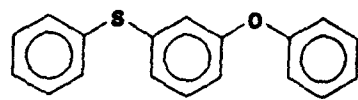
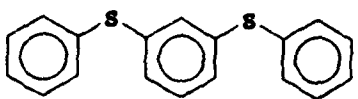
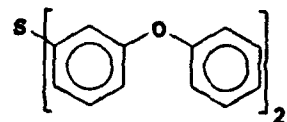
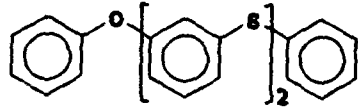
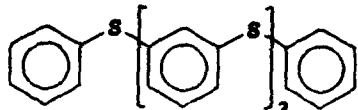
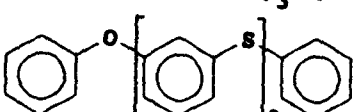
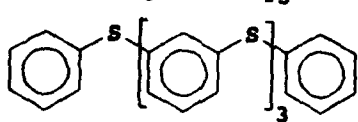
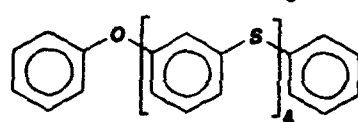
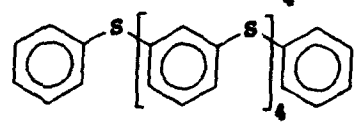
1	
2	
3	
4	
5	
6	
7	
8	
9	
10	
11	

Figure 39. Compound Identification for Figures 37 and 38.

atmosphere. In none of these products is oxygen (from molecular oxygen) included into their structure, as is normally the case for the degradation products of organic compounds in an oxidative environment.

#### (4) Analysis of Higher Molecular Weight Oxidation Products

Isolation of the higher molecular weight compounds (as acetonitrile insolubles) yielded a small amount of a blackish, brittle material that was higher in molecular weight than the homologues but much less than that previously seen with polyphenyl ethers.<sup>31</sup> Furthermore, the amount of this material produced for the PPTEs was at least an order of magnitude less than that found with similarly degraded polyphenyl ethers. FTIR analysis reveals the spectra of these compounds to be nearly identical, as both possess carbonyl absorptions indicative of aromatic ring destruction (Figure 40). Thus, it appears that a similar mechanism produced these products, but that the quantity of material produced indicates that it is a minor reaction path for PPTE. This may explain why the organotin PPE antioxidant was only marginally effective in stabilizing the C-ether lubricant.

#### (5) Degradation Mechanism

The oxidation of thioethers by various peroxy compounds to form sulfoxides and sulfones has been reported.<sup>39</sup> Likewise, the autoxidation of thioethers, which form a complicated mix of compounds including sulfoxides, has been investigated.<sup>39</sup> Diaryl thioethers were reported to be more resistant to oxidation due to a lack of a C-H bond adjacent to the sulfur. In general, the lack of hydrogens that are relatively easily extractable by radicals is an important feature of organic liquid lubricants that possess oxidative stability at high temperatures. Since the high temperature oxidation of PPTE does not produce these sulfoxide and sulfone oxidation products, the question arises as to what mechanism could produce the observed products. A radical mechanism involving homolytic bond scission with successive additions of sulfur-phenyl groups to the basestock components had been previously proposed.<sup>38</sup> However, the lack of significant amounts of certain compounds in either the reacted lubricant or the entrapped volatiles, including benzene, phenyl ether, thiols, various sulfur-phenyl end capped PPTE homologues with internal ether linkages (such as would be produced by reactions with compounds 4 and 5 in Figure 39) and various biphenylated compounds (as occurs with PPEs<sup>31</sup>), argues against such a mechanism. A possible mechanism might involve a nonradical transition state that results in an exchange of the aryl groups bonded to the sulfur, as shown below for the reaction of phenoxyphenyl sulfide with itself:

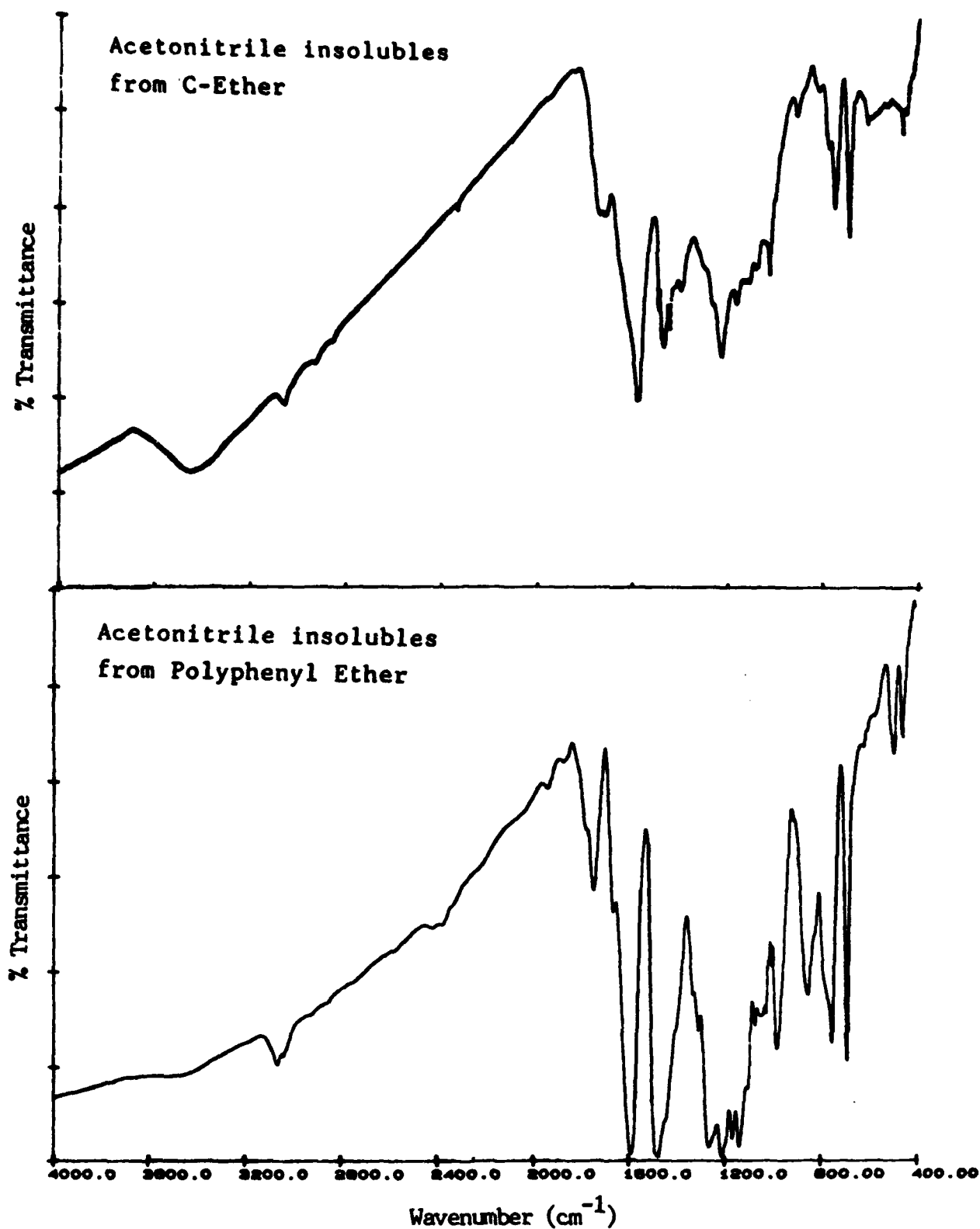
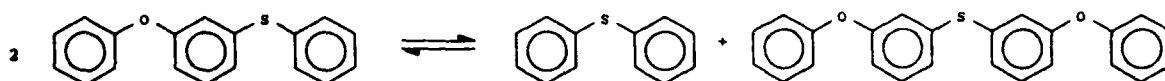


Figure 40. Comparison of FTIR Spectra of the Acetonitrile Insolubles from Oxidized Polyphenyl Thioether (C-Ether) and Oxidized Polyphenyl Ether.



Although no specific mechanism of this type has been found in the literature, this intermolecular rearrangement would account for all of the products observed as well as the retention of the meta-isomer structures. Obviously, the complex interactions between four different components present in this particular PPTE mixture complicates the kinetics of this reaction. The use of model compounds would help determine the general correctness of this mechanism, but none are commercially available. Since the rate of this reaction increases in the presence of oxygen relative to nitrogen, it appears that oxygen, or some minor oxidation product, plays a catalytic role.

#### (6) Basestock Consumption Analysis of Oxidized O-64-20

Quantitative analysis of the PPTE degradation at different temperatures shows that the reaction rate appears to level off after a period of time (Figure 41), thus, mirroring the changes in viscosity. An initial large drop in the concentration of the basestock remaining in the lubricant is observed followed by a decrease in the reaction rate until the basestock concentration seems to be resistant to further changes. From the previously discussed mechanism, it should be obvious that not only can the original basestock components react with each other to produce other basestock components and degradation products, the degradation products can likewise do the same. This complicated interplay of intermolecular rearrangement reactions would seem to ultimately result in a mixture of components that produce a steady state condition for the original basestock components (compounds 3 to 6 in Figure 39). Thus, the measurement of the amount of basestock remaining in the lubricant, which should be a primary measure of the reaction rate, does not yield the degradation rate for PPTEs. This is because it is not possible to differentiate between the basestock components originally present and those produced by the rearrangement reactions. Figure 41 shows that there does not seem to be a single stable composition mixture and that this mixture is a function of the reaction temperature. The reason for this is not apparent. Interestingly, a number of patents were granted that involved increasing the oxidative stability of PPTEs by heating at 230 to 260°C, usually with some kind of metal.<sup>40-42</sup> The stabilization afforded by this process would seem to be at least partially due to the formation of a steady state composition mix as is shown in this work.

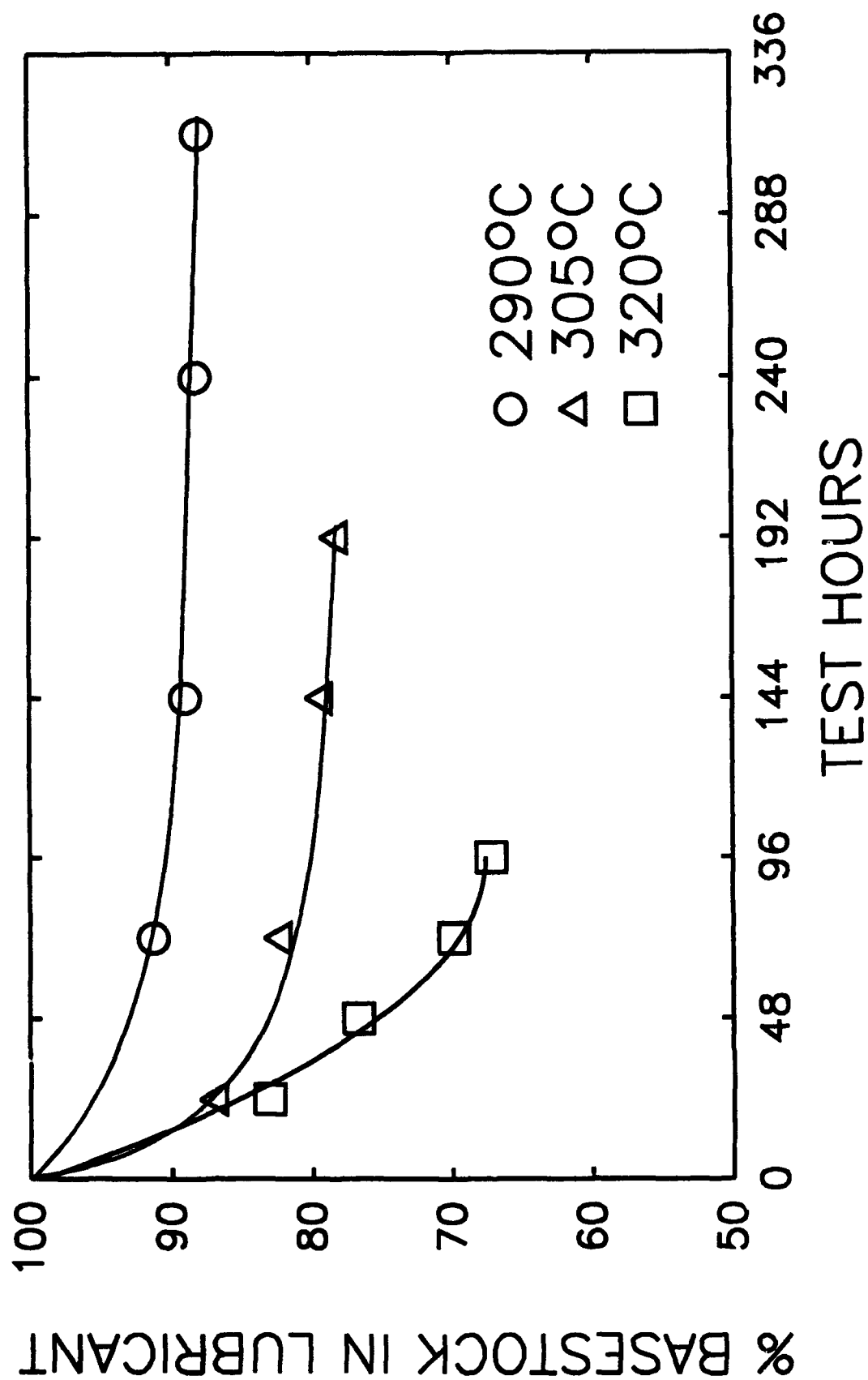


Figure 41. Basestock Consumption of O-64-20 (PPTe) During Corrosion and Oxidation Testing at 290, 305, and 320°C.

## (7) Conclusions

The application of chromatographic methods developed for the analysis of oxidized C-ethers has allowed for a partial explanation for the corrosion and oxidation test behavior of C-ethers. Identification of degradation products indicates that the predominate reaction of C-ether components, even under oxidative conditions, is a thermal rearrangement that produces a homologous series of polyphenyl thioethers. The data suggest that this thermal rearrangement involves a nonradical transition state, contrary to what had been previously proposed. Oxidation reactions similar to those that occur in PPE are present, but constitute a minor reaction route, thus, explaining the general lack of effectiveness of the PPE antioxidant in the C-ether lubricant.

Analysis of the degraded C-ether at various test temperatures indicates that both basestock consumption and viscosity increase undergo a deceleration with stressing time, nearly leveling off. This leveling off is due to an approximate steady state concentration of basestock components. This is proposed to occur as a result of an equal rate of consumption and production of these components in a manner consistent with the proposed thermal rearrangement mechanism.

### i. Stability Testing of Cyclophosphazene Based Fluids

#### (1) Introduction

Previously, it was shown that the cyclophosphazene based high temperature lubricant candidate fluids (TEL-9050, TEL-9071, TEL-90024, TEL-90059, TEL-90063) had a relatively poor oxidative stability as well as a significant corrosion problem for both immersed and vapor phase specimens.<sup>3</sup> Also, it was not possible to obtain reproducible test data for Arrhenius plot development.<sup>3</sup> Reported here are further investigations into the oxidative behavior of other lots of unformulated cyclophosphazene fluids. Corrosion and oxidation testing under various test conditions and alternative test apparatus materials (poly-ethrafluoroethylene (PTFE) and/or nickel) was conducted.

#### (2) Effect of Metal Specimens

A 75 hour 280°C C&O test was conducted on TEL-90013 (basestock) without metal specimens and the results compared to a similar test with specimens. The results (Table 56) show that the metal specimens appear to have stabilized the lubricant. A similar effect had been noted for polyphenyl ether basestock although it had no effect on formulated polyphenyl ethers.<sup>3</sup>

TABLE 56

**CORROSION AND OXIDATION TEST DATA FOR TEL-90013  
AT 280°C, SQUIRES TUBES AND 10 L/H AIRFLOW**

**Without Metal Specimens**

Time h	Viscosity, cSt/40°C	% Visc. Chg. at 40°C	Viscosity, cSt/100°C	% Visc. Chg at 100°C	TAN mg KOH/g
0	212.34	-	10.75	-	0.011
25	275.79	29.9	13.57	26.2	1.12
54	462.12	117.6	18.82	75.1	5.15
75	547.25	157.7	20.99	95.3	7.96

**With Metal**

0	212.34	-	10.75	-	0.011
24	250.18	17.8	12.26	14.0	1.22
48	320.69	50.8	15.08	40.3	2.07
72	399.2	88.0	17.70	64.7	3.43

**Specimen Corrosion Data mg/cm<sup>2</sup>**

Al	Ag	M-St	M-50	Wasp	Ti
0	-4.96	0	0	0	0

### (3) Effect of a PTFE C&O Test Apparatus

It had been previously shown that the degradation products of cyclophosphazene basestock fluids attacked the glass used in the test apparatus, as evidenced by etching of the tip of the glass condenser and high silicon levels in the lubricant.<sup>3</sup> Since this sort of interaction is not desirable and may affect the C&O test results, an all PTFE C&O test apparatus (tube, condenser and aerator tube) was constructed and TEL-90013 (basestock) was C&O tested at 260 and 280°C for 48 hours. The results (Table 57) show that the rate of lubricant degradation increased relative to the all glass apparatus. Furthermore, the 260°C test result showed slightly higher degradation levels than the 280°C test data, an unexpected result. It is possible that the leached silicon from the tip of the glass condenser may be acting as an antioxidant and, thus, stabilizing the fluid in the normal C&O test apparatus. However, it was noted after the first C&O test (at 280°C) that the PTFE tube was permanently stained. Either the PTFE degraded during the test or the degradation products were absorbed or adsorbed onto the PTFE. Since either process would have likely, negatively influenced the results of the second test (at 260°C) it was decided that no further testing would be conducted with this equipment.

### (4) Effect of a Nickel C&O Test Apparatus

Another inert C&O test apparatus was constructed using nickel. Thus nickel sample and aerator tubes were constructed and, along with the previously used PTFE condenser (which was not stained or degraded by the previous testing), was used to C&O test the cyclophosphazene fluid TEL-92026 (basestock). A similar test setup was used by Gumprecht to oxidatively stress perfluoroalkyl ethers,<sup>43</sup> which also produce degradation products that are corrosive to glass. The results of testing at 240, 260, and 280°C (Tables 58-61, Figure 42) show that the degradation level for the lubricant in the nickel apparatus was considerably less than that occurring in a glass apparatus under similar conditions. However, very little difference between the 260 and 280°C data was observed. Again, as with the C-ethers, the lack of normal C&O test behavior precludes the development of Arrhenius data.

### (5) Effect of Different Atmospheres and Condensate Return

The effects of thermal degradation, hydrolysis, oxidation and retention of volatiles on the physical property changes of a cyclophosphazene basestock (TEL-92026) were determined. Thus, a 48 hour 280°C C&O test using the nickel test tube /PTFE condenser test apparatus was performed on this fluid under the following atmospheric conditions: dry nitrogen, moisture saturated nitrogen, air and air without condensate return all at 10 L/h. The air test was repeated in order to check test reproducibility. The results of the testing are shown in Table 62.

TABLE 57

CORROSION AND OXIDATION TEST DATA FOR TEL-90013 WITH  
THE PTFE APPARATUS AND 10 L/H AIRFLOW

## 260°C

Time Hours	Viscosity 40°C, cSt	% Visc. Chg. at 40°C	Viscosity 100°C, cSt	% Visc. Chg. at 100°C
0	212.34	-	10.75	-
24	299.38	41.0	13.73	27.7
48	N.M. <sup>a</sup>	-	25.33	135.6

## 280°C

0	212.34	-	10.75	-
24	286.26	34.8	13.51	25.7
48	657.77	209.8	23.53	118.9

Specimen Corrosion Data, mg/cm<sup>2</sup>

Temp, °C	Al	Ag	M-St	M50	Wasp	Ti
260	+0.04	-1.02	+0.02	+0.02	+0.04	0
280	-0.02	-1.3	+0.02	-0.02	0	-0.02

<sup>a</sup> N.M. = Not Measured

TABLE 58

## C&amp;O TEST DATA FOR TEL-92026 AT 240°C\*

Test Hours	Visc., cSt 40°C	% Visc. Chg. 40°C	Visc., cSt 100°C	% Visc. Chg. 100°C
0	215.30	-	10.91	-
48	218.00	1.3	10.88	0
96	232.33	7.9	11.42	4.7
144	253.26	17.6	12.17	11.6
216	405.62	88.4	16.40	50.3

Specimen Corrosion Data (216 hours)  
Wt. Chg. in mg/cm<sup>2</sup>

Al	Ag	M-St	M-50	Wasp	Ti
0.24	2.70	2.50	1.10	0.80	0.50

\*Nickel tube and aerator, PTFE condenser  
Intermediate sampling, 10 L/h airflow

TABLE 59

C&amp;O TEST DATA FOR TEL-92026 AT 260°C FOR 144 HOURS\*

Test Hours	Visc., cSt 40°C	% Visc. Chg. 40°C	Visc., cSt 100°C	% Visc. Chg. 100°C
0	215.30	-	10.91	-
72	226.96	5.4	11.38	4.3
144	644.52	199	21.80	99.8

Specimen Corrosion Data (144 hours)  
Wt. Chg. in mg/cm<sup>2</sup>

Al	Ag	M-St	M-50	Wasp	Ti
0.14	-0.16	0.16	0.16	0.10	0.10

\*Nickel tube and aerator, PTFE condenser  
Intermediate sampling, 10 L/h airflow

TABLE 60

C&amp;O TEST DATA FOR TEL-92026 AT 260°C FOR 125 HOURS\*

Test Hours	Visc., cSt 40°C	% Visc. Chg. 40°C	Visc., cSt 100°C	% Visc. Chg. 100°C
0	215.30	-	10.91	-
75	258.05	19.9	12.29	12.6
99	359.01	66.7	15.26	39.9
123	602.56	180	21.34	95.6
125	test ended			

Specimen corrosion Data (125 hours)  
Wt. Chg. in mg/cm<sup>2</sup>

Al	Ag	M-St	M-50	Wasp	Ti
0.38	0.02	0.38	0.30	0.18	0.12

\*Nickel tube and aerator, PTFE condenser  
Intermediate sampling, 10 L/h airflow  
Test #2 at 260°C

TABLE 61

## C&amp;O TEST DATA FOR TEL-92026 AT 280°C\*

Test Hours	Visc., cSt 40°C	% Visc. Chg. 40°C	Visc., cSt 100°C	% Visc. Chg. 100°C
0	215.30	-	10.91	-
48	220.15	2.3	10.97	0.6
96	302.61	40.6	13.72	25.8
120	442.22	105.4	17.75	62.7
168	1181.7	449	31.85	192

Specimen Corrosion Data (168 hours)  
Wt. chg. in mg/cm<sup>2</sup>

Al	Ag	M-St	M-50	Wasp	Ti
0	-1.00	0	-0.04	-0.02	0

\*Nickel tube and aerator, PTFE condenser  
Intermediate sampling, 10 L/h airflow

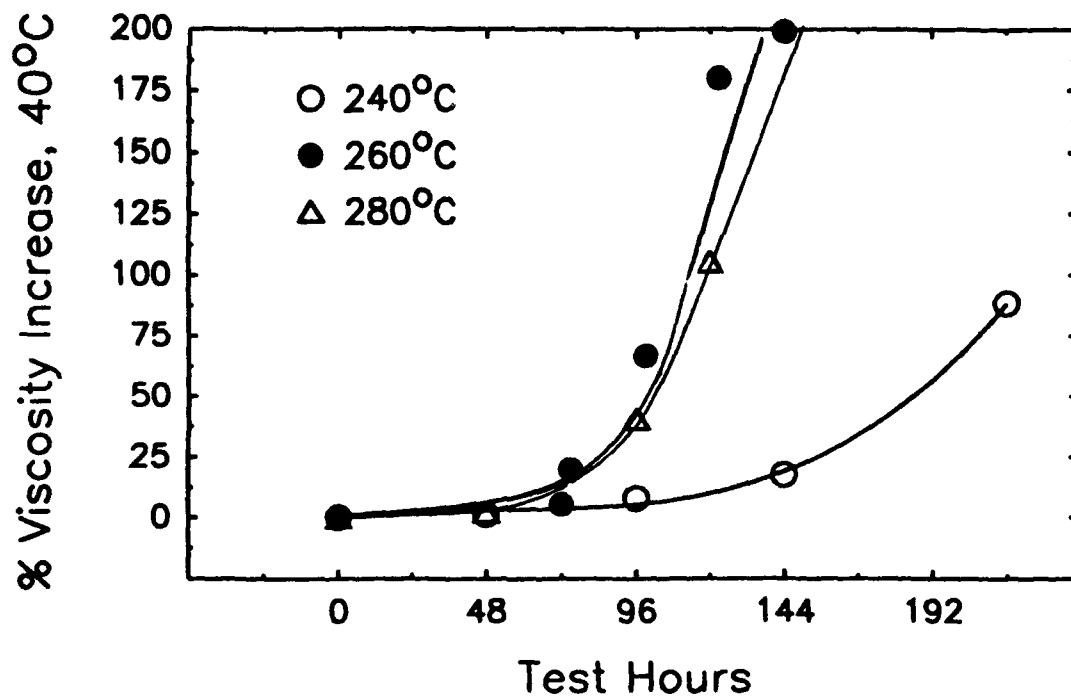
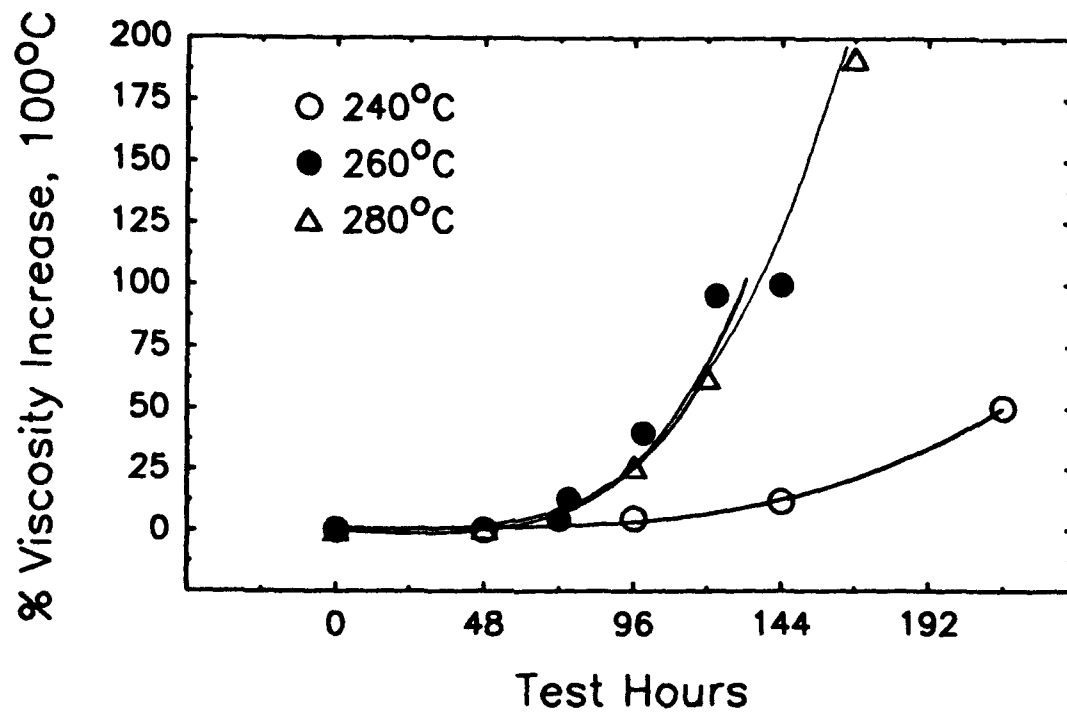


Figure 42. Viscosity Increase for TEL-92026 During Corrosion and Oxidation Testing in the Nickel Test Apparatus.

TABLE 62

THERMAL STRESSING DATA FOR TEL-92026 UNDER DIFFERENT  
TEST CONDITIONS AT 280°C FOR 48 HOURS

	Dry N <sub>2</sub>	Wet N <sub>2</sub>	Air NCR <sup>1</sup>	Air Test 1	Air Test 2
40°C Visc. Inc., %	8.0	8.5	23.1	6.0	6.9
100°C Visc. Inc., %	5.7	5.2	18.1	3.9	4.1
TAN	0.39	0.61	1.01	0.50	0.62
Silver Wt. Chg., <sup>2</sup> mg/cm <sup>2</sup>	0.00	-0.44	-0.66	-1.0	-0.64
Wt. Loss, %	2.0	0.44	3.4	0.4	0.4

<sup>1</sup> No Condensate Return

<sup>2</sup> All other metals had insignificant weight losses

The dry and wet nitrogen tests yielded viscosity increases and TANs that were very similar to those results from the air tests with condensate return. The dry nitrogen test, however, produced no silver corrosion while all other tests produced very significant levels of silver corrosion. The use of water saturated nitrogen did not increase the viscosity increases relative to dry nitrogen, although there was a slight increase in TAN. The air test without condensate return produced significant increases in all physical property changes despite only a moderate increase in weight loss. The duplicate air tests with condensate return reproduced very well resulting in no change in weight loss while TAN and viscosity (100°C) changes were within 0.1 and 0.2, respectively.

A number of things can be inferred from these data. The lack of significant difference between the nitrogen and air tests indicates that most of the degradation in the lubricant is thermal rather than oxidative. The lack of difference in physical property changes between the wet and dry nitrogen indicates that hydrolysis is not a significant degradation route. The lack of condensate return greatly increased the viscosity increase and TAN despite only a small increase in weight loss. This would indicate that the volatiles act as a stabilizer.

#### (6) Conclusions

The use of an inert C&O test apparatus eliminated the uncertainty connected with the reaction of the degradation products of the cyclophosphazene fluid with the test apparatus. While the nickel tube with teflon condenser gave more reproducible C&O test results, anomalous test data were still observed with this setup which precluded the development of Arrhenius plots. Although the exact source of this anomalous behavior could not be pinpointed, the results of various experiments and analyses indicated that thermal degradation is more significant than oxidative degradation, that hydrolysis is insignificant, and that the volatile degradation products can act as a fluid stabilizer. It appears that the retention of volatile components is a significant factor in producing the anomalous data.

#### j. Chemical Analysis of Degraded Cyclophosphazenes

##### (1) Introduction

Because of the anomalous behavior of the cyclophosphazene fluids, an investigation was made into its degradation chemistry. Analytical techniques were developed in order to identify degradation products and the data used to explain the anomalous C&O data.

## (2) Analytical Method Development

The following chromatographic techniques and conditions were used to characterize the degradation products. Gel Permeation Chromatography (GPC): 500, 100 and 50 Angstrom columns; tetrahydrofuran at 1.0 mL/min; UV detection at 254 nm. Gas Chromatography (GC): 25 M X 0.52 mm ID X 0.17  $\mu$ m film thickness of HT-5, fused silica capillary column; direct column injection at 300°C; AED detector at 325°C, oven program, 100 to 325°C at 8°C/minute, 5 minutes final hold. Gas chromatography - mass spectroscopy was used to identify lower boiling degradation products, including entrapped volatiles.

## (3) Background

A description of the development and properties of fluids of the type like TEL-92026 (cyclotriphosphazenes) had been previously published.<sup>44</sup> Considerable information exists in the literature on the general properties of cyclophosphazenes.<sup>45,46</sup> Thermally, the cyclophosphazenes embody some of the characteristics of an equilibrating homologous series; that is the lower cyclo-oligomers are thermally interconvertible with their high polymers. It had been shown<sup>47</sup> that the chlorophosphazene oligomers (trimer, tetramer, etc.) are converted to a high polymer at temperatures from 200 to 300°C. At 350°C (under vacuum), this high polymer converts to lower molecular weight cyclo-oligomers.<sup>47</sup> However, the thermodynamics of this conversion are considerably influenced by the steric interactions of organic groups on the cyclophosphazene ring.<sup>48</sup> Increasing dimensions of the side groups increasingly destabilize the polymeric form. Thus, while the diphenoxyphosphazene cyclo-trimer (similar type compound to those present in TEL-92026) fails to polymerize at 300°C,<sup>49-51</sup> the diphenoxyphosphazene polymer will depolymerize at 100°C to a mixture of lower cyclo-oligomers.<sup>48,52</sup> It appears that interconversion of cyclo-oligomers also occurs. This was shown to occur with tri(heptafluorobutyl)phosphonitrile as a 50% conversion to the tetramer occurred after 50 hours at 340°C.<sup>53</sup> This same process also was proposed to account for the increase in viscosity and decrease in ASTM slope that occurred during thermal stressing of some mixed trimeric (aryl and fluoroalkyl) phosphonitrile hydraulic fluids.<sup>54</sup> Although the literature reveals hydrolytic instability for some cyclophosphazenes (especially perhalogenated), the substitution of bulky organic groups greatly reduces this susceptibility. The following analytical work was undertaken to investigate the degradation of cyclophosphazene lubricants.

#### (4) Analysis of Oxidized Cyclophosphazenes

GPC analysis of oxidized TEL-90013 shows that even for a severely degraded oil (as shown in Figure 43) high molecular weight compounds in the range of those seen in oxidized polyphenyl ethers are not observed. The major degradation products are slightly higher in molecular weight (by GPC, Figure 43) and slightly less volatile (by GC, Figure 44) than the original cyclotrimer basestock compounds. GC-AED analysis reveals that these higher molecular weight compounds contain all of the expected elements (C, N, P, O, F, H).

It seems likely, then, that these compounds are the tetramer form of the cyclophosphazene. Unfortunately, confirmation of the molecular weight cannot be determined due to the inability of conventional mass spectrometers to handle molecular weights greater than 1000 a.m.u. These presumed tetramers are thermal stressing products since the 48 hour dry nitrogen test lubricant sample showed the presence of these compounds.

It is likely, therefore, that most of the viscosity changes in oxidatively stressed cyclophosphazene fluids are due to thermal transformation (and equilibration) of the cyclotrimer to the cyclotetramer, rather than the usual oxidative degradation. A similar type transformation had been previously shown to occur for C-ethers, which involved nonoxidative transformation to both higher and lower chain lengths (see Section h. above). Lower oligomers (monomers and dimers) would not be produced from the cyclophosphazene trimer since these are not stable forms.<sup>45,46</sup> The mechanism of this reaction is not known, although it may involve polyphosphazene intermediates, but it is very conceivable that this reaction could be accelerated or inhibited by some type of catalyst.

GC-MS analysis of the trapped volatiles from a C&O test of a cyclophosphazene fluid (Figure 45) shows that the bulk of the volatiles consists of two phenols, 4-fluorophenol and 3-trifluoromethylphenol. These compounds represent the two pendant groups found on the cyclophosphazene ring<sup>44</sup> and would seem to be thermal degradation products. Other apparent thermal degradation products found include phenoxyphenol and various substituted phenyl ethers. Among the more interesting degradation products found were the various substituted di- and triphenyl phosphates. Since these compounds contain phosphorous from the cyclophosphazene ring, their appearance is indicative of the destruction of the ring and are probably oxidation products. The total amount of material captured, as well as the amount of these degradation products in the lubricant, is very small and, thus, the contribution of these reactions to the total fluid degradation rate is small compared to the aforementioned thermal rearrangement. However, these compounds could have a potential

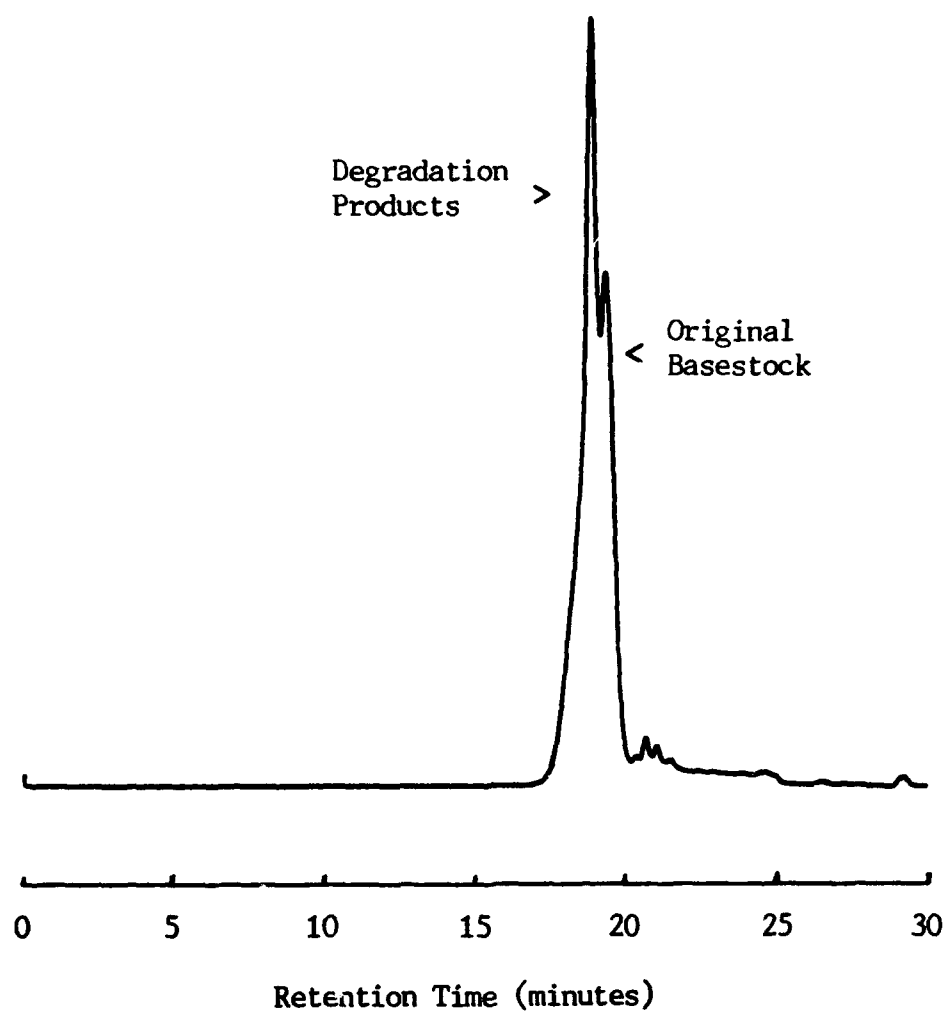


Figure 43. Gel Permeation Chromatogram of an Oxidized Substituted Cyclophosphazene (TEL-90013, 54 Hours at 280°C).

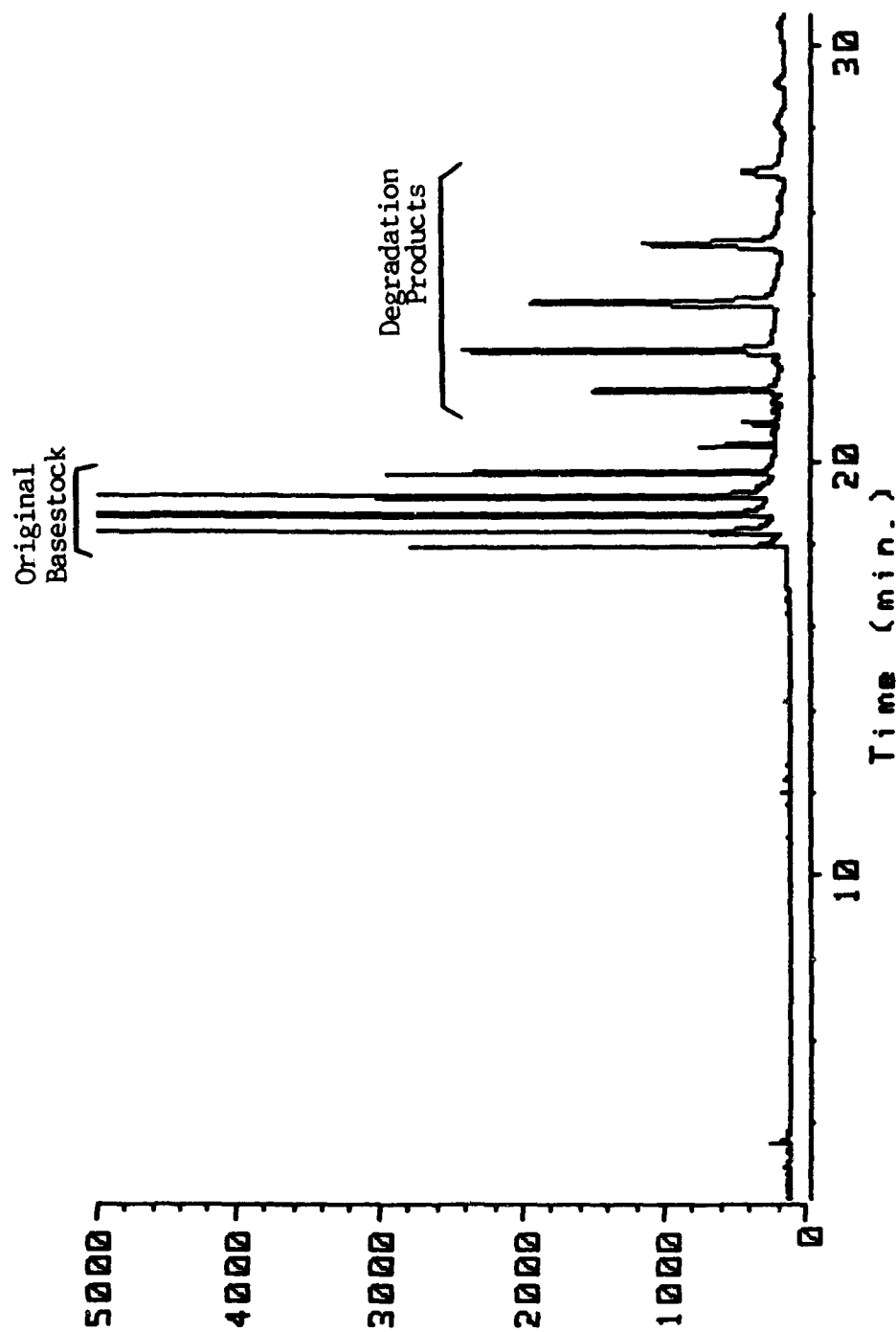


Figure 44. Gas Chromatogram with Atomic Emission Detection (GC-AED) of an Oxidized Substituted Cyclophosphazene (TEL-90013, 54 Hours at 280°C).

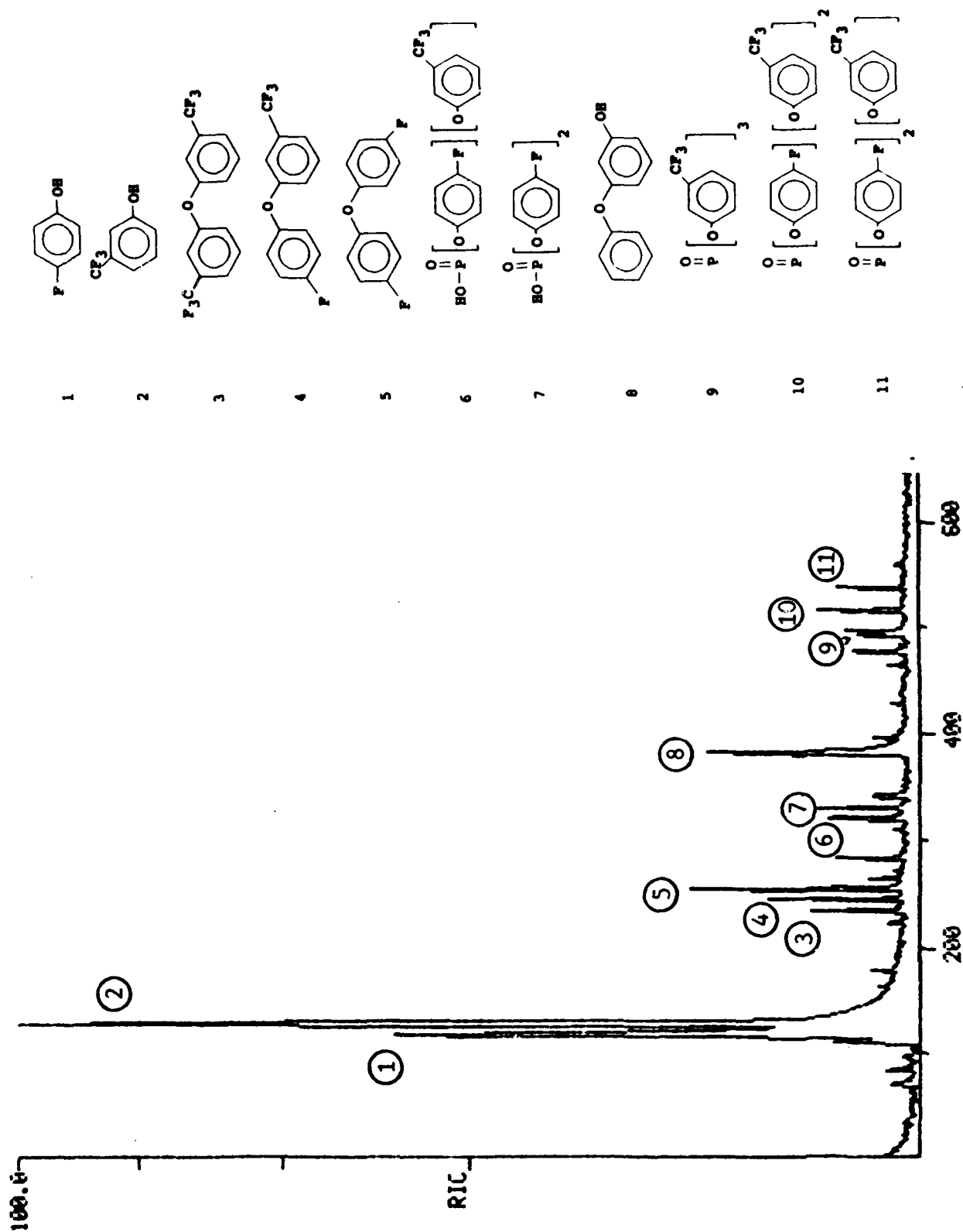


Figure 45. Gas Chromatogram with Mass Spectrometry (GC-MS) of Trapped Volatiles from the Corrosion and Oxidation Test of a Substituted Cyclophosphazene (TEL-90024).

catalytic effect on the rate of this thermal rearrangement and their relative degree of retention in the test cell may affect the test results.

### (5) Conclusions

It appears that the viscosity changes that occur during C&O testing of the cyclophosphazene experimental high temperature lubricants are largely the result of thermal, and to a much lesser extent oxidative, reactions, probably involving the conversion of the cyclotrimer to the cyclotetramer. It is proposed that catalysis of this reaction by external contaminants, or possibly even volatile degradation products, may be responsible for the anomalous C&O test results.

## 3. LUBRICANT DEPOSITION STUDIES

### a. AFAPL Static Coker

#### (1) Introduction

Satisfactory performance of a lubricant requires, among many properties, a low deposition tendency. As previously reported many techniques have been investigated for measuring the deposit forming characteristics of a lubricant.<sup>1</sup> One of these techniques involved the AFAPL Static Coker which has been investigated in depth and used for measuring the deposit forming characteristics of ester based MIL-L-7808 and MIL-L-23699 type lubricants.<sup>2</sup> Further modification and development of the AFAPL Static Coker was conducted<sup>3</sup> and used for investigating the deposition characteristics of high temperature lubricants and fluids. This effort describes the continued use of the AFAPL Static Coker for investigating and measuring the deposit characteristics of various high temperature lubricants and experimental fluids.

#### (2) Apparatus and Test Procedure

The AFAPL Static Coker and general test procedure have been previously described<sup>1-3</sup> and will not be reported here. Any changes made in the test procedure such as test time, temperature or coking surface will be described below where appropriate.

#### (3) Test Lubricants

Lubricants investigated are described in Table 63 and include 4 cSt candidate ester base lubricants and new and prestressed polyphenyl thioether (C-ether). Prestressing consisted of corrosion and oxidation testing and Four-ball wear testing prior to the coking studies.

TABLE 63

DESCRIPTION OF TEST FLUIDS USED IN AFAPL  
STATIC COKER STUDY

Test Fluid	Description	Viscosity at	
		40°C	100°C
O-64-20	POLYPHENYL THIOETHER, C-ETHER	21.71	4.01
O-67-1	Mil-L-87100 Oil (5P4E)	280.3	12.61
O-85-1	Candidate Oil, Ester Base	17.68	4.04
O-86-2	Different Lot of O-85-1	17.63	4.01
O-90-6	Different Lot of O-85-1	17.62	4.00
O-91-13	Candidate Oil, Ester Base	18.51	4.14
TEL-90103	" " "	17.09	3.97
TEL-90104	" " "	17.68	4.00
TEL-91002	" " "	17.69	4.00
TEL-91003	" " "	17.60	4.02
TEL-91005	" " "	17.76	4.04
TEL-91053	" " "	16.70	3.99
TEL-91063	" " "	17.01	4.02
TEL-92036	" " "	18.38	4.10
TEL-92039	" " "	18.04	4.10
TEL-92040	" " "	16.63	3.99
TEL-92041	" " "	17.56	4.10
TEL-92049	" " "	18.25	4.10
TEL-92050	" " "	17.66	4.05
TEL-93003	" " "	17.50	4.09
TEL-93011	" " "	17.58	3.99

#### (4) General Discussion of Data

Appendix A shows the static coking data developed during this study. For most samples and test conditions, three or four tests were conducted with the average of the data being the reported value for the specific lubricant and test condition.

The data in Appendix A shows the detailed test conditions such as type sample, sample size, test temperature coking surface and both test specimen and seal deposits. Although seal deposits are reported as residue, it should be remembered that in most cases for ester base fluids and PTFE seals the deposits can consist of considerable unstressed oil that has crept up the seals which are at a much lower temperature than the surface temperature of the test specimen. For example a seal deposit of 5 mg/g sample could be close to 0.005 grams of oil or one percent of the sample. Using stainless steel seals for high temperature studies of polyphenyl ethers and C-ethers, the deposits on the seals vary more towards breakdown deposit due to higher seal temperatures.

#### (5) High Temperature Ester Base Fluids

AFAPL Static Coker testing was conducted on 19 ester base 4 cSt lubricants with testing being conducted at 300°C, for 3 h test time, and using Teflon seals, stainless steel test surface, 0.5 g sample and temperature programming. Table 64 displays this data showing test specimen deposits (mg/g sample) along with standard deviation of testing. With the exception of three oils (O-86-2, TEL-92039 and TEL-92049) the deposit values of the remaining 16 oils ranged from 9.5 to 15.0 mg/g. The average of all the 16 values was 11.9 mg/g with a standard deviation of 2.0 which shows that these fluids displayed similar static coker values. These values are slightly lower than expected based on previous AFAPL Static Coker studies of ester base lubricants.<sup>2</sup> This is due to the revised testing using temperature programming and the use of stainless steel test specimens which give lower deposits values as shown in Table 65. Lubricants TEL-91002 and TEL-92050 showed the same difference in the coking values of the two test surfaces as previously observed for other ester base fluids.<sup>1,2</sup> Lubricants TEL-92049 and TEL-93003 showed much greater differences between the two test surfaces. Since these differences were also observed for total deposits (test specimen deposits plus seal deposits) these two lubricants appear to be very "test surface" sensitive.

TABLE 64

AFAPL STATIC COKER DATA FOR HIGH TEMPERATURE  
ESTER BASE LUBRICANTS (300°C, 3 H TEST TIME, SS-302  
TEST SURFACE, 0.5 g SAMPLE, PTFE SEALS)

Lubricant	Deposits <sup>1</sup> mg/g	Std Dev. <sup>2</sup>	Type Deposit
O-85-1	9.6	1.5	Dark Varnish to Black Coke
O-86-2	27.6	1.9	Dark Varnish to Black Coke
O-90-6	9.9	0.4	Dark Varnish
O-91-13	10.7	0.8	Brown Coke
TEL-90103	11.4	1.0	Dark Varnish
TEL-90104	13.3	0.8	Dark Varnish
TEL-91002	12.6	0.6	Dark Coke
TEL-91003	14.0	0.6	Dark Varnish
TEL-91005	15.0	0.9	Dark Varnish
TEL-91053	13.8	1.0	Heavy Brown to Black Coke
TEL-91063	15.0	1.0	Brown Coke
TEL-92036	10.1	1.0	Brown Coke
TEL-92039	19.3	2.4	Brown Coke
TEL-92040	11.0	1.0	Brown Coke
TEL-92041	9.5	3.6	Brown Coke
TEL-92049	21.9	2.7	Dark Coke
TEL-92050	12.2	1.7	Brown to Black Coke
TEL-93003	9.9	2.1	Brown Coke
TEL-93011	13.4	3.1	Black Coke

<sup>1</sup>Test Specimen Deposits

<sup>2</sup>Normally 4 Tests

TABLE 65

EFFECT OF TEST SURFACE ON AFAPL STATIC COKING VALUES  
(300°C, 3H TEST TIME, PTFE SEALS, 0.5g SAMPLE)

Lubricant	Specimen Deposits, mg/g	
	Shim Stock Test Spec.	SS-302 Test Spec.
TEL-91002	17.9 ± 1.9	12.6 ± 0.6
TEL-92049	31.2 ± 1.3	21.9 ± 2.7
TEL-92050	14.8 ± 1.7	12.2 ± 1.7
TEL-93003	27.8 ± 0.8	9.9 ± 2.1
TEL-93011	21.7 ± 6.1	13.4 ± 3.1

Testing of six of the 4 cSt lubricants were evaluated under the same test conditions except for increasing the test time. This study was conducted for determining decreases in coking values of the various lubricants by increasing the test time. Data obtained from this study presented in Table 66 show that for five of the six lubricants very little differences in deposits levels exist between 3 and 4 hour test times. Lubricant TEL-90103 showed a much greater test specimen deposit for the 4 hour test. The following data show the differences in test specimen and seal deposits for both the 3 and 4 hour tests:

TABLE 66

EFFECT OF TEST TIME ON AFAPL STATIC COKER VALUES  
(300°C SS-302 TEST SPECIMENS, 0.5g SAMPLE, PTFE SEALS)

<u>Test Time</u>	<u>3 h</u>	<u>4 h</u>
Test Spec. Deposits mg/g	11.4 ± 1.0	17.8 ± 1.3
Seal Deposits, mg/g	15.2 ± 1.3	7.5 ± 1.4
Total Deposits, mg/g	26.6 ± 0.4	25.2 ± 0.9

These differences cannot be explained at this time. The good standard deviation of testing does not indicate a test problem.

The effect of using SS-302 seals in place of the normal PTFE seals used for ester based lubricants is shown in Table 67. The data show that lower deposit values are obtained when using stainless steel seals for both the test specimen and seal deposits. This difference may be caused by changes in the relative rate of evaporation to the rate of degradation since the AFAPL Static Coker is volatility oriented. Also stainless steel seals have more oil creepage, thus, reducing the quantity of oil on the coking surface and subsequently less test specimen coke. Since the steel seals are at a higher temperature the oil would undergo more coking which would reduce weighed seal deposits.

TABLE 67

COMPARISON OF AFAPL STATIC COKER DATA USING  
 SS-302 STEEL SEALS AND PTFE SEALS  
 (STAINLESS STEEL TEST SURFACE, 300°C TEST TEMP & 0.5g SAMPLE)

Lubricant	Deposits, mg/g			
	Stainless Steel Seal		PTFE Seal	
	Specimen	Total	Specimen	Total
O-91-13 (3h)	5.9 ± 0.8	22.2 ± 1.6	10.7 ± 0.8	29.1 ± 9.6
TEL-90104 (3h)	9.7 ± 0.5	11.7 ± 0.7	13.3 ± 0.8	16.2 ± 1.1
TEL-90104 (4h)	10.6 ± 0.6	13.3 ± 1.8	12.5 ± 1.5	15.8 ± 2.9
TEL-91003 (4h)	8.0 ± 1.7	15.1 ± 1.5	14.1 ± 2.9	21.3 ± 2.7

(6) High Temperature Polyphenyl Thioether (C-Ether)

AFAPL Static Coker testing was conducted on fluid O-64-20 (C-Ether) at various test temperatures and test times with data being given in Table 68. The data show that fluid O-64-20 has very low static coker deposit values for test temperatures of 325 to 400°C and for both the 3 and 4 hour test times. These deposit values are very similar to those obtained for 5P4E (polyphenyl ether) lubricant O-67-1 which had a test specimen deposit value of 0.3 mg/g and a total deposit value (test specimen plus seal) of 0.6 mg/g at 375°C test temperature and 3 hour test time. All deposits of O-64-20 consisted of a golden varnish.

The effect of oxidative prestressing on the Static Coker deposit values of O-64-20 fluid was investigated by conducting C&O testing (D 4871 tubes, 10 L/h airflow, condensate return) prior to Static Coker testing. Data obtained from this study given in Table 69 indicate that C&O prestressing increases the deposit forming characteristics of fluid O-64-20. The quantity of coke formed appears to reach a plateau somewhere between 72 and 144 hours of C&O stressing time. The deposits formed during the above testing consisted of light varnish. No significant difference in deposit values existed for the 320°C C&O 48 hour stressed samples obtained using condensate return versus no condensate return. This has been found not true for some fluids previously investigated.<sup>1,2</sup>

Previous research<sup>33</sup> indicated that the use of silver specimens in oxidation tests resulted in two to five times the rate of formation of higher molecular weight compounds relative to steel specimens. This research further implied a correlation between these results and extensive deposition that occurred during bearing rig testing with silver plated cages. A further implication of these results was that increased rates of formation of low volatility higher molecular weight products should result in higher coking deposits, as occurs with C&O stressed polyphenyl ether fluids. As such, various AFAPL Static Coker tests were conducted for determining the effect of silver on deposition characteristics of C-ether O-64-20. Data obtained from this investigation are given in Table 70.

The results for the fresh fluid, tested initially at 375°C for 3 hours, indicated the silver specimen to give a small increase in deposits although no visible coke was observed on either specimen. Lowering the test temperature to 325°C resulted in similar behavior of the silver test specimen having slightly more deposits than the SS-302 specimen. Since silver induced deposition could be more a function of C-ether oxidation products rather

TABLE 68

AFAPL STATIC COKER TEST DATA FOR C-ETHER O-64-20  
USING SS-302 TEST SPECIMEN, 0.5g SAMPLE

Test Temp. °C	Test Time, Hours	Test Spec. Deposits, mg/g	Total Deposits, mg/g
325	4	$0.2 \pm 0.1$	$0.2 \pm 0.1$
375	4	$0.2 \pm 0.1$	$0.2 \pm 0.1$
375	3	$0.2 \pm 0.2$	$0.3 \pm 0.3$
400	3	$0.3 \pm 0.2$	$0.6 \pm 0.6$

TABLE 69

EFFECT OF C&O PRESTRESSING ON AFAPL  
STATIC COKER DEPOSITS OF C-ETHER O-64-20

C&O Prestressing Conditions	Deposit <sup>1</sup> , mg/g	
	Test Specimen	Total
New Oil	0.2 ± 0.2	0.2 ± 0.2
290°C C&O, 72 H	0.6 ± 0.2	1.2 ± 0.3
290°C C&O, 114 H	0.9 ± 0.1	1.8 ± 0.2
290°C C&O, 240 H	0.9 ± 0.1	2.7 ± 0.1
290°C C&O, 312 H	0.9 ± 0.1	1.7 ± 0.1
320°C C&O 24 H	0.8 ± 0.4	1.2 ± 0.7
320°C C&O 48 H	0.8 ± 0.1	0.9 ± 0.1
320°C C&O 48 H(NCR) <sup>2</sup>	0.9 ± 0.1	1.9 ± 0.1
320°C C&O 48 <sup>3</sup>	0.2 ± 0.2	0.2 ± 0.1

<sup>1</sup>Static Coker Testing Conducted at 375°C, 0.5g Sample,  
SS-302 Test Specimen

<sup>2</sup>NCR - No Condensate Return

<sup>3</sup>Static Coker Test Temperature of 400°C

TABLE 70

EFFECT OF USING SILVER TEST SPECIMENS ON  
AFAPL STATIC COKER DEPOSITS OF C-ETHER O-64-20  
(TEST TEMP. 375°C, 3 TEST HOURS, 0.5 g SAMPLE)

Sample	Test Specimen	Deposits, mg/g	
		Test Specimen	Total
O-64-20	Silver	$0.7 \pm 0.3$	$1.1 \pm 0.2$
O-64-20	SS-302	$0.2 \pm 0.2$	$0.3 \pm 0.3$
O-64-20 <sup>1</sup>	Silver	$0.5 \pm 0.2$	$0.5 \pm 0.2$
O-64-20 <sup>1</sup>	SS-302	$0.2 \pm 0.1$	$0.2 \pm 0.1$
O-64-20 48 H, 320°C, C&O	Silver	$3.0 \pm 0.3$	$6.5 \pm 0.5$
O-64-20 48 H, 320°C, C&O	SS-302	$0.8 \pm 0.1$	$0.9 \pm 0.1$
O-64-20 + 1.35% DPBA <sup>2</sup>	Silver	$0.5 \pm 0.0$	$0.5 \pm 0.0$
O-64-20, 48 H, 320°C C&O + 1.35% DPBA	SS-302	$4.2 \pm 0.8$	$6.1 \pm 0.7$
O-64-20, 96 H 320°C C&O + 1.35% DPBA	Silver	$2.6 \pm 0.6$	$3.4 \pm 0.6$
O-64-20, 48 H 320°C C&O + Ag Coupon	SS-302	$0.7 \pm 0.4$	$1.5 \pm 0.6$
O-64-20, 48 H, <sup>1</sup> 320°C C&O Ag Coupon only	SS-302	$2.9 \pm 0.8$	$7.5 \pm 1.0$

<sup>1</sup>Test temperature of 325°C

<sup>2</sup>DPBA - Diphenylborinic anhydride

than the original composition, Static Coker testing was conducted using both type test specimens and a sample of 48 h, 320°C C&O stressed O-64-20 fluid. The results showed an increase in deposits for both type specimens but was much greater for the silver test specimen. Also, a greater deposit value was obtained when using only a silver test coupon during the 48 h C&O testing and subsequent use of a stainless steel coking test surface.

AFAPL Static Coker testing was conducted on samples of new and stressed O-64-20 fluid containing 1.35% (wt) of diphenylborinic anhydride additive (DPBA) which was investigated for reducing silver corrosion during corrosion and oxidation testing. Data obtained from these tests given in Table 70 indicate that the additive DPBA has very little effect on coking values when using either silver or stainless steel test specimens.

The effect of wear metal on the deposition characteristics of fluid O-64-20 was investigated using samples of the fluid after Four-ball wear testing with the results of subsequent Static Coker testing being given in Table 71. The data show that wear debris has no effect on the coking tendency of O-64-20 at the two lower test temperatures. An increase in deposit value did occur for the wear test sample conducted at 315°C.

#### (7) Summary

The coking characteristics of 16 4-cSt ester based lubricants had an average of 11.9 mg/g deposits with a standard deviation of 2.0 which indicate that these fluids (unstressed) have similar coking characteristics when determined using the AFAPL Static Coker. Three 4 cSt oils showed a much greater deposit level.

The use of stainless steel test specimens gave lower deposit values than shim stock test specimens. Stainless steel seals also give both lower test specimen deposits and seal deposits.

Increasing the test time from 3 to 4 hours had very little effect on deposit values of either the 4 cSt lubricants or the C-ether.

The C-ether O-64-20 had very low Static Coking values at test temperatures of 325 to 400°C. Like polyphenyl ether and other lubricants C&O prestressing of the fluid prior to coker testing increased deposit values. No difference in the deposit values occurred when using either condensate or no condensate return during C&O testing.

TABLE 71  
EFFECT OF WEAR METAL ON AFAPL STATIC COKER DEPOSITS  
FOR C-ETHER O-64-20

Four Ball Wear <sup>1</sup> Test Number	Wear Test Temp., °C	Deposits <sup>2</sup> , mg/g	
		Specimen	Total
New Oil	-	0.2 ± 0.1	0.2 ± 0.1
635	150	0.0 ± 0.0	0.0 ± 0.0
633	250	0.0 ± 0.0	0.0 ± 0.0
617	315	1.4 ± 0.3	1.8 ± 0.1
617	315	1.5 ± 0.4	1.7 ± 0.5
617	315	1.1 ± 0.1 <sup>3</sup>	1.5 ± 0.1

<sup>1</sup>Wear Test Conditions: M50 Balls, 3 h Test, 145N Loading

<sup>2</sup>Coker Test Conditions:; 375°C, 0.5g Sample, 3 h, SS-302 Specimens

<sup>3</sup> Test Time of 4 h

The use of silver coking surface had little effect on new O-64-20 fluid but showed an increase in deposit values for C&O stressed O-64-20 fluid compared to the deposit value obtained using SS-302 coking surface. C&O testing using only a silver corrosion coupon gave a much higher deposit value than that obtained using the normal C&O corrosion coupons.

The additive diphenylborinic anhydride (DPBA) used for improving silver corrosion of O-64-20 fluid during C&O testing had little effect on deposit values.

Wear debris samples obtained from four-ball wear testing at 250°C or below had no effect on deposit values. Wear testing at 315°C prior to Static Coker testing gave a significant increase in deposits.

b.     Micro Carbon Residue Tester (MCRT)

(1)    Introduction

Lubricant deposition studies of high temperature lubricants and experimental fluids have been continued using the Micro Carbon Residue Tester (MCRT). This deposition test is somewhat similar to the AFAPL Static Coker where coke is formed under non-flowing lubricant condition. The MCRT simulates "pockets" or "pools" of oil<sup>3</sup> subject to high temperatures where the Static Coker more simulates conditions of thin film coking occurring upon engine shutdown.

(2)    Apparatus and Procedure

The apparatus and test procedure have previously been described in detail.<sup>2</sup> Briefly, the MCRT test unit is essentially a temperature programmable sealed oven so that various heating cycles and test times can be conducted under varying and controlled atmospheric conditions. Test fluid samples are normally placed in glass vials circularly positioned in an aluminum basket.

The normal test procedure involves a one hour presoak at 150°C followed by a 30-hour coking period at 400°C using an air atmosphere (275°C coking temperature for high temperature ester base fluids) and then oven cool down to room temperature using normal static room air cooling. At the end of all tests, the vials are reweighed and the percent weight of coke is determined for each vial. Normally, 12 vials are used for each test and the averages of all values are reported.

### **(3) Test Lubricants**

Lubricants and experimental fluids investigated during this study are presented in Table 63 which are the lubricants and test fluids used in the AFAPL Static Coker study.

### **(4) Results and Discussion of Data**

#### **(a) General**

Appendix A shows the MCRT Coker data developed for the above lubricants. The data include test conditions such as type sample, sample size, test temperature and test hours, type and size of test vial, percent residue, standard deviation and a description of residue or deposits.

#### **(b) High Temperature Ester Base Fluids**

MCRT testing was conducted on 20 ester base 4 cSt lubricants with testing being conducted for 30 hours at 275°C using 3.5 cm vials. Table 72 displays the data showing the percent weight of the deposit, standard deviation of testing and deposit description.

The data in Table 72 show 95% of the samples (14 samples) have MCRT deposit values between 15.0 and 25.1% with an average of  $21.5 \pm 3.3\%$ . Lubricant O-86-2 had a value of 10.4% which is the lowest of all 4 cSt ester base fluids and would be low for MIL-L-7808 fluids which normally have higher volatility and lower MCRT coking characteristics. Lubricant O-86-2, along with lubricant O-91-13, have been reported as being different lots of lubricant O-85-1. The MCRT deposit values for these fluids are 16.4% (O-85-1), 10.4% (O-86-2) and 25.1% (O-91-13) which indicate they are not of the same formulation. C&O evaluations and AFAPL Static Coker testing also showed major differences in these three lubricants. The standard deviation of the MCRT testing is considered very good for deposition testing and in most cases was only 2 to 3 percent of the reported MCRT value. The deposits consisted of light to black varnish and brown to black hard or flaky coke. Some lubricants produced both varnish and coke depending upon deposit location within the test vials.

TABLE 72

**MCRT DEPOSIT VALUES FOR HIGH TEMPERATURE  
ESTER BASE LUBRICANTS  
(275°C, 30 H Test Time, 3.5 CM Vials)**

Lubricant	Deposit % Wt.	Std. Dev <sup>1</sup>	Type Deposits
O-85-1	16.4	± 0.3	Black uniform coke
O-86-2	10.4	± 0.6	Black uniform coke
O-90-6 <sup>2</sup>	15.9	± 0.3	Dark varnish
O-91-13	25.1	± 0.6	Dark varnish & black coke
TEL-90087	22.8	± 0.4	Dark coke
TEL-90103 <sup>2</sup>	24.7	± 0.8	Dark coke
TEL-90104 <sup>2</sup>	17.3	± 0.5	Dark coke
TEL-91002	15.7	± 0.4	Dark varnish
TEL-91003	24.0	± 0.3	Flaky coke
TEL-91005	24.3	± 0.3	Flaky coke
TEL-91053	22.4	± 1.0	Brown coke
TEL-91063	25.1	± 1.6	Brown coke
TEL-92036	24.2	± 0.3	Flaky brown coke
TEL-92039	23.6	± 0.3	Brown coke
TEL-92040	21.9	± 0.4	Brown coke
TEL-92041	21.6	± 0.3	Brown coke
TEL-92049	24.4	± 0.4	Flaky brown coke
TEL-92050	19.0	± 0.4	Dark varnish
TEL-93003	21.0	± 0.3	Dark varnish
TEL-93011	18.4	± 0.3	Brown varnish, black coke

<sup>1</sup>Standard Deviation for 12 vials

<sup>2</sup>Average 2 tests, 12 vial each

(c) High Temperature Polyphenyl Thioether

MCRT testing was conducted on fluid O-64-20 (C-Ether) using both 3.5 cm and 7.5 cm tall vials before and after 4-ball wear testing at two temperatures. All MCRT testing was conducted at 400°C, 30 test hours and 0.5 gram sample. Data obtained from this testing are given in Table 73. Data for polyphenyl ether lubricant O-67-1 are also shown for comparative purposes.

MCRT deposit values for new O-64-20 fluid are higher than that obtained for the polyphenyl ether lubricant using either of the two vial sizes. As expected, the tall vial gave more deposits due to less volatilization of the sample. The data in Table 73 also showed that wear debris has very little effect on the deposit forming tendency of fluid O-64-20 when using the two 4-ball test conditions for developing the wear debris.

(d) Effect of Dilution on MCRT Deposits of Polyphenyl Ether Lubricant O-67-1

MCRT testing was conducted on polyphenyl ether lubricant O-67-1 containing 25% tetrachloroethylene for determining inert solvent dilution effects. Test conditions were 400°C, 30 test hours, 0.5 g sample and 3.5 cm vials. A deposit value of  $3.7 \pm 0.5\%$  wt was obtained with the deposits consisting of coke on the bottom of the vial and varnish on the sides. This value is slightly higher than the value for O-67-1 lubricant ( $2.4 \pm 0.5\%$  by wt) indicating dilution may have a small effect on the MCRT deposit forming tendency of the polyphenyl ether lubricant.

(e) Correlation of MCRT with AFAPL Static Coker

Figure 46 shows the relationship between MCRT coking values and AFAPL Static Coker values for 19 4-cSt ester base lubricants. The data show that no correlation exists between the two tests. For 18 of the 19 lubricants, the deposit values fell within a box having a boundary of about 10 to 20 mg/g Static Coker deposits and 15 to 25% wt MCRT deposits. A greater spread is seen in the MCRT deposit values (16 fluids) than in the Static Coker deposit values. One fluid (O-86-2) showed a much greater Static Coker value relative to the MCRT value than all other fluids. No explanation can be given for this behavior other than its formulation may be vastly different from the other 18 lubricants.

TABLE 73

## MCRT TEST DATA FOR C-ETHER O-64-20

Sample	Type Vial	Deposits % Wt.	Type Deposits
Fresh O-64-20	7.5 cm	$13.6 \pm 0.3$	Varnish
Fresh O-64-20	3.5 cm	$6.7 \pm 0.2$	Varnish
Fresh O-64-20	3.5 cm	$6.7 \pm 0.3$	Varnish
Wear Test # 635 <sup>1</sup>	3.5 cm	$8.2 \pm 0.2$	Dark brown coke
Wear Test # 633 <sup>2</sup>	3.5 cm	$7.9 \pm 0.3$	Dark brown coke
Fresh O-67-1 <sup>3</sup>	3.5 cm	$1.5 \pm 0.8$	Dark Brown Varnish
Fresh O-67-1 <sup>3</sup>	7.5 cm	$11.3 \pm 1.7$	Dark Brown Varnish

<sup>1</sup>Wear Test Temp. of 150°C, 3 h test, 145 N load

<sup>2</sup>Wear Test Temp. of 250°C, 3 h test, 145 N load

<sup>3</sup>Data from Reference 3

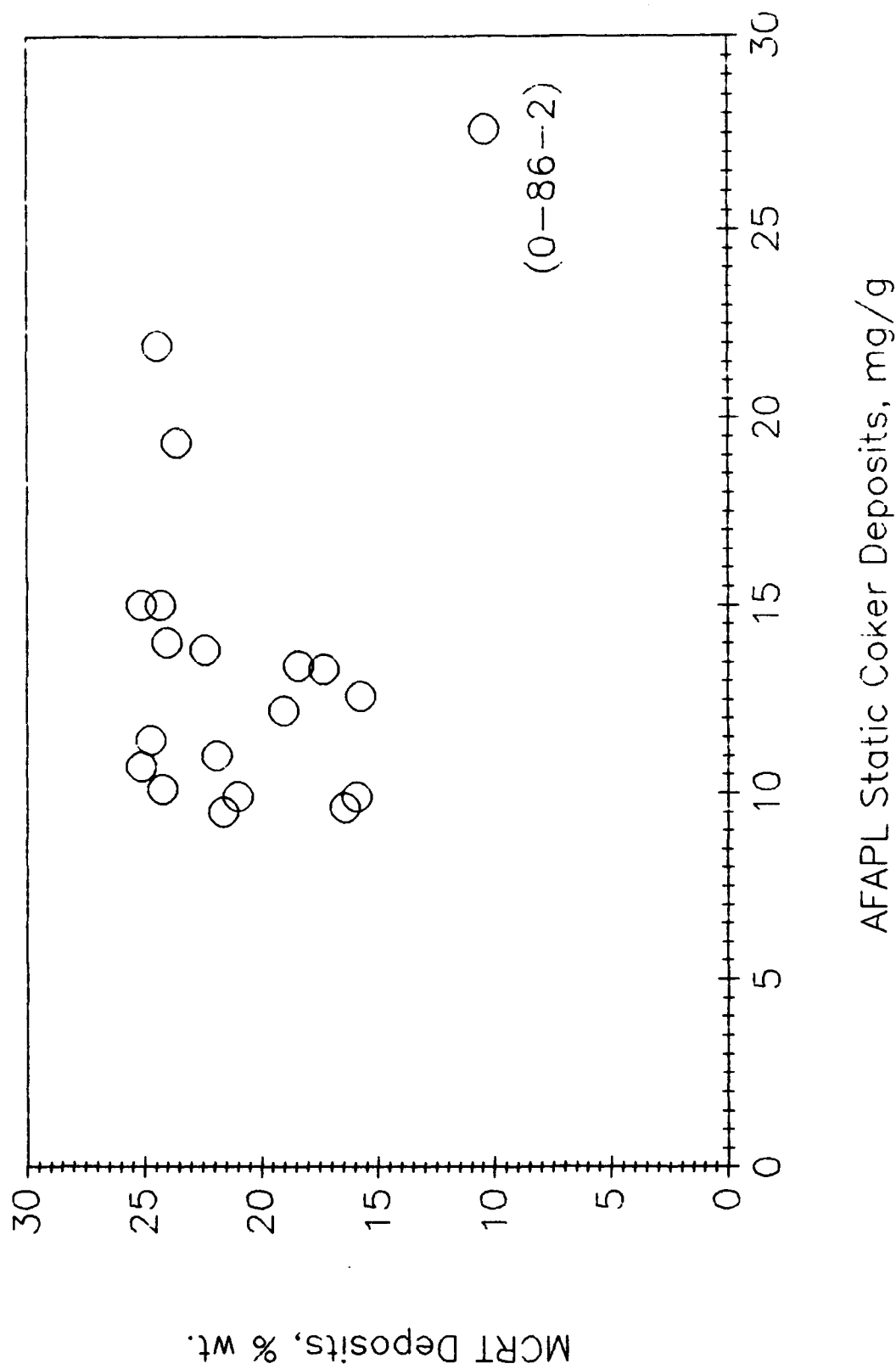


Figure 46. Correlation of AFAPL Static Coker Deposits with MCRT Deposits (New 4 cSt Oils).

(f) Summary

Deposition characteristics of 19 4-cSt ester base candidate lubricants were investigated using the Micro Carbon Residue Tester (MCRT). The deposit values ranged between 15 and 25% weight with the exception of one lubricant which displayed an unusual low value even for lower viscosity (normally higher volatility) MIL-L-7808 lubricants. Three of the fluids reported as being different lots of the same lubricant had major differences in coking values, indicating major formulation differences. The deposits of the 4 cSt lubricants consisted of light to dark varnish to black hard or flaky coke.

MCRT deposit values of the polyphenyl thioether were higher than those obtained on polyphenyl ether lubricant. Four-ball wear test debris had very little effect on the MCRT deposit value.

The addition of 25% (by volume) tetrachloroethylene to the PPE lubricant O-67-1 produced an increase in the MCRT deposit indicating such dilution may have some effect on the deposit forming characteristics of polyphenyl ether lubricant.

4. MINISIMULATOR

a. Introduction

A miniaturized high-temperature turbine engine lubrication system simulator (minisimulator) has been used to evaluate 5P4E basestock, inhibited 5P4E, and an ester. The minisimulator consists of an instrumentation panel, personal computer, and test stand (Figure 47). The test stand is a combination of two separate frames which support the two main components of the minisimulator, a heated lubricant sump and a test head (Figure 48). The fluid is pumped from the sump to the test head where a pair of 30-mm bore, angular contact bearings are spinning while under a mild Hertzian load. The test head is heated above the bulk oil temperature to further stress the test fluid, thereby, causing deposits to form on the components of the test section. This system is designed to operate with as little as a liter of lubricant and has provisions for lubricant sampling and makeup during testing. In addition, the system is corrosion resistant to all the known candidate lubricants and breakdown products.



Figure 47. Wright Laboratory Miniaturized High-Temperature Turbine Engine Lubrication System Simulator.



Figure 48. Minisimulator Test Stand.

**b. Apparatus**

A thorough description of the minisimulator is given in Reference 55, but the basic features of the system bear repeating. The minisimulator has maximum temperature capabilities for bulk oil, bearings, and hot spot of 400°C, 455°C, and 510°C, respectively. Band heaters placed around the test head and oil sump are used to obtain bearing and bulk oil temperatures, respectively, and a cartridge heater can be inserted into a cavity in the rear end cap of the head to produce a hot spot.

The number 2 main shaft bearing of the Allison T-63 turbine engine is used as the test bearing. The bearings have M50 balls and races and a silver-plated ASM-6415 cage. A pair of these bearings are mounted on the test shaft and are preloaded by an Inconel spring to a 100,000 psi Hertzian stress. Lubrication to each bearing is provided by two jets which spray test fluid into the gap between the outer race and cage at a predetermined rate.

**c. Test Method**

To evaluate a liquid lubricant in the minisimulator, 48-hour tests were originally performed using predetermined conditions for temperature, bearing speed, and test fluid flow rate. The test duration was accomplished in three 16-hour segments with a cool-down period between runs. Evaluation of the performance of a liquid from minisimulator testing is made based on deposition characteristics and analyses of oil samples.

Lubricant deposition is quantified by evaluating the oil-exposed surfaces within the test head. As specified in Reference 55, 10-ml samples of oil are drawn from the sump every 4 hours for viscosity and acidity measurements. Equal amounts of fresh fluid are added to the system after each drawn sample to maintain a constant volume, and fresh fluid is also added between test segments to compensate for losses due to deposition or leakage.

Oil samples are also analyzed for concentrations of specific metals. Originally, a total of six metal test coupons (aluminum, silver, titanium, Waspalloy, M50 and mill steel) were placed in the sump for lubricant/material compatibility analysis. The preweighed coupons are evaluated at the completion of each test both visually and for weight changes, but in addition, the oil samples are analyzed for any presence of elements which coincide with the metal coupons (Al, Ag, Ti, Co/Cr, and Fe), the minisimulator Inconel components (Ni/Cr), and the test bearings (Fe and Ag).

Over the course of eight minisimulator tests, refinements to the test procedure have been made to make data interpretation easier and testing more accommodating. The test schedule was shortened to allow the operator to monitor the equipment within the normal working hours of the laboratory. To this end, the three 16-hour test periods were replaced with four 9-hour segments for a reduction in total test duration of 12 hours. The volume for oil samples was reduced to 5 ml and was no longer replenished with fresh fluid to maintain the original sump volume. The diluting effect of periodic additions of fresh fluid interferes with the rate of viscosity increase for the test fluid and complicates analyses of additive depletion (when applicable).

The total amount of lubricant used to charge the sump before a test has been reduced to 850 ml. Because the minisimulator is intended for fluids of limited supply, revisions were made within the sump to accommodate the least amount of fluid that could be used. Limitations on oil volume are dependent on three system characteristics: the amount of tubing required to deliver fluid from the sump to the test head, the volume of the reservoir which allows flow measurements to be made, and the oil level within the sump necessary to keep the metal coupons constantly submerged even during flow rate measurements. The simplest way of reducing the fluid requirement without redesigning the entire system was to mount the metal coupons on several bolts secured to the pump instead of a single bolt. With two coupons per bolt, a total of four bolts would be used allowing two additional metals (bronze and magnesium) to be used to study catalytic effects along with the original six.

Before the start of each test segment, the test head and oil are slowly heated to their predetermined target temperatures while rotating the bearings at 5000 rpm. A ceramic fiber insulating blanket is wrapped around the test head and the oil line supplying the bearings to help maintain target temperatures. Even with these measures, the warm-up procedure can last up to 2 hours. Once the bearings are within approximately 50°C of their target values, the bearing speed is increased to 10,000 rpm, and data acquisition started. Careful monitoring of the minisimulator is necessary to ensure critical areas do not cool or overheat.

During warm-up, the drive motor of the pump is gradually increased until the desired flow rate is achieved (200 ml/minute for all minisimulator tests). Because of in-line pressure transducers, the oil pump must be started at its lowest setting when testing viscous fluids to avoid overstressing the sensors. The purpose of the transducers is to determine whether

the oil jets are clogging. The oil jets are simply 1/8-inch diameter tubes which are capped at one end and have a tiny orifice in the side allowing a high-velocity spray of test fluid to be delivered to the bearings. A pair of transducers are placed in series along the line supplying the oil jets so when a filter element is placed between them, the possibility of the jets clogging (and the bearings operating without lubrication) can be reduced. With two transducers, clogging of the jets will cause a pressure rise in both devices while clogging of the filter will cause a pressure rise in only one of them. Unfortunately, with some high temperature fluids such as PPE, high oil viscosity during start-up prevents the use of a filter.

#### d. Evaluation Procedure

When all test segments are completed, the oil from the sump is recovered and the machine is disassembled. Before cleaning, however, the 12 components of the test section (Figure 49) must first be rated for the severity of resulting deposits. The rating process is taken from the specification MIL-L-27502 and involves assigning values of 0 through 20 to the oil-wetted surfaces of the test head components (a value of 0 for clean parts, a value of 20 for the most severe carbon deposits). A listing of the various deposit types is given in Table 74 including descriptions for each deposit type and the criterion for determining the severity of each deposit. Table 74 also gives the corresponding demerit value for each deposit.

To compare deposits from one test to another, a total demerit rating is calculated for the entire test. The total demerit rating can range from 0 (if all parts were totally free of deposits) to 483 (if all parts were covered with heavy crinkled carbon). The total demerit rating is calculated by averaging the individual ratings for the oil wetted surfaces of the 12 test head components. The individual ratings are found by multiplying demerit values by the percentage of surface area covered by the respective deposit type. These area ratings are summed to account for 100% of the rated surface. The resulting value is multiplied by 10 and then by a weighting factor depending on the part being evaluated. The 12 individual test head ratings are then averaged to give the total demerit rating for the test. A listing of the rated test head components is given in Table 75 along with their respective weighting factors.

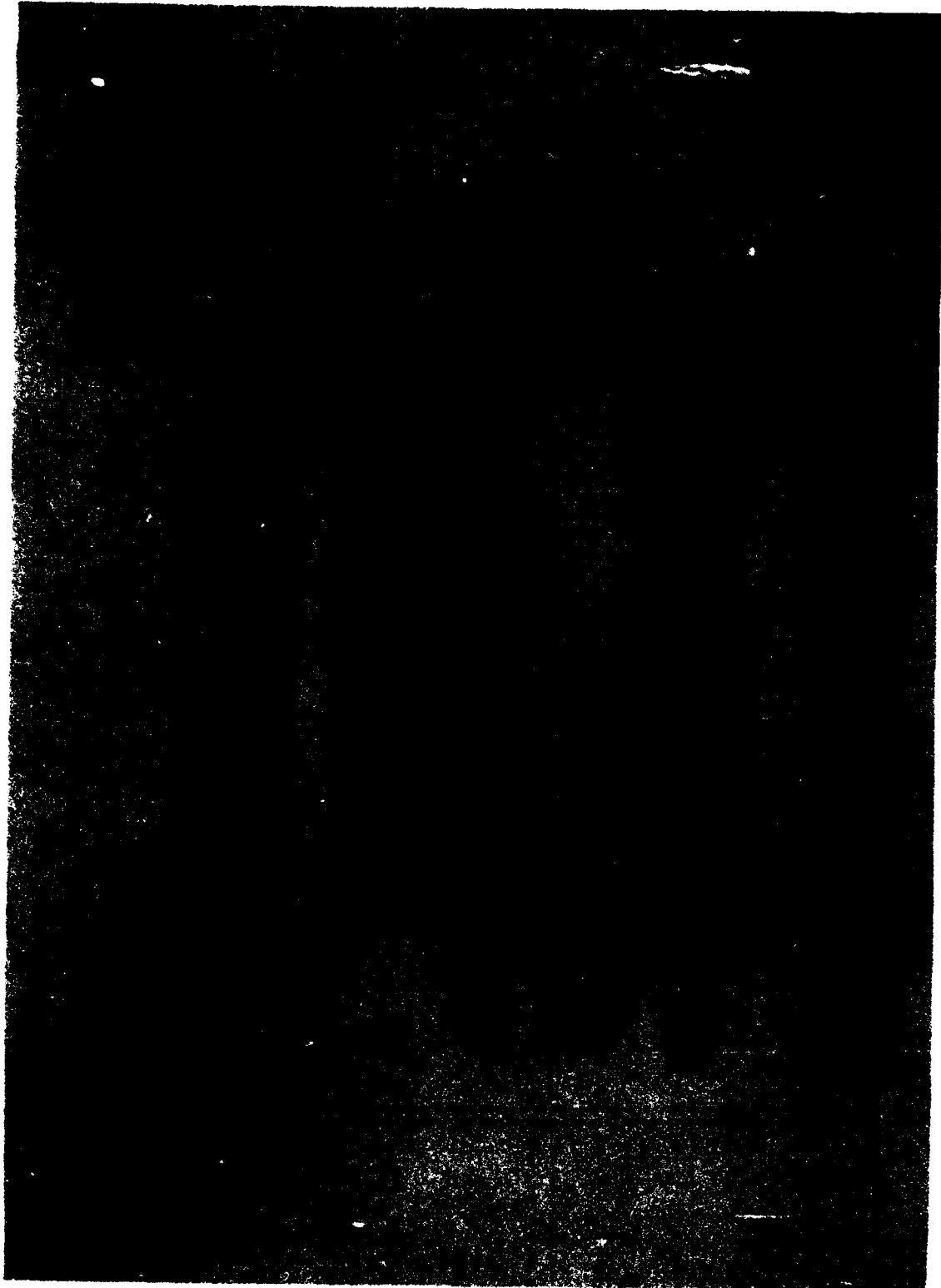


**Figure 49. Minisimulator Test Section Components.**

TABLE 74  
DEPOSIT TYPES AND THEIR DEMERIT VALUES

DEPOSIT	DESCRIPTION	RATING
Varnish	Shiny lacquer-like coating	
Light	Light gold or yellow; translucent	1
Medium	Brown or dark brown; translucent	3
Heavy	Black; opaque	5
Sludge	Shiny, oily emulsion of carbon and oil, usually light brown in color; removable by wiping with a rag	
Light	Less than 1/64 inch thick	6
Medium	Between 1/64 and 3/64 inch thick	7
Heavy	More than 3/64 inch thick	8
Smooth Carbon	Smooth carbonaceous coating; not removable by wiping with a rag	
Light	Less than 1/64 inch thick	9
Medium	Between 1/64 and 3/64 inch thick	10
Heavy	More than 3/64 inch thick	11
Crinkled Carbon	Carbonaceous coating with ridged or uneven surfaces; not removable by wiping with a rag	
Light	Less than 1/64 inch thick	12
Medium	Between 1/64 and 3/64 inch thick	13
Heavy	More than 3/64 inch thick	14
Blistered Carbon	Carbonaceous coating with blistered or bubbled surfaces; not removable by wiping with a rag	
Light	Less than 1/64 inch thick	15
Medium	Between 1/64 and 3/64 inch thick	16
Heavy	More than 3/64 inch thick	17
Flaked Carbon	Carbonaceous coating with flaked, peeling, or broken blisters; not removable by wiping with a rag	
Light	Less than 1/64 inch thick	18
Medium	Between 1/64 and 3/64 inch thick	19
Heavy	More than 3/64 inch thick	20

TABLE 75

**DEMERIT WEIGHTING FACTORS FOR THE COMPONENTS  
OF THE MINISIMULATOR TEST SECTION**

Test Section Component	Weighting Factor
Spacer	1
Oil Slinger	1
#1 End Cover	1
#2 End Cover	1
Test Head	2
Drive Shaft	2
Bearing Retainer	2
Hot Spot Heat Shield	3
#1 Bearing Mount	3
#2 Bearing Mount	3
#1 Bearing	5
#2 Bearing	5

When the sump is disassembled, the metal coupons inside are solvent-cleaned and allowed to air dry before reweighing to determine whether any catalytic reactions took place. The weight changes are reported with respect to the amount of surface area of each coupon. Values above  $0.2 \text{ mg/cm}^2$  are considered significant. No significant weight changes in any of the metal coupons took place during the eight minisimulator tests.

**e. Results**

Table 76 summarizes the results of all minisimulator tests performed to date. Except for the initial test, in which an ester was used, PPE was the test fluid. Tests WLM003 and WLM004 both used an inhibited PPE. The flow rate during test WLM005 was substantially lower than the intended rate of 200 ml/minute because of a pump misalignment. The duration of test WLM008 was cut short due to an oil leak at the start of the third 9-hour segment which depleted 70% of the test fluid.

TABLE 76

## MINISIMULATOR TEST SUMMARY

Test Number	Duration, hours	Fluid	Quantity, mL	Target Temp., °C		Rating
				Oil	Bearing	
WLM001	48	Ester	1200	175	260	78.7
WLM002	48	5P4E	1200	300	360	114.0
WLM003	48	5P4E*	1200	300	360	147.1
WLM004	48	5P4E*	1200	300	360	134.8
WLM005	48	5P4E	1370	300	360	161.6
WLM006	48	5P4E	1370	175	260	8.1
WLM007	36	5P4E	950	300	360	107.9
WLM008	18	5P4E	850	300	360	79.0

\* Inhibited 5P4E

The changes in fluid viscosities during minisimulator tests are shown in Figures 50, 51, and 52. In Figure 50, the oils used in WLM002 (ester) and WLM006 (PPE basestock) are compared. The ester was tested at the limits of its effective temperature range while the PPE was used at the same conditions to allow a one-to-one comparison of their percentage of viscosity increase (as well as their deposition characteristics). Figure 51 compares the plots of two inhibited PPE tests to the basestock fluid. The percent viscosity increases for each of four PPE basestock tests run at high temperature (WLM002, WLM005, WLM007, and WLM008) are compared in Figure 52.

The temperatures given in Table 76 represent targeted values for the bulk oil and bearings. These two quantities, however, do not totally characterize test conditions. The temperature of the oil at the inlet of the oil jets is also an important measure because the test fluid acts as both lubricant and coolant. The oil inlet temperature determines how often the bearing heaters must be powered to compensate for the cooling effect and maintain desired bearing temperature. Bearing temperatures should not be significantly affected by the oil inlet temperature, however, bearing heater cycle time will affect the temperatures of all other test head components. Table 77 compares the average temperature profiles during the eight minisimulator tests performed to their intended target values.

## MINISIMULATOR Oil Comparison

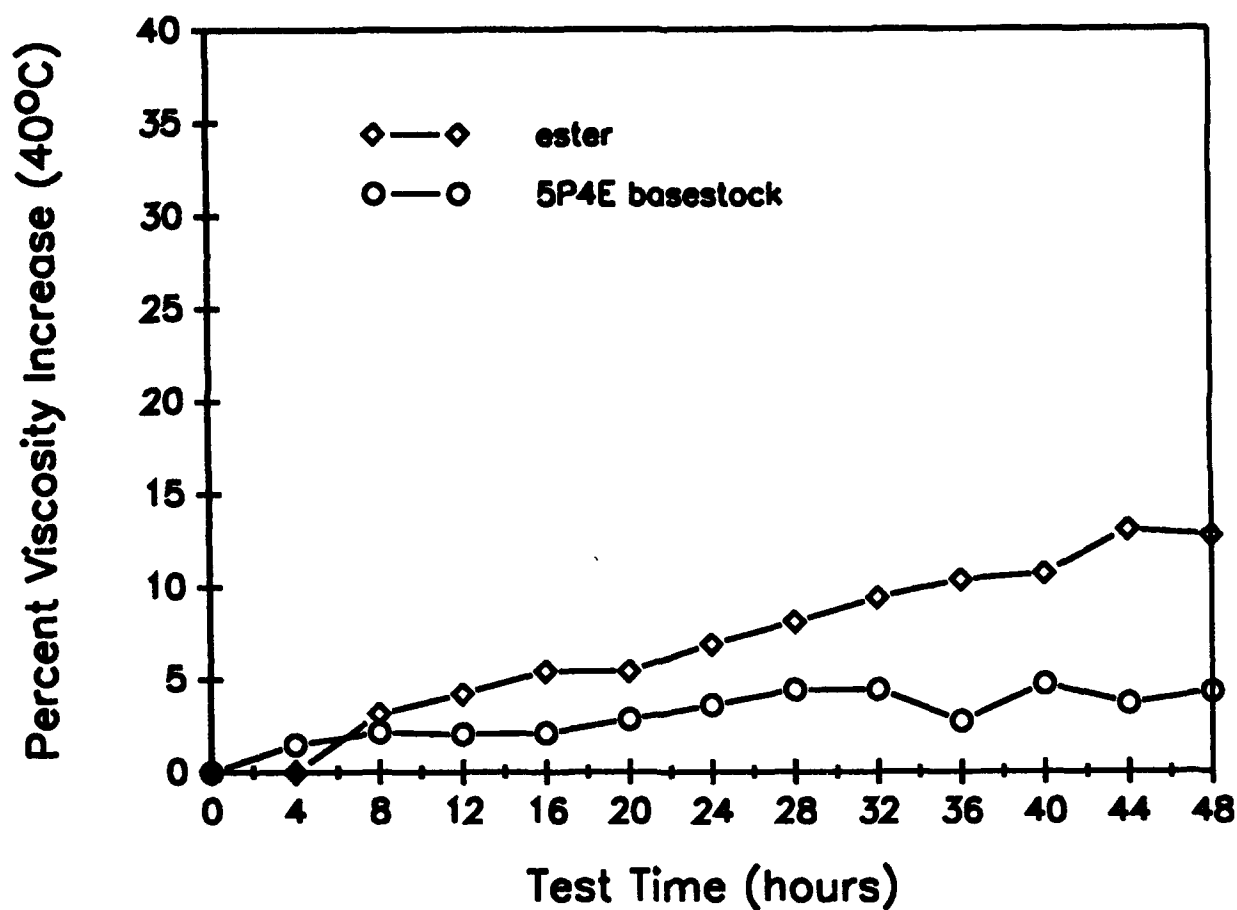


Figure 50. Viscosity Increases for an Ester (O-87-2) and PPE Basestock (O-77-6) During Minisimulator Tests at 175°C Bulk Oil and 260°C Bearing Temperatures.

## MINISIMULATOR Oil Comparison

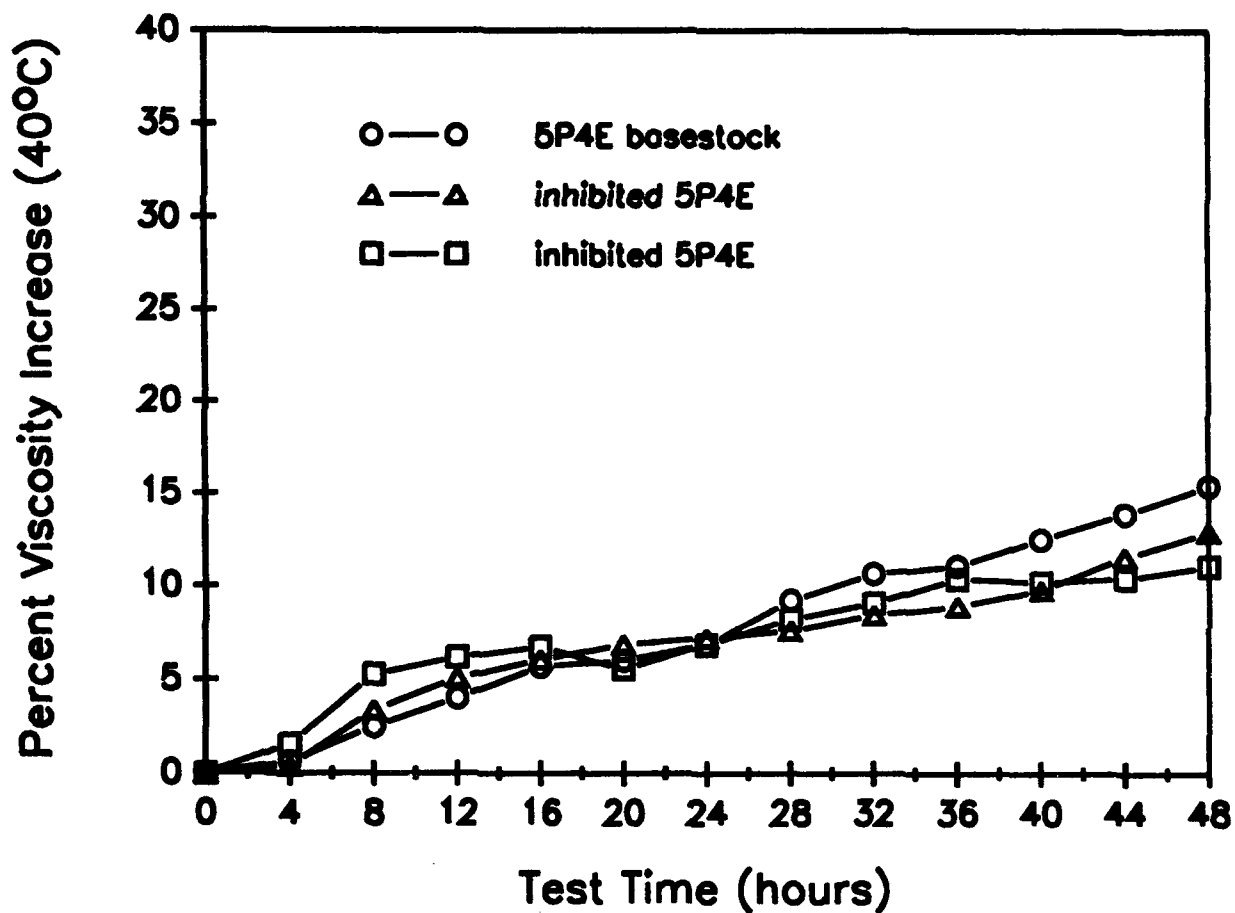


Figure 51. Viscosity Increases for PPE Basestock (O-77-6) and Inhibited PPE (TEL-90102) During Minisimulator Tests at 300°C Bulk Oil and 360°C Bearing Temperatures.

## MINISIMULATOR 5P4E Basestock Comparison

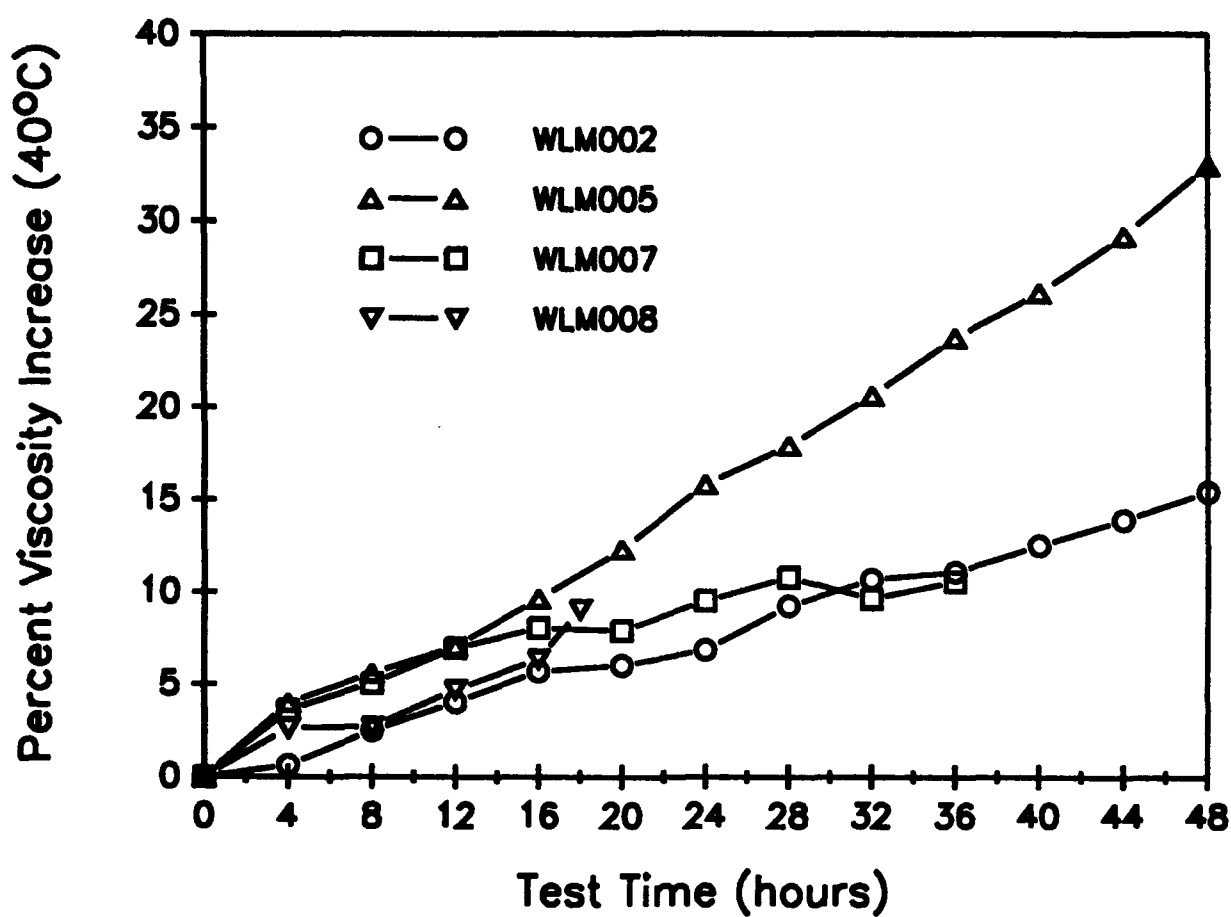


Figure 52. Viscosity Increases During Four Minisimulator Tests of PPE Basestock (O-77-6) at 300°C Bulk Oil and 360°C Bearing Temperatures.

TABLE 77

COMPARISON OF TARGET TEMPERATURES (°C) TO AVERAGE TEMPERATURES (°C)  
FOR CRITICAL SECTION OF THE MINISIMULATOR

Thermocouple Location	Target Temperature	WLM001 Average	WLM006 Average	Target Temperature	WLM002 Average	WLM003 Average	WLM004 Average	WLM005 Average	WLM007 Average	WLM008 Average
Oil Sump	175	176	186	300	301	299	300	299	300	300
Bearing Housing	None	299	337	400	411	380	420	406	409	407
Hot Spot										
Top	None	244	266	460	360	335	368	347	426	439
Bottom	None	244	271	460	365	336	374	345	422	437
#1 Bearing										
Top	260	253	262	360	361	325	365	360	356	351
Bottom	260	248	259	360	361	315	355	354	353	355
#2 Bearing										
Top	260	259	258	360	363	340	360	358	363	359
Bottom	260	247	255	360	356	337	354	350	359	362
#1 Bearing Oil Inlet										
Top	175	169	141	300	290	262	242	219	261	240
Bottom	175	173	166	300	289	246	157	198	265	260
#2 Bearing Oil Inlet										
Top	175	171	160	300	287	254	244	246	250	236
Bottom	175	171	165	300	291	251	228	235	247	248

In tests WLM007 and WLM008, a cartridge heater was inserted into the recess in the rear end cap of the test head to produce a "hot spot" (see Figure 53). The hot spot heater provided a further challenge in maintaining consistent temperature profiles because of the added heat to the test head. For example, a target temperature of 460°C was chosen for the hot spot, but at this temperature, the rear bearing was susceptible to uncontrollable overheating. In order to control overheating, cooling coils were wound into a gap between the rear end cap and the test head. Even with these measures, the hot spot had to be reduced from 460°C to 440°C.

It was stated earlier that the metal coupons submerged in the oil sump had negligible weight changes for all tests. Analysis of the oil samples confirmed that Ti, Al, Cu, and Mg corrosion was not present. However, concentrations of Fe, Ag, Cr, and Ni were consistently detected in most of the oil samples from all tests. The greatest concentrations of these elements during each test are presented in Table 78.

TABLE 78

MAXIMUM ELEMENTAL CONCENTRATIONS IN OIL  
SAMPLES FROM MINISIMULATOR TESTING  
(Tests WLM001-WLM004 by PWMA, Tests WLM005-WLM008 by AE)

Test	PPM			
	Fe	Ag	Cr	Ni
WLM001	*	*	*	*
WLM002	*	*	10.7	2.6
WLM003	1.6	1.1	19.6	3.7
WLM004	1.7	5.2	8.4	1.5
WLM005	1.0	*	7.9	2.4
WLM006	1.2	0	2.8	2.3
WLM007	2.3	*	11.7	2.5
WLM008	2.5	*	15.2	2.3

\* less than 1 ppm

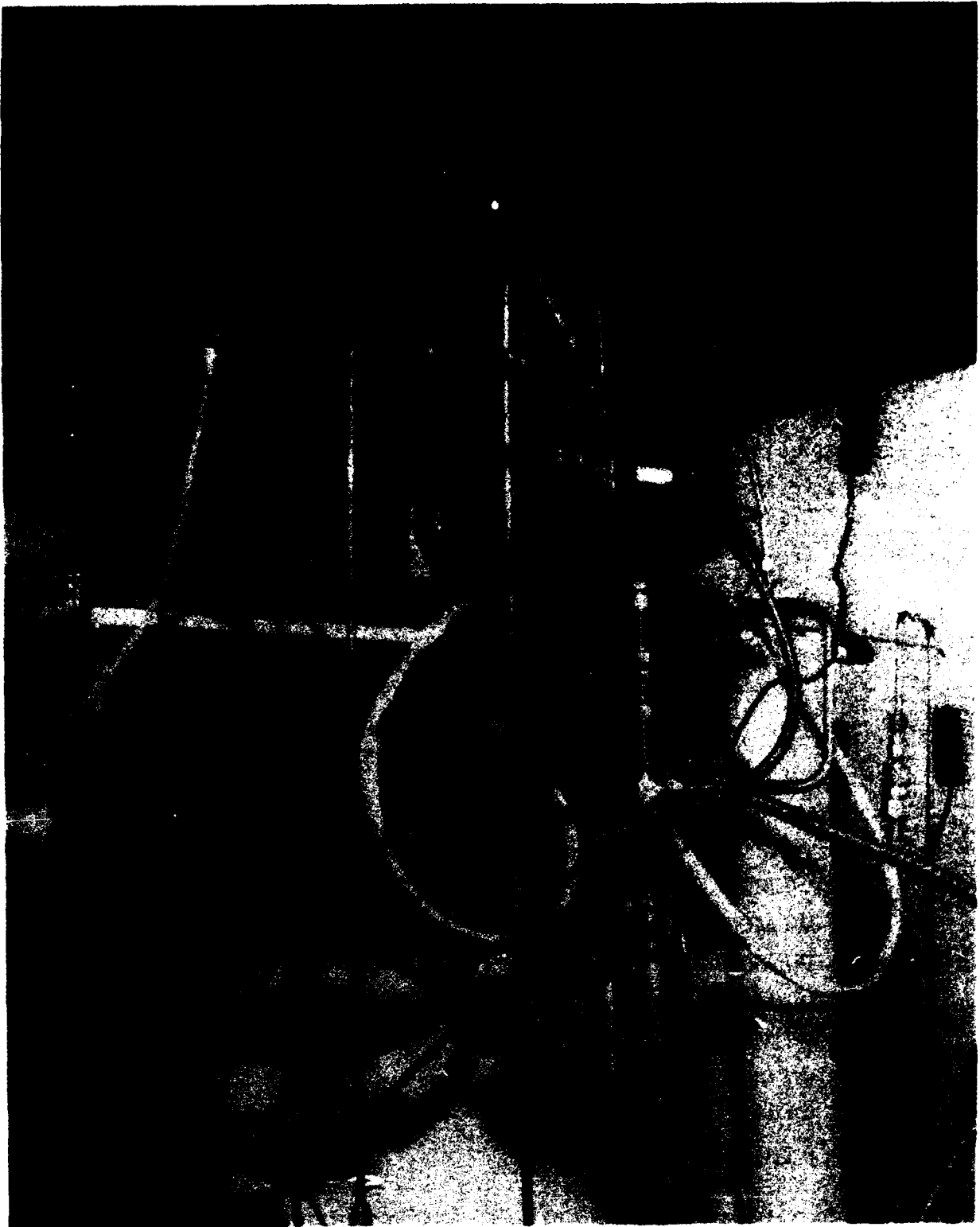


Figure 53. Minisimulator Test Section.

Appreciable amounts of Cr were consistently found in PPE samples from high-temperature tests (300°C bulk oil, 360°C bearing temperatures). Fe concentrations as high as 2.5 ppm and Ni concentrations as high as 3.7 ppm were present in PPE samples also. Trace amounts of Ag were detected in most tests (except for WLM004 which had 5.2 ppm and WLM006 which had zero Ag concentration). Although Fe and Ag comprise three of the eight metal coupons used, their presence in the oil can be attributed to run-in wear of the bearing balls (M50 steel) against the cage (Ag-plated ASM-6415 steel).

The presence of Ni is believed to be attributed to tightening wear of the many Inconel tubes and fittings of the minisimulator. Since Ni and Cr are the primary constituents of Inconel 600, Inconel wear particles in the oil should give approximately 3 times as much Ni as Cr. The disproportionate amount of Cr suggests that Inconel wear may not be responsible for all of the Cr present in samples. In comparing the Cr and Ni concentrations of tests WLM001 and WLM006, PPE samples contained as much as 2.8 ppm of Cr and 2.3 ppm of Ni while only trace amounts of these two elements were present in ester samples although the bulk oil and bearing temperatures were identical during these tests. The disparity in concentration may suggest that some reactivity between the PPE and the Inconel may occur which may account for even higher Cr concentrations when the test temperatures are increased.

#### f. Discussion

To ensure that unblemished surfaces are initially present where deposit will likely form, all of the test head components, except the ball bearings, are thoroughly cleaned and polished after each test. The bearing surfaces cannot be brought back to their original metallic finish, however, and new bearings are used for each test even though no visible bearing wear was detected after any of the minisimulator tests. Interpretation of the surface discoloration of the bearings is difficult because oxidation of the M50 steel darkens formed varnish deposit. Typically, the bearings have varnish deposits on the races and balls and sludge deposits on the exposed faces of the cage, but the severity of the varnish deposits (light, medium, or heavy) is at times only a guess.

The qualitative nature of the deposition rating procedure causes an unavoidable degree of uncertainty with resulting total demerit ratings. In order to provide consistent evaluations, two reviewers rated the parts beginning with WLM007, and the total ratings from each individual review are averaged together. This measure, along with increased efforts to more precisely control critical test section temperatures allows more viable comparisons between tests at identical conditions. Temperature repeatability is essential if the deposition characteristics of different oils are to be compared.

Any comparison of the demerit ratings of tests done at "identical" conditions must take into consideration the exact temperatures maintained during the test as well as the lubricant flow rate. The highest total demerit rating for any test was 161.6 (corresponds to WLM005) which resulted from a steadily decreasing flow rate due to a pump malfunction. A comparison of the ratings for tests WLM002 and WLM005 (both have similar temperature profiles and both used PPE basestock) indicates that the lower flow rate of WLM005 resulted in a total demerit rating increase of 47.6 (see Table 76). Two other tests had high demerit ratings (WLM003 and WLM004), but these tests were characterized by persistent periods of overheating. Although tests WLM003 and WLM004 used an inhibited PPE, the severe deposits formed on some test head components, particularly the bearing housing (see Figure 54), were responsible for their high ratings (see Table 76).

The center of the bearing housing is most susceptible to severe deposit formation because of excess heat accumulation from the bearing heaters. The information in Table 77 indicates that the average test head temperature was greatest during WLM004 (420°C). Since the chosen target value for the test head was 400°C, all high-temperature tests (WLM002, WLM003, WLM004, WLM005, WLM007, and WLM008) had average test head temperatures within 5% of the intended value. Maximum test head temperatures for tests WLM003 and WLM004, however, were as high as 450°C during one of each of their three test periods. To prevent test head overheating from possibly influencing deposition during future tests, measures were taken to better control the test head temperature.

Test head temperature was originally controlled by varying the amount of fiber insulation around the ends of the test head where the bearing heaters were placed. The middle of the test head was left exposed to allow excess heat to escape. Unfortunately, these measures still allowed short periods of overheating to occur, and precise control over the head temperature was impossible to achieve. To gain reliable control over the test head temperature, cooling coils were wrapped around the housing, between the two bearing heaters. The introduction of a compressed airflow with a regulating valve provided some degree of control over cooling. To demonstrate the effectiveness of the cooling coils in reducing instances of test head overheating, two tests have been run using a 400°C test head target temperature. This value was set based on the average values from previous tests, and the only instance of overheating (430°C) occurred during the first 9-hour segment of WLM007 (the first test using the cooling coils).

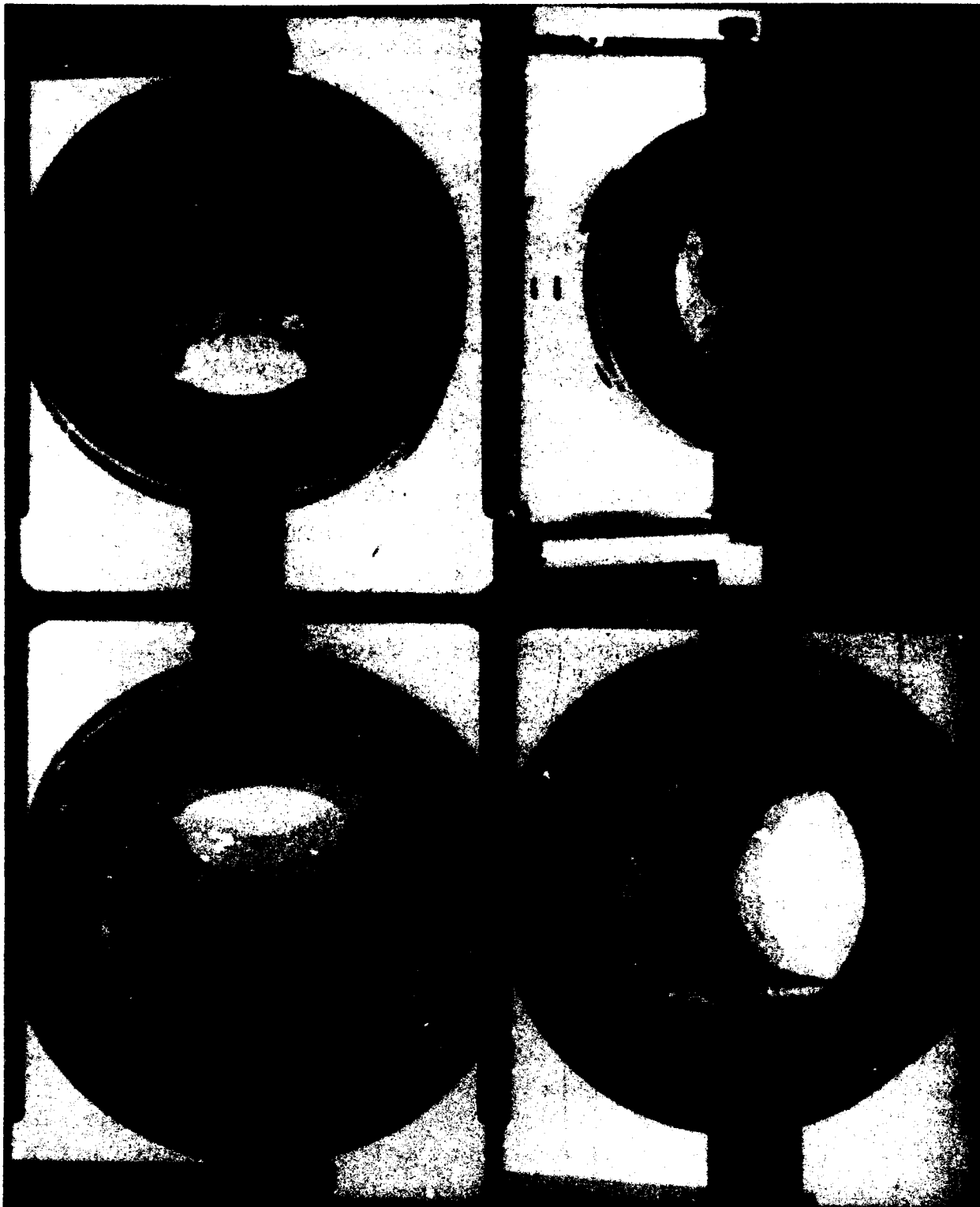


Figure 54. Deposits Within the Test Head from Inhibited PPE (TEL-90102)  
After WLM003.

The selective viscosity increase comparisons made in Figures 50, 51, and 52 are based on the targeted bulk oil and bearing temperatures of each test. Because the total oil volume varied from 1200 ml in initial tests to a final value of 850 ml (see Table 76), the amount of fluid used may impact viscosity measurements as well as deposition within the test head. By lowering the total oil volume, the ratio of fluid in the sump to fluid in the test head is also lowered. Since the test head is considerably hotter than the sump, the test fluid is more severely stressed when reduced oil volumes are used.

In Figure 50, the viscosity increases during tests of an ester (WLM001) and a PPE basestock (WLM006) are compared. The figure indicates that at the same bulk oil and bearing temperatures, the overall viscosity increase of PPE is substantially less than that of the ester. From Table 76, the difference in the total demerit rating between these two tests is even more dramatic (78.7 for the ester and 8.1 of the PPE). However, the total oil volume used in WLM006 was 170 ml greater than test WLM001 (see Table 76). The difference in the oil volumes is due to different sampling procedures. Each oil sample taken from WLM001 was replaced with the same amount of fresh fluid, but an excess 170 ml was used in WLM006 so that no fresh fluid would have to be added to attain the same final oil volume as WLM001. Therefore, despite different initial oil volumes, comparisons of the viscosity increases and demerit ratings for these two tests are still valid.

Figure 51 compares the viscosity increases during two tests of inhibited PPE (WLM003 and WLM004) to a single test of PPE basestock (WLM002). The initial oil volumes and sampling procedure (an equal amount of fresh fluid was added after each sample) were the same for all three tests. The presence of an antioxidant additive in the inhibited PPE did not significantly alter sample viscosities with respect to the basestock fluid. A significant difference does exist between the total demerit ratings for the two inhibited tests and the rating for the basestock test (see Table 76). It was mentioned earlier that test head overheating (by up to 12.5% over the target value) periodically occurred during WLM003 and WLM004. Whether or not it was these excessive thermal stresses or the antioxidant additive that was responsible for the high demerit ratings (severe deposits) of WLM003 and WLM004 remains unclear.

The final comparison of viscosity increases (Figure 52) is for all tests using PPE basestock. Although the total oil volume differs for each of the four tests shown, some general observations can still be made. The dramatic increase in the oil viscosity from test WLM005 can be attributed its reduced flow rate. Earlier, the flow rate during WLM005 was said to be responsible for the large demerit rating as compared with WLM002. A difference in the initial oil volumes for these two tests (see Table 76) is not likely to have contributed to the disparity in

their percent viscosity increases or demerit ratings. Both tests WLM007 and WLM008 used the smallest fluid volumes (950 ml and 850 ml, respectively), yet their viscosity increases are similar to WLM002 within the same time period although stresses on the fluid were greater.

The shortened durations of WLM007 and WLM008 do indicate that deposit formation is somewhat time dependent. From Table 76, the rating for the 18-hour WLM008 test is 79.0, the rating for the 36-hour WLM007 test is 107.9, and the rating for the 48-hour WLM002 test is 114.0. The small difference in the ratings between the 36-hour and 48-hour tests suggests that the evolution of deposits (from varnish to sludge to the various types of carbon) ceases after a certain time for given conditions.

#### g. Conclusions

Although the minisimulator cannot fully duplicate an actual engine environment, it still allows screening of high-temperature fluids under reasonable operating conditions. Tests establish the capability of a fluid to provide lubrication without excessive thermal or oxidative degradation. The deposit types formed on minisimulator components can be used not only to rank tests, but to provide an example of the deposit severity likely to be generated by the next generation of turbine engines. More tests, however, must still be done to establish the repeatability of both the testing procedure as well as the rating procedure before other candidate fluids are tested. Once sufficient baseline tests have been run, other avenues of testing can be explored such as inerting the test head and sump, increasing the axial load to induce wear, and varying test conditions to better qualify their effect on deposit formation.

### 5. LUBRICANT FOAMING

#### a. Introduction

The importance of the foaming characteristics of turbine engine lubricants has been previously discussed<sup>56</sup> with excessive foaming and aeration causing increased gear and bearing temperatures, a decrease in lubrication, oil pump cavitation and, in some cases, loss of oil "overboard" through oil system breather vents. Early efforts in the investigation and developments of test methods for measuring lubricant foaming were directed toward normal mineral oils and ester base lubricants requiring relative large sample volumes. Test methods developed during these studies are described by Federal Test Method 791, Method 3213 (Static Foam Test) and by Method 3214 (Dynamic Foam Test). A small volume 25 mL test method was developed<sup>1,2</sup> for use in the investigation of the foaming and aeration characteristics of experimental fluids where large sample volumes are not available. Recent studies<sup>3</sup> resulted in

the development of foam and aeration testing capability up to 200°C for use in the evaluation of high temperature lubricants and experimental fluids.

This study describes continued effort for improving high temperature foam testing capability and the evaluation of various fluids representing different chemical classes of potential lubricants with respect to foaming and aeration characteristics at high temperatures.

#### b. Test Apparatus and Procedure

Two test methods were used during the course of this study. Federal Test Method 3213 was modified by varying the test temperature from the normal 80°C to 200°C for high temperature lubricants and experimental fluids. This was accomplished by using a high temperature viscosity oil bath containing inhibited polyphenyl ether as the bath oil. The bath was modified to accept either the normal 500 cc foam test graduated cylinder or the small volume 250 cc foam test graduated cylinder. An air preheating coil was used in the bath to insure correct oil test temperature during aeration. The small volume test<sup>2</sup> conducted at 200°C incorporated the revised aeration procedure of initiating testing at a low airflow rate (100 cc/min) and increasing the airflow after foam stabilization to various airflow levels until an airflow of 1000 cc/min is obtained. Foam testing using both sample sizes were conducted using the ASTM diffuser stone (Method 3213) and 13/16 inch diameter five micrometer pore size metal sparger (25 mL test). Testing of advanced ester based 4 cSt lubricants were conducted at the normal 80°C test temperature using both the Federal Test Method 3213 and 25 mL test if sufficient sample existed.

#### c. Test Lubricants

Nineteen high temperature lubricants and experimental fluids were investigated during this phase of the program and are described in Table 79 which also includes four lubricants that were previously evaluated.<sup>3</sup> Appendix A gives detailed foaming data for the lubricants and fluids investigated.

#### d. Results and Discussion

##### (1) High Temperature Ester Base Fluids

Foam and aeration data obtained on 18 ester base fluids are given in Table 80. Eight of the samples showed very low foaming values (<20 mL) for either test and both airflow rates. These fluids had good oil/foam interfaces and foam collapse times usually below 10 seconds. Six of the samples showed low foaming values with very low (<10 s) collapse times

TABLE 79

## DESCRIPTION OF FLUIDS USED IN FORMING STUDIES

Fluid	Description	Viscosity, cSt	
		40°C	100°C
O-67-1	MIL-L-8700 Oil (5P4E)	280.3	12.61
O-85-1	Candidate Oil, Ester Base	17.68	4.04
O-86-2	Different Lot of O-85-1	17.63	4.01
O-90-6	Different Lot of O-85-1	17.62	4.00
O-91-13	Candidate Oil, Ester Base	18.51	4.14
TEL-9050 <sup>1</sup>	Experimental Fluid	214.3	10.88
TEL-90001 <sup>1</sup>	Experimental Fluid	235.4	16.25
TEL-90024 <sup>1</sup>	Inhibited TEL-9050 Type Fluid	193.4	10.66
TEL-90087	Candidate Oil, Ester Base	17.65 <sup>2</sup>	3.94 <sup>2</sup>
TEL-90103	Candidate Oil, Ester Base	17.09	3.97
TEL-90104	Different Lot of O-85-1	17.68	4.00
TEL-91001	Modified TEL-8039	289.2	12.67
TEL-91002	Candidate Oil, Ester Base	17.69	4.00
TEL-91005	Candidate Oil, Ester Base	17.76	4.04
TEL-91063	Candidate Oil, Ester Base	17.01	4.02
TEL-92036	Candidate Oil, Ester Base	18.38	4.10
TEL-92039	Candidate Oil, Ester Base	18.04	4.10
TEL-92040	Candidate Oil, Ester Base	16.63	3.99
TEL-92041	Candidate Oil, Ester Base	17.56	4.10
TEL-92049	Candidate Oil, Ester Base	18.25	4.10
TEL-92050	Candidate Oil, Ester Base	17.66	4.05
TEL-93003	Candidate Oil, Ester Base	17.50	4.09
TEL-93011	Candidate Oil, Ester Base	17.58	3.99

<sup>1</sup>Foam Testing conducted during Interim Reporting Period, Ref. F-3

<sup>2</sup> Viscosity values for different lot

TABLE 80

**FOAMING CHARACTERISTICS OF HIGH TEMPERATURE  
ESTER BASE LUBRICANTS**

(Test Temperature of 80°C, Foam Values in mL)

Fluid	25 mL Volume Airflow cc/min			Fed. Test # 3213 Airflow, cc/min		
	500	1000	Comment	500	1000	Comment
O-85-1	6	8	a <sup>1</sup>	5	8	a <sup>1</sup>
O-86-2	4	18	a <sup>1</sup>	6	8	a <sup>1</sup>
O-90-6	5	6	a <sup>1</sup>	5	8	a <sup>1</sup>
O-91-13	6	8	a <sup>1</sup>	7	10	a <sup>1</sup>
TEL-90087	-	-	-	41	68	a
TEL-90103	28	48	b <sup>2</sup>	I/S <sup>3</sup>	I/S	-
TEL-90104	6(45) <sup>4</sup>	8(50)	b	200	305	b
TEL-91002	4	5	a	7	11	a
TEL-91005	40	42	b	220	300	b
TEL-91005 <sup>5</sup>	64	66	b	210	290	b
TEL-90063	9	13	a	10	15	a
TEL-92036	6	12	a	5	10	a
TEL-92039	1	4	a	I/S	I/S	-
TEL-92040	5	8	a	"	"	-
TEL-92041	6	8	a	"	"	-
TEL-92049	4	5	a	"	"	-
TEL-92050	4	2	a	"	"	-
TEL-93003	2	6	a	5	8	a
TEL-93011	6	38	a	I/S	I/S	-

<sup>1</sup>a: Good oil/foam interface

<sup>2</sup>b: No oil/foam interface

<sup>3</sup>I/S: Insufficient sample

<sup>4</sup>: Oil had questioned oil/foam interface.

Values in ( ) includes severe aeration

<sup>5</sup>TEL-91005: Repeat test

using the small volume test. However, insufficient samples prevented testing using Method 3213. Three fluids showed severe aeration (milkshaking) when using both tests and produced high foaming values. The correlation between the two tests for fluids having severe aeration was different than previously determined.<sup>2</sup> This difference could be due to different types of formulated oils or a difference between technicians in determining the existence of an oil/foam interface.

## (2) High Temperature Nonester Base Fluids

Foam testing was conducted on one high temperature nonester base fluid (TEL-91001) during the latter part of the research program. Data obtained are shown in Table 81 along with foaming data previously obtained on these type fluids.<sup>3</sup> The purpose of including this data is for comparing the foaming characteristics of different classes of fluids.

Foaming characteristics of TEL-91001 appear to be slightly greater than the other 5P4E fluid O-67-1. Although, the use of either the ASTM diffuser stone or the 5 micrometer pore size metal sparger is allowed for testing MIL-L-7808 lubricants, the data obtained on the fluid TEL-91001 show that there may be different foaming data obtained between the two since severe aeration (milkshaking) occurred when using the sparger but not the diffuser stone. The data in Table 81 show that the two 5P4E base fluids have lower foaming characteristics than the three non-5P4E base fluids.

### e. Summary

Foam Testing conducted on high temperature ester base lubricants gave low foaming values and good correlation between the small volume test and Method 3213 for fluids having good oil/foam interfaces. For the lubricants having high aeration characteristics, both tests gave higher foaming values but not the expected correlation as previously obtained.

Foam testing of experimental nonpolyphenyl ether type fluids gave higher foaming values than the MIL-L-87100 type fluids at 200°C. Data obtained for one fluid indicated a difference in foaming values may be obtained between using the ASTM diffuser stone and the 5 micrometer 13/16 inch diameter metal sparger.

**TABLE 81**  
**FOAMING CHARACTERISTICS OF HIGH TEMPERATURE**  
**NON-ESTER BASE FLUIDS**  
 (Test Temperature of 200°C, Foam Values in mL)

Fluid	25 mL Volume Test			Fed. Test Method # 3213		
	Airflow cc/min			Airflow, cc/min		
	500	1000	Comment	500	1000	Comment
O-67-1	8	34	a, <sup>1</sup> 6s <sup>2</sup>	13	15	a, 4s
TEL-9050	155	177	a, 15s	ND <sup>3</sup>	ND	-
TEL-90001	140	100	a, 15s	"	"	
TEL-90024	>200	>200	a, 20s	"	"	
TEL-91001 <sup>4</sup>	9	88	b, <sup>5</sup> 4s	"	"	
TEL-91001 <sup>6</sup>	15	51	a, 3s		"	

<sup>1</sup>a: Oil/foam interface

<sup>2</sup>6s: Foam collapse time in seconds

<sup>3</sup>ND: Not determined

<sup>4</sup>TEL-91001: Test using 5 micrometer pore size, 13/16" dia sparger

<sup>5</sup>b: No clear oil/foam interface

<sup>6</sup>TEL-91001: Test using ASTM diffuser stone

### SECTION III

#### DEVELOPMENT OF IMPROVED LUBRICATION SYSTEM HEALTH MONITORING TECHNIQUES

##### 1. FERROSCAN 310

###### a. Introduction

A ferrous wear metal detector, the Ferroskan 310, has been evaluated. The 310 unit is an update of the Ferroskan 210 model which was evaluated previously.<sup>3</sup> The device is an in-line sensor designed to replace a section of tubing in which there is an oil flow. The Ferroskan system was initially tested by circulating oil and introducing measured quantities of Fe powder. Small quantities of oil were taken after each addition to compare the actual Fe concentration to the output of the 310 unit. The Ferroskan system essentially monitors the rate change of magnetic flux as oil passes through the sensor tube. The Ferroskan output is, thus, a change in frequency per time unit although the data are nondimensionalized and given the name relative debris number (RDN). The RDN, unfortunately, is a qualitative measure which is influenced by the temperature as well as the oil speed.

###### b. Results and Discussion

###### (1) Effect of Oil Velocity

Figure 55 (Test 46) shows the RDN versus time graph for oil being circulated by a pump driven with a variable speed motor. Four motor speeds were used to determine the effect on the RDN increases for three consecutive 5-mg additions of 10-20 micron Fe particles. The percentages shown above each of the four sets of additions correspond to the amount of power supplied to the variable speed drive. The equivalent oil velocities corresponding to these percentages and for the diameter of the sensor tube used are 2.00, 3.25, 3.45, and 3.65 m/s. All of these speeds are within the 1 to 5 m/s range set by the manufacturer as acceptable velocities for the 310 system. At 20% of the maximum motor speed, the rises in the RDN caused by each of the three Fe additions decrease sharply. The changes in the RDN before and after the three additions are 24, 22, and 23. These values are the differences from the highest RDN after an addition and the lowest RDN before that addition. In terms of the actual concentration of Fe in ppm, for the 1200 ml of oil used, the concentration rises by 4.9 ppm after each addition. Although the 310 unit indicates the Fe concentration decreases after each addition, the sensitivity (given by the RDN change) is essentially constant.

# TEST 46

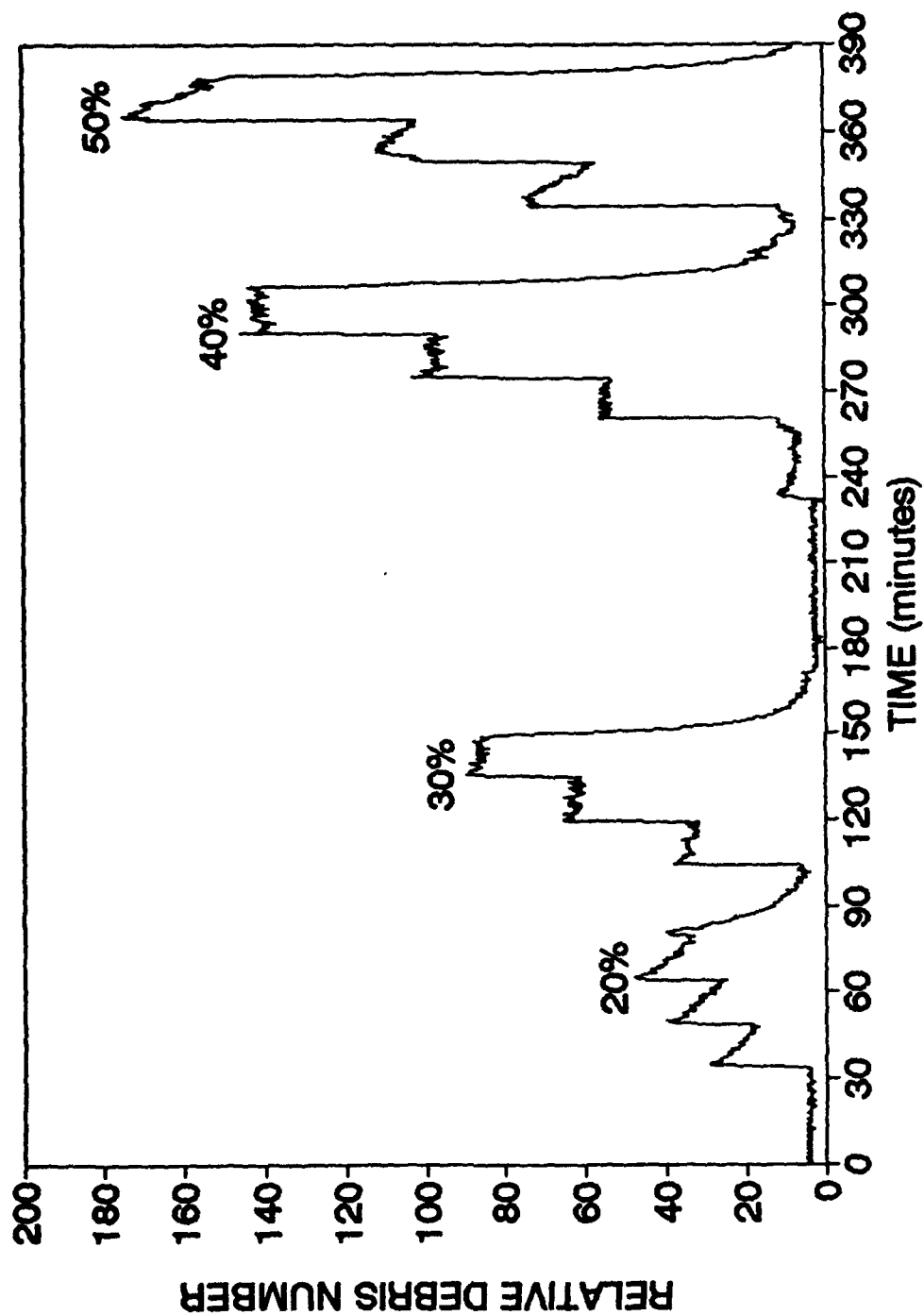


Figure 55. Ferrosan Output of Oil Spiked with Three 5-mg Additions of 5-10 Micron Fe Powder for Each of the Four Pumping Outputs Shown.

At the 30 and 40% motor speeds, the RDN changes still remained essentially constant, but the RDN levels themselves remained constant, also. For the 30% motor speed, the rises in RDN were 32, 33, and 29, respectively, while the rises for 40% were 45, 50, and 50. At 50% of the maximum motor speed, the sensitivity of the 310 unit varied. The RDN changes for this speed were 63, 55, and 73, respectively. Although sensitivity increases, the RDN values no longer remain steady like they did at the 30 and 40% speeds. It should be pointed out that although the data in Figure 55 were taken continuously, the Fe particles added at each motor speed were collected with a magnet before increasing the motor speed to a higher level. Most of the data collected during these extraction periods was omitted from Figure 55 to avoid confusion.

## (2) Effect of Temperature

The effect of temperature on the RDN can be seen in Figure 56. In this test, oil with some initial concentration of Fe began circulating at room temperature. The initial RDN was approximately 150 but rose to 600 as the temperature increased to 50°C from friction caused by the pump. The oil was circulating at a rate of 2.75 m/s, and one addition of 100 mg of 5-10 micron Fe powder was introduced after the equilibrium temperature was reached. The levels of the RDN appear steady before and after the addition. To quantify the variation, 80 minutes worth of data before and after the addition were averaged, and their standard deviations calculated. Before the addition, the average RDN was 609.7 with a standard deviation of 6.3. After the addition, the average RDN rose to 701.1 with a standard deviation of 7.1.

Unlike some of the data of Figure 55, there is no substantial decay in the RDN once an addition had been made. Based on the minimum and maximum RDN values before and after the addition, an RDN increase of 129 results from the 100-mg Fe addition. Another way of interpreting the increase of the RDN is by comparing the averaged values for the RDN before and after the addition. This "average" difference of 91.4 is considerably less than the "min/max" difference of 129, but the averaging procedure includes all data points compared to only two data points to compute the difference between the minimum and maximum values.

## (3) Effect of Particle Size Using 5-10, 10-20, and 20-30 Micron Fe Powder

The next three tests were performed to compare the ferrosan responses to different ranges of Fe particle size. An excessive number of Fe additions were made to determine whether sensitivity loss takes place at higher Fe concentrations. Unlike Test 27 (Figure 56), only 30-mg additions were made into the 4-gallon volume of oil circulating at 2.75

## TEST 27

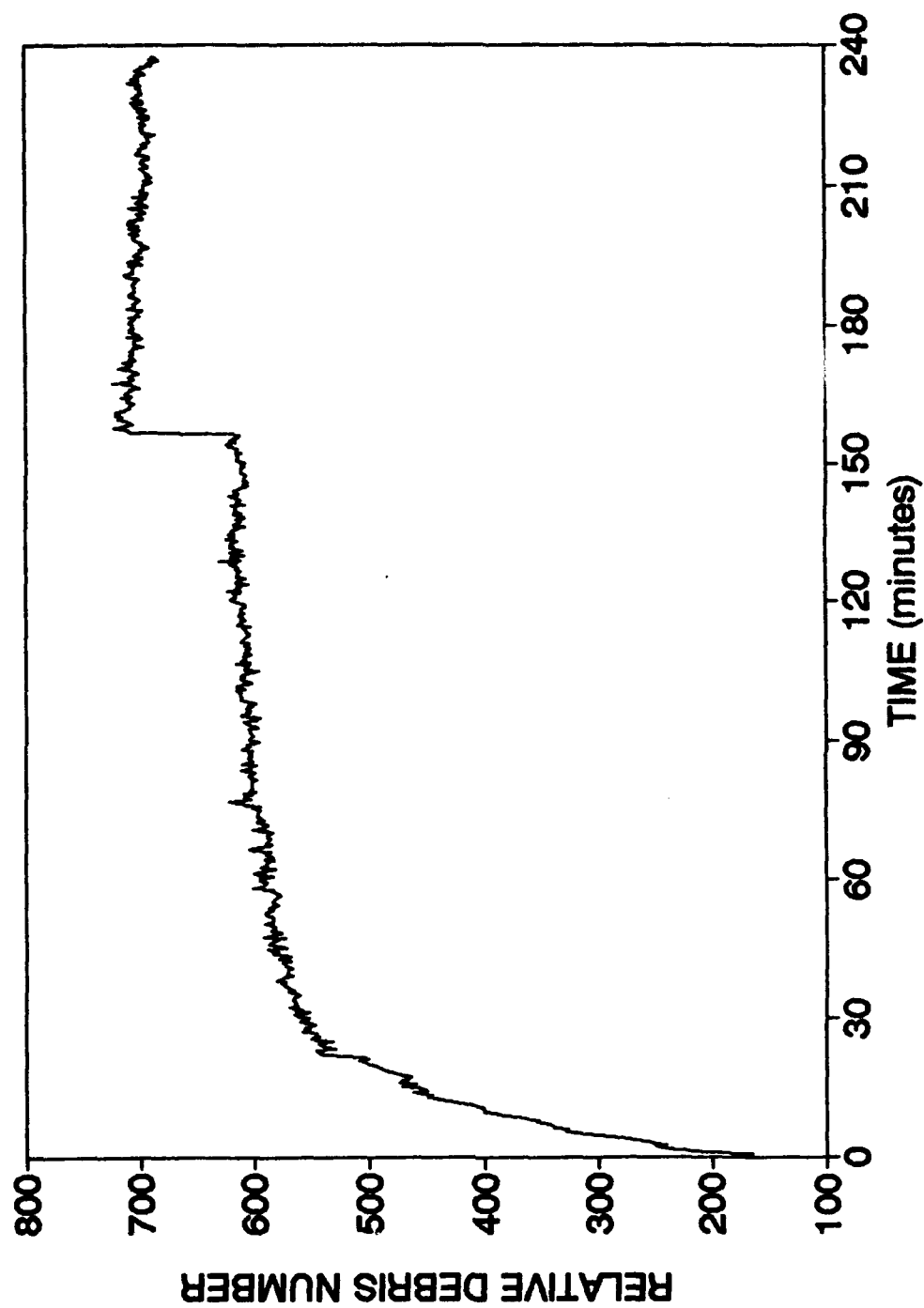


Figure 56. Ferrosan Output for Oil Circulating at 2.75 m/s with One 100-mg Addition of 5-10 Micron Fe Powder.

m/s resulting in an Fe concentration increase of 2.3 ppm for each addition (compared to a 7.8 ppm increase for the 100-mg addition of Test 27). The three tests, numbers 34, 35, and 36, all began with RDN readings of about 100 and at least 20 additions of Fe powder were made. The first addition of each test was made after the temperature had stabilized and subsequent additions were made at 10-minute intervals.

Figure 57 shows the RDN versus time graph for additions of 5-10 micron Fe particles. A noticeable decline of the RDN readings takes place after the initial rise for each addition. Like the data of Test 27, the averages and standard deviations of each "step" in Figure 58 are computed. The largest standard deviation is only 6.79, but the range of RDN changes based on the difference of averaged RDN readings varies from 15.8 to 51.5. The RDN changes for each addition are plotted in Figure 58 along with the Fe concentration. The concentration was determined by ADM-AA analyses of oil samples (less than 10 mL) taken intermittently throughout the test. Figure 58 compares the two methods of quantifying the increase in the RDN caused by additions of Fe particles. The differences in the averages of the RDN before and after each Fe addition are represented by squares while triangles give the differences between the lowest RDN reading before an addition and the highest RDN reading after an addition.

Figure 59 shows the RDN versus time graph for additions of 10-20 micron Fe particles. Compared to the RDN readings of Figure 57, less of a decline occurs after each Fe addition. The standard deviations of the average RDN readings for each step are less than 5, and the RDN differences of the averages of adjacent steps are shown in Figure 60 along with the minimum to maximum RDN change and the sampled Fe concentration.

The responses of the 310 system to 20-30 micron Fe particle additions are shown in Figure 61. The decline in RDN after each Fe addition is greatest for the large particles used in Test 36, and is evidenced by the standard deviations as high as 8.15 for average RDN readings. Figure 62 again compares the average and min/max RDN increases corresponding to each Fe addition along with the Fe concentration from oil samples.

To better compare the methods used to quantify the RDN changes of Tests 34 through 36, linear regressions were performed on the data shown in Figures 58, 60, and 62. Table 82 shows the coefficients,  $m$  and  $b$ , corresponding to the linear equation,  $y = mx + b$ , which represents the best fit for the data scatter. The  $y$  variable in this equation refers to either type of RDN increase or the absolute sampled concentration while  $x$  refers to the number of

## TEST 34

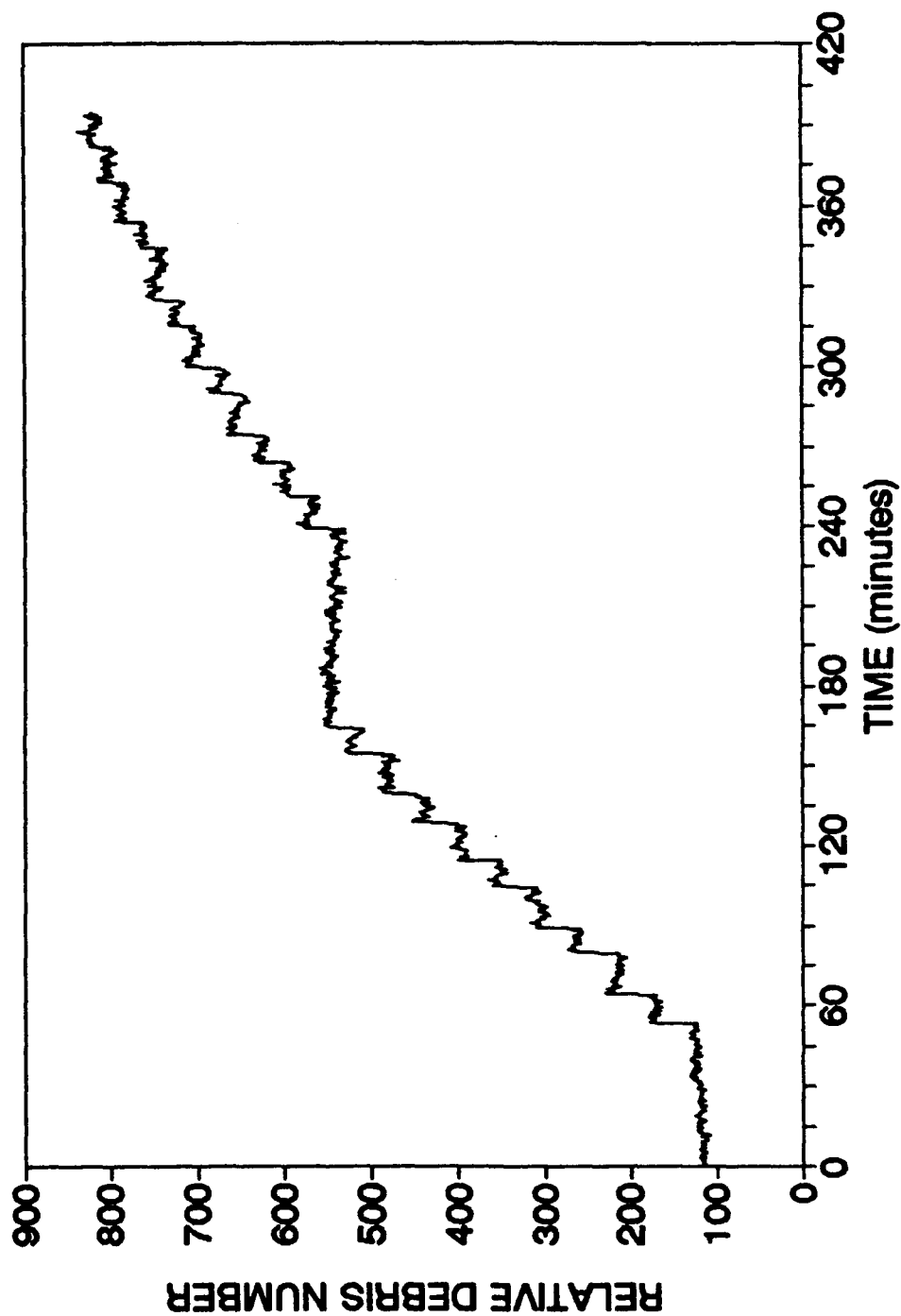


Figure 57. Ferrosan Output for Oil Circulating at 2.75 m/s with 22 30-mg Additions of 5-10 Micron Fe Powder.

# TEST 34

## 5-10 micron Fe

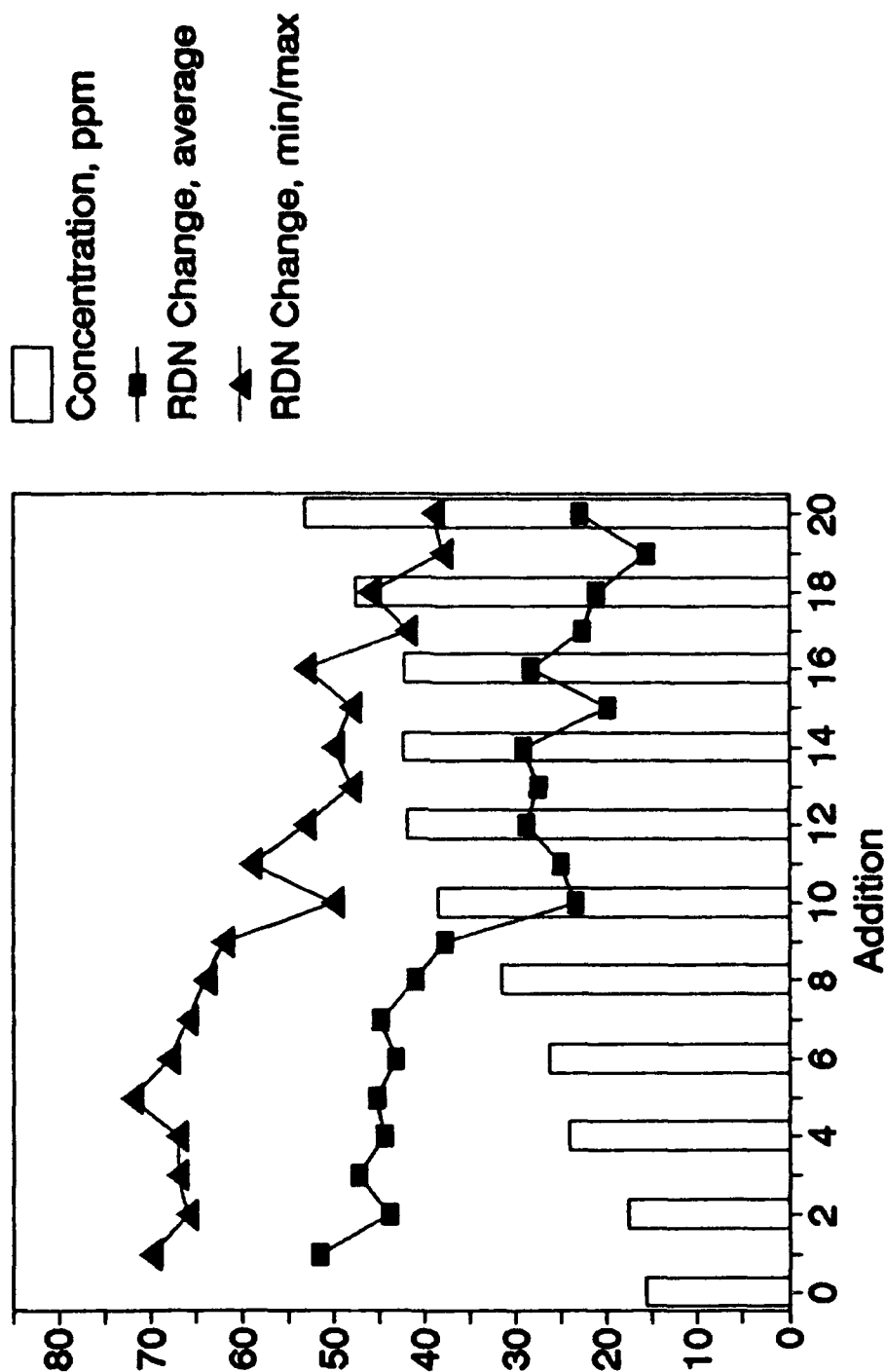


Figure 58. Comparison of the Relative Debris Number Increases for 5-10 Micron Fe Particles Based on the Average Values and the Minimum and Maximum Values of Adjacent "Steps" in Figure 57.

## TEST 35

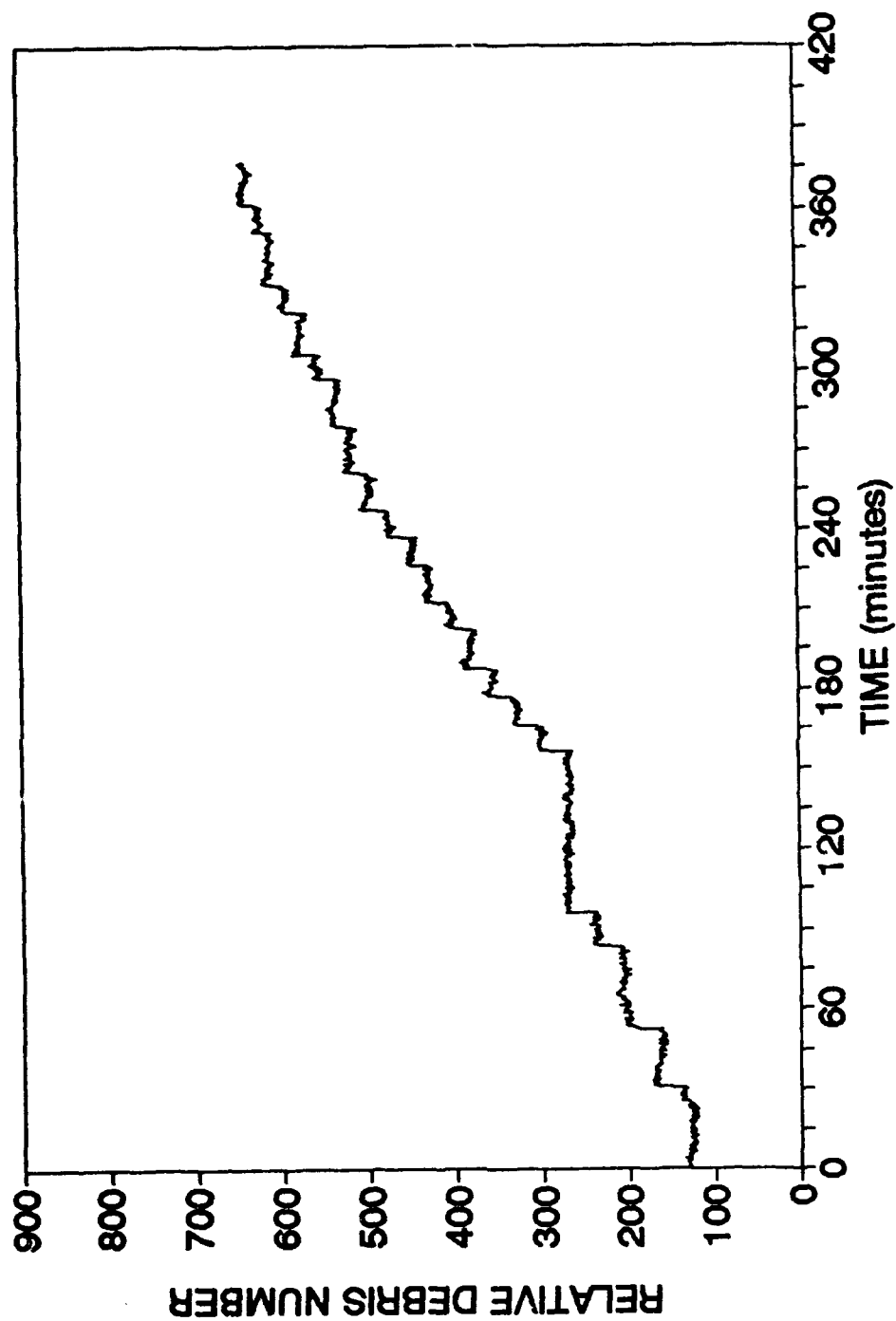


Figure 59. Ferrosan Output for Oil Circulating at 2.75 m/s with 21 30-mg Additions of 10-20 Micron Fe Powder.

# TEST 35

## 10-20 micron Fe

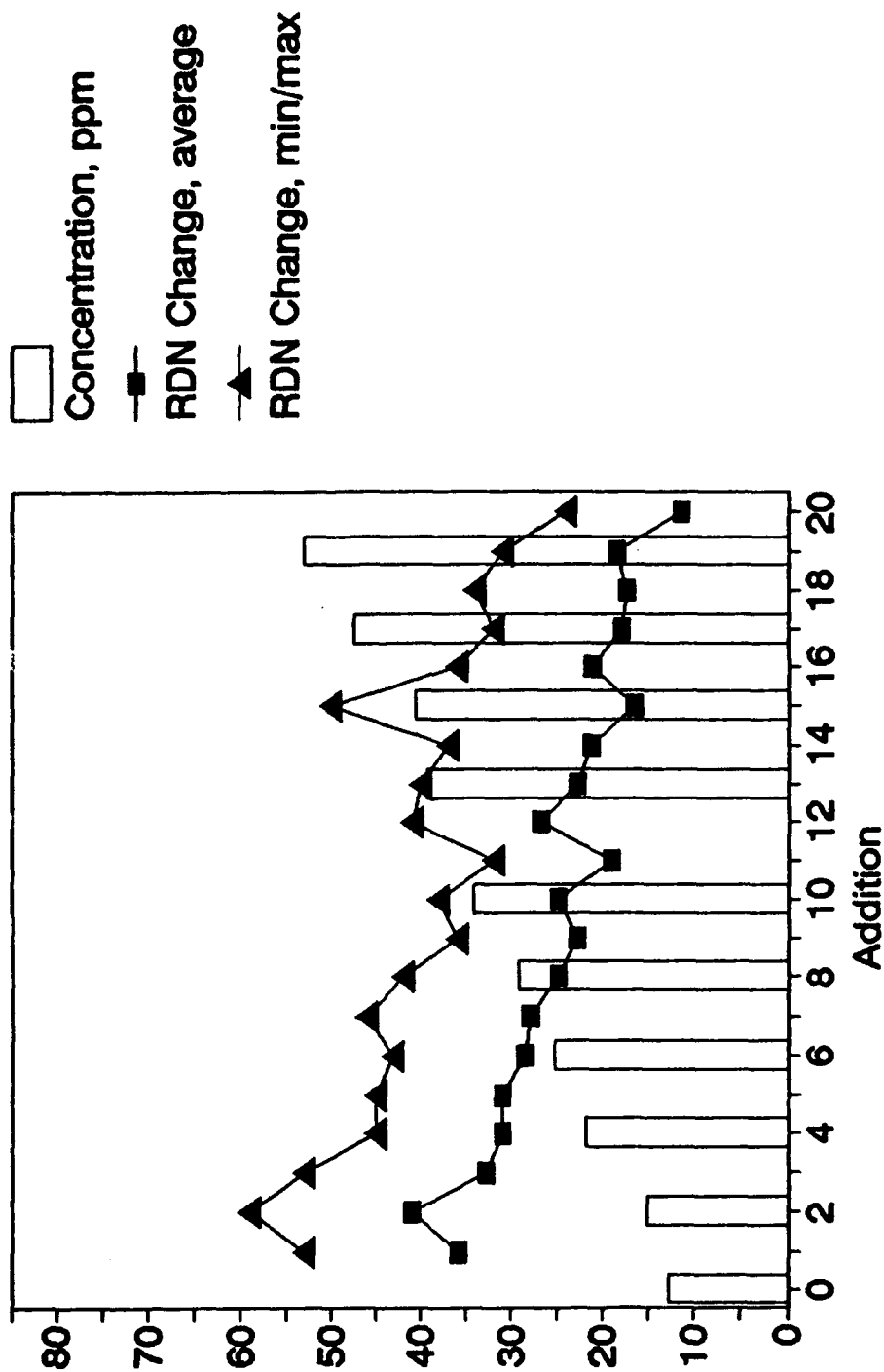


Figure 60. Comparison of the Relative Debris Number Increases for 10-20 Micron Fe Particles Based on the Average Values and the Minimum and Maximum Values of Adjacent "Steps" in Figure 59.

## TEST 36

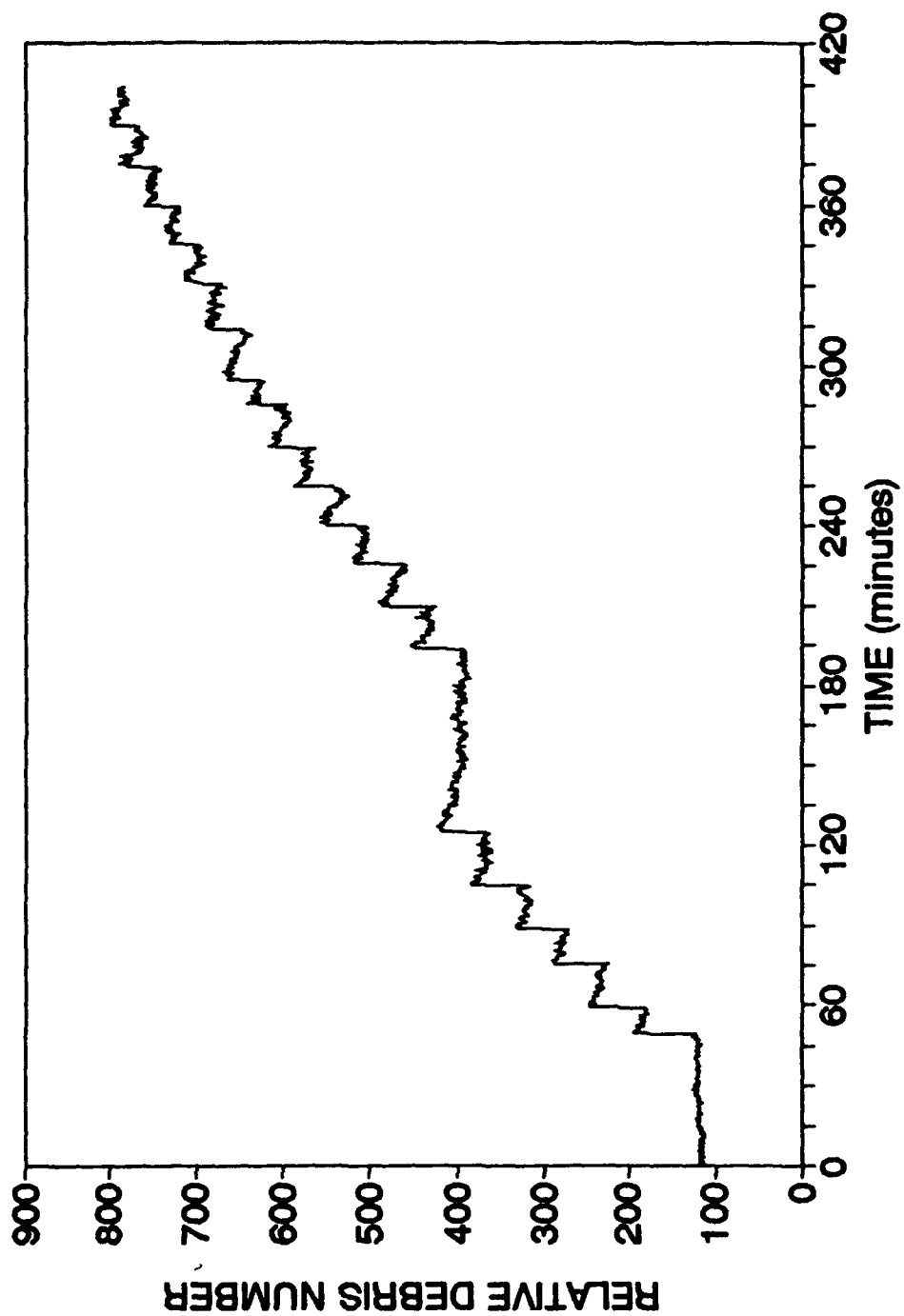


Figure 61. Ferrosan Output for Oil Circulating at 2.75 m/s with 20 30-mg Additions of 20-30 Micron Fe Powder.

# TEST 36

## 20-30 micron Fe

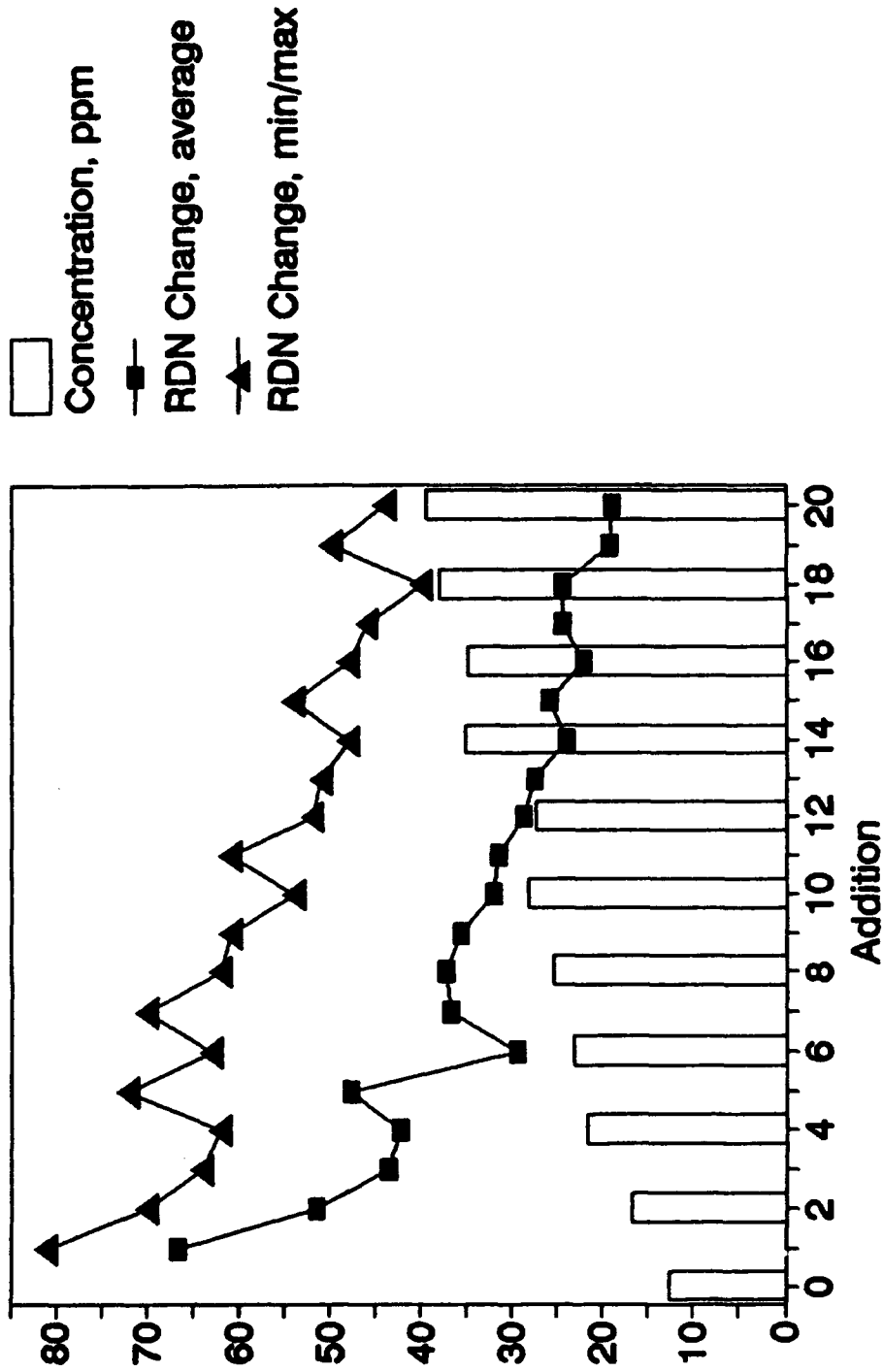


Figure 62. Comparison of the Relative Debris Number Increases for 20-30 Micron Fe Particles Based on the Average Values and the Minimum and Maximum Values of Adjacent "Steps" in Figure 61.

TABLE 82

**COEFFICIENTS FOR LINEAR REGRESSIONS  
FOR THE DATA IN FIGURES 58, 60, AND 62**

Test Number	y (parameter)	m (slope)	b (y-intercept)
34	min/max RDN	$-1.73 \pm 0.15$	$74.59 \pm 3.91$
34	average RDN	$-1.72 \pm 0.17$	$51.28 \pm 4.46$
34	ppm	$1.83 \pm 0.11$	$16.28 \pm 2.37$
35	min/max RDN	$-1.19 \pm 0.20$	$53.33 \pm 5.22$
35	average RDN	$-1.14 \pm 0.11$	$36.66 \pm 2.86$
35	ppm	$2.04 \pm 0.07$	$12.65 \pm 1.38$
36	min/max RDN	$-1.64 \pm 0.18$	$74.90 \pm 4.54$
36	average RDN	$-1.84 \pm 0.21$	$52.85 \pm 5.38$
36	ppm	$1.29 \pm 0.08$	$14.63 \pm 1.62$

30-mg additions made. The slope, m, of the equation indicates the rate of change of RDN increases or concentration with respect to the number of additions made. The y intercept, b, indicates the initial RDN rise or concentration level.

The slope values given in Table 82 indicate that the trend for RDN increases is essentially the same whether the average RDNs are used or the whether min/max values are used. Test 36 has the greatest discrepancy between its min/max and average RDN slopes (0.20) but this difference is within the standard error range of both coefficients. Comparison of the m and b values for RDN changes of all three tests indicates that the response of the 310 unit is the same for 5-10 micron particles as it is for 20-30 micron particles. In contrast, 10-20 micron particles gave not only lower rates of change (m-values) but also had diminished responses (b-values). Because of the disparity in the results from the intermediate 10-20 micron particles with respect to the results from both larger and smaller particle ranges, Test 35 was repeated.

The results of the second test of 10-20 micron Fe particles are shown in Figure 63. Although the beginning RDN level is roughly 100 greater than either of the three previous tests, the initial Fe concentration was only 12.72 ppm. This level is essentially identical to the initial concentration of the first test of 10-20 micron Fe particles (12.91 ppm). As with the previous tests, the averages for each step of Figure 63 were calculated, and the greatest standard deviation was 5.58 (compared to 4.71 for Test 35).

# TEST 37

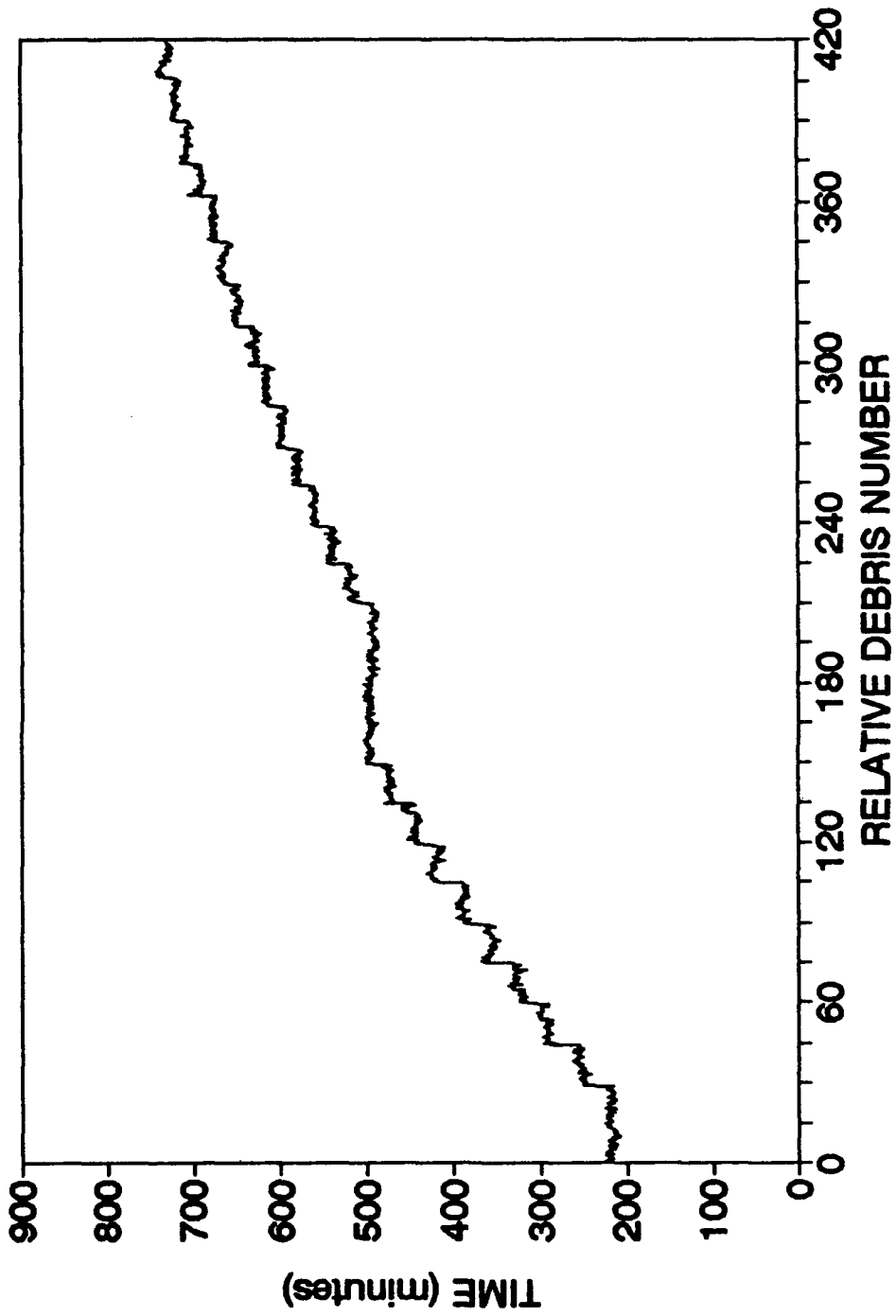


Figure 63. Ferrosan Output for Oil Circulating at 2.75 m/s with 24 30-mg Additions of 10-20 Micron Fe Powder.

The average and min/max RDN changes of Test 37 are plotted in Figure 64 along with the Fe concentrations of oil samples. In comparing Figure 64 to Figure 60, the data for both the average RDN increases and the concentration are found to be very close. The min/max RDN change is also similar for the two plots except between the 12th and 16th additions. To better see the differences and the similarities of Tests 35 and 37, regression analyses were done for the data of Figure 64 and given in Table 83 along with the previously shown values corresponding to Test 35.

TABLE 83  
COEFFICIENTS FOR LINEAR REGRESSIONS DONE  
ON THE DATA OF FIGURES 60 AND 64

Test Number	y (parameter)	m (slope)	b (y-intercept)
35	min/max RDN	$-1.19 \pm 0.20$	$53.33 \pm 5.22$
37	min/max RDN	$-1.74 \pm 0.14$	$59.28 \pm 3.63$
35	average RDN	$-1.14 \pm 0.11$	$36.66 \pm 2.86$
37	average RDN	$-1.28 \pm 0.10$	$37.04 \pm 2.67$
35	ppm	$2.04 \pm 0.07$	$12.65 \pm 1.38$
37	ppm	$2.19 \pm 0.09$	$12.73 \pm 1.81$

Table 83 indicates that the repeatability of all of the initial values (y-intercepts) is excellent. Repeatability of the average RDN increase and ppm change (slopes) is also good but the repeatability of min/max RDN increase change is poor. Nonetheless, the initial RDN rise based either on the min/max or average difference is again shown to be significantly less than the corresponding values for either the 5-10 or 20-30 micron ranges which indicates that the Ferrosan is less sensitive to the intermediate 10-20 micron Fe particles.

Although the concentration of Fe increased by a controlled amount in each of Tests 34 to 37 (2.3 ppm for each 30-mg addition), the ppm slopes in Tables 82 and 83 do not quite reflect that level of increase. For example, 20-30 micron Fe particles gave a measured concentration increase of only 1.29 ppm per addition made. The fact that this value is considerably lower than any for the other corresponding particle sizes suggests that the large 20-30 micron particles are difficult to keep in suspension, and oil samples taken for analyses may not have had representative concentration levels. The same argument is valid to a lesser extent for the smaller particle ranges and helps to explain why each ppm slope is below the theoretical amount of 2.3 ppm per addition.

# TEST 37

## 10-20 micron Fe

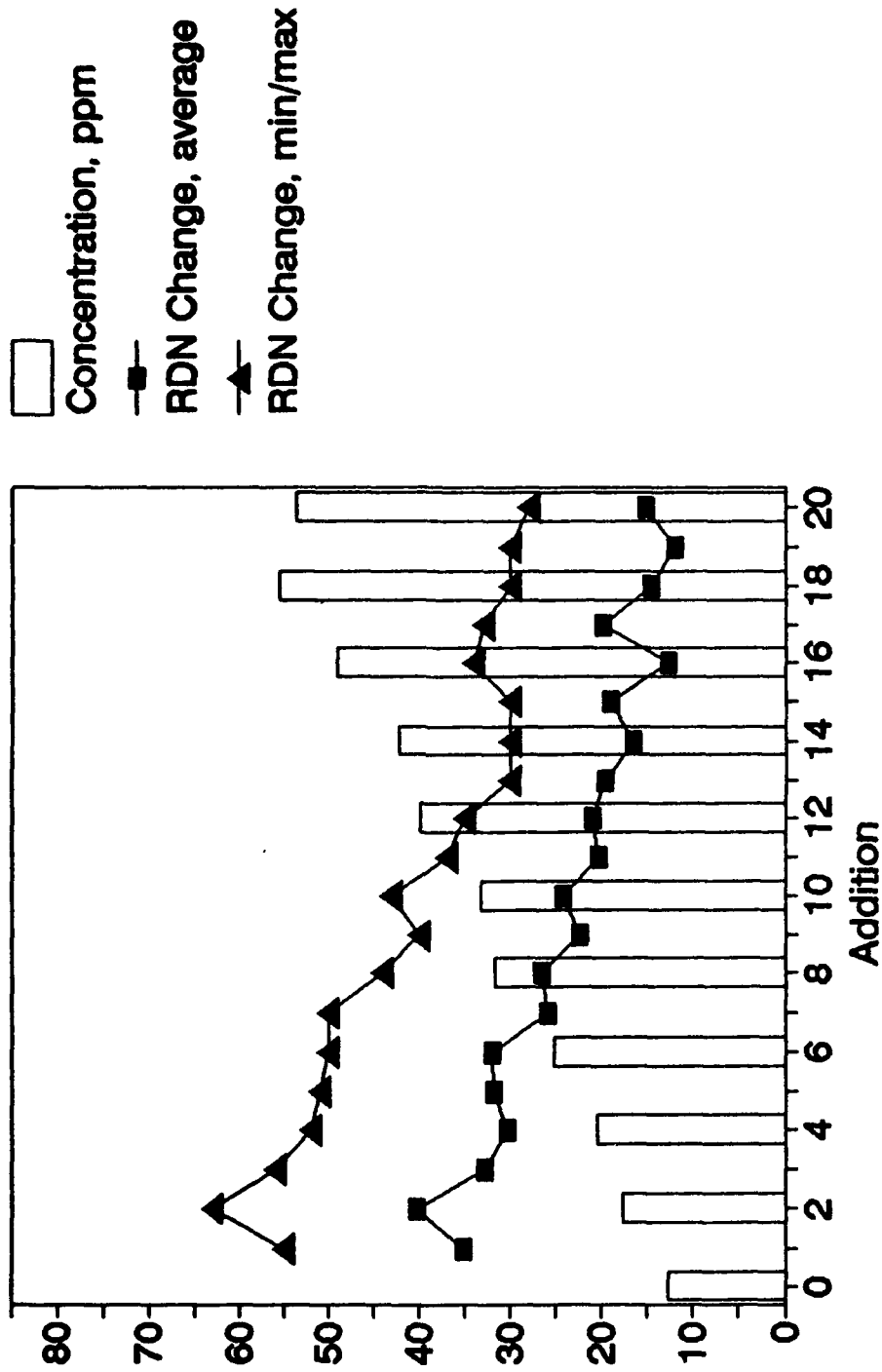


Figure 64. Comparison of the Relative Debris Number Increases for 10-20 Micron Fe Particles Based on the Average Values and the Minimum and Maximum Values of Adjacent "Steps" in Figure 63.

While particle size has been shown to affect the response of the Ferroscan unit, RDN readings have also been seen to steadily decrease with increasing concentration (Figures 58, 60, 62, and 64). Although the slopes for the RDN change regressions provide insight into the rate of sensitivity loss, it is essential to determine which method (either the difference between minimum and maximum RDNs or averages of consecutive RDN levels) is most appropriate for measuring concentration increases. The data of Tables 82 and 83 indicate that either method is justifiable for 5-10 and 20-30 micron particles, but a significant discrepancy exists between the min/max RDN change slopes for Tests 35 and 37. Because of this difference, the decrease in the average differences will be used. The sensitivity loss is given in Table 84 and is calculated by dividing the RDN increase per addition by the concentration increase per addition.

TABLE 84  
SENSITIVITY LOSS OF THE FERROSCAN 310  
FOR VARIOUS FE PARTICLE SIZES

Test Number	particle range, microns	sensitivity loss RDN per ppm
34	5-10	$0.75 \pm 0.07$
35	10-20	$0.50 \pm 0.05$
36	20-30	$0.80 \pm 0.09$
37	10-20	$0.56 \pm 0.04$

The sensitivity loss shown in Table 84 is calculated using the theoretical increase in Fe concentration (2.3 ppm). The values shown indicate that the sensitivity loss for small particles (5-10 micron) is similar to the loss in large particles (20-30 micron). The sensitivity from intermediate-sized particles (10-20 micron) is less affected by the concentration, however, and this value is consistent for both Tests 35 and 37. It should again be noted that this evaluation is qualitative because of the dependence of the RDN to both oil temperature and oil speed.

Sensitivity loss can be attributed primarily to magnetized Fe which collects in the sensor tube. The sensor tube was cleaned after every test with a white paper towel, and significant amounts of Fe were consistently collected. This problem of Fe magnetization is inherent to the 310 system and probably can only be minimized by using very fast oil speeds. Unfortunately, the manufacturer limits the effective oil speed to 5 m/s which may not cause sufficient turbulence to keep debris off the walls of the sensor tube.

#### **(4) Effect of Wear from a Wear Metal Generator on RDN**

Despite the Ferroskan system's inability to sustain constant RDN increases at increasing Fe concentrations, the unit was placed in line with a controlled wear test to evaluate its ability to monitor a dynamic system. The three-ball-on-disk (TBOD) wear test was chosen for this evaluation due to its simple geometry which allows oil to be easily delivered to and from the test chamber (see Figure 65). Appropriate test conditions were determined by running baseline tests which established the amount of wear resulting for the given loads and rotational speeds used.

In order to monitor the RDN of the oil within a TBOD test, a total of three pumps were necessary to circulate the test fluid. One pump circulated the bulk of the oil from a small reservoir through the Ferroskan sensor and back. The second pump took oil from the reservoir and delivered it to the wear test chamber. Finally, the third pump took oil out of the test chamber and put it back in the reservoir. This set-up was necessary to accommodate the velocity requirements of the 310 unit.

Initially, a 5-hour duration was used for the TBOD tests. Increases to the load were made periodically during the test to determine the ability of the 310 unit to sense increased wear rates. In order to compare RDN data from the Ferroskan to an actual record of specimen wear, an LVDT was used to monitor the vertical position of the ball fixture relative to its initial position. Additionally, to ensure significant amounts of wear would be generated, the specimen balls used were made of a much harder material (M-50 steel) than the disk material (1018 steel).

The wear results for a 5-hour TBOD test are shown in Figure 66. The initial load of 30 kg was increased by 20 kg at the 100 and 200-minute marks. During the first 100 minutes, initial run-in wear takes place but eventually wear stops. Increasing the load to 50 kg initiated the wear process again, but the slope of the wear curve begins to level to zero again. The final 100-minute segment reflects a nearly linear wear rate.

Ideally, the RDN data collected for this TBOD test should mirror the output shown in Figure 66. Because of the sensitivity problems seen in previous tests, the actual output, shown in Figure 67, is hardly a mirror image of Figure 66. The RDN versus time data does, however, clearly distinguish the points during the test where the load was increased and the wear rate correspondingly increased. Unfortunately, sensitivity causes a drop in the RDN readings during the first 100-minute portion when, in fact, the RDN level should have stayed

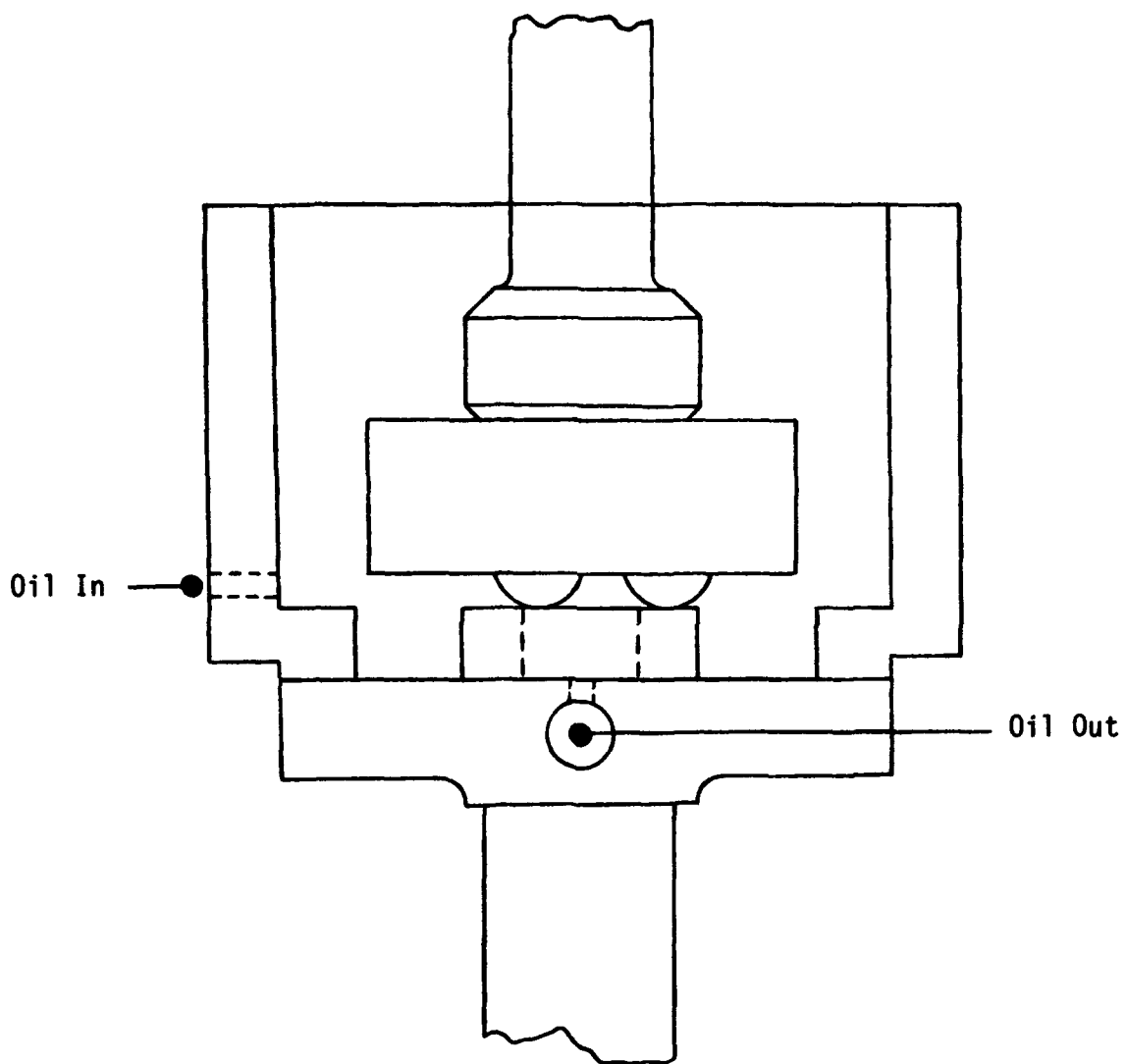


**Figure 65. Three-Ball-on-Disk Wear Test Configuration for a Circulating Oil Flow.**

# TEST 58

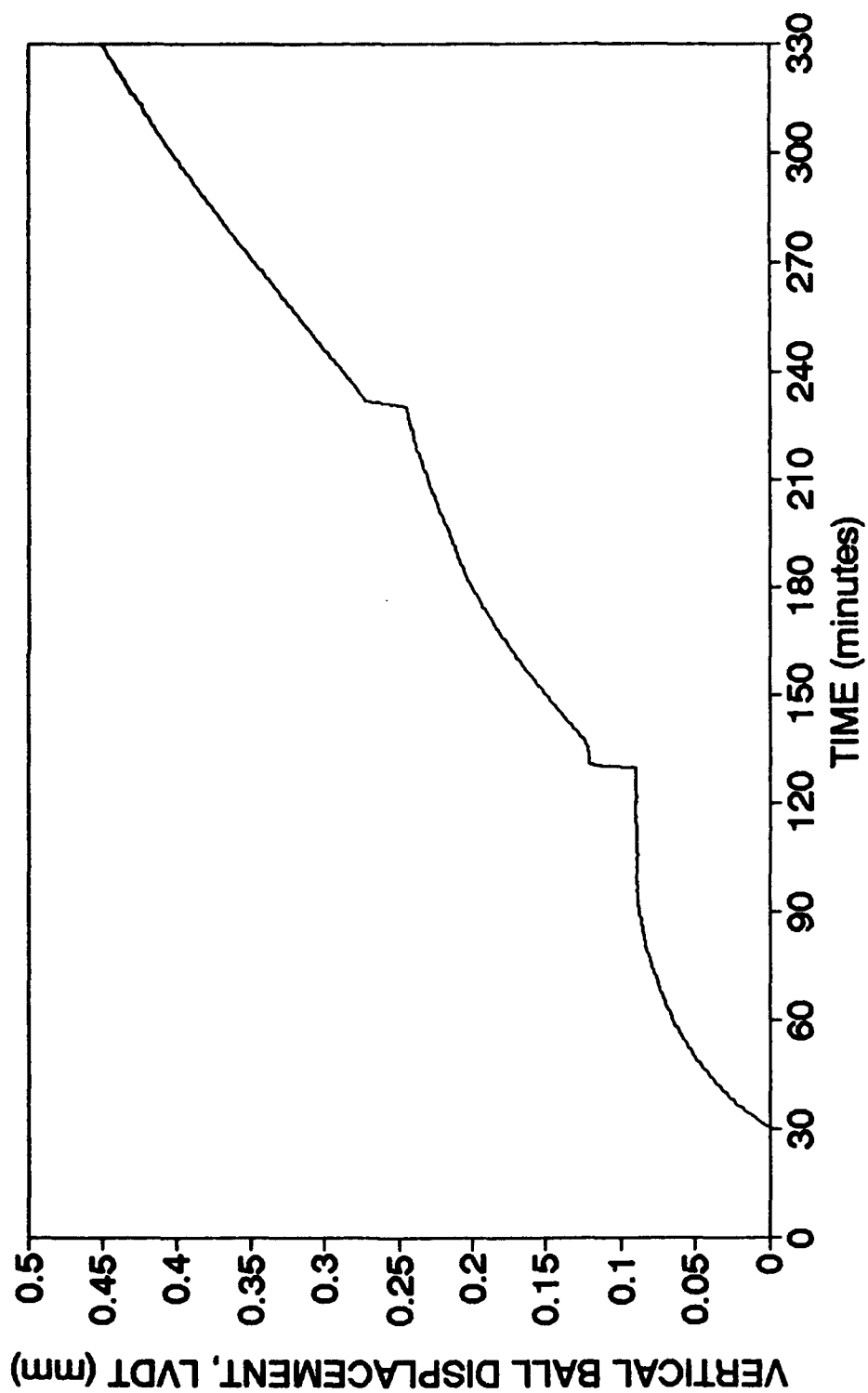


Figure 66. Wear Rate During a Three-Ball-on-Disk Test Given by the Vertical Displacement of the Ball Specimens (1018 Steel Disk, M50 Steel Balls, 250 rpm, Successive Loads of 30, 50, and 70 kg).

# TEST 58

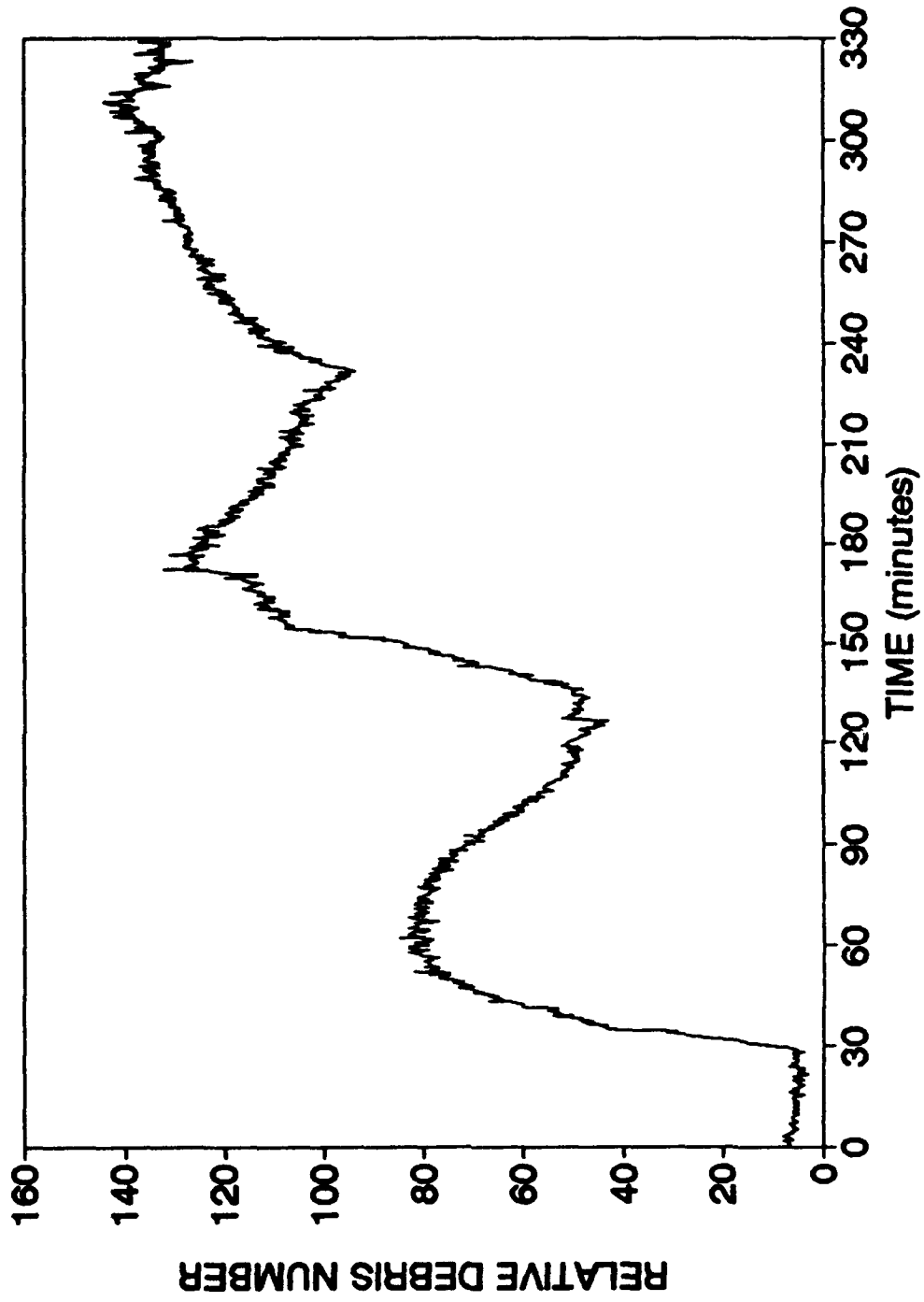


Figure 67. Ferrosan Output During the 5-Hour TBOD Test of Figure 66.

constant. The sensitivity worsens during the second 100-minute period because the RDN decreases in spite of the fact that wear had only started to level off. Finally, during the last segment, RDN levels appear to level off while the wear rate remained constant.

An oil sample was taken after the wear test of Figures 65 and 66 was completed. The Fe concentration in this sample was 958.4 ppm. The fact that RDN output for this test was only as high as 140 indicates that sensitivity loss is apparently higher for actual wear debris than for the 5-10, 10-20, and 20-30 micron Fe particles tested earlier. The wear debris from several TBOD wear tests was analyzed to establish the particles' size distribution. The Fe concentrations found after various filtrations of the wear debris are compared in Figure 68. Since no discernable drop in the concentration from any of the three tests occurs with filter sizes greater than 5 microns, the majority of the wear debris must be less than 5 microns.

(5) Effect of Particles Less than 5 Micron on RDN

Since no testing had been done to determine the effectiveness of the Ferroscan in monitoring particles below 5 microns, a supply of less than 5-micron Fe particles was prepared using a 5-micron sieve, and fixed amounts of these particles were fed into an oil flow just as had been done for larger particle size ranges. Figure 69 shows the RDN versus time plot for four 5-mg additions of less than 5 micron Fe particles in a volume of 500 ml. Because only a small quantity of particles was obtained, the number of additions was limited. Nonetheless, the RDN increases for each addition were again calculated based upon the average readings and the minimum to maximum readings and are listed in Table 85.

TABLE 85

RDN INCREASES FROM FOUR ADDITIONS  
OF LESS THAN 5 MICRON FE PARTICLES

Addition Number	average RDN increase	min/max RDN increase
1	3.812	8
2	9.701	14
3	9.410	14
4	5.350	9

# TBOD WEAR PARTICLE COMPARISON

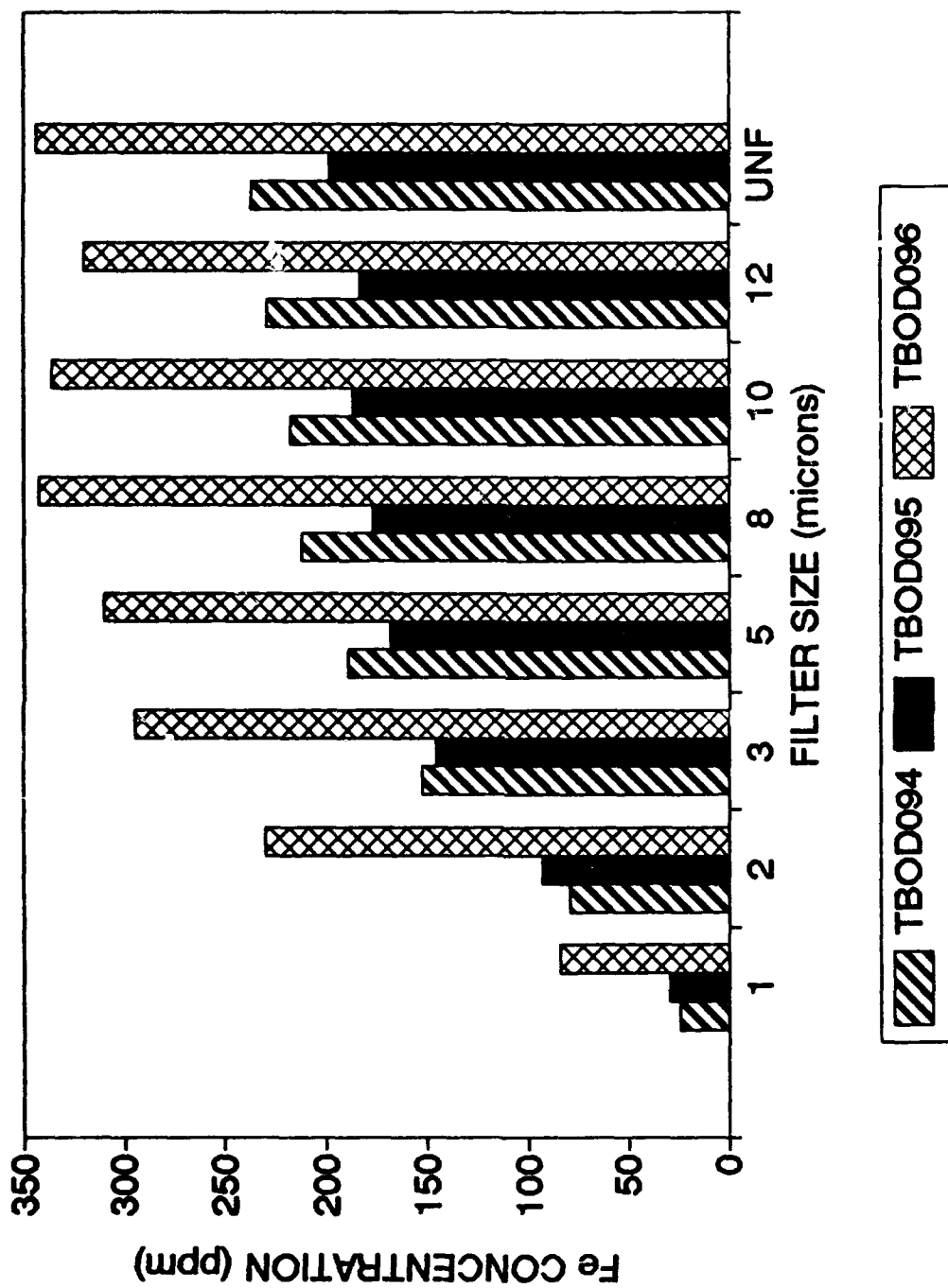


Figure 68. Wear Particle Size Distribution for Three TBOD Tests.

## TEST 54

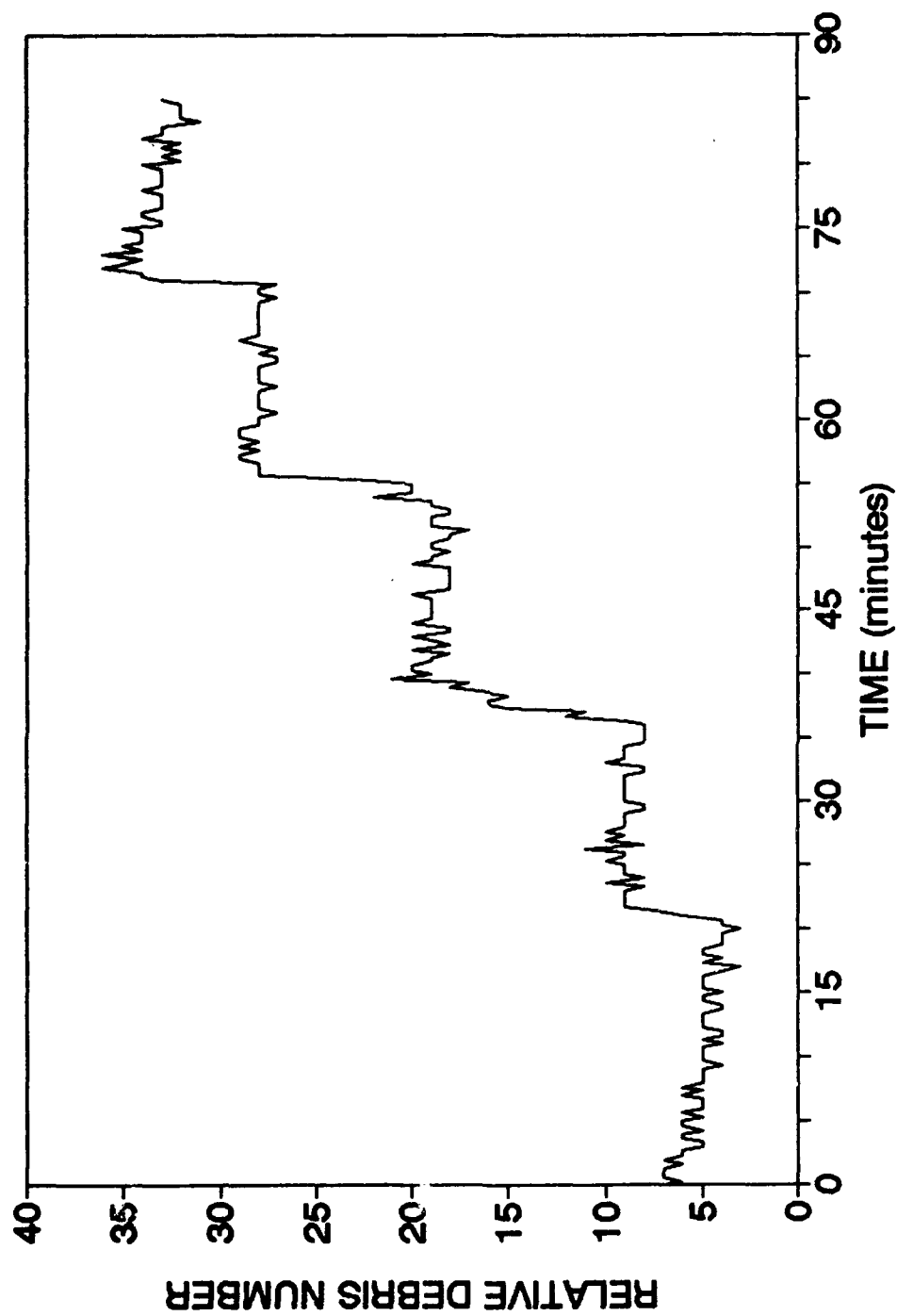


Figure 69. Ferrosan Output for Oil Circulating at 1.5 m/s with Four 5-mg Additions of Less Than 5 Micron Fe Particles.

Although the four RDN responses represent a drastically smaller statistical sampling than previous tests of larger Fe particles, a linear regression was again used to try to quantify the relationship between Fe concentration and RDN response. The equation  $y = mx + b$  corresponding to the average RDN difference (y) after each addition (x) has coefficients, m and b, of  $0.43 \pm 1.58$  and  $5.99 \pm 3.54$ , respectively. For the minimum to maximum RDN difference, the value for m is  $0.30 \pm 1.74$ , and the value for b is  $10.50 \pm 3.89$ .

Qualitatively, the Ferroskan response for these small particles is good judging by the relative "flatness" of each level in Figure 69. Quantitatively, the response is poor based on the large error range for the coefficients of either the average or min/max RDN increase regression. Comparison of the RDN response for less than 5 micron particles to the RDN response for the three larger particle size ranges cannot legitimately be made since the linear velocity of the oil was substantially slower (only 1.5 m/s). The response might otherwise have been expected to be greater since each 5-mg addition into the 500 ml of oil used for Test 54 (Figure 69) represents a greater concentration increase (11.8 ppm compared to 2.3 ppm). The oil velocity was chosen to be 1.5 m/s because the manufacturer indicates that this value represents the optimum oil speed for the 310 system, and this speed was used exclusively during TBOD testing with the Ferroskan in-line.

#### (6) Effect of Wear Debris from TBOD on RDN

Despite the inconsistent rise in RDN levels for each addition, the RDN output for less than 5 micron Fe particles is not representative of the behavior seen for actual wear debris (Figure 67). The noticeable RDN declines during the monitoring of Test 58 are not at all seen in Test 54. As a result, the wear debris from a TBOD test was collected, and Test 54 was repeated with 5-mg additions of the collected debris instead of laboratory-grade Fe powder. The results of this test (Test 56) are shown in Figure 70.

The responses for each 5-mg addition of TBOD wear debris shown in Figure 70 differs drastically from those observed for the less than 5-micron Fe powder (Figure 69). Unlike Test 54, the initial RDN response for each addition of wear debris is large and decreases immediately. To better compare the two tests, the average and min/max RDN increases for Test 56 are listed in Table 86.

# TEST 56

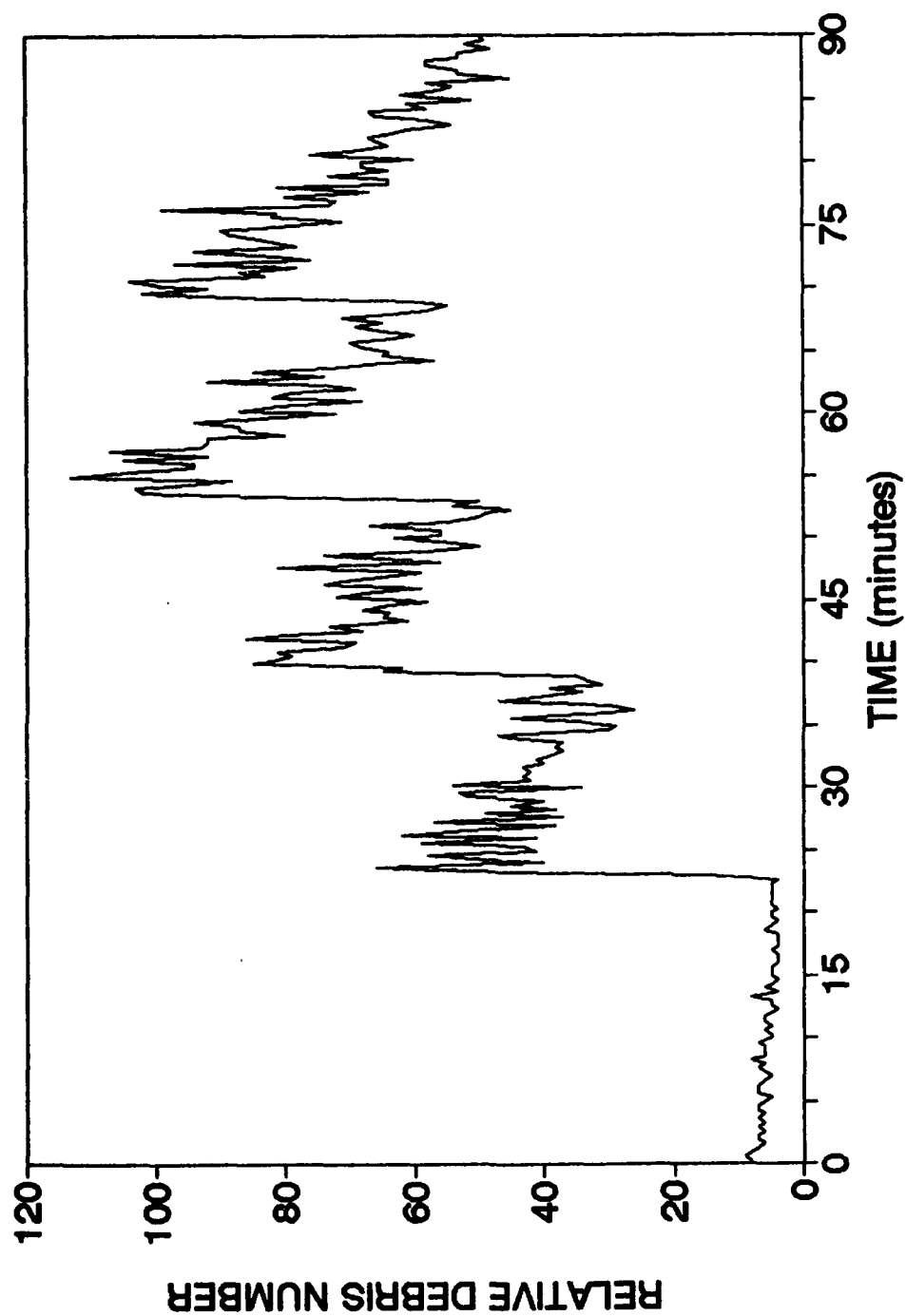


Figure 70. Ferrosan Output for Oil Circulating at 1.5 m/s with Four 5-mg Additions of TBOD Wear Particles.

TABLE 86

## RDN INCREASES FROM FOUR ADDITIONS OF TBOD WEAR PARTICLES

Addition Number	average RDN increase	min/max RDN increase
1	36.26	62
2	22.53	60
3	15.16	68
4	-9.67	49

The differences between the average RDN values of each level in Figure 70 decrease until the average RDN level after the fourth addition is actually less than the previous level. The minimum-to-maximum RDN changes are better behaved, but a decline still occurs after the fourth addition. A linear regression of the average RDN increase versus addition data gives  $m$  and  $b$  coefficients of  $-14.5 \pm 2.4$  and  $52.4 \pm 5.4$ , respectively. For the min/max RDN increase,  $m$  is  $-3.1 \pm 3.8$ , and  $b$  is  $67.5 \pm 8.4$ . Comparison of the  $y$ -intercepts ( $b$ ) from Tests 54 and 56 reveals the difference in the responses of the Ferrosan for the pure Fe particles and the 1018 steel wear particles generated during a TBOD test. The initial RDN level found from the regression of the data of Table 86 (Test 56) is nearly nine times greater based on the average RDN increases and more than 6 times greater based on the min/max RDN increases. Since the size of TBOD wear particles has been shown to be less than 5 microns, the increased sensitivity displayed by the Ferrosan unit with true wear particles may be due to the alloying elements within 1018 steel. Thus, different types of steels will likely produce varying responses from the 310 system.

The high rate of loss in the RDN after each addition in Test 56 (Figure 70) is consistent with the results of the monitored TBOD test (Test 58). The fact that the final concentration of Fe in an oil sample analyzed after Test 58 showed a level of 958.4 ppm despite a peak RDN of only about 140 which indicates that the 310 system had reached a sort of saturation point. The cause of this RDN-limiting phenomenon must be attributed to the magnetization of the wear debris itself which allows it to collect within the sensor tube and, thus, dull the Ferrosan ability to detect free particles as they pass through. Since actual wear particles (like the 1018 steel disk) proved more easily detectable to the Ferrosan than commercially pure Fe powder, the true wear particles appear to be more susceptible to induced magnetic fields and, thus, more likely to become magnetized and cause decreased sensitivity.

## **(7) Effect of Test Duration on RDN**

The final test of the Ferrosan system was again performed in conjunction with a TBOD wear test. For this test, however, the duration was reduced to 90 minutes in an effort to minimize sensitivity loss by debris magnetization. Conditions are otherwise identical to those used for Test 58 except that load increases of 10 kg were made at 30, 45, and 60 minutes into the test. The graph of the vertical ball displacement versus time is shown in Figure 71. Appropriate rises in the wear rate can be seen at the points where load increases are made. Figure 71 also includes the Fe concentrations found in oil samples taken at the designated points during the test. Figure 72 shows the RDN during the same time period of Figure 71.

Figures 71 and 72, although not identical, do express the same information about the wear history of the TBOD test. During the time of the initial 30-kg load (the first 30 minutes of the wear test), the RDN curve rises but levels out and begins to decrease slightly while the vertical ball displacement rises parabolically. After the load is increased to 40 kg, the RDN curve begins to assume again a positive slope, and the LVDT data show an increase in its slope. With 50 kg of load, the slope of the RDN curve becomes greater as does the displacement slope. During the final loading period, the RDN curve continues to keep roughly the same slope, but data scatter increases and the RDN eventually appears to level off during the last 10 minutes of the test. The slope of the displacement curve again increases slightly and stays constant throughout the same time period.

The Fe concentrations noted in Figure 71 were positioned in the graph so that their values are proportionate to the y-axis scale. Therefore, the rate of the concentration rise also concurs with both the ball displacement data and the RDN data. It is worthwhile to note that the Fe concentration increases continuously throughout Test 59 to a final value of 394.9 ppm. In comparing the final concentrations and RDN of Test 58 to Test 59, the RDN max-out at the same level (about 140) even though the Fe concentration of Test 58 is more than twice that of Test 59. This disparity again suggests that the 310 unit has a saturation point at least for the conditions and ferrous particles of Tests 58 and 59.

### **c. Conclusions**

It has been shown that the Ferrosan can effectively monitor a controlled, dynamic wear process. Its effectiveness diminishes, however, when high amounts of wear are being generated over an amount of time measured in hours rather than minutes. Magnetization of existing wear debris decreases the unit ability to sense additional quantities. The output from

# TEST 59

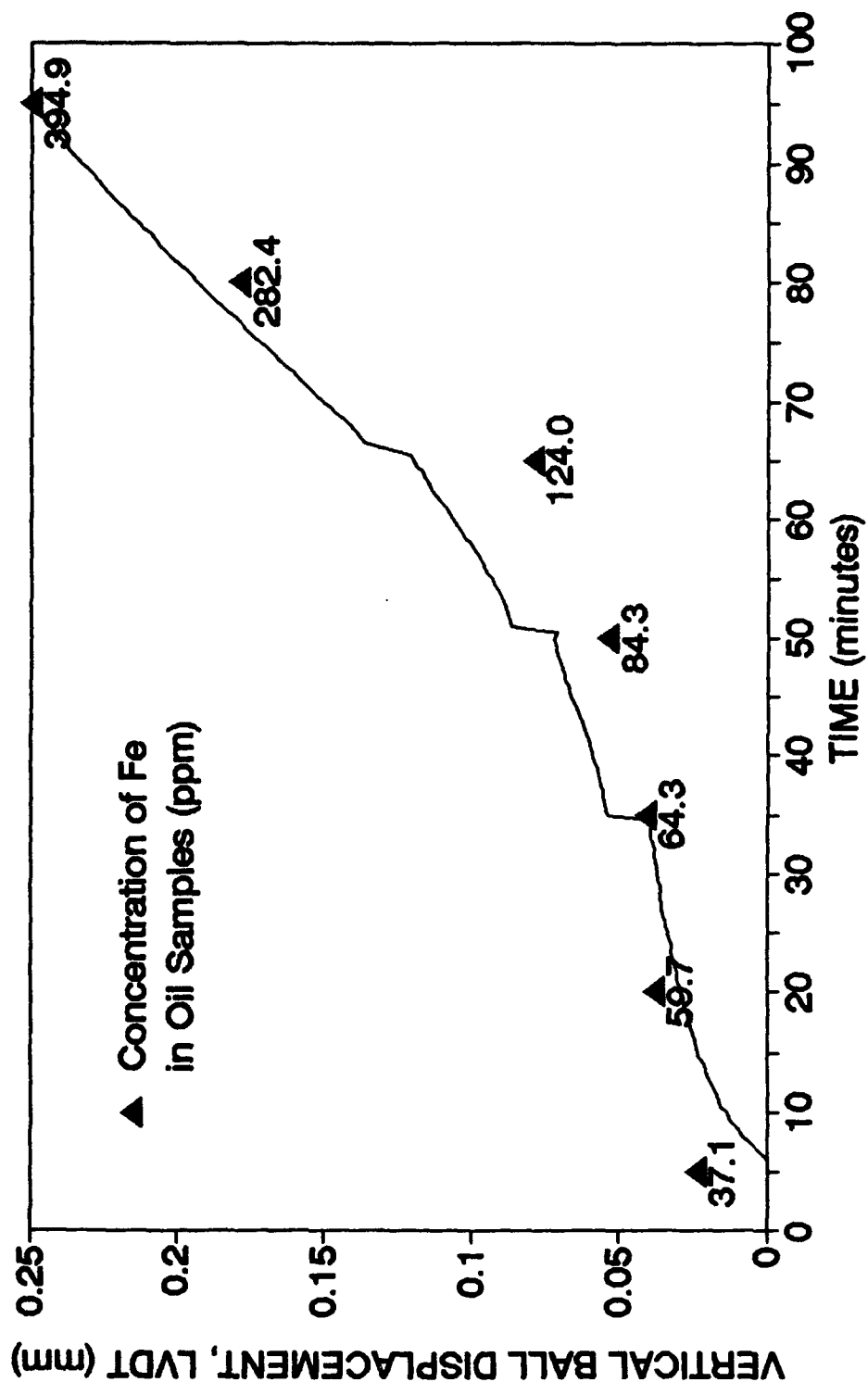


Figure 71. Wear Rate During a Three-Ball-on-Disk Test Given by the Vertical Displacement of the Ball Specimens (1018 Steel Disk, M50 Steel Balls, 250 rpm, Successive Loads of 30, 40, 50, 50, and 60 kg).

# TEST 59

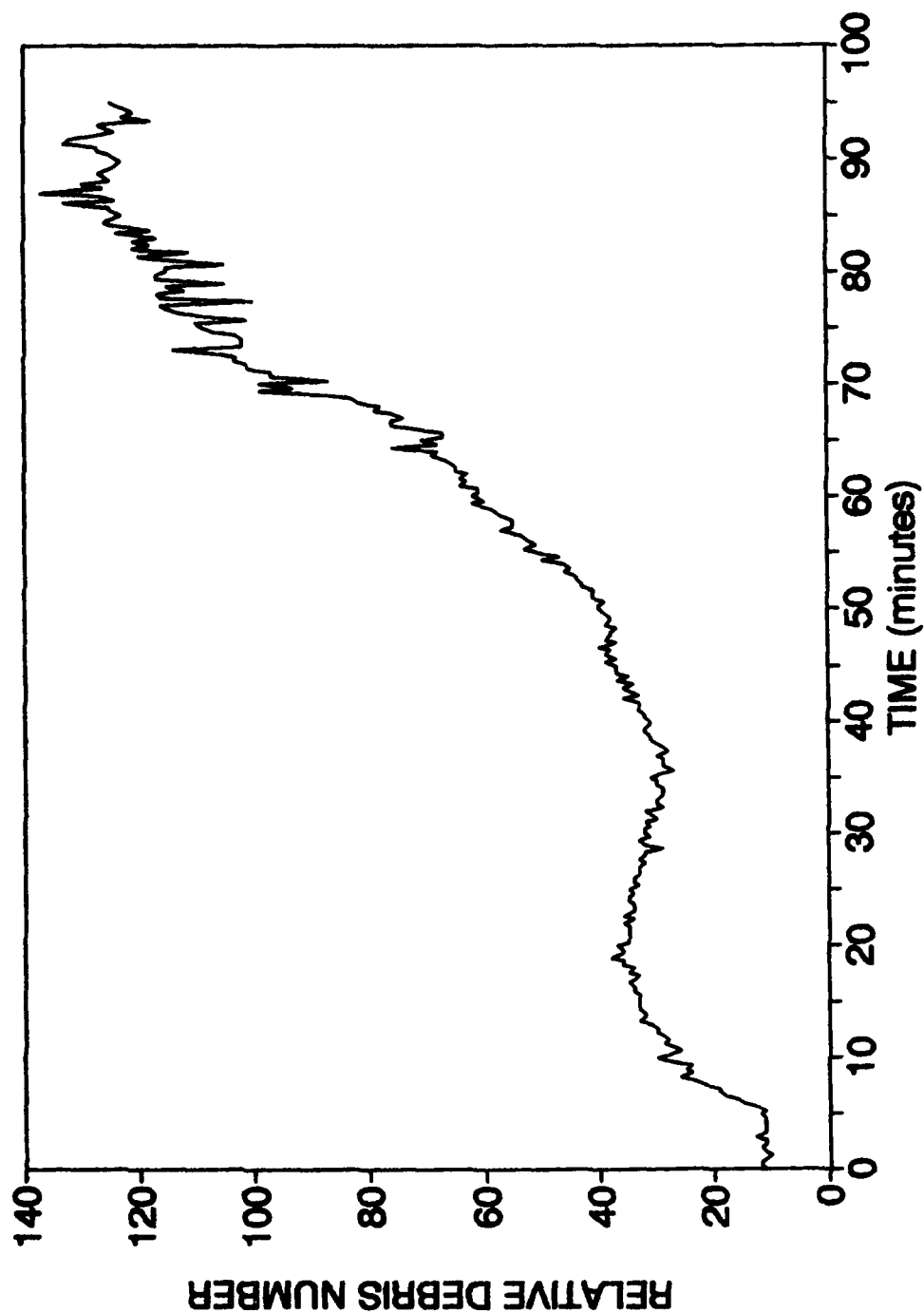


Figure 72. Ferrosan Output During the 90-Minute TBOD Test of Figure 71.

the 310 system has been seen to be affected strongly by temperature, oil velocity, and type of ferrous material. Particle size has also been shown to affect sensitivity but to a lesser degree.

#### d. Summary

The Ferrosan 310 system has been evaluated based on additions of Fe particles of into a circulating oil stream. The sensitivity of the 310 unit was seen to increase with increasing temperature and oil velocity. Fe particle sizes of 5 to 10 microns, 10 to 20 microns, and 20 to 30 microns were tested extensively to determine whether the system sensitivity is size dependent. Similar results were obtained for the 5 to 10 and 20 to 30 micron particles, but the 10 to 20 micron Fe particles showed less of a response from the sensor.

Testing of these particles size ranges also revealed that the 310 unit loses sensitivity with increasing Fe concentration. This sensitivity loss was most apparent during a three-ball-on-disk wear test monitored by the Ferrosan. Reducing the duration of the wear test allowed the data of the 310 unit to better match the measured wear during the test, but the sensor has a saturation-point which prevents monitoring of high Fe concentration levels.

## 2. METALSCAN MARK 3

#### a. Introduction

A second wear metal sensor has been purchased for evaluation. The Metalscan Mark 3 system, like the Ferrosan 310, an in-line sensor which is designed to replace a section of tubing in an oil flow system, was also evaluated. In contrast to the 310, the Mark 3 is a particle counter, not an indicator of the concentration of wear metal. However, the Mark 3 has the added capacity of being able to detect conductive, nonferrous debris and distinguishes ferrous wear metal from nonferrous wear metal.

The Mark 3 monitors both ferrous and nonferrous channels simultaneously although the output of only one channel can be displayed on the CRT at a time. The system is designed to detect large wear particles typical during abnormal wear. Ferrous particles can be detected as small as 125 microns, and nonferrous particles can be detected down to 225 microns. The Mark 3 can also distinguish the size ranges for wear particles. The range for ferrous particles is 125 to 160 microns, 160 to 185 microns, and greater than 185 microns.

System limitations require oil temperature to be below 190°C and oil pressure to be below 3450 kPa. In addition, particle counting is influenced by vibration of the sensor and

aeration of the oil. Like the Ferrosan 310, the Mark 3 requires oil velocity to be within a specific range (0.6 m/s to 6.0 m/s).

The Mark 3 has been installed in an oil loop for testing. The system consists of a pump powered by a 2-hp motor which circulates oil to and from a 7-gallon reservoir. The oil lines consist of 1-inch stainless steel tubing, and the oil flow rate can be adjusted by opening a valve of a bypass line. The Mark 3 sensor tube is placed in the primary return line to the reservoir. A filter is included in the system and is placed immediately after the sensor tube to capture particles after they have been counted.

Only some basic testing has been done with the Mark 3. The reservoir was filled with 15 L of MIL-L-7808 oil and pumped through the sensor at two different flow rates to check whether false counting occurred. Oil velocities were measured when the bypass is closed ( $3.94 \pm 0.04$  m/s through the sensor) and when the bypass is open ( $1.46 \pm 0.11$  m/s through the sensor). False particle counts have been recorded when the oil flow through the sensor is at its maximum, but the false counts are only for the ferrous channel. At the system minimum oil velocity, no false counts are detected for either ferrous or nonferrous channels.

Initial testing of the Mark 3 will be performed by making periodic additions of a variety of metals into the oil flow. After establishing the sensor ability to discriminate between ferrous and nonferrous metals and verifying that responsiveness is equal for a variety of different nonferrous metals, the Mark 3 will be used to monitor a wear test like the TBOD. In order to generate appropriate-sized wear debris for the Mark 3, the TBOD test used to evaluate the Ferrosan 310 would have to be replaced with some sort of bearing test in which the bearing is heavily loaded and rotating at a high rate of speed for its size (i.e., large DN). By doing so, the onset of a fatigue failure will quickly result, and spalling will cause large bearing wear particles to be available for detection by the Mark 3.

### 3. IMPACT OF FILTRATION ON SECONDARY WEAR

#### a. Introduction

A study was undertaken to determine the extent that wear particles present in a lubrication system contribute to further wear. This study of secondary wear began by first devising an oil circulation system into and out of a controlled wear test. The three-ball-on-disk (TBOD) wear test was again chosen as the method for generating wear metal because its simplified geometry and test fixtures allow oil to flow through the wear areas and sweep away most of the wear particles generated (Figure 65).

The three-pump set-up described in Section 1.b.(4) above was used to circulate the oil into and out of the test chamber. Previously, the Ferrosan 310 sensor was in-line with the larger of the three pumps, but this device was replaced with a filter housing for selective filtration of particles greater than 3 microns, greater than 5 microns, and greater than 10 microns. A schematic of the oil flow network is shown in Figure 73.

**b. Preliminary Testing**

To ensure adequate wear would take place, three M50 steel balls ( $R_c$  60) were slid against an ASTM 1018 steel disk ( $R_c$  20) for each test. Initial tests using a MIL-L-7808 type lubricant (0-82-3) were conducted at rotational speeds of 250 rpm (for a linear sliding velocity of approximately 0.3 m/s) and loads of 40 kg. Tests were conducted at room temperature although pumping caused the oil temperature to rise to approximately 35°C. The wear rates for three baseline tests are shown in Figure 74 by the vertical displacement of the test balls. Figure 74 indicates substantial variation for the three tests. Further indication of repeatability difficulties are seen when the friction coefficients throughout each of the three tests are compared (Figure 75).

Despite the variations in the three baseline tests, the TBOD tests were repeated with a filter placed in-line with the circulating oil. Filter sizes of 10, 5, and 3 microns were used, and two tests were performed for each size filter. The results for the wear rates and friction coefficients from the tests of the 10-micron filter are shown in Figures 76 and 77, respectively. Like the baseline tests, substantial variation exists between these two tests with the 10-micron filter. The same data are presented in Figures 78 and 79 for the 5-micron filter. Repeatability of both the wear rates and friction coefficients is improved, but in comparison to the baseline tests, the effect of the filter cannot be seen. Finally, the data for the 3-micron filter are given in Figures 80 and 81. As with the 10-micron filter, substantial variation exists between the results of the two tests using the 3-micron filter.

Since no discernable change in the wear behavior is seen with filtration, the test procedure was reevaluated. The 40-kg load chosen for baseline tests ensured that wear continued throughout the majority of the 5-hour test duration. At some point during most of these tests, a levelling of the wear rate curve occurs indicating a hydrodynamic separation of the wear surfaces. This hydrodynamic oil film is precisely what is needed to observe the effects of secondary wear because without separation of the contact surfaces, existing wear debris cannot enter into the wear region and contribute to the wear process.

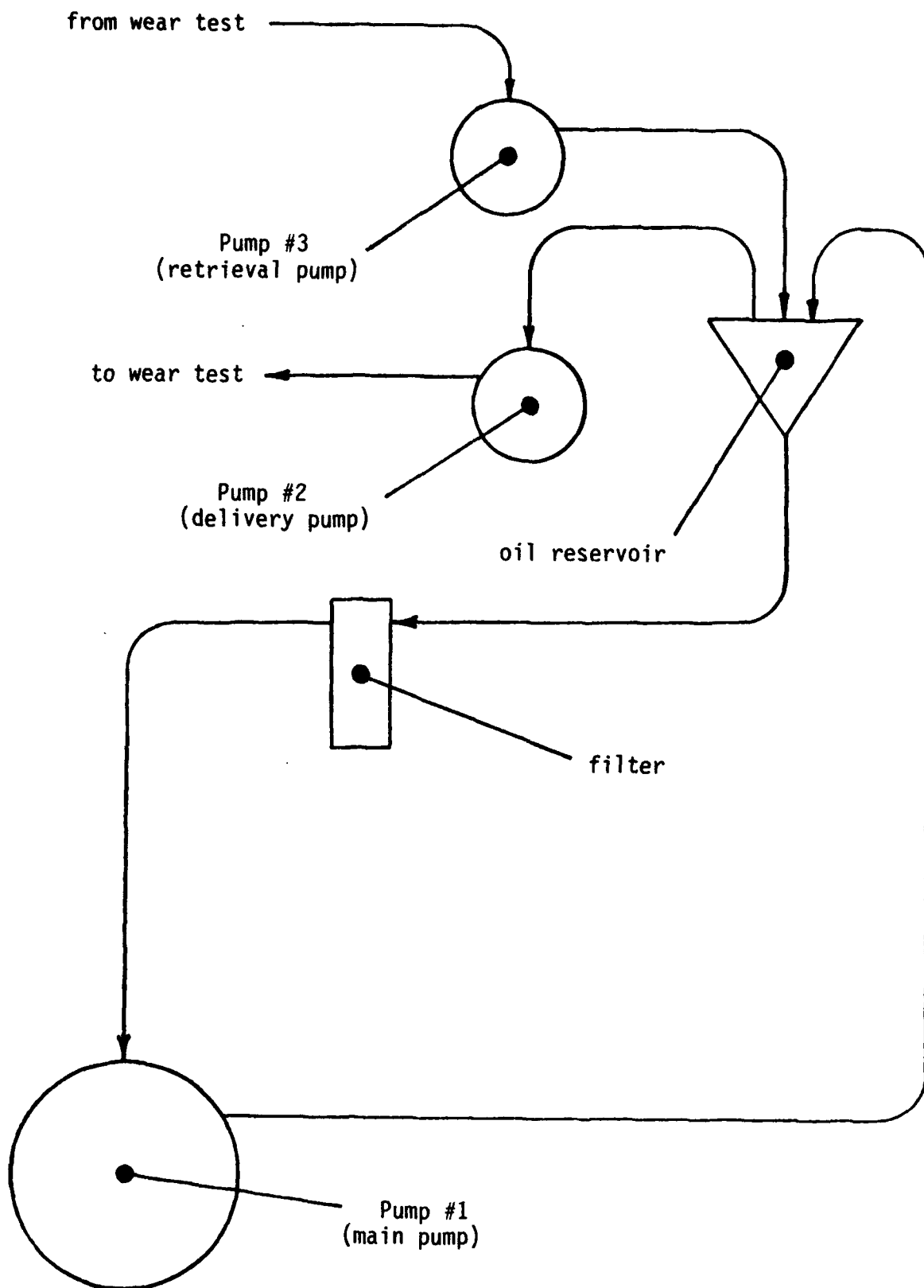


Figure 73. Oil Flow Network for TBOD Testing With Filtration.

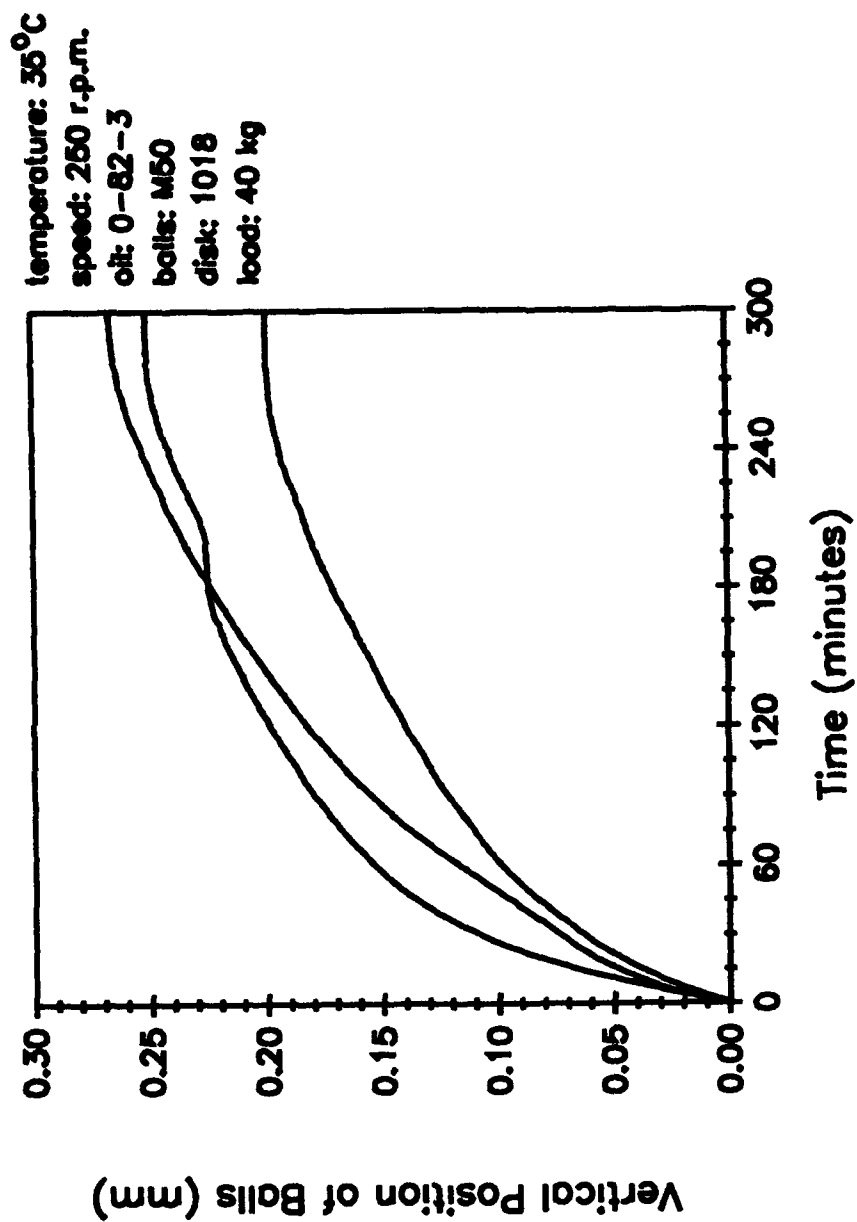


Figure 74. Comparison of the Wear Rates of Three Unfiltered TBOD Tests Run at the Same Operating Conditions.

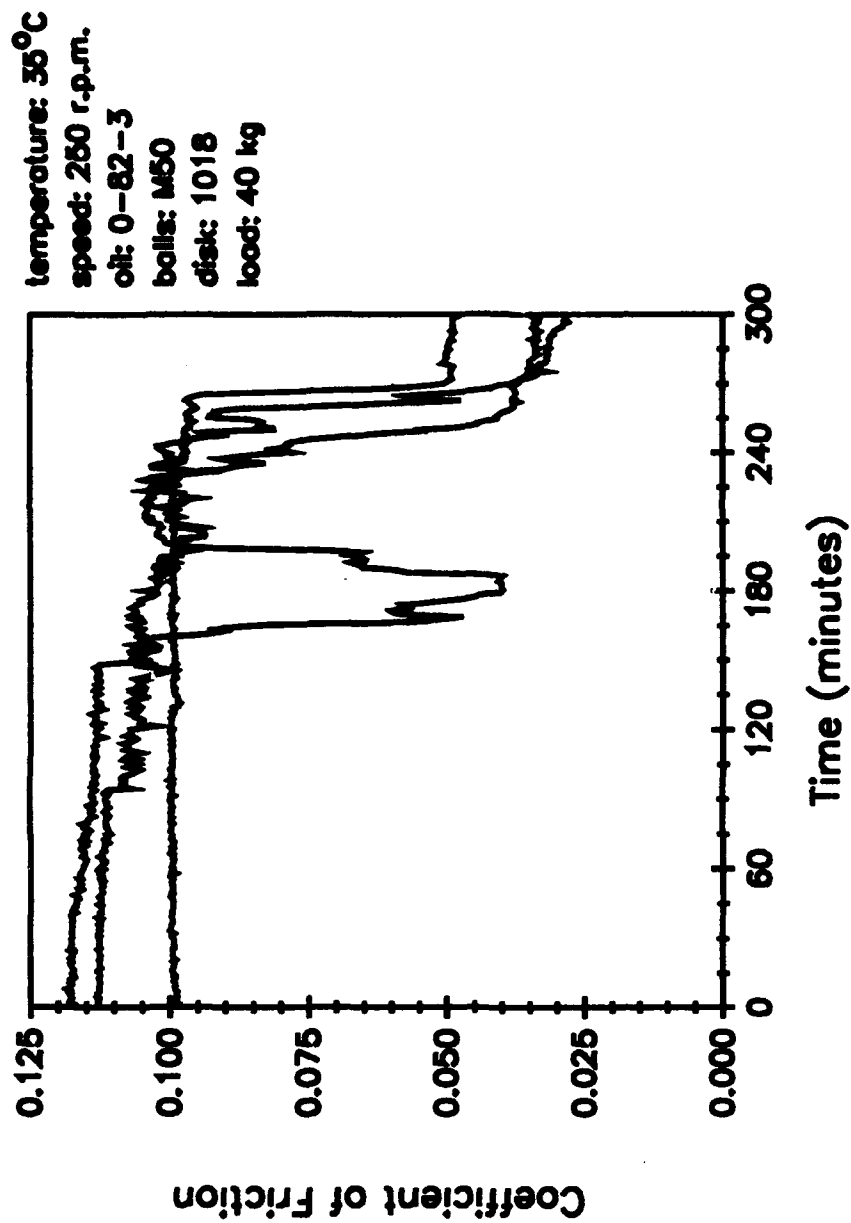


Figure 75. Comparison of the Friction Coefficients During the Three TBOD Tests of Figure 74.

temperature: 35°C  
speed: 250 r.p.m.  
oil: 0-82-3  
balls: M50  
disk: 1018  
load: 40 kg

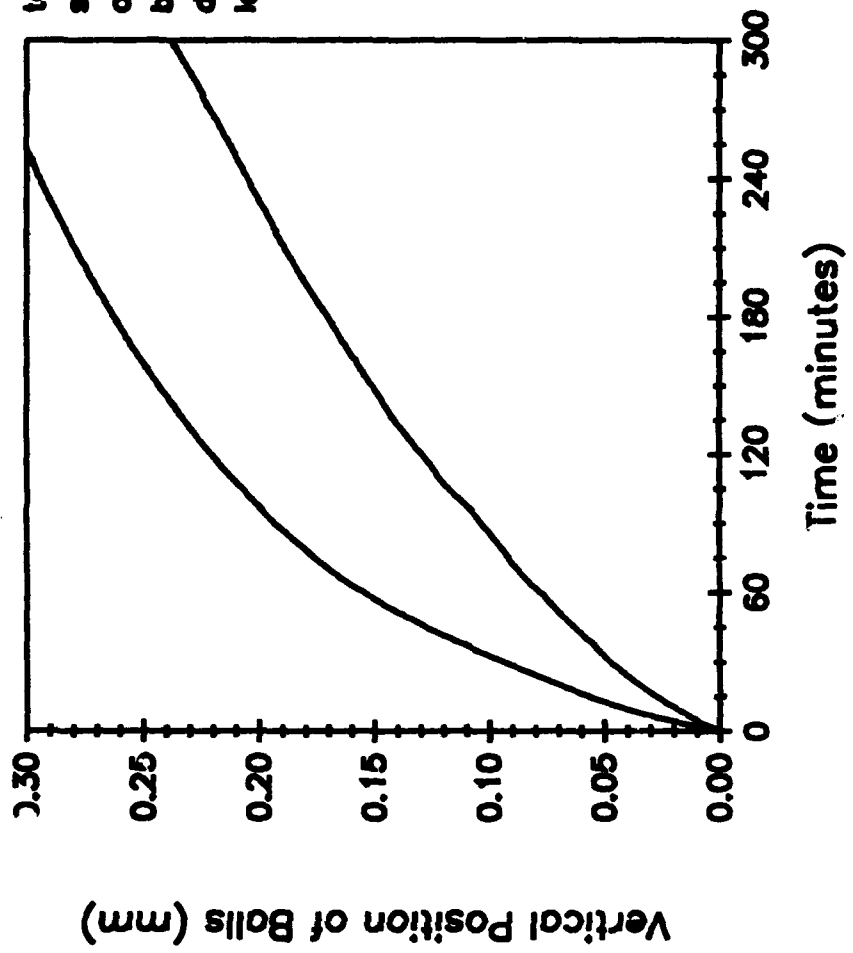


Figure 76. Comparison of the Wear Rates of Two TBOD Tests Run at the Same Conditions as Those in Figure 74 but with a 10-Micron Filter.

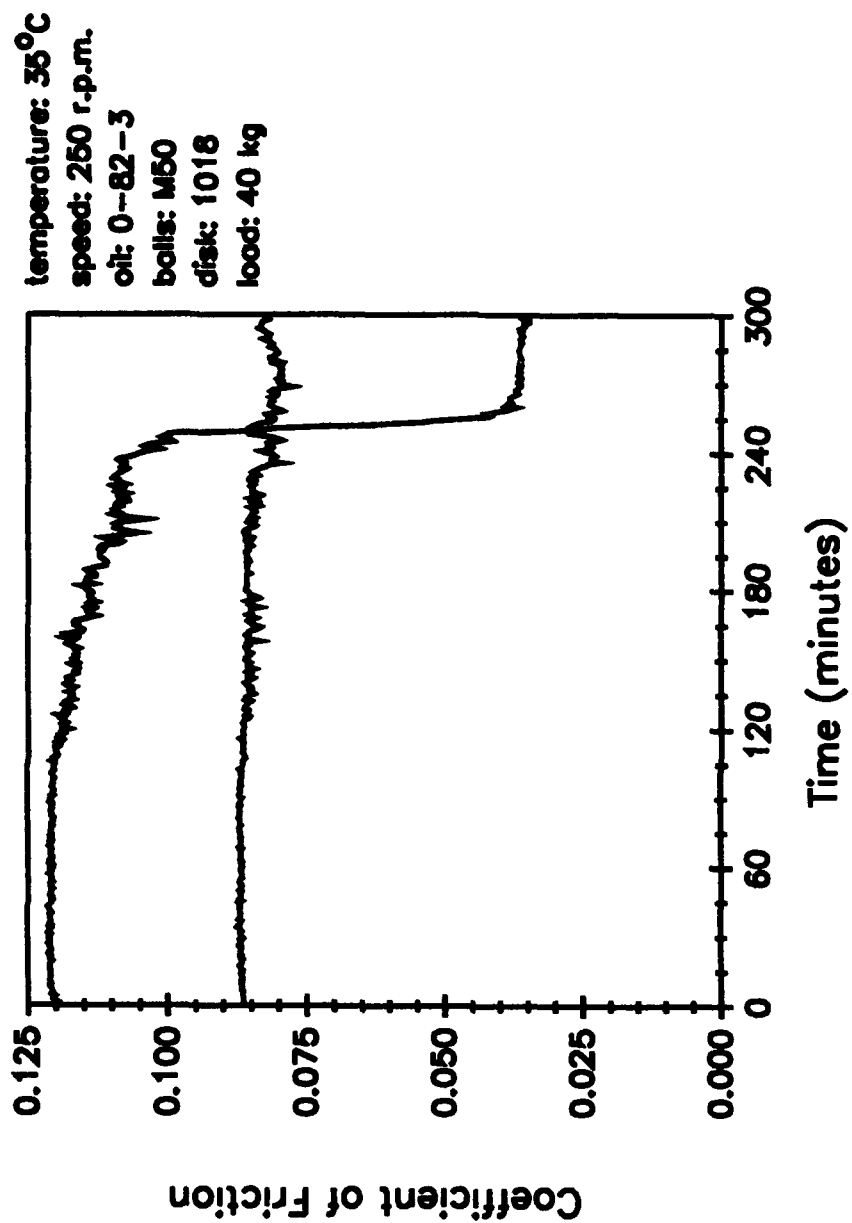


Figure 77. Comparison of the Friction Coefficients During the Two TBOD Tests of Figure 76.

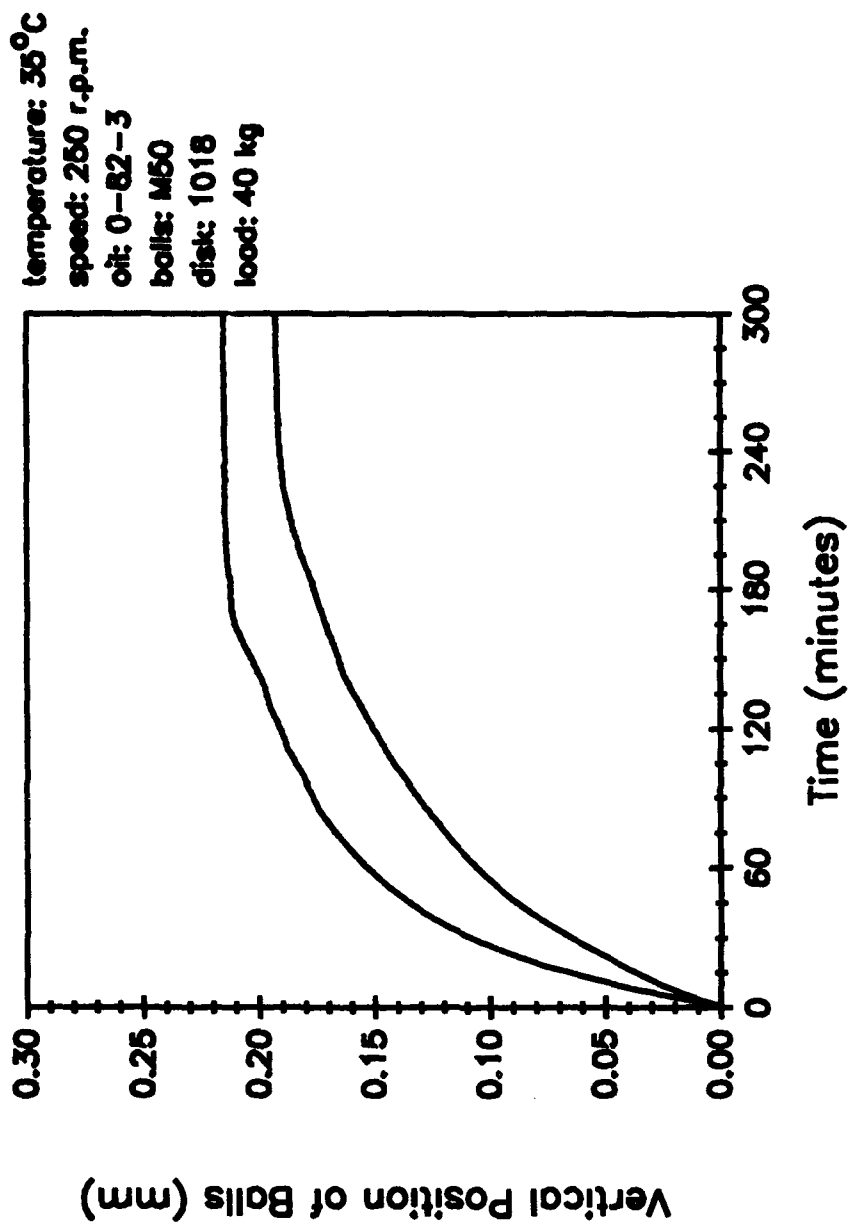


Figure 78. Comparison of the Wear Rates of Two TBOD Tests Run at the Same Conditions as Those in Figure 74 but with a 5-Micron Filter.

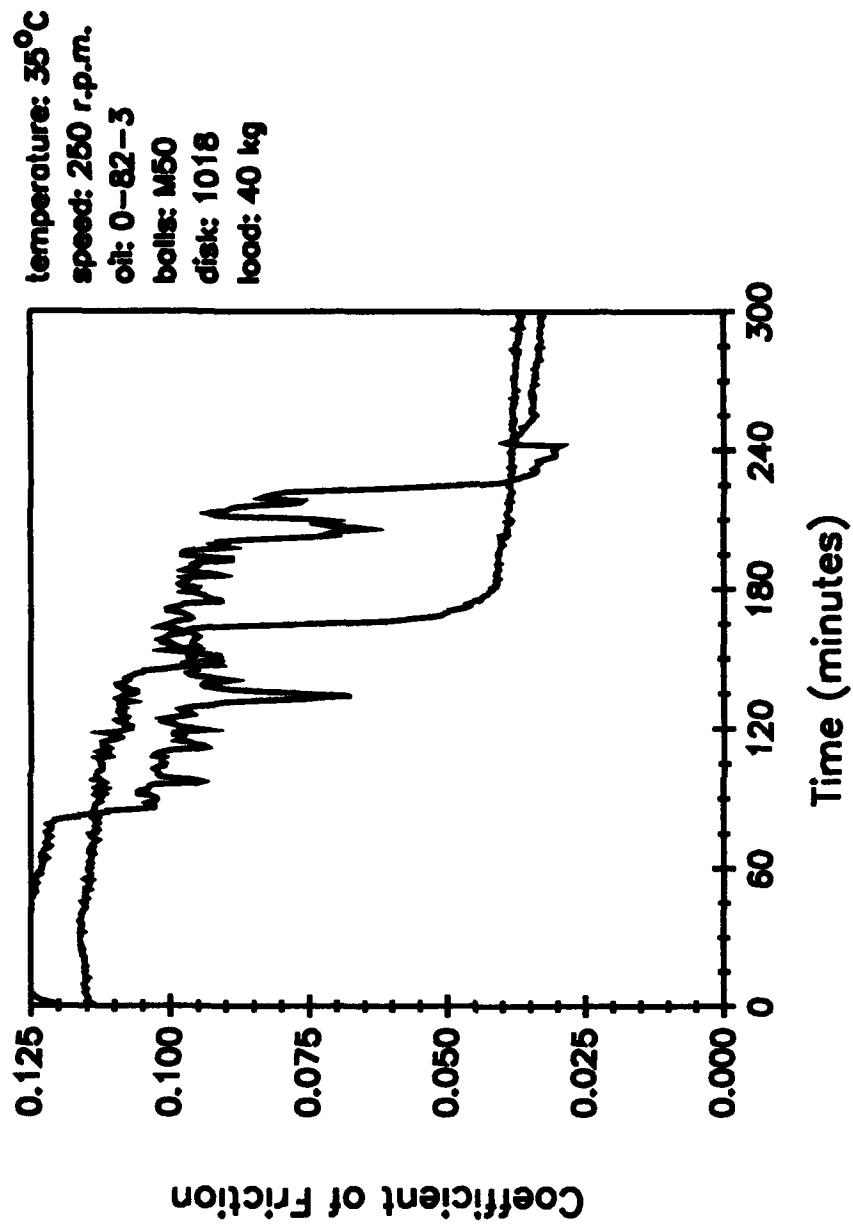


Figure 79. Comparison of the Friction Coefficients During the Two TBOD Tests of Figure 78.

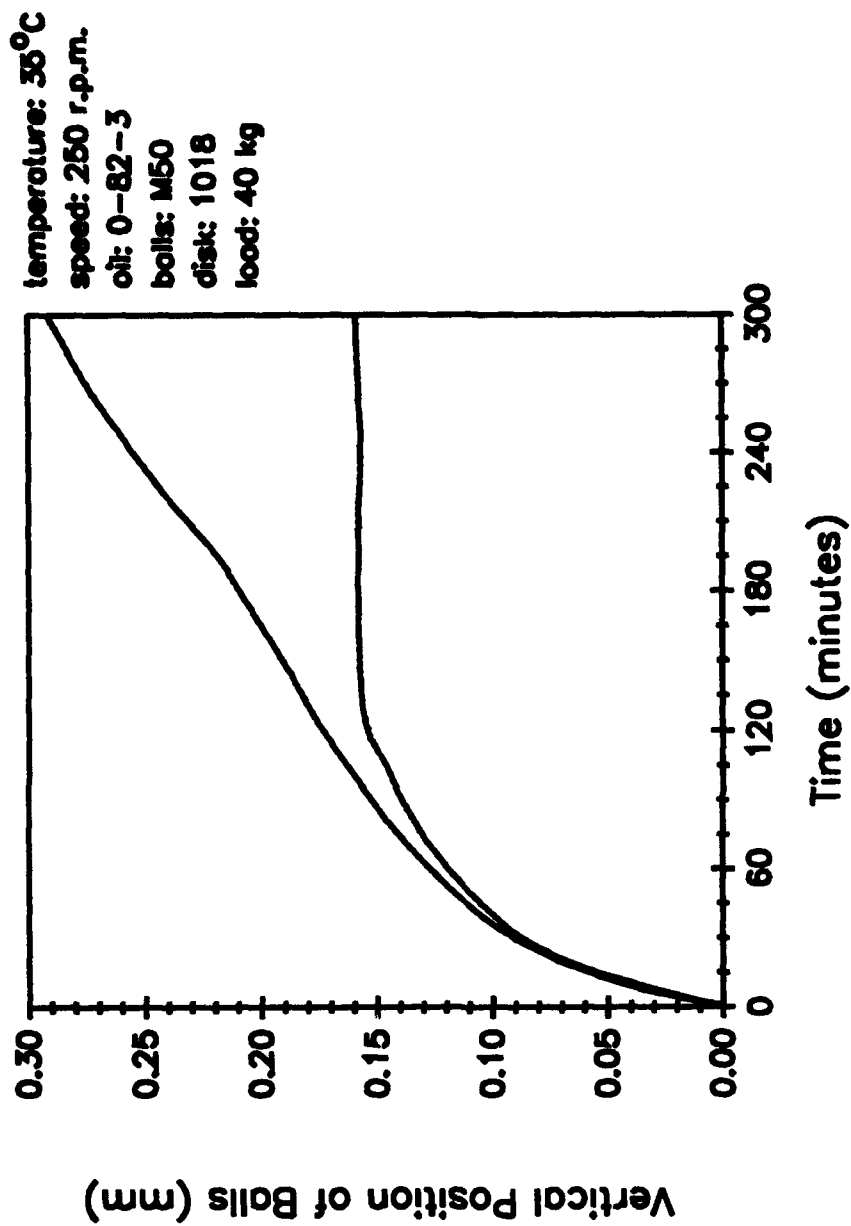


Figure 80. Comparison of the Wear Rates of Two TBOD Tests Run at the Same Conditions as Those in Figure 74 but with a 3-Micron Filter.

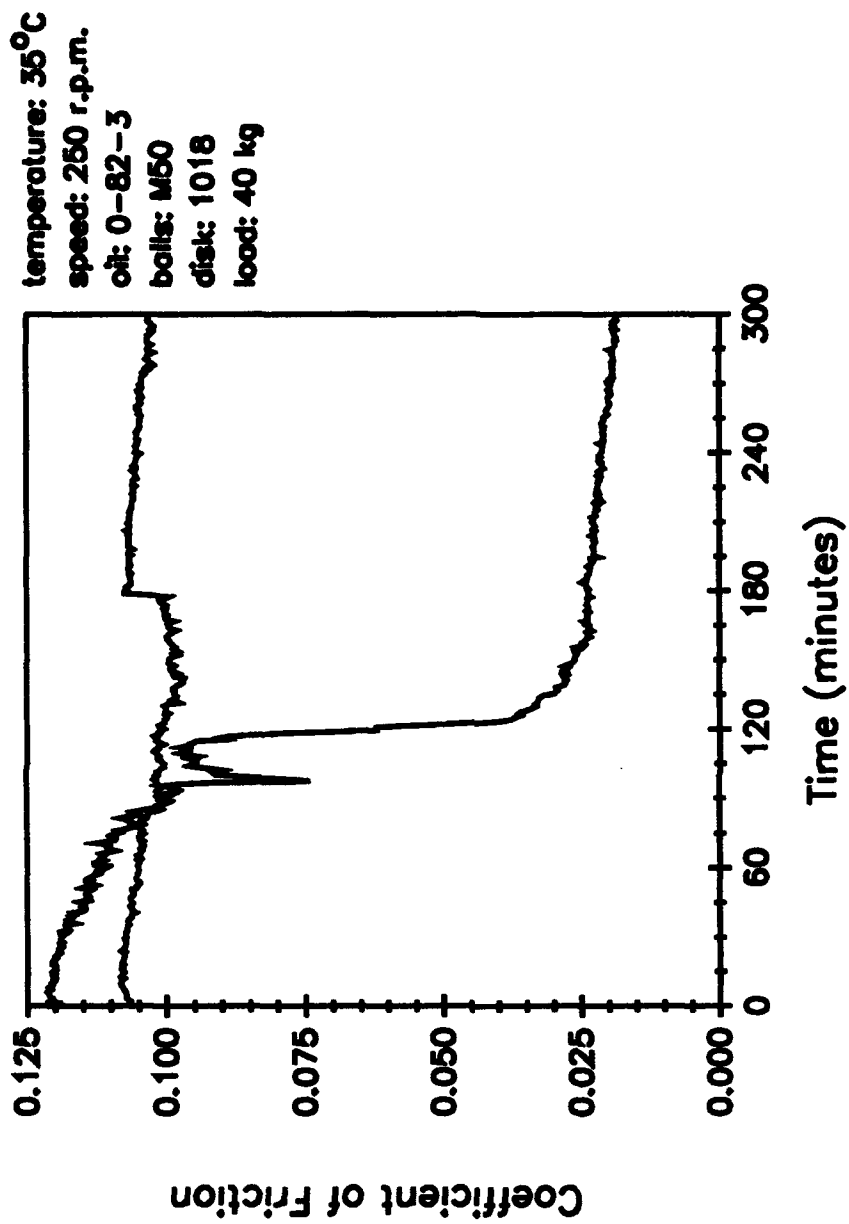


Figure 81. Comparison of the Friction Coefficients During the Two TBOD Tests of Figure 80.

To allow wear particles an opportunity to freely circulate into contact areas, hydrodynamic lubrication must be induced during baseline tests and sufficient time must be given for hydrodynamic separation in order to see an effect. Therefore, a TBOD test was conducted with a confined oil volume of 75 ml and a reduced load of 30 kg. The oil temperature was controlled at 50°C, and the test was allowed to run for 50 hours. Figure 82 gives the wear rate during this test.

Figure 82 indicates that after initial run-in wear, the wear rate assumes the form of a step function. Each step is a period of hydrodynamic separation during which existing wear particles can come between the contact surfaces and eventually cause a period of accelerated wear. This increase in wear stops when the contact surfaces grow large enough to again be supported by a hydrodynamic film, and the process starts over.

Filtration of the formed wear particles during TBOD Test 139 (Figure 82) should ensure that the initial hydrodynamic separation continues uninterrupted. To establish the contribution of secondary wear, a test was again performed with a circulating oil flow and a 3-micron filter at the same load and speed as TBOD Test 139. Unlike TBOD Test 139, the filtration test was allowed to run 66.7 hours (4000 minutes) without an outside heat source. Figure 83 shows the wear rate data on the same vertical scale used for Figure 82. Except for one increase in the wear rate at approximately the 1000-minute mark, hydrodynamic lubrication is maintained throughout the entire test.

Since the tests of Figures 82 and 83 were not done at exactly the same conditions (TBOD Test 139 used a confined oil volume of 75 ml at 50°C while TBOD Test 140 used a circulating oil volume of 1200 ml without heating), a repeat of TBOD Test 140 was performed without filtration. The wear rate during this test is shown in Figure 84 and reveals the same wear trends that were observed for the confined oil volume test of Figure 82.

#### c. 20-Hour TBOD Tests

Based on the results of the 66.7-hour test of Figure 83, a duration of 20 hours would give sufficient time to see any secondary wear effects after the onset of hydrodynamic separation. A battery of 20-hour TBOD tests were completed using 3, 5, and 10 micron filters as well as no filter to establish repeatability and compare the effectiveness of increasingly finer filtrations. As will be shown, three characteristic wear regimes have occurred during these 20-hour tests and prevented repeatable data even from duplicate tests performed at exactly the same conditions.

# TBOD 139

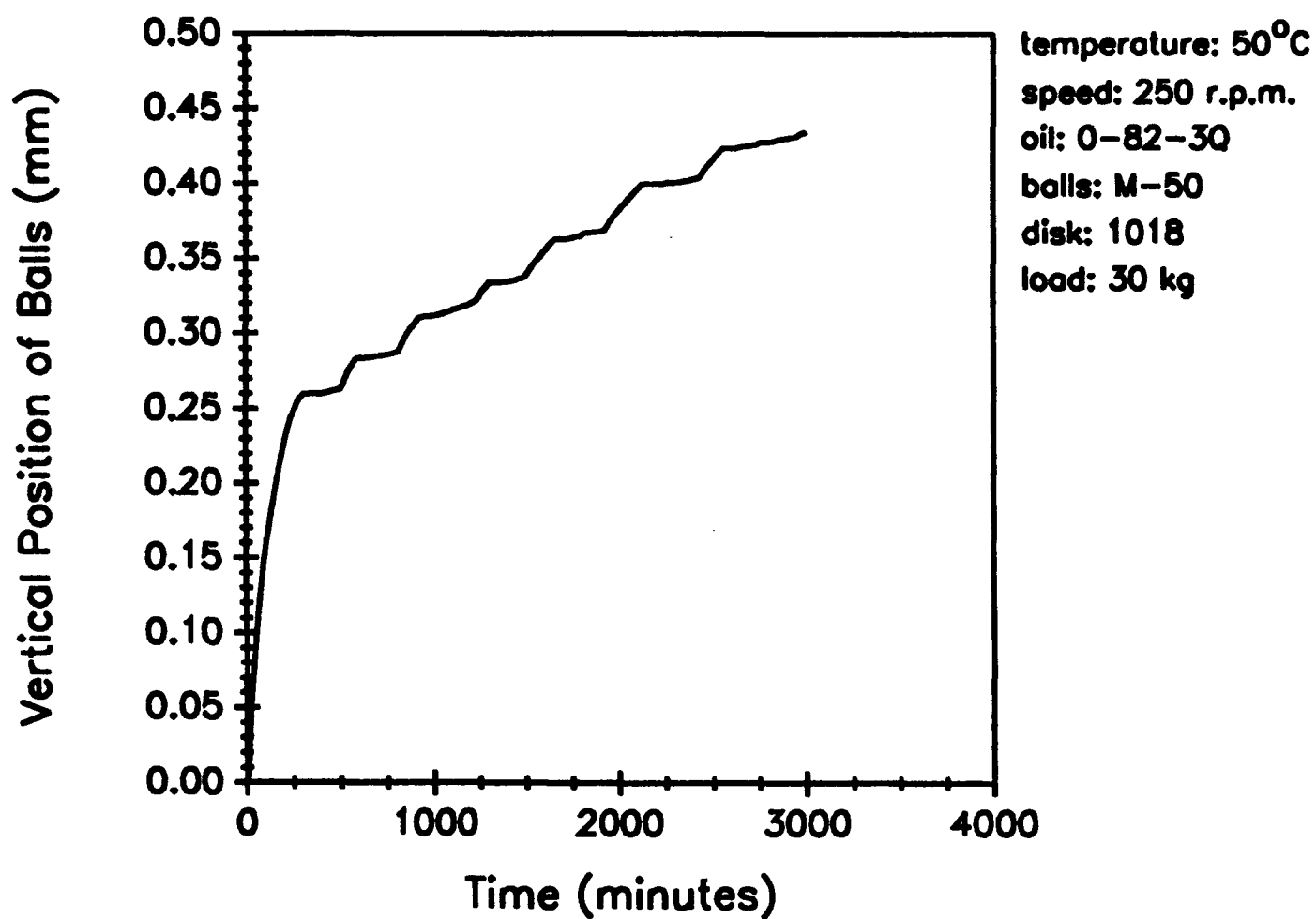


Figure 82. Wear Rate During a 50-Hour TBOD Test with a Confined Oil Volume of 75 mL.

# TBOD 140

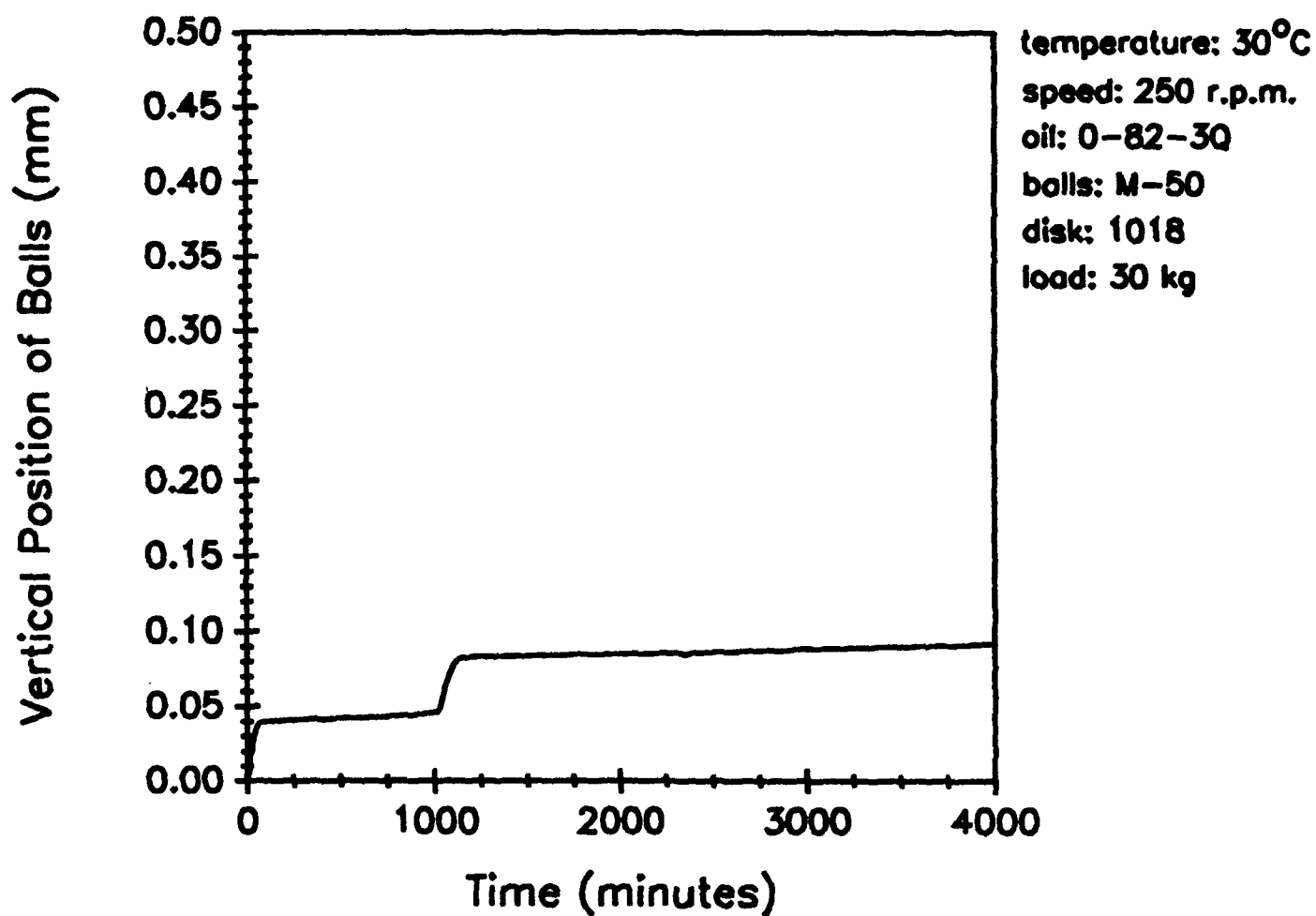


Figure 83. Wear Rate During a 66.7-Hour TBOD Test with Oil Circulated Through a 3-Micron Filter.

# TBOD 141

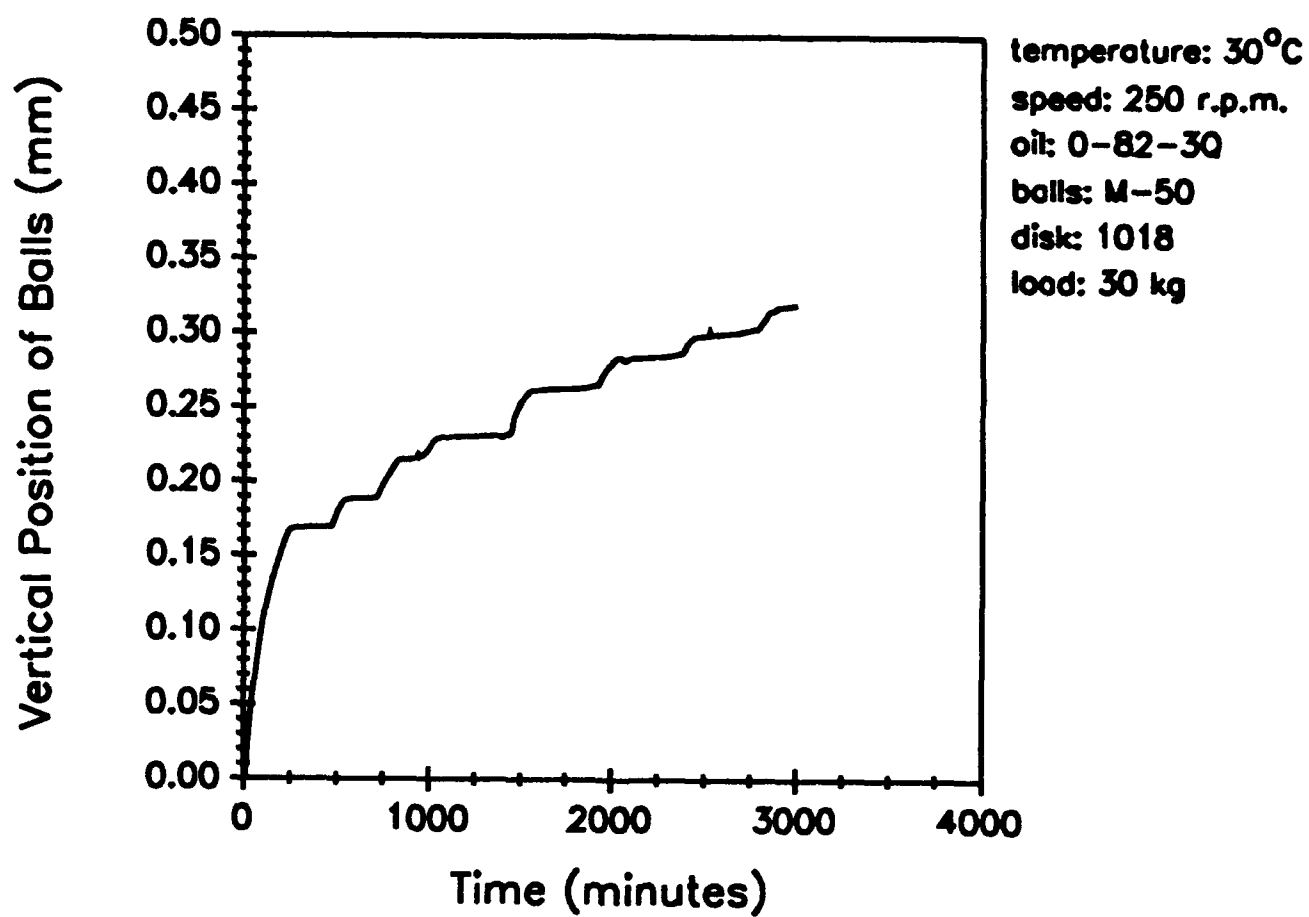


Figure 84. Wear Rate During a 50-Hour TBOD Test with Oil Circulated without Filtration.

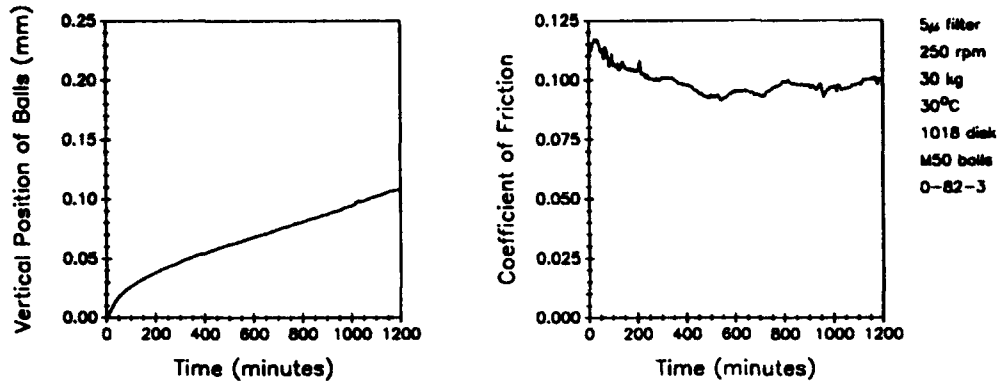
The results from the TBOD tests are again presented in terms of the wear rate and the friction coefficient. Figure 85 shows the wear rate and friction coefficient curves for all of the TBOD tests which exhibited both a near linear wear rate as well as steady coefficients of friction. The three tests shown in Figure 85 consist of a test where no filtration was done (85b), where a 5-micron filter was used (85a), and where a 10-micron filter was used (85c).

The second characteristic wear regime seen during these TBOD tests was similar to the first in terms of the shape of the wear rate curves, but the friction coefficients fluctuated dramatically throughout the tests. Five tests showed such behavior and are presented in Figure 86. Three of these tests were from 3-micron filtration (Figures 86b, 86c, and 86d), one from 5-micron filtration (86a), and one from 10-micron filtration (86e). Although the coefficients of friction do vary tremendously during these tests, the curves indicate a gradual decrease in the average values over the length of the tests.

Finally, the last of the three characteristic wear regimes is the same as that of the preliminary tests shown in Figures 82 through 84. In these tests, initial run-in wear is very large (in comparison to the other two wear regimes) but the large resulting scar areas allow hydrodynamic separation to take place and wear to cease. The presence of wear particles in the oil, however, cause run-in wear to be periodically reinstated. During the run-in portions, friction coefficients are high, but during the periods of hydrodynamic separation, the coefficient of friction is dramatically lowered. Figure 87 shows the friction and wear data of the remaining tests which all exhibited extended periods of hydrodynamic separation. Figures 87c, 87d, and 87e are from tests using a 3-micron filter while Figures 87a, 87b, and 87f all used a 10-micron filter.

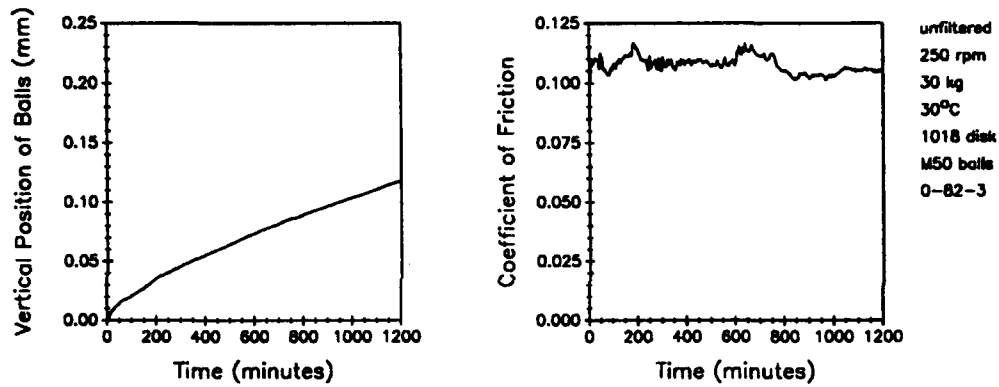
The results of the wear data of these tests are summarized in Table 87. The wear is first presented by volume based on measurements of the resulting scars on the balls. Disk wear is also given by the weight loss during the test. Wear on the ball specimens was negligible since the balls are much harder than the disks.

### TBOD 158



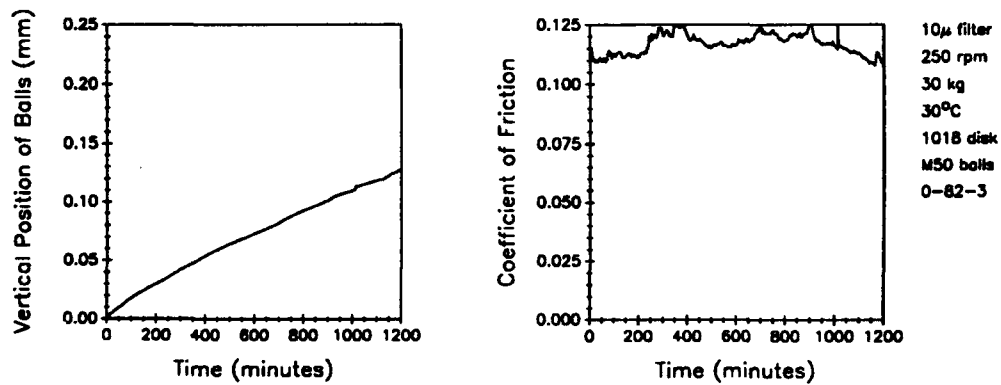
a. 5-micron filter

### TBOD 163



b. unfiltered

### TBOD 167



c. 10-micron filter

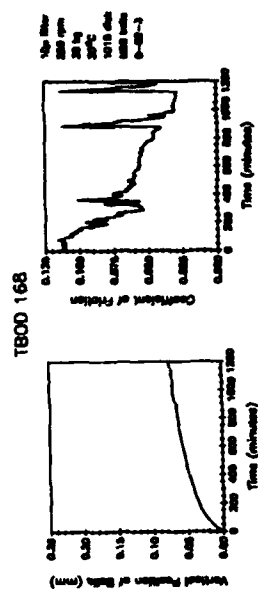
**Figure 85. Constant Wear and Constant Friction Coefficient Curves for Three TBOD Tests with Filtration.**



b. 3-micron filter



d. 3-micron filter



e. 10-micron filter

a. 5-micron filter

c. 3-micron filter

Figure 86. Constant Wear and Varying Friction Coefficient Curves for Five TBOD Tests with Filtration.

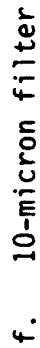
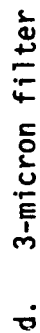
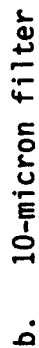


**Figure 87. Varying Wear and Varying Friction Coefficient Curves for Six TBOD Tests with Filtration.**

TABLE 87

**TBOD WEAR FROM 20-HOUR TESTS OF M50 BALLS  
AND 1018 DISKS USING FILTERED MIL-L-7808**

Test Number	Figure Number	Filter Size (microns)	Total Wear (mm <sup>3</sup> )	Disk Weight Loss, grams
158	85	5	12.48	0.091
163	85	none	11.60	0.104
167	85	10	13.50	0.120
157	86	5	7.64	0.070
160	86	3	9.20	0.082
161	86	3	6.40	0.049
165	86	3	8.14	0.057
168	86	10	7.08	0.052
155	87	10	27.00	0.242
156	87	10	39.27	0.343
159	87	3	33.93	0.308
162	87	3	27.45	0.247
164	87	3	37.93	0.343
166	87	10	19.96	0.185

The data of Table 87 do not reveal a discernable effect from filtration since substantial wear variations exist for identical tests exhibiting the same wear regime. For example, the three tests of Figure 87 which had 3-micron filtration have wear volumes ranging from 27.45 mm<sup>3</sup> to 37.93 mm<sup>3</sup> and disk wear ranging from 0.247 grams to 0.343 grams. The other three tests from Figure 87 used a 10-micron filter and the variation in wear was even more pronounced (19.96 mm<sup>3</sup> to 39.27 mm<sup>3</sup> and 0.185 grams to 0.343 grams). For the wear regime demonstrated in Figure 86, three other tests with 3-micron filtration can be compared. For these tests (160, 161, and 165) the wear volumes ranged from 6.40 mm<sup>3</sup> to 9.20 mm<sup>3</sup> while the disk wear varied from 0.049 grams to 0.082 grams.

TBOD testing has consistently shown variations in the length and relative amounts of run-in wear. In order to ensure that hydrodynamic separation occurred during testing, another batch of tests was performed with preworn disks. The existing wear scars on these disks varied, but with even a small initial contact area, run-in wear has a head start and some period of hydrodynamic separation should be expected.

Filter sizes of 3, 5, and 10 microns are used in three of the five new tests. The fourth test was performed using the 3-micron filter together with a magnetic flow meter (to remove those wear particles smaller than 3 microns). The fifth test was done without the use of any filter. Except for filter size, all tests were performed under the same conditions.

Figure 88 shows the friction and wear results from a 20-hour TBOD test without filtration. The shape of the curve in Figure 88a indicates initial run-in wear which lasted for 200 minutes and was followed by four periods where the wear temporarily ceased. By comparing Figure 88b to Figure 88a, the friction coefficient is seen to drop dramatically during the four, no-wear periods.

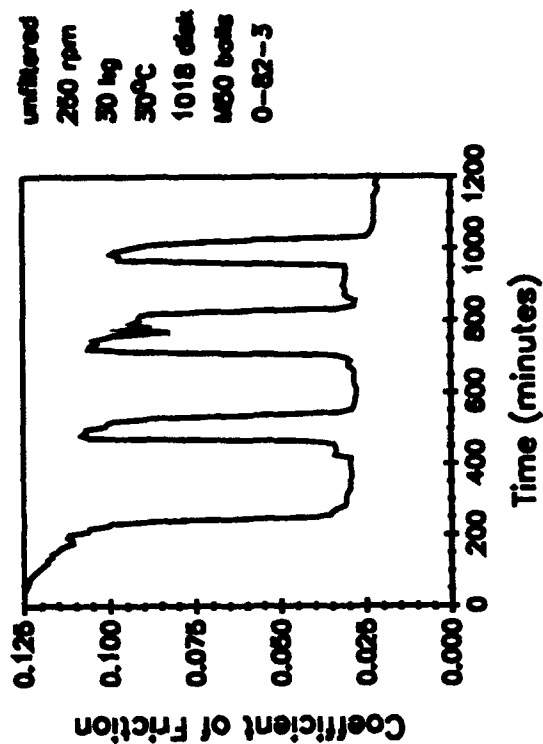
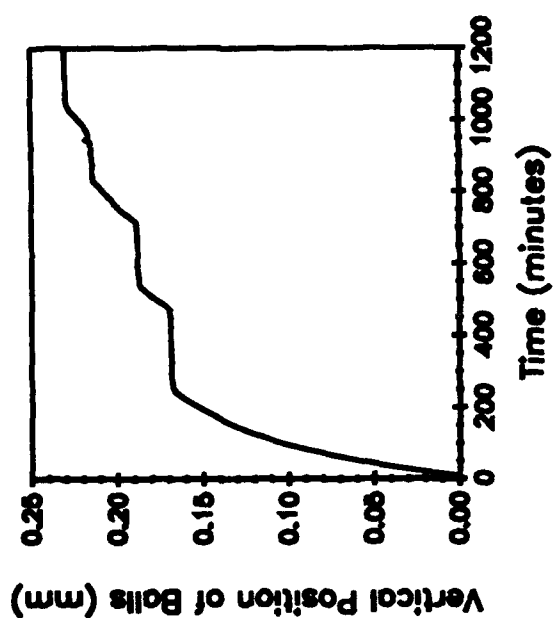
The reduction in the friction coefficient results from hydrodynamic separation of the balls/disk contact. The three spikes seen in Figure 88b indicate that the hydrodynamic separation is interrupted and wear resumes. Figure 88a confirms the onset of wear at these three points during the test. Furthermore, the slopes of the curve at each of the three points are similar to the slope before the onset of the first hydrodynamic period, indicating additional run-in wear. The presence of all of the wear debris generated during the test of Figure 88 allowed run-in wear to be reinstated three times.

The next test was performed with a 10-micron filter, and the results are given in Figure 89. Although the displacement and friction curves are similar to Figure 88, the 10-micron filter caused only two additional periods of run-in after initial hydrodynamic separation.

The third and fourth tests used a 5-micron and 3-micron filter, and their results are presented in Figures 90 and 91, respectively. By further reducing the size of existing wear particles in the oil, the two additional run-in periods of Figure 89 are reduced to only one for Figures 90 and 91. Further, the 3-micron filter prevented additional wear until about the 950-minute mark (Figure 91) while the 5-micron filter allowed additional wear at about the 500-minute mark (Figure 90).

The results from the final test are given in Figure 92. In this test, the 3-micron filter was used in addition to an in-line magnetic element in an effort to eliminate particles below 3-microns in size. As the curves in Figure 92 indicate, the removal of all wear debris allowed hydrodynamic separation to continue uninterrupted for the entire 20-hour test duration.

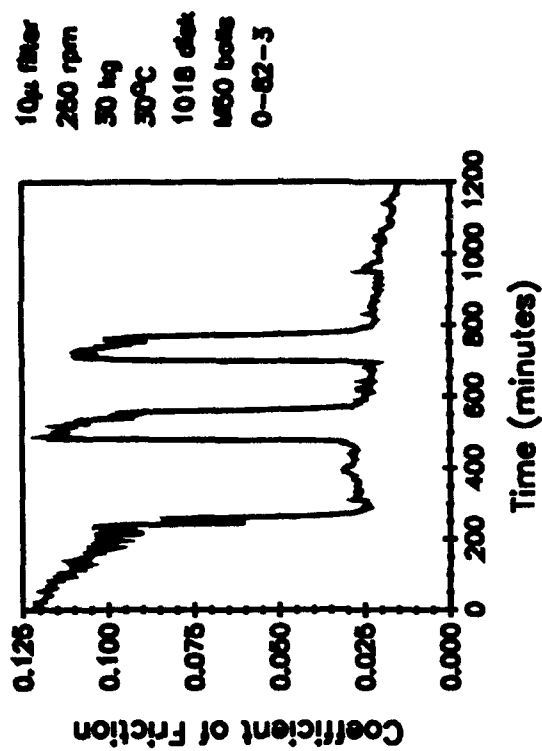
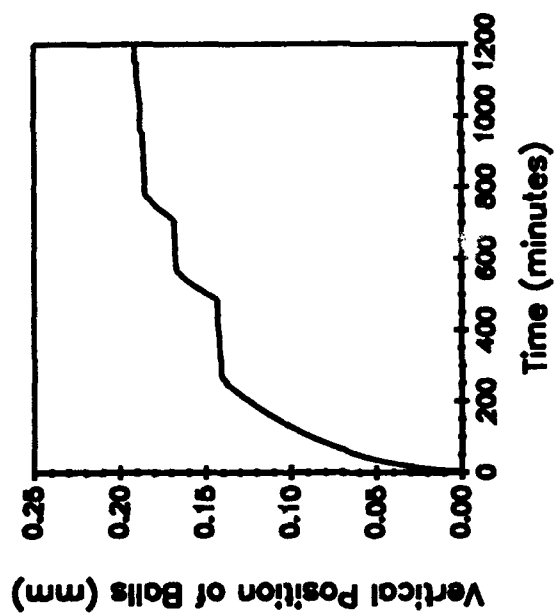
# TBOD



unfiltered  
250 rpm  
30 kg  
30°C  
1018 disk  
M50 balls  
0-82-3

Figure 88. Friction and Wear Results from TBOD Testing without Filtration.

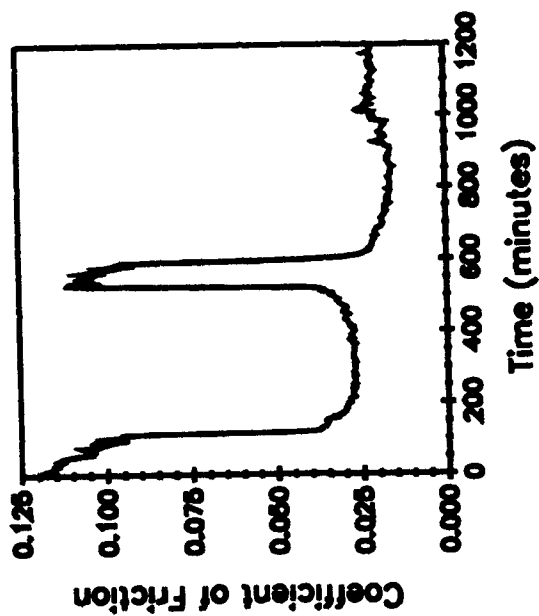
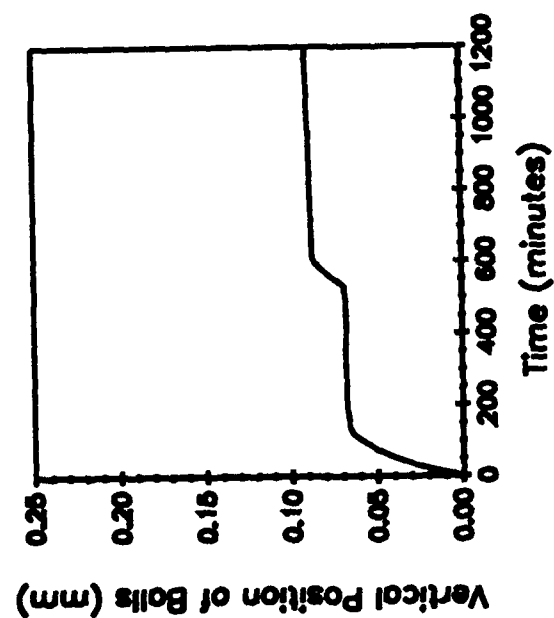
# TBOD



10µ filter  
250 rpm  
30 kg  
30°C  
1018 disk  
1650 balls  
0-82-3

Figure 89. Friction and Wear Results from TBOD Testing with a 10-Micron Filter.

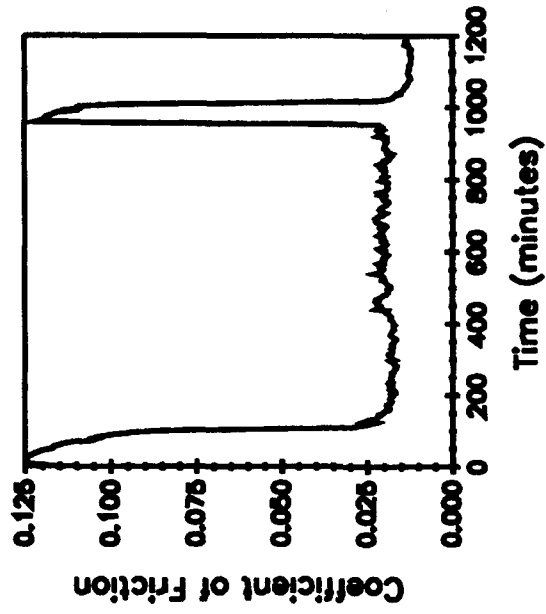
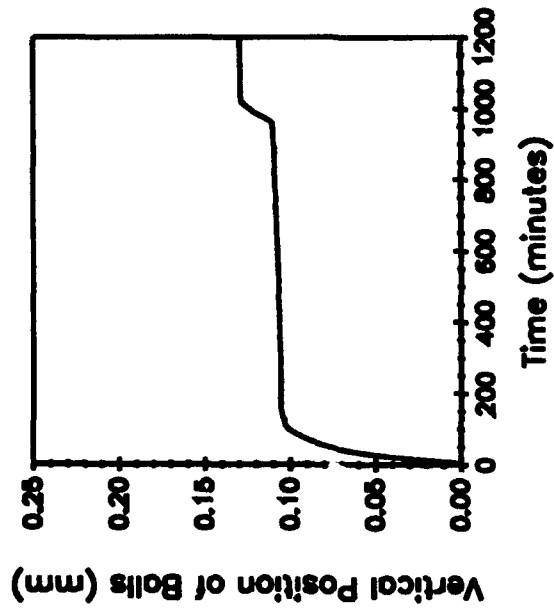
# TBOD



5µm filter  
250 rpm  
30 kg  
30°C  
1018 disk  
M50 balls  
0-52-3

Figure 90. Friction and Wear Results from TBOD Testing with a 5-Micron Filter.

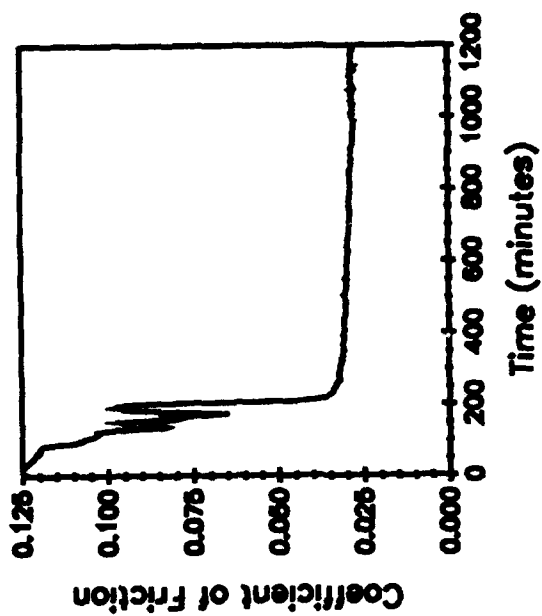
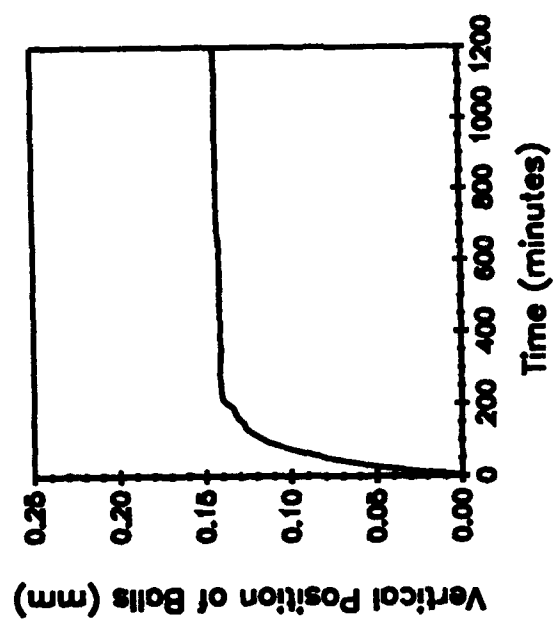
# TBOD



3µ filter  
250 rpm  
30 kg  
30°C  
1018 disk  
M50 balls  
0-82-3

Figure 91. Friction and Wear Results from TBOD Testing with a 3-Micron Filter.

## TBOD



3µ filter •  
280 rpm  
30 kg  
30°C  
1018 disk  
M50 balls  
0-52-3

Figure 92. Friction and Wear Results from TBOD Testing with a 3-Micron Filter and an In-Line Magnet.

**d. Conclusions**

Filtration seems to be effective in reducing instances of secondary wear (i.e., renewed run-in wear) in TBOD tests using preworn disks. Quantitative results are not available because the preworn disks used varied in initial wear volumes. In addition, repeatability has not yet been established for the apparent trends from Figures 89 through 92.

**e. Future Work**

In order to address the above two issues, future TBOD filtration tests will be performed under revised conditions. A new battery of tests will be done using preworn disks with a large enough wear scar that hydrodynamic separation should occur immediately with the loading and rotational speed previously used (30-kg, 245 rpm). The disks will be worn down so that they all having approximately the same beginning scar sizes and profiles, and initial wear volumes for the test disks will be calculated for comparison to final wear volumes.

By inducing hydrodynamic separation right from the start of the test, primary wear will have already taken place so that no wear particles will be present to cause secondary wear. It will, therefore, be necessary to add wear debris. This procedure should allow for improved repeatability since in all previous tests, wear debris showed an affinity to the test balls and collected around the ball scars even during 3-micron filtration. With clean test balls and preworn disks, wear particles of a known size collected from previous TBOD tests (i.e., less than 3 microns, less than 5 microns, or less than 10 microns) can be introduced in a known concentration. Any subsequent wear will result because of these additions and the repeatability difficulties of variations in initial run-in wear (Figures 85, 86, and 87) should be avoided.

## SECTION IV

### CANDIDATE HIGH TEMPERATURE LUBRICANT DIAGNOSTIC DEVICES

#### 1. HP-DSC FOR SCREENING OF HIGH TEMPERATURE LUBRICANTS

The use of high pressure differential scanning calorimetry (HP-DSC) for determining the relative oxidative stability of high temperature lubricants was investigated. Because of the small amount of lubricant (5 to 10 mg) used by this technique as well as the quick analysis time (<1 hour), HP-DSC could be used as a condition monitoring device or assist in determining oxidation test analysis temperatures and sampling times for limited supply experimental lubricants.

##### a. Background

DSC has been successfully used for evaluating the relative oxidative stability of lubricating oils.<sup>57-59</sup> This technique, which measures relative heat flow as a function of time or temperature, takes advantage of the fact that oxidation of a lubricant is basically an exothermic process. An idealized DSC thermogram<sup>57</sup> of a lubricant (Figure 93) reveals that a sudden exothermic rise in the baseline is observed due to the rapid oxidation (breakpoint) of the oil at the point of total antioxidant depletion. The stable period before oxidation onset (induction time) is proportional to the oxidative stability of the lubricant. DSC is often performed at high pressures (200-1000 psi) in order to lower the evaporation rate and increase the rate of oxygen diffusion into the lubricant which helps to sharpen the "onset of oxidation" peak.

High temperature lubricants, such as PPEs, would not be expected to display the same behavior as conventional lubricants due to the fact that the former contain inorganic, nonvolatile antioxidants that apparently are not consumed during oxidative stressing. In order to compare the HP-DSC behavior of high temperature lubricants with their bulk phase oxidation behavior, the HP-DSC analysis results of various PPE lubricants under different test conditions are correlated with lubricant degradation as determined by posttest sample analysis by gel permeation chromatography (GPC).

##### b. Experimental

HP-DSC experiments were performed on various PPE lubricants using a Dupont Model 910 DSC with high pressure accessory and the thermal analyst 2100 system for data analysis. The DSC cell was jumped to the particular test temperature (which took 3 to 4 minutes) and held for one hour. The cell was initially pressurized to 500 psi (air) in the constant volume

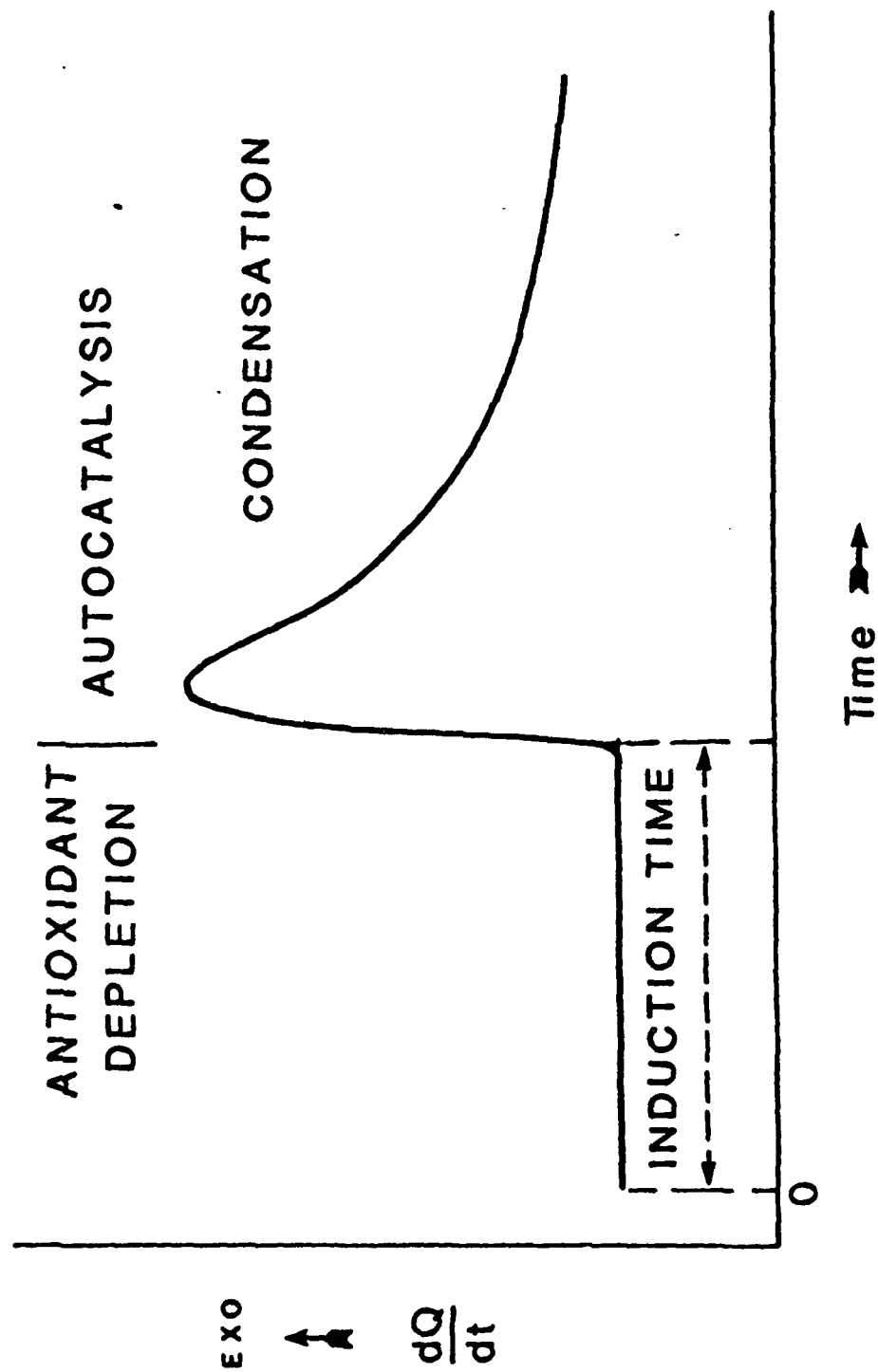


Figure 93. Typical DSC Thermogram of a Lubrication Oil (from Reference 57).

mode, meaning that the cell was pressurized and then sealed which of course resulted in a rise in the final pressure upon reaching the set temperature. Because of the rapid temperature jump, the instrument naturally displayed large signal imbalances due to the sample and reference pans being out of equilibrium and, thus, the thermograms in this report are shown after 10 minutes of test time when the signal had stabilized. Approximately 5 to 10 mg (weighed) of lubricant was used for each analysis. Upon completion of each test, the sample pan was removed from the cell as quickly as possible, the contents dissolved in THF and then analyzed by GPC for molecular weight average data.

c. Limitations of GPC Analysis on HP-DSC Samples

GPC data were found to correlate very well with the viscosity increases of C&O tested PPEs and, thus, was a good indicator of lubricant degradation. Unfortunately, GPC cannot be used to indicate the degree of oxidation of PPE during HP-DSC testing as with bulk oxidation tests. This is because the percent of lubricant lost to evaporation, which is very low in corrosion/oxidation tests due to a large mass/surface area ratio as well as the use of condensers, was found to be very large under the conditions used here for the HP-DSC, even at 500 psi. Since the high molecular weight oxidation products are not volatile, this results in an artificial increase in their concentration relative to the basestock and, thus, gives GPC posttest analysis data that would indicate higher degradation levels than actually have occurred. Therefore, GPC will be used here only as an approximate indicator of lubricant oxidation.

d. HP-DSC Analysis of O-67-1 at Various Temperatures

HP-DSC was used to analyze fresh O-67-1 (5P4E + Antioxidant) at final set temperatures of 320, 360 and 400°C (Figure 94) and the posttest samples analyzed by GPC. The baseline of the 320°C thermogram is flat, displaying no endothermic or exothermic behavior. Despite this, GPC analysis indicated a mild degree of oxidation. At 360°C, the thermogram displays a gradual baseline rise while GPC indicates a fairly high degree of oxidation (this sample was solid but still soluble in THF). The 400°C thermogram more resembles a typical lubricant thermogram (as in Figure 93) with a large broad exotherm. The residual sample was a blackish, THF insoluble solid (essentially coke). These data indicate that the observed exotherm is due to coking and not to an oxidative breakpoint as is seen with conventional lubricants. These data agree with previous research into inhibited 5P4E oxidation mechanisms which suggested that no breakpoint of the oil occurs but that a gradual acceleration in oxidation is observed due to the oxidative instability of the high molecular weight oxidation products that accumulate in the oil. Therefore, it is not known if the apparent induction time in the 400°C thermogram shows any relationship to the oxidative stability of the oil.

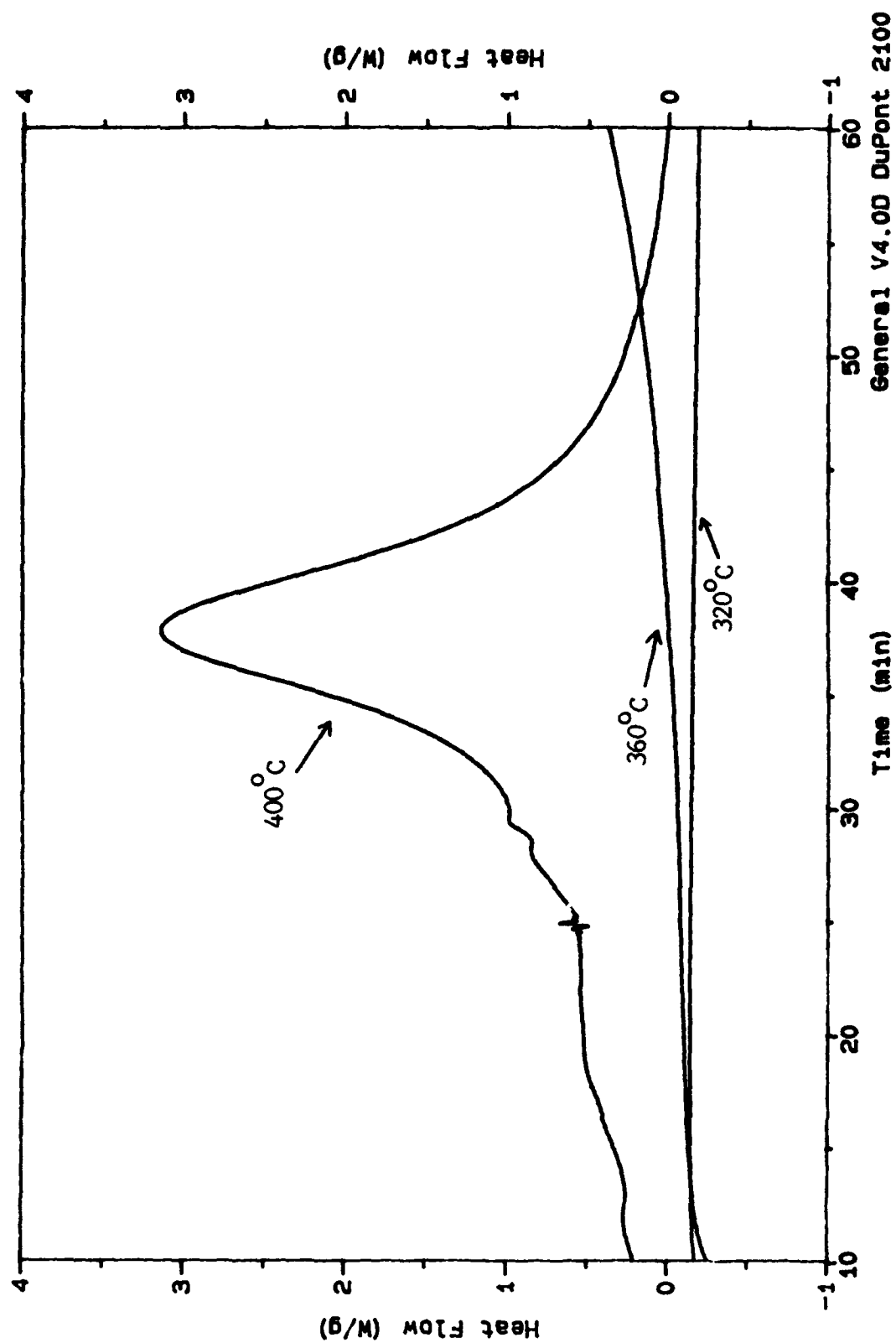


Figure 94. HP-DSC Thermograms of O-67-1 at 320, 360 and 400°C.

e. HP-DSC Analysis of Prestressed O-67-1

Since it appears that the HP-DSC induction time for O-67-1 does not correlate well with the oxidative stability of the lubricant, an attempt was made to relate the amount of baseline rise to the condition of the lubricants. The 360°C thermograms for the 5P4E basestock (O-77-6), formulated 5P4E (O-67-1) and two O-67-1 lubricants from the 320°C corrosion and oxidation test (144 and 216 hours) revealed that the absolute amount of baseline rise increases as the oxidative condition of the oil deteriorates (Figure 95). The basestock shows a steeper rise than the formulated PPEs due to its higher rate of oxidation. The posttest residue of the two prestressed O-67-1 samples and the basestock were THF insoluble black solids. Again, these data show that no correlation exists between the oxidative stability of O-67-1 and any observable HP-DSC induction time. However, an approximate correlation does exist between the oxidative degradation of the lubricant and the amount of baseline rise, which is due to the decreased stability of O-67-1 and the resultant increased oxidation rate.

f. HP-DSC Analysis of TEL-8085 and TEL-8087

TEL-8085 and TEL-8087 (5P4E with different levels of a new antioxidant) are later batches of TEL-8039 and TEL-8040 and were shown to have superior oxidative stability properties than O-67-1. It was also shown that the antioxidant in these formulations completely inhibited the formation of the high molecular weight components (HMW-2) that were thought to be responsible for the oxidative acceleration observed in O-67-1 (see October 1988 Monthly Progress Report). Further work on these formulations has been hindered due to room storage instability of its additive. And indeed the two samples of TEL-8085 and TEL-8087 used in this study contained a layer of material on the bottom of the bottle that was probably due to the additive falling out of the lubricant. Prior to HP-DSC testing, the two lubricants were heated, ultrasonicated and shaken well in order to resuspend this material. HP-DSC analysis was made on these two formulations at 360°C. The thermogram of TEL-8085 (Figure 96) displayed a basically flat baseline while leaving a posttest yellowish oily residue that was shown by GPC to be mildly oxidized PPE. The thermogram of TEL-8087, however, displayed a very large baseline rise while leaving a blackish, THF insoluble residue. It appears that it was possible to resuspend the additive in TEL-8085 but not the additive in TEL-8087.

In order to demonstrate if the additive is unstable after oxidative stressing, a previously stressed TEL-8040 sample (C&O at 330°C, 24 hours) was analyzed by HP-DSC. The thermogram (Figure 96) shows similar behavior to TEL-8085 (slightly endothermic) while leaving a similar type residue. Although this is not a definitive experiment, these data suggest

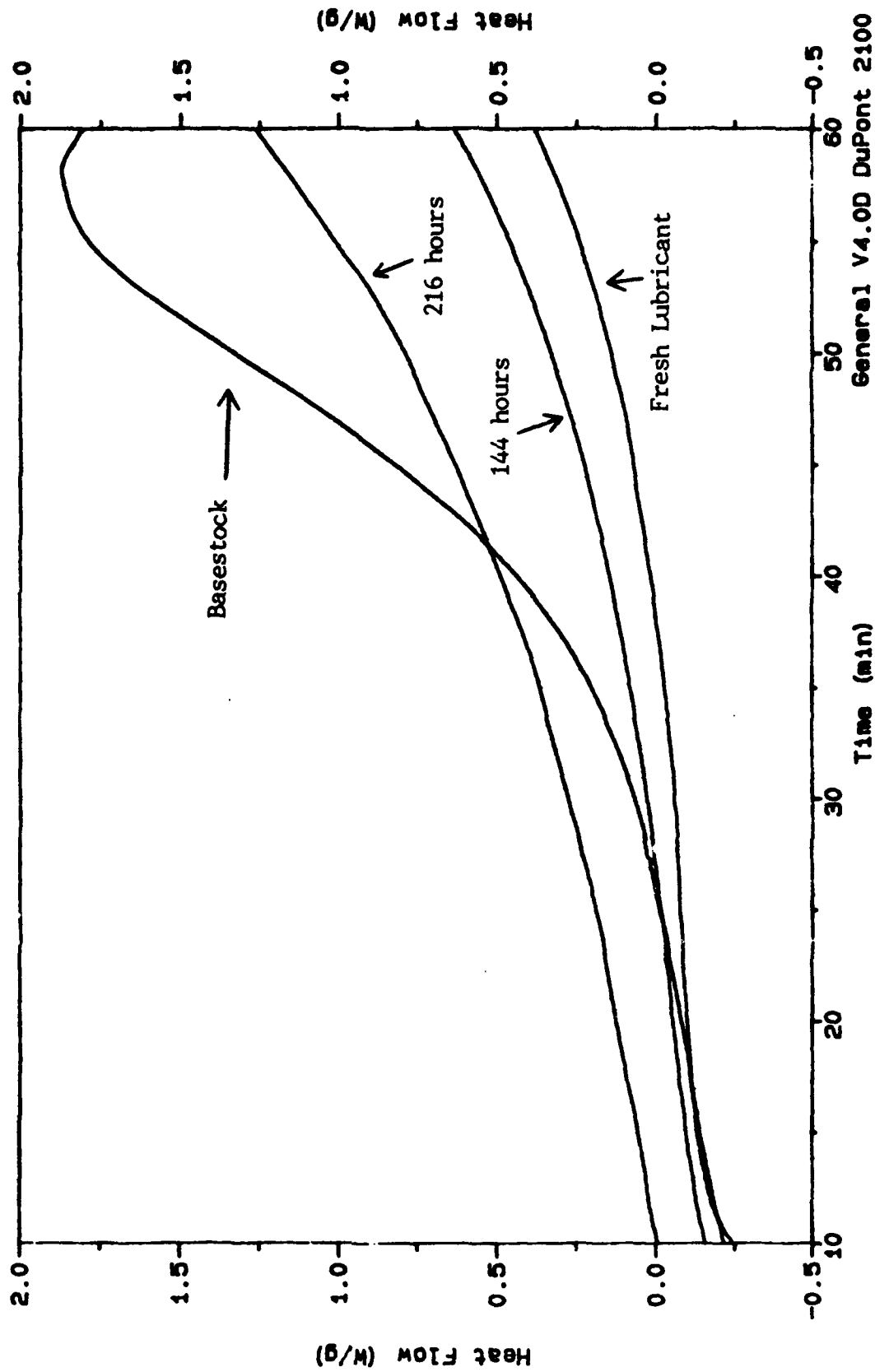


Figure 95. HP-DSC Thermograms of Fresh PPE (O-67-1), Basestock (O-77-6) and C&O Tested O-67-1 at 320°C for 144 Hours and 216 Hours.

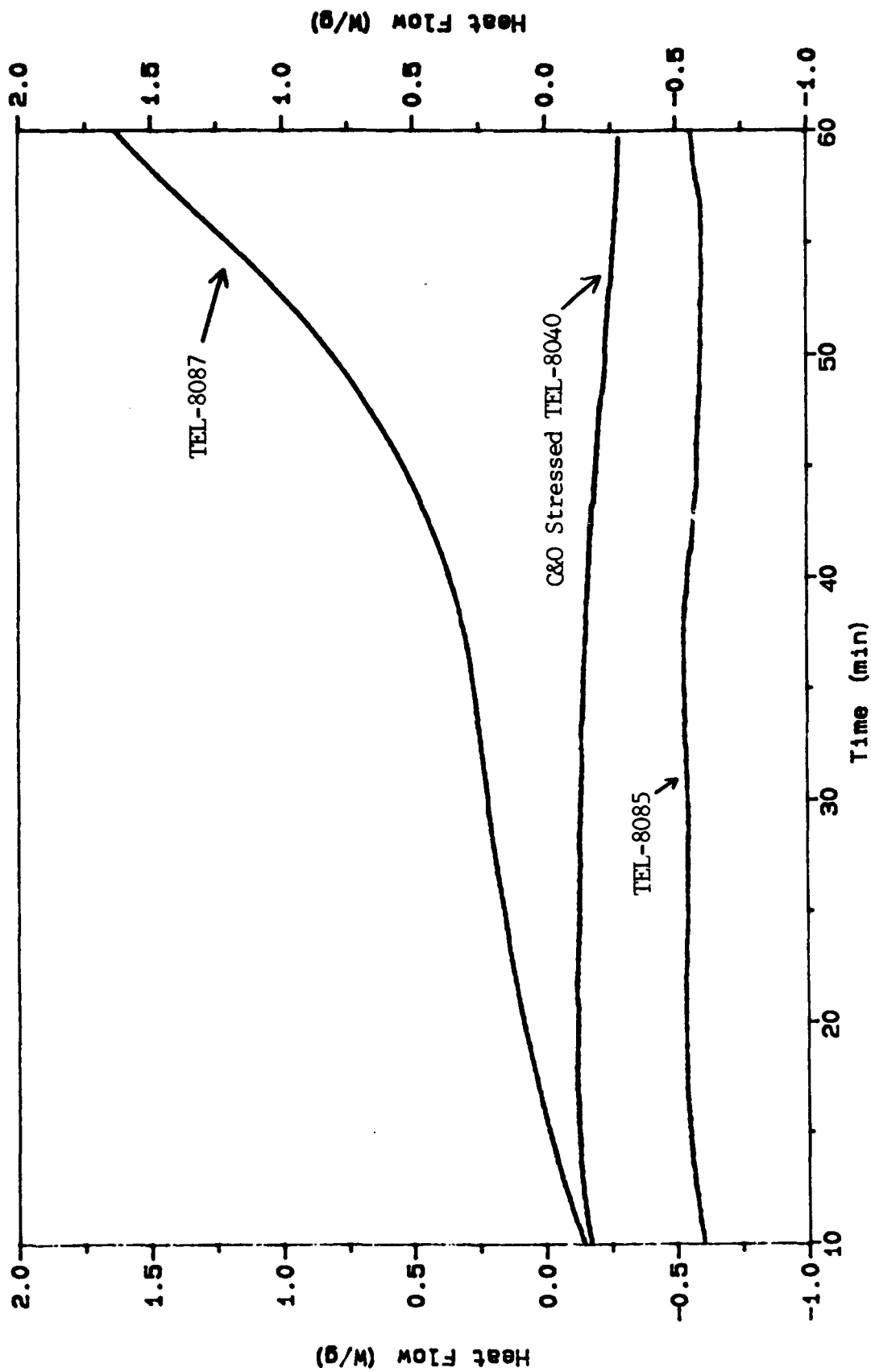


Figure 96. HP-DSC Thermograms at 360°C for TEL-8085, TEL-8087 and C&O Tested TEL-8040 (330°C, 24 Hours).

that prestressing these formulations may help to stabilize their additive, particularly since the above prestressed sample had been stored approximately for 2 years after C&O testing prior to HP-DSC testing. It may be that this additive undergoes a similar chemical transformation as was shown with the organotin antioxidant in O-67-1.<sup>31</sup> However, due to the proprietary nature of the additive in these fluids, no investigation of this type was conducted.

These data show that these formulations display superior oxidative stability to that of O-67-1 when the additive is properly dispersed. Furthermore, the lack of an exotherm (baseline rise) indicates that oxidation, as defined by the uptake of oxygen, is completely inhibited by the additive in these formulations.

#### g. Conclusions

It appears that based on the evidence reported here that high-pressure differential scanning calorimetry (HP-DSC) would not be very useful as an oxidative stability screening device for high temperature lubricants. Despite the use of high pressures, which inhibits evaporation and theoretically should accelerate oxidation, it was found that the evaporation rate for PPEs far exceeded the oxidation rate. More importantly, the fact that PPE lubricants use antioxidants that are not depleted during oxidative stressing (as opposed to antioxidants in conventional lubricants) resulted in thermograms that generally did not give induction times proportional to oxidative lubricant life. In fact, it was found for PPEs that the large exotherm, normally associated with the rapid oxidation of conventional lubricants, was due to coking processes that occurred a considerable time after the lubricant had deteriorated to the point of solidification. Finally, formulation differences (O-67-1 vs. TEL-8085) resulted in drastically different HP-DSC behavior among the PPEs tested. Since variations in the formulation of PPEs resulted in different HP-DSC behavior, it can be reasonably expected that other formulations of high temperature lubricants (perfluoropolyethers among others) would also yield their own peculiar type of nonstandard behavior.

Despite its limitations as a general oxidative stability screening device, HP-DSC may have some use as a research tool. HP-DSC was able to demonstrate the exothermic nature of the oxidative degradation of O-67-1 compared to the apparently heat driven degradation of TEL-8085 (TEL-8039). This had been previously indicated by research conducted on the oxidative inhibition properties of the additives in these two formulations. Also, this work indicated the possibility of prestressing the TEL-8085 and TEL-8087 lubricants in order to stabilize its additive.

## SECTION V

### TRIBOLOGICAL EVALUATION OF CANDIDATE FLUIDS

#### 1. FOUR-BALL TEST

##### a. Material Comparison with PPE

##### (1) M50, 52100, Si<sub>3</sub>N<sub>4</sub>, and Brass

Earlier work shows that the amount of wear which results from four-ball testing of PPE is material dependent.<sup>3</sup> The materials used as the ball specimens for the four-ball test included 52100 and M50 steels as well as brass and Si<sub>3</sub>N<sub>4</sub>. These tests used a quantity of 35 mL of fluid at a bulk oil temperature of 150°C, and the upper ball was rotated at 1200 rpm under a 15-kg load. Based on the size and shape of the lower ball wear scars, the 52100 balls incurred an order of magnitude less wear than M50 balls, which have superior material properties. To further study the four-ball wear characteristics of materials lubricated with PPE, more tests of the various ball specimens were performed at temperatures of 75, 250, and 31 °C.

The first test series were done at 75°C with multiple tests performed on brass balls, M50 balls, 52100 balls, and Si<sub>3</sub>N<sub>4</sub> balls. Individual tests were done with different material combinations as well. These tests used either M50, 52100, or Si<sub>3</sub>N<sub>4</sub> top balls with three lower balls of either of the other two materials. The test results are compared in Figure 97 based on the total wear scar volumes. Since the first four tests were repeated at least twice, error bars are included to show the variation in scarring.

Si<sub>3</sub>N<sub>4</sub> has the least wear, and 52100 had the second least amount of wear of the four test series using balls of a single material. The M50 tests give the greatest amount of wear, but the variation for this series is tremendous. The large error bars result from two distinct scar sizes being formed on M50 balls at 75°C. For a total of four tests of M50 balls run at this temperature, all tests generated circular lower ball wear scars but in two tests, the scar diameter was approximately 2.14 mm while the other two tests had diameters of only 1.51 mm. For this reason, it is unclear whether or not brass balls wear less or more than M50 balls at 75°C with PPE.

Substituting Si<sub>3</sub>N<sub>4</sub> for either 52100 or M50 greatly reduces the wear when compared to the steel on steel results. The combinations of one Si<sub>3</sub>N<sub>4</sub> on either three M50s or

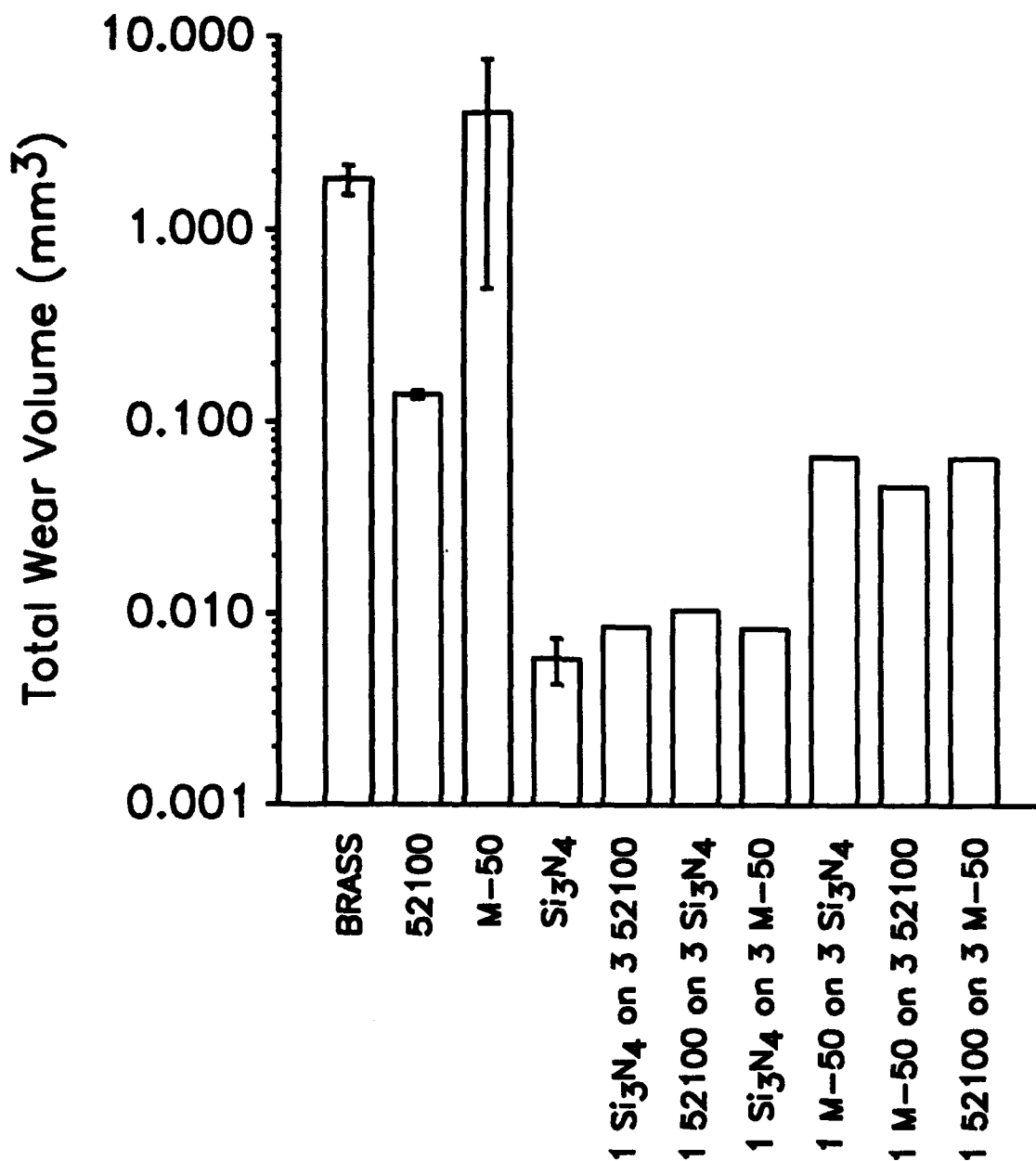


Figure 97. Total Four-Ball Wear for Various Specimen Materials Lubricated with O-67-1 at 75°C (3-Hour Tests at 1200 rpm with 145-N Loads).

three 52100s and one 52100 on three  $\text{Si}_3\text{N}_4$ s are within the same order of magnitude as the  $\text{Si}_3\text{N}_4$  on  $\text{Si}_3\text{N}_4$  tests. The three remaining combinations (one M50 on either three  $\text{Si}_3\text{N}_4$ s or three 52100s and one 52100 on three M50s) produced similar amounts of wear which are about the same order of magnitude as the 52100 on 52100 tests.

To more easily compare the change in material wear caused by PPE when the temperature is increased, the results obtained at 150°C are again presented. In Figure 98, the 10 material combinations used in Figure 97 are now ranked at 150°C. The ranking is essentially unchanged except that the M50 on 52100 combinations have two orders of magnitude more wear than at 75°C. At 150°C, these tests generated the same order of wear that M50 on M50 incurs. Overall, four-ball wear is increased at 150°C for 9 out of the 10 ball combinations tested. The exception is the one M50 on three  $\text{Si}_3\text{N}_4$  test which gave about the same wear at 150°C that it did at 75°C.

At 250°C, brass balls cannot be used due to material softening. In addition, the combinations of 52100 with M50 and  $\text{Si}_3\text{N}_4$  were not tested. Figure 99 ranks the five remaining combinations on a linear scale and again indicates that four-ball wear on M50 balls is greater than the other tested materials. The least wear takes place for one M50 on three  $\text{Si}_3\text{N}_4$  balls although the 52100/52100 and one  $\text{Si}_3\text{N}_4$  on three M50 are nearly as low.

Figure 100 shows the material ranking at 315°C. Because of loss of hardness at this temperature, 52100 balls could not be tested. The  $\text{Si}_3\text{N}_4$ /M50 combinations continue to have less wear than either  $\text{Si}_3\text{N}_4$  on  $\text{Si}_3\text{N}_4$  or M50 on M50. In terms of the average wear from multiple tests,  $\text{Si}_3\text{N}_4$  on  $\text{Si}_3\text{N}_4$  has more four-ball wear at 315°C than M50 on M50.

To better see the four-ball wear versus temperature trends for the various M50/ $\text{Si}_3\text{N}_4$  combinations of Figures 97 through 4, these data are consolidated in Figure 101. The M50 on M50 tests given by the circles produced consistently high wear from 75 to 315°C. The  $\text{Si}_3\text{N}_4$  on  $\text{Si}_3\text{N}_4$  tests shown by the triangles initially have little wear at the low temperature end but wind up having the same amount of wear as the M50 on M50 tests at the high temperature extreme, an increase of three orders of magnitude. The least wear as well as the least variation in wear over the entire temperature range is attained when a  $\text{Si}_3\text{N}_4$ /M50 combination (shown by squares and diamonds).

## (2) M50 versus 52100 at 50°C

It is a general rule that with increasing material hardness comes a reduction in wear. However, four-ball wear of M50 steel at the selected test temperatures

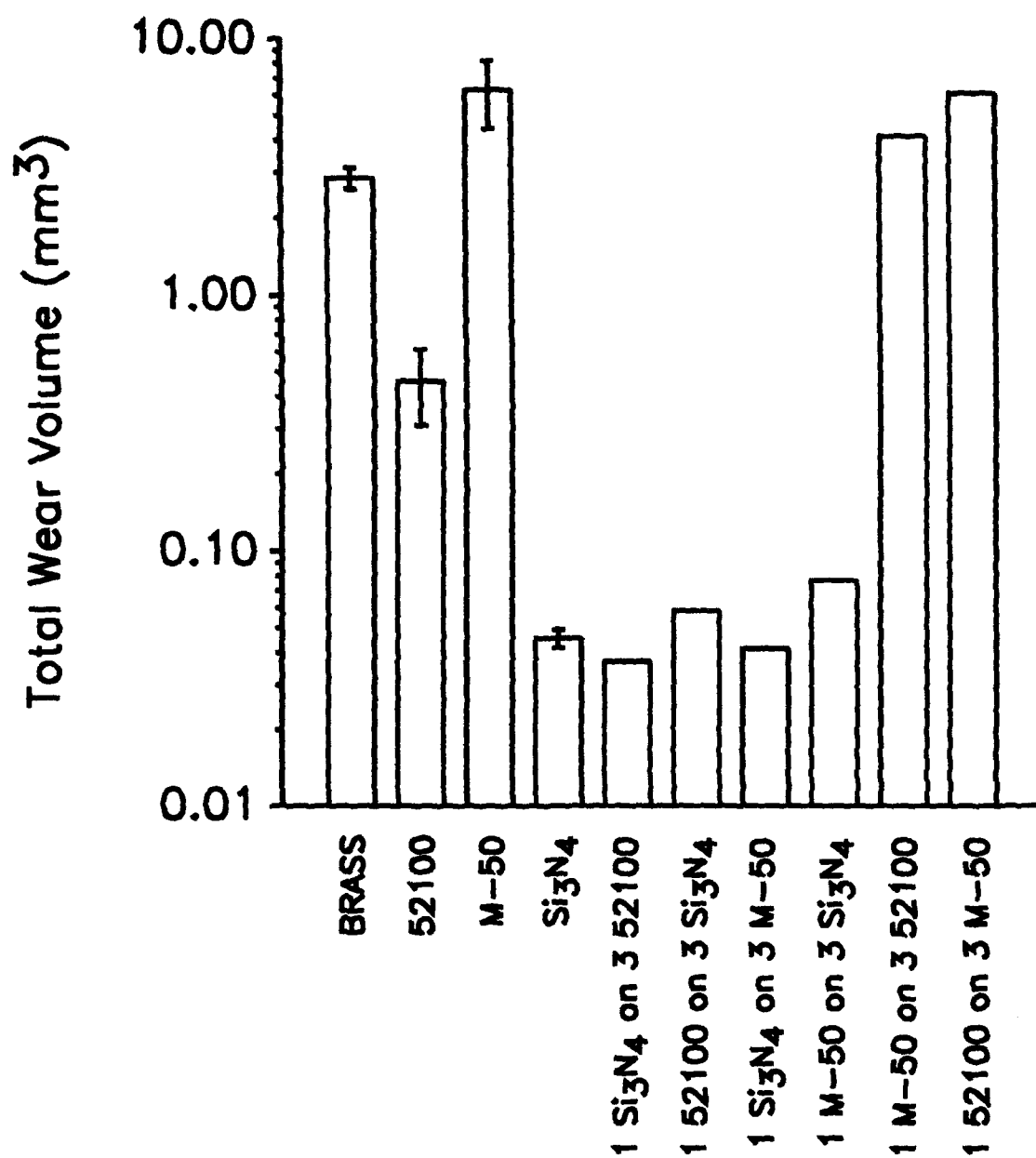


Figure 98. Total Four-Ball Wear for Various Specimen Materials Lubricated with O-67-1 at 150°C (3-Hour Tests at 1200 rpm with 145-N Loads).

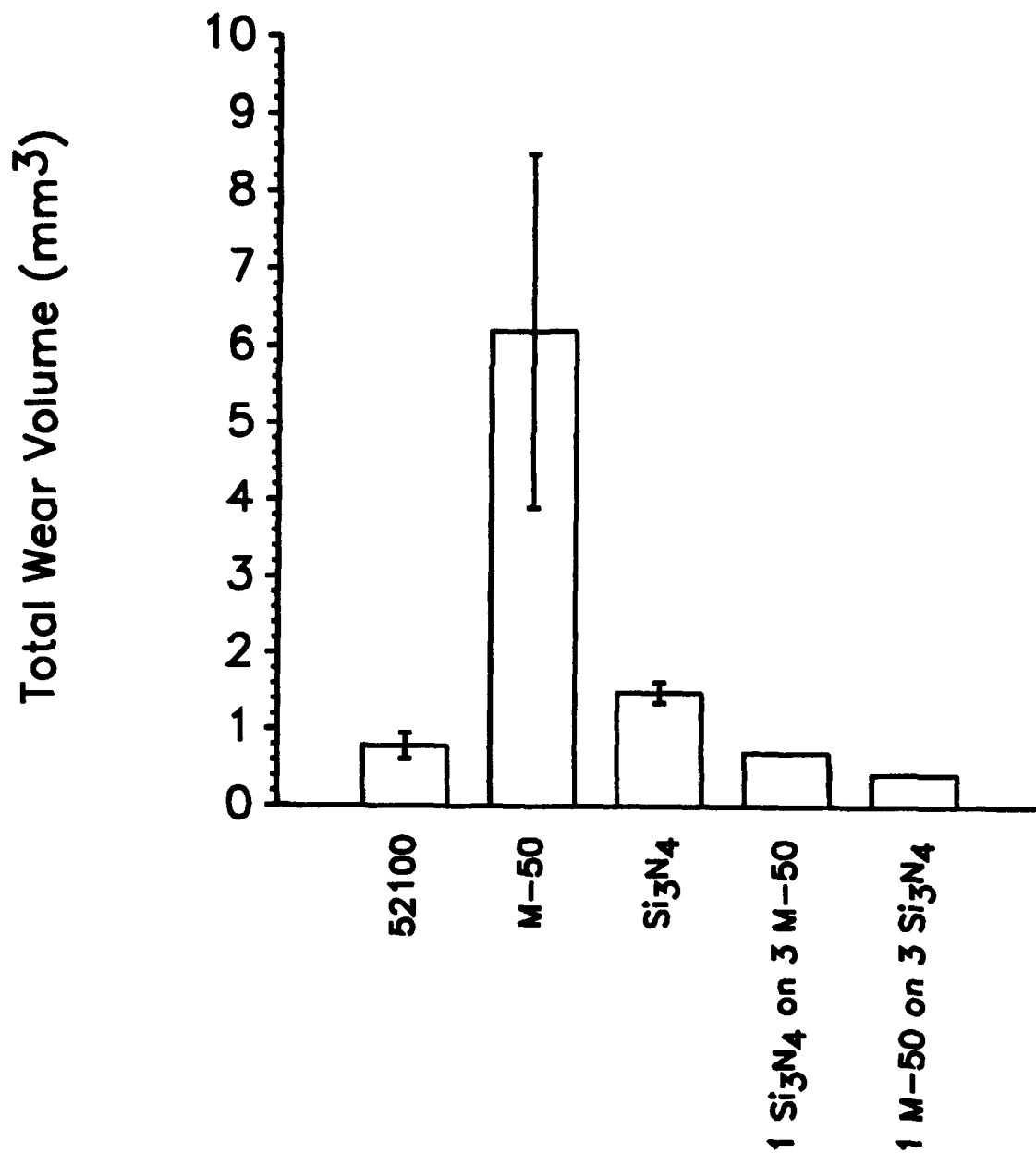


Figure 99. Total Four-Ball Wear for Various Specimen Materials Lubricated with O-67-1 at 250°C (3-Hour Tests at 1200 rpm with 145-N Loads).

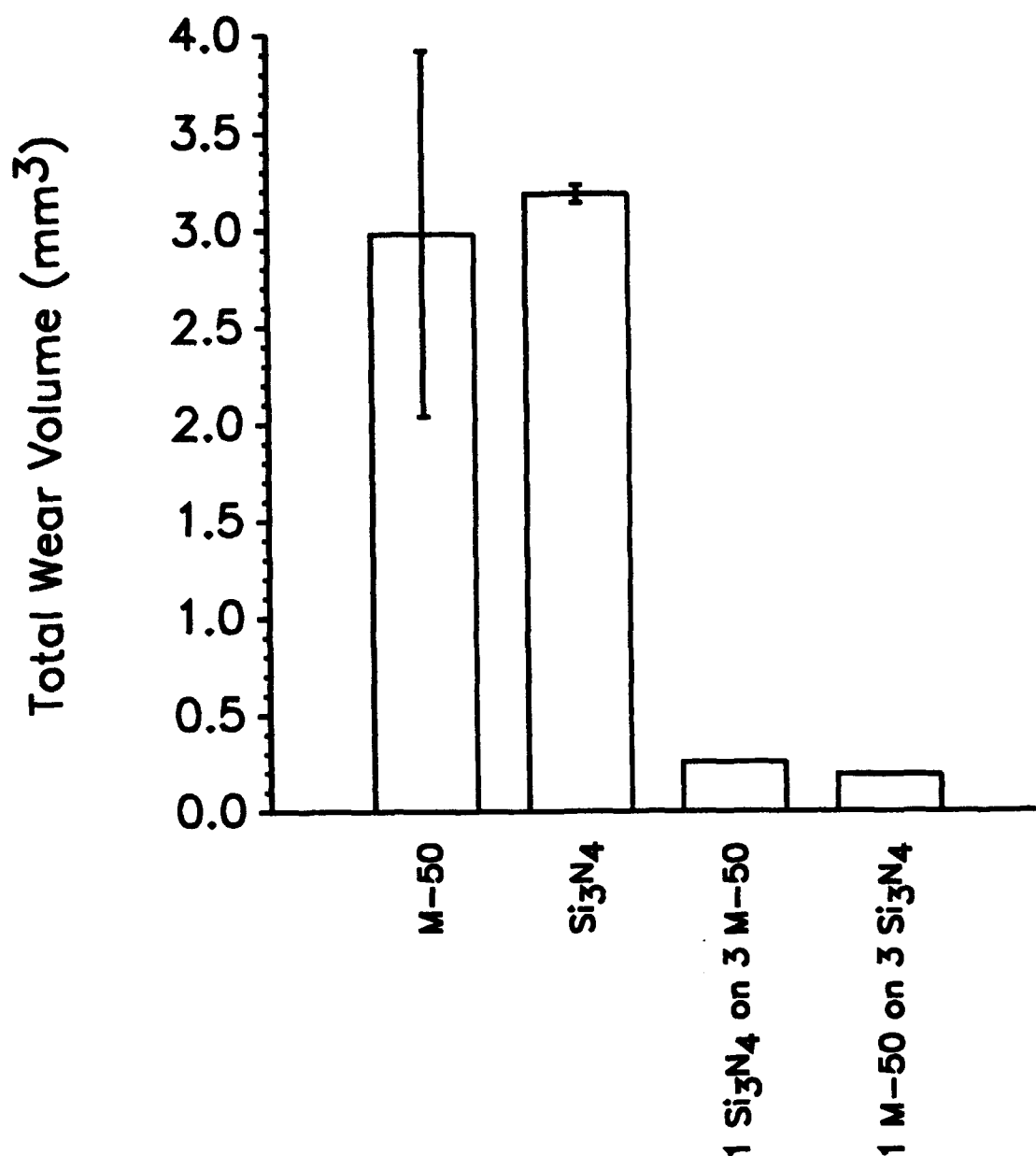


Figure 100. Total Four-Ball Wear for Various Specimen Materials Lubricated with O-67-1 at 315°C (3-Hour Tests at 1200 rpm with 145-N Loads).

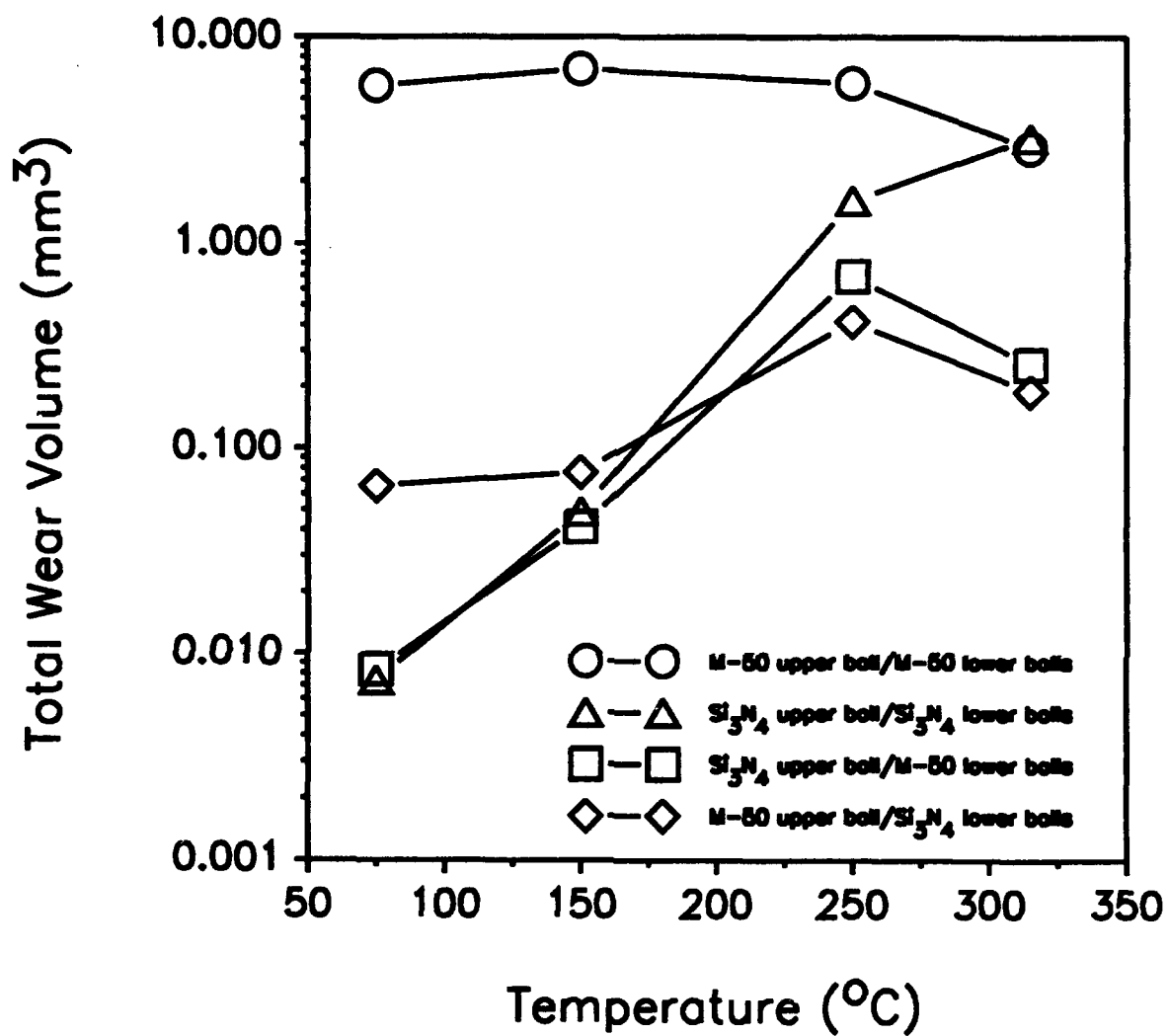


Figure 101. Total Four-Ball Wear Versus Temperature for M50/Si<sub>3</sub>N<sub>4</sub> Ball Combinations Lubricated with O-67-1 (3-Hour Tests at 1200 rpm with 145-N Loads).

reported is consistently greater than for softer 52100 steel when PPE is the test fluid. To pursue this anomaly, additional four ball experiments were conducted at 50°C to compare these materials at a temperature where their respective hardness is essentially equal.

The variation of hardness as a function of temperature is displayed in Figure 102. The difference between the hardness of the three bearing steels diminishes as the temperature decreases. With tests having already been performed at 75°C, M50 and 52100 four-ball specimens were tested at 50°C because this temperature is the lowest which can be accurately controlled.

The 50°C-four-ball test results for the 52100 and M50 specimens are presented in Figures 103 and 104, respectively, along with all other tests performed at 75, 150, 250, and 315°C. As shown, the experimental data for 52100 steel demonstrate good repeatability and the wear versus temperature curve follows a linear trend. In addition, the wear volumes throughout the temperature range remain small (less than 1 mm<sup>3</sup>). These characteristics all indicate the existence of a stable tribological environment within the 52100/PPE sliding contact.

In contrast to the 52100 four-ball tests, the performance of M50 is quite the opposite. The poor repeatabilities and large wear volumes seen in Figure 104 are a direct consequence of scuffing. It seems that the bulk-hardness of the test specimens has little to do with the total four-ball wear for PPE and these materials. In particular, the total wear scar volumes at 50°C for the two steels differ significantly although their respective hardness are the same at this temperature.

Despite the data scatter of M50 tests throughout the whole temperature range investigated, four-ball wear seems to increase with temperature until perhaps 200°C but then decreases with increasing temperature. This reduction may be attributed to the formation of a protective film within the tribo-contacts. In similar work, Spar and Damasco<sup>11</sup> used the four-ball test to study PPE using M10 tool steel balls. Figure 105 reveals a reduction of wear after reaching a critical temperature level. Moreover, the effect of load diminished at high-temperature as a result of a change in the wear mechanism likely caused by tribo-chemical reactions. Table 88 lists the chemical composition of various steels. Compared to 52100, both M10 and M50 contain more than twice the amount of chromium and also appreciable amounts of vanadium. Both of these elements are corrosive and reactive in nature, and it is quite possible for them to initiate and catalyze chemical a reaction under the extreme conditions of EHD or boundary lubrication.

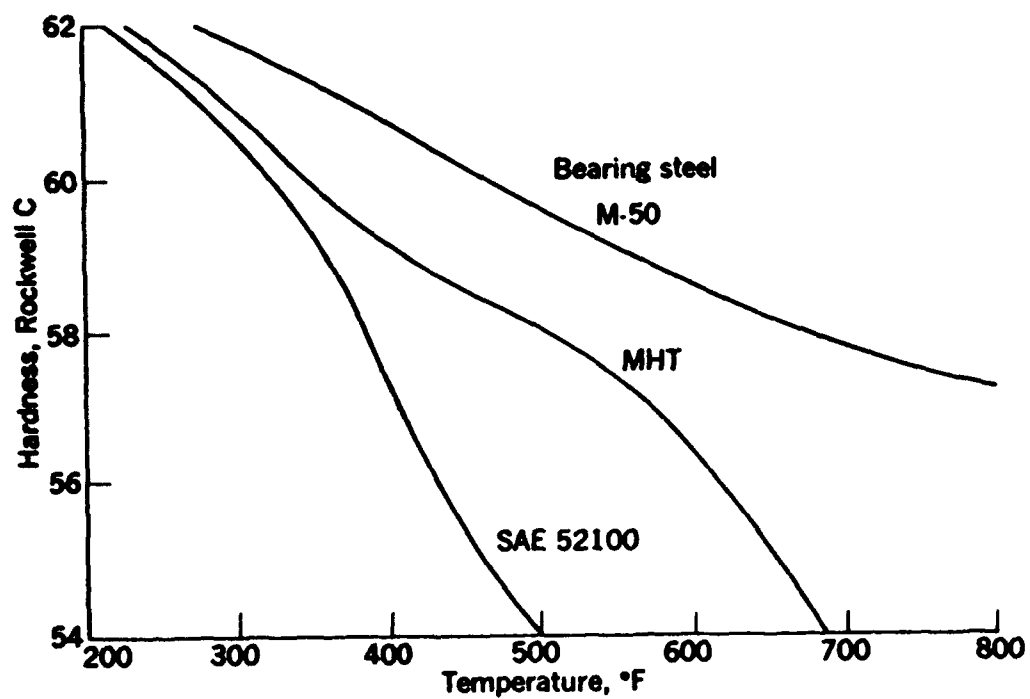


Figure 102. Hardness as a Function of Temperature for Three Bearing Steels (from Advanced Bearing Technology).

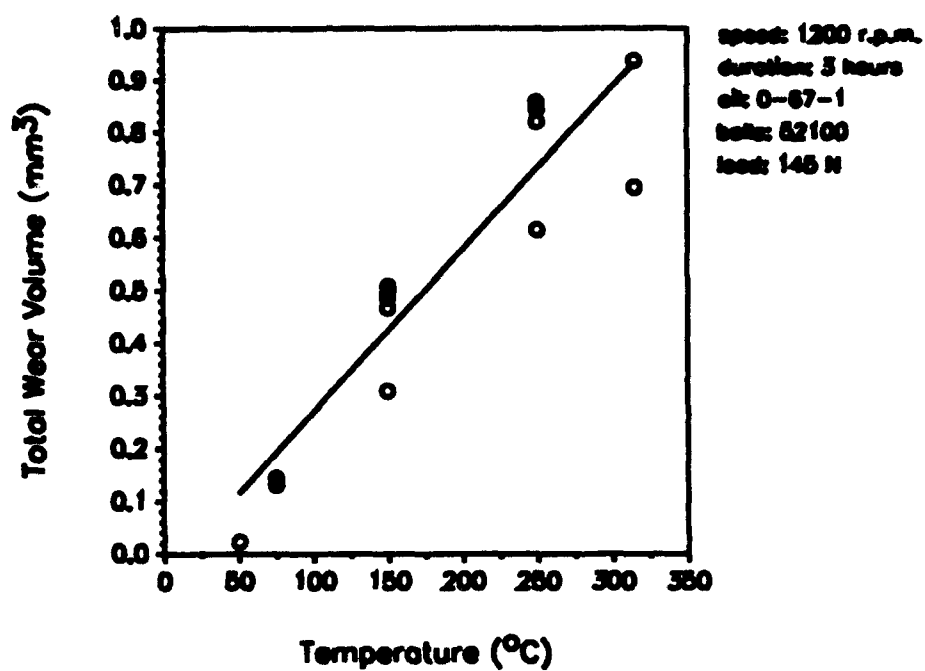


Figure 103. Total Four-Ball Wear Versus Temperature for 52100 Steel Balls.

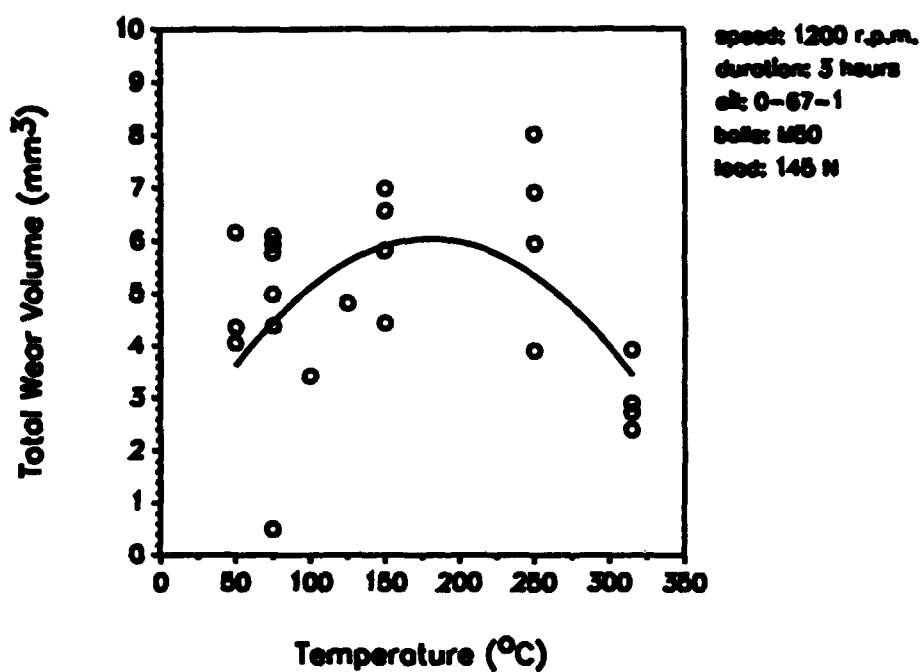


Figure 104. Total Four-Ball Wear Versus Temperature for M50 Steel Balls.

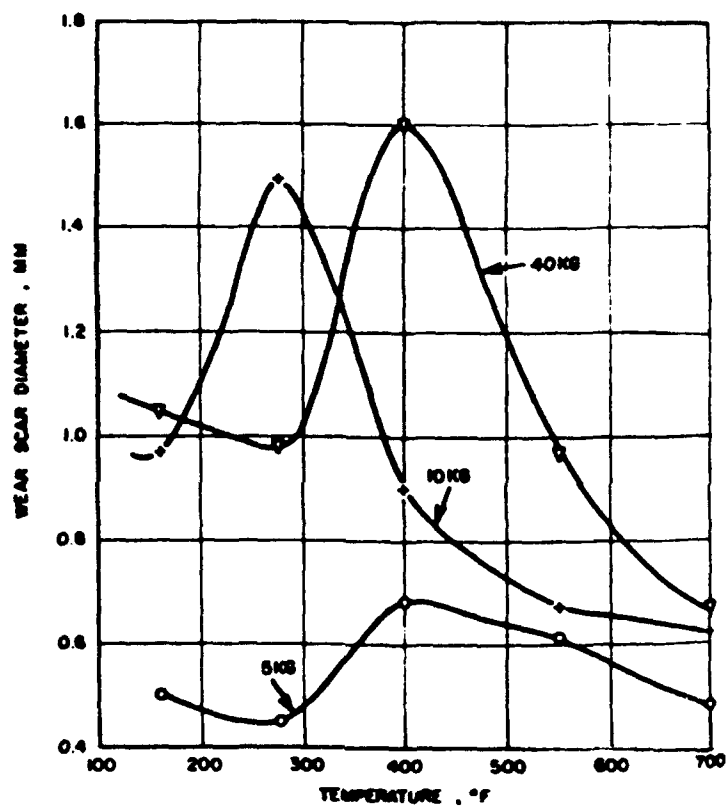


Figure 105. Wear Scar Size Versus Temperature for Four-Ball Tests of Polyphenyl Ether (1-Hour Tests at 600 rpm in Nitrogen with M10 Balls) (from Reference 11).

TABLE 88

## CHEMICAL COMPOSITION OF SELECTED STEELS

Designation	Max operat- ing tempera- ture °C	Composition, %							Other Remarks	
		C	Mn	Si	Cr	Ni	Mo	W		V
Through-Hardening Steels										
52100	150	300	0.98-1.10	0.25-0.45	0.15-0.30	1.30-1.60	...	...	...	Most popular bearing steels; must be protected from atmospheric corrosion by oil film
50100	120	250	0.98-1.10	0.25-0.45	0.15-0.30	0.40-0.60	...	...	...	Used for small section parts such as needle rollers
51100	120	250	0.98-1.10	0.25-0.45	0.15-0.30	0.90-1.15	...	...	...	Used for small section parts such as needle rollers
52100 modified	150	300	0.90-1.05	0.95-1.25	0.50-0.70	0.90-1.15	...	...	...	For heavy sections; hardenability increased by increased Mn
M50	425	800	0.77-0.85	0.20-0.35	0.10-0.25	3.75-4.25	<0.10	4.0-4.5	<0.25 0.90-1.10	Most popular tool steel grade; grinds well; high wear resistance; available as consumable-electrode vacuum melted stock
M10	535	1000	0.85	0.20-0.40	0.20-0.40	4.0	...	8.0	...	2.0
M1	535	1000	0.75-0.85	0.20-0.40	0.20-0.40	3.25-4.50	...	7.75-9.25	1.15-1.85	0.90-1.30
M2	535	1000	0.78-0.88	0.20-0.40	0.20-0.40	3.25-4.50	...	4.50-5.50	5.50-6.75	1.60-2.20
Co modified	535	1000	1.07	0.30	0.02	4.40	...	3.9	6.30	2.0
5.2 Co Superior hot hardness to Mo-base steels										

The peculiar behavior of PPE may be best characterized by its formation of semisolid or solid film (due to glass transition) inside the contact junction. Alsaad et al.<sup>13</sup> have done extensive research on the glass transitions of lubricants (see Figures 106 and 107). It is believed that under ordinary EHD or boundary lubrication conditions, 5P4E could form solid-like film within the tribo-contacts. Because of this phase transition, the physical as well as rheological properties of this lubricant will change accordingly, thus, rendering some unusual phenomenon in its tribo-behavior.

Thus, the *in-situ* solid-film formation of the 5P4E-based fluid (0-67-1) appears to be the prevailing cause in the wear mechanism. Generally speaking, the wear rates are more strongly dependent on the predominant wear mechanisms (or wear modes) rather than on the specimen hardness. It seems that this solid-film has good compatibility with 52100 steel tribo-surfaces. However, asperity hardness may play an important role in wear because of formed films. Even for bulk oil temperatures as low as 50°C, the temperature within the sliding contacts could be well above 200°C where the hardness of 52100 steel is less than that of M50. The relatively low hardness of the 52100 tribo-surface may create a compatible environment for solid films by acting as a cushion.

#### b. Four-Ball Scarring

The data corresponding to the M50/M50 tests of Figures 97 through 100 had consistently wide error bands at each temperature. The variation of wear scar volume results from the large variation in wear scars formed on M50 balls lubricated with PPE. Although the variation in scarring was addressed in earlier work,<sup>3</sup> the trends seen in the wear scars of M50 balls bear further mentioning.

The degree of top ball wear during a four-ball test has a direct result on the shape of the lower ball wear scars.<sup>60</sup> From four-ball testing of M50 specimens with PPE, three characteristic scar types were observed which account for three possible categories of four-ball wear. These three categories are primary lower ball wear, primary upper ball wear, and a combination of primary upper ball and primary lower ball wear which varies along the length of the scar.

The first wear category, primary lower ball wear, is the most typical result of four-ball testing. The scars formed on the lower balls are circular because wear of the upper ball is negligible. With primary upper ball wear, however, the lower ball scars are elliptical instead of circular. While primary upper ball wear would only seem to occur when the upper ball

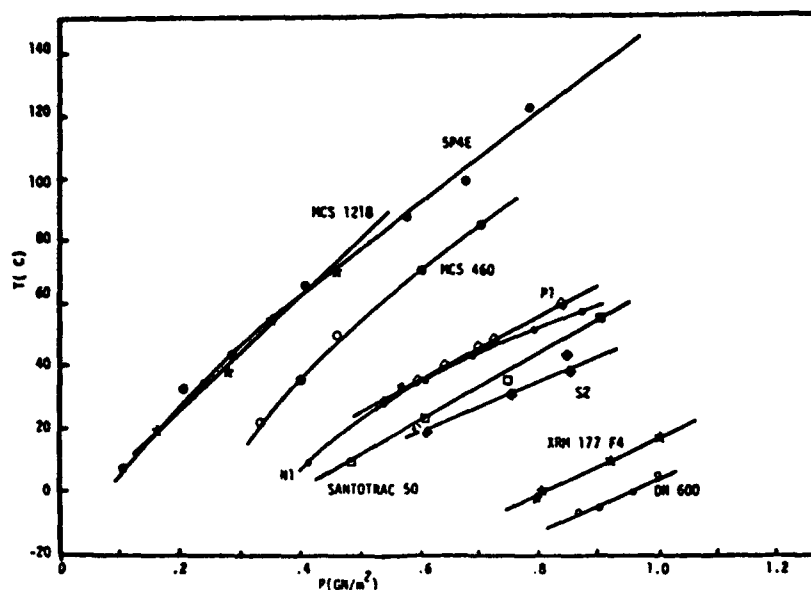


Figure 106. Glass Transition by Isothermal Compression from Liquid (Dilatometry) (from Reference 13).

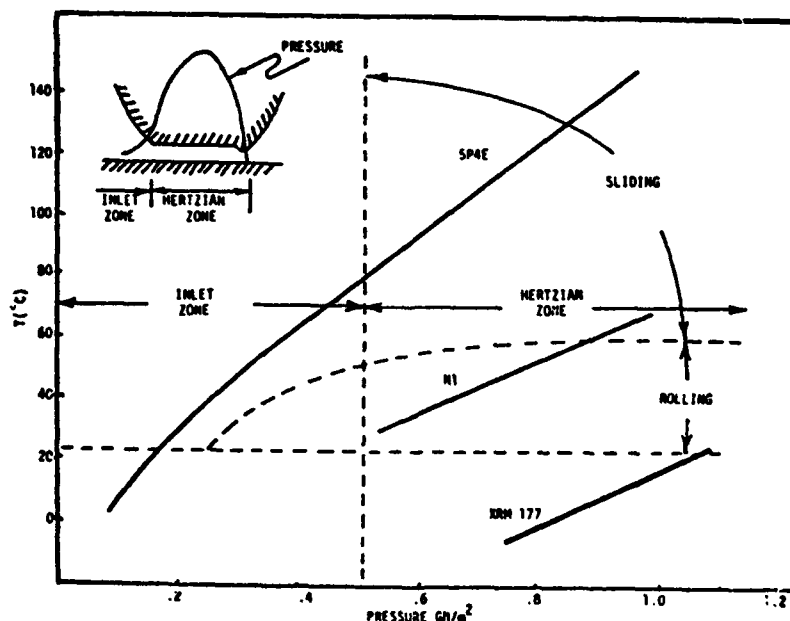


Figure 107. Heuristic Estimates of the Relationship Between Conditions in an EHD Contact and Glass-Liquid Phase Diagrams of Three Lubricants (Lubricant Supply Temperature about 20°C) (from Reference 13).

material differs from the three lower balls, such scarring can in fact occur when four identical test balls are used. Finally, when the scarred surfaces are exceptionally jagged, the shapes of the lower ball scars can take on very unusual geometries which are neither circular nor elliptical. In this instance, the primary wearing ball(s) is determined by the width of the wear scar at any point along its length.

Surface profiles of the upper ball scars from the tests of M50 balls at 75, 150, 250, and 315°C are given in Figure 108, 109, 110, and 111 to show the representative scarring for each of the three categories of four-ball wear. The two traces shown in Figure 108 represent identical tests in which very little upper ball wear took place. Because the wear is so small, it is difficult to actually tell where the worn surface ends. Through optical measurements of the lower ball scars, the average value for the length of the first profile is 1.51 mm and 2.14 mm for the second. This large variation in size was typical for PPE tested on M50 balls at 75°C; all scars which were formed were either round and small (about 1.51 mm in diameter) or round and large (about 2.14 mm in diameter).

Variation in scarring was not unique to 75°C-tests, however. According to Figure 109, the scars from 150°C-tests have approximately the same lengths but drastically different surfaces. Despite this difference, both scars can be categorized as having a combination of upper and lower ball wear that varies along the length of the scar. The large peaks near the ends of the first profile and the large peak in the middle of the second profile (which was too large to fit on the surface trace) correspond to points where most of the original upper ball surface still exists (or primary lower ball wear). All other points along the scar reflect the amount of material that the lower ball removed from the upper ball (or primary upper ball wear). The scars formed on M50 balls at 150°C from PPE varied tremendously in shape but not in length.

At 250°C, wear scars are more consistent in size as well as shape. Figure 110 shows two surface profiles, each of which exemplifies primary upper ball wear to nearly the same depth and length. Although total four-ball wear for these two tests differs considerably (see Figure 99), small differences in the wear scars during primary upper ball wear result in large differences in wear volume calculations.

Figure 111 shows a final profile done on the upper ball from a test at 315°C. Only one trace is shown because the scar category at 315°C is the same as 150°C, a combination of primary upper and lower ball wear that varies along the length of the scar. The variation in scar depth is perhaps less severe at 315°C which may account for the small variation seen in the wear scar volumes shown in Figure 100.

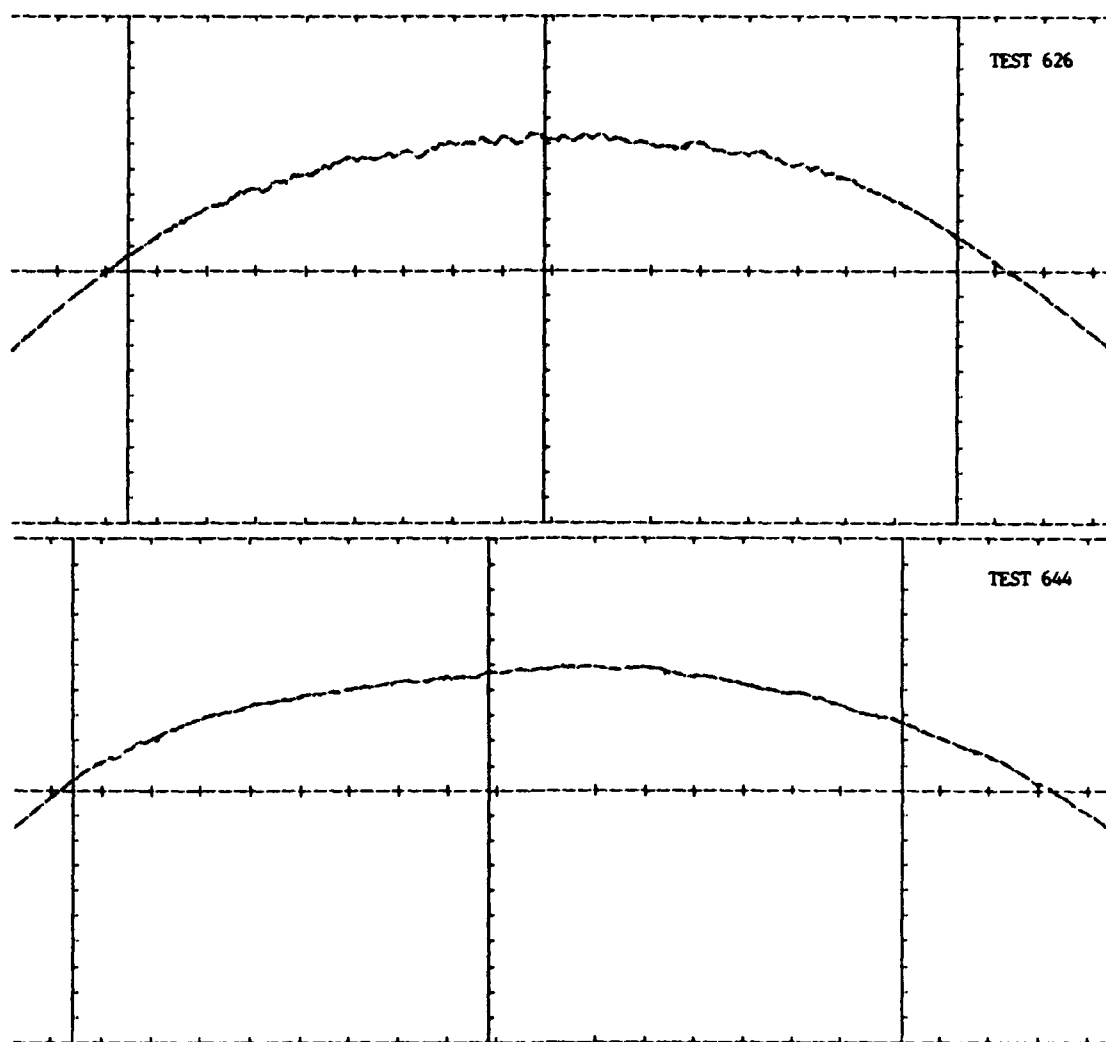


Figure 108. Surface Profiles of the Upper Ball Wear Scars from Two Four-Ball Tests of O-67-1 at 75°C (M50 Balls, 3-Hour Tests, 1200 rpm, 145-N Load, 0.1 mm per Division Horizontal Scale, 0.01 mm per Division Vertical Scale).

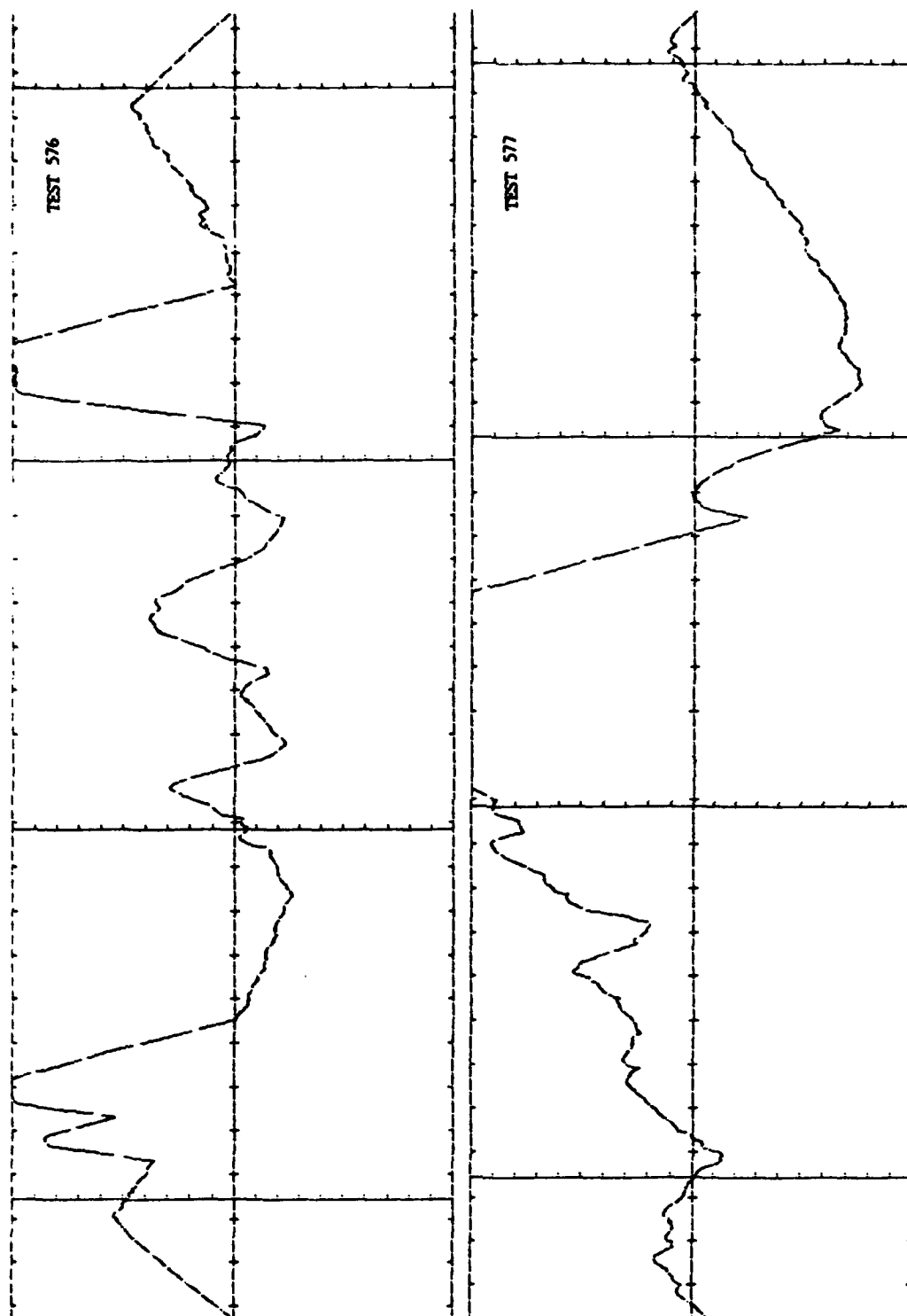


Figure 109. Surface Profiles of the Upper Ball Wear Scars from Two Four-Ball Tests of O-67-1 at 150°C (M50 Balls, 3-Hour Tests 1200 rpm, 145-N Load, 0.1 mm per Division Horizontal Scale, 0.01 mm per Division Vertical Scale).

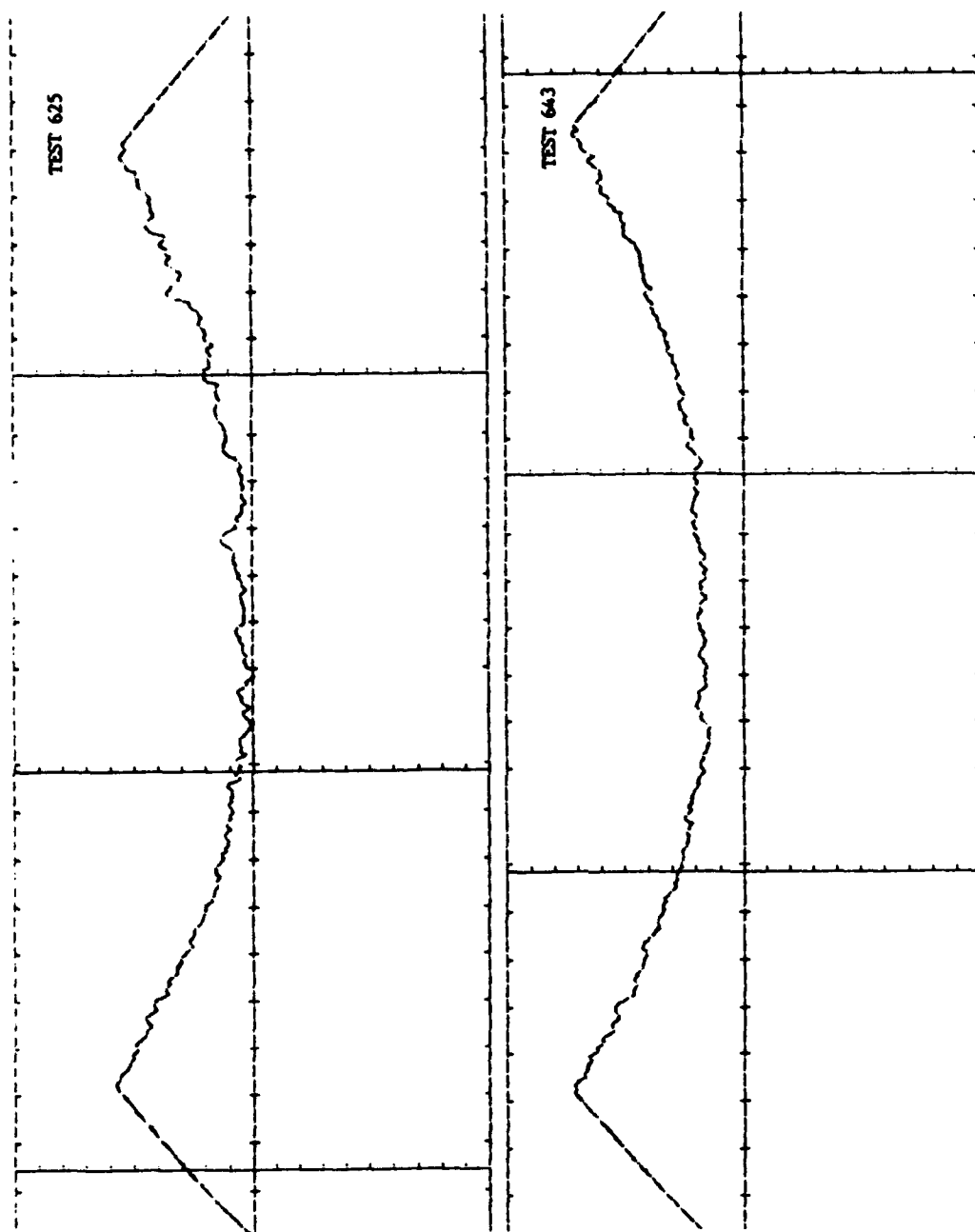


Figure 110. Surface Profiles of the Upper Ball Wear Scars from Two Four-Ball Tests of O-67-1 at 250°C (M50 Balls, 3-Hour Tests, 1200 rpm, 145-N Load, 0.1 mm per Division Horizontal Scale, 0.01 mm per Division Vertical Scale).

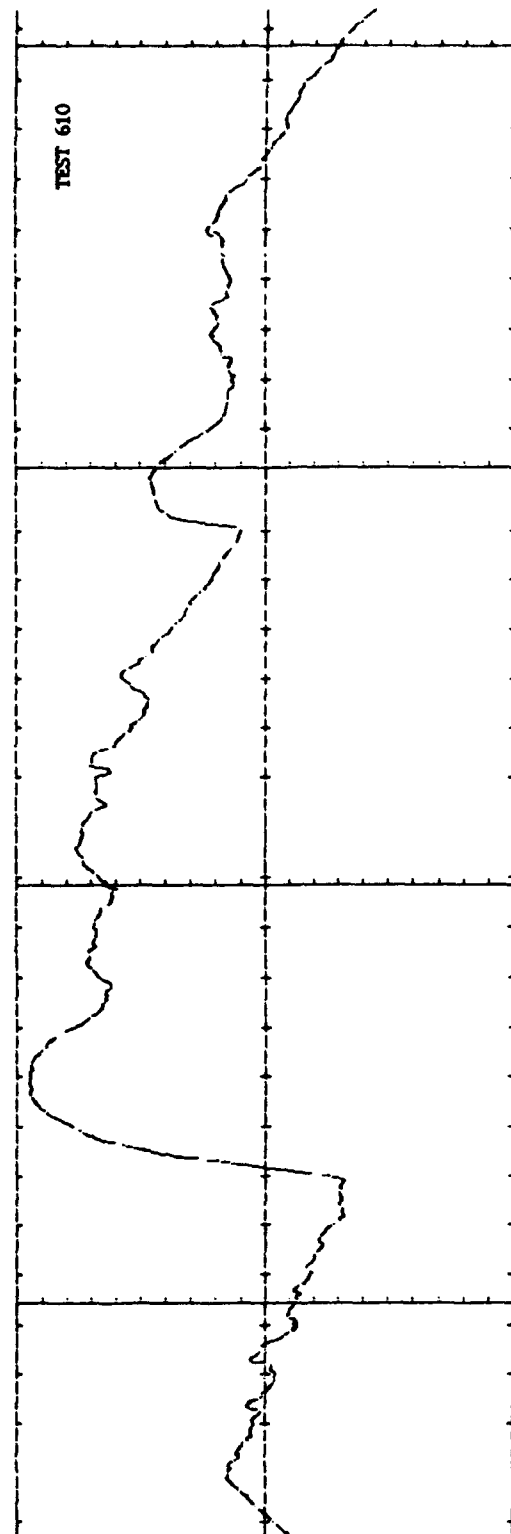


Figure 111. Surface Profile of the Upper Ball Wear Scar from a Four-Ball Test of O-67-1 at 315°C (M50 Balls, 3-Hour Test, 1200 rpm, 145-N Load, 0.1 mm per Division Horizontal Scale, 0.01 mm per Division Vertical Scale).

### c. Wear Versus Temperature Comparison of Candidate Fluids

Just as previous work had been done in comparing four-ball tests of different materials at 150°C, a comparison of various candidate fluids was made at temperatures of 150 and 250°C. To better understand the temperature dependence of four-ball wear for these fluids, additional tests with M50 balls were performed at 315°C. The total four-ball wear versus temperature plots for three 5P4E fluids are shown in Figure 112. The trends for the three 5P4E fluids are nearly identical from 150 to 250°C, showing a reduction in wear as the temperature is raised. At 315°C, the two inhibited fluids (TEL-90012 and TEL-90101) show a continued reduction in four-ball wear while the basestock (0-77-6) causes an increase. Overall, (TEL-91001) gives the least four-ball wear throughout the temperature range investigated.

In Figure 113, the total four-ball wear versus temperature plots of three experimental fluids are shown. With the range of the vertical axes in Figure 113 ranging from 0.0005 to 1 mm<sup>3</sup> on a logarithmic scale, the total four-ball wear of these experimental fluids is substantially less than the 5P4E fluids (whose wear volumes ranged from 0 to 10 mm<sup>3</sup> on a linear scale). At 150°C, each experimental fluid has very little wear. At 250°C, TEL-9050 and TEL-90063 have dramatic rises in wear, and at 315°C very little change takes place. The TEL-90059 fluid has a less pronounced rise in wear at 250°C but does incur a drastic increase at 315°C. The TEL-90063 fluid has the least wear at the temperature extremes while the TEL-90059 fluid has the least wear at the intermediate temperature.

The wear versus temperature comparisons shown in Figure 114 are for the three fluids TEL-90028, 0-64-20, and 0-66-26. As with the 5P4E fluids, the wear volumes associated with TEL-90028 (an inhibited 6P5E) are large although they hardly vary from 150 to 315°C. 0-64-20 (a C-ether) appears to have a linearly increasing wear versus temperature trend that remains an order of magnitude less than the PPEs. 0-66-26 (a perfluoropolyalkyl ether, PFAE) is even an order of magnitude lower than C-ether, and like the two inhibited 5P4E fluids shown earlier, least wear is produced at 315°C.

The four-ball wear of two PPE mixtures was also investigated between 150 and 315°C. The viscosities of both mixtures are substantially less than neat PPE and were blended in order to lower the pour point of PPE. The first mixture is a 3:1 combination of PPE basestock and trichloroethylene (TCE). The effect of TCE on four-ball wear can be seen in Figure 115. Figure 115 compares the wear versus temperature trend of the TCE-diluted basestock to undiluted basestock. Although the temperatures of these tests would soon cause the TCE in solution to evaporate, a significant reduction in wear does take place at 150 and 315°C when TCE is present.

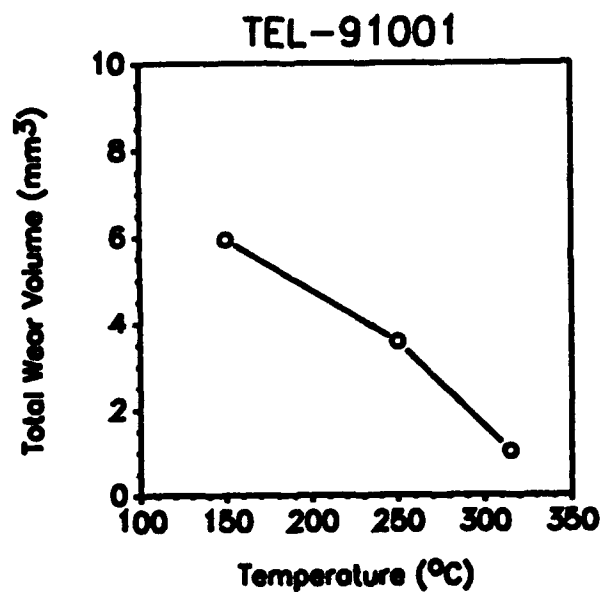
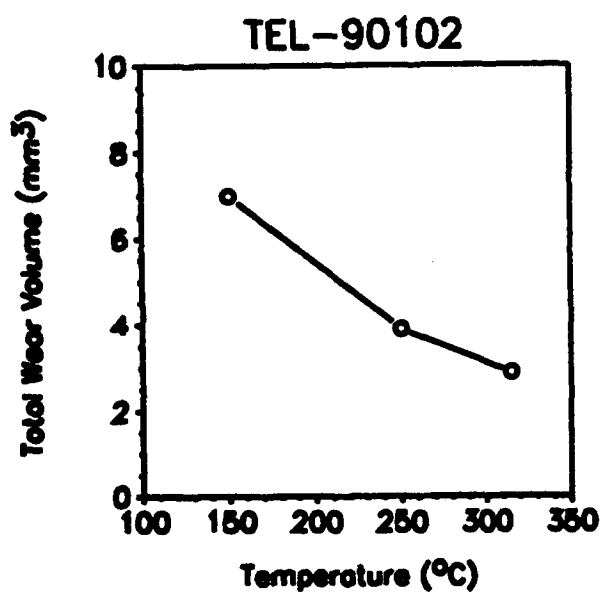
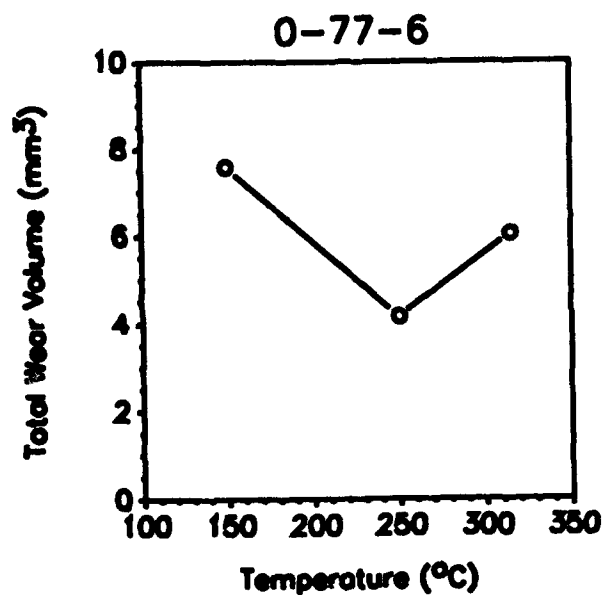


Figure 112. Four-Ball Wear Versus Temperature Curves for Three 5P4E Polyphenyl Ethers (M50 Balls, 3-Hour Tests, 1200 rpm, 145-N Load).

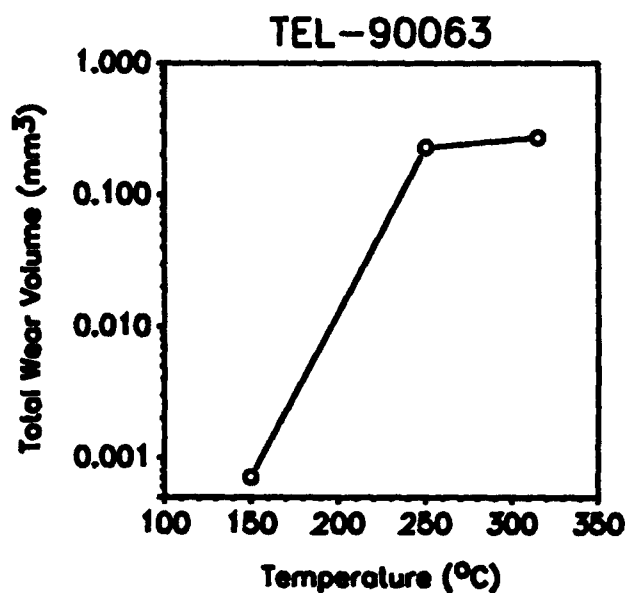
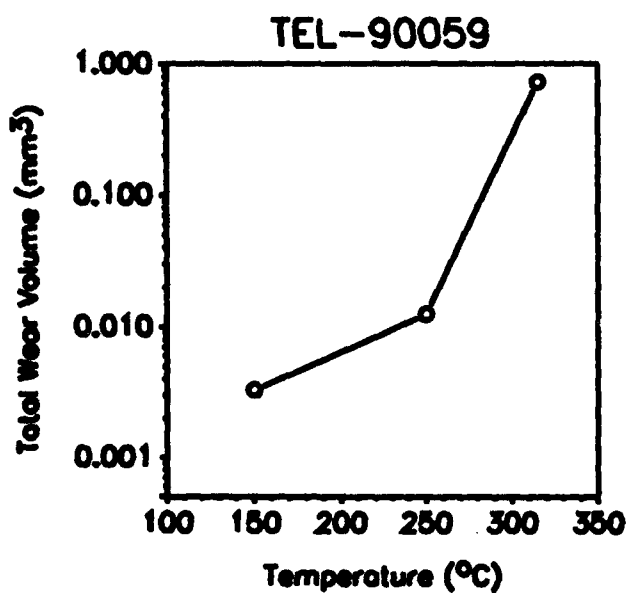
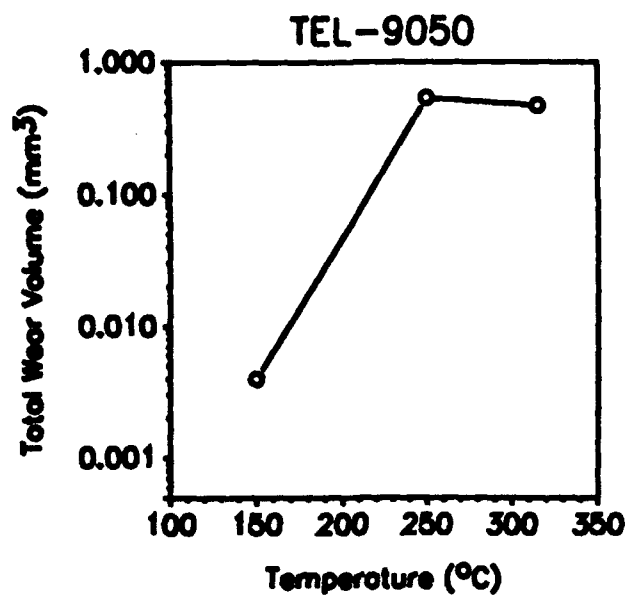


Figure 113. Four-Ball Wear Versus Temperature Curves for Three Experimental Fluids (M50 Balls, 3-Hour Tests, 1200 rpm 145-N Load).

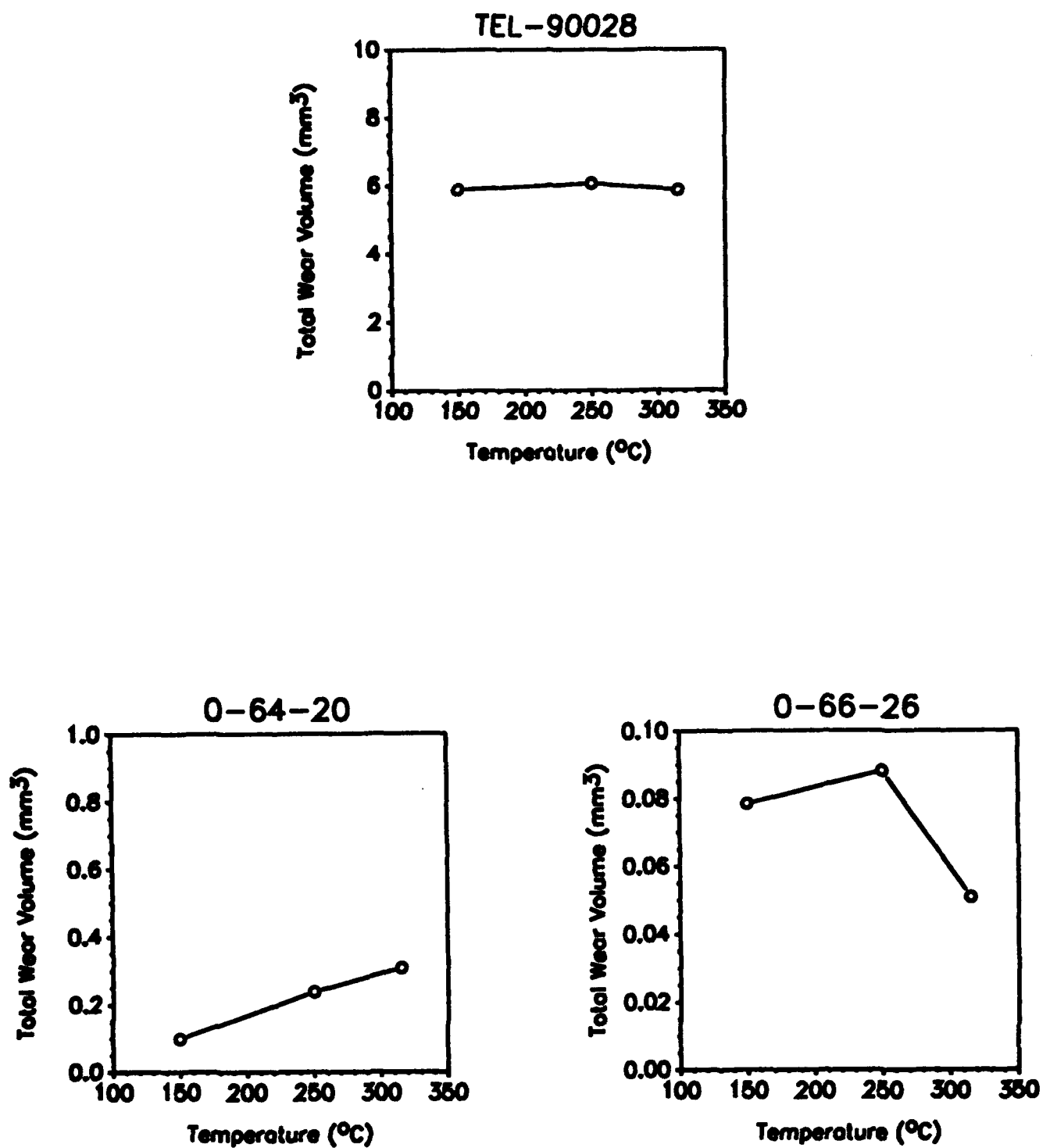


Figure 114. Four-Ball Wear Versus Temperature Curves for a 6P5E Polyphenyl Ether, a C-Ether, and a Perfluoropolyalkyl Ether (M50 Balls, 3-Hour Tests, 1200 rpm, 145-N Load).

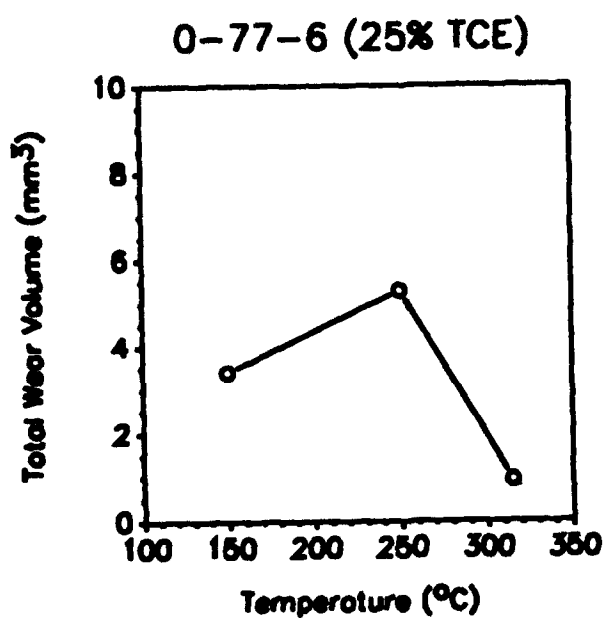
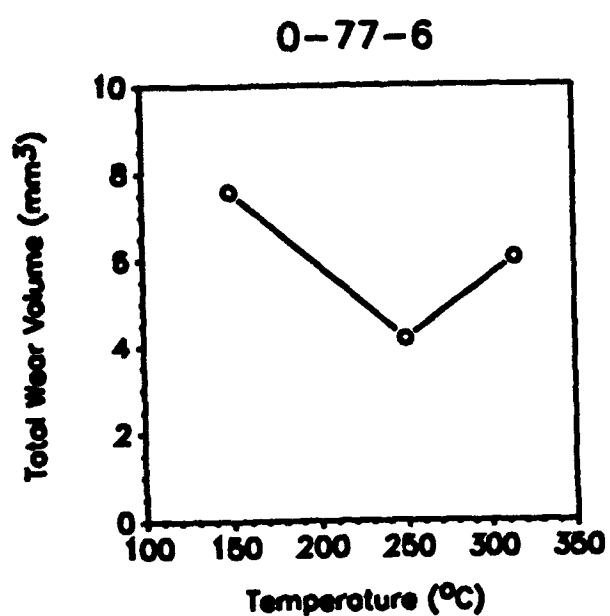


Figure 115. Four-Ball Wear Versus Temperature Curves for Polyphenyl Ether Basestock with and without Trichloroethylene Dilution.

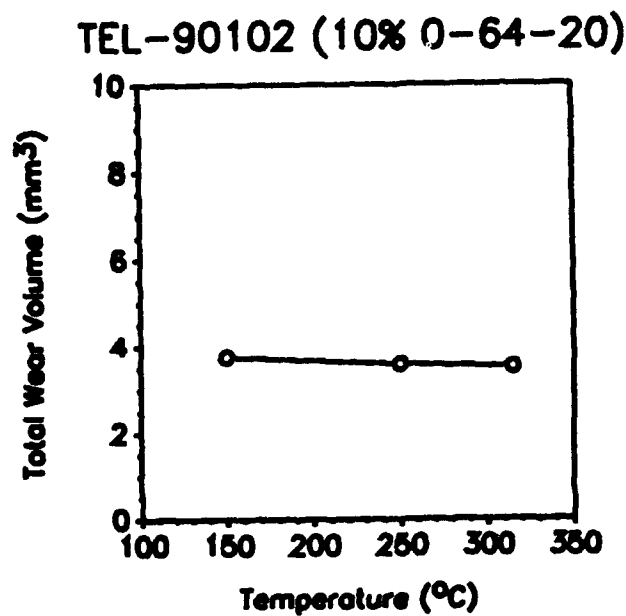
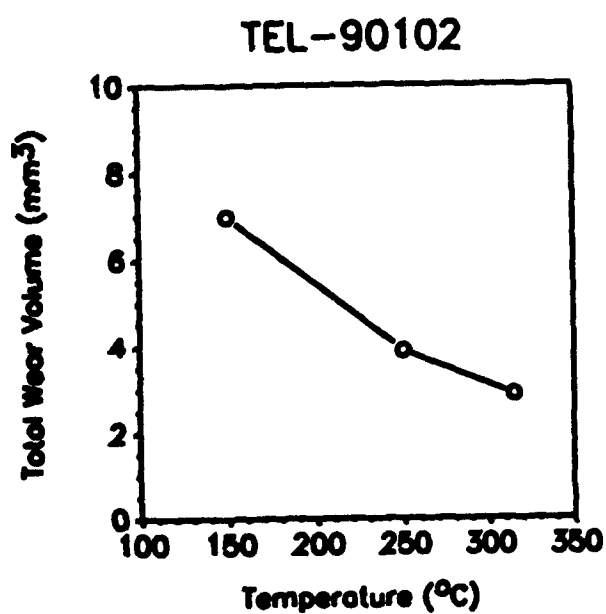


Figure 116. Four-Ball Wear Versus Temperature Curves for Inhibited Polyphenyl Ether with and without C-Ether Dilution.

Figure 116 compares the four-ball wear versus temperature relations of inhibited PPE and a 9:1 mixture of inhibited PPE and C-ether. The mixture has less four-ball wear than tests of neat TEL-90102 at each of three test temperatures. The PPE/C-ether mixture gives roughly the same amount of wear at each of the test temperatures.

d. TCE-Diluted PPE

Surface analyses previously done on the wear scars on 52100 balls lubricated with PPE indicated a chlorine presence.<sup>3</sup> Analyses of M50 balls tested at identical conditions showed no presence of chlorine, however. In similar tests of M50 specimens where an air flow was introduced into the test cup, four ball wear was reduced, and chlorine was detected at the surfaces. Since four-ball wear of M50 balls was consistently greater than the wear of 52100 balls at identical conditions for PPE, the chlorine presence might provide antiwear properties. Indeed, the work of Gong and his colleagues showed that chlorine can improve a lubricant load carrying capacity.<sup>61</sup>

Four-ball testing of PPE diluted with trichloroethylene (TCE) had been done on 52100 balls tested at 75, 150, 250, and 315°C. The presence of this chlorinated solvent, however, did nothing to inhibit wear. Nonetheless, the tests of M50 balls with the 3:1 PPE to TCE solution shown in Figure 115 were analyzed to determine the surface elements on the wear scar. These analyses did not reveal the presence of chlorine even for the tests at 150 and 315°C (where less wear took place). The reduction of four-ball wear for the TCE-diluted tests may have been due to the absence of sludge accumulations around the lower ball wear scars. Tests of PPE normally have these characteristic sludge build-ups, and the reduction in wear may have been caused by the TCE ability to keep deposits in solution or prevent them entirely.

e. ASTM Four-Ball Testing

All the four-ball testing and wear evaluations that have been done were based on the premise that more information could be gleaned from longer test durations and higher temperatures than those dictated by ASTM D 4172. Because of the variations in scarring that result from testing at high temperature, wear volumes were used to compare the tests rather than the average size of the wear scars, the measure dictated by ASTM D 4172. The basis for choosing a 3-hour test duration can be justified by the two plots shown in Figure 117.

Using the absolute vertical position of the upper ball of the four-ball configuration as a measure of the wear rate, Figure 117 compares a test of TCE-diluted PPE to a test of PPE with an antiwear additive. After one hour, the dashed line (representing TCE-diluted PPE) falls

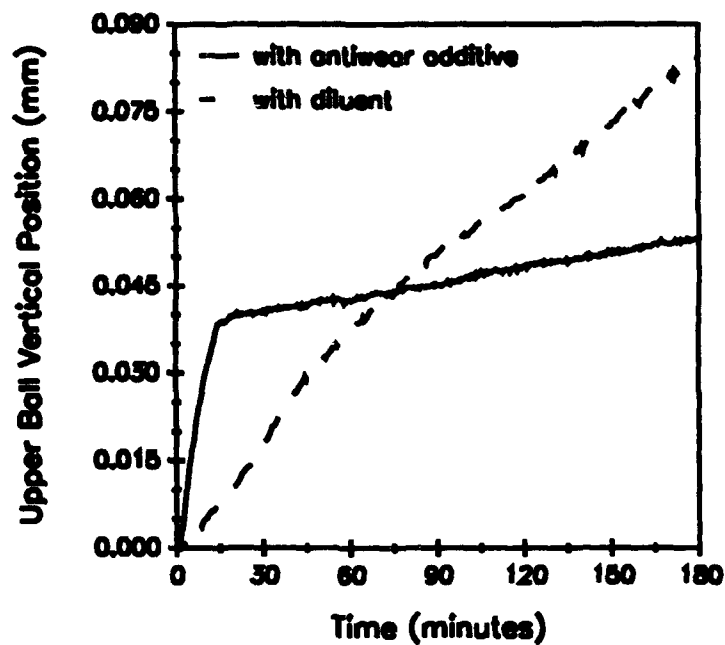


Figure 117. Four-Ball Wear Rates for Two Identically Tested Fluids Presented Using the Displacement of the Upper Ball Versus Test Time.

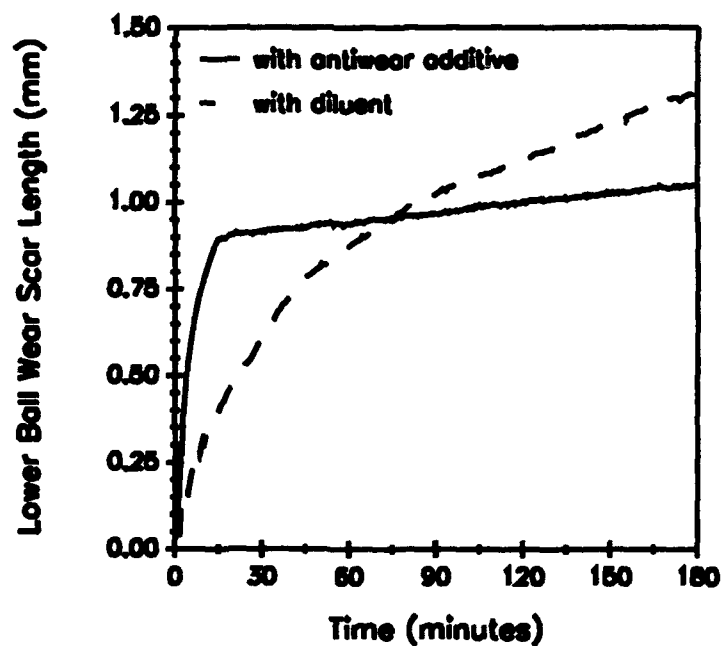


Figure 118. Four-Ball Wear Scar Length Versus Test Time Calculated from the Data of Figure 117.

below the solid line (representing PPE with an antiwear additive). A relationship was previously devised which allows the length of a four-ball wear scar to be calculated from the vertical displacement of the upper test specimen.<sup>3</sup> Using this relation, a plot of scar length versus test time can be constructed using the data of Figure 117. The results are shown in Figure 118.

Like the data of Figure 117, the trace for the TCE-diluted PPE is below that of the PPE with the antiwear additive at the one-hour mark. Because the test was allowed to run a total of three hours, the presence of the antiwear additive causes the final scar length to be less than that for the PPE-dilution. Because of high run-in wear, the scars from the test of the PPE/additive combination would have indicated more wear than the PPE/diluent combination for any test time below about 75 minutes. To avoid misleading data, a duration of three hours was chosen for comparison based on the wear rates of initial tests of candidate fluids.

In order for a comprehensive evaluation of the candidate fluids to be made, a battery of tests was completed according to ASTM D 4172. Figure 119 ranks 10 candidate fluids based on the average size (width and length) of the lower ball scars from one-hour tests at 75°C. Although the load and speed agree with ASTM D 4172, the ball specimens remained M50 steel instead of 52100 steel. The ranking lists the fluids in increasing order of scar size (left to right).

The PFAE fluid, 0-64-20, produces the smallest scars followed by the three experimental fluids, TEL-90059, TEL-90063, and TEL-90013 (a different supply of TEL-9050). TCE-diluted 5P4E basestock is next in the ranking, followed by the 10% mixture of 0-64-20 in inhibited 5P4E and neat 0-64-20. The largest scars in the ranking correspond to neat PPE formulations. Both of the inhibited 5P4Es (TEL-90102 and TEL-91001) generate similar sized wear scars slightly larger than those for the 0-64-20 fluid and the 0-64-20/TEL-90102 mixture. The 5P4E basestock (0-77-6) creates significantly larger scars than the inhibited 5P4Es, but the largest scars formed are from inhibited 6P5E (TEL-90028).

#### f. Summary

The various PPE fluids produced the highest four-ball wear of any of the candidate fluids. The scarring of M50 balls is temperature dependent, and the variety of scars formed always fell within one of three categories, primary lower ball wear, primary upper ball wear, and a combination of primary upper ball and primary lower ball wear that varies along the length of the scar. In four-ball tests of PPE where M50 is slid against another ball material, wear was less than tests of only M50 specimens. Si<sub>3</sub>N<sub>4</sub>/M50 combinations yield the least four-ball wear from 75°C through 315°C, and exclusively produce scars that exhibit primary lower ball wear.

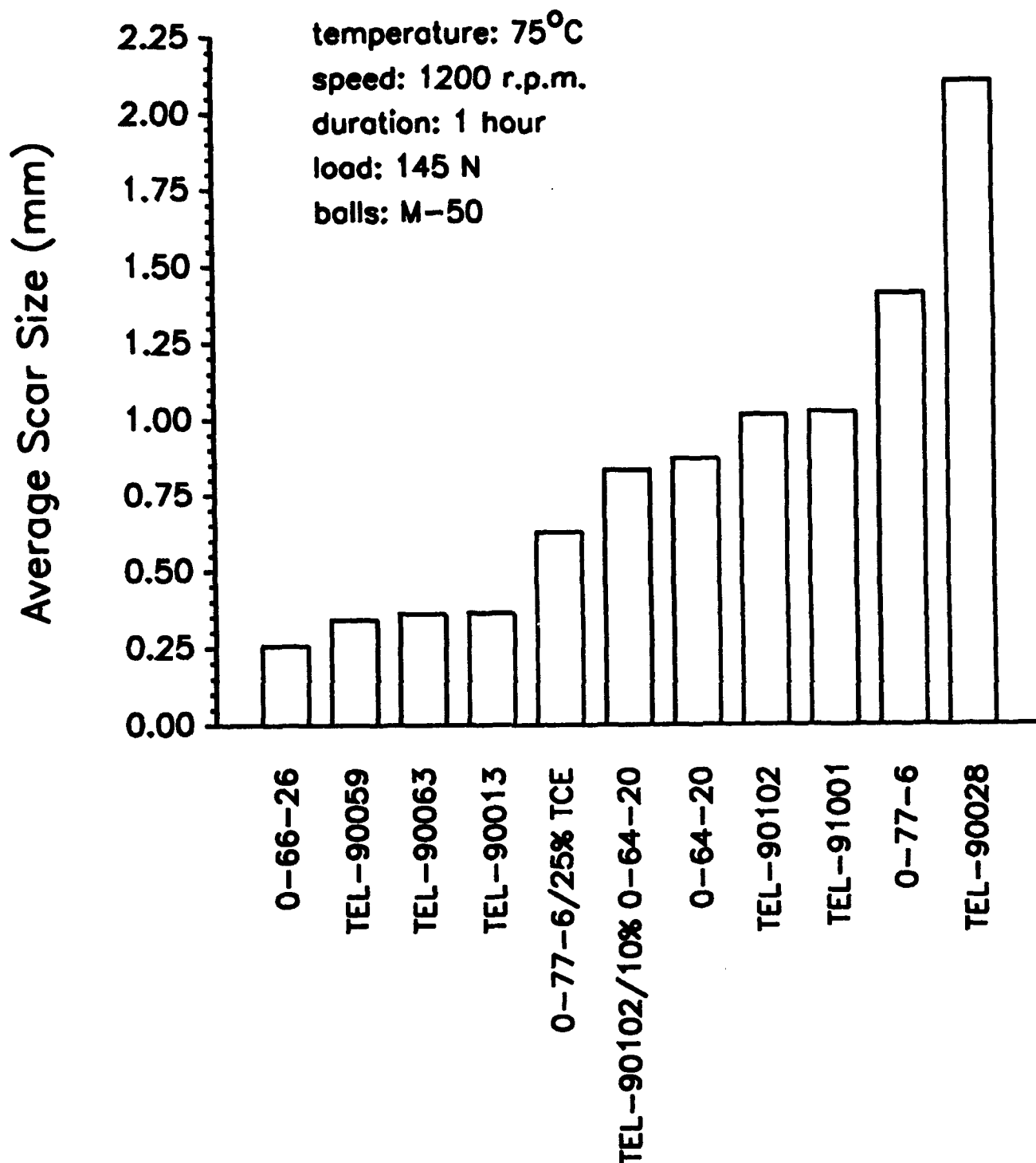


Figure 119. Ranking of Fluids by the Average Scar Diameter After Four-Ball Testing at the Conditions in ASTM D 4172.

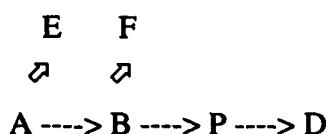
Increasing temperature lowered four-ball wear for inhibited 5P4E, TCE-diluted 5P4E, and PFAE. In comparing the results to ASTM test procedure, the greatest wear takes place with 6P5E and the least wear takes place for PFAE. When the four-ball test is to be used for comparing one fluid to another, the wear rates of each test should be considered so that appropriate durations are chosen.

## 2. THREE-BALL-ON-DISK (TBOD) TEST

### a. Introduction

Due to some fundamental differences existing in reaction mechanisms of liquid lubricants, three predominant chemical reaction domains are commonly recognized in liquid-lubricated systems. These are: (1) the flooded bulk reservoir or oil sump, (2) the thin lubricant film region, and (3) the dynamic tribo-contacts. In bulk lubricant reservoir, diffusion limitations of certain reactive species from the nearby gas phase (i.e., oxygen from the surrounding air) could complicate the overall reaction kinetics significantly. However, diffusion-controlling kinetics do not appear in areas where only a thin film of lubricant is being formed.<sup>29</sup>

Chemical conversions taking place *under either the bulk or the thin-film lubricant circumstances* are generally in a "static" reaction manner. In contrast, lubricants within tribo-contacts are subjected to extreme "dynamic" shearing action. Although the detail of reaction kinetics is extremely complex, a simplified first-order kinetic model of organic lubricant oxidation has, nevertheless, been attempted in the Penn State microoxidation test as follows.<sup>29</sup>



where,

- A : fresh liquid lubricant
- E : evaporated (A) in the vapor phase
- B : the primary oxidation products in the liquid phase
- F : evaporated (B) in the vapor phase
- P : the high-molecular-weight condensation polymers in the liquid phase
- D : sludge and varnish deposits

The rate limiting step is  $A \rightarrow B$ , which is usually 10 to 100 times slower than the subsequent reaction steps in the liquid phase. The relative magnitudes of these reaction rates are dependent upon the severity of the reaction conditions and the pool of reaction participants as well.

In the early 1940s, Shaw<sup>62</sup> proposed a mechanically activated chemical reaction mechanism following his study of a metal-cutting process wherein some organometallic compounds, which are extremely difficult to be synthesized under any conventional circumstance, were being produced. Since then, many highly stable organic compounds have also been found to readily undergo chemical conversions to form high molecular weight polymeric materials inside the tribological contacts.<sup>34,63,64</sup> Therefore, a general consensus has been reached that the kind of reaction condition experienced by the lubricant film interposed between two tribo-surfaces must be extraordinarily intense.

The process of lubricated wear is primarily governed by mechanical and chemical stresses in association with the thermal stress inside the tribo-junction. In general, these three stresses act jointly, and their combined effect determines the degree of friction, wear, and lubricant consumption of the junction. As a rough description of the condition within a conventional rubbing contact: the junction temperature is around 250 to 450°C, pressure could be as high as 3 GPa, and shear rate is usually from  $10^5$  to  $10^7 \text{ sec}^{-1}$  order of magnitude. In addition, mechanical deformation of the rubbing contacts can produce surface structural defects which, in turn, could promote the catalytic activity of the tribo-surface and possibly emit energetic and charged particles to speed up the chemical reaction in the contact region.<sup>65</sup>

A direct consequence of the collective action among all those stressing factors mentioned above is that the degradation rate of lubricant within the "dynamic" conjunction is unusually high. In many cases, the reaction products grow to their ultimate configuration (insoluble deposits) immediately, rather than going through some intermediate stages as outlined in the kinetic model obtained from the "static" Penn State microoxidation test.<sup>34,63,64,66</sup>

One other critical aspect of tribochemistry is that surface adsorbed species, such as polar lubricant additives, can be preferentially drawn into the contact zone, thus, attaining a much larger concentration inside the tribo-junction than otherwise in the bulk or thin-film conditions. This situation may result in accelerated consumption of those additive species within the contact region.<sup>14</sup>

Because of the primary importance of the three chemical reaction domains discussed so far, almost all of the laboratory bench tests have been designed to simulate one or more of these situations. In other words, liquid lubricants are being widely evaluated in one of the following ways: (1) "static" bulk oil testing, (2) "static" thin lubricant film testing, and (3) "dynamic" tribological testing.<sup>27</sup> Difficulties have arisen when one attempts to link the results obtained from these three different tests. Obviously, there exist variations in their reaction mechanisms, but in many cases the nature of each test apparatus differs so greatly that numerous system artifacts have been introduced into the process of data correlation. In order to minimize this externally induced complexity the development of an experimental device which is capable of performing all these tasks under the "same" environment is highly desirable.

Another major concern in the tribology community is the diversity of measuring wear. An excellent survey of this matter has been given by Blau.<sup>67</sup> The continuing practice of using myriad wear units, and the inconsistent ways of measuring wear have already created confusion for data comparison in tribology literature. To alleviate this painful burden, some well-defined and effective wear measuring techniques were pursued. A procedure for wear volume calculation has already been developed by this laboratory.<sup>60</sup>

In this section, a newly developed three-ball-on-disk (TBOD) bench technique will be presented, where lubricants are exposed to "dynamic" sliding contacts. Events of lubricant degradation occurring both inside and outside the sliding contacts are investigated via a microsample TBOD test. Experimental data of friction, wear, lubricant consumption, and tribochemistry are integrated to elucidate the lubricated wear process within the tribo-contacts. It should be noted that results from this microsample technique should be interpreted within the scope of thin-film liquid tribology; although the tribochemistry could remain similar, extreme caution must be exercised in extrapolating the meaning to fully flooded fluid conditions. Improved measurements of wear volume can be achieved through the use of a TBOD contact geometry compared to the popular four-ball wear test. This TBOD device is also designed for "static" bulk or thin-film oxidation testing.

#### b. Experimental Development

The basic features of the test apparatus are shown in Figure 120. A three-ball-on-disk (TBOD) contact arrangement, where three rotating balls slide against a flat disk surface, is adapted to a multispecimen wear tester. The original design was modified to accommodate a custom-made disk holder for contamination-free handling of the disk specimens and for retainment of liquid lubricant as well. The quantity of lubricant required in this

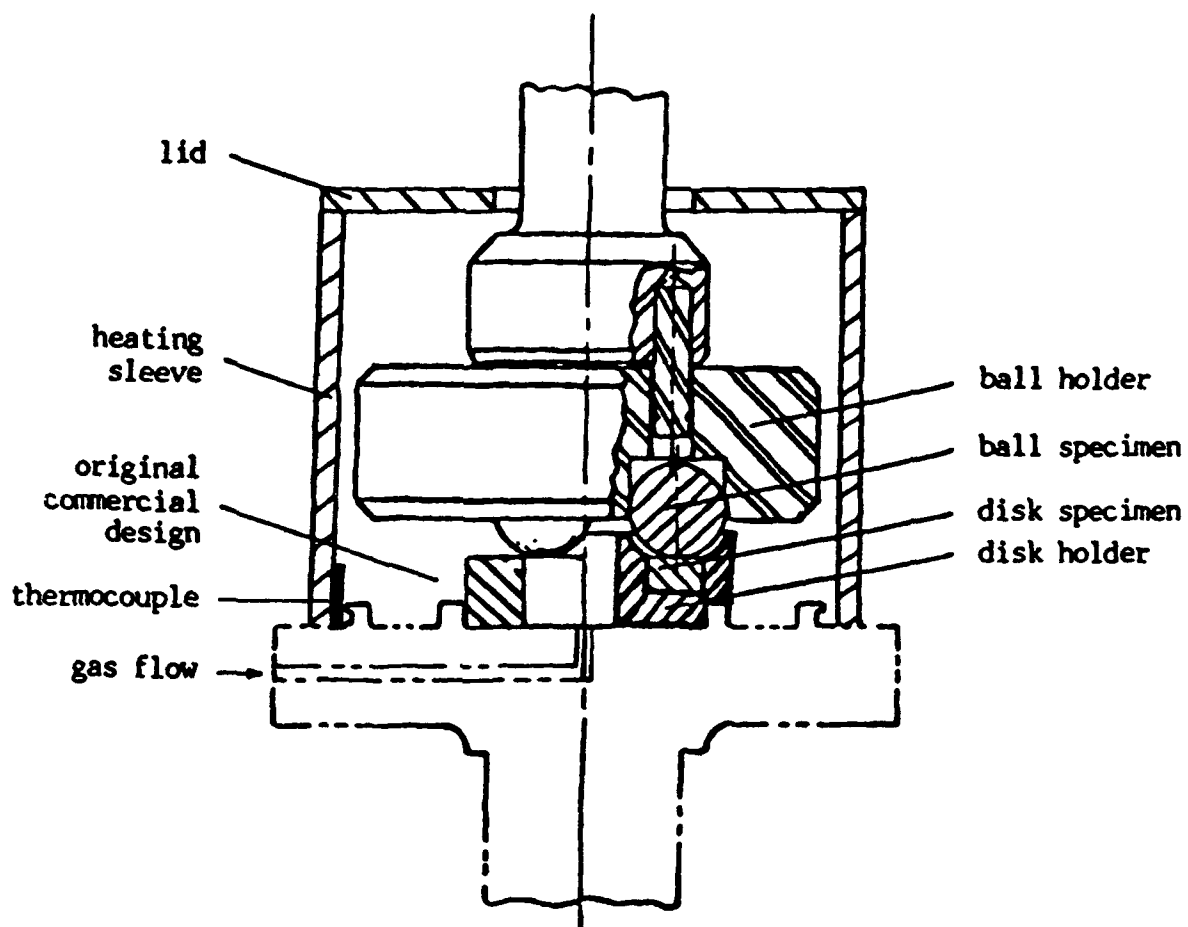


Figure 120. A Schematic Diagram of the Three-Ball-on-Disk (TBOD) Wear Test Device.

"dynamic" TBOD test may be varied from several cubic millimeters to about a half cubic centimeter, which is sufficient to cover the whole lubrication spectrum anywhere from a starvation regime to a fully flooded situation. A heating sleeve and a thermocouple are provided for temperature control. The temperature control error is within  $\pm 1^\circ\text{C}$ . If it is desirable, a gas flow can be introduced into the system through the opening at the bottom of the test chamber.

When micro-sample tests are being performed at high temperatures, a specially indented disk surface is employed to prevent lubricant migration due to its reduced viscosity. A cross-sectional profile of this disk surface is shown in Figure 121, together with a still photo of all test specimens and holders. The disk holder and disk specimens are notched so that a small key can be inserted to lock the disk in position during the test.

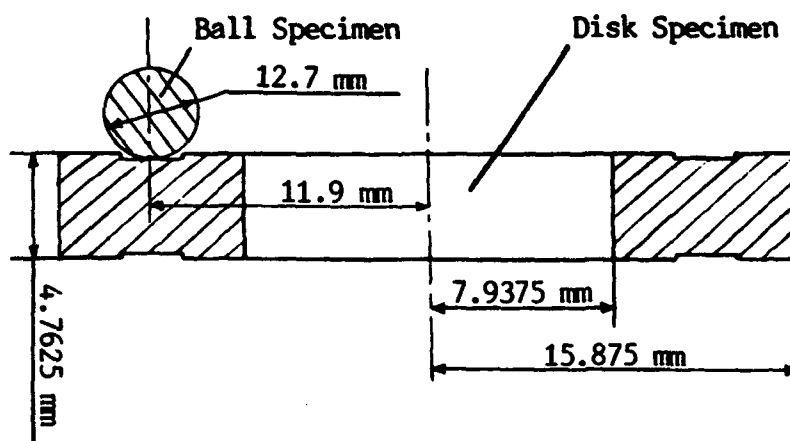
After a careful screening study, the following experimental parameters have been selected for the current TBOD test. A high temperature tool steel, M50, is utilized as the tribo-material for both the disk and the 12.7 mm (or 0.5 inch) diameter ball specimens. The inner and outer diameters of the disk specimen are 15.875 mm and 31.75 mm, respectively; and the disk thickness is 4.7625 mm. Table 89 lists the chemical composition and some physical properties of the M50 steel.

Brief descriptions and viscosity measurements of all test lubricants are presented in Table 90. These lubricants are: three 5P4E polyphenyl ethers (O-77-6, TEL-90102 and TEL-91001), two 3 cSt. ester fluids (O-77-10 and O-90-10), a cyclophosphazene (TEL-90013), and a C-ether (O-64-20). Among them, O-77-6, O-77-10, and TEL-90013 are single-compound basestocks. TEL-90102 and TEL-91001 are two inhibited 5P4Es, which contain only antioxidant additives. It should be made clear here the thermal-oxidative stability of TEL-91001 is superior to that of TEL-90102 according to our existing record.<sup>31</sup> O-90-10 is a fully formulated ester lubricant with a complete package of additives. The last fluid, O-64-20, is a C-ether mixture consisting mainly of two principal components with distinctive molecular weights, the lower fraction 3P2E C-ethers labeled "component 1" and the higher fraction 4P3E C-ethers named "component 2" hereafter.

Baseline of the TBOD test is established from the experimental data of O-77-6, a well-known high temperature basestock with oxidative stability at temperatures as high as  $295^\circ\text{C}$ .<sup>3</sup> An adequate amount of test lubricant is needed in order to sustain a reasonable test duration so that enough wear products could be generated for analysis. Too much lubricant, on the other hand, could cause poor resolution of the small tribo-induced changes within the fluid body. As a compromise, a sample size of  $20\text{ mm}^3$  has been chosen in this work. A ball rotating



( a )



( b )

Figure 121. Components of TBOD: (a) TBOD Test Head Assembly and (b) Profile of the Indented Disk Surface.

TABLE 89

## CHEMICAL COMPOSITION AND PHYSICAL PROPERTIES OF THE M50 STEEL

Chemical Element	Weight %
Carbon	0.77 - 0.85
Manganese	0.20 - 0.35
Silicon	0.10 - 0.25
Chromium	3.75 - 4.25
Molybdenum	4.00 - 4.50
Vanadium	0.90 - 1.10
Nickel	0.10 max.
Tungsten	0.25 max.
Phosphorus	0.015 max.
Sulfur	0.015 max.
Iron	Balance

Physical Property	Magnitude
Specific Gravity	7.87
Density (g/cm <sup>3</sup> )	7.971
Young's Modulus (GPa)	204
Hardness (Rockwell C)	61
Tensile Strength (GPa)	2.8
Yield Strength (GPa)	2.3

**TABLE 90**  
**A LIST OF THE TEST LUBRICANTS**

Code Name	Description	Viscosity (cSt)	
		40°C	100°C
O-77-6	5P4E Polyphenyl Ether	280.8	12.52
TEL-90102	Inhibited O-77-6	283.0	12.77
TEL-91001	Inhibited O-77-6	289.2	12.67
O-77-10	3 cSt Ester Fluid	11.79	3.12
O-90-10	Formulated O-77-10	12.51	3.16
TEL-90013	Cyclophosphazene	212.3	10.75
O-64-20	C-Ether	21.7	4.01

speed of 200 rpm coupled with the 23.8 mm disk wear track diameter is able to offer a moderate sliding speed of 0.25 m/s, which may promote elastohydrodynamic (EHD) or mixed film lubrication during the test (as supported by the friction and wear data from the TBOD test).

The logic behind the test configuration of using three balls and a plane disk is that three contacting points define a flat surface. A relatively heavy load of 22.68 kg dead weight (provides an initial Hertzian contact pressure of 1.048 GPa) is being applied. Under this loading, three nearly equal ball scars and an essentially uniform wear track have been produced, which implies adequate specimen alignment during the test. A universal joint presented between the rotating spindle and the ball holder ensures proper specimen alignment. To lower lubricant evaporation loss, no dynamic gas flow of any kind has been introduced into the test chamber. TBOD tests have been carried out at temperatures of 30, 150, 250°C, and under an ambient atmosphere.

Prior to each TBOD test, the test specimens are soaked in clean toluene and sonicated for 15 minutes. The retrieved specimens are subsequently rinsed by reagent grade hexane, and air dried. The specimen holders and other components inside the test chamber are also cleaned by toluene and hexane. A micro syringe, cleaned by reagent grade hexane, is used to deliver the lubricant sample into the anticipated wearing location on the disk surface. The test rig is then assembled and brought up to the designated test temperature. It requires approximately 15 or 20 minutes for the system to reach 150 or 250°C, respectively. Once the desired temperature is attained, the already loaded TBOD tester is started immediately. The running time is preset for every experiment. However, the longest possible test duration at each temperature setting is limited by a sudden rise of frictional torque or seizure in the tribosystem, which indicates that the degraded lubricant is too thick and can no longer effectively circulate into the three sliding contacts.<sup>14</sup>

The friction torque is measured by a strain gauge located 2 cm away from the rotating axis. The friction coefficient can be calculated using the torque, the radius of disk wear track, and the applied load. While the torque can be continuously monitored throughout the entire run, the wear information is obtained only at the end of each test. A procedure of wear volume calculation for both ball and disk specimens has been adapted from a wear model designed for the four-ball wear test.<sup>60</sup> A linear variable displacement transducer (LVDT) was employed to record the vertical displacement of three balls during the test. The vertical ball displacement is used together with the wear scar sizes for wear volume determination. The total wear volume, the sum of every individual measurements from all three balls and one disk, is standardized as the representative wear measurement. The relative share of the wear from the

balls or the disk specimen can be interpreted through a dimensionless scar surface parameter, beta (for beta calculation see Appendix B). When beta is 0, there is no disk wear, and the ball wear represents 100 % of the total wear. Conversely, a beta value of 1 means that there is no ball wear, and the disk wear represents 100 % of the total wear.

At the conclusion of each test run, the residual of lubricant sample is recovered by washing with 3 cm<sup>3</sup> tetrahydrofuran (THF), and the solution is then analyzed by gel permeation chromatography (GPC) to examine the molecular weight distribution of the tested lubricant. Comparison of the GPC chromatogram of the TBOD stressed sample with that of a fresh lubricant standard not only reveals the degree of lubricant consumption, but also provides useful information concerning lubricant tribochemistry during the TBOD test.

### c. Results and Discussion

#### (1) O-77-6

The 5P4E polyphenyl ether basestock (O-77-6), with a well-established literature data base, is adopted as the reference fluid in this study. Experiments of the O-77-6 fluid have been carried out at all three levels of temperatures: 30, 150, and 250°C.

##### (a) Lubricant Degradation

The TBOD-stressed O-77-6 is analyzed in a GPC apparatus, and the quantitative measure of lubricant consumption is based on the difference between the GPC peak area of the stressed sample and the peak area of the fresh standard. Figure 122 shows the results of lubricant consumption as a function of TBOD test duration. Every plotted data point in the figure represents a single completed test. The experimental results suggest that the amount of lubricant consumed is linearly proportional to the time of TBOD test. In other words, a constant rate of consumption can be constructed for each temperature. It is also clear that the consumption rate of 5P4E increases rapidly with the test temperature. The average rate at each test temperature has been calculated and is presented as follows:  $3.8 \times 10^{-3}$  mm<sup>3</sup>/min at 30°C,  $7.8 \times 10^{-2}$  mm<sup>3</sup>/min at 150°C, and  $2.4 \times 10^{-1}$  mm<sup>3</sup>/min at 250°C.

It should be mentioned that the actual temperature of lubricant sample during the TBOD test might be considerably higher than the monitored chamber temperature due to frictional heating. For this reason, the observed rate of lubricant consumption should include (1) lubricant "dynamic" reaction within the sliding junctions, (2) "static" reaction taking place outside the sliding junctions, and (3) possible evaporation loss of O-77-6 especially at a chamber temperature of 250°C since the TBOD system is not completely sealed.

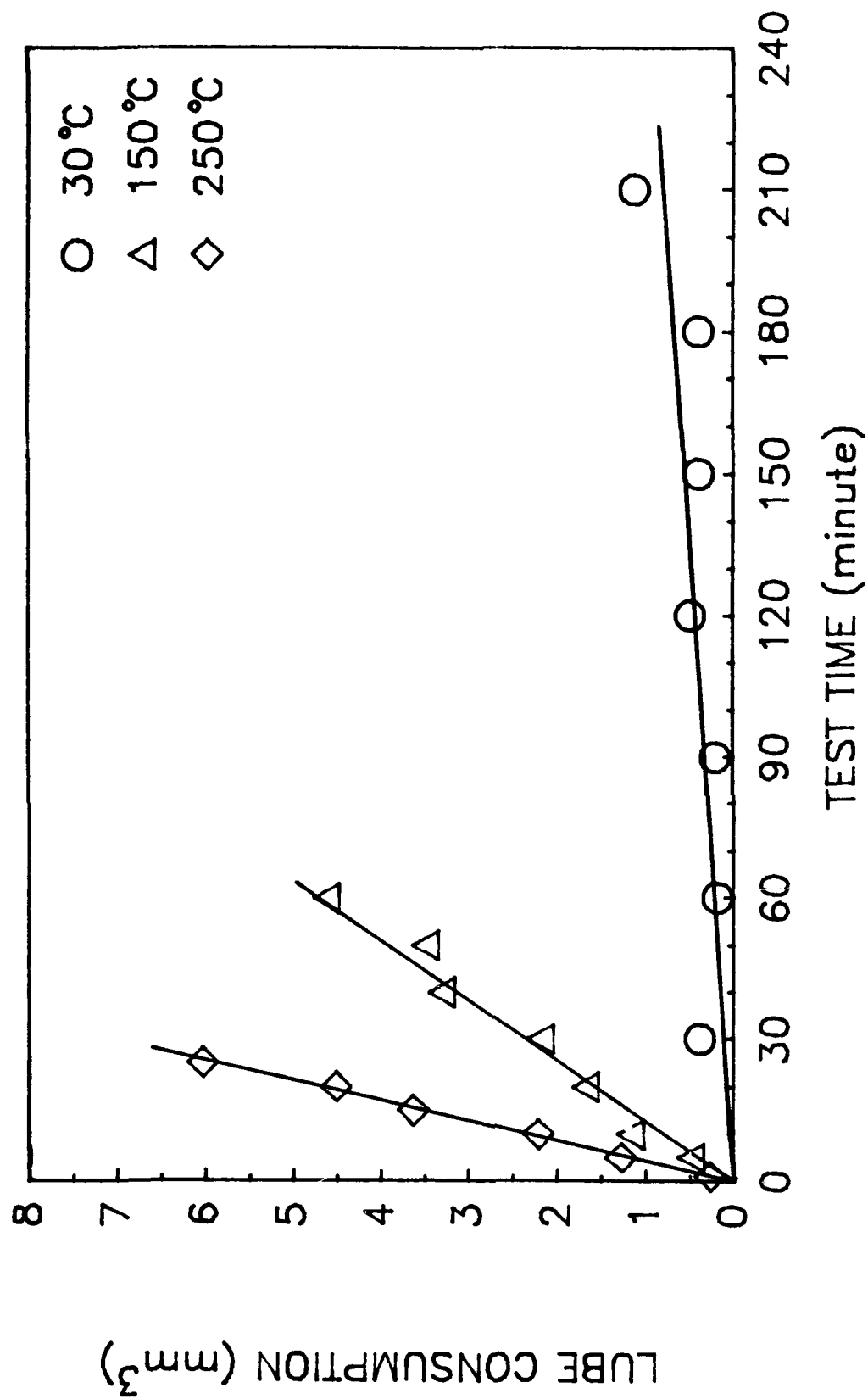


Figure 122. Consumption Rates of O-77-6 at 30, 150 and 250°C. Rotating Speed: 200 rpm; Load: 22.68 kg; Lubricant Volume: 20 mm<sup>3</sup>.

Examples of GPC chromatograms of the TBOD tested samples together with the fresh standard are displayed in Figure 123. In this figure, the abscissa refers to molecular weight distribution where the higher end of molecular weight is placed on the left side of each chromatogram peak and the lower end is located on the right side. The height of the peak represents the quantity of the material bearing that particular molecular weight. Because of the shallow yield of the THF soluble high molecular weight (HMW) reaction products, chromatograms of the longest (or the limiting) TBOD duration obtained at each test temperature are being used in the plot in order to enhance the signal of the HMW species. The selected chromatographic scale is intended to show both the existence of the HMW fraction and its magnitude relative to the main O-77-6 peak.

The HMW signal appears clearly in the chromatogram of 210-minute TBOD test at 30°C, and this signal is also visible in the chromatogram of 25-minute TBOD test at 250°C. However, the THF soluble HMW materials are hardly seen in the case of 60-minute TBOD test at 150°C. Moreover, it should be noted that the THF soluble HMW products generated at 30°C are different from those of 250°C; the 30°C HMW species are "bigger" molecules (located further left on the abscissa) than their counterparts from 250°C. In a separate study using a bulk corrosion/oxidation test (ASTM method D4636) at 320°C, GPC results of a moderately stressed O-77-6 sample gave similar THF soluble HMW products as those found at 250°C from the TBOD testing. However, when the O-77-6 sample had severely degraded to form sludge and deposits in the corrosion/oxidation test, its GPC chromatogram showed two distinctive HMW peaks each corresponds to the HMW peak found in either 30°C or 250°C TBOD test.

For the 250°C TBOD test, the THF soluble HMW fraction is likely to be generated from "static" chemical conversion in the hot periphery of the tribo-junction. Other degradation products created in this TBOD test should be THF insolubles of extremely large molecular weights. These THF insoluble deposits have probably formed under the excessively stressed condition within the sliding contacts. The THF soluble HMW species from the 30°C TBOD test are not easy to be interpreted. Since "static" chemical reaction of 5P4E outside the sliding junctions is unlikely at such a low temperature, the only place for lubricant reaction is within the real contacts. Combination of severe junction condition and possible glass transition of 5P4E<sup>13</sup> may be the principal cause for those "bigger" HMW THF solubles.

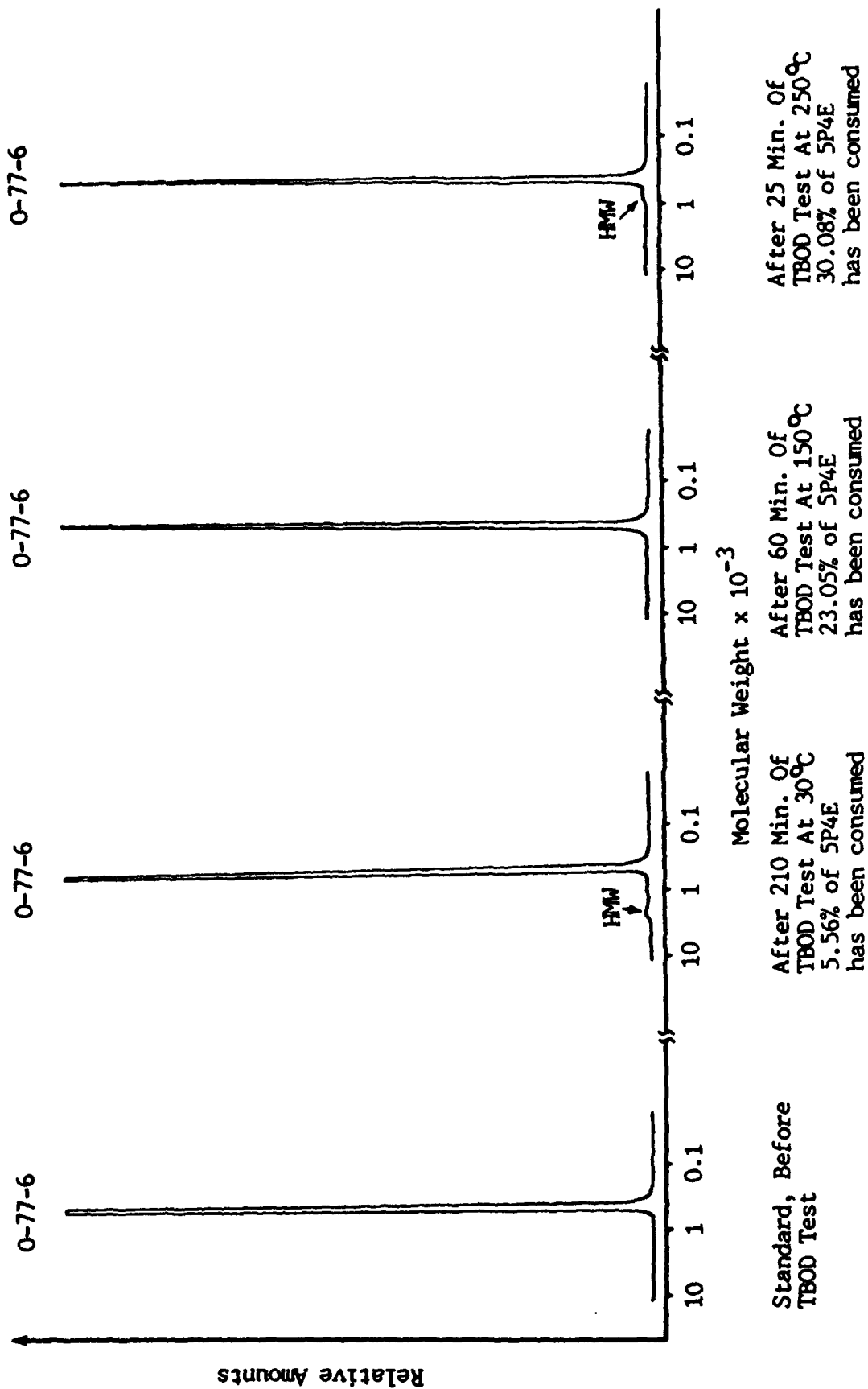


Figure 123. GPC Chromatograms of O-77-6, Showing Build-up of the Tetrahydrofuran Soluble High Molecular Weight (HMW) Wear Products.

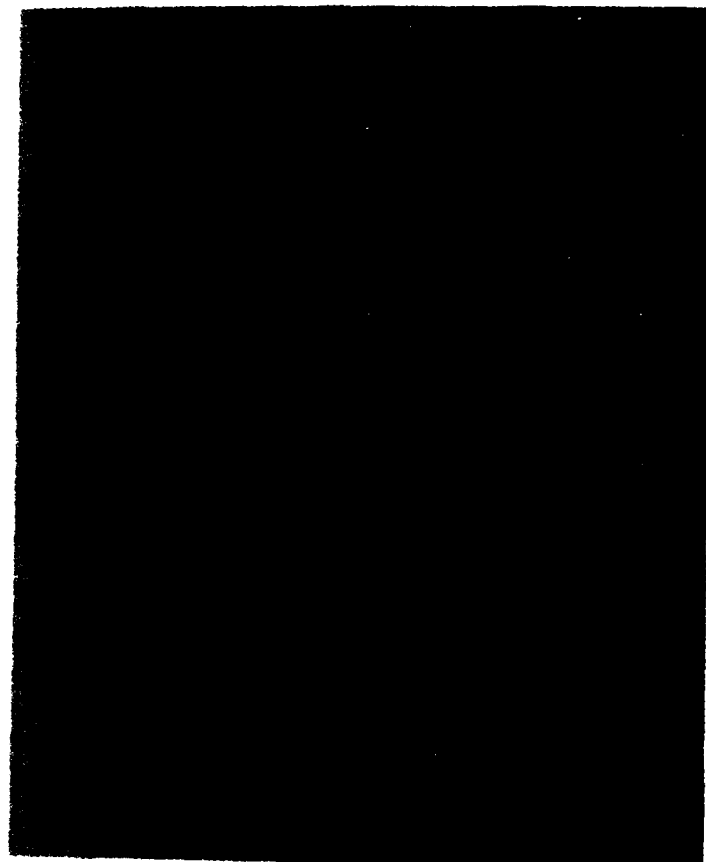
## (b) Wear

According to a previous wear program developed for the four-ball wear test,<sup>60</sup> wear volumes of four-ball specimens can be accurately estimated whenever circular or elliptical wear scars are being produced. Although these scar shapes are common in general, irregular scar geometries can be generated when four-ball testing is done at high-temperatures.<sup>3</sup> With M50 specimens, we have discovered that the wear scars from 5P4E-based fluids exhibit very peculiar shapes like the one pictured in Figure 124(a). The jagged edges of this scar reflect the dramatic roughness of the worn surfaces. The exact reason for such kind of scar shape is not thoroughly understood; however, the distribution pattern of the internal stresses experienced by the four-ball rubbing surfaces might play an important role in this matter.<sup>68</sup>

Without the complication of the horizontal load component as in the four-ball test, all of the load in the TBOD test is vertically applied on the tribo-surfaces. Furthermore, if the radius of curvature of the wearing track (or halo) is large enough and/or the sliding speed is not too high, the tribological state of a TBOD junction could well approach that of a linear sliding condition. Hence, the possible factors that may attribute to irregular wear scars would be substantially eliminated, thereby, ensuring consistent wear volume measurements. Indeed, this has proven to be the case in the current TBOD test (see the scar shape in Figure 124(b)).

The wear results of the TBOD test are presented in Figure 125, in which the total wear volume is plotted against the TBOD test time. For the 30°C-tests, wear initially increases proportionally with the running time until the transition point at 120-minute of the TBOD test, at that moment it then begins to level off. This transition is probably due to hydrodynamic lift created by the thickened 5P4E film after stressing for 120 minutes in the TBOD test.<sup>14</sup> The gradual increase in the area of the contact region (or reducing of contact pressure) during the TBOD test may also provide additional increase in lubricant film thickness within the sliding junctions. Despite data scatter, linear functionality between wear volume and test duration can nevertheless be established for tests conducted at 150 and 250°C. Interestingly enough, the wear rate at 250°C seems smaller than that at 150°C. Similar results were also found in an earlier study by us using the four-ball machine. This may have something to do with the extent of glass transition of the 5P4E within the sliding junctions.<sup>13</sup>

Optical measurements of the ball wear scars were made for determining the wear volumes of the balls and disk. The scar length and width measurements were used to generate the surface profile parameter, beta, for each test. The values of the beta



(a)



(b)

Figure 124. Photomicrographs of Ball Wear Scars: (a) From the Four-Ball Test. Lubricant: 5P4E; Test Specimen: M50 Balls; Temperature: 150°C; Rotating Speed: 1200 rpm; Load: 14.74 kg; Lubricant Volume: 30 cm<sup>3</sup>; Test Duration: 180 min., (b) From the TBOD Test. Lubricant: 5P4E; Test Specimen: M50 Balls and Disk; Temperature: 150°C; Rotating Speed: 200 rpm; Load: 22.68 kg; Lubricant Volume: 20 mm<sup>3</sup>; Test Duration: 60 min.

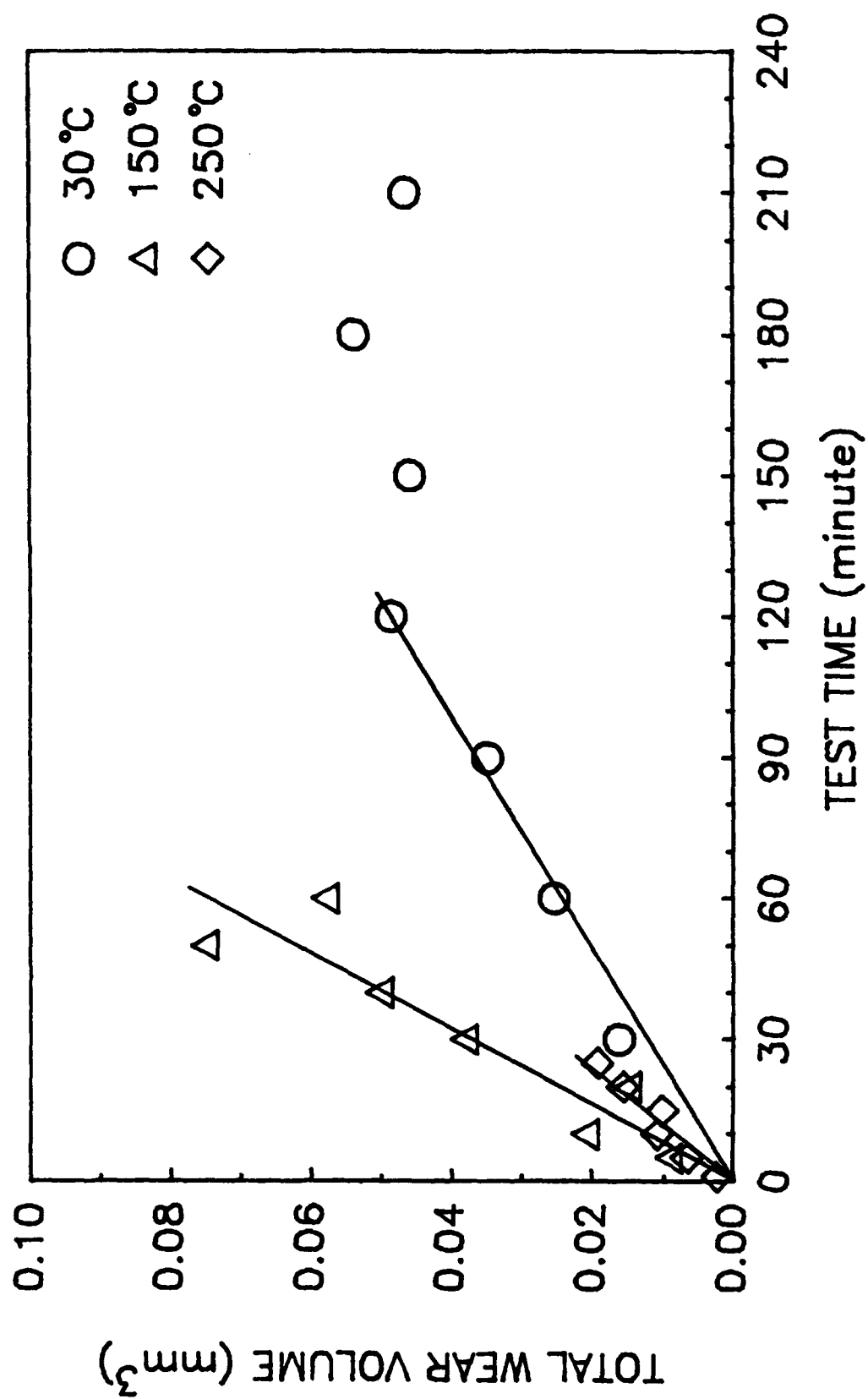


Figure 125. Wear Rates of M50 Specimens at 30, 150, and 250°C. Rotating Speed: 200 rpm; Load: 22.68 kg; Lubricant Volume: 20 mm<sup>3</sup>.

parameter are plotted versus test time in Figure 126. It was stated earlier that the beta parameter indicates the proportion of ball wear to total wear. Figure 127 shows the variation of this wear ratio (wear volume of the three balls divided by the total wear volume) with respect to the beta parameter. In this plot two curves have been included to show that the ratio of ball wear to total wear is both scar shape (i.e., beta) and scar size dependent. The 0.5-mm and 1.0-mm scar lengths encompass all scar sizes generated during this part of the work.

### (c) Friction

For each individual TBOD test, an (arithmetic) average coefficient of friction is calculated based on all of the friction measurements registered throughout the test. The friction data are plotted against their corresponding test time in Figure 128. It appears that the average coefficient of friction stays approximately constant at each temperature level regardless of how long their test durations might be, provided that all tests are completed prior to the moment of seizure (or the sudden jump of friction). The rank of the friction magnitude for all three temperatures is consistent with the rank of the wear rate shown in Figure 125. The frictional coefficient decreased in the order of the following temperatures:  $150 > 250 > 30^{\circ}\text{C}$ .

### (2) O-77-6, O-77-10, and O-90-10

For the fully formulated ester fluid (O-90-10) its field application temperature is typically around  $150^{\circ}\text{C}$ . The choice of this operating temperature is largely due to its relatively low thermal-oxidative stability and highly volatile nature compared with other high temperature lubricants. Because of that reason TBOD evaluation of ester fluids (O-77-10 and O-90-10) has been performed at  $150^{\circ}\text{C}$ , and their results will be discussed next in conjunction with the data obtained from the 5P4E polyphenyl ether basestock, O-77-6.

### (a) Friction and Wear

The TBOD friction data of these three lubricants are shown in Figure 129. Within the range of data scattering, the constant friction levels of both ester fluids are very close. It is also clear that the friction coefficient of the O-77-6 lubricant is nearly double those seen from the ester fluids. A plot of total wear volume versus test duration is presented in Figure 130, where the wear rate of O-77-10 is slightly higher than that of O-90-10. For the two ester lubricants, wear rates are generally very low, and their wear volumes reach to approximately constant levels after 5 minutes into the TBOD test. The wear rate of O-77-6 lubricated specimens is, however, much larger compared with those of the ester fluids.

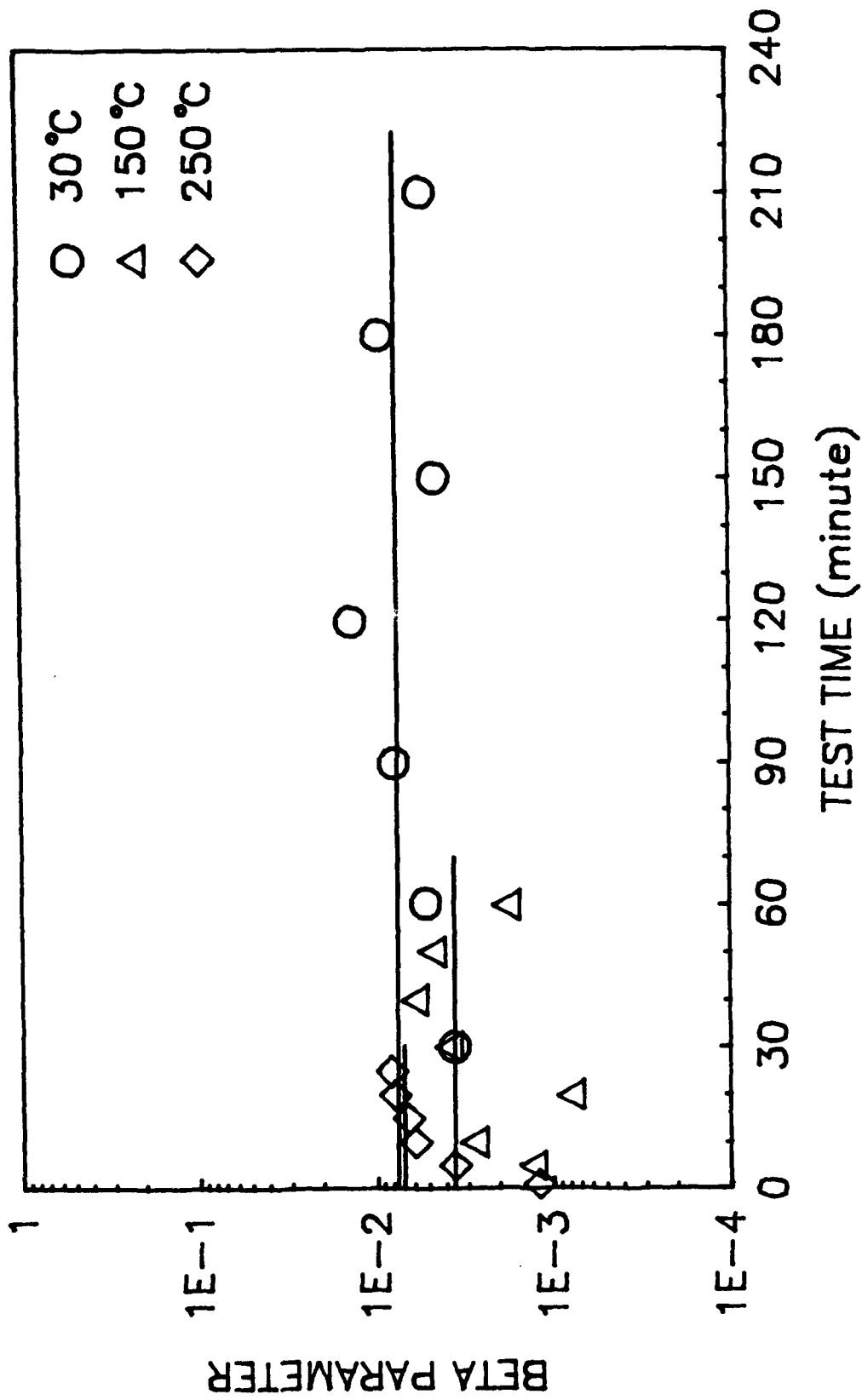


Figure 126. Beta Values Corresponding to the Wear Data Presented in Figure 125.

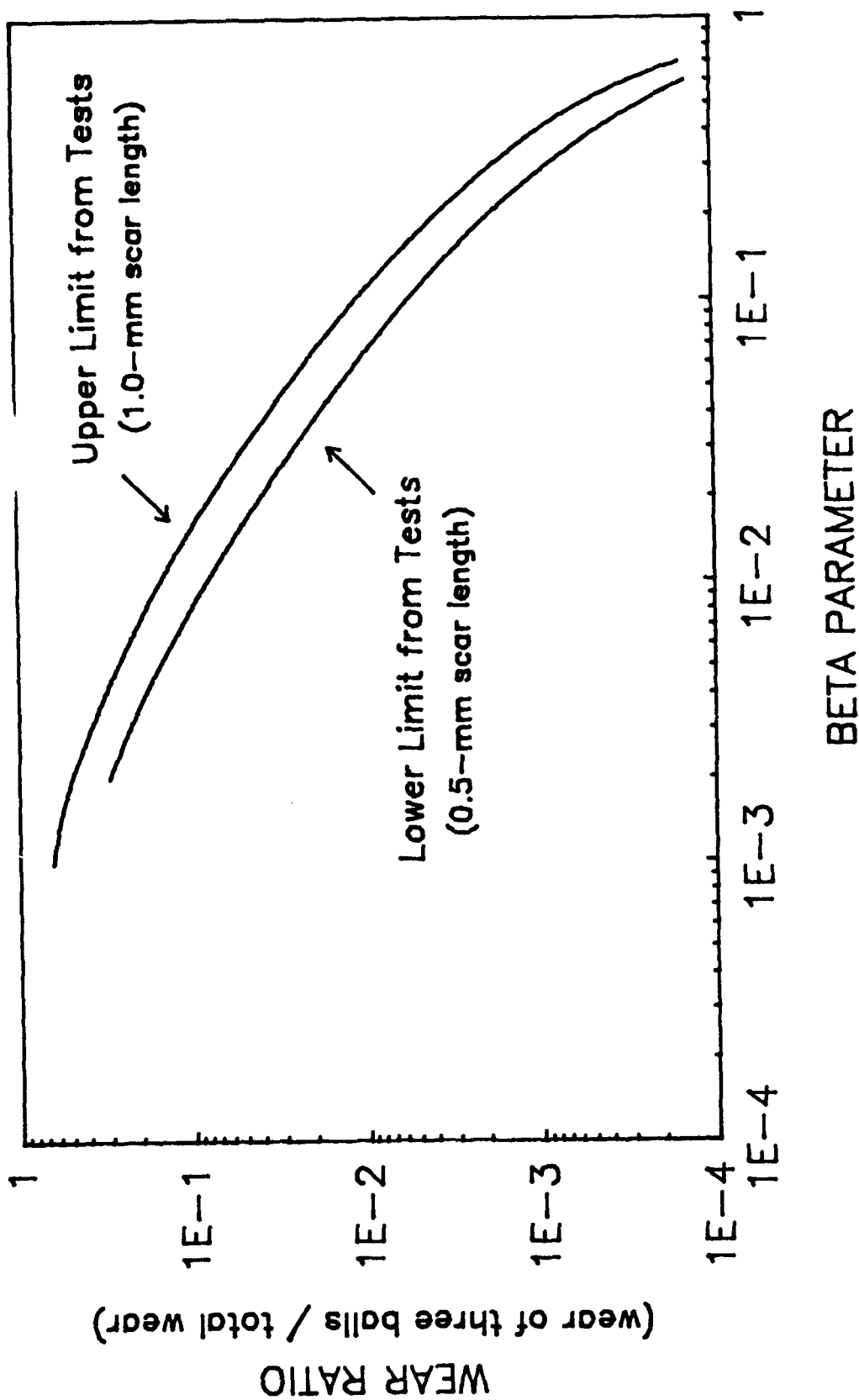


Figure 127. Wear Ratio (Wear of Three Balls/Total Wear) as a Function of the Beta Parameter for a Fixed Scar Length. The Limits of Scar Lengths Observed from the Experiment are Indicated.

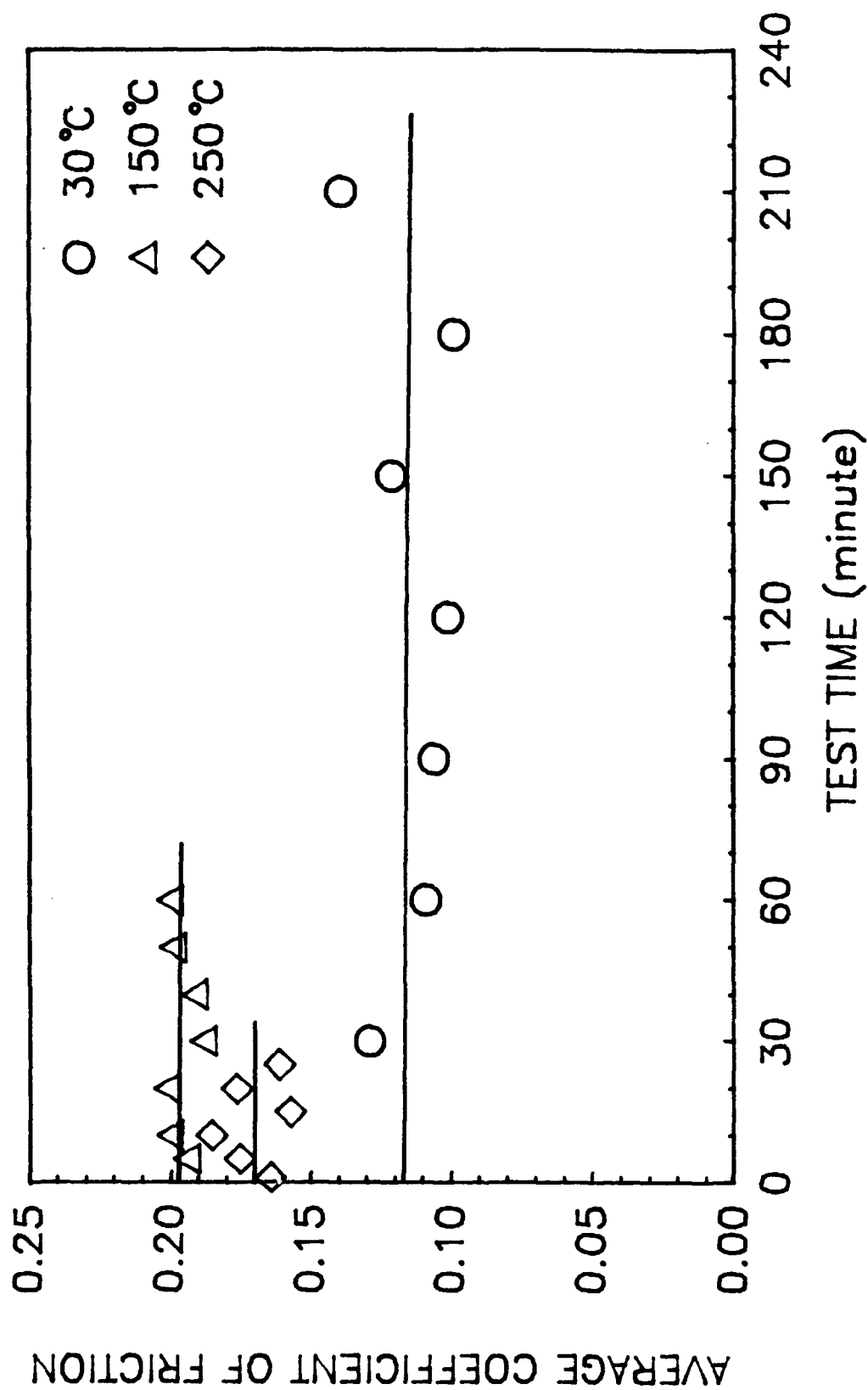


Figure 128. Coefficient of Friction at 30, 150, and 250°C. Rotating Speed: 200 rpm; Load: 22.68 kg; Lubricant Volume: 20 mm<sup>3</sup>.

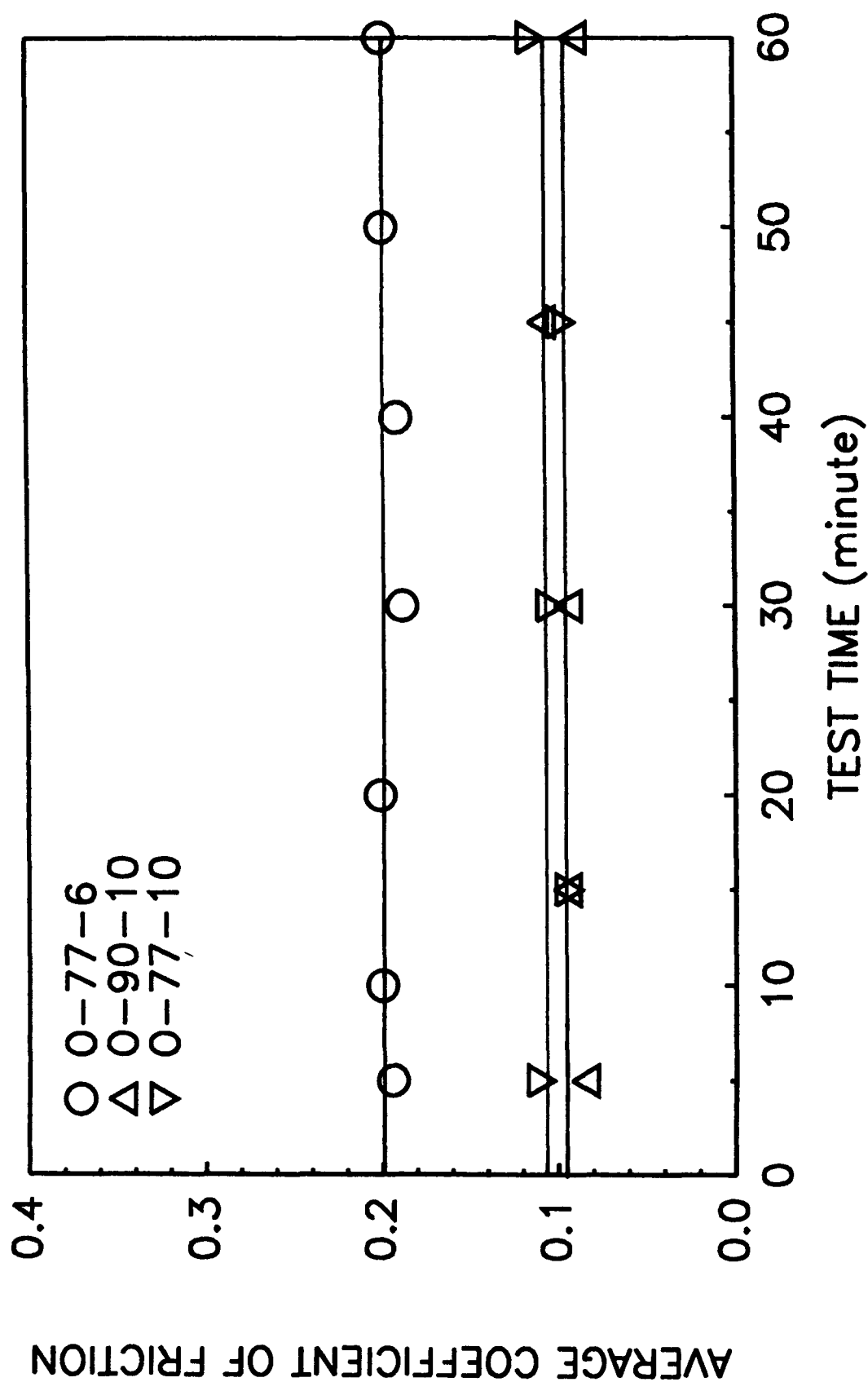


Figure 129. Coefficient of Friction at 150°C. Rotating Speed: 200 rpm; Load: 22.68 kg; Lubricant Volume: 20 mm<sup>3</sup>.

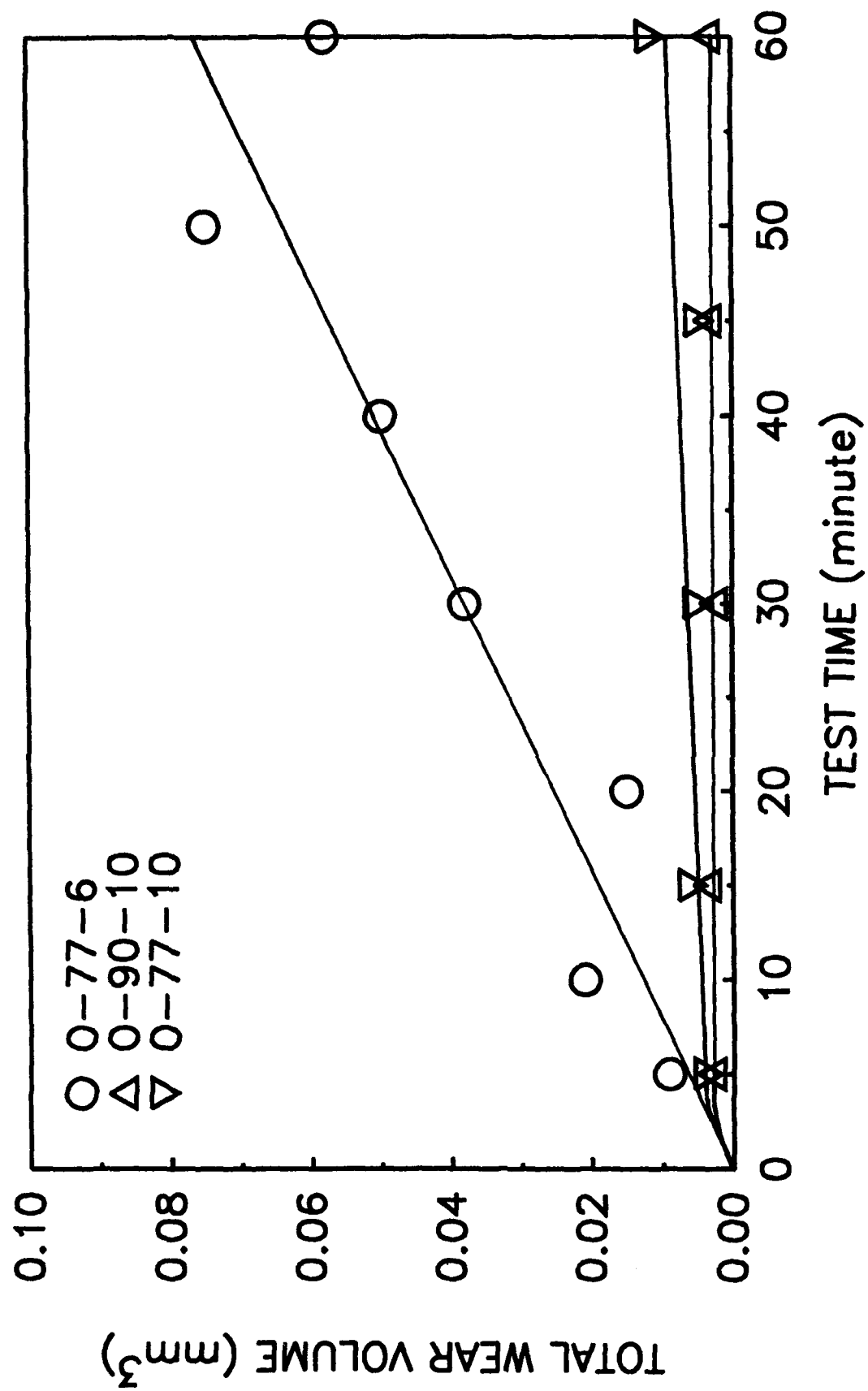


Figure 130. Wear Rates of M50 Specimens at 150°C. Rotating Speed: 200 rpm; Load: 22.68 kg; Lubricant Volume: 20 mm<sup>3</sup>.

### (b) Lubricant Consumption and Tribochemistry

Illustrated in Figure 131, the consumption rate of O-90-10 is slightly higher than that of O-77-10. Furthermore, the difference in lubricant consumption between the ester fluids and the polyphenyl ether basestock (O-77-6) is also not as striking as those observed in their friction and wear plots. The somewhat higher consumption rate of O-77-6 may be associated with its larger friction (heat) and wear (catalytic surface area) magnitudes. GPC chromatograms of the stressed lubricant samples and their related standards are displayed in Figure 132. THF soluble high molecular weight reaction products are hardly detected from these chromatograms.

It should be mentioned that for the experimental condition employed here, it is very difficult to differentiate these two ester fluids in terms of their friction, wear, and lubricant consumption characteristics. Although the ester basestock (O-77-10) seems to have slightly more wear than its fully formulated version (O-90-10), the lubricant consumption rate of O-77-10 is shown to be little less than that of O-90-10.

### (3) O-77-6, TEL-90102, TEL-91001, TEL-90013, and O-64-20

Since all five enlisted lubricants are considered as high temperature candidate fluids, they have been tested under the most intensive TBOD condition of 250°C.

#### (a) Friction

A plot of average coefficients of friction vs. their corresponding TBOD running times is presented in Figure 133. From each test fluid its average friction measurements are about the same in magnitude for the various test durations. The friction level of TEL-91001 is very close to that of O-77-6. Other than that, differences among these test fluids are quite clear in general. The rank of friction for the five lubricants is in the following decreasing order: TEL-90102 > TEL-91001 > O-77-6 > O-64-20 > TEL-90013.

#### (b) Wear

Figure 134 shows the wear data of M50 specimens lubricated by the five fluids. While a constant wear rate can be established in all other cases, the TEL-90013 lubricated M50 yielded a wear curve with gradual reduction of the wear rate with TBOD test time. This decrease of wear rate indicates some kind of antiwear capability of TEL-90013 towards the M50 sliding surface.

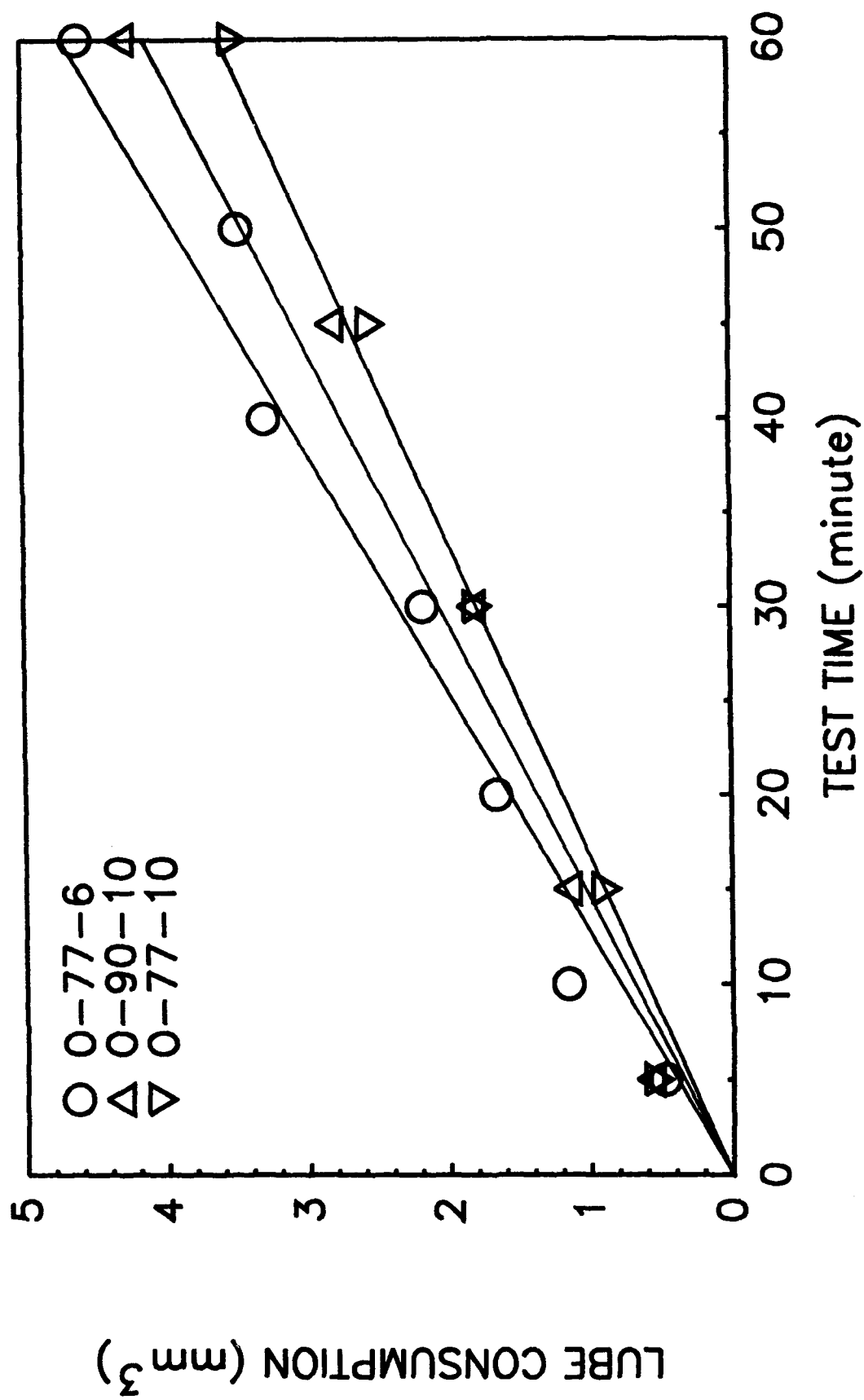


Figure 131. Lubricant Consumption Rates at 150°C. Rotating Speed: 200 rpm; Load: 22.68 kg; Lubricant Volume: 20  $\text{mm}^3$ .

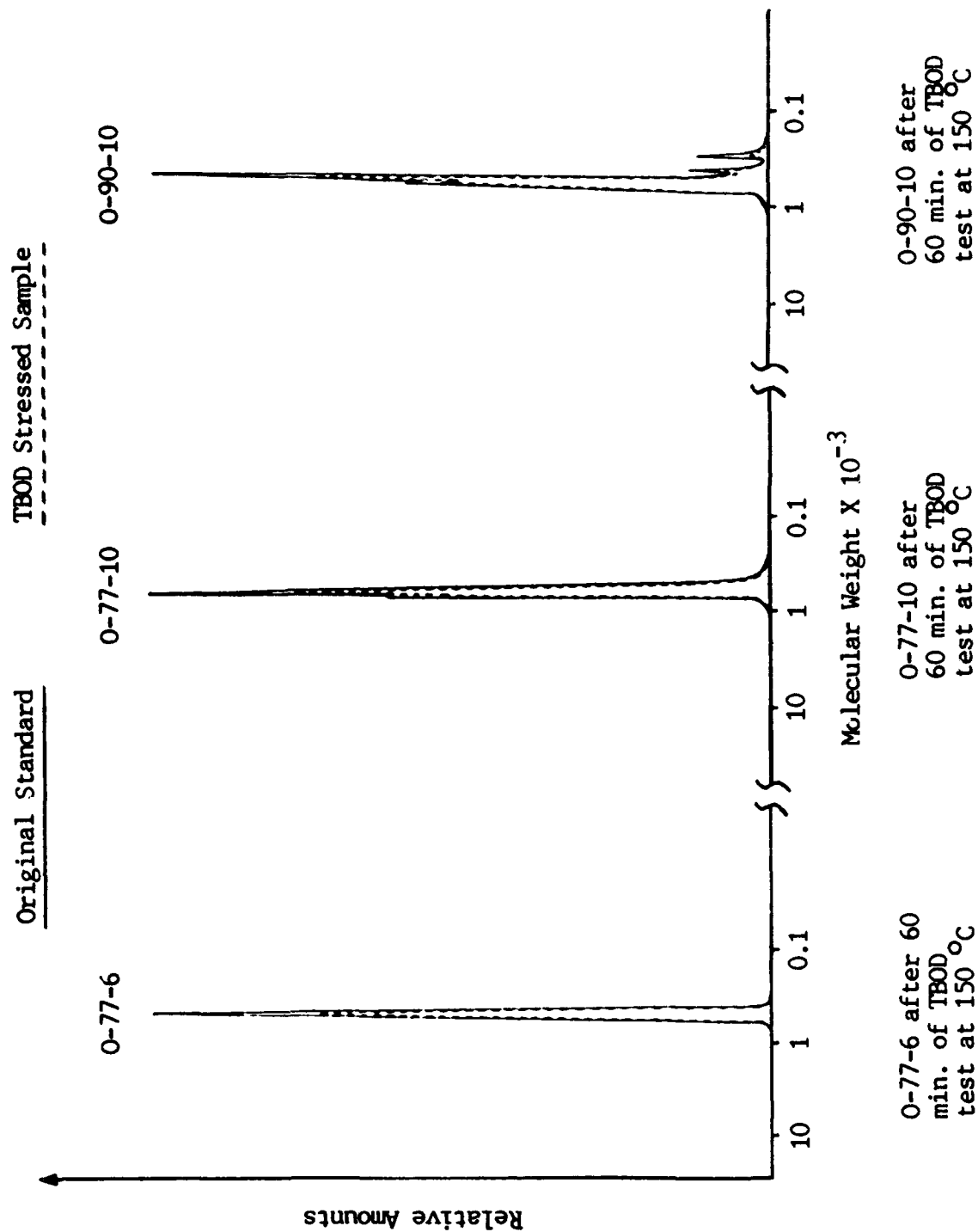


Figure 132. GPC Chromatograms of the Three Tested Fluids, Together with Their Corresponding Fresh Standards.

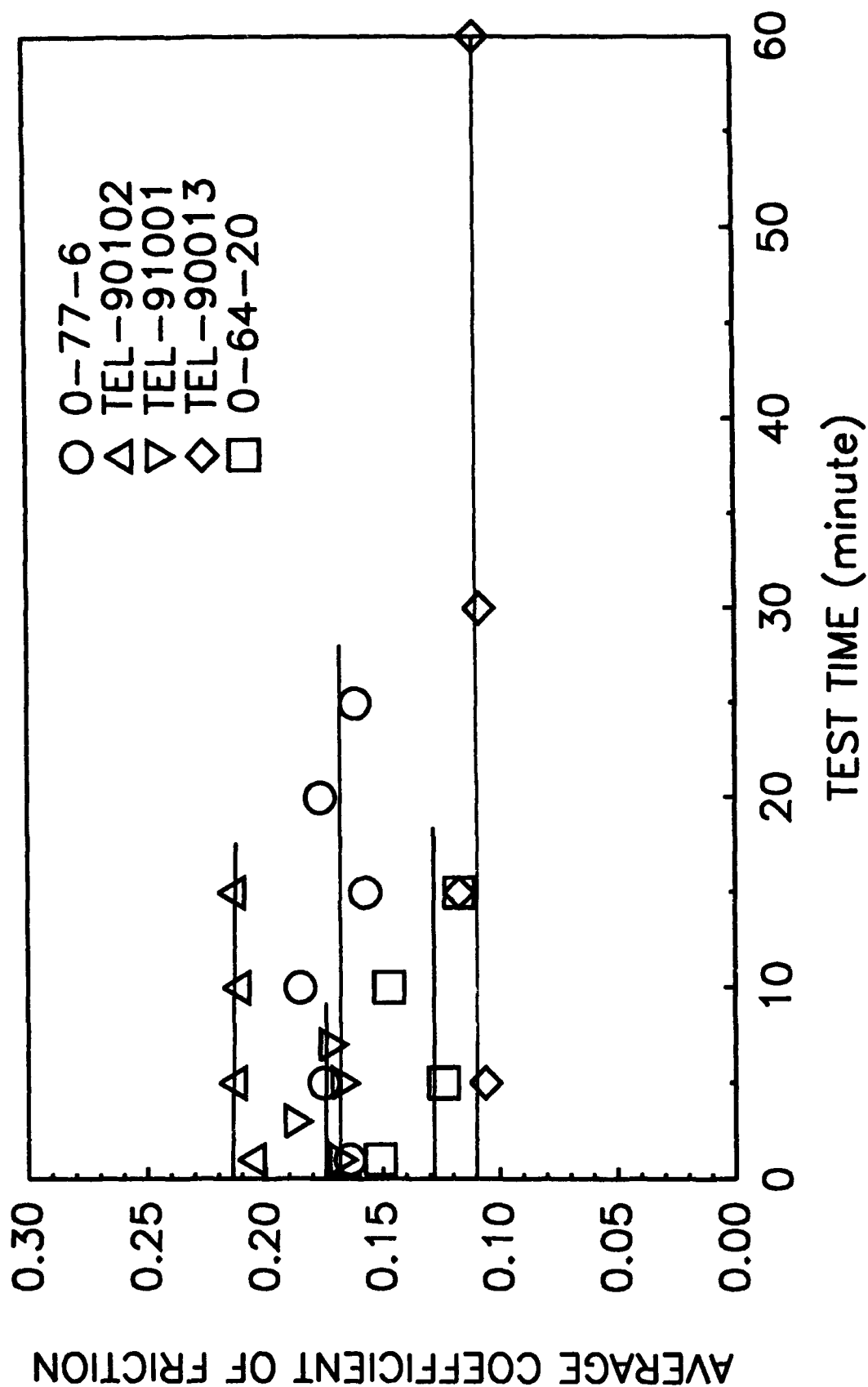


Figure 133. Coefficient of Friction for the Five Test Fluids. Rotating Speed: 200 rpm; Load: 22.68 kg; Lubricant Volume: 20 mm<sup>3</sup>; Temperature: 250°C.

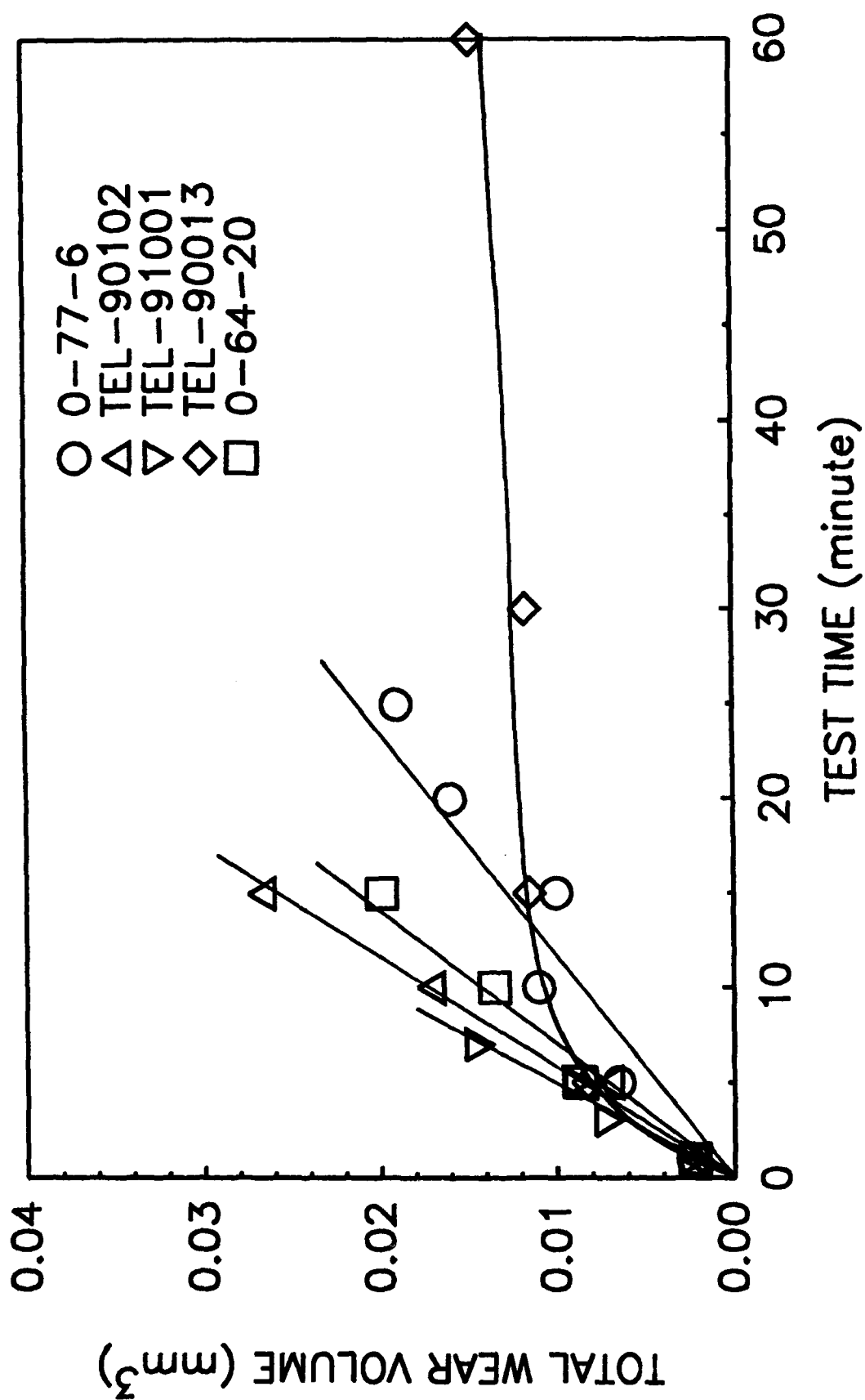


Figure 134. Total Wear Volume of M50 Specimens. Rotating Speed: 200 rpm; Load: 22.68 kg; Lubricant Volume: 20 mm<sup>3</sup>; Temperature: 250°C.

For the sake of confirmation, a graph of wear scar diameter against test time is also included (see Figure 135). The formula used for scar diameter calculation is:  $\text{scar diameter} = (\text{scar length} \times \text{scar width})^{1/2}$  which is based on the area equivalency of an elliptic shape with a perfect circle. The same pattern of the TEL-90013 wear curve shown in Figure 134 also appears in this plot. A comparison of Figure 134 and Figure 135 reveals the advantages of using total wear volume instead of scar diameter as the standard wear measurement. The wear rate of O-64-20 is slightly higher than that of O-77-6, which is consistent with previous studies conducted by other researchers.<sup>69</sup> For the four lubricants with linear relationship presented in Figure 134, the wear rates decreased in the order of TEL-91001 > TEL-90102 > O-64-20 > O-77-6. Notably, the wear rates of inhibited polyphenyl ethers are higher than that of the polyphenyl ether basestock.

#### (c) Lubricant Thickening Due To Wear Debris

In a previous publication,<sup>14</sup> a mechanistic model was proposed for the seizure phenomenon in the microsample test. It was believed that a liquid lubricant sample could turn into a semisolid or grease-like material as a result of its thermal-oxidative degradation. The lubricant reaction products, the high molecular weight polymer species, could act like a grease thickener to trap the fresh lubricant from recirculating into the contact junctions. Figure 134, however, shows that the longest attainable TBOD duration for each lubricant (or, the time-to-seizure) is strongly influenced by its corresponding specimen wear rate. A good comparison can be made from the three polyphenyl ether fluids since their rheological properties are nearly identical. Among the three, TEL-91001 produces a very high wear rate and, thus, a brief period of time-to-seizure (of only 7 minutes). On the other hand, the wear rate of the O-77-6 lubricated specimen is quite low; also, a relatively prolonged period of time-to-seizure (25 minutes) is obtained. Both the wear rate and the time-to-seizure from the TEL-90102 case are intermediate. It looks like that the build-up of wear particles does have some influence on lubricant thickening.

#### (d) Lubricant Tribochemistry

As seen previously, the extent of lubricant degradation and its related tribochemistry in the TBOD test can be determined through the use of the gel permeation chromatography (GPC) technique. GPC chromatograms of the TBOD stressed lubricant samples are exhibited in Figure 136, together with their original fresh standards. To achieve the best resolution for the minimal yield of wear products, GPC chromatogram for the longest TBOD duration for each test fluid is used in this figure.

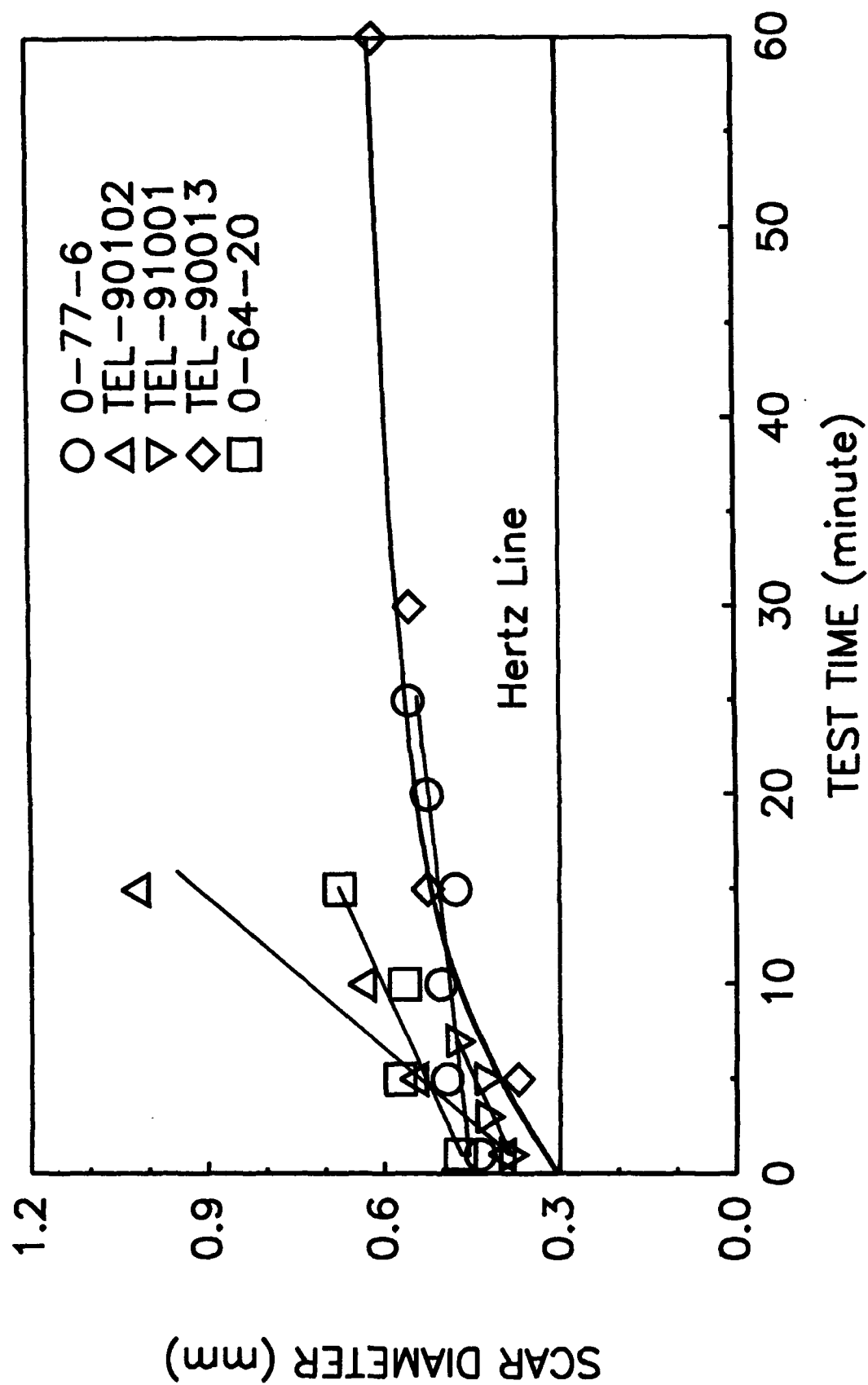


Figure 135. Wear Scar Diameter of M50 Balls. Rotating Speed: 200 rpm; Load: 22.68 kg; Lubricant Volume: 20 mm<sup>3</sup>; Temperature: 250°C.

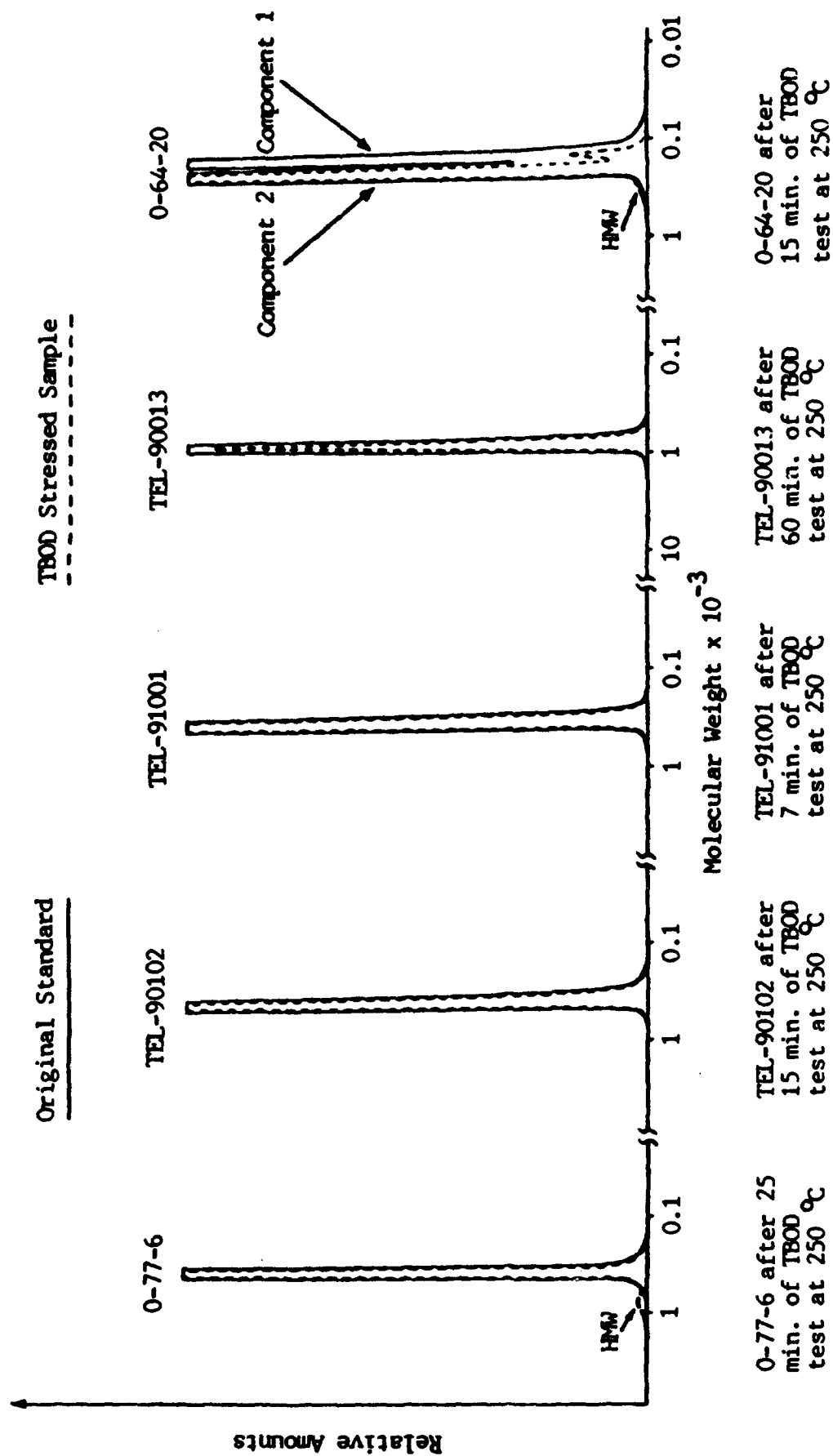


Figure 136. GPC Chromatograms of the Five Test Fluids, Showing Build-up of the THF Soluble HMW Wear Products.

A small amount of THF soluble high molecular weight (HMW) reaction products has been produced from the polyphenyl ether basestock (O-77-6) after stressing for 25 minutes in the TBOD apparatus. However, none of these HMW polymeric materials were observed in the TEL-90102 and TEL-91001 chromatograms. Obviously, the reaction products from the two inhibited polyphenyl ether fluids are, largely, THF insolubles of extremely high molecular weights. These deposits were filtered out (which can be seen on the filter paper) before the GPC analysis; hence, they could not be detected in the GPC chromatograms. It is highly possible that the THF insoluble wear deposits are being generated from the "dynamic" rubbing junctions under extreme reaction conditions. The relatively low molecular weight products (the THF soluble HMW materials), on the other hand, could be the result of "static" chemical conversion taking place in the vicinity around the actual sliding contacts.

Since friction coefficients observed from the O-77-6 TBOD tests are almost the same as those in the TEL-91001 tests, temperatures inside and outside the sliding junctions of the two cases should be very close. For TEL-91001, due to its highly stable nature, reaction is unlikely to proceed under the "static" condition outside the tribo-contacts generating no THF soluble HMW products. Within the tribo-contacts, the extreme junction environment could rapidly convert the fresh lubricant to THF insoluble deposits; if this is true for TEL-91001 (the inhibited polyphenyl ether), it should also be true for the less stable O-77-6 (the polyphenyl ether basestock). The only difference here is O-77-6 also reacts under the "static" condition because of its reduced stability. It is clear that the reaction condition outside the contact junction is adequate to trigger the O-77-6 reaction, but not yet severe enough to cause changes in TEL-91001. Relative to TEL-91001, TEL-90102 is oxidatively less stable according to our previous results from a bulk oxidation test.<sup>31</sup> Even with a higher frictional level, and a doubled TBOD test period of TEL-91001, THF soluble HMW materials were still not observed in the GPC analysis of TEL-90102.

The above discussion of the polyphenyl ether results suggests that although the Penn State kinetic model, described in the introduction, can be exercised successfully in dealing with the "static" reactions outside the sliding junctions, its form may be reduced to simply,  $A \rightarrow D$ , when applied to the much severe "dynamic" situation inside the tribo-contacts.

Arguments used for the inhibited polyphenyl ether fluids are also appropriate for TEL-90013, in which THF soluble HMW materials were not found. Different from other lubricants, the GPC chromatogram of O-64-20 contains a lower molecular weight peak (component 1) and a higher molecular weight peak (component 2). Traces of THF soluble

HMW products can be seen from its GPC chromatogram. Furthermore, preferential consumption of the lower fraction (component 1) of O-64-20 is evident.

(e) Lubricant Consumption

The scale of lubricant consumption is shown as a function of the TBOD duration in Figure 137. As suggested by the data in this figure, other than O-64-20, the amount of lubricant consumed is linearly proportional to the time of TBOD test, or a constant rate of consumption is obtained. For the three polyphenyl ether fluids (O-77-6, TEL-90102, and TEL-91001), their experimental data largely overlapped. In other words, within the experimental data scatter, their consumption rates could be considered approximately equal. Because the volatility characteristics of these polyphenyl ether fluids are very much alike, their evaporation rates during the TBOD test should be similar. Also, "static" reaction of the polyphenyl ether fluids is strongly limited in the TBOD test. So that, the consumption rates of these three polyphenyl ethers inside the "dynamic" junctions are about the same, which indicates that the effectiveness of the antioxidant additive is somewhat diminished under the extreme condition of the "dynamic" tribo-contacts. This agrees with recent findings made by Klaus et al.,<sup>70</sup> that antioxidant additives can be rendered ineffective if intensity of the reaction condition surpassed certain maximum limit.

Compared with the polyphenyl ether fluids, TEL-90013 has a smaller consumption rate, which may have something to do with its high molecular weight (see Figure 136). In contrast, the consumption rate of O-64-20 is much higher than those of polyphenyl ether fluids, and its molecular weight is the lowest relative to the other lubricants. As expected, the rate of lubricant consumption is approximately in an inverse proportion to the molecular weight of the test fluid.<sup>71</sup>

Unlike the others, the O-64-20 rate of consumption decreases with time. It should be noted that significant quantity of O-64-20 evaporates during the "static" heating and cooling periods of the test, in addition to its normal depletion which is a direct result of the actual TBOD test. The "static" loss of O-64-20 is represented by the data point allocated at zero test time in Figure 137. A breakdown of the total consumption rate of O-64-20 into two major components has been made in Figure 138. It is obvious that the lower molecular weight fraction (component 1) in O-64-20 is mainly responsible for the large evaporation loss. Interestingly, a constant rate of consumption is observed for the higher molecular weight fraction (component 2), a rate that is very much compatible with those found from the polyphenyl ether fluids in Figure 137.

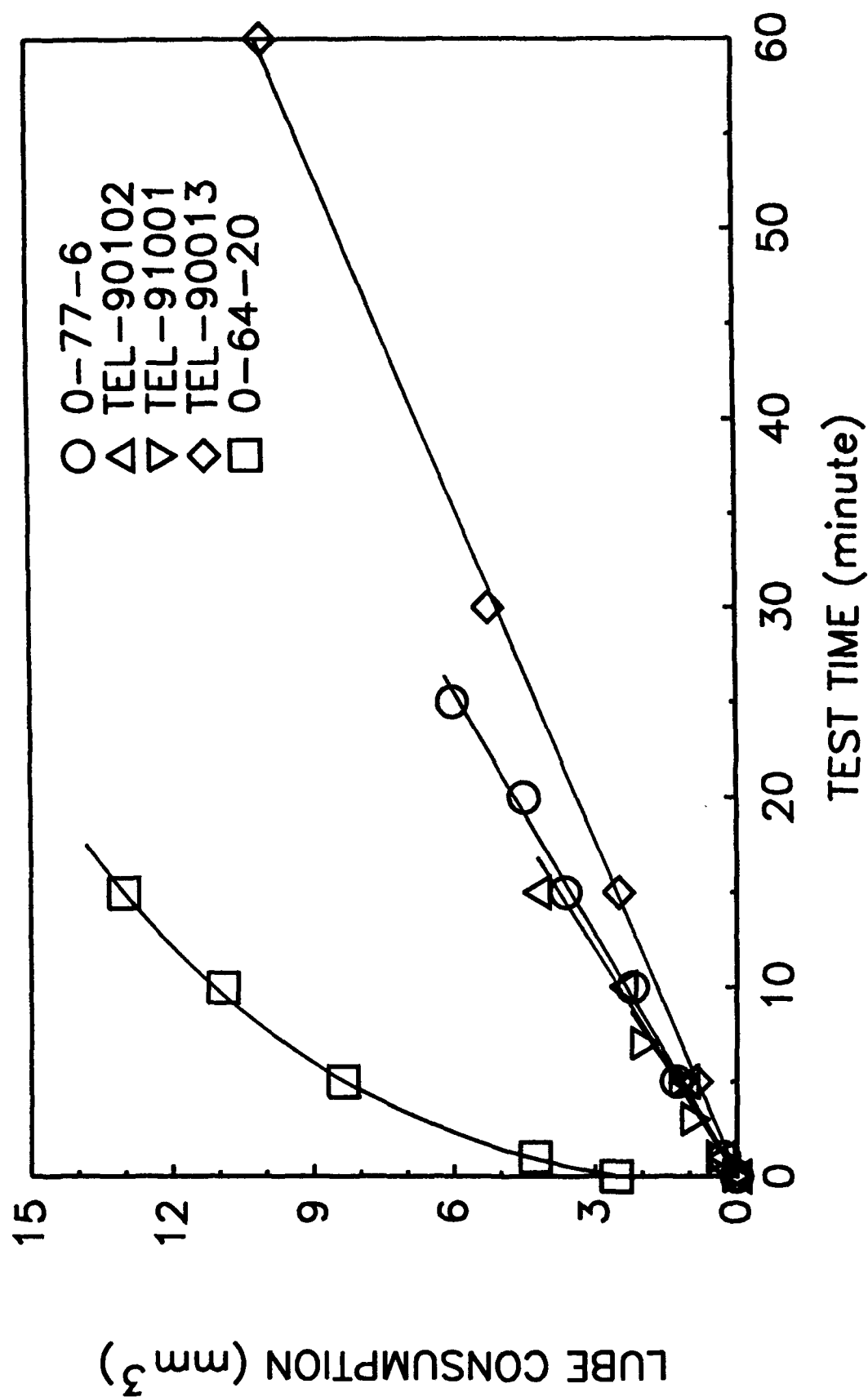


Figure 137. Lubricant Consumption of the Five Test Fluids. Rotating Speed: 200 rpm; Load: 22.68 kg; Lubricant Volume: 20 mm<sup>3</sup>; Temperature: 250°C.

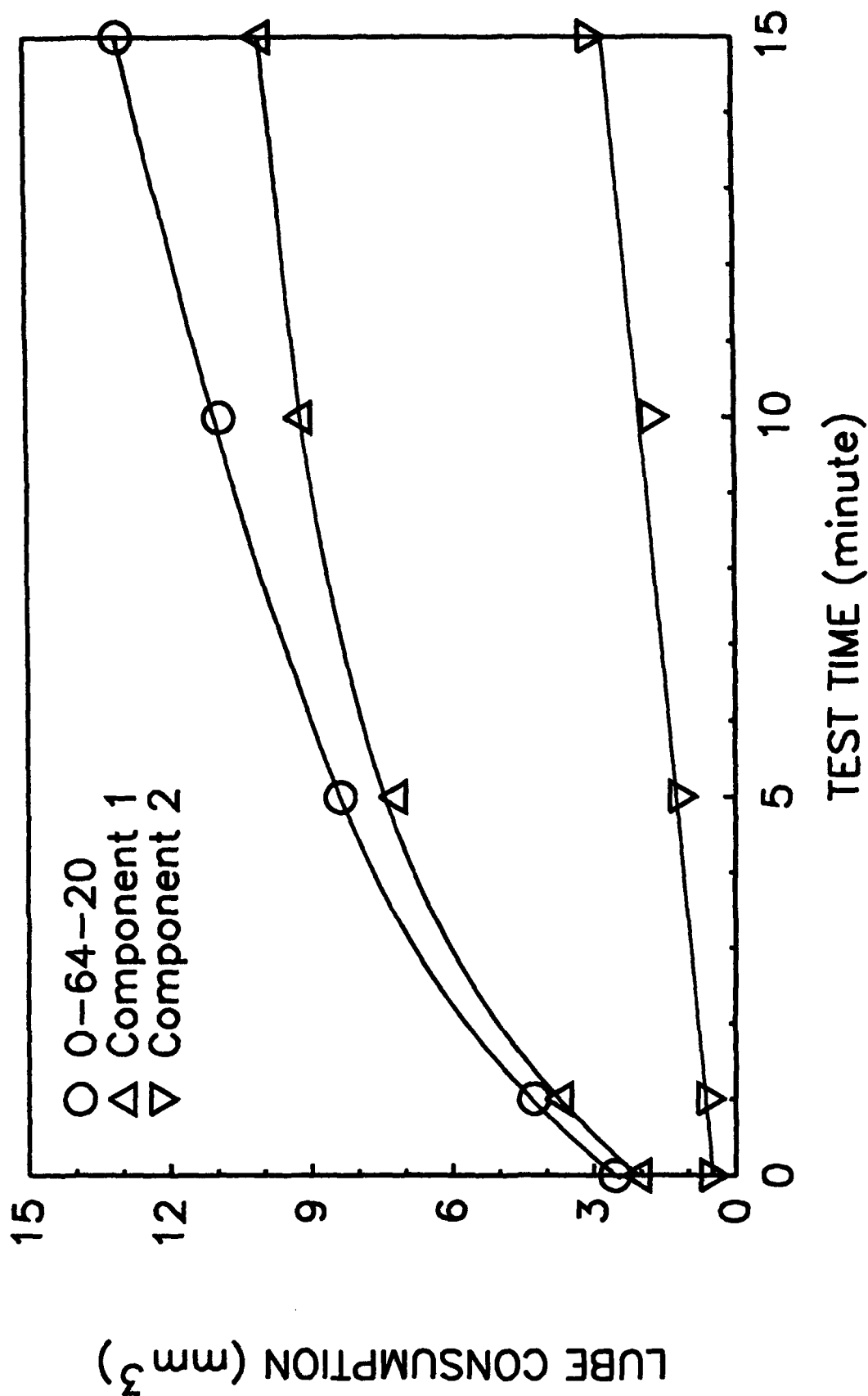


Figure 138. A Breakdown of the Total Consumption of O-64-20 into Two Major Components. Rotating Speed: 200 rpm; Load: 22.68 kg; Lubricant Volume: 20 mm<sup>3</sup>; Temperature: 250°C.

The magnitudes of lubricant consumption rates for the five fluids discussed here can be arrayed as: O-64-20 > TEL-91001  $\approx$  TEL-90102  $\approx$  O-77-6 > TEL-90013.

d. Summary

A three-ball-on-disk (TBOD) "dynamic" wear test has been developed to evaluate high temperature liquid lubricants. The TBOD bench test method is capable of generating an integrated set of tribo-information including friction, wear, lubricant consumption, tribochemistry, and so on. Since all of these tribo-measurements originate from a single test condition, they are intrinsically related to each other. As a result this technique could be very helpful in understanding the complex nature of friction and wear processes occurring in liquid lubricated systems. Well-defined wear scars of circular and elliptical shapes are exclusively produced in this TBOD test, which is crucial for precise wear volume calculation. Besides the "dynamic" TBOD test used in this research, "static" bulk and thin-film oxidation tests could also be performed using the same apparatus.

(1) O-77-6

The THF soluble HMW materials discovered in the 30°C TBOD test of O-77-6 are different from those of the 250°C TBOD test. The consumption rate of O-77-6 rises rapidly with the test temperature. The average rate at each test temperature was calculated and is presented as follows:  $3.8 \times 10^{-3} \text{ mm}^3/\text{min}$  at 30°C,  $7.8 \times 10^{-2} \text{ mm}^3/\text{min}$  at 150°C, and  $2.4 \times 10^{-1} \text{ mm}^3/\text{min}$  at 250°C. Friction and wear of the 250°C test are lower than those obtained from the 150°C test. At 250°C, possible formation of chemical film within the sliding junction, and changes in physical properties of the M50 steel as well as the 5P4E basestock (i.e., diminished glassy formation at higher temperature) may be considered for the explanation of this reversed temperature effect. Furthermore, the high friction and wear, coupled with relatively large degree of data scattering witnessed at 150°C of the TBOD test may suggest the occurrence of possible scuffing during the test. Both friction and wear values decrease in the order of the following temperatures: 150 > 250 > 30°C.

(2) O-77-6, O-77-10, and O-90-10

For ester fluids, their TBOD experiments were carried out at 150°C. Friction, wear, and lubricant consumption properties of these ester lubricants are very similar to each other; indeed, under present TBOD test condition it is hard to see any clear difference between the two ester fluids in terms of those properties. Comparing with ester fluids, the 5P4E polyphenyl ether basestock (O-77-6) demonstrates much higher coefficient of friction and wear

volume. However, the consumption rate of O-77-6 is only slightly above those from the ester fluids.

(3) O-77-6, TEL-90102, TEL-91001, TEL-90013, and O-64-20

These five lubricants have been evaluated at 250°C of the TBOD test. Among them, TEL-90013 gave the best overall performance: the smallest consumption rate, the lowest coefficient of friction, a good wear characteristic, and the longest attainable TBOD duration. These excellent properties of TEL-90013 can be related to its sizable molecular weight, and to some functional elements involved in its chemical makeup, such as phosphorus, oxygen, nitrogen, aryl and other cyclic groups.<sup>44</sup> Interesting observations were made for the O-64-20 fluid, where the extent of preferential depletion of its lower molecular weight fraction (component 1) is quantified.

Experimental data of the polyphenyl ether fluids (O-77-6, TEL-90102, and TEL-91001) have offered a number of significant insights into the lubricated contacts. It is very likely that the THF insoluble wear deposits are, largely, being formed inside the "dynamic" sliding junctions. The relatively low molecular weight products (the THF soluble HMW materials), on the other hand, could be the consequence of "static" chemical reactions taking place in the hot periphery of the real tribo-contacts. Another important observation is that the lubricant consumption rates of these polyphenyl ether fluids are almost the same. Based on their similar volatilities and very limited "static" reactions, the "dynamic" consumption rates of these polyphenyl ethers from the rubbing junctions should also be very close. This infers that the antioxidant additive is ineffective when exposed to the harsh environment inside the "dynamic" contact.

The friction magnitudes of the five test fluids can be placed in a descending order of TEL-90102 > TEL-91001 > O-77-6 > O-64-20 > TEL-90013. For the four lubricants with linear functionality shown in Figure 134, the order of their wear rates is TEL-91001 > TEL-90102 > O-64-20 > O-77-6. Finally, the lubricant consumption rates of the five fluids can be arranged in the following sequence: O-64-20 > TEL-91001 ≈ TEL-90102 ≈ O-77-6 > TEL-90013.

f. Advantages

(1) Only a very small quantity of lubricant is needed for each TBOD test. This minimal volume of test fluid could not only lower the cost but also allow running many tests on the same lubricant from a single batch, thus, avoiding possible complication due to

material property variations from different batches. Another advantage of this test in requiring a small quantity of lubricant is that it will accommodate newly developed lubricant in short supply.

(2) Both balls and disk specimens are reusable. The worn disk surface can easily be refinished for further experiments. Because of the simple geometries of the test specimens (ball and disk), they are readily accessible commercially and at a relatively low cost for both metal and ceramic materials.

(3) Because this test can accommodate small amounts of lubricant down to 20 mm<sup>3</sup>, a short test duration is sufficient to achieve measurable lubricant degradation.

(4) With the tested balls undisturbed in the holder, the ball holder can be easily placed under a conventional microscope. Accurate measurements of the ball wear scars can be made without a special optical adapter which is required for the four-ball test. This is particularly useful for some sequential test procedures where the same pair of mated wear surfaces is used repeatedly for each additional step of the test.

### 3. THREE-BALL ROLLING FATIGUE (TBRF) TEST

#### a. Introduction

The advent of highly clean and nearly flawless steels in recent years signifies a turning point for fatigue mechanisms of rolling bearings. That is, the inclusion induced sub-surface fatigue has been replaced by the surface or near-surface failure mechanisms initiated largely by foreign particulates to form three-body contacts.<sup>72,73</sup> Lubricant-borne solid particles, when being overrolled inside a contact junction, can produce local stress concentrates, thus, create surface defects which, in turn, become precursors for the eventual fatigue failure. These liquid-suspended solid debris could originate from several different sources: wear chips generated by operating machine parts, contaminants from the immediate working environment, or carried over through production processes. Consequently, they represent variety of materials with diverse particle sizes and shapes.<sup>74</sup>

All known lubricant-borne particulates may be sorted into three general groups: (1) ductile particles (i.e., various metal wear debris), (2) brittle particles (i.e., sand, glass, and coal dust), and (3) tough particles (i.e., diamond, and ceramic materials such as alumina, silicon nitride, silicon carbide).<sup>74</sup> Mechanisms of surface damages caused by those solid particles, unfortunately, are not all clear. There still exist many unanswered questions. For instance, it has been observed experimentally that relatively soft debris is capable to indent much harder raceway

surfaces, and sharp indentations yielded from friable debris do not always lead to the same proportion of fatigue life reduction.<sup>72,75-77</sup>

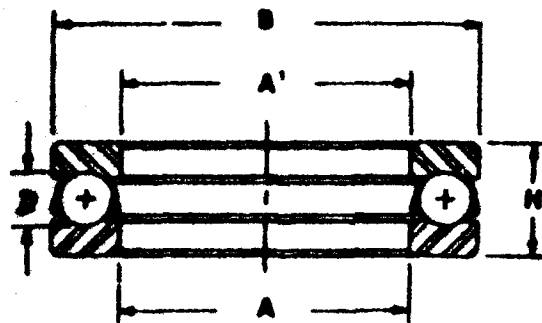
There is a growing need to address these issues, and current research activities in rolling fatigue failure are geared toward this general direction.

b. Experimental Development

A thrust rolling test rig has been adapted to the Falex machine in a fashion similar to the sliding three-ball-on-disk (TBOD) introduced earlier. Test specimens used in this rolling apparatus were manufactured by INA Bearing Company, Inc. Geometry and size of the actual balls and races are shown in Figure 139. It was our intention to choose small ball bearings so that the overall surface area exposed to the rolling action is at its minimal. Also, the total number of balls in the purchased bearing was reduced from its original 12 to a minimum of 3, which provides the highest possible Hertzian contact pressure within the rolling junctions. Owing to all these considerations, the resulted three-ball rolling fatigue (TBRF) contacts could be effectively stressed within a relatively short period of time.

Both ball and racetrack are made of 52100 steel with a hardness anywhere between Rc 60 and Rc 64. The ball retainer is fabricated from 1008 carburized steel (a type of low carbon steel). Five weight percent of solid powders is suspended in a 3 cSt ester basestock (O-77-10) to form a nonhomogeneous solution. Test results of this solution are then compared with those obtained from the pure O-77-10 to determine the impact of solid particulates on the fatigue failure of 52100 rolling surfaces. Powders made from  $\text{Si}_3\text{N}_4$ , Fe, Ti and Al, with three different sets of particle size distribution (less than 10, 10-20, and 20-30 microns), are used in this study.

After a number of trials, the following experimental condition has been established. A vertical load of 317.5 kg (or 700 lbs., the limiting capacity of the Falex machine) is applied in the TBRF test, which gives approximately 720 ksi initial Hertzian pressure in the three rolling contacts. Rotating speed of the top spindle is 500 rpm, and the temperature of the test chamber is maintained at 30°C. About 2 cm<sup>3</sup> of the test solution is used in each experiment. This combination of speed, temperature, and sample volume is adequate to prevent test fluid from being thrown out of its container by the centrifugal force generated during the test. As noted in the TBRF experiment, possible basestock degradation and the rising 52100 wear debris in the lubricant sample could influence the final test results. In order to minimize these unwanted complications the longest running time of the TBRF test is restricted for 300 minutes.



$A = 12.78 \text{ (mm)}$   
 $A' = 13.4874 \text{ (mm)}$   
 $B = 30.96 \text{ (mm)}$   
 $D = 4.7752 \text{ (mm)}$   
 $H = 14.30 \text{ (mm)}$

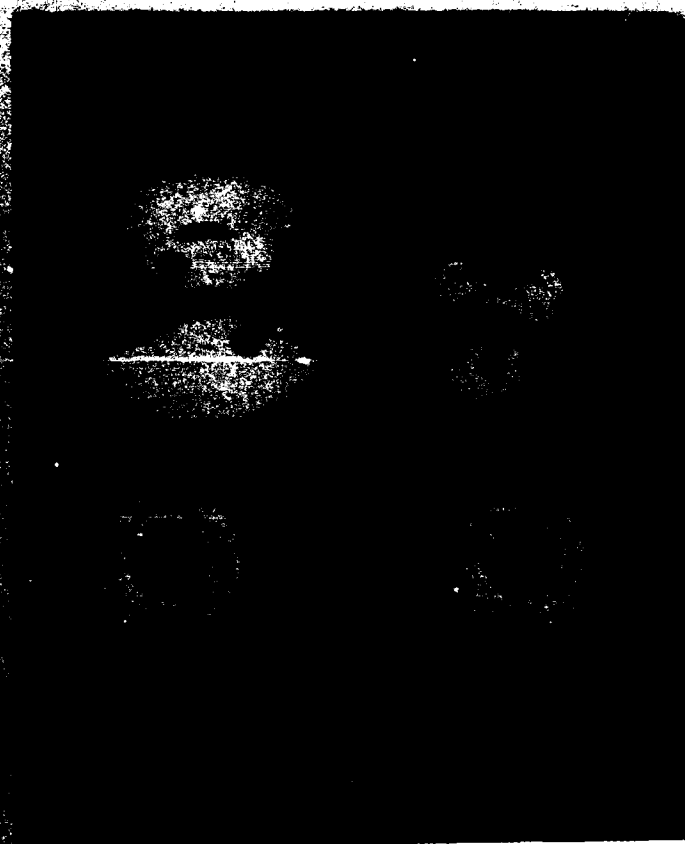


Figure 139. A Schematic Diagram of the Rolling Bearing Used in the TBRF Test, Together with a Still Photo of the Actual Bearing Components and Their Holders.

Prior to each TBRF test, specimens and the top and bottom holders are washed by toluene and hexane in sequence. The cleansed parts are then air-dried. After applying the lubricant sample the test rig is assembled. TBRF experiment was conducted under ambient atmosphere with no forced air flow introduced into the test chamber. Condition of the test is monitored by a frictional torque sensor, a strain gauge. The test is terminated whenever a sudden increase of torque is registered. This sudden increase of frictional torque indicates spallation and/or other forms of fatigue failure of the rolling surfaces. Duration of the TBRF test is recorded and used as a symbolic measure of the fatigue life of the rolling components.

### c. Results and Discussion

When pure O-77-10 ester basestock (without the presence of solid powders) was used in the TBRF test, no spallation or any other forms of fatigue damage was observed on the bearing surfaces after a 300-minute test period. Limited experimental data of the four blends of nonhomogeneous solutions are summarized in Table 91. The bar signs in the table reflect that these data points are not available due to insufficient quantity of powders for the TBRF test. It should be emphasized that because of low thermal stress (30°C) and short test duration (300 minutes or less), the extent of basestock degradation was very small. In other words, chemical and rheological characteristics of the liquid medium remained approximately same throughout the test. The relatively large concentration of solid powder (5 % by weight) present in the ester fluid was intended to overshadow possible influence of the tribo-induced 52100 wear debris on the fatigue life of the rolling elements.

According to the metal handbook and other accessible references, both Young's Modulus and Yield Strength of these powder materials supposedly decrease in the following order:  $\text{Si}_3\text{N}_4 > \text{Fe} > \text{Ti} > \text{Al}$ . The test results demonstrated that fatigue life of 52100 specimens increases with the particle size of the suspended powders ( $\text{Si}_3\text{N}_4$  and Al). As a note, in all cases spallation and other surface damages occurred only on racetracks, but were not found on the surfaces of three tested balls. The long lasting fatigue lives from the TBRF tests of Fe and Ti powders are difficult to understand. The high specific gravities of these two materials (Fe: 7.87, Ti: 4.54, in comparison with  $\text{Si}_3\text{N}_4$ : 3.28, and Al: 2.70) may indicate less suspension tendency of their particles in the extremely thin 3 cSt. ester fluid. Hence, the effective particle concentration in the test solution could drop continuously as the test proceeds. In fact, sizable portion of the Fe or Ti particles had been recovered from the gap between the bottom racetrack and its holder when the TBRF test was completed. By merely comparing the data of  $\text{Si}_3\text{N}_4$  with those of Al, we can see that fatigue life decreases with increase in hardness and toughness of the solid powders.

TABLE 91

## A SUMMARY OF THE TBRF TEST RESULTS

III II	I	Si <sub>3</sub> N <sub>4</sub>	Fe	Ti	Al
	< 10	101	--	--	--
	10 - 20	136	> 300	> 300	150
	20 - 30	170	--	--	> 300

I: Material of the Suspended Particles  
 II: Particle Size (micron)  
 III: Fatigue Life (minute)

d. Summary

A three-ball rolling fatigue (TBRF) test has been developed. This TBRF method is used to investigate the effect of lubricant-borne solid particulates on the fatigue life of rolling elements. Solid powders made from four materials ( $\text{Si}_3\text{N}_4$ , Fe, Ti, and Al) were studied in a 3 cSt. ester basestock (O-77-10).

e. Conclusions

From the test results of  $\text{Si}_3\text{N}_4$  and Al powders, it appears that fatigue life of 52100 race surface increases with particle size. This may be interpreted like that the bigger the particles, the less the chance they can enter the rolling contacts. Moreover, as expected the hard  $\text{Si}_3\text{N}_4$  powder caused more surface damage on the raceways than does the much softer aluminum ones.

## **APPENDIX A**

### **LUBRICANT PERFORMANCE TEST DATA**

Appendix A contains lubricant test data obtained during the development of improved methods for measuring lubricant performance and presented in Section II of this report. Tables A-1 through A-5 list Squires oxidative test data for the 4 cSt ester fluids, corrosion and oxidation data for the high temperature lubricant candidate fluids, static and MCRT coking data and foaming data. Squires oxidative stability data curves for the 4 cSt ester fluids along with their Arrhenius plots are presented in Figures A-1 through A-25.

TABLE A-1  
SQUIRES OXIDATIVE TEST DATA

LUBRICANT AND TEST TEMP.	LUBRICANT PROPERTY	TEST HOURS						
		New oil	24	48	75	96	120	168
TEL-9076  210°C	Weight Loss, %		8.1	14.4	20.8	24.0	26.8	40.4
	COBRA Reading	2	133	185	188	196	>200	194
	Total Acid No.	0.26	0.60	0.74	1.08	1.21	1.43	2.28
	Viscosity @40°C, cst	17.76	ND	ND	ND	ND	ND	ND
	40°C Visc Change, %		ND	ND	ND	ND	ND	ND
	Viscosity @100°C, cs	4.04	4.40	4.55	4.71	4.84	4.92	5.44
	100°C Visc Change, %		8.9	12.6	16.6	19.8	21.8	34.7
	Toluene Insol, % wt	ND	ND	ND	ND	ND	ND	ND
	Visual Appearance of Deposits		No deposits					
LUBRICANT AND TEST TEMP.	LUBRICANT PROPERTY	TEST HOURS						
		New oil	168	192	241			
TEL-9076 b (a) 210°C	Weight Loss, %		41.2	48.6	67.8			
	COBRA Reading	2	ND	ND	ND			
	Total Acid No.	0.26	2.52	2.66	13.47			
	Viscosity @40°C, cst	17.76	ND	ND	ND			
	40°C Visc Change, %		ND	ND	ND			
	Viscosity @100°C, cs	4.04	5.69	6.11	ND			
	100°C Visc Change, %		40.8	51.2	ND			
	Toluene Insol, % wt	ND	ND	ND	ND			
	Visual Appearance of Deposits							
LUBRICANT AND TEST TEMP.	LUBRICANT PROPERTY	TEST HOURS						
		New oil	72	120				
TEL-9076  215°C	Weight Loss, %		27.7	41.8				
	COBRA Reading		182	183				
	Total Acid No.	0.26	1.25	2.19				
	Viscosity @40°C, cst	17.76	ND	ND				
	40°C Visc Change, %		ND	ND				
	Viscosity @100°C, cs	4.04	4.95	5.77				
	100°C Visc Change, %		22.5	42.8				
	Toluene Insol, % wt	ND	ND	ND				
	Visual Appearance of Deposits		None	SLT.VARN.				

(a) - continuation of TEL-9076 210°C

LUBRICANT AND TEST TEMP.	LUBRICANT PROPERTY	TEST HOURS						
		New oil	24	48	92			
TEL-9076  220°C	Weight Loss, %		11.7	20.9	59.8			
	COBRA Reading	ND	188	190	174			
	Total Acid No.	0.26	1.11	1.83	2.50			
	Viscosity @40°C, cst	17.76	ND	ND	ND			
	40°C Visc Change, %		ND	ND	ND			
	Viscosity @100°C, cs	4.04	4.50	4.77	5.71			
	100°C Visc Change, %		11.3	18.1	41.3			
	Toluene Insol, % wt	ND	ND	ND	ND			
	Visual Appearance of Deposits		None	NONE	SLIGHT			

**SQUIRES OXIDATIVE TEST DATA**

LUBRICANT AND TEST TEMP.	LUBRICANT PROPERTY	TEST HOURS						
		Rev Oil	24	48	72	96	124	144
O-91-13  205°C	Weight Loss, g		7.4	13.3	19.5	25.1	31.5	33.3
	COMRA Reading	ND	ND	ND	ND	ND	ND	ND
	Total Acid No.	0.29	0.24	0.53	0.72	1.74	2.24	2.04
	Viscosity @40 C, cst	18.51	21.59	23.24	24.57	27.12	30.17	32.57
	40 C Visc Change, %		16.6	25.6	32.7	46.5	63.8	76.0
	Viscosity @100 C, cs	4.14	4.60	4.82	4.99	5.33	5.69	5.67
	100 C Visc Change, %		11.1	16.4	20.5	28.7	37.4	37.0
	Toluene Insol, g wt	ND	ND	ND	ND	ND	ND	ND
	Visual Appearance of Deposits							
LUBRICANT AND TEST TEMP.	LUBRICANT PROPERTY	TEST HOURS						
		Rev Oil	216					
O-91-13 b (g) 205 C	Weight Loss, g		49.9					
	COMRA Reading	ND	ND					
	Total Acid No.	0.29	4.10					
	Viscosity @40 C, cst	18.51	65.53					
	40 C Visc Change, %		254.0					
	Viscosity @100 C, cs	4.14	9.60					
	100 C Visc Change, %		131.9					
	Toluene Insol, g wt	ND	ND					
	Visual Appearance of Deposits							

(a) - times continued from 144 hours

LUBRICANT AND TEST TEMP.	LUBRICANT PROPERTY	TEST HOURS						
		Rev Oil	24	48	60	72	96	120
O-91-13  210°C	Weight Loss, g		9.2	16.4	22.7	29.8	38.2	42.0
	COMRA Reading	ND	ND	ND	ND	ND	ND	ND
	Total Acid No.	0.29	0.66	1.09	1.34	6.22	5.03	ND
	Viscosity @40 C, cst	18.51	21.89	24.17	25.93	40.23	45.50	ND
	40 C Visc Change, %		18.3	30.6	40.1	117.3	145.8	ND
	Viscosity @100 C, cs	4.14	4.65	4.96	5.20	6.73	7.42	ND
	100 C Visc Change, %		12.3	19.8	25.6	62.6	79.2	ND
	Toluene Insol, g wt	ND	ND	ND	ND	ND	ND	ND
	Visual Appearance of Deposits							
LUBRICANT AND TEST TEMP.	LUBRICANT PROPERTY	TEST HOURS						
		Rev Oil	144					
O-91-13 b (g) 210 C	Weight Loss, g		50.7					
	COMRA Reading	ND	ND					
	Total Acid No.	0.29	ND					
	Viscosity @40 C, cst	18.51	ND					
	40 C Visc Change, %		ND					
	Viscosity @100 C, cs	4.14	ND					
	100 C Visc Change, %		ND					
	Toluene Insol, g wt	ND	ND					
	Visual Appearance of Deposits							

(a) - Test times continued from 120 hours

LUBRICANT AND TEST TEMP.	LUBRICANT PROPERTY	TEST HOURS						
		Rev Oil	24	48	72			
O-91-13  220°C	Weight Loss, g		13.2	33.1	47.4			
	COMRA Reading	ND	ND	ND	ND			
	Total Acid No.	0.29	1.15	5.21	ND			
	Viscosity @40 C, cst	18.51	23.59	49.79	ND			
	40 C Visc Change, %		27.4	169.0	ND			
	Viscosity @100 C, cs	4.14	4.86	7.79	ND			
	100 C Visc Change, %		17.4	88.2	ND			
	Toluene Insol, g wt	ND	ND	ND	ND			
	Visual Appearance of Deposits							

**SQUIRES OXIDATIVE TEST DATA**

LUBRICANT AND TEST TEMP.	LUBRICANT PROPERTY	TEST HOURS						
		New Oil	48	96	192	216	288	336
TEL-90087  197°C	Weight Loss, g		16.2	22.8	34.2	36.1	41.9	43.5
	COBRA Reading	1.67	200+	200+	200+	200+	200+	200+
	Total Acid No.	.80	.30	.66	.89	.73	ND	ND
	Viscosity @40 C, cst	17.48	21.49	23.88	28.59	29.51	32.79	35.92
	40 C Visc Change, %		22.9	36.6	63.6	68.8	87.6	105.5
	Viscosity @100 C, cs	4.02	4.615	5.008	5.561	5.718	6.136	6.54
	100 C Visc Change, %		14.8	24.6	38.3	42.2	52.6	62.7
	Toluene Insol, g wt	ND	ND	ND	ND	ND	ND	ND
	Visual Appearance of Deposits							
LUBRICANT AND TEST TEMP.	LUBRICANT PROPERTY	TEST HOURS						
		New Oil	28	52	79	104	128	148
TEL-90087 (g) 210°C	Weight Loss, g		NA	NA	30.5	36.5	42.7	45.6
	COBRA Reading	1.67	195	>200	>200	>200	>200	>200
	Total Acid No.	.80	.49	.63	1.10	1.27	1.46	1.62
	Viscosity @40 C, cst	17.48	21.85	24.27	27.76	25.28	34.72	39.60
	40 C Visc Change, %		25.0	38.8	58.8	ND	98.6	126.5
	Viscosity @100 C, cs	4.02	4.61	4.97	5.47	5.85	6.33	6.94
	100 C Visc Change, %		14.7	23.6	36.1	45.5	57.5	72.6
	Toluene Insol, g wt	ND	ND	ND	ND	ND	ND	ND
	Visual Appearance of Deposits							

(a) - Same as O-98-6 (lower temperatures of test)

LUBRICANT AND TEST TEMP.	LUBRICANT PROPERTY	TEST HOURS						
		New Oil	169	192				
TEL-90087b (g) 210°C	Weight Loss, g		ND	ND				
	COBRA Reading	ND	ND	ND				
	Total Acid No.	0.80	ND	ND				
	Viscosity @40 C, cst	17.48	45.48	55.48				
	40 C Visc Change, %		160.2	217.3				
	Viscosity @100 C, cs	4.02	ND	ND				
	100 C Visc Change, %		ND	ND				
	Toluene Insol, g wt	ND	ND	ND				
	Visual Appearance of Deposits							
LUBRICANT AND TEST TEMP.	LUBRICANT PROPERTY	TEST HOURS						
		New Oil	24	48	73	96	120	165
TEL-90087  225°C	Weight Loss, g		19.5	33.8	44.4	53.6	61.7	73.5
	COBRA Reading	1.67	24	197	>200	>200	>200	>200
	Total Acid No.	.80	.82	1.32	2.23	4.13	6.53	10.48
	Viscosity @40 C, cst	17.48	24.34	30.95	40.17	63.18	120.8	ND
	40 C Visc Change, %		39.2	77.1	129.8	261.4	591.8	ND
	Viscosity @100 C, cs	4.02	4.99	6.165	6.95	9.47	14.57	69.27
	100 C Visc Change, %		24.1	53.3	72.9	135.6	262.4	1623
	Toluene Insol, g wt	ND	ND	ND	ND	ND	ND	ND
	Visual Appearance of Deposits							

(a) - Continued from 149 hours

SQUIERS OXIDATIVE TEST DATA

LUBRICANT AND TEST TEMP.	LUBRICANT PROPERTY	TEST HOURS						
		New Oil	19	27	48	68	116	168
TEL-90103  210°C	Weight Loss, %		9.4	13.4	17.2		36.6	45.9
	COBRA Reading	6.5	93	121	158	>200	>200	>200
	Total Acid No.	0.34	0.06	0.18	0.27	0.51	1.25	ND
	Viscosity @40°C, cst	17.09	ND	ND	ND	ND	ND	ND
	40°C Visc Change, %		ND	ND	ND	ND	ND	ND
	Viscosity @100°C, cs	3.97	4.56	4.70	4.91	5.37	6.15	7.14
	100°C Visc Change, %		14.6	18.4	23.7	35.0	54.8	79.8
	Toluene Insol, % wt	ND	ND	ND	ND	ND	ND	ND
	Visual Appearance of Deposits		oil in blower tube					light varnish
LUBRICANT AND TEST TEMP.	LUBRICANT PROPERTY	TEST HOURS						
		New Oil	19	27	48	68	122	
TEL-90103  225°C	Weight Loss, %		19.1	26.6	35.9	ND	67.0	
	COBRA Reading	6.5	173	>200	>200	>200	>200	
	Total Acid No.	0.34	0.41	0.55	1.24	1.69	3.80	
	Viscosity @40°C, cst	17.09	ND	ND	ND	ND	ND	
	40°C Visc Change, %		ND	ND	ND	ND	ND	
	Viscosity @100°C, cs	3.97	4.99	5.36	5.99	6.99	ND	
	100°C Visc Change, %		25.7	35.0	50.9	76.1	ND	
	Toluene Insol, % wt	ND	ND	ND	ND	ND	ND	
	Visual Appearance of Deposits		oil in blower head	oil in blower head				
LUBRICANT AND TEST TEMP.	LUBRICANT PROPERTY	TEST HOURS						
		New Oil	7	24	49	56		
TEL-90103  235°C	Weight Loss, %		7.4	26.2	38.4	50.0		
	COBRA Reading	6.5	171	>200	>200	>200		
	Total Acid No.	0.34	0.33	1.08	3.04	4.22		
	Viscosity @40°C, cst	17.09	ND	ND	ND	ND		
	40°C Visc Change, %		ND	ND	ND	ND		
	Viscosity @100°C, cs	3.97	4.56	5.62	7.60	10.28		
	100°C Visc Change, %		14.9	41.4	91.4	158.9		
	Toluene Insol, % wt	ND	ND	ND	ND	ND		
	Visual Appearance of Deposits							

**SQUIRES OXIDATIVE TEST DATA**

LUBRICANT AND TEST TEMP.	LUBRICANT PROPERTY	TEST HOURS						
		New Oil	72	144	240	288	312	360
TEL-91002  205°C	Weight Loss, g		14.9	26.9	46.2	54.7	55.2	64.0
	COBRA Reading	ND	ND	ND	ND	ND	ND	ND
	Total Acid No.	0.02	0.36	0.67	1.06	1.96	2.02	2.09
	Viscosity @40 C, cst	17.73	19.20	20.73	26.48	30.88	32.72	ND
	40 C Visc Change, %		7.7	16.9	49.4	74.2	84.6	ND
	Viscosity @100 C, cs	3.99	4.19	4.41	5.14	5.67	5.88	6.59
	100 C Visc Change, %		5.0	10.5	28.8	42.1	47.4	65.2
	Toluene Insol, % wt	ND	ND	ND	ND	ND	ND	ND
Visual Appearance of Deposits								
LUBRICANT AND TEST TEMP.	LUBRICANT PROPERTY	TEST HOURS						
		New Oil	527					
TEL-91002B (g) 205°C	Weight Loss, g		89.2					
	COBRA Reading	ND	ND					
	Total Acid No.	0.02	4.09					
	Viscosity @40 C, cst	17.73	ND					
	40 C Visc Change, %		ND					
	Viscosity @100 C, cs	3.99	ND					
	100 C Visc Change, %		ND					
	Toluene Insol, % wt	ND	ND					
Visual Appearance of Deposits								

(a) - Test times continued from 360 hours

LUBRICANT AND TEST TEMP.	LUBRICANT PROPERTY	TEST HOURS						
		New Oil	48	96	168	216	263	
TEL-91002  215°C	Weight Loss, g		15.6	39.5	52.3	64.0	79.5	
	COBRA Reading	ND	ND	ND	ND	ND	ND	
	Total Acid No.	0.02	0.33	0.68	1.91	3.10	5.79	
	Viscosity @40 C, cst	17.73	19.30	22.30	28.00	39.91	ND	
	40 C Visc Change, %		8.9	25.8	57.9	125.1	ND	
	Viscosity @100 C, cs	3.99	4.21	4.60	5.33	6.67	ND	
	100 C Visc Change, %		5.5	15.3	33.6	67.2	ND	
	Toluene Insol, % wt	ND	ND	ND	ND	ND	ND	
Visual Appearance of Deposits								
LUBRICANT AND TEST TEMP.	LUBRICANT PROPERTY	TEST HOURS						
		New Oil	48	72	96	168		
TEL-91002  220°C	Weight Loss, g		20.7	41.8	48.2	78.9		
	COBRA Reading	ND	ND	ND	ND	ND		
	Total Acid No.	0.02	0.53	1.04	6.42	ND		
	Viscosity @40 C, cst	17.73	19.90	23.24	47.67	ND		
	40 C Visc Change, %		12.2	31.1	169	ND		
	Viscosity @100 C, cs	3.99	4.31	4.73	7.29	ND		
	100 C Visc Change, %		8.0	18.6	82.7	ND		
	Toluene Insol, % wt	ND	ND	ND	ND	ND		
Visual Appearance of Deposits								
LUBRICANT AND TEST TEMP.	LUBRICANT PROPERTY	TEST HOURS						
		New Oil	24	48	72	96		
TEL-91002  225°C	Weight Loss, g		13.2	34.1	48.0	67.2		
	COBRA Reading	ND	ND	ND	ND	ND		
	Total Acid No.	0.02	0.35	0.85	6.33	ND		
	Viscosity @40 C, cst	17.73	19.16	21.92	71.48	ND		
	40 C Visc Change, %		8.1	23.6	303	ND		
	Viscosity @100 C, cs	3.99	4.19	4.57	9.45	ND		
	100 C Visc Change, %		5.0	14.5	137	ND		
	Toluene Insol, % wt	ND	ND	ND	ND	ND		
Visual Appearance of Deposits								

**SQUIRES OXIDATIVE TEST DATA**

LUBRICANT AND TEST TEMP.	LUBRICANT PROPERTY	TEST HOURS						
		New Oil	24	48	72	96	152	333
TEL-91003  210°C	Weight Loss, %		5.1	10.6	14.3	21.6	31.1	63.7
	COBRA Reading	ND	ND	ND	ND	ND	ND	ND
	Total Acid No.	0.02	0.16	0.53	0.64	0.86	1.56	6.36
	Viscosity @40°C, cst	17.60	ND	ND	ND	ND	ND	ND
	40°C Visc Change, %		ND	ND	ND	ND	ND	ND
	Viscosity @100°C, cs	4.02	4.18	4.36	4.44	4.58	1.93	11.09
	100°C Visc Change, %		4.0	8.5	10.4	13.9	22.6	175.9
	Toluene Insol, % wt	ND	ND	ND	ND	ND	ND	ND
	Visual Appearance of Deposits							
LUBRICANT AND TEST TEMP.	LUBRICANT PROPERTY	TEST HOURS						
		New Oil	24	48	72	96	137	
TEL-91003  225°C	Weight Loss, %		10.9	21.8	28.3	35.6	50.1	
	COBRA Reading	2	36	53	69	93	128	
	Total Acid No.	0.02	0.44	0.82	1.45	2.12	4.39	
	Viscosity @40°C, cst	17.60	ND	ND	ND	ND	ND	
	40°C Visc Change, %		ND	ND	ND	ND	ND	
	Viscosity @100°C, cs	4.02	4.35	4.62	4.91	5.24	7.76	
	100°C Visc Change, %		8.2	14.9	22.1	30.5	93.1	
	Toluene Insol, % wt	ND	ND	ND	ND	ND	ND	
	Visual Appearance of Deposits							
LUBRICANT AND TEST TEMP.	LUBRICANT PROPERTY	TEST HOURS						
		New Oil	26	49	72	96		
TEL-91003  235°C	Weight Loss, %		19.3	32.6	48.2	68.0		
	COBRA Reading	2	62	95	123	NA		
	Total Acid No.	0.02	0.89	2.61	4.95	12.05		
	Viscosity @40°C, cst	17.60	ND	ND	ND	ND		
	40°C Visc Change, %		ND	ND	ND	ND		
	Viscosity @100°C, cs	4.02	4.65	5.51	8.01	ND		
	100°C Visc Change, %		15.7	37.1	99.3	ND		
	Toluene Insol, % wt	ND	ND	ND	ND	ND		
	Visual Appearance of Deposits							

**SQUIRES OXIDATIVE TEST DATA**

LUBRICANT AND TEST TEMP.	LUBRICANT PROPERTY	TEST HOURS						
		New Oil	49	102	144	192	266	339
TEL-91005  195°C	Weight Loss, %		14.2	23.9	28.0	36.0	42.9	47.6
	COBRA Reading	2	>200	ND	ND	ND	ND	ND
	Total Acid No.	0.00	0.34	0.43	0.57	0.95	1.19	1.38
	Viscosity @40 C, cst	17.76	22.33	25.40	26.95	29.67	34.79	38.12
	40°C Visc Change, %		25.7	43.0	51.7	67.1	99.9	200.5
	Viscosity @100 C, cs	4.04	4.73	5.15	5.36	5.68	6.35	6.77
	100°C Visc Change, %		17.1	27.5	32.7	40.6	57.2	67.6
	Toluene Insol, % wt	ND	ND	ND	ND	ND	ND	ND
	Visual Appearance of Deposits							
LUBRICANT AND TEST TEMP.	LUBRICANT PROPERTY	TEST HOURS						
		New Oil	409	460				
TEL-91005b (g) 195°C	Weight Loss, %		60.7	63.8				
	COBRA Reading	ND	ND	ND				
	Total Acid No.	0.00	1.47	2.45				
	Viscosity @40 C, cst	17.76	ND	ND				
	40°C Visc Change, %		ND	ND				
	Viscosity @100 C, cs	4.04	ND	ND				
	100°C Visc Change, %		ND	ND				
	Toluene Insol, % wt	ND	ND	ND				
	Visual Appearance of Deposits		deposits	were at	8.5 in.	from bot.	of tube.	

(a) - test times cont. from 339 hours

LUBRICANT AND TEST TEMP.	LUBRICANT PROPERTY	TEST HOURS						
		New Oil	26	72	96	168	192	200
TEL-91005  210°C	Weight Loss, %		17.3	30.7	41.7	55.7	57.1	61.0
	COBRA Reading	2	>200	ND	ND	ND	ND	ND
	Total Acid No.	0.00	0.35	0.93	1.14	2.43	3.08	ND
	Viscosity @40 C, cst	17.76	23.17	28.68	33.66	53.74	63.66	ND
	40°C Visc Change, %		30.5	61.5	89.5	202.6	260.3	ND
	Viscosity @100 C, cs	4.04	4.86	5.59	6.19	8.55	9.57	ND
	100°C Visc Change, %		20.3	38.3	53.2	111.6	136.9	ND
	Toluene Insol, % wt	ND	ND	ND	ND	ND	ND	ND
	Visual Appearance of Deposits							
LUBRICANT AND TEST TEMP.	LUBRICANT PROPERTY	TEST HOURS						
		New Oil	24	48	72	97		
TEL-91005  225°C	Weight Loss, %		23.7	38.1	46.5	56.2		
	COBRA Reading	2	>200	ND	ND	ND		
	Total Acid No.	0.00	0.89	1.72	2.38	3.35		
	Viscosity @40 C, cst	17.76	26.55	34.76	43.92	64.66		
	40°C Visc Change, %		49.5	95.7	147.3	264.1		
	Viscosity @100 C, cs	4.04	5.30	6.33	7.44	9.71		
	100°C Visc Change, %		31.2	56.7	84.2	140.4		
	Toluene Insol, % wt	ND	ND	ND	ND	ND		
	Visual Appearance of Deposits							

**SQUIRES OXIDATIVE TEST DATA**

LUBRICANT AND TEST TEMP.	LUBRICANT PROPERTY	TEST HOURS						
		New Oil	24	48	72	126	168	264
TEL-91053  200°C	Weight Loss, %		9.3	17.3	20.9	29.6	36.5	49.1
	COBRA Reading	ND	ND	ND	ND	ND	ND	ND
	Total Acid No.	0.55	-----	-----	-----	0.17	0.45	1.05
	Viscosity @40 C, cst	16.70	18.89	20.27	21.05	22.67	24.33	28.06
	40 C Visc change, %		13.1	21.4	26.1	35.8	45.7	68.0
	Viscosity @100 C, cs	3.99	4.34	4.55	4.66	4.92	5.21	5.71
	100 C Visc Change, %		8.8	14.0	16.8	23.3	30.6	43.1
	Toluene Insol, % wt	ND	ND	ND	ND	ND	ND	ND
Visual Appearance of Deposits								
LUBRICANT AND TEST TEMP.	LUBRICANT PROPERTY	TEST HOURS						
		New Oil	336	412	525			
TEL-91053b  (g) 200°C	Weight Loss, %		51.7	64.6	ND			
	COBRA Reading	ND	ND	ND	ND			
	Total Acid No.	0.55	1.26	1.87	4.22			
	Viscosity @40 C, cst	16.70	29.26	36.61	ND			
	40 C Visc change, %		75.2	119.2	ND			
	Viscosity @100 C, cs	3.99	5.87	6.83	ND			
	100 C Visc Change, %		42.9	71.1	ND			
	Toluene Insol, % wt	ND	ND	ND	ND			
Visual Appearance of Deposits								

(a) - test times cont.

LUBRICANT AND TEST TEMP.	LUBRICANT PROPERTY	TEST HOURS					
		New Oil	24	72	144	240	
TEL-91053  210°C	Weight Loss, %		14.0	29.6	44.2	63.2	
	COBRA Reading	ND	ND	ND	ND	ND	
	Total Acid No.	0.55	-----	0.41	1.41	3.28	
	Viscosity @40 C, cst	16.70	19.78	23.04	27.71	43.43	
	40 C Visc Change, %		18.4	38.0	65.9	160.1	
	Viscosity @100 C, cs	3.99	4.47	4.95	5.62	7.69	
	100 C Visc Change, %		12.0	24.1	40.9	92.7	
	Toluene Insol, % wt	ND	ND	ND	ND	ND	
Visual Appearance of Deposits							
LUBRICANT AND TEST TEMP.	LUBRICANT PROPERTY	TEST HOURS					
		New Oil	24	72	120		
TEL-91053  220°C	Weight Loss, %		19.2	42.0	56.2		
	COBRA Reading	ND	ND	ND	ND		
	Total Acid No.	0.55	0.18	1.78	4.48		
	Viscosity @40 C, cst	16.70	21.24	29.24	49.68		
	40 C Visc Change, %		27.2	75.1	197.6		
	Viscosity @100 C, cs	3.99	4.69	5.84	8.42		
	100 C Visc Change, %		17.5	46.4	111.0		
	Toluene Insol, % wt	ND	ND	ND	ND		
Visual Appearance of Deposits							

**SEVING OXIDATIVE TEST DATA**

LUBRICANT AND TEST TEMP.	LUBRICANT PROPERTY	TEST HOURS						
		Rev Oil	48	96	144	168	192	222
TEL-91063  205°C	Weight Loss, %		16.6	29.8	37.7	39.3	44.0	46.1
	COBRA Reading	2.0	140	200	>200	>200	>200	>200
	Total Acid No.	0.06	0.56	1.16	1.50	1.75	1.93	2.52
	Viscosity @40°C, cSt	17.01	21.12	23.04	26.17	27.44	29.67	32.20
	40°C Visc Change, %		24.2	40.3	53.9	61.3	74.4	89.3
	Viscosity @100°C, cSt	4.02	4.63	5.03	5.36	5.53	5.95	6.16
	100°C Visc Change, %		15.2	25.1	33.3	37.6	48.0	53.2
	Toluene Insol, % wt	ND	ND	ND	ND	ND	ND	ND
Visual Appearance of Deposits								
LUBRICANT AND TEST TEMP.	LUBRICANT PROPERTY	TEST HOURS						
		Rev Oil	240	312				
TEL-91063b (a) 205°C	Weight Loss, %		50.1	62.3				
	COBRA Reading	2	>200	>200				
	Total Acid No.	0.06	2.71	5.15				
	Viscosity @40°C, cSt	17.01	35.40	ND				
	40°C Visc Change, %		100.6	ND				
	Viscosity @100°C, cSt	4.02	6.57	ND				
	100°C Visc Change, %		63.5	ND				
	Toluene Insol, % wt	ND	ND	ND				
Visual Appearance of Deposits								

(a) - test times cont. from 222 hours

LUBRICANT AND TEST TEMP.	LUBRICANT PROPERTY	TEST HOURS						
		Rev Oil	48	96	129	175	199	213
TEL-91063  210°C	Weight Loss, %		19.7	34.4	38.8	51.5	59.2	55.5
	COBRA Reading	2	154	>200	>200	>200	ND	ND
	Total Acid No.	0.06	0.73	1.30	1.74	3.06	4.10	3.71
	Viscosity @40°C, cSt	17.01	21.01	25.23	27.15	36.31	45.79	42.40
	40°C Visc Change, %		20.2	48.3	59.0	113.5	169.2	149.7
	Viscosity @100°C, cSt	4.02	4.73	5.20	5.53	6.69	7.04	7.46
	100°C Visc Change, %		17.7	29.3	37.5	66.4	95.5	85.6
	Toluene Insol, % wt	ND	ND	ND	ND	ND	ND	ND
Visual Appearance of Deposits								
LUBRICANT AND TEST TEMP.	LUBRICANT PROPERTY	TEST HOURS						
		Rev Oil	220					
TEL-91063b (a) 210°C	Weight Loss, %		55.9					
	COBRA Reading							
	Total Acid No.	0.06	4.92					
	Viscosity @40°C, cSt	17.01	49.27					
	40°C Visc Change, %		190.6					
	Viscosity @100°C, cSt	4.02	8.25					
	100°C Visc Change, %		105.2					
	Toluene Insol, % wt	ND	ND					
Visual Appearance of Deposits								

(a) - test times cont. from 213 hours

LUBRICANT AND TEST TEMP.	LUBRICANT PROPERTY	TEST HOURS						
		Rev Oil	24	40	56	64	80	99
TEL-91063  220°C	Weight Loss, %		12.8	24.9	35.3	35.3	47.6	51.7
	COBRA Reading	2	170	>200	>200	>200	>200	ND
	Total Acid No.	0.06	0.62	0.95	1.69	1.57	3.04	3.66
	Viscosity @40°C, cSt	17.01	20.79	23.29	26.10	26.69	35.30	30.66
	40°C Visc Change, %		22.2	36.9	53.9	56.9	107.5	127.3
	Viscosity @100°C, cSt	4.02	4.57	4.93	5.35	5.39	6.57	6.97
	100°C Visc Change, %		13.7	22.6	33.1	34.1	63.4	73.5
	Toluene Insol, % wt	ND	ND	ND	ND	ND	ND	ND
Visual Appearance of Deposits								
LUBRICANT AND TEST TEMP.	LUBRICANT PROPERTY	TEST HOURS						
		Rev Oil	117					
TEL-91063b (a) 220°C	Weight Loss, %		56.4					
	COBRA Reading							
	Total Acid No.	0.06	ND					
	Viscosity @40°C, cSt	17.01	ND					
	40°C Visc Change, %		ND					
	Viscosity @100°C, cSt	4.02	ND					
	100°C Visc Change, %		ND					
	Toluene Insol, % wt	ND	ND					
Visual Appearance of Deposits								

(a) - test times cont. from 99 hours

**SQUIRES OXIDATIVE TEST DATA**

LUBRICANT AND TEST TEMP.	LUBRICANT PROPERTY	TEST HOURS						
		New Oil	48	96	120	144	168	192
TEL-92036 (a) 205°C	Weight Loss, %		10.6	19.7	22.6	30.6	38.8	37.5
	CONRA Reading	ND	ND	ND	ND	ND	ND	ND
	Total Acid No.	0.04	0.77	1.18	1.33	2.52	4.23	ND
	Viscosity @40°C, cst	18.38	22.08	24.62	25.66	29.70	46.35	ND
	40°C Visc Change, %		20.1	34.0	39.6	61.6	152.2	ND
	Viscosity @100°C, cs	4.10	4.68	5.02	5.13	5.64	7.53	ND
	100°C Visc Change, %		14.2	22.4	25.1	37.6	83.7	ND
	Toluene Insol, % wt	ND	ND	ND	ND	ND	ND	ND
	Visual Appearance of Deposits							
LUBRICANT AND TEST TEMP.	LUBRICANT PROPERTY	TEST HOURS						
		New Oil	24	48	72	96		
TEL-92036 215°C	Weight Loss, %		10.8	26.0	36.8	46.1		
	CONRA Reading	ND	ND	ND	ND	ND		
	Total Acid No.	0.04	0.83	6.40	6.37	ND		
	Viscosity @40°C, cst	18.38	22.34	42.77	69.05	ND		
	40°C Visc Change, %		21.6	132.7	275.7	ND		
	Viscosity @100°C, cs	4.10	4.68	6.99	9.66	ND		
	100°C Visc Change, %		14.2	70.5	135.6	ND		
	Toluene Insol, % wt	ND	ND	ND	ND	ND		
	Visual Appearance of Deposits							

(a) - not enough oil for three temperatures

**SQUIRES OXIDATIVE TEST DATA**

LUBRICANT AND TEST TEMP.	LUBRICANT PROPERTY	TEST HOURS						
		New Oil	24	72	96	120	149	197
TEL-92039  205°C	Weight Loss, %		6.0	12.4	16.7	20.0	24.2	30.7
	COBRA Reading	ND	ND	ND	ND	ND	ND	ND
	Total Acid No.	0.27	0.03	0.51	0.43	0.74	0.83	1.40
	Viscosity @40°C, cst	18.04	19.90	21.34	22.17	22.93	23.81	26.23
	40°C Visc Change, %		10.3	18.3	22.9	27.1	32.0	45.4
	Viscosity @100°C, cs	4.10	4.39	4.58	4.70	4.81	4.94	5.26
	100°C Visc Change, %		7.1	11.7	14.6	17.3	20.5	28.3
	Toluene Insol, % wt	ND	ND	ND	ND	ND	ND	ND
	Visual Appearance of Deposits							
LUBRICANT AND TEST TEMP.	LUBRICANT PROPERTY	TEST HOURS						
		New Oil	264	312				
TEL-92039b (g) 205°C	Weight Loss, %		41.0	54.1				
	COBRA Reading	ND	ND	ND				
	Total Acid No.	0.27	2.15	2.64				
	Viscosity @40°C, cst	18.04	32.21	46.28				
	40°C Visc Change, %		78.6	156.5				
	Viscosity @100°C, cs	4.10	6.20	7.72				
	100°C Visc Change, %		51.2	88.3				
	Toluene Insol, % wt	ND	ND	ND				
	Visual Appearance of Deposits							

(a) - Test time continued from 197 hours

LUBRICANT AND TEST TEMP.	LUBRICANT PROPERTY	TEST HOURS						
		New Oil	24	72	116	168	186	
TEL-92039  215°C	Weight Loss, %		8.7	21.7	32.4	49.2	58.9	
	COBRA Reading	ND	ND	ND	ND	ND	ND	
	Total Acid No.	0.27	0.15	0.86	2.28	5.05	ND	
	Viscosity @40°C, cst	18.04	20.56	23.72	29.16	57.49	95.73	
	40°C Visc Change, %		14.0	31.5	61.6	218.7	430.7	
	Viscosity @100°C, cs	4.10	4.48	4.91	5.61	8.85	12.53	
	100°C Visc Change, %		9.3	19.8	36.8	116	206	
	Toluene Insol, % wt	ND	ND	ND	ND	ND	ND	
	Visual Appearance of Deposits							
LUBRICANT AND TEST TEMP.	LUBRICANT PROPERTY	TEST HOURS						
		New Oil	24	48	72	80	96	
TEL-92039  225°C	Weight Loss, %		11.9	24.2	36.2	39.1	55.3	
	COBRA Reading	ND	ND	ND	ND	ND	ND	
	Total Acid No.	0.27	0.53	2.07	4.37	ND	ND	
	Viscosity @40°C, cst	18.04	21.62	25.73	36.59	ND	ND	
	40°C Visc Change, %		19.8	42.6	102.8	ND	ND	
	Viscosity @100°C, cs	4.10	4.60	5.15	6.51	ND	ND	
	100°C Visc Change, %		12.2	25.6	58.8	ND	ND	
	Toluene Insol, % wt	ND	ND	ND	ND	ND	ND	
	Visual Appearance of Deposits							

**SQUIRES OXIDATIVE TEST DATA**

LUBRICANT AND TEST TEMP.	LUBRICANT PROPERTY	TEST HOURS						
		New Oil	48	97	144	166	240	288
TEL-92040  205°C	Weight Loss, %		16.3	26.9	36.0	39.2	50.7	49.4
	COBRA Reading	ND	ND	ND	ND	ND	ND	ND
	Total Acid No.	0.11	0.40	0.89	0.89	1.06	1.55	1.79
	Viscosity @40°C, cst	16.63	20.17	22.92	25.13	26.30	32.10	31.37
	40°C Visc Change, %		21.3	37.8	51.1	58.2	93.5	88.6
	Viscosity @100°C, cs	3.99	4.56	4.88	5.22	5.39	6.16	6.10
	100°C Visc Change, %		14.3	22.3	30.8	35.1	54.4	52.9
	Toluene Insol, % wt	ND	ND	ND	ND	ND	ND	ND
	Visual Appearance of Deposits							
LUBRICANT AND TEST TEMP.	LUBRICANT PROPERTY	TEST HOURS						
		New Oil	480					
TEL-92040b (g) 205°C	Weight Loss, %		63.6					
	COBRA Reading	ND	ND					
	Total Acid No.	0.11	4.48					
	Viscosity @40°C, cst	16.63	ND					
	40°C Visc Change, %		ND					
	Viscosity @100°C, cs	3.99	9.96					
	100°C Visc Change, %		150					
	Toluene Insol, % wt	ND	ND					
	Visual Appearance of Deposits							

(a) - Test times continued from 288 hours

LUBRICANT AND TEST TEMP.	LUBRICANT PROPERTY	TEST HOURS						
		New Oil	48	72	96	168	192	216
TEL-92040  215°C	Weight Loss, %		21.2	28.9	42.6	50.8	58.1	64.4
	COBRA Reading	ND	ND	ND	ND	ND	ND	ND
	Total Acid No.	0.11	0.62	0.89	1.41	2.61	3.35	4.51
	Viscosity @40°C, cst	16.63	21.57	23.40	26.68	34.23	ND	ND
	40°C Visc Change, %		29.7	40.7	60.4	105.8	ND	ND
	Viscosity @100°C, cs	3.99	4.70	4.97	5.43	6.43	7.46	ND
	100°C Visc Change, %		17.8	24.6	36.1	61.2	87.0	ND
	Toluene Insol, % wt	ND	ND	ND	ND	ND	ND	ND
	Visual Appearance of Deposits							
LUBRICANT AND TEST TEMP.	LUBRICANT PROPERTY	TEST HOURS						
		New Oil	240					
TEL-92040b (g) 215°C	Weight Loss, %		67.7					
	COBRA Reading	ND	ND					
	Total Acid No.	0.11	6.25					
	Viscosity @40°C, cst	16.63	ND					
	40°C Visc Change, %		ND					
	Viscosity @100°C, cs	3.99	ND					
	100°C Visc Change, %		ND					
	Toluene Insol, % wt	ND	ND					
	Visual Appearance of Deposits							
LUBRICANT AND TEST TEMP.	LUBRICANT PROPERTY	TEST HOURS						
		New Oil	24	48	72	96		
TEL-92040  225°C	Weight Loss, %		17.5	37.5	41.2	52.7		
	COBRA Reading	ND	ND	ND	ND	ND		
	Total Acid No.	0.11	0.71	1.47	2.40	4.78		
	Viscosity @40°C, cst	16.63	21.35	25.63	29.51	46.77		
	40°C Visc Change, %		28.4	54.1	77.5	181.0		
	Viscosity @100°C, cs	3.99	4.57	5.27	5.85	7.90		
	100°C Visc Change, %		14.5	32.1	46.6	98.0		
	Toluene Insol, % wt	ND	ND	ND	ND	ND		
	Visual Appearance of Deposits							

**SQUIRES OXIDATIVE TEST DATA**

LUBRICANT AND TEST TEMP.	LUBRICANT PROPERTY	TEST HOURS						
		New Oil	48	96	168	216	336	528
TEL-92041  205°C	Weight Loss, %		13.7	22.5	34.4	39.7	56.6	79.5
	COBRA Reading	ND	ND	ND	ND	ND	ND	ND
	Total Acid No.	0.03	0.61	0.81	0.75	0.78	1.67	3.74
	Viscosity @40 C, cst	17.56	21.12	23.27	25.54	27.03	36.30	ND
	40 C Visc Change, %		20.3	32.5	45.4	53.9	107.0	ND
	Viscosity @100 C, cs	4.10	4.55	4.79	5.19	5.30	6.58	ND
	100 C Visc Change, %		11.0	16.0	26.6	31.2	60.5	ND
	Toluene Insol, % wt	ND	ND	ND	ND	ND	ND	ND
	Visual Appearance of Deposits							
LUBRICANT AND TEST TEMP.	LUBRICANT PROPERTY	TEST HOURS						
		New Oil	48	72	96	168	216	240
TEL-92041  215°C	Weight Loss, %		20.9	34.2	41.6	53.6	65.8	70.2
	COBRA Reading	ND	ND	ND	ND	ND	ND	ND
	Total Acid No.	0.03	0.97	1.02	1.15	2.42	3.72	ND
	Viscosity @40 C, cst	17.56	22.25	24.86	27.64	36.89	ND	ND
	40 C Visc Change, %		26.7	41.6	57.4	110.0	ND	ND
	Viscosity @100 C, cs	4.10	4.74	5.09	5.61	6.66	ND	ND
	100 C Visc Change, %		15.6	24.2	36.8	62.4	ND	ND
	Toluene Insol, % wt	ND	ND	ND	ND	ND	ND	ND
	Visual Appearance of Deposits							
LUBRICANT AND TEST TEMP.	LUBRICANT PROPERTY	TEST HOURS						
		New Oil	24	48	72	96		
TEL-92041  225°C	Weight Loss, %		16.4	37.4	46.0	63.1		
	COBRA Reading	ND	ND	ND	ND	ND		
	Total Acid No.	0.03	1.19	1.46	4.25	ND		
	Viscosity @40 C, cst	17.56	21.79	27.40	47.68	ND		
	40 C Visc Change, %		24.1	56.0	172.0	ND		
	Viscosity @100 C, cs	4.10	4.65	5.41	7.67	ND		
	100 C Visc Change, %		13.4	32.0	87.1	ND		
	Toluene Insol, % wt	ND	ND	ND	ND	ND		
	Visual Appearance of Deposits							

**SQUIRES OXIDATIVE TEST DATA**

LUBRICANT AND TEST TEMP.	LUBRICANT PROPERTY	TEST HOURS						
		New Oil	48	96	192	264	336	408
TEL-92049  195°C	Weight Loss, %		7.0	15.8	21.7	30.1	37.2	40.5
	COBRA Reading	ND	ND	ND	ND	ND	ND	ND
	Total Acid No.	0.03	0.51	0.74	0.97	1.38	1.89	2.06
	Viscosity @40°C, cst	10.25	21.25	23.16	24.43	27.10	30.53	32.24
	40°C Visc Change, %		16.4	26.9	33.9	48.5	67.3	76.7
	Viscosity @100°C, cs	4.10	4.52	4.72	4.96	5.35	5.76	5.92
	100°C Visc Change, %		10.2	15.1	21.0	30.5	40.5	44.4
	Toluene Insol, % wt	ND	ND	ND	ND	ND	ND	ND
	Visual Appearance of Deposits							
LUBRICANT AND TEST TEMP.	LUBRICANT PROPERTY	TEST HOURS						
		New Oil	528					
TEL-92049b (g) 195°C	Weight Loss, %		60.5					
	COBRA Reading	ND	ND					
	Total Acid No.	0.03	3.00					
	Viscosity @40°C, cst	10.25	ND					
	40°C Visc Change, %		ND					
	Viscosity @100°C, cs	4.10	7.47					
	100°C Visc Change, %		82.2					
	Toluene Insol, % wt	ND	ND					
	Visual Appearance of Deposits							

(a) - times continued from 408 hours

LUBRICANT AND TEST TEMP.	LUBRICANT PROPERTY	TEST HOURS						
		New Oil	48	96	120	144	168	192
TEL-92049  205°C	Weight Loss, %		10.1	14.4	21.9	26.8	36.3	37.6
	COBRA Reading	ND	ND	ND	ND	ND	ND	ND
	Total Acid No.	0.03	0.96	1.63	1.81	2.69	3.84	4.06
	Viscosity @40°C, cst	10.25	22.26	24.18	26.16	27.95	41.28	ND
	40°C Visc Change, %		22.0	32.5	43.3	53.2	126.0	ND
	Viscosity @100°C, cs	4.10	4.66	4.91	5.15	5.43	6.94	6.99
	100°C Visc Change, %		13.7	19.8	25.6	32.4	69.3	70.5
	Toluene Insol, % wt	ND	ND	ND	ND	ND	ND	ND
	Visual Appearance of Deposits							
LUBRICANT AND TEST TEMP.	LUBRICANT PROPERTY	TEST HOURS						
		New Oil	24	48	72	96		
TEL-92049  215°C	Weight Loss, %		9.0	21.6	33.0	47.9		
	COBRA Reading	ND	ND	ND	ND	ND		
	Total Acid No.	0.03	0.86	2.06	7.08	ND		
	Viscosity @40°C, cst	10.25	21.74	26.00	53.22	ND		
	40°C Visc Change, %		19.1	42.5	192.0	ND		
	Viscosity @100°C, cs	4.10	4.60	5.07	8.10	ND		
	100°C Visc Change, %		12.2	23.7	97.6	ND		
	Toluene Insol, % wt	ND	ND	ND	ND	ND		
	Visual Appearance of Deposits							

**SQUIRES OXIDATIVE TEST DATA**

LUBRICANT AND TEST TEMP.	LUBRICANT PROPERTY	TEST HOURS						
		Rev Oil	48	144	216	288	336	480
TEL-92050  205°C	Weight Loss, %		9.2	27.7	37.2	49.6	56.9	77.5
	COBRA Reading	ND	ND	ND	ND	ND	ND	ND
	Total Acid No.	0.03	0.53	0.85	1.49	1.68	2.22	4.22
	Viscosity @40 C, cst	17.66	19.41	22.31	25.77	30.11	36.12	ND
	40 C Visc Change, %		9.9	26.3	45.9	70.5	105	ND
	Viscosity @100 C, cs	4.05	4.24	4.63	5.19	5.66	6.44	ND
	100 C Visc Change, %		4.7	14.3	28.2	39.8	59.0	ND
	Toluene Insol, % wt	ND	ND	ND	ND	ND	ND	ND
Visual Appearance of Deposits								
LUBRICANT AND TEST TEMP.	LUBRICANT PROPERTY	TEST HOURS						
		Rev Oil	48	96	168	264		
TEL-92050  215°C	Weight Loss, %		14.2	36.2	49.1	78.6		
	COBRA Reading	ND	ND	ND	ND	ND		
	Total Acid No.	0.03	0.52	0.76	1.29	4.15		
	Viscosity @40 C, cst	17.66	19.83	23.23	29.80	ND		
	40 C Visc Change, %		12.3	31.5	68.7	ND		
	Viscosity @100 C, cs	4.05	4.33	4.77	5.62	ND		
	100 C Visc Change, %		6.9	17.8	38.8	ND		
	Toluene Insol, % wt	ND	ND	ND	ND	ND		
Visual Appearance of Deposits								

LUBRICANT AND TEST TEMP.	LUBRICANT PROPERTY	TEST HOURS						
		Rev Oil	24	48	72	96	120	167
TEL-92050  220°C	Weight Loss, %		8.8	21.6	25.2	35.0	41.1	68.9
	COBRA Reading	ND	ND	ND	ND	ND	ND	ND
	Total Acid No.	0.03	0.57	0.80	1.06	1.90	5.25	ND
	Viscosity @40 C, cst	17.66	19.46	20.97	22.08	25.05	33.10	ND
	40 C Visc Change, %		10.2	18.7	25.0	41.9	87.4	ND
	Viscosity @100 C, cs	4.05	4.25	4.45	4.60	4.99	5.92	8.63
	100 C Visc Change, %		4.9	9.9	13.6	23.2	46.2	113
	Toluene Insol, % wt	ND	ND	ND	ND	ND	ND	ND
Visual Appearance of Deposits								
LUBRICANT AND TEST TEMP.	LUBRICANT PROPERTY	TEST HOURS						
		Rev Oil	24	48	72			
TEL-92050  225°C	Weight Loss, %		11.7	20.9	47.2			
	COBRA Reading	ND	ND	ND	ND			
	Total Acid No.	0.03	0.82	0.95	3.62			
	Viscosity @40 C, cst	17.66	20.40	21.82	34.04			
	40 C Visc Change, %		15.5	23.6	206			
	Viscosity @100 C, cs	4.05	4.39	4.55	8.19			
	100 C Visc Change, %		8.4	12.4	102			
	Toluene Insol, % wt	ND	ND	ND	ND			
Visual Appearance of Deposits								

TABLE A-2  
CORROSION AND OXIDATION TEST DATA

LUBRICANT SAMPLE SIZE TEST TEMP.	LUBRICANT PROPERTY	TEST HOURS				
		New Oil	48			
C-59-9 51.4 grams 320°C	Viscosity @40C, cst	64.76	86.10			
	40C Visc Change, %		33.0			
	Viscosity @100C, cst	6.24	7.24			
	100C Visc Change, %		16.0			
	Total Acid Number % Insolubles					
Squires Tube	Visual Appearance of Deposits					
	Test Variations					
CORROSION DATA, Wt. Change mg/cm						
Test Hrs.	Al	Ag	M-St	M-50	Wasp	Ti
48	0.00	-0.04	0.02	-0.02	-0.04	-0.04
LUBRICANT SAMPLE SIZE TEST TEMP.	LUBRICANT PROPERTY	TEST HOURS				
		New Oil	24	48	72	96
O-64-20 51.8 grams 260°C	Viscosity @40C, cst	21.71	24.12	25.16	29.36	
	40C Visc Change, %		11.1	15.9	35.2	
	Viscosity @100C, cst	4.01	4.22	4.31	4.65	
	100C Visc Change, %		5.2	7.5	16.0	
	Total Acid Number % Insolubles					
Squires Tube	Visual Appearance of Deposits					
	Test Variations					
CORROSION DATA, Wt. Change mg/cm						
Test Hrs.	Al	Ag	M-St	M-50	Wasp	Ti
96	0.00	-0.50	0.04	0.08	0.06	0.00
CORROSION DATA, Wt. Change mg/cm						
Test Hrs.	Al	Ag	M-St	M-50	Wasp	Ti
96	0.00	-0.50	0.04	0.08	0.06	0.00

## CORROSION AND OXIDATION TEST DATA

LUBRICANT SAMPLE SIZE TEST TEMP.	LUBRICANT PROPERTY	TEST HOURS					
		New Oil	72	144	240	312	
O-64-20	Viscosity @40C, cst	21.71	26.06	27.64	29.87	30.93	
	40C Visc Change, %		20.0	27.3	37.6	42.5	
	Viscosity @100C, cst	4.01	4.36	4.53	4.71	4.83	
	100C Visc Change, %		8.7	13.0	17.5	20.5	
	Total Acid Number						
49.2 grams 290 °C	% Insolubles						
	Visual Appearance of Deposits						
CORROSION DATA, Wt. Change mg/cm							
		Test Hrs.	Al	Ag	M-St	M-50	Ti
		312	0.00	-1.76	0.02	0.06	-0.02
LUBRICANT SAMPLE SIZE TEST TEMP.	LUBRICANT PROPERTY	TEST HOURS					
		New Oil	24	72	144	192	
O-64-20	Viscosity @40C, cst	21.71	24.01	25.50	28.30	29.39	
	40C Visc Change, %		10.6	17.5	30.4	35.4	
	Viscosity @100C, cst	4.01	4.20	4.37	4.62	4.69	
	100C Visc Change, %		4.7	9.0	15.2	17.0	
	Total Acid Number						
54.3 grams 305 °C	% Insolubles						
	Visual Appearance of Deposits						
CORROSION DATA, Wt. Change mg/cm							
		Test Hrs.	Al	Ag	M-St	M-50	Ti
		192	0.20	-1.58	0.04	0.08	0.02

## CORROSION AND OXIDATION TEST DATA

LUBRICANT SAMPLE SIZE TEST TEMP.	LUBRICANT PROPERTY	TEST HOURS				
		New Oil	48			
O-64-20 (a) 30.7 grams 320°C	Viscosity @40C, cst	21.71	26.44			
	40C Visc Change, %		21.8			
	Viscosity @100C, cst	4.01	4.46			
	100C Visc Change, %		11.2			
	Total Acid Number					
	% Insolubles					
	Visual Appearance of Deposits					
CORROSION DATA, Wt. Change mg/cm						
		Test Hrs.	Al	Ag	M-St	M-50
		48	0.00	-1.44	0.12	0.14
						Wasp
						0.10
						Ti
						0.08
TEST HOURS						
O-64-20 31.9 grams 320°C	Viscosity @40C, cst	21.71	26.81			
	40C Visc Change, %		23.5			
	Viscosity @100C, cst	4.01	4.56			
	100C Visc Change, %		13.7			
	Total Acid Number					
	% Insolubles					
	Visual Appearance of Deposits					
CORROSION DATA, Wt. Change mg/cm						
		Test Hrs.	Al	Ag	M-St	M-50
		48	0.18	-0.38	0.02	0.16
						Wasp
						0.02
						Ti
						0.04
TEST HOURS						
CORROSION DATA, Wt. Change mg/cm						
		Test Hrs.	Al	Ag	M-St	M-50
		48	0.18	-0.38	0.02	0.16
						Wasp
						0.02
						Ti
						0.04

(a) - 0.06% Phenylphosphinic acid and 0.07% Perfluoroglutaric acid

## CORROSION AND OXIDATION TEST DATA

LUBRICANT SAMPLE SIZE TEST TEMP.	LUBRICANT PROPERTY	TEST HOURS				
		New Oil	48			
O-64-20	Viscosity @40C, cst	21.71	25.12			
	40C Visc Change, %		15.7			
	Viscosity @100C, cst	4.01	4.36			
	100C Visc Change, %		8.7			
	Total Acid Number					
30.3 grams	% Insolubles					
	Visual Appearance of Deposits					
Test Variations						
100% relative Additive A added						
CORROSION DATA, Wt. Change mg/cm						
Test Hrs.	Al	Ag	M-St	M-50	Wasp	Ti
48	0.00	-0.30	0.00	-0.04	0.00	-0.04
LUBRICANT SAMPLE SIZE TEST TEMP.	LUBRICANT PROPERTY	TEST HOURS				
		New Oil	48			
O-64-20 (a)	Viscosity @40C, cst	21.74	41.86			
	40C Visc Change, %		92.6			
	Viscosity @100C, cst					
	100C Visc Change, %					
	Total Acid Number					
14.1 grams	% Insolubles					
	Visual Appearance of Deposits					
Test Variations						
Squires Tube Silver coupon only						
CORROSION DATA, Wt. Change mg/cm						
Test Hrs.	Al	Ag	M-St	M-50	Wasp	Ti
48	n/a	-0.30	n/a	n/a	n/a	n/a

(a) - 1% 4-Aminopyrazolo[3,4-d]pyrimidine

## CORROSION AND OXIDATION TEST DATA

LUBRICANT SAMPLE SIZE TEST TEMP.	LUBRICANT PROPERTY	TEST HOURS				
		New Oil	48			
O-64-20 18.2 grams 320°C	Viscosity @40C, cst	21.74	28.57			
	40C Visc Change, %		31.4			
	Viscosity @100C, cst	4.01	4.62			
	100C Visc Change, %		15.2			
	Total Acid Number					
	% Insolubles					
	Visual Appearance of Deposits					
<u>Test Variations</u>						
Squires tube Silver coupon only						
		CORROSION DATA, Wt. Change mg/cm				
Test Hrs.		Al	Ag	M-St	M-50	Wasp
48		n/a	-0.26	n/a	n/a	n/a
Ti						
n/a						
LUBRICANT SAMPLE SIZE TEST TEMP.	LUBRICANT PROPERTY	TEST HOURS				
		New Oil	24	48	72	96
O-64-20 (a) 48.7 grams 320°C	Viscosity @40C, cst	21.96	25.71	26.77	28.01	28.81
	40C Visc Change, %		17.1	21.9	27.6	31.2
	Viscosity @100C, cst	3.99	4.41	4.64	4.55	5.41
	100C Visc Change, %		10.5	16.3	14.0	35.6
	Total Acid Number					
	% Insolubles					
	Visual Appearance of Deposits					
<u>Test Variations</u>						
Squires Tube						
		CORROSION DATA, Wt. Change mg/cm				
Test Hrs.		Al	Ag	M-St	M-50	Wasp
96		0.00	-0.48	-0.28	0.00	-0.02
Ti						
0.00						

(a) - 1.35% Diphenylborinic anhydride

CORROSION AND OXIDATION TEST DATA

LUBRICANT SAMPLE SIZE TEST TEMP.	LUBRICANT PROPERTY	TEST HOURS				
		New Oil	48	96		
O-64-20 (a) 19.7 grams 320°C	Viscosity @40C, cst	21.71	n/a	n/a		
	40C Visc Change, %		n/a	n/a		
	Viscosity @100C, cst	4.01	n/a	n/a		
	100C Visc Change, %		n/a	n/a		
	Total Acid Number					
	% Insolubles					
Squires Tube Silver coupon only	Visual Appearance of Deposits					
	Test Variations					
	CORROSION DATA, Wt. Change mg/cm					
	Test Hrs.	Al	Ag	M-St	M-50	Wasp
	48	n/a	-0.28	n/a	n/a	n/a
	96	n/a	-0.62	n/a	n/a	n/a
O-64-20 (b) 16.8 grams 320°C	Viscosity @40C, cst	21.74	32.72			
	40C Visc Change, %		50.5			
	Viscosity @100C, cst	4.01	4.97			
	100C Visc Change, %		23.9			
	Total Acid Number					
	% Insolubles					
Squires Tube Silver coupon only	Visual Appearance of Deposits					
	Test Variations					
	CORROSION DATA, Wt. Change mg/cm					
	Test Hrs.	Al	Ag	M-St	M-50	Wasp
	48	n/a	-0.04	n/a	n/a	n/a

(a) - Fresh Ag coupon after 48 h  
 (b) - 1.35% Diphenylborinic anhydride

**CORROSION AND OXIDATION TEST DATA**

LUBRICANT SAMPLE SIZE TEST TEMP.	LUBRICANT PROPERTY	TEST HOURS					
		New Oil	24	48	72	96	
O-64-20 (a) 46.0 grams 320°C	Viscosity @40C, cst	21.82	25.07	26.39	27.11	28.35	
	40C Visc Change, %		14.9	20.9	24.2	29.9	
	Viscosity @100C, cst	3.99	4.34	4.48	4.53	4.64	
	100C Visc Change, %		8.8	12.3	13.5	16.3	
	Total Acid Number						
	% Insolubles						
Squires Tube	Visual Appearance of Deposits						
	Test Variations						
CORROSION DATA, Wt. Change mg/cm							
Test Hrs.	Al	Ag	M-St	M-50	Wasp	Ti	
96	0.00	-0.28	-0.36	-0.50	-0.02	0.00	
LUBRICANT SAMPLE SIZE TEST TEMP.	LUBRICANT PROPERTY	TEST HOURS					
		New Oil	24	48	72	96	
O-64-20 53.6 grams 320°C	Viscosity @40C, cst	21.71	24.76	26.37	28.29	28.75	
	40C Visc Change, %		14.1	21.5	30.3	32.4	
	Viscosity @100C, cst	4.01	4.33	4.43	4.60	4.65	
	100C Visc Change, %		8.0	10.5	14.7	16.0	
	Total Acid Number						
	% Insolubles						
Squires Tube	Visual Appearance of Deposits						
	Test Variations						
CORROSION DATA, Wt. Change mg/cm							
Test Hrs.	Al	Ag	M-St	M-50	Wasp	Ti	
96	0.02	-1.96	0.04	0.08	-0.02	0.02	

(a) - 0.5% Diphenylborinic anhydride

# CORROSION AND OXIDATION TEST DATA

LUBRICANT SAMPLE SIZE TEST TEMP.	LUBRICANT PROPERTY	TEST HOURS			
		New Oil	24	48	
O-64-20 (a) 50.5 grams 320 C	Viscosity @40C, cst	21.71	24.75	25.79	
	40C Visc Change, %		14.0	18.8	
	Viscosity @100C, cst	4.01	4.31	4.39	
	100C Visc Change, %		7.5	9.5	
	Total Acid Number	0.01	0.00	0.00	
	% Insolubles		0	0	
Visual Appearance of Deposits					
CORROSION DATA, Wt. Change mg/cm					
	Test Hrs.	Al	Ag	M-St	Wasp
	48	0.15	-0.68	0.06	0.06
					Ti
					0.04
LUBRICANT SAMPLE SIZE TEST TEMP.	LUBRICANT PROPERTY	TEST HOURS			
		New Oil	48	72	96
O-64-20 38.0 grams 320 C	Viscosity @40C, cst	21.71	27.36	31.06	36.41
	40C Visc Change, %		26.0	43.1	67.7
	Viscosity @100C, cst	4.01	4.55	4.85	5.24
	100C Visc Change, %		13.5	20.9	30.7
	Total Acid Number				
	% Insolubles				
Visual Appearance of Deposits					
CORROSION DATA, Wt. Change mg/cm					
	Test Hrs.	Al	Ag	M-St	Wasp
	72	0.04	-0.84	0.00	0.08
					Ti
					0.00
LUBRICANT SAMPLE SIZE TEST TEMP.	LUBRICANT PROPERTY	TEST HOURS			
		New Oil	48	72	96
O-64-20 38.0 grams 320 C	Viscosity @40C, cst	21.71	27.36	31.06	36.41
	40C Visc Change, %		26.0	43.1	67.7
	Viscosity @100C, cst	4.01	4.55	4.85	5.24
	100C Visc Change, %		13.5	20.9	30.7
	Total Acid Number				
	% Insolubles				
Visual Appearance of Deposits					
CORROSION DATA, Wt. Change mg/cm					
	Test Hrs.	Al	Ag	M-St	Wasp
	72	0.04	-0.84	0.00	0.08
					Ti
					0.00
LUBRICANT SAMPLE SIZE TEST TEMP.	LUBRICANT PROPERTY	TEST HOURS			
		New Oil	48	72	96
O-64-20 38.0 grams 320 C	Viscosity @40C, cst	21.71	27.36	31.06	36.41
	40C Visc Change, %		26.0	43.1	67.7
	Viscosity @100C, cst	4.01	4.55	4.85	5.24
	100C Visc Change, %		13.5	20.9	30.7
	Total Acid Number				
	% Insolubles				
Visual Appearance of Deposits					
CORROSION DATA, Wt. Change mg/cm					
	Test Hrs.	Al	Ag	M-St	Wasp
	72	0.04	-0.84	0.00	0.08
					Ti
					0.00
LUBRICANT SAMPLE SIZE TEST TEMP.	LUBRICANT PROPERTY	TEST HOURS			
		New Oil	48	72	96
O-64-20 38.0 grams 320 C	Viscosity @40C, cst	21.71	27.36	31.06	36.41
	40C Visc Change, %		26.0	43.1	67.7
	Viscosity @100C, cst	4.01	4.55	4.85	5.24
	100C Visc Change, %		13.5	20.9	30.7
	Total Acid Number				
	% Insolubles				
Visual Appearance of Deposits					
CORROSION DATA, Wt. Change mg/cm					
	Test Hrs.	Al	Ag	M-St	Wasp
	72	0.04	-0.84	0.00	0.08
					Ti
					0.00

(a) - no sludge, coke, varnish

## CORROSION AND OXIDATION TEST DATA

LUBRICANT SAMPLE SIZE TEST TEMP.	LUBRICANT PROPERTY	TEST HOURS				
		New Oil	48	72	96	
O-64-20  34.4 grams  320 C	Viscosity @40C, cst	21.71	26.40	29.47	31.18	
	40C Visc Change, %		21.6	35.7	43.6	
	Viscosity @100C, cst	4.01	4.48	4.73	4.89	
	100C Visc Change, %		11.7	17.9	21.9	
	Total Acid Number					
	% Insolubles					
	Visual Appearance of Deposits					
Test Variations						
No Metal Specimens						
CORROSION DATA, Wt. Change mg/cm						
		Test Hrs.	Al	Ag	M-St	Ti
		No Data				
LUBRICANT SAMPLE SIZE TEST TEMP.	LUBRICANT PROPERTY	TEST HOURS				
		New Oil	48	VP		
O-64-20  31.4 grams  320 C	Viscosity @40C, cst	21.71	25.76			
	40C Visc Change, %		18.7			
	Viscosity @100C, cst	4.01	4.42			
	100C Visc Change, %		10.2			
	Total Acid Number	0.00	0.00			
	% Insolubles					
	Visual Appearance of Deposits					
Test Variations						
Squires Tube Vapor Phase Corrosion						
CORROSION DATA, Wt. Change mg/cm						
		Test Hrs.	Al	Ag	M-St	Ti
		48	0.06	-0.30	0.14	0.04
		VP	0.02	-0.06	0.06	0.02

**CORROSION AND OXIDATION TEST DATA**

LUBRICANT SAMPLE SIZE TEST TEMP.	LUBRICANT PROPERTY	TEST HOURS					
		New Oil	24				
O-77-6 (a) 54.6 grams 280°C	Viscosity @40C, cst	218.2	236.5				
	40C Visc Change, %		8.4				
	Viscosity @100C, cst	11.42	11.80				
	100C Visc Change, %		3.3				
	Total Acid Number						
	% Insolubles						
Visual Appearance of Deposits							
<u>Test Variations</u>							
Squires Tube							
No Metal Specimens							
CORROSION DATA, Wt. Change mg/cm							
		Test Hrs.	Al	Ag	M-St	M-50	Wasp
		No Data					Ti
LUBRICANT SAMPLE SIZE TEST TEMP.	LUBRICANT PROPERTY	TEST HOURS					
		New Oil	24				
O-77-6 (b) 57.3 grams 280°C	Viscosity @40C, cst	216.4	256.4				
	40C Visc Change, %		18.5				
	Viscosity @100C, cst	11.37	12.86				
	100C Visc Change, %		13.1				
	Total Acid Number	0.00	0.49				
	% Insolubles						
Visual Appearance of Deposits							
<u>Test Variations</u>							
Squires Tube							
No Metal Specimens							
CORROSION DATA, Wt. Change mg/cm							
		Test Hrs.	Al	Ag	M-St	M-50	Wasp
		No Data					Ti

(a) - 5% TPP

(b) - 5% TPP & 0.15% TPT

LUBRICANT SAMPLE SIZE TEST TEMP.	LUBRICANT PROPERTY	TEST HOURS						
		New Oil	24					
O-77-6 (a) 61.2 grams  280°C	Viscosity @40C, cst							
	40C Visc Change, %							
	Viscosity @100C, cst							
	100C Visc Change, %							
	Total Acid Number							
	% Insolubles							
	Visual Appearance of Deposits		oil too thick to test					
<u>Test Variations</u>								
10% TCP and 0.15% TPT								
		Test Hrs.	Al	Ag	M-St	M-50	Wasp	Ti
		No Data						
LUBRICANT SAMPLE SIZE TEST TEMP.	LUBRICANT PROPERTY	TEST HOURS						
		New Oil	24					
O-77-6 (b) 53.6 grams  280°C	Viscosity @40C, cst	219.4						
	40C Visc Change, %							
	Viscosity @100C, cst	11.34						
	100C Visc Change, %							
	Total Acid Number							
	% Insolubles							
	Visual Appearance of Deposits							
<u>Test Variations</u>								
Squires Tube								
No Metal Specimens								
		Test Hrs.	Al	Ag	M-St	M-50	Wasp	Ti
		No Data						
<u>CORROSION DATA, Wt. Change mg/cm</u>								

357

LUBRICANT SAMPLE SIZE TEST TEMP.	LUBRICANT PROPERTY	TEST HOURS						
		New Oil	24					
O-77-6 (a) 49.4 grams 300°C	Viscosity @40C, cst	211.1	294.8					
	40C Visc Change, %		39.7					
	Viscosity @100C, cst	11.45	12.89					
	100C Visc Change, %		12.6					
	Total Acid Number % Insolubles	0.00	0.02					
	Visual Appearance of Deposits							
<u>Test Variations</u> Squires Tube No Metal Specimens								
CORROSION DATA, Wt. Change mg/cm								
		Test Hrs.	Al	Ag	M-St	M-50	Wasp	Ti
		No Data						
LUBRICANT SAMPLE SIZE TEST TEMP.	LUBRICANT PROPERTY	TEST HOURS						
		New Oil	24					
O-77-6  51.5 grams 300°C	Viscosity @40C, cst	273.3	309.5					
	40C Visc Change, %		13.2					
	Viscosity @100C, cst	12.56	13.13					
	100C Visc Change, %		4.5					
	Total Acid Number % Insolubles	0.00	0.03					
	Visual Appearance of Deposits							
<u>Test Variations</u> Squires Tube No Metal Specimens								
CORROSION DATA, Wt. Change mg/cm								
		Test Hrs.	Al	Ag	M-St	M-50	Wasp	Ti
		No Data						

358

## CORROSION AND OXIDATION TEST DATA

LUBRICANT SAMPLE SIZE TEST TEMP.	LUBRICANT PROPERTY	TEST HOURS				
		New Oil	48			
O-77-6  57.0 grams  320 C	Viscosity @40C, cst	110.9	722.1			
	40C Visc Change, %		551.3			
	Viscosity @100C, cst	8.73	20.26			
	100C Visc Change, %		132.1			
	Total Acid Number % Insolubles	0.00	11.7			
Visual Appearance of Deposits						
Test Variations						
Squires Tube 20% TPP						
CORROSION DATA, Wt. Change mg/cm						
Test Hrs.	Al	Ag	M-St	M-50	Wasp	Ti
48	0.74	-1.00	0.68	0.60	0.30	0.34
TEST HOURS						
O-77-6  57.1 grams  320 C	Viscosity @40C, cst	136.1	-			
	40C Visc Change, %		-			
	Viscosity @100C, cst	9.55	-			
	100C Visc Change, %		-			
	Total Acid Number % Insolubles	0.00				
Visual Appearance of Deposits						
Test Variations						
Squires Tube 20% TPP						
CORROSION DATA, Wt. Change mg/cm						
Test Hrs.	Al	Ag	M-St	M-50	Wasp	Ti
48	13.54	17.30	12.98	11.30	10.20	11.48

## CORROSION AND OXIDATION TEST DATA

LUBRICANT SAMPLE SIZE TEST TEMP.	LUBRICANT PROPERTY	TEST HOURS				
		New Oil	24			
O-77-6  60.6 grams  320 C	Viscosity @40C, cst	110.7	283.3			
	40C Visc Change, %		155.8			
	Viscosity @100C, cst	8.74	12.80			
	100C Visc Change, %		46.5			
	Total Acid Number	0.00	0.06			
	% Insolubles					
	Visual Appearance of Deposits					
<u>Test Variations</u>						
Squires Tube 20% TPP						
		CORROSION DATA, Wt. Change mg/cm				
		Test Hrs.	Al	Ag	M-St	Wasp
		24	0.00	-0.20	0.12	0.02
						Ti
						0.08
<u>Test Variations</u>						
Squires Tube 20% TPP						
		CORROSION DATA, Wt. Change mg/cm				
		Test Hrs.	Al	Ag	M-St	Wasp
		24	0.34	-0.88	0.12	0.10
						Ti
						0.10

LUBRICANT SAMPLE SIZE TEST TEMP.	LUBRICANT PROPERTY	TEST HOURS			
O-77-6 43.1 grams 320°C	Viscosity @40C, cst	New Oil	24		
	40C Visc Change, %	235.1			
	Viscosity @100C, cst	11.68			
	100C Visc Change, %				
	Total Acid Number				
	% Insolubles				
	Visual Appearance of Deposits				
<u>Test Variations</u>					
Squires Tube					
7% TCP; oil too thick to test					
		Test Hrs.	Al	Ag	M-St
		24	1.70	0.18	0.58
					M-50
					0.70
					Wasp
					0.30
					Ti
					0.28
LUBRICANT SAMPLE SIZE TEST TEMP.	LUBRICANT PROPERTY	TEST HOURS			
O-77-6 (a) 53.8 grams 320°C	Viscosity @40C, cst	New Oil	18		
	40C Visc Change, %	212.5			
	Viscosity @100C, cst	11.28			
	100C Visc Change, %				
	Total Acid Number				
	% Insolubles				
	Visual Appearance of Deposits				
<u>Test Variations</u>					
Squires Tube					
No Metal Specimens					
		Test Hrs.	Al	Ag	M-St
		No Data			
					M-50
					Wasp
					Ti

**(a) - oil too thick to test**

LUBRICANT SAMPLE SIZE TEST TEMP.	LUBRICANT PROPERTY	TEST HOURS			
		New Oil	18		
O-77-6 (a) 53.7 grams 320°C	Viscosity @40C, cst	214.4			
	40C Visc Change, %				
	Viscosity @100C, cst	11.32			
	100C Visc Change, %				
	Total Acid Number				
	% Insolubles				
	Visual Appearance of Deposits				
<u>Test Variations</u> Squires Tube No Metal Specimens					
CORROSION DATA, Wt. Change mg/cm					
		Test Hrs.	Al	Ag	M-St
		No Data			
					Wasp
					Ti

LUBRICANT SAMPLE SIZE TEST TEMP.	LUBRICANT PROPERTY	TEST HOURS			
		New Oil	24		
O-77-6 (b) 51.0 grams 320°C	Viscosity @40C, cst	170.4	287.8		
	40C Visc Change, %		68.9		
	Viscosity @100C, cst	10.47	13.37		
	100C Visc Change, %		27.7		
	Total Acid Number	0.00	0.44		
	% Insolubles				
	Visual Appearance of Deposits				
<u>Test Variations</u> Squires Tube No Metal Specimens					
CORROSION DATA, Wt. Change mg/cm					
		Test Hrs.	Al	Ag	M-St
		No Data			
					Wasp
					Ti

362

**CORROSION AND OXIDATION TEST DATA**

LUBRICANT SAMPLE SIZE TEST TEMP.	LUBRICANT PROPERTY	TEST HOURS					
		New Oil	24				
O-77-6 (a) 52.2 grams 320 °C	Viscosity @40C, cst	215.7	535.2				
	40C Visc Change, %		148.1				
	Viscosity @100C, cst	11.41	17.75				
	100C Visc Change, %		55.6				
	Total Acid Number	0.00	0.88				
		% Insolubles					
		Visual Appearance of Deposits					
		Test Variations					
Squires Tube No Metal Specimens		CORROSION DATA, Wt. Change mg/cm					
		Test Hrs.	Al	Ag	M-St	Wasp	Ti
		No Data					
LUBRICANT SAMPLE SIZE TEST TEMP.	LUBRICANT PROPERTY	TEST HOURS					
		New Oil	24				
O-77-6 56.1 grams 320 °C	Viscosity @40C, cst	169.2	220.9				
	40C Visc Change, %		30.6				
	Viscosity @100C, cst	10.39	11.76				
	100C Visc Change, %		13.2				
	Total Acid Number	0.00	0.35				
		% Insolubles					
		Visual Appearance of Deposits					
		Test Variations					
Squires Tube 10% TPP		CORROSION DATA, Wt. Change mg/cm					
		Test Hrs.	Al	Ag	M-St	Wasp	Ti
		24	0.06	-0.26	0.12	0.10	-0.02

(a) - 5% TPP

## CORROSION AND OXIDATION TEST DATA

LUBRICANT SAMPLE SIZE TEST TEMP.	LUBRICANT PROPERTY	TEST HOURS				
		New Oil	24			
O-77-6 56.4 grams 320°C	Viscosity @40C, cst	110.8	133.3			
	40C Visc Change, %		20.3			
	Viscosity @100C, cst	8.75	9.52			
	100C Visc Change, %		8.8			
	Total Acid Number	0.00	0.74			
	% Insolubles					
	Visual Appearance of Deposits					
CORROSION DATA, Wt. Change mg/cm						
Squires Tube 20% TPP	Test Variations	Test Hrs.	Al	Ag	M-St	Wasp
		24	0.04	-0.02	0.22	0.18
						Ti
						0.02
CORROSION DATA, Wt. Change mg/cm						
Squires Tube 25% TPP	Test Variations	Test Hrs.	Al	Ag	M-St	Wasp
		24	0.08	0.32	0.30	0.14
						Ti
						0.02

LUBRICANT SAMPLE SIZE TEST TEMP.	LUBRICANT PROPERTY	New Oil	24	TEST HOURS				
O-77-6 (a) 36.7 grams  320°C	Viscosity @40C,cst	204.4						
	40C Visc Change, %							
	Viscosity @100C,cst	10.71						
	100C Visc Change, %							
	Total Acid Number	0.00	14.4					
	% Insolubles							
	Visual Appearance of Deposits							
	Test Variations							
<b>Squires Tube</b>								
<b>10% TPP &amp; 10% TPPO</b>								
		Test Hrs.	Al	Ag	M-St	M-50	Ti	
		24	0.14	-1.86	0.12	0.28	0.06	
LUBRICANT SAMPLE SIZE TEST TEMP.	LUBRICANT PROPERTY	New Oil	24	TEST HOURS				
O-77-6 (b) 37.1 grams  320°C	Viscosity @40C,cst	87.64						
	40C Visc Change, %							
	Viscosity @100C,cst	7.56						
	100C Visc Change, %							
	Total Acid Number	0.00	29.0					
	% Insolubles							
	Visual Appearance of Deposits							
	Test Variations							
<b>30% TPP &amp; 10% TPPO</b>								
		Test Hrs.	Al	Ag	M-St	M-50	Ti	
		24	0.16	-2.14	0.12	0.35	0.02	

(a) - oil too thick to test  
(b) - oil too thick to test

## CORROSION AND OXIDATION TEST DATA

LUBRICANT SAMPLE SIZE TEST TEMP.	LUBRICANT PROPERTY	TEST HOURS				
		New Oil	24			
O-77-6  35.1 grams  320°C	Viscosity @40C, cst	110.9	300.7			
	40C Visc Change, %		171.0			
	Viscosity @100C, cst	8.72	13.59			
	100C Visc Change, %		55.9			
	Total Acid Number	0.00	12.9			
	% Insolubles					
	Visual Appearance of Deposits					
Test Variations						
Squires Tube 20% TPP						
		Test Hrs.	Al	Ag	M-St	M-50
		24	2.12	1.30	0.32	0.30
						0.16
CORROSION DATA, Wt. Change mg/cm						
LUBRICANT SAMPLE SIZE TEST TEMP.	LUBRICANT PROPERTY	TEST HOURS				
		New Oil	24			
O-77-6  33.0 grams  320°C	Viscosity @40C, cst	110.5	360.4			
	40C Visc Change, %		226.2			
	Viscosity @100C, cst	8.72	14.78			
	100C Visc Change, %		69.5			
	Total Acid Number	0.00	11.7			
	% Insolubles					
	Visual Appearance of Deposits					
Test Variations						
Squires Tube 20% TPP						
		Test Hrs.	Al	Ag	M-St	M-50
		24	0.40	0.94	0.32	0.26
						0.18
CORROSION DATA, Wt. Change mg/cm						
		Test Hrs.	Al	Ag	M-St	M-50
		24	0.40	0.94	0.32	0.26
						0.18

## CORROSION AND OXIDATION TEST DATA

LUBRICANT SAMPLE SIZE TEST TEMP.	LUBRICANT PROPERTY	TEST HOURS				
		New Oil	24			
O-77-6 59.5 grams 320°C	Viscosity @40C, cst	88.65	92.78			
	40C Visc Change, %		4.7			
	Viscosity @100C, cst	7.61	7.73			
	100C Visc Change, %		1.6			
	Total Acid Number	0.00	0.39			
	% Insolubles					
	Visual Appearance of Deposits					
Test Variations						
Squires Tube						
Nitrogen						
30% TPP & 10% TPPO						
CORROSION DATA, Wt. Change mg/cm						
	Test Hrs.	Al	Ag	M-St	Wasp	Ti
	24	0.04	0.00	0.02	0.06	0.04
LUBRICANT						
O-77-6 57.8 grams 320°C	LUBRICANT PROPERTY	New Oil	24			
	Viscosity @40C, cst	128.6	128.0			
	40C Visc Change, %		-0.4			
	Viscosity @100C, cst	8.87	9.26			
	100C Visc Change, %		4.4			
	Total Acid Number	0.00	0.00			
	% Insolubles					
	Visual Appearance of Deposits					
Test Variations						
Squires Tube						
Nitrogen						
19% TPP						
CORROSION DATA, Wt. Change mg/cm						
	Test Hrs.	Al	Ag	M-St	Wasp	Ti
	24	0.04	0.02	0.04	0.00	0.02

## CORROSION AND OXIDATION TEST DATA

LUBRICANT SAMPLE SIZE TEST TEMP.	LUBRICANT PROPERTY	TEST HOURS				
		New Oil	24			
O-77-6  54.2 grams  320°C	Viscosity @40C, cst	115.0	118.7			
	40C Visc Change, %		3.1			
	Viscosity @100C, cst	8.86	8.90			
	100C Visc Change, %		0.5			
	Total Acid Number	0.00	32.6			
	% Insolubles					
	Visual Appearance of Deposits					
Test Variations						
Squires Tube Nitrogen 1% TPP, moist nitrogen						
		Test Hrs.	Al	Ag	M-St	M-50
		24	2.44	-0.04	0.54	0.56
						Wasp
						0.92
						1.46
						Ti
						0.70
CORROSION DATA, Wt. Change mg/cm						
O-77-6 (a) 55.1 grams  320°C	Viscosity @40C, cst	87.75	96.63			
	40C Visc Change, %		10.1			
	Viscosity @100C, cst	7.59	7.81			
	100C Visc Change, %		2.9			
	Total Acid Number	0.00	ND			
	% Insolubles					
	Visual Appearance of Deposits					
Test Variations						
Squires Tube Nitrogen 30% TPP & 10% TPPO						
		Test Hrs.	Al	Ag	M-St	M-50
		24	ND	1.06	-10.5	0.84
						Wasp
						0.86
						0.70
						Ti
						0.70
CORROSION DATA, Wt. Change mg/cm						

(a) - moist nitrogen, Al coupon dissolved

CORROSION AND OXIDATION TEST DATA

LUBRICANT SAMPLE SIZE TEST TEMP.	LUBRICANT PROPERTY	TEST HOURS				
		New Oil	24	48		
O-77-6  56.5 grams  320°C	Viscosity @40C, cst	81.90	104.2	214.4		
	40C Visc Change, %		27.2	161.7		
	Viscosity @100C, cst	7.36	8.69	12.11		
	100C Visc Change, %		18.1	64.5		
	Total Acid Number % Insolubles	0.00	1.78	4.46		
Visual Appearance of Deposits						
Test Variations						
Squires Tube 30% TPP & 10% TPPP						
CORROSION DATA, Wt. Change mg/cm						
Test Hrs.		Al	Ag	M-St	M-50	Wasp
24		0.10	-1.26	0.20	0.24	0.04
Ti						0.10
O-77-6 (a) 109.1 grams  320°C	Viscosity @40C, cst					
	40C Visc Change, %					
	Viscosity @100C, cst					
	100C Visc Change, %					
	Total Acid Number % Insolubles					
Visual Appearance of Deposits						
Test Variations						
From can G						
CORROSION DATA, Wt. Change mg/cm						
Test Hrs.		Al	Ag	M-St	M-50	Wasp
24		0.00	0.00	0.02	0.00	0.00
Ti						-0.02

(a) - Duplicate of test run 4-12-88

# CORROSION AND OXIDATION TEST DATA

LUBRICANT SAMPLE SIZE TEST TEMP.	LUBRICANT PROPERTY	TEST HOURS				
		New Oil	24	48		
TEL-90013  56.0 grams  260°C	Viscosity @40C, cst	212.3	299.4			
	40C Visc Change, %		41.0			
	Viscosity @100C, cst	10.75	13.73	25.33		
	100C Visc Change, %		27.7	135.6		
	Total Acid Number					
	% Insolubles					
	Visual Appearance of Deposits					
<u>Test Variations</u> All TEFLON Apparatus						
		Test Hrs.	Al	Ag	M-St	M-50
		48	0.04	-1.02	0.02	0.04
						Ti
						0.00
CORROSION DATA, Wt. Change mg/cm						
LUBRICANT SAMPLE SIZE TEST TEMP.	LUBRICANT PROPERTY	TEST HOURS				
		New Oil	48			
TEL-90013  41.2 grams  260°C	Viscosity @40C, cst	212.3	378.9			
	40C Visc Change, %		78.5			
	Viscosity @100C, cst	10.75	15.90			
	100C Visc Change, %		47.9			
	Total Acid Number	0.01	3.74			
	% Insolubles					
	Visual Appearance of Deposits					
<u>Test Variations</u> Squires Tube Nickel set-up; TEFLON condenser						
		Test Hrs.	Al	Ag	M-St	M-50
		48	-0.02	-0.32	0.00	-0.04
						Wasp
						0.02
						Ti
						-0.02
CORROSION DATA, Wt. Change mg/cm						

## CORROSION AND OXIDATION TEST DATA

LUBRICANT SAMPLE SIZE TEST TEMP.	LUBRICANT PROPERTY	TEST HOURS				
		New Oil	24	48		
TEL-90013  59.8 grams  280°C	Viscosity @40C, cst	212.3	286.3	657.8		
	40C Visc Change, %		34.8	209.8		
	Viscosity @100C, cst	10.75	13.51	23.53		
	100C Visc Change, %		25.7	118.9		
	Total Acid Number					
	% Insolubles					
	Visual Appearance of Deposits					
Test Variations						
All TEFLON Apparatus						
		CORROSION DATA, Wt. Change mg/cm				
		Test Hrs.	Al	Ag	M-St	Wasp
		48	-0.02	-1.30	0.02	0.00
						Ti
						-0.02
TEST HOURS						
LUBRICANT SAMPLE SIZE TEST TEMP.	LUBRICANT PROPERTY	New Oil	48			
		212.3	425.4			
		40C Visc Change, %	100.3			
		Viscosity @100C, cst	17.49			
		100C Visc Change, %	62.7			
38.8 grams  280°C	Total Acid Number	0.01	2.69			
	% Insolubles					
	Visual Appearance of Deposits					
Test Variations						
Squires Tube						
Nickel set-up; TEFLON condenser						
		CORROSION DATA, Wt. Change mg/cm				
		Test Hrs.	Al	Ag	M-St	Wasp
		48	-0.02	-0.72	0.06	0.02
						Ti
						0.02

# CORROSION AND OXIDATION TEST DATA

LUBRICANT SAMPLE SIZE TEST TEMP.	LUBRICANT PROPERTY	TEST HOURS				
		New Oil	25	54	75	
TEL-90013 59.9 grams 280°C	Viscosity @40C, cst	212.3	275.8	462.1	547.3	
	40C Visc Change, %		29.9	117.6	157.7	
	Viscosity @100C, cst	10.75	13.57	18.82	20.99	
	100C Visc Change, %		26.2	75.1	95.3	
	Total Acid Number					
	% Insolubles					
	Visual Appearance of Deposits					
Test Variations						
No Metal Specimens						
		CORROSION DATA, Wt. Change mg/cm				
		Test Hrs.	Al	Ag	M-St	Wasp
		No Data				Ti
TEST HOURS						
TEL-90013 59.8 grams 280°C	Viscosity @40C, cst	New Oil	24	48	72	
	40C Visc Change, %	212.3	250.2	320.7	399.2	
	Viscosity @100C, cst		17.8	50.8	88.0	
	100C Visc Change, %	10.75	12.26	15.08	17.7	
	Total Acid Number	0.01	14.0	40.3	64.7	
	% Insolubles		1.22	2.07	3.43	
	Visual Appearance of Deposits					
Test Variations						
Squires Tube						
		CORROSION DATA, Wt. Change mg/cm				
		Test Hrs.	Al	Ag	M-St	Wasp
		72	0.00	-4.96	0.00	0.00
						Ti
						0.00

## CORROSION AND OXIDATION TEST DATA

LUBRICANT SAMPLE SIZE TEST TEMP.	LUBRICANT PROPERTY	TEST HOURS				
		New Oil	24	48		
TEL-90013 50.0 grams 290 C	Viscosity @40C, cst	212.3	409.4	ND		
	40C Visc Change, %		92.8	ND		
	Viscosity @100C, cst	10.75	17.81	ND		
	100C Visc Change, %		65.7	ND		
	Total Acid Number					
	% Insolubles					
	Visual Appearance of Deposits					
Test Variations						
Squires Tube						
All TEFLON apparatus						
CORROSION DATA, Wt. Change mg/cm						
	Test Hrs.	Al	Ag	M-St	M-50	Wasp
	48	0.00	-1.86	-0.02	0.08	-0.02
						Ti
						0.14
TEST HOURS						
TEL-90101 48.7 grams 320 C	Viscosity @40C, cst	288.4	325.7			
	40C Visc Change, %		12.9			
	Viscosity @100C, cst	12.94				
	100C Visc Change, %					
	Total Acid Number					
	% Insolubles					
	Visual Appearance of Deposits					
Test Variations						
Squires Tube						
CORROSION DATA, Wt. Change mg/cm						
	Test Hrs.	Al	Ag	M-St	M-50	Wasp
	48	0.00	-0.04	0.02	-0.02	0.04
						Ti
						-0.06

## CORROSION AND OXIDATION TEST DATA

LUBRICANT SAMPLE SIZE TEST TEMP.	LUBRICANT PROPERTY	TEST HOURS				
		New Oil	48			
TEL-90102 50.0 grams 320°C	Viscosity @40C, cst	59.89	73.21			
	40C Visc Change, %		22.2			
	Viscosity @100C, cst	6.64	7.30			
	100C Visc Change, %		9.9			
	Total Acid Number % Insolubles	0.01	0.06			
Visual Appearance of Deposits						
Test Variations						
Squires Tube						
50% 90102 + 50% 0-64-20 (VOL)						
		Test Hrs.	Al	Ag	M-St	M-50
		48	0.00	-0.28	0.02	0.02
						Wasp
						0.04
						Ti
						0.06
LUBRICANT SAMPLE SIZE TEST TEMP.	LUBRICANT PROPERTY	TEST HOURS				
		New Oil	48	48vap		
TEL-90102 (a) 51.7 grams 320°C	Viscosity @40C, cst	282.9	329.1			
	40C Visc Change, %		16.3			
	Viscosity @100C, cst	12.77	13.52			
	100C Visc Change, %		5.9			
	Total Acid Number % Insolubles					
Visual Appearance of Deposits						
Test Variations						
Squires Tube						
Vapor Phase Corrosion						
20% (vol) Methyl propionate						
		Test Hrs.	Al	Ag	M-St	M-50
		48	0.00	0.02	0.08	0.04
		48vap	0.00	0.02	0.00	0.00
						Wasp
						0.00
						Ti
						0.00

(a) - No initial condensate return

LUBRICANT SAMPLE SIZE TEST TEMP.	LUBRICANT PROPERTY	TEST HOURS						
		New Oil	48	48vap				
TEL-90102 (a) 51.1 grams 320°C	Viscosity @40C,cst	282.9	324.9					
	40C Visc Change, %		14.8					
	Viscosity @100C,cst	12.77	13.41					
	100C Visc Change, %		5.0					
	Total Acid Number							
	% Insolubles							
Visual Appearance of Deposits								
<u>Test Variations</u> Squires Tube Vapor Phase Corrosion 20% (vol) Propyl formate								
TEL-90102 (b) 50.0 grams 320°C	LUBRICANT PROPERTY	New Oil	48	48vap				
		282.9	326.8					
			15.5					
		12.77	13.52					
			5.9					
Total Acid Number								
% Insolubles								
Visual Appearance of Deposits								
<u>Test Variations</u> Squires Tube Vapor Phase Corrosion 20% (vol) Trichloroethylene								
LUBRICANT PROPERTY		Test Hrs.	Al	Ag	M-St	M-50	Wasp	Ti
48		48	0.02	-0.04	0.02	0.08	0.00	0.04
48vap		48vap	-0.02	0.02	0.02	-0.02	0.04	0.04
CORROSION DATA, Wt. Change mg/cm								
LUBRICANT PROPERTY		New Oil	48	48vap				
282.9		282.9	326.8					
40C Visc Change, %			15.5					
Viscosity @100C,cst		12.77	13.52					
100C Visc Change, %			5.9					
Total Acid Number								
% Insolubles								
Visual Appearance of Deposits								
CORROSION DATA, Wt. Change mg/cm								
LUBRICANT PROPERTY		Test Hrs.	Al	Ag	M-St	M-50	Wasp	Ti
48		48	-0.02	-0.04	0.04	-0.02	0.00	0.00
48vap		48vap	0.00	0.02	0.00	0.00	-0.04	0.00
CORROSION DATA, Wt. Change mg/cm								

375

## CORROSION AND OXIDATION TEST DATA

LUBRICANT SAMPLE SIZE TEST TEMP.	LUBRICANT PROPERTY	TEST HOURS					
		New Oil	48	48vap			
TEL-90102 (a) 54.5 grams 320°C	Viscosity @40C,cst	282.9	-	-			
	40C Visc Change, %		-				
	Viscosity @100C,cst	12.77	-	-			
	100C Visc Change, %		-				
	Total Acid Number						
	% Insolubles						
	Visual Appearance of Deposits		oil too thick to test				
<u>Test Variations</u>							
Squires Tube Vapor Phase Corrosion 20% (vol)1-bromopropane							
		Test Hrs.	Al	Ag	M-St	Wasp	Ti
		48	-	-	-	-	-
		48vap	-	-	-	-	-
LUBRICANT SAMPLE SIZE TEST TEMP.	LUBRICANT PROPERTY	TEST HOURS					
		New Oil	48	48vap			
TEL-90102 (b) 55.1 grams 320°C	Viscosity @40C,cst	282.9	326.8				
	40C Visc Change, %		15.5				
	Viscosity @100C,cst	12.77	13.45				
	100C Visc Change, %		5.3				
	Total Acid Number						
	% Insolubles						
	Visual Appearance of Deposits						
<u>Test Variations</u>							
Squires Tube Vapor Phase Corrosion 20%(vol) Propyl formate							
		Test Hrs.	Al	Ag	M-St	Wasp	Ti
		48	0.00	-0.06	-0.02	0.02	0.00
		48vap	0.00	0.00	0.00	-0.08	-0.02

(a) - condensate return throughout test

(b) - No initial condensate return

LUBRICANT SAMPLE SIZE TEST TEMP.	LUBRICANT PROPERTY	TEST HOURS			
		New Oil	48	48vap	
TEL-90102 (a) 58.1 grams 320°C	Viscosity @40C, cst	282.9	327.1		
	40C Visc Change, %		15.6		
	Viscosity @100C, cst	12.77	13.54		
	100C Visc Change, %		6.0		
	Total Acid Number				
	% Insolubles				
	Visual Appearance of Deposits				
<u>Test Variations</u>					
Squires Tube					
Vapor Phase Corrosion					
20% (vol) 1-bromopropane					
		Test Hrs.	Al	Ag	M-St
		48	-0.02	-0.06	0.00
		48vap	0.00	0.04	0.04
		CORROSION DATA, Wt. Change mg/cm			
				M-50	Wasp
				0.06	0.04
				0.04	-0.04
					0.02
		TEST HOURS			
LUBRICANT SAMPLE SIZE TEST TEMP.	LUBRICANT PROPERTY	New Oil	48		
TEL-90102 (b) 52.8 grams 320°C	Viscosity @40C, cst	282.9			
	40C Visc Change, %				
	Viscosity @100C, cst	12.77			
	100C Visc Change, %				
	Total Acid Number				
	% Insolubles				
	Visual Appearance of Deposits		oil too thick to test		
<u>Test Variations</u>					
Squires Tube					
Vapor Phase Corrosion					
20% (vol) Diglyme					
		Test Hrs.	Al	Ag	M-St
		48	-	-	-
		CORROSION DATA, Wt. Change mg/cm			
				M-50	Wasp
				-	-
					-

(a) - No initial condensate return

## CORROSION AND OXIDATION TEST DATA

LUBRICANT SAMPLE SIZE TEST TEMP.	LUBRICANT PROPERTY	TEST HOURS				
		New Oil	48	48vap		
TEL-90102 (a) 54.1 grams 320°C	Viscosity @40C, cst	282.9	343.5			
	40C Visc Change, %		21.4			
	Viscosity @100C, cst	12.77	13.79			
	100C Visc Change, %		8.0			
	Total Acid Number					
	% Insolubles					
Squires Tube Vapor Phase Corrosion 20% (vol) Diglyme	Visual Appearance of Deposits					
	Test Variations					
LUBRICANT SAMPLE SIZE TEST TEMP.	LUBRICANT PROPERTY	CORROSION DATA, Wt. Change mg/cm				
		Test Hrs.	Al	Ag	M-St	Wasp
TEL-90102 (b) 56.1 grams 320°C	Viscosity @40C, cst	48	0.00	0.40	0.00	0.02
	40C Visc Change, %	48vap	0.00	-0.02	0.06	-0.04
	Viscosity @100C, cst					
	100C Visc Change, %					
	Total Acid Number					
	% Insolubles					
Squires Tube Vapor Phase Corrosion 20% (vol) Methyl propionate	Visual Appearance of Deposits					
	Test Variations					
LUBRICANT SAMPLE SIZE TEST TEMP.	LUBRICANT PROPERTY	TEST HOURS				
		New Oil	48	48vap		
TEL-90102 (b) 56.1 grams 320°C	Viscosity @40C, cst	282.9	324.6			
	40C Visc Change, %		14.7			
	Viscosity @100C, cst	12.77	13.53			
	100C Visc Change, %		6.0			
	Total Acid Number					
	% Insolubles					
Squires Tube Vapor Phase Corrosion 20% (vol) Methyl propionate	Visual Appearance of Deposits					
	Test Variations					
LUBRICANT SAMPLE SIZE TEST TEMP.	LUBRICANT PROPERTY	CORROSION DATA, Wt. Change mg/cm				
		Test Hrs.	Al	Ag	M-St	Wasp
TEL-90102 (b) 56.1 grams 320°C	Viscosity @40C, cst	48	0.00	0.00	0.08	0.04
	40C Visc Change, %	48vap	0.00	0.04	0.02	-0.02
	Viscosity @100C, cst					
	100C Visc Change, %					
	Total Acid Number					
	% Insolubles					
Squires Tube Vapor Phase Corrosion 20% (vol) Methyl propionate	Visual Appearance of Deposits					
	Test Variations					

(a) - No initial condensate return

(b) - Condensate return throughout test

**CORROSION AND OXIDATION TEST DATA**

LUBRICANT SAMPLE SIZE TEST TEMP.	LUBRICANT PROPERTY	TEST HOURS				
		New Oil	48	48VAP		
TEL-90102 (a) 50.7 grams 320°C	Viscosity @40C, cst	282.9	331.5			
	40C Visc Change, %		17.2			
	Viscosity @100C, cst	12.77	13.54			
	100C Visc Change, %		6.0			
	Total Acid Number % Insolubles					
Visual Appearance of Deposits						
<u>Test Variations</u>						
Squires Tube Vapor Phase Corrosion 20% (VOL) 2-pentanone						
		Test Hrs.	Al	Ag	M-St	Wasp
		48	0.00	0.02	0.06	0.08
		48VAP	-0.02	0.02	-0.02	-0.02
						Ti
						0.02
						0.04
LUBRICANT SAMPLE SIZE TEST TEMP.	LUBRICANT PROPERTY	TEST HOURS				
		New Oil	48	48VAP		
TEL-90102 (b) 52.1 grams 320°C	Viscosity @40C, cst	282.9	330.6			
	40C Visc Change, %		16.8			
	Viscosity @100C, cst	12.77	13.54			
	100C Visc Change, %		6.0			
	Total Acid Number % Insolubles					
Visual Appearance of Deposits						
<u>Test Variations</u>						
Squires Tube Vapor Phase Corrosion 20% (vol) Propyl acetate						
		Test Hrs.	Al	Ag	M-St	Wasp
		48	0.02	0.00	0.02	0.02
		48VAP	0.02	-0.02	0.00	-0.02
						Ti
						0.02
						0.04

(a) - No initial condensate return  
(b) - No initial condensate return

LUBRICANT SAMPLE SIZE TEST TEMP.	LUBRICANT PROPERTY	TEST HOURS			
		New Oil	48	48VAP	
TEL-90102 (a) 53.5 grams 320°C	Viscosity @40C, cst	282.9	365.3		
	40C Visc Change, %		29.1		
	Viscosity @100C, cst	12.77	14.29		
	100C Visc Change, %		11.9		
	Total Acid Number				
	% Insolubles				
	Visual Appearance of Deposits				
<u>Test Variations</u> Squires Tube Vapor Phase Corrosion 20% (vol) 2-pentanone					
LUBRICANT SAMPLE SIZE TEST TEMP.	LUBRICANT PROPERTY	CORROSION DATA, Wt. Change mg/cm			
		Test Hrs.	Al	Ag	M-St
TEL-90102 (b) 51.1 grams 320°C	Viscosity @40C, cst	48	0.04	0.08	Wasp
	40C Visc Change, %	48VAP	0.00	0.08	0.06
	Viscosity @100C, cst				0.02
	100C Visc Change, %				0.00
	Total Acid Number				
	% Insolubles				
	Visual Appearance of Deposits				
<u>Test Variations</u> Vapor Phase Corrosion 20% (vol) Ethylbenzene					
LUBRICANT SAMPLE SIZE TEST TEMP.	LUBRICANT PROPERTY	TEST HOURS			
		New Oil	48	48vap	
TEL-90102 (b) 51.1 grams 320°C	Viscosity @40C, cst	282.9	380.7		
	40C Visc Change, %		34.5		
	Viscosity @100C, cst	12.77	14.59		
	100C Visc Change, %		14.3		
	Total Acid Number				
	% Insolubles				
	Visual Appearance of Deposits				
<u>Test Variations</u> Vapor Phase Corrosion 20% (vol) Ethylbenzene					
LUBRICANT SAMPLE SIZE TEST TEMP.	LUBRICANT PROPERTY	CORROSION DATA, Wt. Change mg/cm			
		Test Hrs.	Al	Ag	M-St
TEL-90102 (b) 51.1 grams 320°C	Viscosity @40C, cst	48	0.00	0.00	Wasp
	40C Visc Change, %	48vap	0.00	-0.08	-0.10
	Viscosity @100C, cst			0.02	0.00
	100C Visc Change, %			0.00	0.02
	Total Acid Number				
	% Insolubles				
	Visual Appearance of Deposits				
<u>Test Variations</u> Vapor Phase Corrosion 20% (vol) Ethylbenzene					

(a) - condensate return throughout test

LUBRICANT SAMPLE SIZE TEST TEMP.	LUBRICANT PROPERTY	TEST HOURS			
TEL-90102 (a) 58.0 grams 320°C	Viscosity @40C, cst	New Oil	48	48VAP	
	40C Visc Change, %	282.9	335.1		
	Viscosity @100C, cst		18.4		
	100C Visc Change, %	12.77	13.68		
	Total Acid Number		7.1		
	% Insolubles				
	Visual Appearance				
	of Deposits				
	Test Variations				
	Squires Tube				
CORROSION DATA, Wt. Change mg/cm					
Squires Tube Vapor Phase Corrosion 20% (vol) Ethylbenzene	Test Hrs.	Al	Ag	M-St	M-50
	48	0.02	-0.08	0.02	0.04
	48VAP	-0.02	0.04	0.06	0.00
Ti					
TEL-90102 (b) 49.6 grams 320°C	Viscosity @40C, cst	New Oil	48	48vap	
	40C Visc Change, %	282.9	344.2		
	Viscosity @100C, cst		21.6		
	100C Visc Change, %	12.77	13.83		
	Total Acid Number		8.3		
	% Insolubles				
	Visual Appearance				
	of Deposits				
	Test Variations				
	Squires Tube				
CORROSION DATA, Wt. Change mg/cm					
Squires Tube Vapor Phase Corrosion 20% (vol) Butyl propionate	Test Hrs.	Al	Ag	M-St	M-50
	48	0.02	0.00	0.06	0.00
	48vap	0.00	0.00	0.02	0.00
Ti					
	Wasp				
	0.00				
	0.00				

381

LUBRICANT SAMPLE SIZE TEST TEMP.	LUBRICANT PROPERTY	New Oil	48	48vap	TEST HOURS
TEL-90102 (a) 51.9 grams  320°C	Viscosity @40C,cst	282.9	332.1		
	40C Visc Change, %		17.4		
	Viscosity @100C,cst	12.77	13.59		
	100C Visc Change, %		6.4		
	Total Acid Number				
	% Insolubles				
Visual Appearance of Deposits					
<u>Test Variations</u>					
Squires Tube					
Vapor Phase Corrosion					
20% (vol) Butyl propionate					
CORROSION DATA, Wt. Change mg/cm					
	Test Hrs.	Al	Aq	M-St	Wasp
	48	-0.06	-0.04	0.00	0.00
	48vap	-0.04	-C.02	0.02	0.00
					Ti
					0.02
					-0.02
LUBRICANT SAMPLE SIZE TEST TEMP.	LUBRICANT PROPERTY	New Oil	48	48vap	TEST HOURS
TEL-90102 (b) 49.8 grams  320°C	Viscosity @40C,cst	282.9	331.9		
	40C Visc Change, %		17.3		
	Viscosity @100C,cst	12.77	13.55		
	100C Visc Change, %		6.1		
	Total Acid Number				
	% Insolubles				
Visual Appearance of Deposits					
<u>Test Variations</u>					
Squires Tube					
Vapor Phase Corrosion					
20% (vol) Propyl acetate					
CORROSION DATA, Wt. Change mg/cm					
	Test Hrs.	Al	Aq	M-St	Wasp
	48	0.00	0.00	0.02	0.02
	48vap	0.00	0.00	0.02	0.02
					Ti
					0.00
					-0.02

**(a) - No initial condensate return**

## CORROSION AND OXIDATION TEST DATA

LUBRICANT SAMPLE SIZE TEST TEMP.	LUBRICANT PROPERTY	TEST HOURS				
		New Oil	48			
TEL-90102 (a) 32.4 grams 320 C	Viscosity @40C, cst	282.9	407.7			
	40C Visc Change, %		44.1			
	Viscosity @100C, cst	12.77	15.17			
	100C Visc Change, %		18.8			
	Total Acid Number					
	% Insolubles					
	Visual Appearance of Deposits		M-st and M-50 black			
Test Variations						
Rolling 4-ball test #0003 unfilt						
CORROSION DATA, Wt. Change mg/cm						
		Test Hrs.	Al	Ag	M-St	Wasp
		48	0.04	0.00	0.14	0.08
						Ti
						0.04
TEST HOURS						
TEL-90102 34.7 grams 320 C	Viscosity @40C, cst	New Oil	24			
	40C Visc Change, %	112.5	-			
	Viscosity @100C, cst	8.83	-			
	100C Visc Change, %		-			
	Total Acid Number	0.00	15.84			
	% Insolubles					
	Visual Appearance of Deposits					
Test Variations						
Squires Tube 20% TPP						
CORROSION DATA, Wt. Change mg/cm						
		Test Hrs.	Al	Ag	M-St	Wasp
		24	0.54	-2.64	0.72	0.42
						Ti
						0.20

(a) - blk. deposits located at half in. from oil surface

# CORROSION AND OXIDATION TEST DATA

LUBRICANT SAMPLE SIZE TEST TEMP.	LUBRICANT PROPERTY	TEST HOURS				
		New Oil	24			
TEL-90102  59.0 grams  320 C	Viscosity @40C, cst	112.6	-			
	40C Visc Change, %		-			
	Viscosity @100C, cst	9.6	-			
	100C Visc Change, %		-			
	Total Acid Number	0.00	20.4			
	% Insolubles					
	Visual Appearance of Deposits					
Test Variations						
Squires Tube 20ATPP						
		CORROSION DATA, Wt. Change mg/cm				
		Test Hrs.	Al	Ag	M-St	Wasp
		24	1.44	6.84	0.48	0.46
						Ti
						0.08
TEST HOURS						
TEL-90102  53.6 grams  320 C	Viscosity @40C, cst	New Oil	48			
	40C Visc Change, %	282.9	327.5			
	Viscosity @100C, cst	12.77	15.7			
	100C Visc Change, %		13.46			
	Total Acid Number		5.4			
	% Insolubles					
	Visual Appearance of Deposits					
Test Variations						
Squires Tube						
		CORROSION DATA, Wt. Change mg/cm				
		Test Hrs.	Al	Ag	M-St	Wasp
		48	0.00	-0.04	0.00	-0.02
						Ti
						0.00

# CORROSION AND OXIDATION TEST DATA

LUBRICANT SAMPLE SIZE TEST TEMP.	LUBRICANT PROPERTY	TEST HOURS				
		New Oil	24			
TEL-90102 (a) 34.4 grams 320 C	Viscosity @40C, cst	239.5				
	40C Visc Change, %					
	Viscosity @100C, cst	11.78				
	100C Visc Change, %					
	Total Acid Number					
	% Insolubles					
	Visual Appearance of Deposits		heavy coke granular deposits			
CORROSION DATA, Wt. Change mg/cm						
		Test Hrs.	Al	Ag	M-St	Wasp
		24	0.72	-0.06	0.86	0.12
						Ti
						0.58
LUBRICANT SAMPLE SIZE TEST TEMP.	LUBRICANT PROPERTY	TEST HOURS				
		New Oil	24			
TEL-90102 34.9 grams 320 C	Viscosity @40C, cst	206.6				
	40C Visc Change, %					
	Viscosity @100C, cst	10.45				
	100C Visc Change, %					
	Total Acid Number	0.02	2.31			
	% Insolubles					
	Visual Appearance of Deposits					
CORROSION DATA, Wt. Change mg/cm						
		Test Hrs.	Al	Ag	M-St	Wasp
		24	0.34	0.68	0.36	0.10
						Ti
						0.06

(a) - oil too thick to test

## CORROSION AND OXIDATION TEST DATA

LUBRICANT SAMPLE SIZE TEST TEMP.	LUBRICANT PROPERTY	TEST HOURS					
		New Oil	48				
TEL-90102 42.2 grams 320 C	Viscosity @40C, cst	282.9	340.2				
	40C Visc Change, %		20.2				
	Viscosity @100C, cst	12.77					
	100C Visc Change, %						
	Total Acid Number						
	% Insolubles						
	Visual Appearance of Deposits						
Test Variations							
Squires Tube							
CORROSION DATA, Wt. Change mg/cm							
		Test Hrs.	Al	Ag	M-St	M-50	Ti
		48	0.00	0.00	0.04	0.02	0.00
TEST HOURS							
TEL-90102 33.0 grams 320 C	Viscosity @40C, cst	New Oil	48				
	40C Visc Change, %						
	Viscosity @100C, cst						
	100C Visc Change, %						
	Total Acid Number						
	% Insolubles						
	Visual Appearance of Deposits						
Test Variations							
Squires Tube							
CORROSION DATA, Wt. Change mg/cm							
		Test Hrs.	Al	Ag	M-St	M-50	Ti
		48	0.00	0.00	0.08	0.00	0.00
						-0.02	0.00

# CORROSION AND OXIDATION TEST DATA

LUBRICANT SAMPLE SIZE TEST TEMP.	LUBRICANT PROPERTY	TEST HOURS				
		New Oil	48			
TEL-90102 (a) 53.2 grams 320 C	Viscosity @40C, cst	299.4	455.4			
	40C Visc Change, %		52.1			
	Viscosity @100C, cst	10.69	15.67			
	100C Visc Change, %		46.6			
	Total Acid Number	0.00	0.03			
	% Insolubles					
	Visual Appearance of Deposits					
Test Variations						
Squires Tube Filtered with silver membrane						
CORROSION DATA, Wt. Change mg/cm						
		Test Hrs.	Al	Ag	M-St	Wasp
		48	0.00	0.00	0.06	0.02
						0.02
Ti						
0.02						
LUBRICANT						
SAMPLE SIZE TEST TEMP.	LUBRICANT	TEST HOURS				
	PROPERTY	New Oil	48			
TEL-90102 53.8 grams 320 C	Viscosity @40C, cst	314.2	378.1			
	40C Visc Change, %		20.3			
	Viscosity @100C, cst	10.87	14.35			
	100C Visc Change, %		32.0			
	Total Acid Number	0.01	0.0			
	% Insolubles					
	Visual Appearance of Deposits					
Test Variations						
Squires Tube Recovered from mini-simulator						
CORROSION DATA, Wt. Change mg/cm						
		Test Hrs.	Al	Ag	M-St	Wasp
		48	0.02	0.02	0.04	0.00
						0.00
						0.00

(a) - Recovered from mini-simulator

**CORROSION AND OXIDATION TEST DATA**

LUBRICANT SAMPLE SIZE TEST TEMP.	LUBRICANT PROPERTY	TEST HOURS				
		New Oil	48	VAP48		
TEL-91001 (a) 52.9 grams 320°C	Viscosity @40C, cst	10.25	10.71			
	40C Visc Change, %		4.5			
	Viscosity @100C, cst	2.54	2.59			
	100C Visc Change, %		2.0			
	Total Acid Number					
Squires Tube Vapor Phase Corrosion With 50% Diphenyl ether	% Insolubles					
	Visual Appearance of Deposits					
	Test Variations					
CORROSION DATA, Wt. Change mg/cm						
Test Hrs.	Al	Ag	M-St	M-50	Wasp	Ti
48	-0.02	-0.06	-0.02	0.00	-0.02	0.00
VAP48	0.00	-0.04	-0.06	-0.04	0.00	0.00
TEST HOURS						
New Oil	48	48vap				
10.25	10.88					
	6.2					
2.54	2.65					
	4.3					
CORROSION DATA, Wt. Change mg/cm						
Test Hrs.	Al	Ag	M-St	M-50	Wasp	Ti
48	0.00	-0.04	0.06	0.00	-0.04	0.00
48vap	-0.04	-0.10	-0.06	-0.04	-0.04	-0.04

- (a) - VAPOR PHASE TEST  
(b) - Temperature of oil monitored; Repeat of test #141

## CORROSION AND OXIDATION TEST DATA

LUBRICANT SAMPLE SIZE TEST TEMP.	LUBRICANT PROPERTY	TEST HOURS					
TEL-91001  39.8 grams  320°C	New Oil	48	240				
	Viscosity @40C, cst	289.2	300.2	332.2			
	40C Visc Change, %	3.8	14.9				
	Viscosity @100C, cst	12.67	12.96	13.43			
	100C Visc Change, %	2.3	6.0				
	Total Acid Number						
% Insolubles			0.098				
Visual Appearance of Deposits							
CORROSION DATA, Wt. Change mg/cm							
	Test Hrs.	Al	Ag	M-St	M-50	Wasp	Ti
	240	0.26	0.02	0.20	0.20	0.00	0.04
LUBRICANT SAMPLE SIZE TEST TEMP.	LUBRICANT PROPERTY	TEST HOURS					
TEL-91001  50.3 grams  320°C	New Oil	48	VAP48				
	Viscosity @40C, cst	11.05	11.53				
	40C Visc Change, %	4.3					
	Viscosity @100C, cst	2.81	2.88				
	100C Visc Change, %	2.5					
	Total Acid Number						
% Insolubles							
Visual Appearance of Deposits	Visc.-30F	12766	(initial)				
	Visc.-30F	16792	(48 hrs.)				
	-30F Visc	Chg=31.5%					
CORROSION DATA, Wt. Change mg/cm							
Test Variations	Test Hrs.	Al	Ag	M-St	M-50	Wasp	Ti
	48	-0.02	-0.12	0.12	0.04	0.00	-0.02
	VAP48	-0.04	0.00	0.00	0.02	-0.04	0.00
Squires Tube							
Vapor Phase Corrosion							
50% Diphenyl sulfide							

## CORROSION AND OXIDATION TEST DATA

LUBRICANT SAMPLE SIZE TEST TEMP.	LUBRICANT PROPERTY	TEST HOURS						
		New Oil	24	72	123	192	310	
TEL-91001 63.7 grams 340 C	Viscosity @40C, cst	289.2	300.2	319.8	344.1	390.5	497.9	
	40C Visc Change, %		3.8	10.6	19.0	35.0	72.2	
	Viscosity @100C, cst	12.67	12.94	13.31	13.73	14.45	17.11	
	100C Visc Change, %		2.1	5.1	8.4	14.1	35.0	
	Total Acid Number % Insolubles	0.00					0.00	
	Visual Appearance of Deposits						GRAY DEP ON GLASS & METAL	
CORROSION DATA, Wt. Change mg/cm								
	Test Hrs.	Al	Ag	M-St	M-50	Wasp	Ti	
	310	0.00	0.00	0.22	0.30	0.04	0.04	
LUBRICANT SAMPLE SIZE TEST TEMP.	LUBRICANT PROPERTY	TEST HOURS						
		New Oil	24	48	72	110	131	145
TEL-91001 65.1 grams 350 C	Viscosity @40C, cst	289.2	305.4	334.0	379.7	429.8	464.8	492.6
	40C Visc Change, %		5.6	15.5	31.3	48.6	60.7	70.3
	Viscosity @100C, cst	12.67	13.04	13.61	14.25	15.11	15.55	15.92
	100C Visc Change, %		2.9	7.4	12.5	19.3	22.7	25.7
	Total Acid Number % Insolubles	0.00						0.00
	Visual Appearance of Deposits						GRAY DEP	
CORROSION DATA, Wt. Change mg/cm								
	Test Hrs.	Al	Ag	M-St	M-50	Wasp	Ti	
	145	0.00	-0.06	0.30	0.14	-0.04	0.00	

**CORROSION AND OXIDATION TEST DATA**

LUBRICANT SAMPLE SIZE TEST TEMP.	LUBRICANT PROPERTY	TEST HOURS					
		New Oil	24	48	98	120	
TEL-91001 (a) 63.2 grams 360 C	Viscosity @40C, cst	289.2	314.4	350.1	469.5	527.8	
	40C Visc Change, %		8.7	21.1	62.3	82.5	
	Viscosity @100C, cst	12.67	13.33	13.94	15.64	16.43	
	100C Visc Change, %		5.2	10.0	23.4	29.7	
	Total Acid Number % Insolubles	0.00				0.00	
	Visual Appearance of Deposits					deposit in oil	
CORROSION DATA, Wt. Change mg/cm							
		Test Hrs.	Al	Ag	M-St	Wasp	Ti
		120	-0.02	0.00	0.14	0.22	-0.04
LUBRICANT SAMPLE SIZE TEST TEMP.	LUBRICANT PROPERTY	TEST HOURS					
		New Oil	48	96	144	216	
	Viscosity @40C, cst	215.3	218.0	232.3	253.3	405.6	
	40C Visc Change, %		1.3	7.9	17.6	88.4	
	Viscosity @100C, cst	10.91	10.88	11.42	12.17	16.40	
TEL-92026 (b) 72.5 grams 240 C	100C Visc Change, %		0.0	4.7	11.6	50.3	
	Total Acid Number % Insolubles						
	Visual Appearance of Deposits						
CORROSION DATA, Wt. Change mg/cm							
		Test Hrs.	Al	Ag	M-St	Wasp	Ti
		216	0.24	2.70	2.50	1.10	0.80
Test Variations							
Squires Tube							
Nickel set-up, TEFLON condenser							

- (a) - Thermocouple in fluid  
(b) - test discontinued, power out

## CORROSION AND OXIDATION TEST DATA

LUBRICANT SAMPLE SIZE TEST TEMP.	LUBRICANT PROPERTY	TEST HOURS				
		New Oil	72	144		
TEL-92026 75.1 grams 260°C	Viscosity @40C, cst	215.3	226.9	644.5		
	40C Visc Change, %		5.4	199.4		
	Viscosity @100C, cst	10.91	11.38	21.8		
	100C Visc Change, %		4.3	99.8		
	Total Acid Number % Insolubles					
Visual Appearance of Deposits						
Test Variations						
Squires Tube Nickel set-up; TEFLON condenser		CORROSION DATA, Wt. Change mg/cm				
		Test Hrs.	Al	Ag	M-St	Wasp
		144	0.14	-0.16	0.16	0.10
						Ti 0.10
TEST HOURS						
TEL-92026 75.8 grams 260°C	Viscosity @40C, cst	215.3	258.1	359.0	602.6	END
	40C Visc Change, %		19.9	66.7	180	
	Viscosity @100C, cst	10.91	12.29	15.26	21.34	
	100C Visc Change, %		12.6	39.9	95.6	
	Total Acid Number % Insolubles					
Visual Appearance of Deposits						
Test Variations						
Squires Tube Nickel tube; TEFLON condenser		CORROSION DATA, Wt. Change mg/cm				
		Test Hrs.	Al	Ag	M-St	Wasp
		125	0.38	0.02	0.38	0.18
						Ti 0.12

## CORROSION AND OXIDATION TEST DATA

LUBRICANT SAMPLE SIZE TEST TEMP.	LUBRICANT PROPERTY	TEST HOURS				
		New Oil	48			
TEL-92026 (a) 50.3 grams 280°C	Viscosity @40C, cst	215.3	232.6			
	40C Visc Change, %		8.0			
	Viscosity @100C, cst	10.91	11.53			
	100C Visc Change, %		5.7			
	Total Acid Number	0.00	0.39			
	% Insolubles					
	Visual Appearance of Deposits					
Test Variations						
Squires Tube						
Nitrogen						
Dry Nitrogen						
CORROSION DATA, Wt. Change mg/cm						
	Test Hrs.	Al	Ag	M-St	M-50	Wasp
	48	-0.02	0.00	0.00	0.02	0.00
	Ti					0.00
LUBRICANT						
TEL-92026 (b) 48.3 grams 280°C	Viscosity @40C, cst	215.3	233.5			
	40C Visc Change, %		8.5			
	Viscosity @100C, cst	10.91	11.48			
	100C Visc Change, %		5.2			
	Total Acid Number	0.00	0.61			
	% Insolubles					
	Visual Appearance of Deposits					
Test Variations						
Squires Tube						
Nitrogen						
Wet Nitrogen						
CORROSION DATA, Wt. Change mg/cm						
	Test Hrs.	Al	Ag	M-St	M-50	Wasp
	48	0.00	-0.44	-0.02	0.04	0.02
	Ti					0.02

(a) - Nickel Tube and Aerator, TEFLON Condenser

(b) - Nickel Tube and Aerator, TEFLON Condenser

**CORROSION AND OXIDATION TEST DATA**

LUBRICANT SAMPLE SIZE TEST TEMP.	LUBRICANT PROPERTY	TEST HOURS				
		New Oil	48			
TEL-92026 (a) 49.7 grams 280°C	Viscosity @40C, cst	215.3	264.9			
	40C Visc Change, %		23.1			
	Viscosity @100C, cst	10.91	12.91			
	100C Visc Change, %		18.3			
	Total Acid Number	0.00	1.01			
	% Insolubles					
Visual Appearance of Deposits						
Test Variations						
Squires Tube						
No Condensate Return						
CORROSION DATA, Wt. Change mg/cm						
		Test Hrs.	Al	Ag	M-St	M-50
		48	-0.02	-0.66	0.02	0.02
						Wasp
						0.00
						Ti
						-0.02
TEST HOURS						
TEL-92026 (b) 50.8 grams 280°C	Viscosity @40C, cst	215.3	230.0			
	40C Visc Change, %		6.9			
	Viscosity @100C, cst	10.91	11.36			
	100C Visc Change, %		4.1			
	Total Acid Number	0.00	0.62			
	% Insolubles					
Visual Appearance of Deposits						
Test Variations						
Squires Tube						
CORROSION DATA, Wt. Change mg/cm						
		Test Hrs.	Al	Ag	M-St	M-50
		48	0.02	-0.64	0.04	0.04
						Wasp
						0.02
						Ti
						0.02

- (a) - Nickel tube and aerator  
(b) - Nickel tube and aerator , TEFLON condenser

**CORROSION AND OXIDATION TEST DATA**

LUBRICANT SAMPLE SIZE TEST TEMP.	LUBRICANT PROPERTY	TEST HOURS				
		New Oil	48			
TEL-92026 (a) 50.5 grams 280°C	Viscosity @40C, cst	215.3	228.2			
	40C Visc Change, %		6.0			
	Viscosity @100C, cst	10.91	11.33			
	100C Visc Change, %		3.9			
	Total Acid Number % Insolubles	0.00	0.50			
Squires Tube	Visual Appearance of Deposits					
	Test Variations					
CORROSION DATA, Wt. Change mg/cm						
		Test Hrs.	Al	Ag	M-St	M-50
		48	-0.02	-1.00	-0.02	0.00
						Wasp
						0.02
						Ti
						0.00
TEST HOURS						
TEL-92026 (b) 77.1 grams 280°C	Viscosity @40C, cst	New Oil	48	96	120	168
	40C Visc Change, %	215.3	220.2	302.6	442.2	1182
	Viscosity @100C, cst		2.3	40.6	105.4	449
	100C Visc Change, %	10.91	10.97	13.72	17.75	31.85
	Total Acid Number % Insolubles	0.00	0.6	25.8	62.7	192
Squires Tube	Visual Appearance of Deposits					
	Test Variations					
CORROSION DATA, Wt. Change mg/cm						
		Test Hrs.	Al	Ag	M-St	M-50
		168	0.00	-1.00	0.00	-0.04
						Wasp
						-0.02
						Ti
						0.00

(a) - Nickel Tube and Aerator, TEFLON Condenser  
(b) - Intermediate sampling

TABLE A-3  
AFAPL STATIC COKEP TEST DATA  
SPECIMEN TYPE USED: 1 = SHIM STOCK; 2 = SS-302; 3 = SILVER

Test #	Oil	Specimen	Temp, C	Time, Min	Size, g	Specimen mg/g		Seal mg/g		Average		Std Dev	Total mg/g		Average	Std Dev	Description of coke
						Residue	Residue	Residue	Residue				Residue	Residue			
407	TEL-91001	2	400	100	0.69	0.43	0	0	0	0	0		0.43	0	0		Stainless seals
408		2			0.72	0.20	0	0	0	0	0		0.20	0	0		Light gold varnish
409		2			0.71	0.14	0	0	0	0	0		0.14	0	0		Stainless seals
410	0-66-20 408 320	2	400	100	0.71	0.39	0	0	0	0	0		0.39	0	0		Stainless seals
411		2			0.75	0.27	0	0	0	0	0		0.27	0	0		Light gold varnish
412		2			0.72	0.26	0.13	0.13	0.13	0.07	0.07		0.27	0.13	0.11		Stainless seals
413		2			0.75	0	0	0	0	0	0		0	0	0		Light gold varnish
414	TEL-90103	2	300	100	0.82	14.5	3.39	3.39	3.39	3.09	3.09		17.09	21.03	10.00		Stainless seals
415		2			0.48	16.24	2.69	2.69	2.69	3.09	3.09		16.32	17.06	2.07		Dark varnish
416		2			0.48	13.62	2.30	2.30	2.30	3.09	3.09		12.14	12.06	2.07		Stainless seals
417		2			0.48	13.97	2.30	2.30	2.30	3.09	3.09		12.06	12.06	2.07		Dark, even varnish
418	TEL-90104	2	300	100	0.85	9.69	2.30	2.30	2.30	3.09	3.09		13.01	13.01	11.72		Stainless seals
419		2			0.55	9.22	7.52	7.52	7.52	1.72	1.72		15.1	15.1	1.49		Thin varnish
420	TEL-91003	2	300	240	0.82	9.49	6.81	6.81	6.81	0.04	0.04		16.34	16.34	1.49		Stainless seals
421		2			0.52	9.7	6.31	6.31	6.31	1.72	1.72		18.97	18.97	4.09		Thin varnish
422		2			0.51	9.26	7.82	7.82	7.82	2.33	2.33		21.35	21.35	1.04		Stainless seals
423	TEL-91005	2	300	240	0.45	8.72	9.06	9.06	9.06	2.75	2.75		14.03	14.03	1.04		Dark seal
424		2			0.54	9.11	14.51	14.51	14.51	2.05	2.05		11.20	11.20	1.04		Stainless seals
425		2			0.48	7.05	12.40	12.40	12.40	8.62	8.62		17.00	17.00	1.27		Dark varnish
426		2			0.47	15.23	3.69	3.69	3.69	2.75	2.75		24.89	24.89	0.9		TEL-90105 seals
427	TEL-90104	2	300	240	0.34	10.94	3.97	3.97	3.97	7.49	7.49		26.04	26.04	3.2		Dark varnish
428		2			0.5	9.93	9.38	9.38	9.38	1.43	1.43		24.15	24.15	17.48		TEL-90105 seals
429		2			0.52	10.9	7.81	7.81	7.81	7.09	7.09		19.76	19.76	2.7		Varnish
430	TEL-90103	2	300	240	0.51	7.23	7.81	7.81	7.81	1.18	1.18		1.75	1.75	1.39		Stainless seals
431		2			0.51	7.63	8.45	8.45	8.45	0.63	0.63		1.1	1.1	0.44		Gold varn, coke spots
432		2			0.49	8.64	9.23	9.23	9.23	0.97	0.97		1.92	1.92			
433		2			0.51	8.31	9.98	9.98	9.98	0.77	0.77						
434		2			0.45	8.31	9.98	9.98	9.98	0.82	0.82						
435		2			0.53	19.19	5.7	5.7	5.7	0.63	0.63						
436	TEL-90103	2	300	240	0.53	16.72	9.19	9.19	9.19	0.63	0.63						
437		2			0.54	10.49	7.55	7.55	7.55	0.63	0.63						
438		2			0.52	16.62	17.76	17.76	17.76	0.63	0.63						
439	0-85-1	2	300	240	0.53	10.54	9.22	9.22	9.22	0.63	0.63						
440		2			0.53	11.20	4.25	4.25	4.25	0.63	0.63						
441		2			0.51	9.79	10.73	10.73	10.73	0.63	0.63						
442		2			0.55	9.82	6.85	6.85	6.85	0.63	0.63						
443	TEL-91003	2	300	240	0.53	13.91	5.76	5.76	5.76	0.63	0.63						
444		2			0.63	9.75	5.76	5.76	5.76	0.63	0.63						
445		2			0.36	15.12	5.76	5.76	5.76	0.63	0.63						
446		2			0.51	15.77	2.94	2.94	2.94	0.63	0.63						
447	0-66-20	2	375	240	0.51	1.02	0.47	0.47	0.47	0.63	0.63						
448		2			0.5 ml	0.47	0.63	0.63	0.63	0.63	0.63						
449		2			0.5 ml	0.47	0.63	0.63	0.63	0.63	0.63						
450		2			0.5 ml	0.97	0.97	0.97	0.97	0.63	0.63						

# STATIC COKER TEST DATA

Test #	Oil	Specimen	Temp, C	Time, Min	Size, g	Specimen mg/g Residue	Average	Std Dev	Seal mg/g Residue	Average	Std Dev	Total mg/g Residue	Average	Std Dev	Description of coke
451	TEL-90104	2	300	240	0.58	11.31	12.52	1.52	2.57	3.25	1.39	13.88	15.76	2.88	TEFLON seals
452		2			0.47	12.02			2.32			14.33			Thick coke
453		2			0.64	14.23			4.85			19.07			TEFLON seals
454	O-86-2	2	300	240	0.64	25.86			3.29			29.15			Thick coke
455		2			0.61	31.52			4			35.51			TEFLON seals
456		2			0.61	30.26	29.21	2.97	3.62	3.64	0.35	33.88	32.85	3.3	Thick coke
457	TEL-91005	2	300	240	0.54	16.06			7.01			23.05			TEFLON seals
458		2			0.54	16.17			2.04			18.22			Thick coke
459		2			0.54	15.64	15.95	0.28	9.97	6.31	3.96	25.51	22.26	3.71	Stainless seals
460	WT 617 O-64-20	2	375	240	0.66	1.07			0.46			1.52			Stainless seals
461		2			0.79	1.02			0.51			1.53			Stainless seals
462		2			0.78	1.16	1.08	0.07	0.39	0.45	0.06	1.54	1.53	0.01	Stainless seals
463	O-64-20	2	375	240	0.65	0.3			0			0.3			Golden varnish
464		2			0.67	0.15			0			0.15			Stainless seals
465		2			0.62	0.16	0.21	0.09	0	0	0	0.16	0.21	0.09	Golden varnish
466	O-64-20 MCR	2	375	240	0.51	0.98			0			0.98			Stainless seals
467	48B 320C	2	375	240	0.57	0.88			0			0.88			Stainless seals
468		2			0.53	0.94	0.93	0.05	0	0	0	0.94	0.83	0.05	Specks of coke
469	TEL-91005	2	300	240	0.5 ml	12.3			6.7			19.02			TEFLON seals
470		2			0.5 ml	9.36			2.97			11.23			TEFLON seals
471		2			0.5 ml	9.05	9.9	2.1	2.22	3.93	2.42	11.27	13.84	4.49	TEFLON seals
472	O-90-6	2	300	240	0.5 ml	10.07			5.13			15.19			Stainless seals
473		2			0.5 ml	12.21			4.74			16.95			Stainless seals
474		2			0.5 ml	10.88	11.05	1.08	4.66	4.48	0.25	15.55	15.9	0.93	Stainless seals
475	O-64-20312H 290	2	375	180	0.59	1.02			0.68			1.69			Specks of coke
476		2			0.64	0.78			0.93			1.71			Stainless seals
477		2			0.61	0.82	0.87	0.13	1.15	0.92	0.24	1.96	1.79	0.15	Specks of coke
478	O-64-20240H 290	2	375	180	0.46	0.86			0.86			1.73			Stainless seals
479		2			0.49	0.82			1.02			1.84			Stainless seals
480		2			0.61	0.92	0.83	0.03	0.92	0.9	0.1	1.65	1.73	0.1	Specks of coke
481	O-64-20144H 290	2	375	180	0.5	0.95			0.95			1.9			Stainless seals
482		2			0.47	0.43	0.94	0.07	0.6	0.78	0.25	1.6	1.75	0.21	Stainless seals
483	O-64-20 72H 290	2	375	180	0.53	0.75			0.64			1.07			Stainless seals
484		2			0.55	0.54	0.57	0.17	0.54	0.65	0.11	1.08	1.22	0.25	Stainless seals
485	O-64-20	2	350	180	0.49	0			0			0			Stainless seals
486		2			0.55	0			0			0			Stainless seals
487		2			0.47	0			0			0			Stainless seals
488	O-91-13	2	300	180	0.38	6.79			14.37			21.16			Stainless seals
489		2			0.45	5.76			15.6			21.39			Coke and varnish
490		2			0.35	5.15	5.91	0.83	18.9	16.29	2.34	24.06	22.2	1.61	TEFLON seals
491	O-91-13	2	300	180	0.35	11.46			28.65			40.1			Stainless seals
492		2			0.36	9.96			14.67			24.63			Ring dk, brown coke
493		2			0.42	10.61	10.68	0.75	12.03	18.45	8.93	22.44	29.12	9.56	TEFLON seals
494	TEL-91053	2	300	180	0.48	12.95			8.53			21.3			Stainless seals
495		2			0.49	14.59			10.51			25.46			Heavy coke
496		2			0.5	13.59	13.83	1.03	8.39	9.08	1.24	21.99	22.92	2.23	
497		2			0.5	13.59			8.39			21.99			

# STATIC COKER TEST DATA

Test #	Oil	Specimen	Temp, C	Time, Min	Size, g	Specimen mp/g			Seal mp/g			Total mp/g			Description of coke		
						Residue	Average	Std Dev	Residue	Average	Std Dev	Residue	Average	Std Dev			
498	O-86-2	2	300	180	0.4	27.22	27.56	1.09	0.24	0.38	1.06	35.46	35.94	0.92	THYLON seals		
499					0.39	29.6			7.4			37			Ring dk, brown coke		
500					0.41	25.06			9.51			35.37	35.94	0.92	THYLON seals		
501	TEL-90104	2	300	180	0.46	12.95			3.95			16.9					
502					0.49	12.69			2.25			14.94					
503					0.44	14.2			2.40			16.68	16.17	1.07	Heavy coke		
504	TEL-90103	2	300	180	0.37	10.67			16.13			26.82			THYLON seals		
505					0.4	12.02			14.27			26.3	26.56	0.37	Rings of coke		
506	O-85-1	2	300	180	0.47	10.67			8.75			19.42			THYLON seals		
507					0.39	8.49			13.37			21.86	20.64	1.73	Heavy coke		
508	O-90-6	2	300	180	0.45	9.46			9.83			15.39			THYLON seals		
509					0.45	10.03			6.13			17.16					
510					0.47	9.62			5.94			19.45					
511					0.49	10.42			7.13			16.55	17.41	1.71	Heavy dk, brown coke		
512	TEL-91005	2	300	180	0.52	15.05			14.28			29.33			THYLON seals		
513					0.44	13.98			16.28			30.26					
514					0.47	13.85			11.35			27.19	28.93	1.57	Heavy dk, brown coke		
515	TEL-91003	2	300	180	0.45	13.27			6.86			20.13			THYLON seals		
516					0.5	14.41			11.61			24.03					
517					0.5	13.68			9.66			23.34	23.17	2.95	Heavy coke		
518	O-64-20	2	375	180	0.5	0			0.2			0.7			Stainless seals		
519					0.43	0.47			0.23			0.42	0.44	0.25			
520					0.48	0			0.22			0.63			Stainless seals		
521	O-64-20	2	375	180	0.48	0.42			0.21			2					
522	OC, 24h, 320C				0.45	1.11			0.09			1.03	1.22	0.71	Specs of coke		
523					0.58	0.86			0.17			2.01			Stainless seals		
524	O-64-20	2	375	180	0.4	0.84			1.17			2.48					
525	OC, 48h, 320C				0.41	0.99			1.49			1.55					
526					0.39	0.86			0.69			1.43	1.87	0.47	Specs of coke		
527	WT 617	2	375	180	0.55	0.72			0.72			1.5			Stainless seals		
528					0.57	1.5			0			2.3					
529	O-64-20	2	375	180	0.52	1.91			0.38			1.39	1.73	0.5	Specs of coke		
530					0.5	1.19			0.2			1.96			Stainless seals		
531	WT 617	2	375	180	0.56	1.07			0.09			1.65					
532	O-64-20	2	375	180	0.54	1.65			0			1.67	1.76	0.14	Specs of coke		
533					0.48	1.67			0			1.74			Stainless seals		
534					0.46	1.09			0.65			0					
535	WT 633	2	375	180	0.53	0			0			0					
536	O-64-20				0.53	0			0			0			No coke		
537					0.52	0			0			0	0	0	Stainless seals		
538					0.55	0			0			0					
539	WT 635	2	375	180	0.56	0			0			0			No coke		
540	O-64-20				0.66	0			0			0	0	0	Stainless seals		
541					0.56	0			0			0					
542					0.58	0			0			0			No coke		
543	O-64-20	3	375	180	0.62	0.64			0.32			0.96	1.07	0.39	Specs of coke		
544					0.62	0.43			0.43			0.87			Stainless seals		
545					0.53	0.64			0.16			0.8					
546					0.61	1.15			0.49			1.64					

# STATIC COKER TEST DATA

Test #	Oil	Specimen	Temp, C	Time, Min	Size, g	Specimen mg/g Residue	Average	Std Dev	Seal mg/g Residue	Average	Std Dev	Total mg/g Residue	Average	Std Dev	Description of cokes
547	0-64-20 *	3	375	100	0.47	3.16	2.95		2.95			6.12			Stainless seals
548	OC, 48h, 320C				0.49	3.04	3.00		3.00			6.74			
549	Ag coupon only				0.5	2.99	3.38		3.38			5.97			
550	0-64-20	3	375	100	0.55	3.00	3.00	0.44	3.00	3.5		7.06	6.47	0.51	Feu specks of coke Stainless seals
551	+1.35% DPMH **				0.63	0.48	0		0			0.48			
552	0-64-20	3	375	100	0.90	0.52	0		0			0.52			
553	+1.35% DPMH **				0.65	0.46	0		0			0.46			No coke Stainless seals
554	0-64-20 *	3	375	100	0.60	3.14	1.05		1.05			2.92			
555	OC, 96h, 320C				0.51	2.92	0		0			3.17			
556	+1.35% DPMH **				0.5	2.30	0.79		0.79			3.25	3.20	0.55	Feu specks bl coke Stainless seals
557	Ag coupon only	3	375	100	0.61	1.79	1.66	0.62	1.66	0.83		0.36			
558	0-64-20				0.56	0.34	0		0			0.75			
559					0.66	0.75	0		0			0.59			
560					0.51	0.30	0		0			0.47	0.34	0.17	No coke Stainless seals
561	0-64-20 *	2	375	100	0.63	0.47	0		0			0.92			
562	OC, 48h, 320C				0.49	4.08	2.44		2.44			6.35			
563	+1.35% DPMH **				0.49	3.07	3.28		3.28			5.31			
564	Ag coupon only				0.54	4.77	0.74	1.10	0.74	1.9		5.67	6.11	0.65	Small amt brown coke Stainless seals
565	0-64-20	2	375	100	0.53	4.53	1.13		1.13			1.69			
566	0-64-20 *				0.47	0.35	0.85		0.85			2.13			
567	OC, 48h, 320C				0.52	0.76	0.76		0.76			1.53			
568	Ag coupon only				0.53	0.30	0.30	0.22	0.30	0.71		0.76	1.53	0.57	Feu specks bl coke Stainless seals
570	0-64-20 *	2	325	100	0.51	3.71	4.3		4.3			8.01			
571	OC, 48h, 320C				0.48	2.74	3.98		3.98			7.2			
572	Ag coupon only				0.5	3.4	3.8		3.8			0.36			
573	0-64-20				0.43	1.04	6.67	1.42	6.67	4.59		0.36	7.51	0.97	Black coke Stainless seals
574		2	325	100	0.59	0.34	0		0			0.34			
575					0.59	0.17	0		0			0.17			
576					0.55	0.34	0		0			0.36			
577					0.55	0	0		0			25.53	0.22	0.17	No coke TSP/LON seals
578	TEL-91063	2	300	100	0.49	15.42	12.1		12.1			20.00			
579					0.39	16.00	14		14			29.2			
580					0.4	14.6	15.53	1.92	15.53	12.01		29.26	28.77	1.54	Thick dk, brown coke TSP/LON seals
581	TEL-92036	2	300	100	0.38	13.71	4		4			13.32			
582					0.53	9.32	4		4			11.25			
583					0.48	9.79	1.46		1.46			13.92			
584					0.46	11.74	2.17		2.17			13.41	12.90	1.03	Dark, brown coke TSP/LON seals
585	TEL-91002	1	300	100	0.48	9.49	3.92	1.1	3.92	2.89		19.94			
586					0.53	18.8	4.14		4.14			24.05			
587					0.44	17.18	6.07		6.07			23.20			
588					0.55	17.6	5.60		5.60			25.39			
589	TEL-91002	2	300	100	0.53	21.03	4.26	1.1	4.26	5.26		16.7	23.17	2.01	Dark, brown coke TSP/LON seals
590					0.46	12.29	2.41		2.41			17.75			
591					0.44	12.97	4.78		4.78			16.06			
592					0.54	13.44	2.61		2.61			16.06			
593					0.45	11.72	5.09	1.22	5.09	3.73		27.49	16.33	1.11	Dark, brown coke TSP/LON seals
594	TEL-92039	2	300	100	0.42	15.41	12.1		12.1			36.28			
595					0.42	19.79	16.5		16.5			31.0			
596					0.38	19.01	12		12			25.77			
597					0.5	22.15	3.6	4.7	3.6	11.1		30.34	4.00		Dark, brown coke

# STATIC COKER TEST DATA

Test #	Oil	Specimen	Temp, C	Time, Min	Size, g	Specimen mp/g Residue		Average	Std Dev	Seal mp/g Residue		Average	Std Dev	Total mp/g Residue		Average	Std Dev	Description of coke
598	TEL-92040	2	300	100	0.47	10.24	15.4	15.4		15.4	25.59	25.59		25.59		25.59	Dark, brown coke TSP/08 seals	
599					0.51	9.91	14.7	14.7		14.7	24.57	24.57		24.57		24.57		
600					0.5	12.24	16.3	16.3		16.3	28.5	28.5		28.5		28.5		
601	TEL-92041	2	300	100	0.45	11.67	14.6	14.6	0.7	14.6	26.27	26.27	1.44	26.27	1.44	26.27	Dark, brown coke TSP/08 seals	
602					0.53	4.51	14.7	14.7		14.7	19.18	19.18		19.18		19.18		
603					0.45	12.19	9.6	9.6		9.6	21.94	21.94		21.94		21.94		
604					0.51	7.65	10.8	10.8		10.8	16.45	16.45		16.45		16.45		
605	TEL-92049	1	300	100	0.51	13.67	7.8	7.8	2.5	7.8	21.48	21.48	1.48	21.48	1.48	21.48	Dark, brown coke TSP/08 seals	
606					0.52	29.76	6.34	6.34		6.34	36.09	36.09		36.09		36.09		
607					0.5	33.26	8.67	8.67		8.67	41.93	41.93		41.93		41.93		
608					0.50	31.16	11.53	11.53		11.53	42.69	42.69		42.69		42.69		
609	TEL-92049	2	300	100	0.53	30.78	7.10	7.10	1.97	7.10	37.96	37.96	2.74	37.96	2.74	37.96	Dark, brown coke TSP/08 seals	
610					0.52	19.29	10.5	10.5		10.5	29.79	29.79		29.79		29.79		
611					0.54	20.72	9.8	9.8		9.8	30.52	30.52		30.52		30.52		
612	TEL-92050	1	300	100	0.50	25.99	6.87	6.87	1.57	6.87	32.45	32.45	1.12	32.45	1.12	32.45	Dark, brown coke TSP/08 seals	
613					0.43	12.98	15.3	15.3		15.3	28.29	28.29		28.29		28.29		
614					0.45	13.85	12.41	12.41		12.41	27.26	27.26		27.26		27.26		
615					0.45	16.98	8.59	8.59		8.59	23.57	23.57		23.57		23.57		
616	TEL-92050	2	300	100	0.49	17.49	7.93	7.93	3.13	7.93	25.43	25.43	1.6	25.43	1.6	25.43	Dark, brown coke TSP/08 seals	
617					0.54	10.9	8.49	8.49		8.49	19.59	19.59		19.59		19.59		
618					0.56	15.12	7.65	7.65		7.65	22.76	22.76		22.76		22.76		
619					0.55	11.15	10.03	10.03		10.03	21.21	21.21		21.21		21.21		
620	TEL-93003	1	300	100	0.54	11.75	8.8	8.8	0.05	8.8	20.56	20.56	1.15	20.56	1.15	20.56	Dark, brown coke TSP/08 seals	
621					0.54	27.92	6.89	6.89		6.89	34.8	34.8		34.8		34.8		
622					0.51	26.7	4.75	4.75		4.75	31.45	31.45		31.45		31.45		
623	TEL-93003	2	300	100	0.49	28.64	5.11	5.11	0.94	5.11	33.75	33.75	1.4	33.75	1.4	33.75	Dark, brown coke TSP/08 seals	
624					0.46	7.99	11.09	11.09		11.09	19.07	19.07		19.07		19.07		
625					0.47	7.7	10.09	10.09		10.09	17.75	17.75		17.75		17.75		
626					0.47	12.67	9.51	9.51		9.51	22.10	22.10		22.10		22.10		
627	TEL-93011	1	300	100	0.57	11.21	11.74	11.74	1.03	11.74	22.95	22.95	2.04	22.95	2.04	22.95	Dark, brown coke TSP/08 seals	
628					0.43	11.05	15.43	15.43		15.43	26.49	26.49		26.49		26.49		
629					0.52	10.86	6.4	6.4		6.4	17.26	17.26		17.26		17.26		
630					0.46	5.02	10.7	10.7		10.7	15.72	15.72		15.72		15.72		
631	TEL-93011	2	300	100	0.43	14.1	13.4	13.4	3.9	13.4	27.5	27.5	6.11	27.5	6.11	27.5	Dark, brown coke TSP/08 seals	
632					0.5	9.69	4.24	4.24		4.24	13.93	13.93		13.93		13.93		
633					0.49	6.67	4.25	4.25		4.25	10.92	10.92		10.92		10.92		
634					0.52	9.19	5.17	5.17		5.17	14.35	14.35		14.35		14.35		
635					0.48	9.91	8.47	8.47	2.01	8.47	18.38	18.38	3.06	18.38	3.06	18.38	Dark, brown coke	

\* GC test run using only Ag coupon

\*\* diphenyl benzidine embedded

\* OC test run  
using only Ag  
coupon

\*\* diphenyl  
barbital  
anhydride

TABLE A-4  
MCRT COKING TEST DATA

VIAL TYPE USED: 1 = 7.5 CM GLASS VIAL; 2 = 3.5 CM GLASS VIAL

Test	Oil Sample	Temp C	Hrs	Size Grams	Vial Type	Gas Type	% Res	Std. Dev.	Residue Description	Coke Color
235	TEL-90103	275	30	0.5	2	AIR	22.64	0.51	crystal coke	dark
236	TEL-90104	275	30	0.5	2	AIR	18.26	0.74	crystal coke	dark
237	O-64-20	400	30	0.5	1	AIR	13.58	0.3	thick, flaky var	dark
238	O-64-20	400	30	0.5	2	AIR	6.66	0.23	coke deposits	dark
239	TEL-91005	275	30	0.5	2	AIR	24.31	0.34	flaky varnish	dark
240	TEL-91003	275	30	0.5	2	AIR	24.01	0.28	varnish	brown-black
241	TEL-90104	275	30	0.5	2	AIR	16.24	0.28	uniform varnish	black
242	TEL-90103	275	30	0.5	2	AIR	26.82	1.04	flaky	black
243	O-85-1	275	30	0.5	2	AIR	16.38	0.32	uniform varnish	black
244	O-90-6	275	30	0.5	2	AIR	16.08	0.26	uniform varnish	black
245	O-86-2	275	30	0.5	2	AIR	10.42	0.58	varnish	black
246	O-64-20 OC, 48h, 320	400	30	0.5	2	AIR	6.67	0.3	coke & varnish	black
247	O-91-13	275	30	0.5	2	AIR	25.06	0.6	coke&flaky varn	brown to black
248	TEL-91053	275	30	0.5	2	AIR	22.4	0.95	heavy coke	black
249	O-64-20 WT 635	400	30	0.5	2	AIR	8.18	0.15	heavy coke	black
250	O-64-20 WT 633	400	30	0.5	2	AIR	7.89	0.26	varnish & coke	dark brown
251	TEL-91063	275	30	0.5	2	AIR	25.07	1.62	uniform varnish	dark brown
252	TEL-92036	275	30	0.5	2	AIR	24.24	0.28	flaky varnish	dark brown
253	TEL-92039	275	30	0.5	2	AIR	23.59	0.34	heavy coke	dark brown
254	TEL-92040	275	30	0.5	2	AIR	21.93	0.44	shiny varnish	dark brown
255	TEL-92041	275	30	0.5	2	AIR	21.62	0.31	shiny varnish	dark brown
256	TEL-92050	275	30	0.5	2	AIR	18.95	0.4	shiny varnish	dark brown
257	TEL-91002	275	30	0.5	2	AIR	15.72	0.37	shiny varnish	dark brown
258	TEL-92049	275	30	0.5	2	AIR	24.44	0.4	shiny varnish	dark brown
259	TEL-93003	275	30	0.5	2	AIR	20.99	0.3	shiny varnish	dark brown
260	TEL-93011	275	30	0.5	2	AIR	18.38	0.33	shiny varnish	dark brown

**TABLE A-5**  
**LUBRICANT FOAMING TEST DATA WITH VARIABLE TEST CONDITIONS**

SAMPLE No.	TEST TEMP C	AIRFLOW cc/min	AERATION TIME @ AIRFLOW min.	VOLUME			FOAM COLLAPSE TIME sec.
				OIL ml	OIL & FOAM ml	FOAM ml	
TEL-91035	80	500	5	12	70	58	4
25-ml test		1000	15	10	74	64	5
TEL-91035	80	500	5	45	261	216	5
FTM3213	(200ML)	1000	15	30	365	335	8
TEL-91036	80	500	5	12	52	40	3
25-ml test		1000	15	10	53	43	3
TEL-91036	80	500	5	50	265	215	5
FTM3213	(200ML)	1000	15	35	405	370	10
TEL-91003	80	500	5	20	38	18	3
25-ml test		1000	15	16	42	26	3
TEL-91003	80	500	5	40	245	205	6
FTM3213	(200ML)	1000	15	25	250	225	6
TEL-91005	80	500	5	16	56	40	3
25-ml test		1000	15	12	54	42	3
TEL-91005	80	500	5	50	260	210	5
FTM3213	(200ML)	1000	15	35	325	290	6
TEL-91005	80	500	5	40	262	222	5
FTM3213	(200ML)	1000	15	25	325	300	6
TEL-90103	80	500	5	20	48	28	2
25-ml test		1000	15	12	60	48	3
TEL-90104	80	500	5	40	46	6	2
25-ml test		1000	15	42	50	8	2
TEL-90104	80	500	25	50	250	200	4
FTM3213	(200ML)	1000	25	45	350	305	10
O-85-1	80	500	5	38	44	6	2
25-ml test		1000	15	40	48	8	2
O-85-1	80	500	5	235	240	5	4
FTM3213	(200ML)	1000	5	250	258	8	3
O-86-2	80	500	5	36	40	4	ND
25-ml test		1000	15	26	44	18	3
O-86-2	80	500	5	226	232	6	2
FTM3213	(200ML)	1000	15	235	243	8	2
O-90-6	80	500	5	38	43	5	2
25-ml test		1000	15	42	48	6	2
O-90-6	80	500	10	235	240	5	3
FTM3213	(200ML)	1000	20	246	254	8	3
TEL-91002	80	500	15	35	44	9	3
25-ml test		1000	10	40	46	6	3
TEL-91002	80	500	15	238	243	5	9
FTM3213	(200ml)	1000	10	252	261	9	10
TEL-91001	200	500	20	14	102	88	8
25-ml test	11/16spar	1000	30	10	194	184	16
TEL-91001	200	500	20	39	54	15	3
25-ml test	13/16spar	1000	20	17	68	51	3
TEL-91001	200	500	20	41	50	9	2
25-ml test	ASTMstone	1000	5	ND	88	49	4
O-91-13	80	500	5	37	42	5	2
25-ml test		1000	5	40	48	8	2
O-91-13	80	500	10	235	242	7	2
FTM3213	(200ml)	1000	5	250	260	10	3
TEL-91053	80	500	5	39	44	5	3
25-ml test		1000	10	17	58	41	4
TEL-91063	80	500	5	33	42	9	2
25-ml test		1000	10	34	47	13	2
TEL-91063	80	500	10	235	245	10	3
FTM3213	(200mL)	1000	5	248	263	15	4
TEL-92036	80	500	5	40	46	6	3
25-ml test		1000	5	40	52	12	4
TEL-92036	80	500	5	240	245	5	3
FTM3213	(200mL)	1000	5	250	260	10	4

TABLE A-5 (CONCLUDED)

SAMPLE No.	TEST TEMP C	AIRFLOW cc/min	AERATION TIME & AIRFLOW min.	VOLUME			FOAM COLLAPSE TIME sec.
				OIL ml	OIL & FOAM ml	FOAM ml	
TEL-92039	80	500	15	39	40	1	1
25-ml test		1000	15	40	44	4	1
TEL-92039	80	500	15	235	239	4	2
FTM3213 (200ml)		1000	15	248	255	7	2
TEL-92040	80	500	15	36	41	5	4
25-ml test		1000	15	40	48	8	4
TEL-92041	80	500	15	41	46	5	4
25-ml test		1000	15	44	52	8	4
TEL-92049	80	500	15	38	42	4	1
25-ml test		1000	15	38	46	8	1
TEL-92050	80	500	15	40	44	4	1
25-ml test		1000	15	46	48	2	2
TEL-91000	80	500	20	38	42	4	retest 1
25-ml		1000	20	40	45	5	1
TEL-91	80	500	15	235	242	7	retest 2
FTM3213 (200ml)		1000	15	246	255	9	2
TEL-93003	80	500	30	230	235	5	1
FTM3213 (200ML)		1000	30	240	248	8	2
TEL-93003	80	500	15	36	38	2	1
25-ml test		1000	15	38	44	6	2
TEL-93011	80	500	30	38	44	6	3
25-ml test		1000	30	14	52	38	3

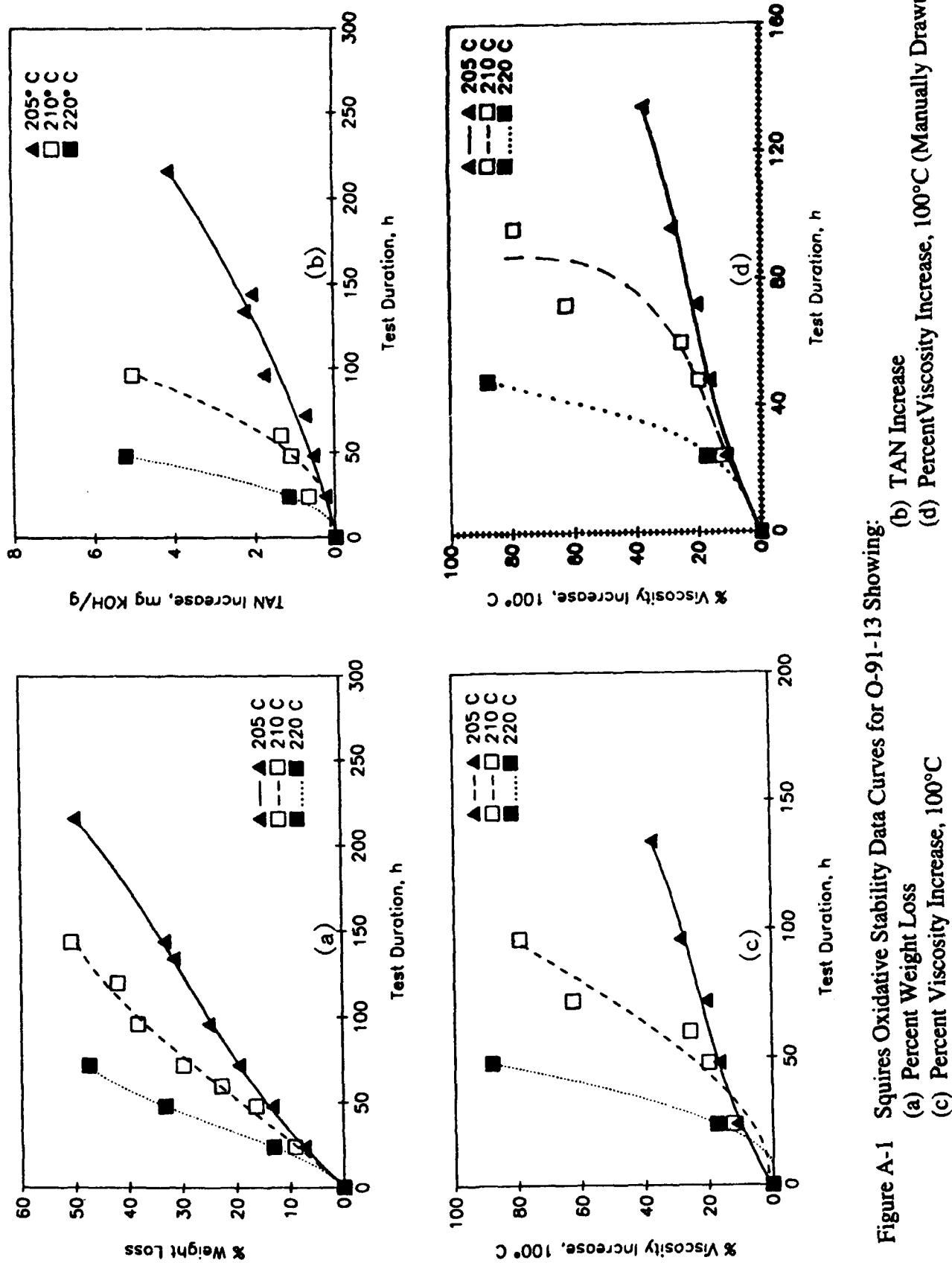


Figure A-1 Squires Oxidative Stability Data Curves for O-91-13 Showing:

(a) Percent Weight Loss

(b) TAN Increase

(c) Percent Viscosity Increase, 100°C

(d) Percent Viscosity Increase, 100°C (Manually Drawn)

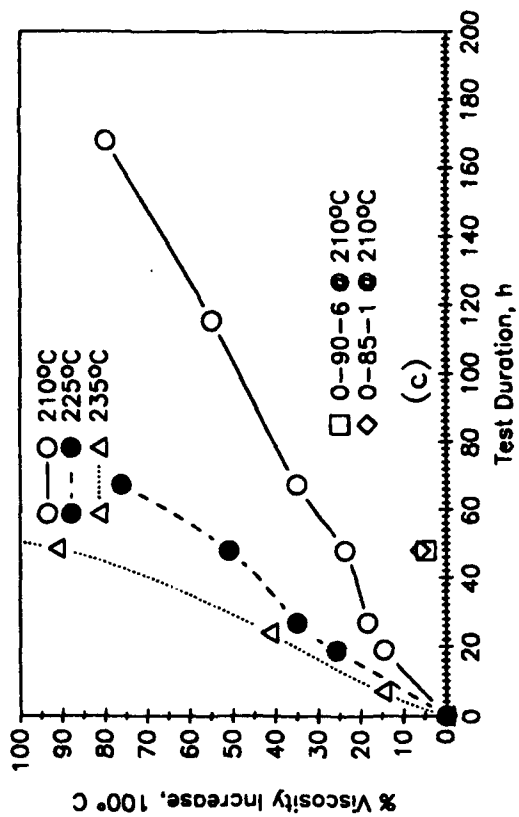
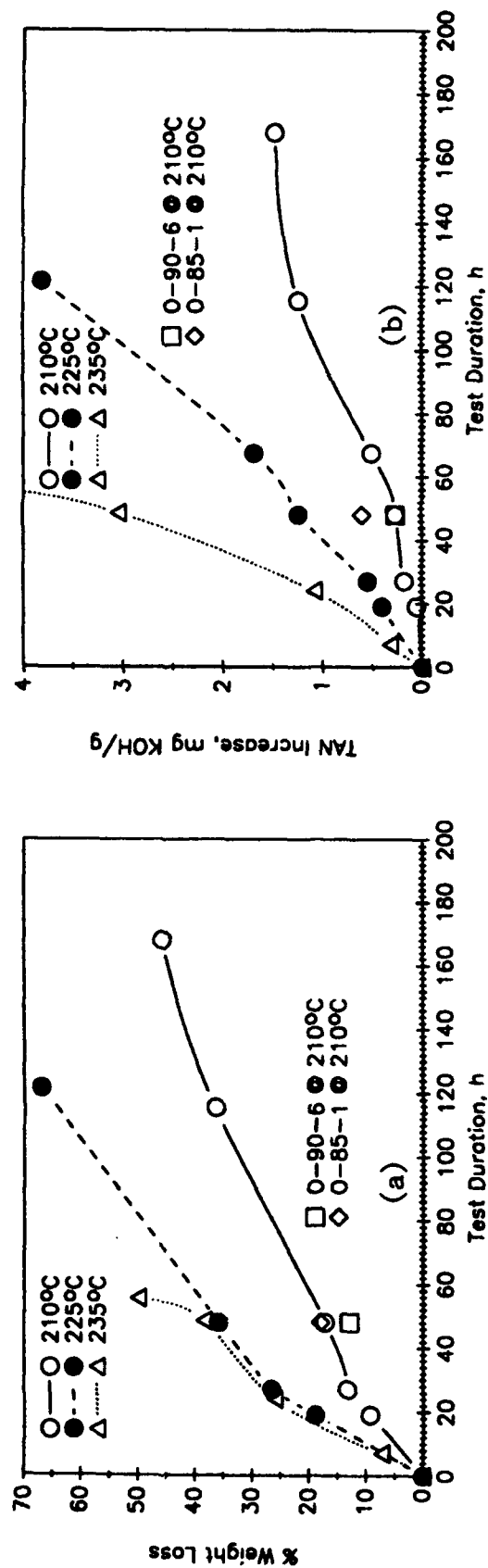


Figure A-2 Squires Oxidative Stability Data Curves for TEL-90103 Showing:  
 (a) Percent Weight Loss  
 (b) TAN Increase  
 (c) Percent Viscosity Increase, 100°C

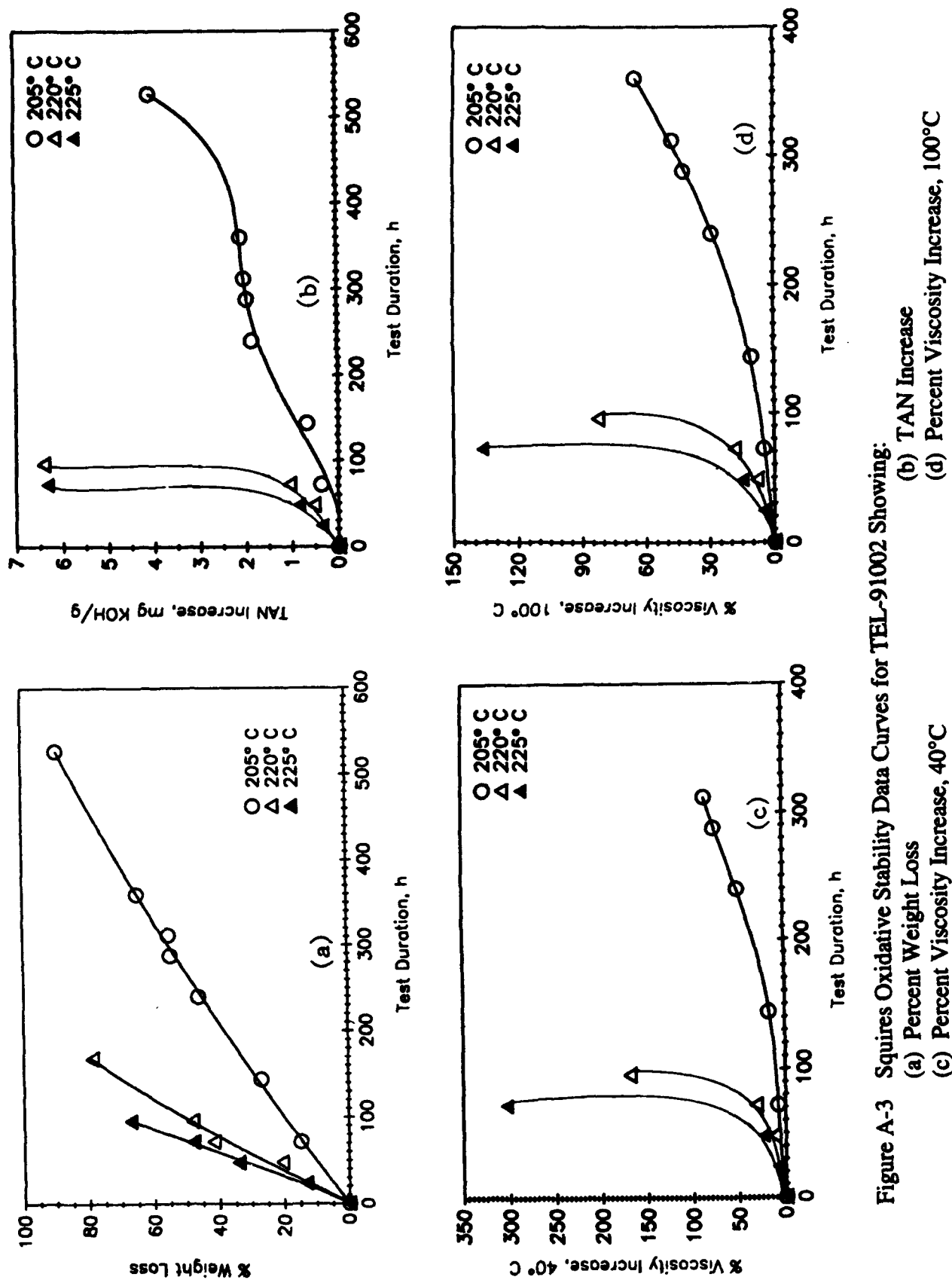


Figure A-3 Squires Oxidative Stability Data Curves for TEL-91002 Showing:

(a) Percent Weight Loss

(c) Percent Viscosity Increase, 40°C

(b) TAN Increase

(d) Percent Viscosity Increase, 100°C

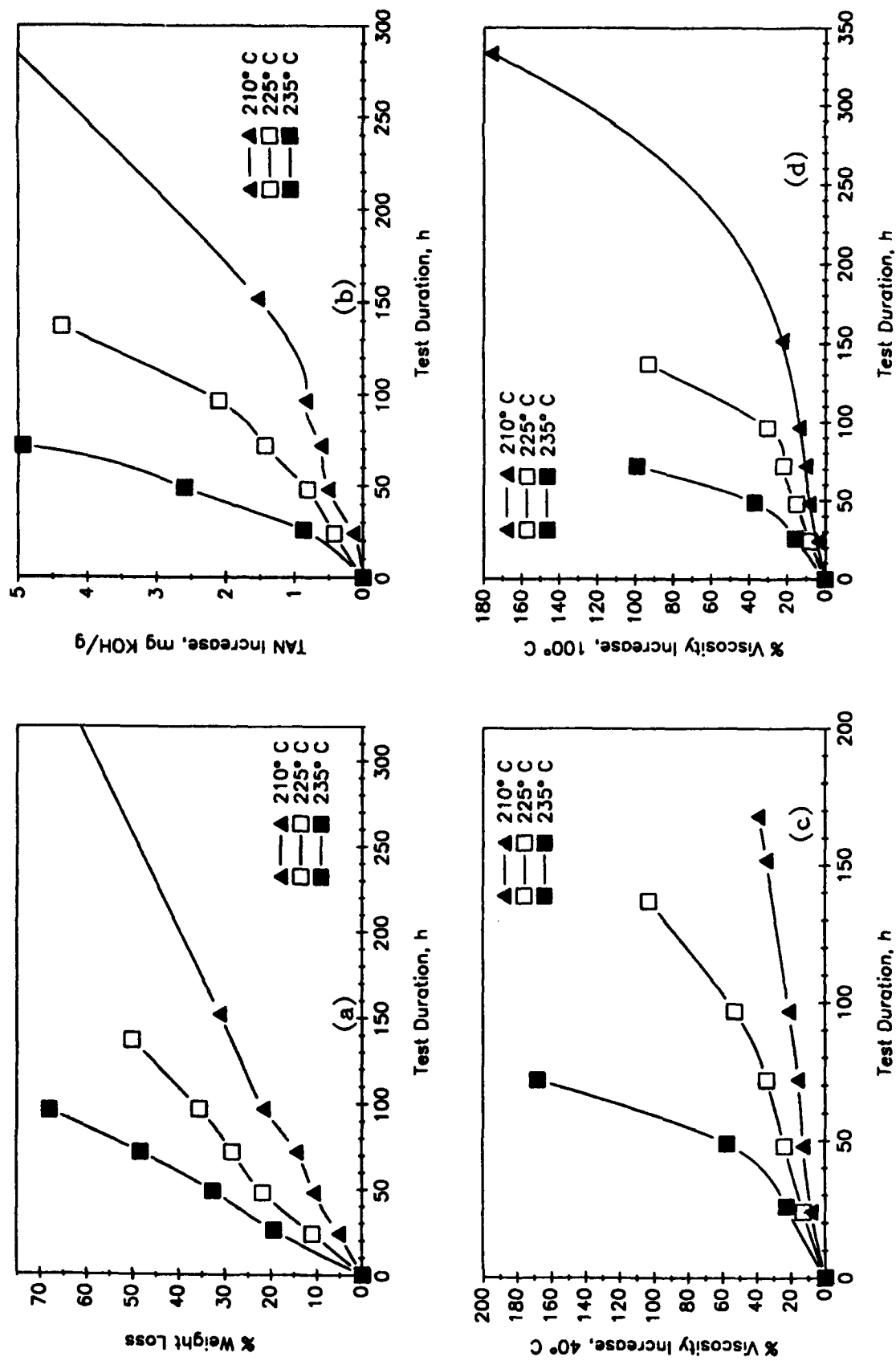


Figure A-4 Squires Oxidative Stability Data Curves for TEL-91003 Showing:

(a) Percent Weight Loss

(b) TAN Increase

(c) Percent Viscosity Increase, 40°C

(d) Percent Viscosity Increase, 100°C

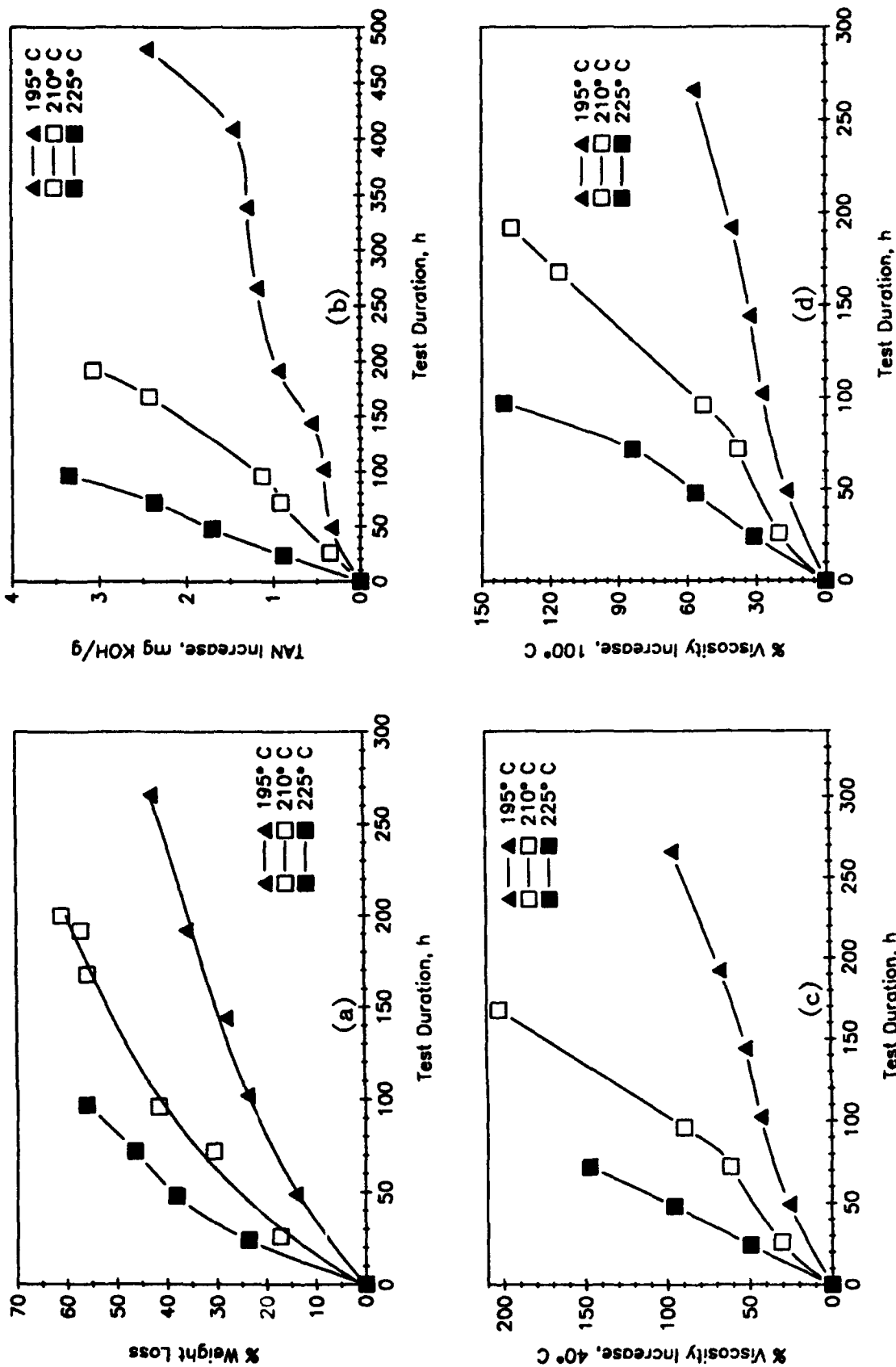


Figure A-5 Squires Oxidative Stability Data Curves for TEL-91052 Showing:

(a) Percent Weight Loss  
(c) Percent Viscosity Increase, 40°C

(b) TAN Increase  
(d) Percent Viscosity Increase, 100°C

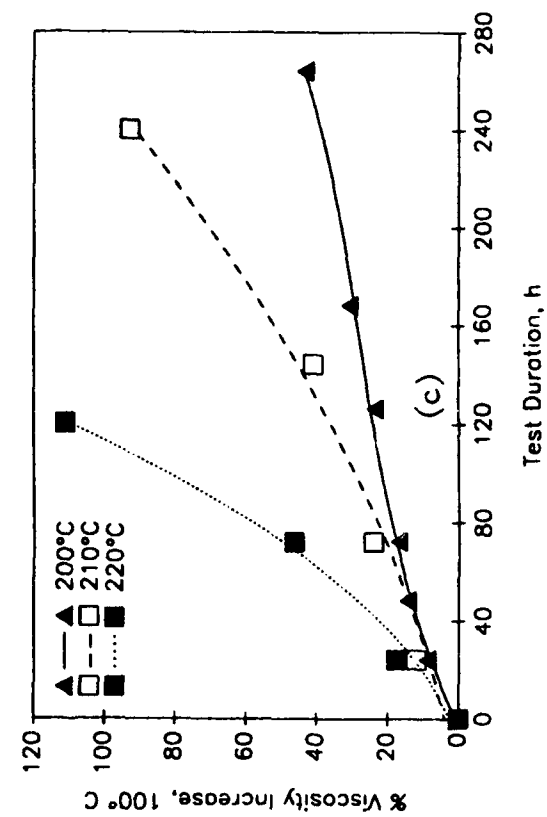
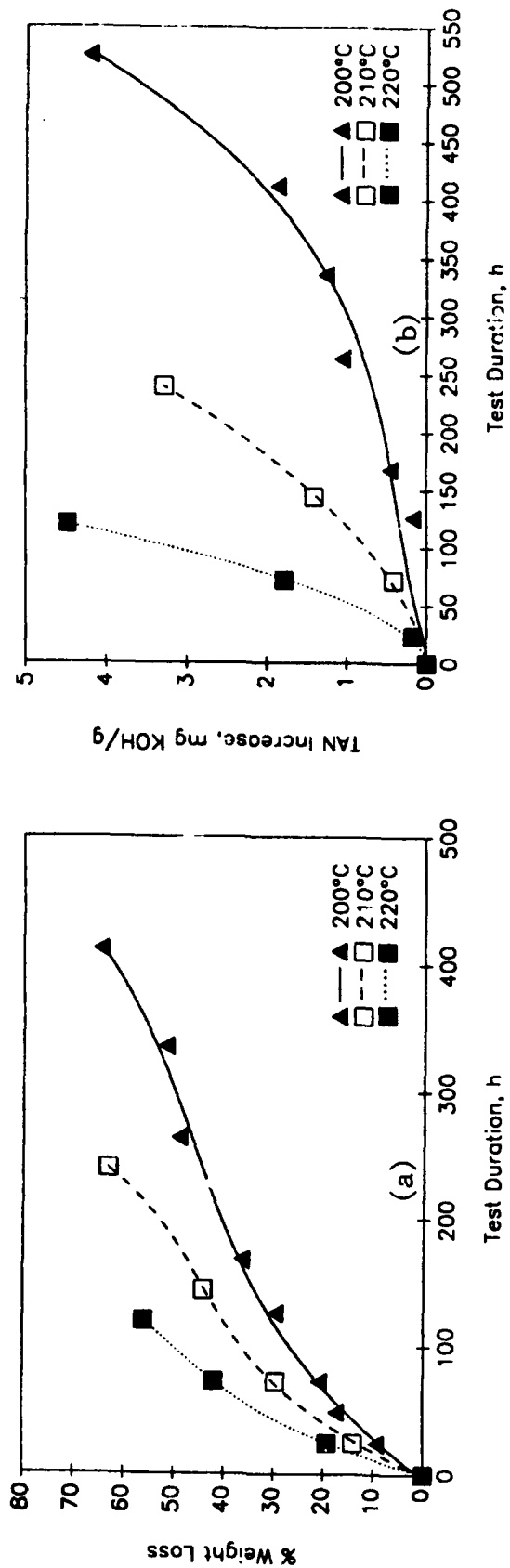


Figure A-6 Squires Oxidative Stability Data Curves for TEL-91053 Showing:  
 (a) Percent Weight Loss  
 (b) TAN Increase  
 (c) Percent Viscosity Increase, 100°C

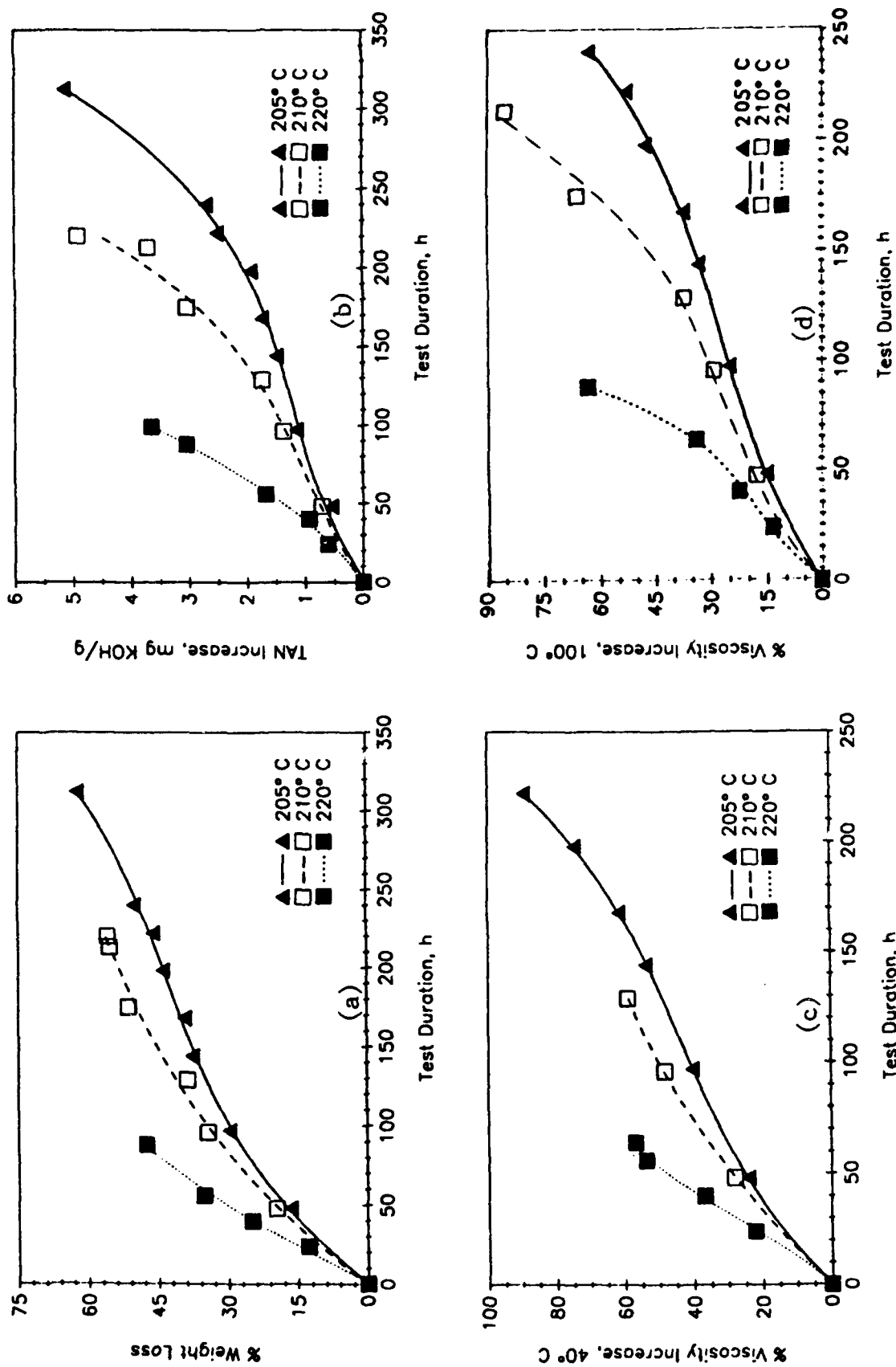


Figure A-7 Squires Oxidative Stability Data Curves for TEL-91063 Showing:

(a) Percent Weight Loss

(b) TAN Increase

(c) Percent Viscosity Increase, 40°C

(d) Percent Viscosity Increase, 100°C

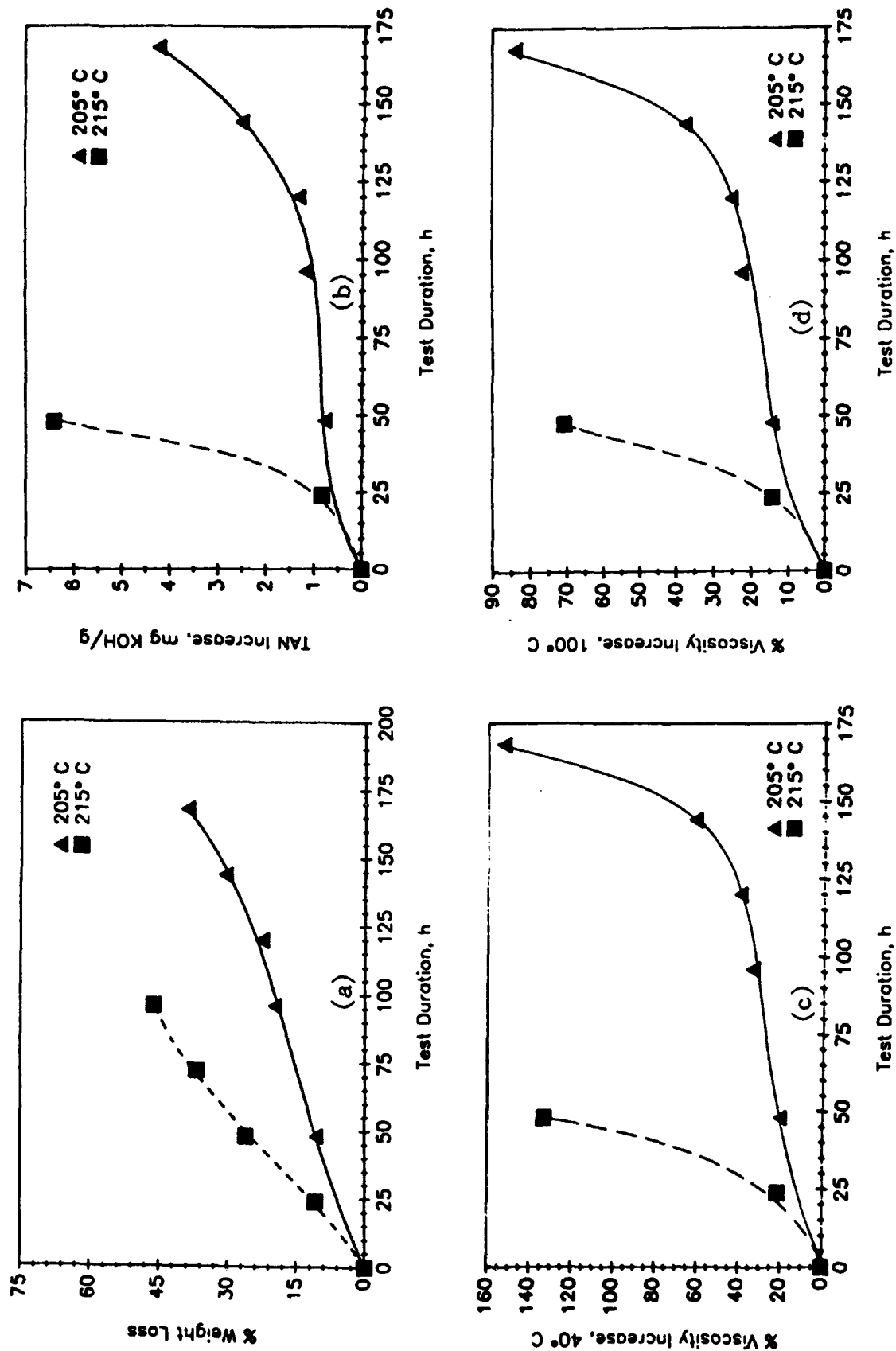


Figure A-8 Squires Oxidative Stability Data Curves for TEL-92036 Showing:

(a) Percent Weight Loss

(b) TAN Increase

(c) Percent Viscosity Increase, 40°C

(d) Percent Viscosity Increase, 100°C

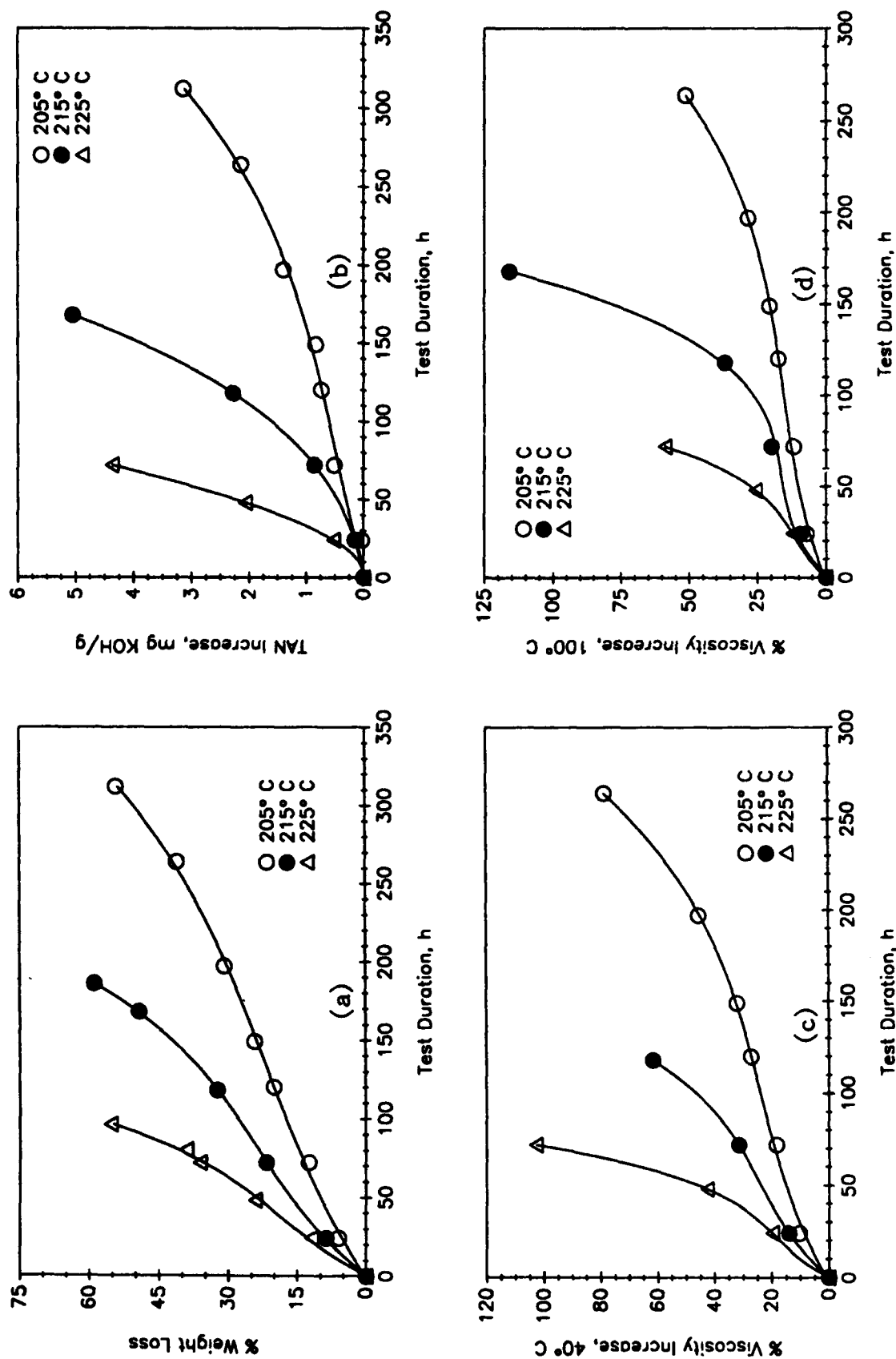


Figure A-9 Squires Oxidative Stability Data Curves for TEL-92039 Showing:

(a) Percent Weight Loss

(b) TAN Increase

(c) Percent Viscosity Increase, 40°C

(d) Percent Viscosity Increase, 100°C

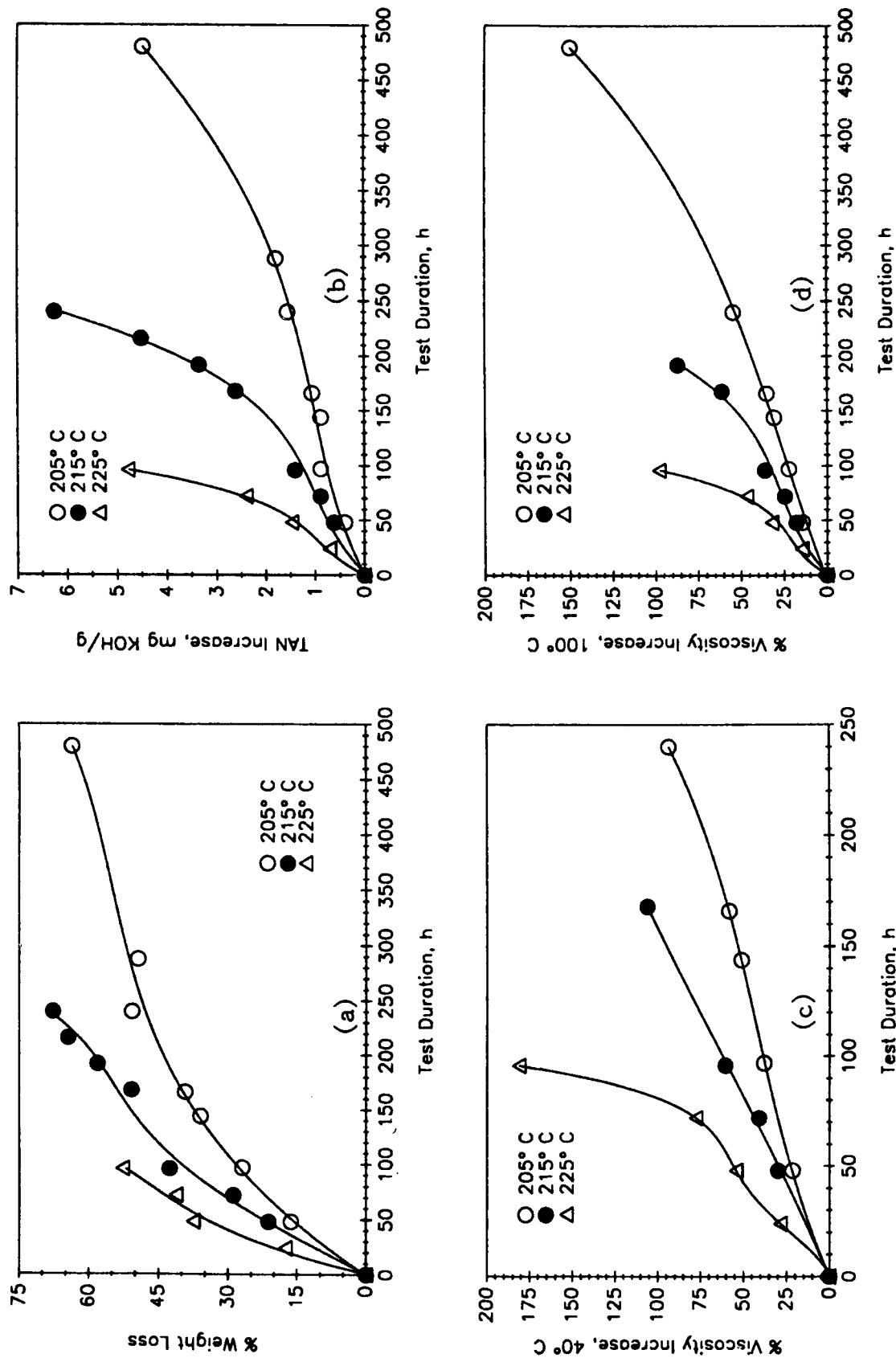


Figure A-10 Squires Oxidative Stability Data Curves for TEL-92040 Showing:  
 (a) Percent Weight Loss  
 (b) TAN Increase  
 (c) Percent Viscosity Increase, 40°C  
 (d) Percent Viscosity Increase, 100°C

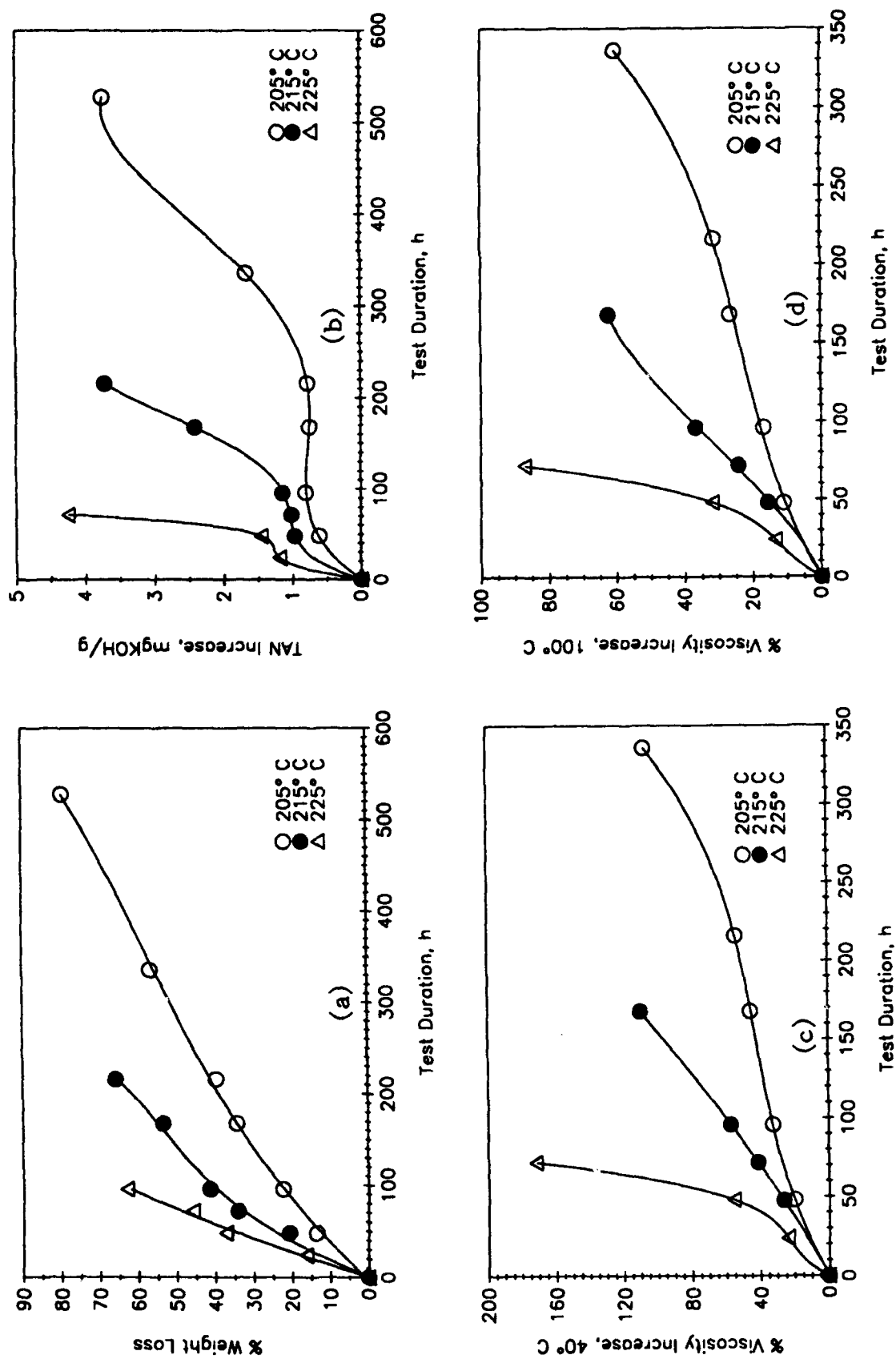


Figure A-11 Squires Oxidative Stability Data Curves for TEL-92041 Showing:  
 (a) Percent Weight Loss  
 (c) Percent Viscosity Increase, 40°C  
 (b) TAN Increase  
 (d) Percent Viscosity Increase, 100°C

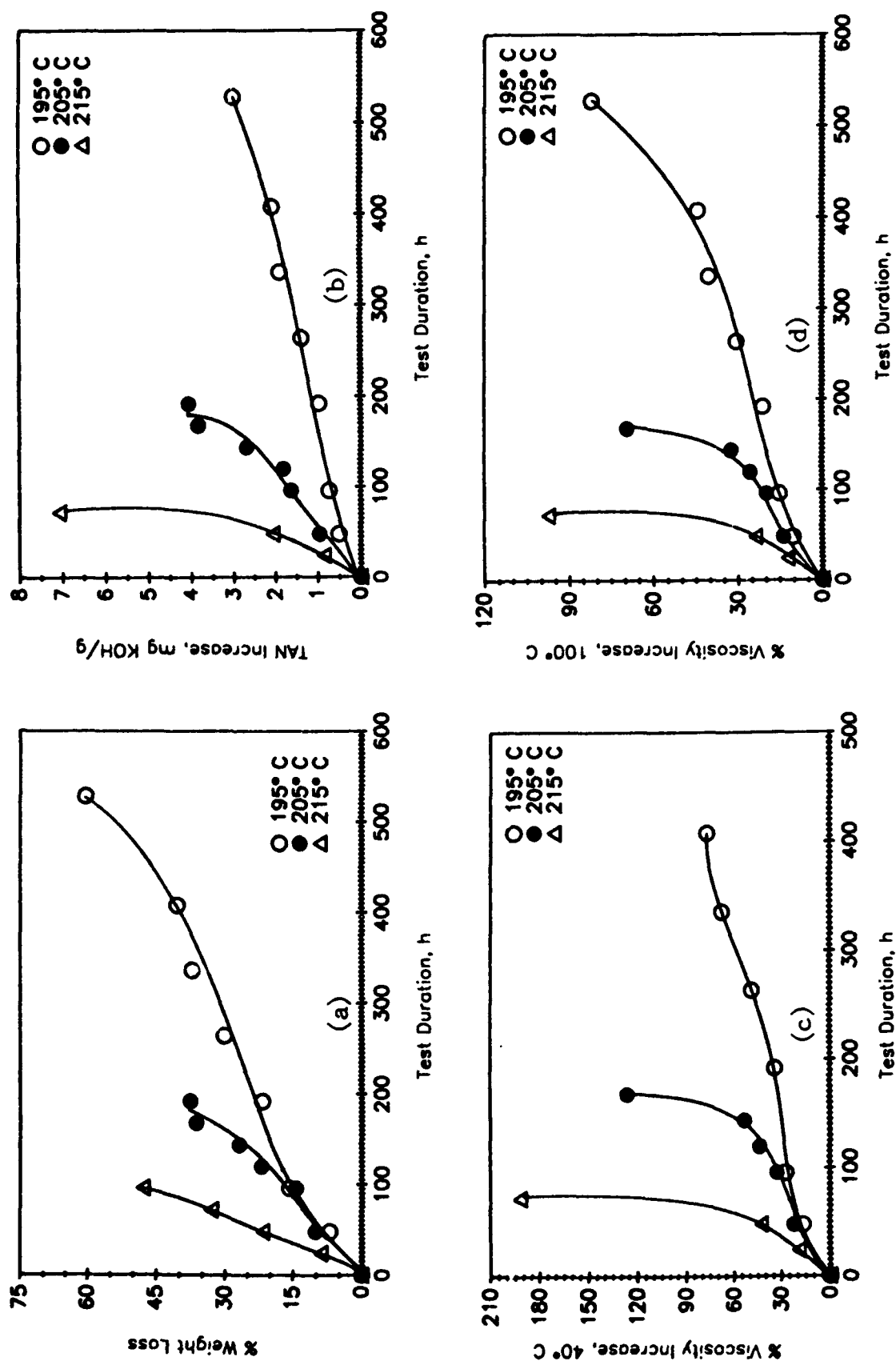


Figure A-12 Squires Oxidative Stability Data Curves for TEL-92049 Showing:  
 (a) Percent Weight Loss  
 (b) TAN Increase  
 (c) Percent Viscosity Increase, 40°C  
 (d) Percent Viscosity Increase, 100°C

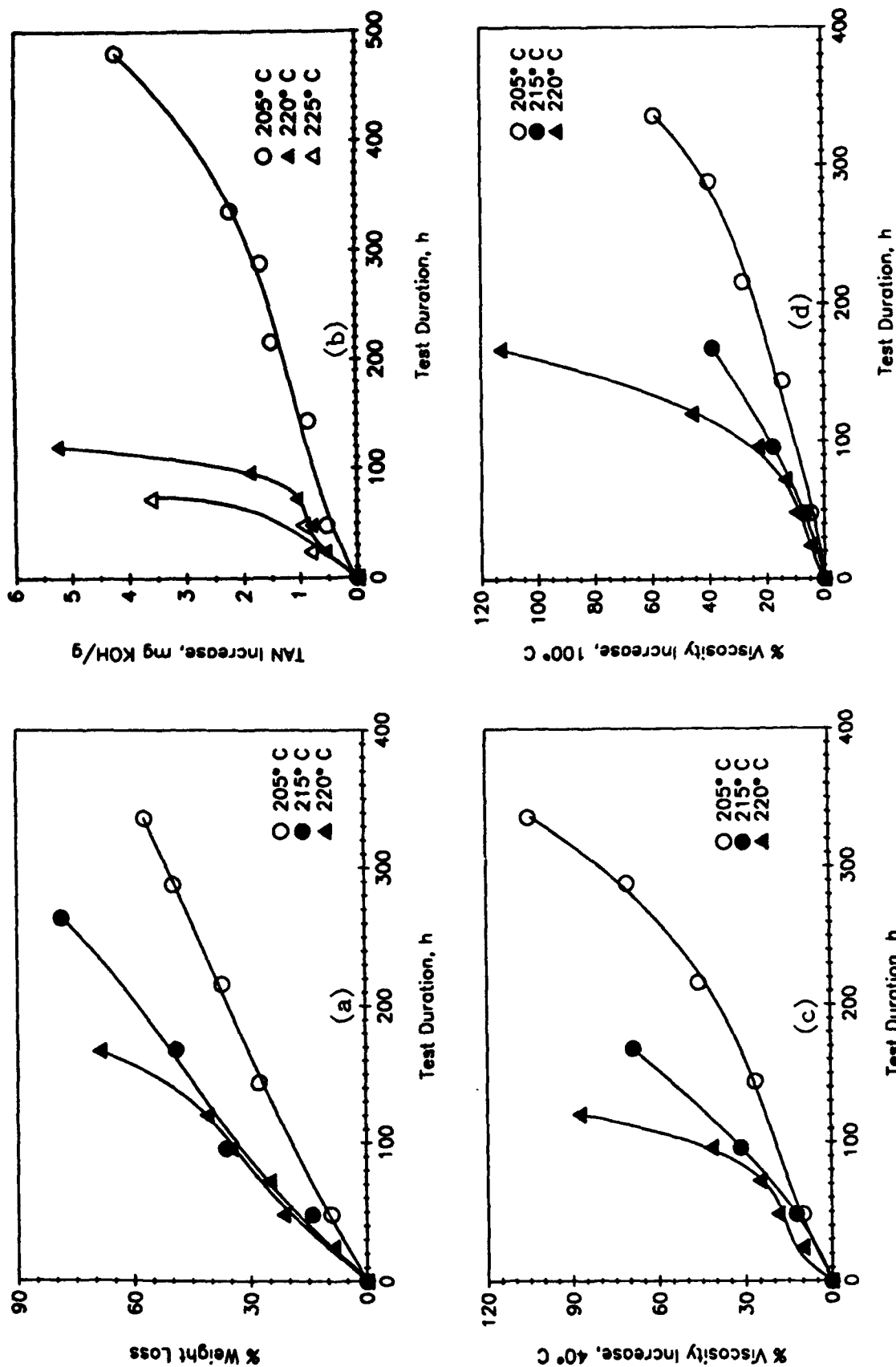


Figure A-13 Squires Oxidative Stability Data Curves for TEL-92050 Showing:

(a) Percent Weight Loss

(b) TAN Increase

(c) Percent Viscosity Increase, 40°C

(d) Percent Viscosity Increase, 100°C

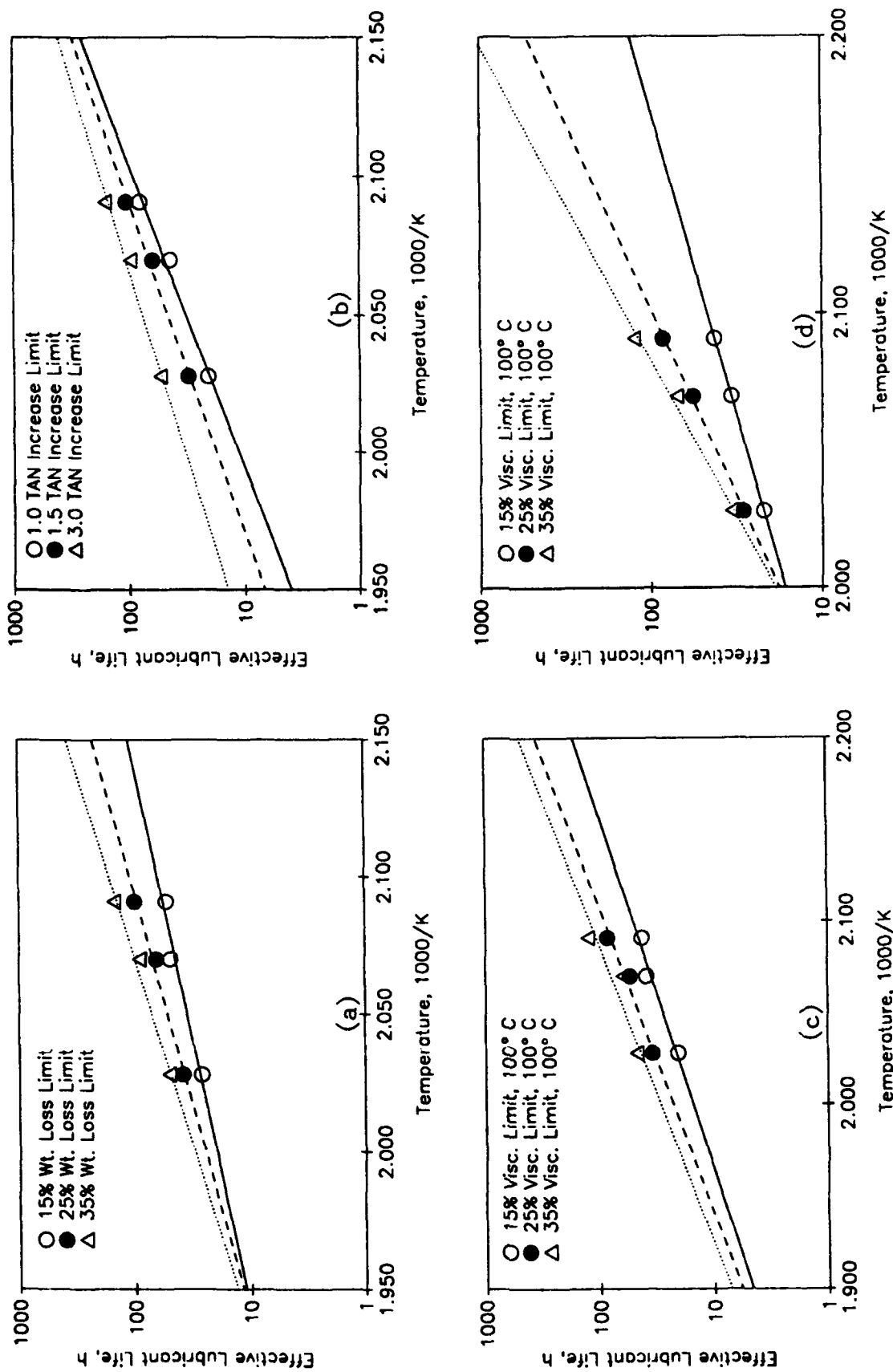


Figure A-14 Effective Lubricant Life as a Function of Temperature for O-91-13 Based on:

(a) Percent Weight Loss Limits

(b) TAN Increase Limits

(c) Percent Viscosity Change at 100°C

(d) Percent Viscosity Change at 100°C

(Data Points from Manually Drawn Curves of Fig. A-1)

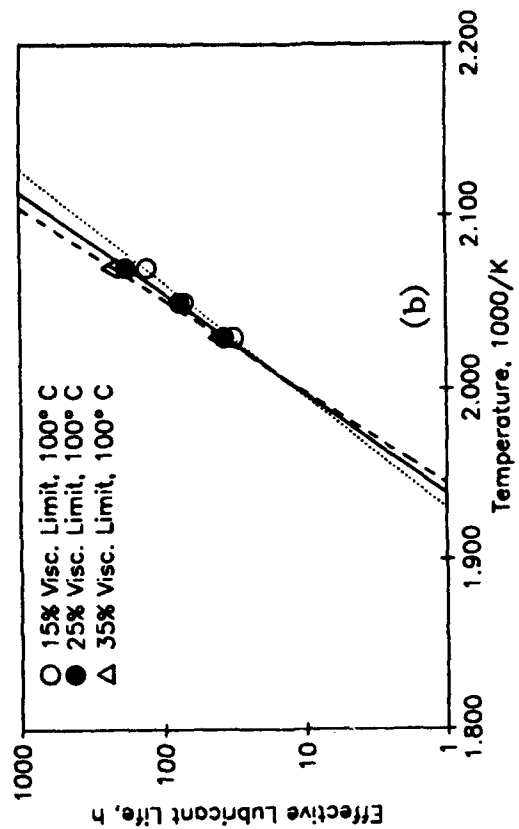
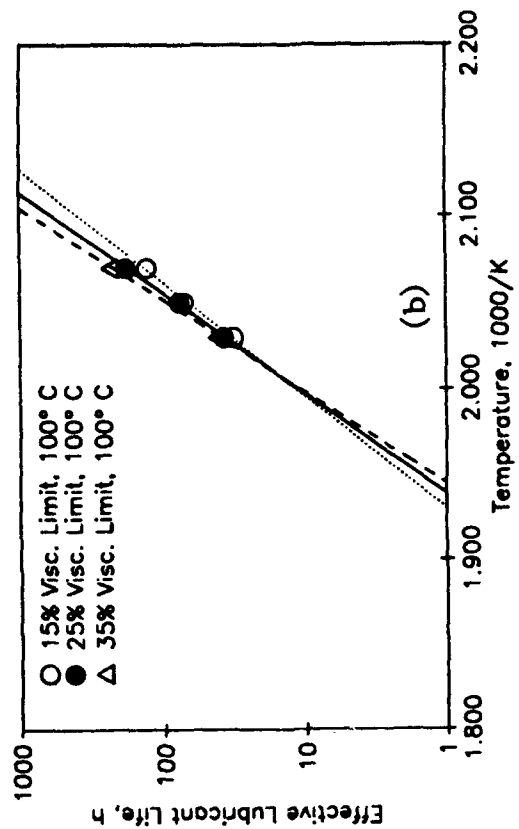


Figure A-15 Effective Lubricant Life as a Function of Temperature for O-90-6 Based on:  
 (a) Percent Weight Loss Limits  
 (b) Percent Viscosity Change at 100°C

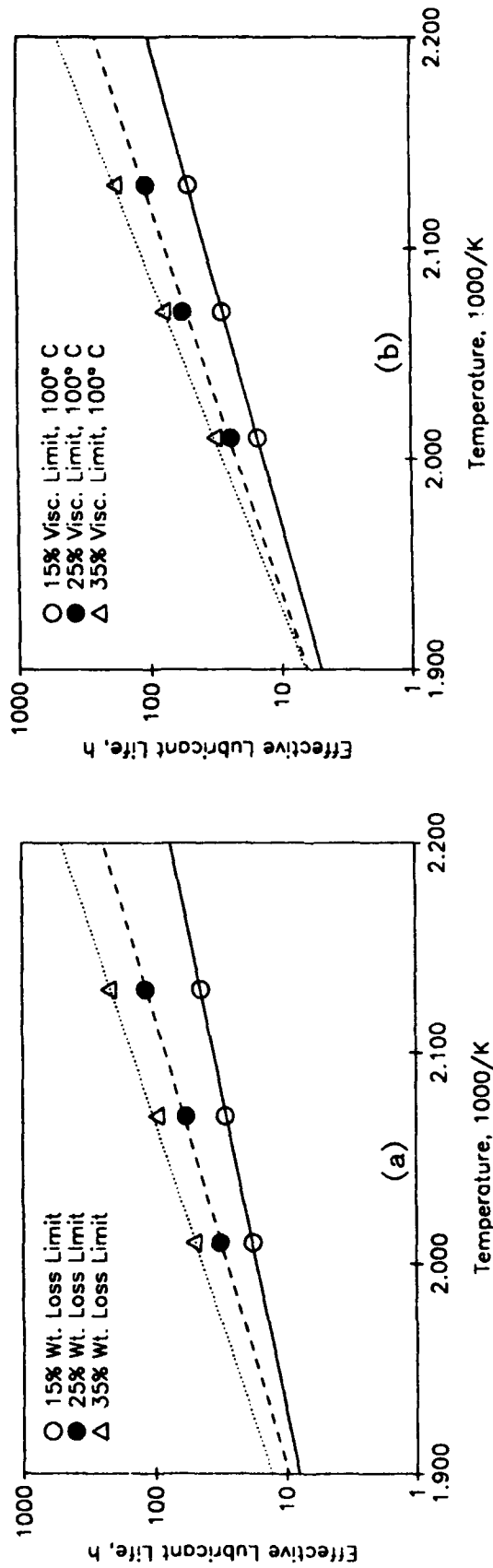


Figure A-16 Effective Lubricant Life as a Function of Temperature for TEL-90087 Based on:  
 (a) Percent Weight Loss Limits  
 (b) Percent Viscosity Change at 100°C

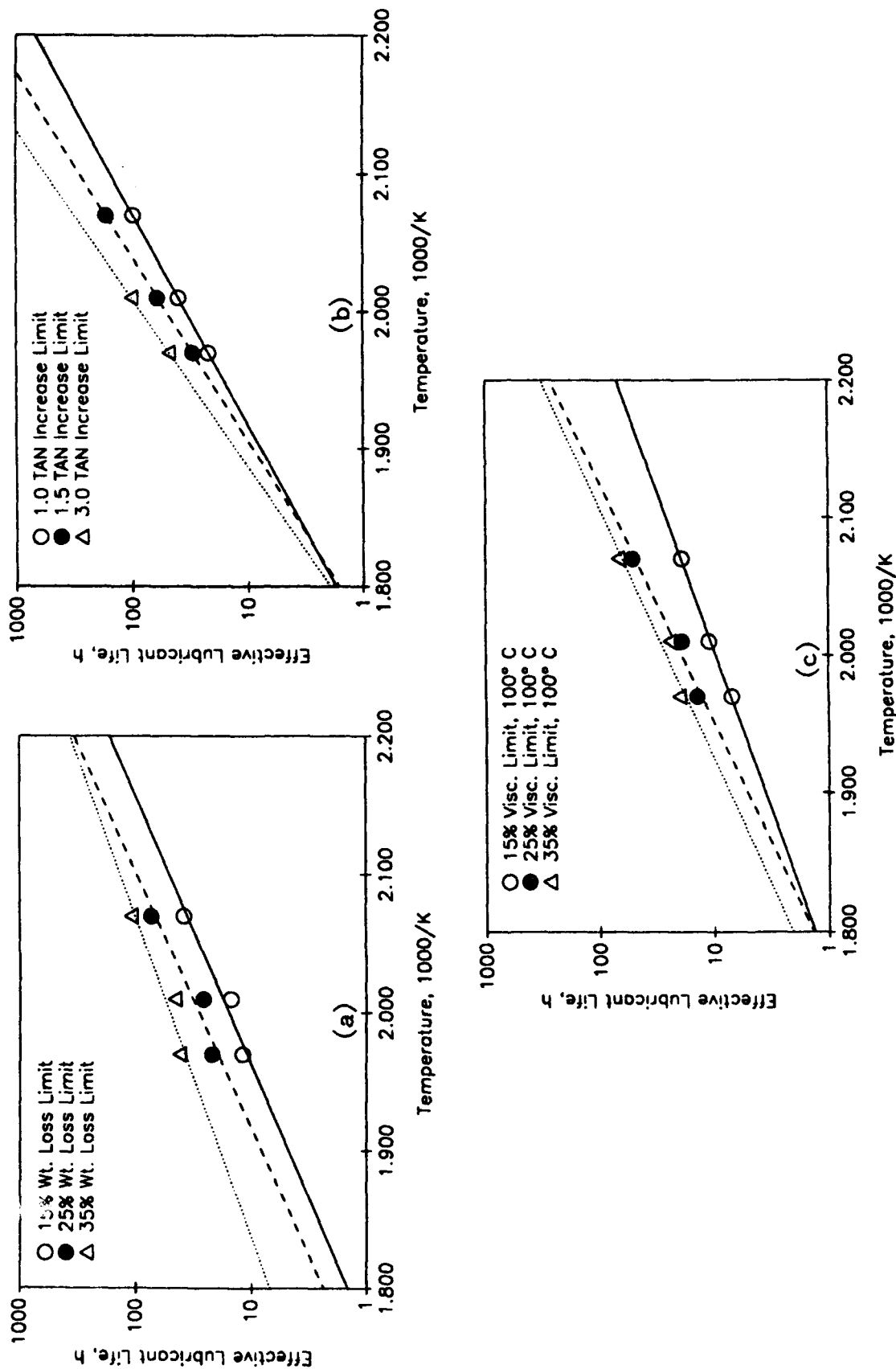


Figure A-17 Effective Lubricant Life as a Function of Temperature for TEL-90103 Based on:  
 (a) Percent Weight Loss Limits  
 (b) TAN Increase Limits  
 (c) Percent Viscosity Change at 100°C

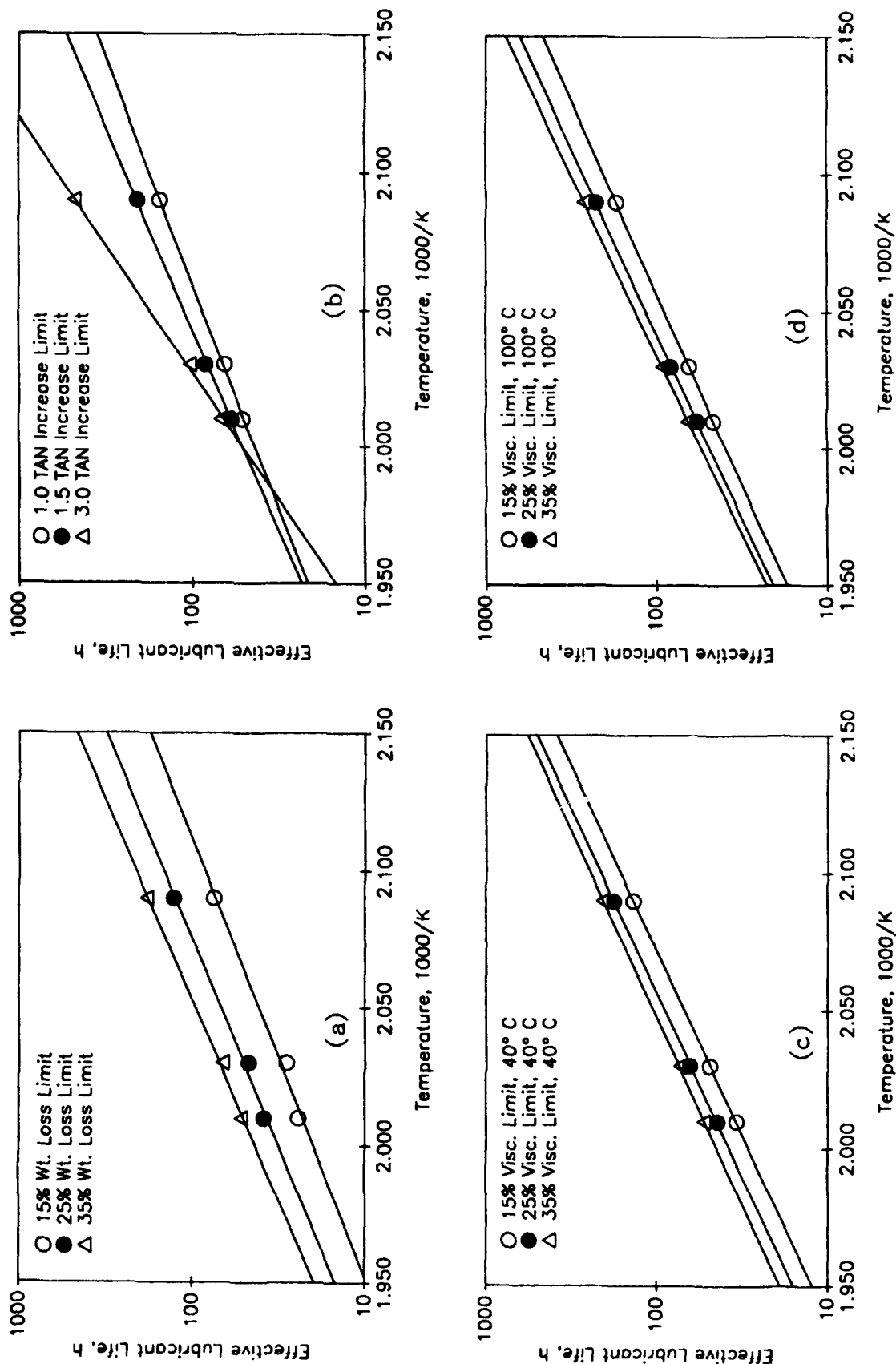


Figure A-18 Effective Lubricant Life as a Function of Temperature for TEL-91002 Based on:  
 (a) Percent Weight Loss Limits  
 (b) TAN Increase Limits  
 (c) Percent Viscosity Change at 40°C  
 (d) Percent Viscosity Change at 100°C

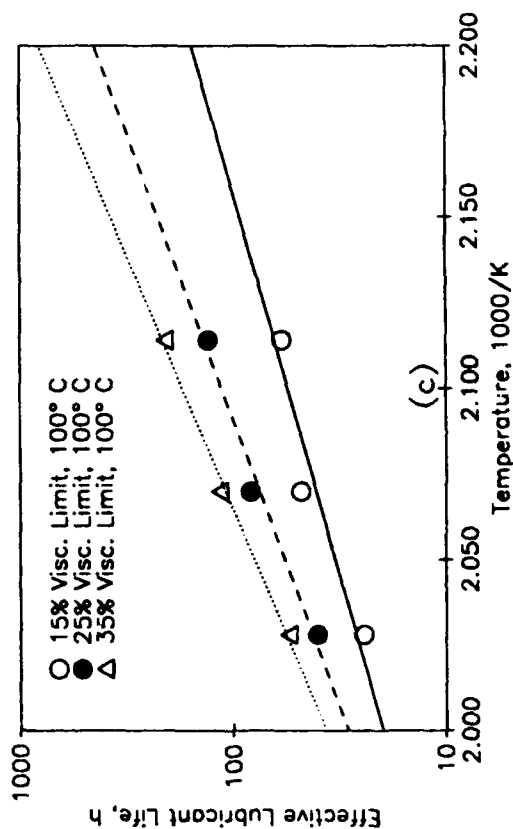
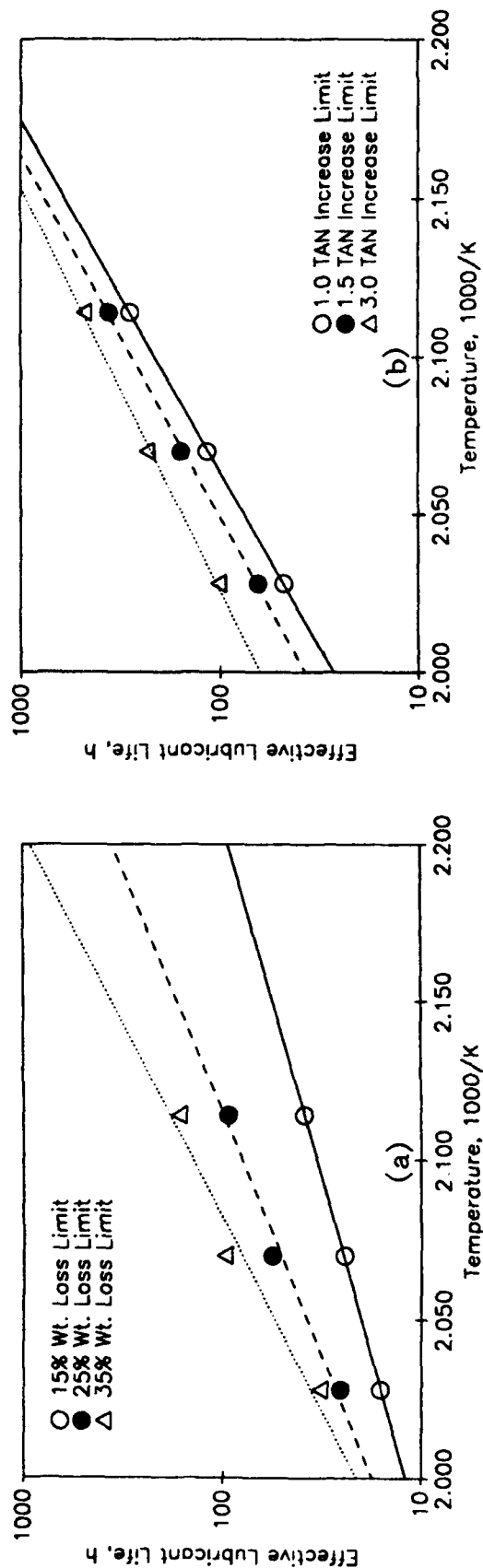


Figure A-19 Effective Lubricant Life as a Function of Temperature for TEL-91053 Based on:

(a) Percent Weight Loss Limits

(b) Percent Viscosity Change at 100°C

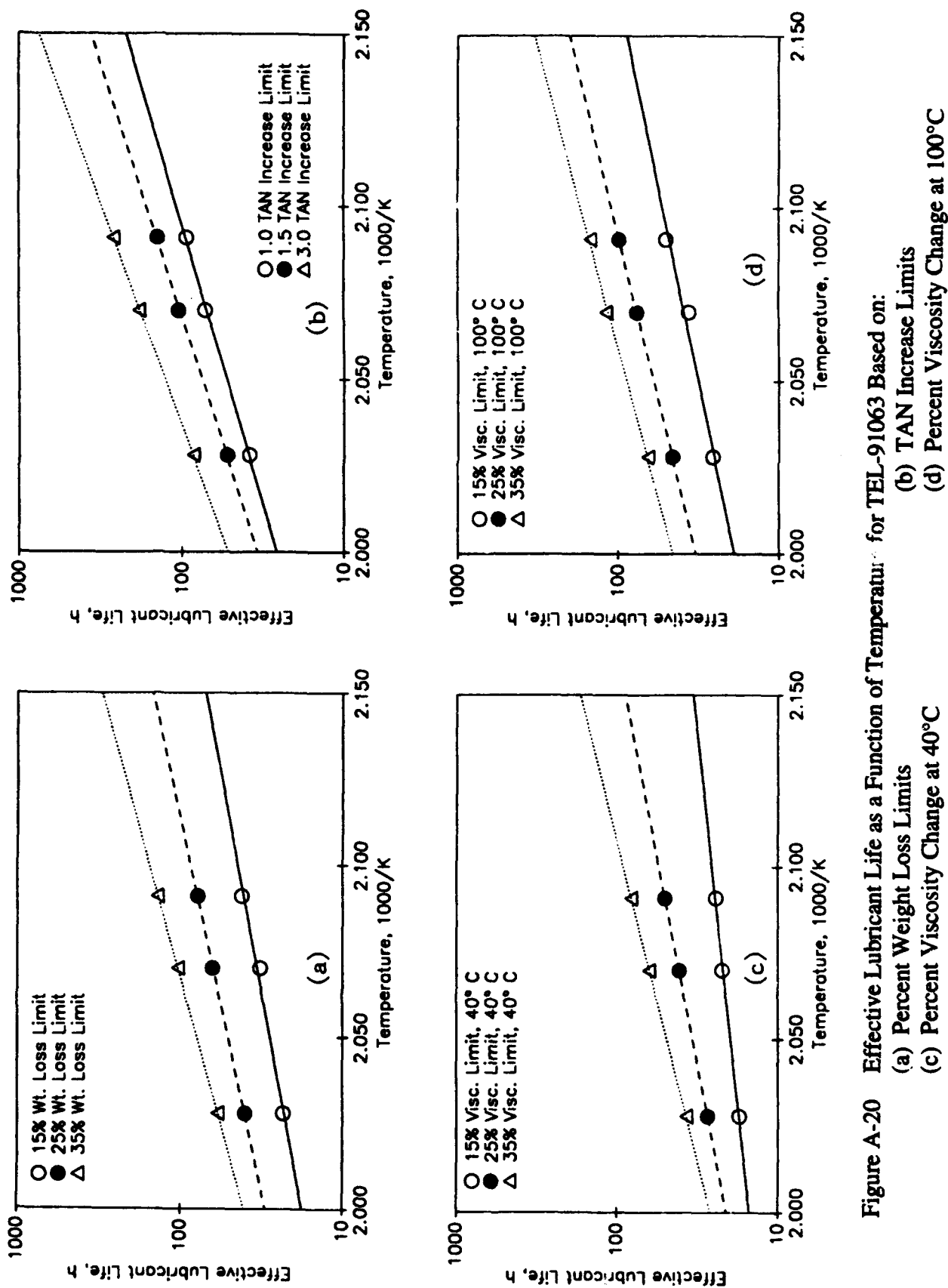


Figure A-20 Effective Lubricant Life as a Function of Temperature for TEL-91063 Based on:  
 (a) Percent Weight Loss Limits  
 (b) TAN Increase Limits  
 (c) Percent Viscosity Change at 40°C  
 (d) Percent Viscosity Change at 100°C

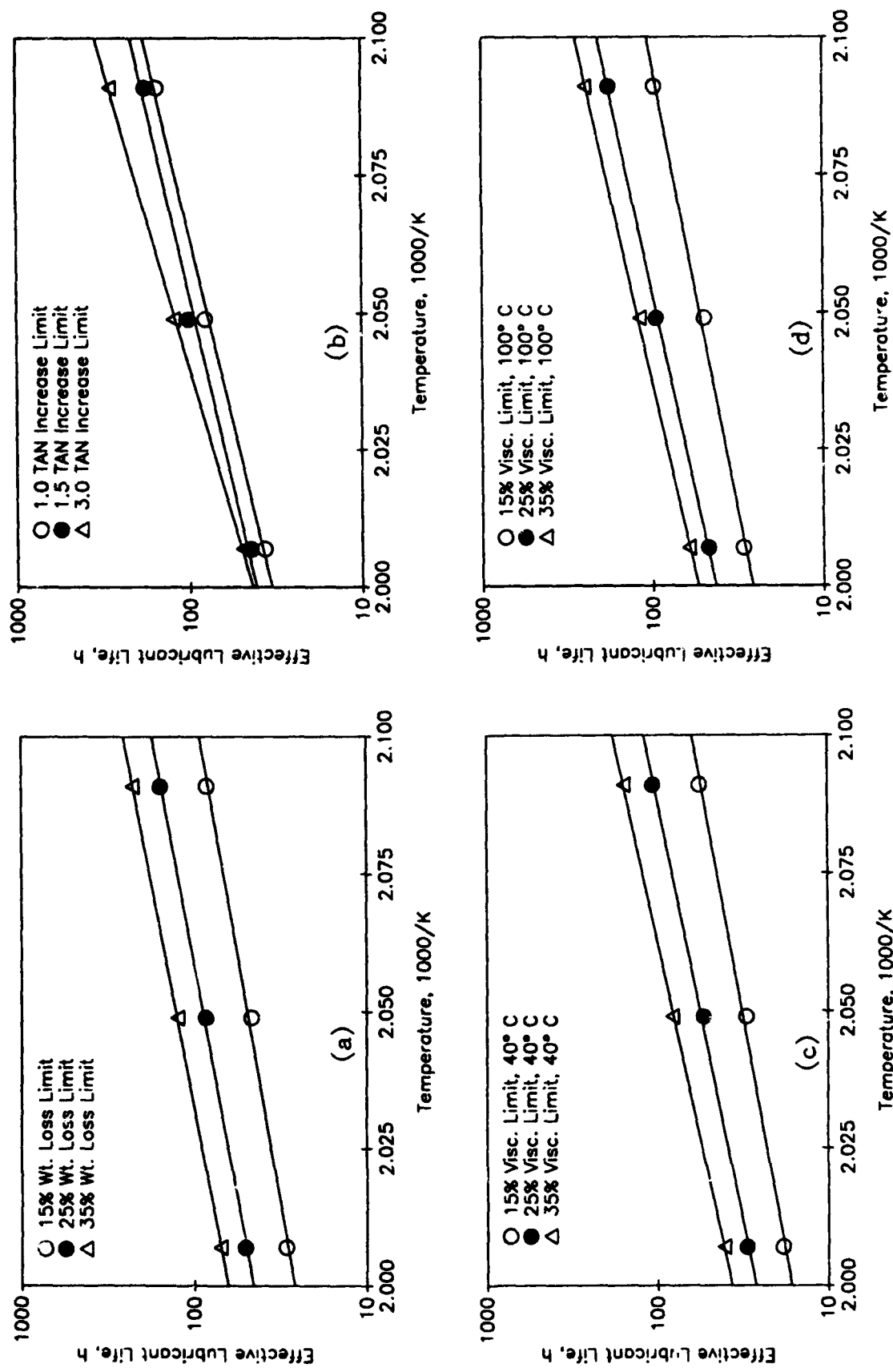


Figure A-21 Effective Lubricant Life as a Function of Temperature for TEL-92039 Based on:  
 (a) Percent Weight Loss Limits  
 (b) TAN Increase Limits  
 (c) Percent Weight Loss Limits  
 (d) Percent Viscosity Change at 100°C

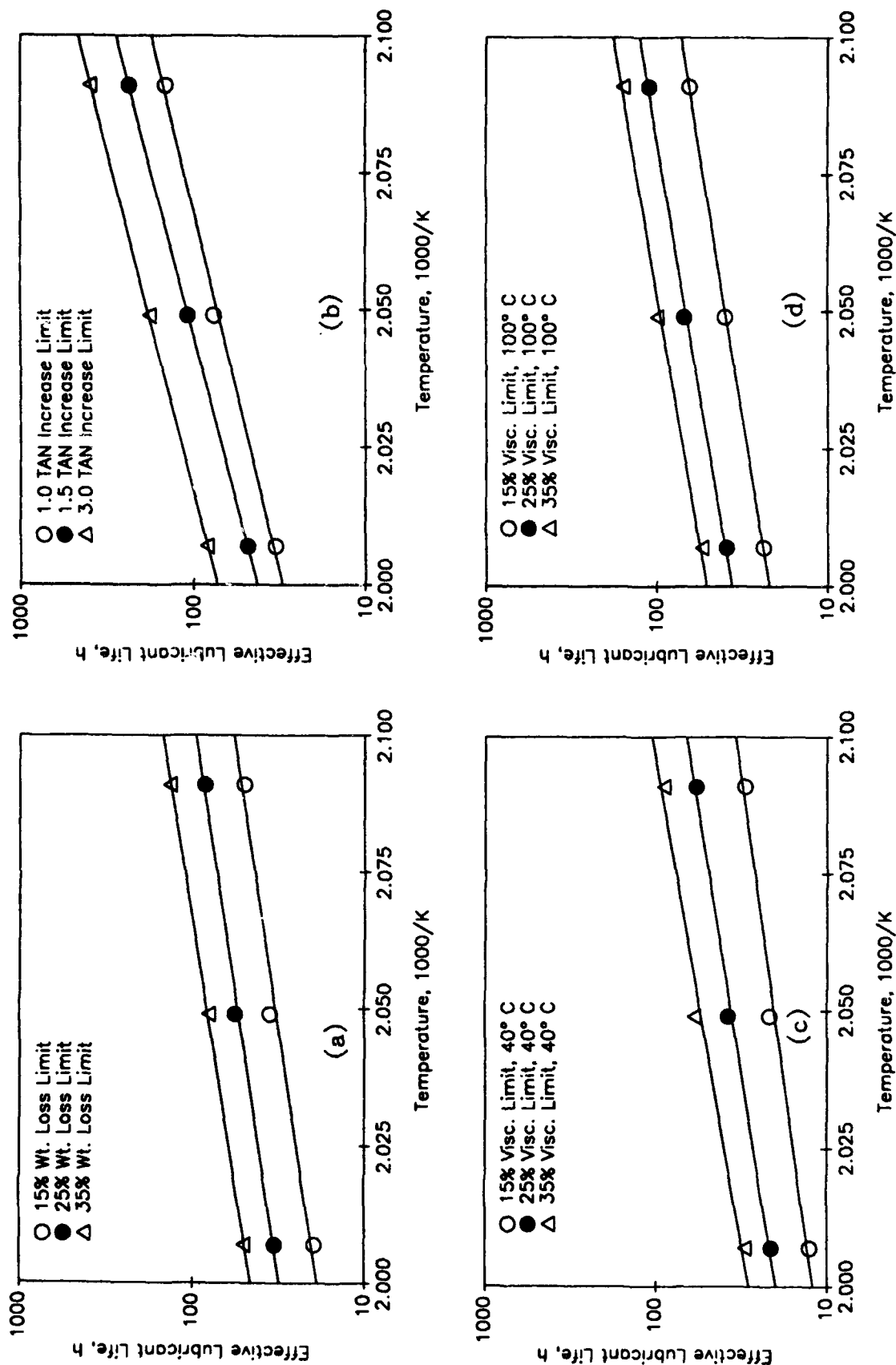


Figure A-22 Effective Lubricant Life as a Function of Temperature for TEL-92040 Based on:

(a) Percent Weight Loss Limits

(b) TAN Increase Limits

(c) Percent Viscosity Change at 40°C

(d) Percent Viscosity Change at 100°C

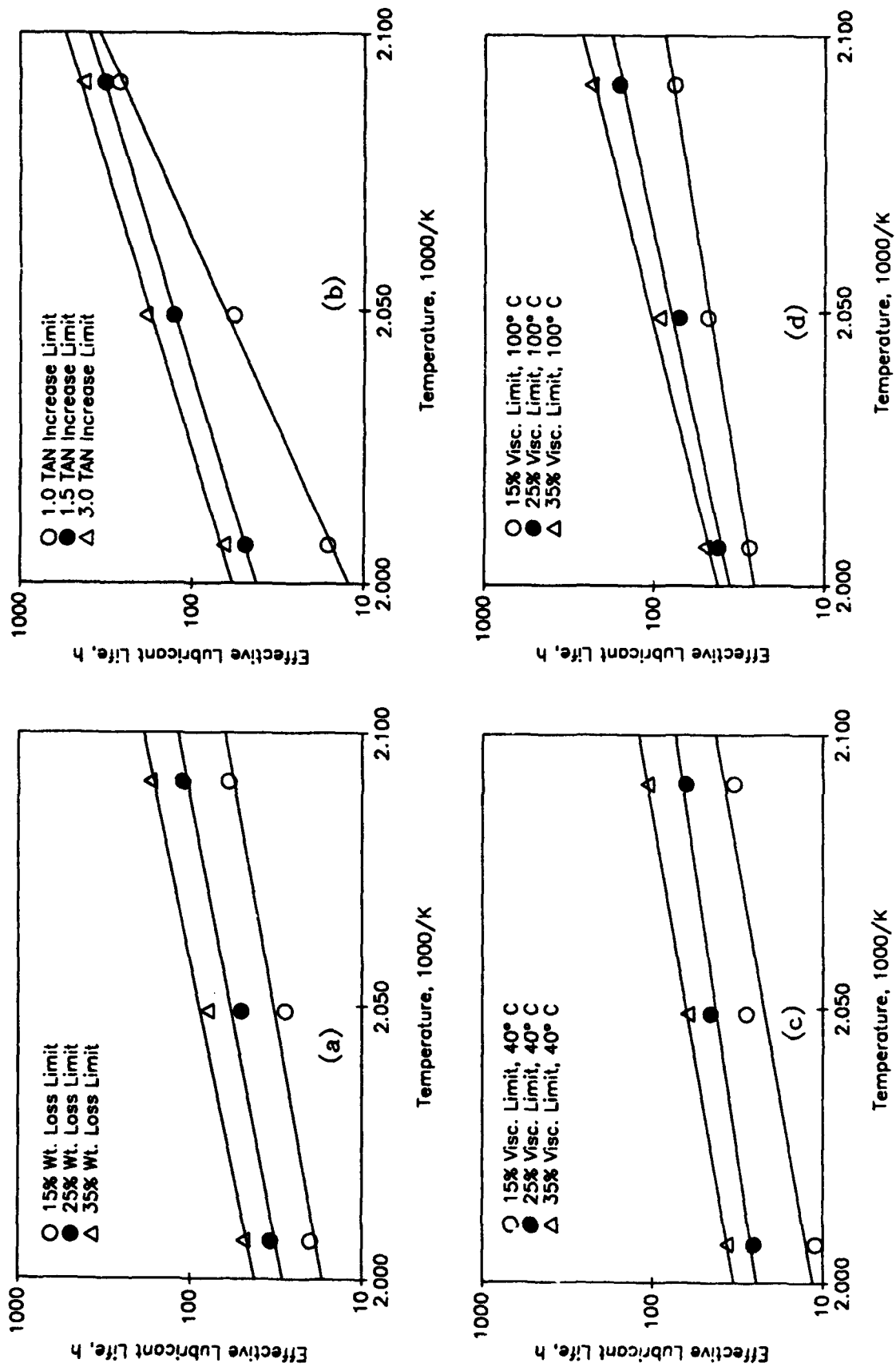


Figure A-23 Effective Lubricant Life as a Function of Temperature for TEL-92041 Based on:  
 (a) Percent Weight Loss Limits  
 (b) TAN Increase Limits  
 (c) Percent Viscosity Change at 40°C  
 (d) Percent Viscosity Change at 100°C

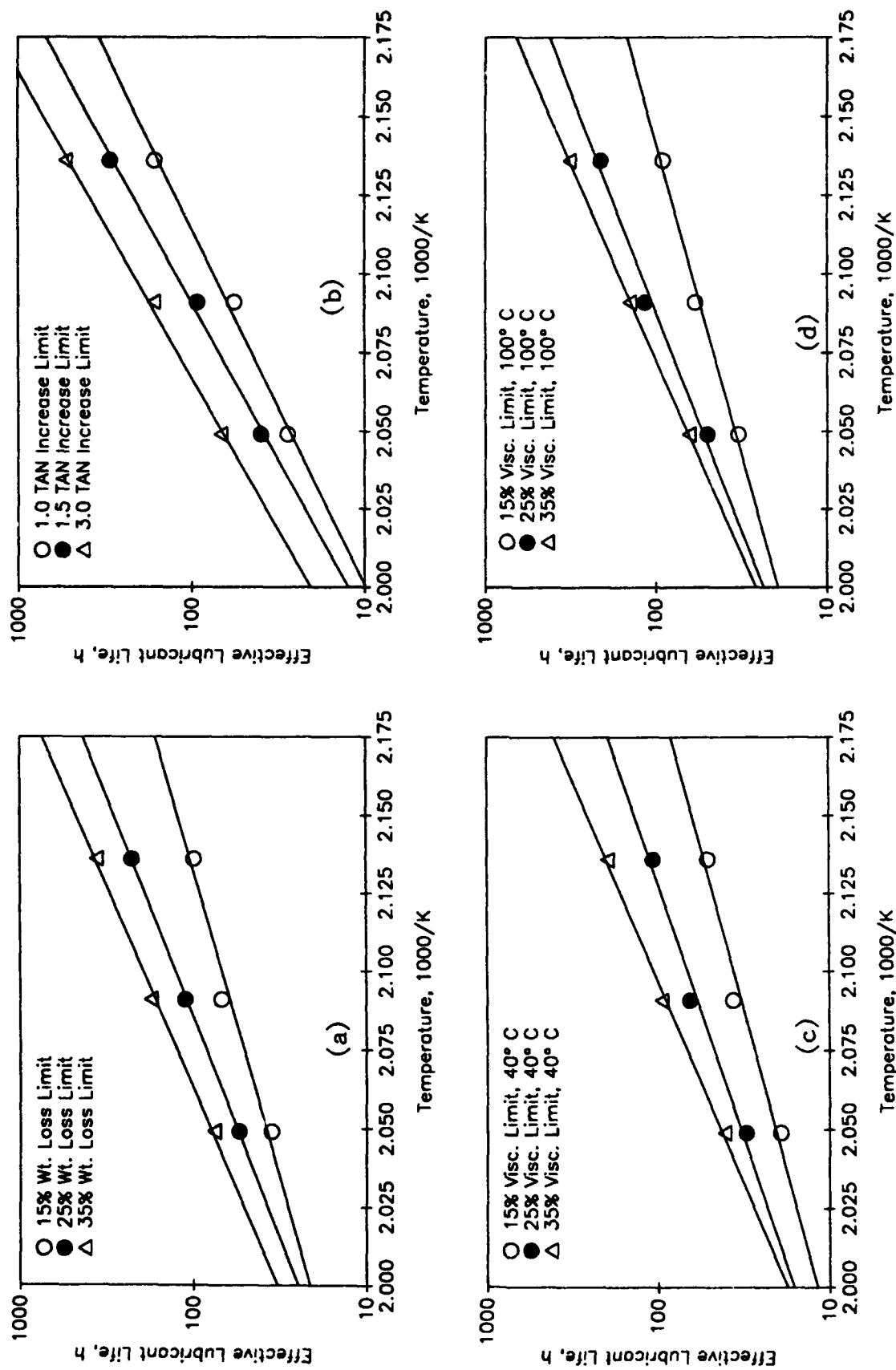


Figure A-24 Effective Lubricant Life as a Function of Temperature for TEL-92049 Based on:  
 (a) Percent Weight Loss Limits  
 (b) TAN Increase Limits  
 (c) Percent Viscosity Change at 40°C  
 (d) Percent Viscosity Change at 100°C

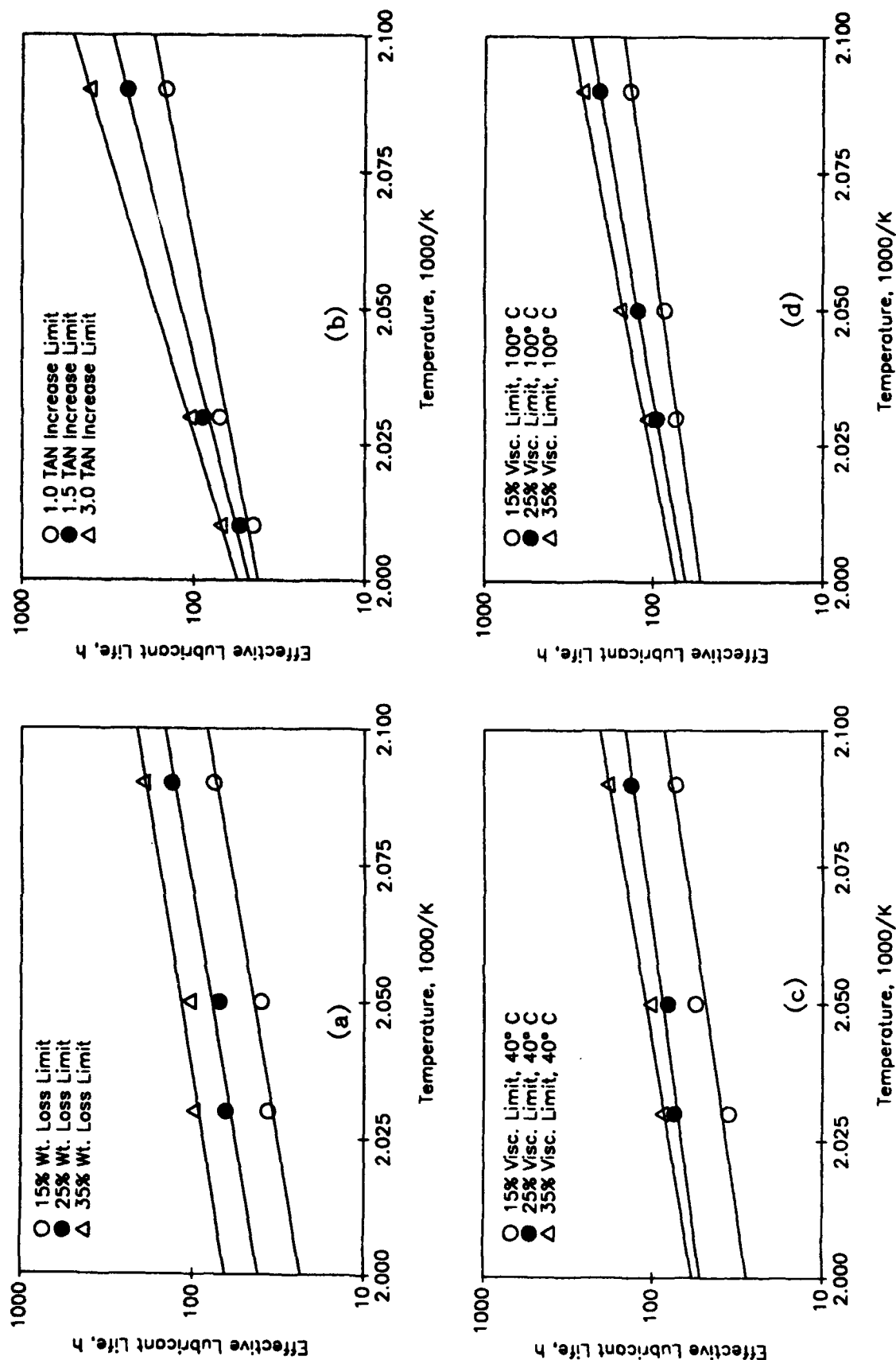


Figure A-25 Effective Lubricant Life as a Function of Temperature for TEL-92050 Based on:  
 (a) Percent Weight Loss Limits  
 (b) TAN Increase Limits  
 (c) Percent Viscosity Change at 40°C  
 (d) Percent Viscosity Change at 100°C

## APPENDIX B

### DETERMINATION OF THE BETA PARAMETER FOR THREE-BALL-ON-DISK WEAR SCARS

#### 1. INTRODUCTION

The geometry of the three-ball-on-disk test configuration was examined to develop a method to calculate the wear volumes of disk and ball specimens by the size and shape of the scars on the balls. Previously,<sup>3</sup> a relationship was found between the length of the lower ball wear scar normal to the direction of sliding to the relative displacement of the top ball for the four-ball wear test. Using the same procedure for analyzing the four-ball wear model, new relationships can be derived for the simpler geometry of the TBOD test.

#### 2. THREE-BALL-ON-DISK GEOMETRY, COORDINATE AXES

Figure B-1 shows the geometry of the disk and one ball, before and after wear, in the x-y plane. As wear proceeds, the vertical distance between the unworn disk surface and the ball center changes from  $k_0$  to  $k$ . The region bounded by the original disk and ball surfaces between points p1 and p2 represents the cross-section of the material that must be removed or deformed in order to allow the center of the upper ball to move from  $k_0$  to  $k$ . If the balls do not deform and the disk does not wear, the profile of the ball scars would be exactly represented by the disk profile. This ideal case will be referred to as the "geometric intersection." In actuality, the balls will undergo some elastic deformation and the disk will have some measure of wear. To represent the cross-section in either case, the points p1 and p2 must be located, and the profile connecting these points must be accurately modeled.

#### 3. SCAR END POINTS

There are two factors that influence the location of p1 and p2, wear and elastic deformation. First, assume that the balls wear without deformation so that the end points of the scar will be the same as p1 and p2 in Figure B-1. This assumption will be true regardless of the relative amount of disk and ball wear. In this case, the end points are directly related to the upper ball position.

By assuming that the end points of the actual scar profile correspond to points p1 and p2 of Figure B-1, the coordinates of these points can be found by solving for the unknown side of a

right triangle with a hypotenuse of  $R$  and one side of length  $k$ . The relationship between the chord,  $c$ , connecting  $p_1$  and  $p_2$  and the distance between the disk and balls is:

$$c = 2\sqrt{R^2 - k^2} \quad B1$$

Equation B1 has been derived by neglecting the contribution of elastic deformation to the scar size. Since deformation does take place, the resulting contact area causes the centers of the specimens to approach one another. For a load of 147 N, the displacement is approximately 0.0026 mm, and the corresponding Hertz diameter is 0.2552 mm (calculated using the appropriate equations and graphs from Boresi and Sidebottom, Advanced Mechanics of Materials, John Wiley and Sons, Inc., New York (1985), pp 599-621). If this displacement from deformation is inserted into Equation B1, the resulting chord length is calculated to be 0.3616 mm. This value is the small scar limit below which Equation B1 does not apply. Scar sizes greater than this value will diminish the effect of Hertz deformations because for a chord length of 0.2552 the volume which could be attributed to wear is only 0.0001 mm<sup>3</sup>.

#### 4. DERIVATION OF SCAR EQUATION

With the end points of the scar located, the only region left to model is the path connecting  $p_1$  and  $p_2$ . From Figure B-1, it is apparent that the scar surface must lie somewhere between the original unworn disk surface and the original unworn ball surface. If the assumption is made that the scar cross-section normal to sliding is circular, the scar profile may be represented by the surface,  $s$ , shown in Figure B-2. The equation for the circle may be found by forming a linear combination of the disk surface and the ball surface between  $p_1$  and  $p_2$ . Let:

$$\beta_1(x^2 + y^2 - R^2) + \beta_2(y - k) = 0 \quad B2$$

where  $\beta_1$  and  $\beta_2$  are weighting functions such that:

$$\beta_1 + \beta_2 = 1 \quad B3$$

Let:

$$\beta = \beta_1 = 1 - \beta_2 \quad (0 \leq \beta \leq 1) \quad \text{B4}$$

so that Equation B2 becomes:

$$\beta(x^2 + y^2 - R^2) + (1 - \beta)(y - k) = 0 \quad \text{B5}$$

Dividing Equation B5 by  $\beta$  gives:

$$x^2 + y^2 - R^2 + \left(\frac{1 - \beta}{\beta}\right)(y - k) = 0 \quad \text{B6}$$

By substituting:

$$\delta = \frac{1 - \beta}{\beta} \quad \text{B7}$$

Equation B6 can be easily rearranged to fit the equation of a circle:

$$x^2 + \left(y + \frac{\delta}{2}\right)^2 = R^2 + \delta\left(k + \frac{\delta}{4}\right) \quad \text{B8}$$

Equation B8 is the three-ball-on-disk equivalent to the scar equation derived for the four-ball test.<sup>3</sup> Equation B8 generates the profile circle illustrated in Figure B-2. From this figure, delta is a measure of the distance from the center of the profile circle,  $s$ , to the center of the ball. Where beta is a dimensionless profile parameter, delta is a dimensionless radius of curvature parameter. When beta is 1, delta is 1, and the radius of curvature of the scar equation is the radius of the ball. When beta is 0, delta is infinite, and the radius of curvature is infinitely long so that the scar equation reduces to the equation of the disk.

## 5. USING THE BALL SCAR WIDTH TO DETERMINE A POINT ON THE SCAR PROFILE

The beta parameter in Equation B5 can be chosen so that the surface,  $s$ , of Figure B-2 will intersect points  $p_1$  and  $p_2$  and model the position of the interface between the disk and balls. Beta averages the peaks and valleys of actual profiles so that accurate volume calculations can be made even from rough scars.

In order to arrive at a value for beta, another point on the profile circle is needed. For a convenient reference, the point  $q$  shall be located half-way between  $p_1$  and  $p_2$ . The points  $p_3$  and  $p_4$  are introduced to correspond to the width at the middle of the ball scar so that the  $z$  coordinate of  $p_3$  is  $w/2$  and the  $z$  coordinate of  $p_4$  is  $-w/2$ . The  $y$  coordinates of  $p_3$ ,  $p_4$ , and  $q$  are identical because these points all lie along the deepest part of the disk wear track. Figure B-3 shows a section of the ball cut in the  $y$ - $z$  plane at  $x = 0$  along with the points  $p_3$ ,  $q$ , and  $p_4$ . The equation of the unworn ball surface in this plane is:

$$y^2 + z^2 = R^2 \quad \text{B9}$$

With the  $z$  coordinate at either  $p_3$  or  $p_4$ , the value for  $y$  is calculated to be:

$$y = \sqrt{R^2 - \left(\frac{w}{2}\right)^2} \quad \text{B10}$$

Therefore, the scar equation has a solution at the coordinates:

$$\left(0, \sqrt{R^2 - \left(\frac{w}{2}\right)^2}, 0\right) \quad \text{B11}$$

By inserting the coordinates of point  $q$  into Equation B8 and rearranging Equation B1 in order to substitute for  $k$ , the following relation for delta (expressed solely in terms of the known quantities  $R$ ,  $c$ , and  $w$ ) results:

$$\delta = \frac{\left(\frac{w}{2}\right)^2}{\sqrt{R^2 - \left(\frac{w}{2}\right)^2} - \sqrt{R^2 - \left(\frac{c}{2}\right)^2}} \quad \text{B12}$$

Beta can finally be calculated by rearranging Equation B7 into the form:

$$\beta = \frac{1}{\delta + 1} \quad \text{B13}$$

Figure B-4 illustrates the relationship between scar length and width for various values of the beta parameter. As beta varies from 0 to 1, the ball scars become increasingly elliptical, changing from a circle when beta is 0 to a line (no scar) when beta is 1.

## 6. DISK WEAR VOLUME

The wear volume of the disk was found by calculating the area of the portion of  $s$  which intersects with the original disk surface. This area is merely a circular cap, and the wear volume is calculated by multiplying the area by the circumference of the circle in which the three balls rotate.

## 7. BALL WEAR VOLUME

The ball wear volume is calculated by first dividing up the scar region into  $n$  increments along the  $y$  axis. The scar region varies between  $y = k$  and Equation B10, and the areas in the  $x$ - $z$  plane at each  $y$  increment must be calculated. Examples of these areas are shown in Figure B-5 for two increments. The first area corresponds to the  $y$  value at the lowest point in the disk wear track (Equation B10). No area exists at this  $y$  value because there is only a line in the  $x$ - $z$  plane. In contrast, the area at  $y = k$  corresponds to a circle since this plane represents the periphery of the unworn ball. All other cross-sections between these  $y$  values will resemble the third area shown in Figure B-5. This area can be calculated by first finding the area of the rectangular portion and then adding the areas of the two circular caps.

The volume of the remaining portion of the ball in the scar region is calculated by averaging the areas between adjacent cross-sections and multiplying this value by the thickness of the increment. All of these incremental volumes are summed and the volume of wear is found by subtracting this remaining volume from the volume of a spherical cap defined by the original disk surface. The sensitivity of volume calculations on the correct value of beta is illustrated in Figure B-6. The volumes were calculated at various ball displacements by assuming different values for beta. Although the wear volumes for the extremes of the beta parameter (0 and 1) is tremendous, a dramatic difference can be seen within the range from 0.00 to 0.10. By referring to Figure B-4, a beta of 0.1 gives a ratio of width to length of approximately 0.645 (the slope of the curve for this beta value). Calculations of the total wear volume, therefore, are exceedingly sensitive to the ellipticity of the ball scars.

## 8. CONCLUSION

From the geometry of the three-ball-on-disk configuration, the ball scar length normal to the direction of sliding is found to be a function of only the upper ball displacement. The ball scar width (parallel to sliding direction) is related to the amount of disk wear. The degree of disk wear determines the curvature of the interface between upper and lower balls normal to sliding (assuming that the profile can be fitted by a circular arc).

A dimensionless surface parameter, beta, defines the circle that approximates the scar profiles. Beta can be determined after a test by measuring the lengths and widths of the scars on the balls. The average beta value for the three balls can then be used to calculate the wear volumes for both disk and balls.

In addition to the accurate quantification of wear for the three-ball-on-disk test, the wear model developed by this geometrical analysis can also be applied to the pin-on-disk test. For hemispherically-tipped riders, the geometric description for these two tests is identical.

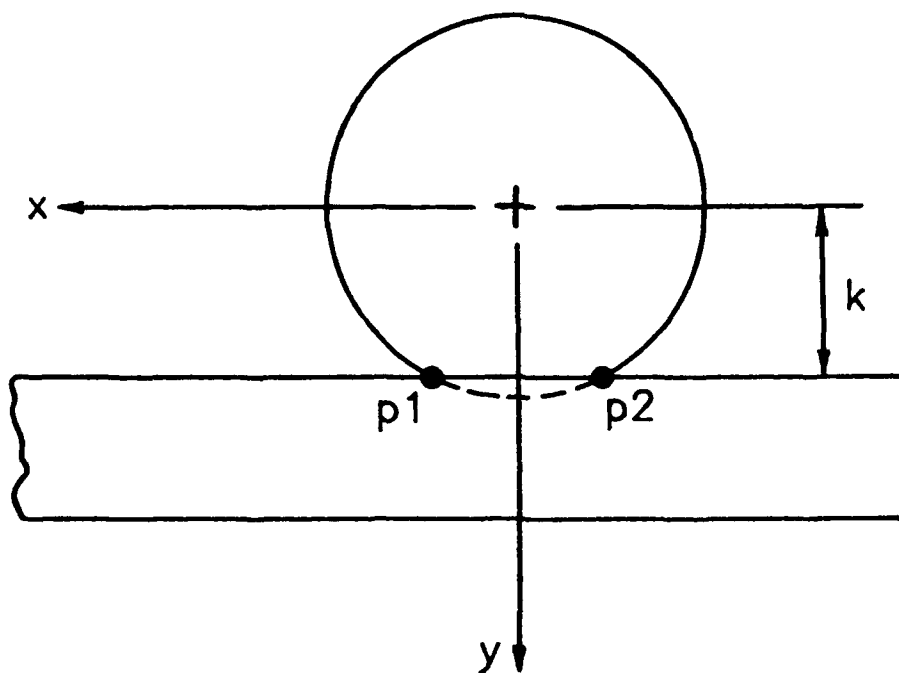
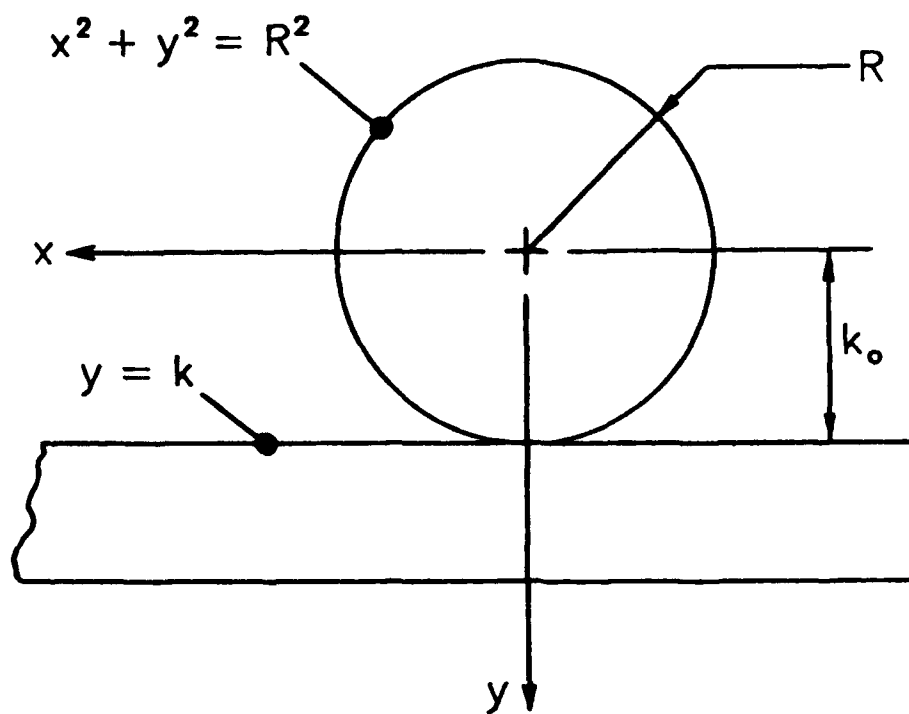


Figure B-1. TBOD Configuration Showing One Ball Before and After Wear.

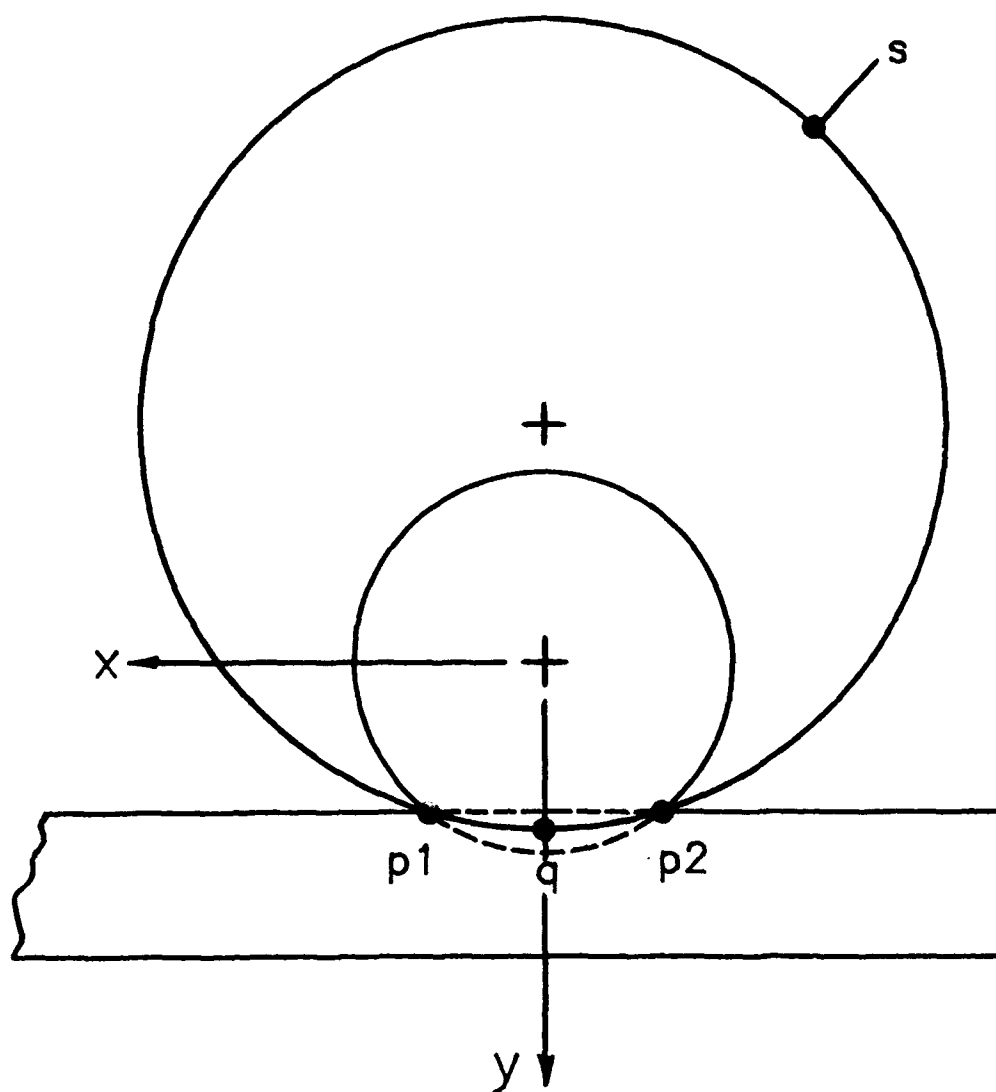
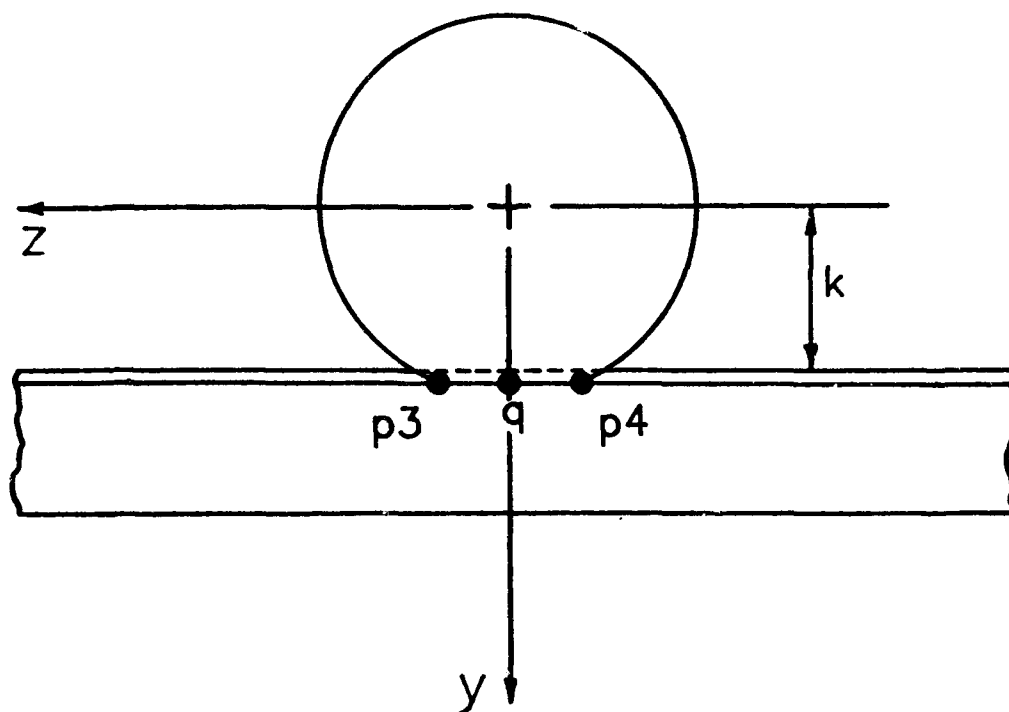


Figure B-2. Scar Surface,  $s$ , Corresponding to Wear on Both the Ball and the Disk.



**Figure B-3. Cross-Section of the Ball and Disk at the Deepest Part of the Disk Wear Track (Ball Slides in the +z Direction).**

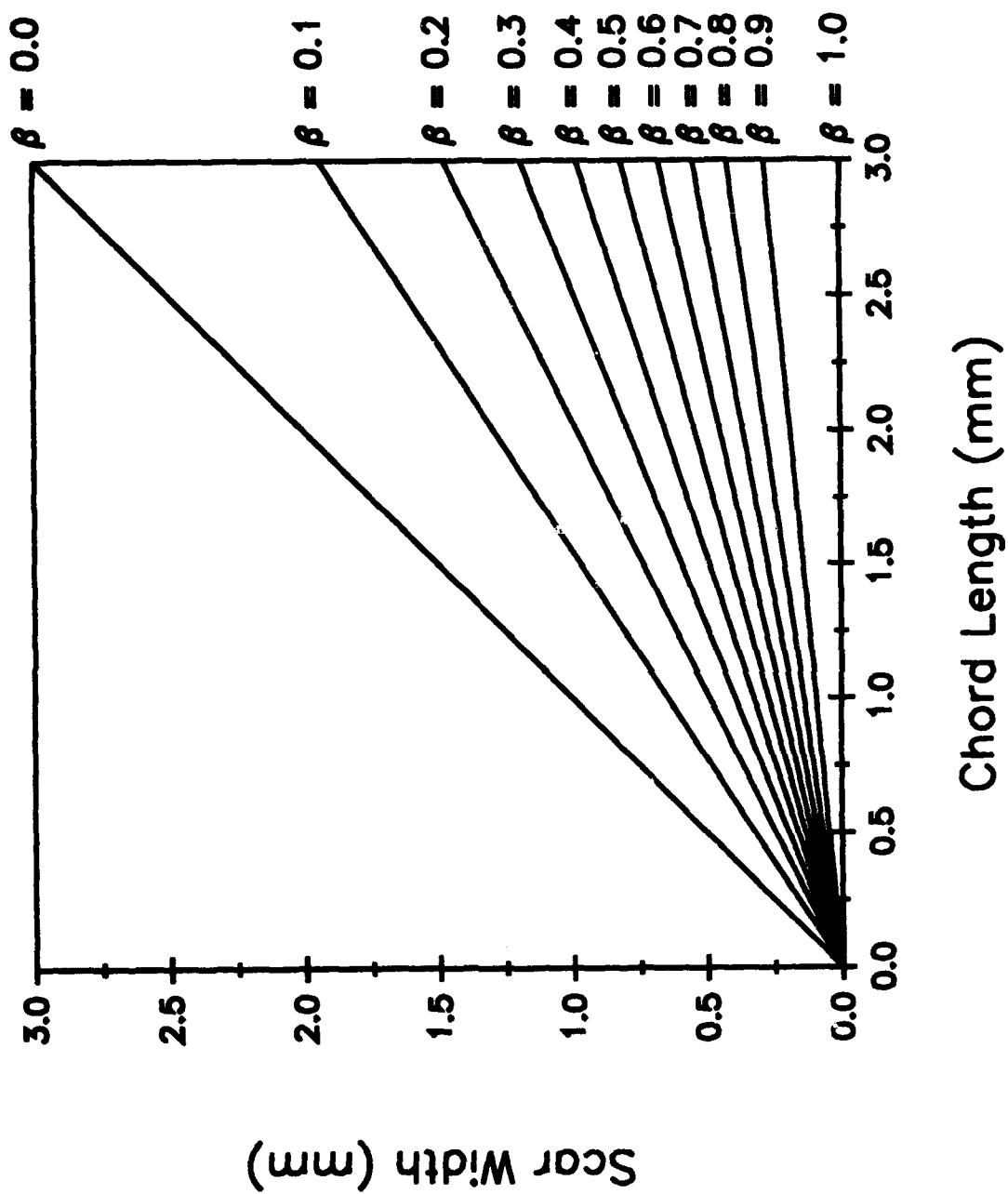
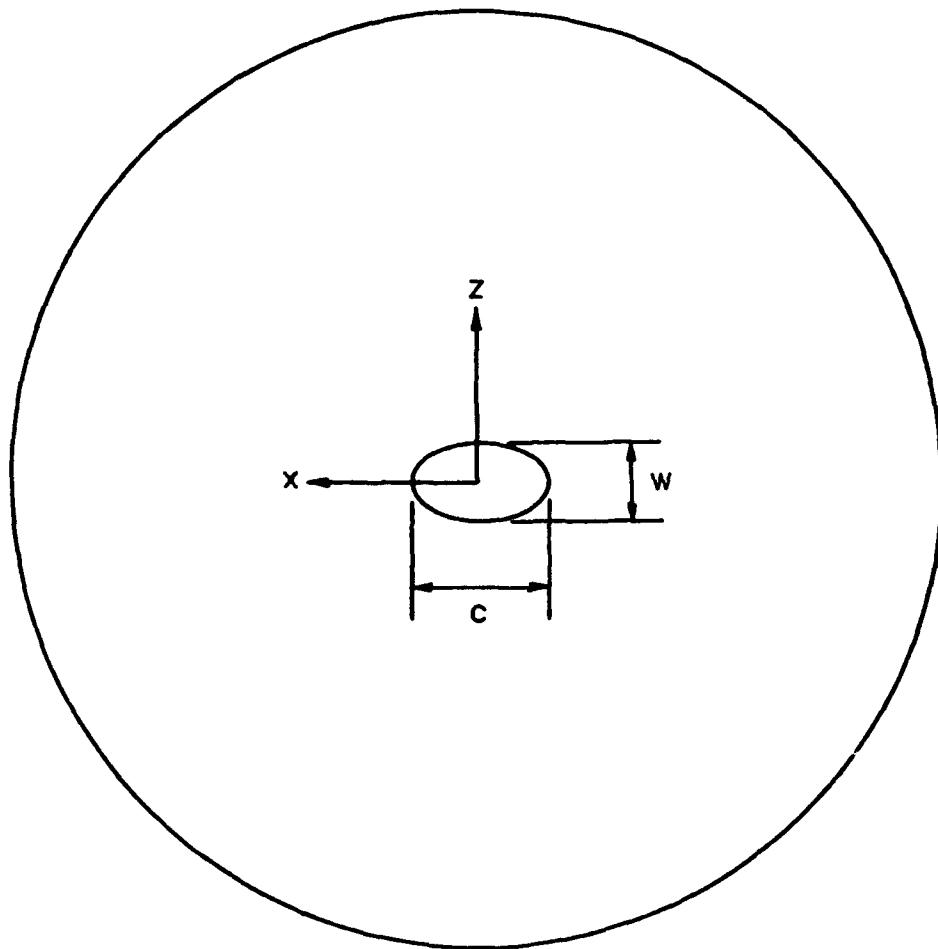


Figure B-4. Relationship Between Scar Width and Chord Length for Selected Values of Beta Ranging from 0 to 1.



$$\odot y = y' = \sqrt{R^2 - \left(\frac{w}{2}\right)^2}$$

$$\bullet y = y'' = k$$

$$\odot y' \geq y \geq y''$$

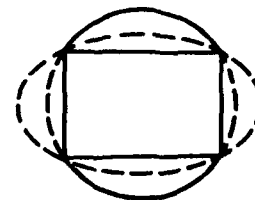
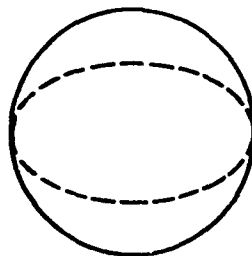
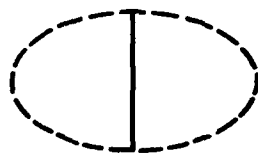


**Figure B-5. View of Scarred Ball (Looking in -y Direction) Along with Cross-Sections of the Scar Region in Different x-z Planes.**

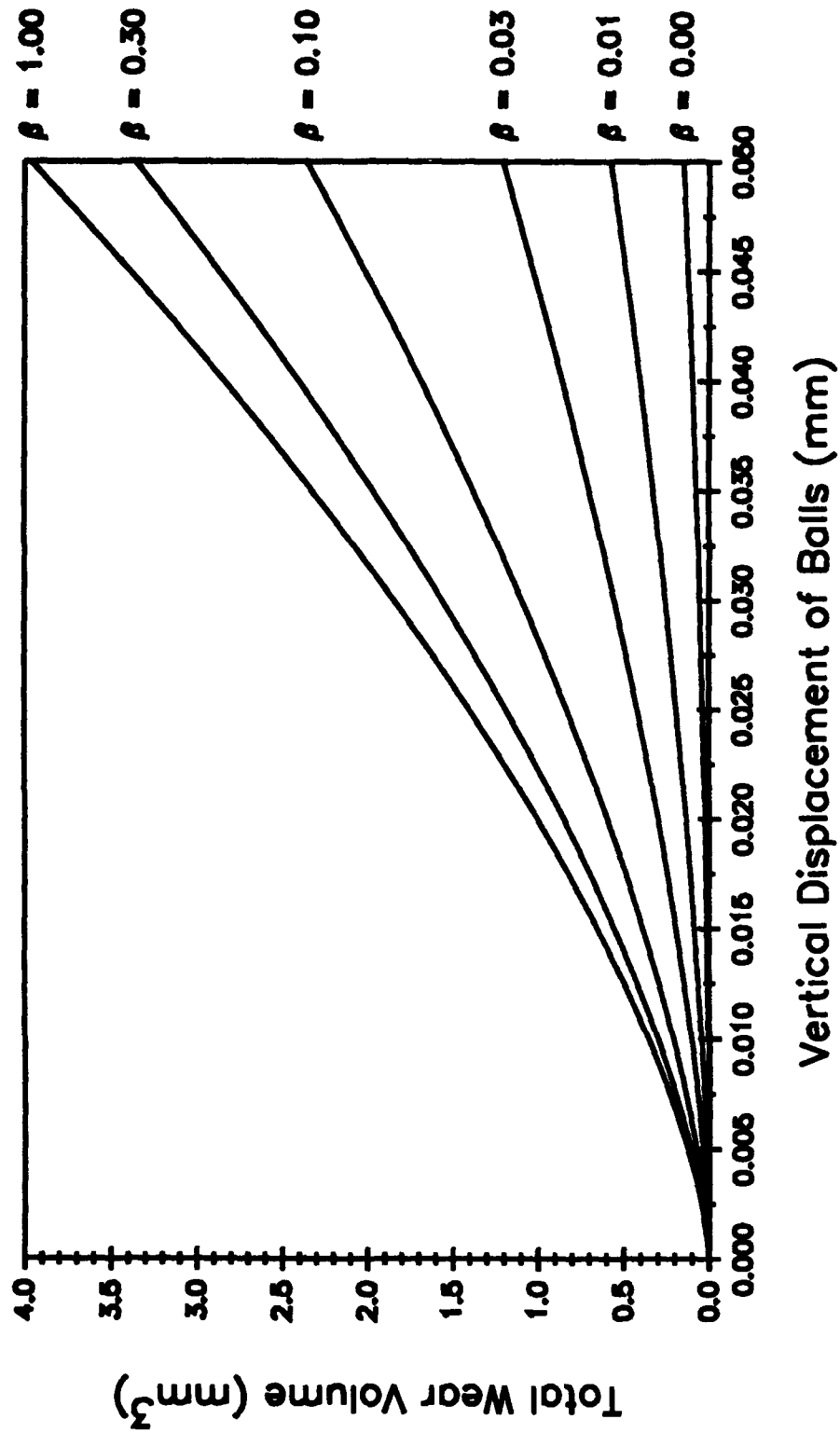


Figure B-6. Sensitivity of Volume Calculations to the Beta Parameter.

## REFERENCES

1. Saba, C.S., Smith, H.A., Keller, M.A., Jain, V.J. and Kauffman, R.E., "Lubricant Evaluation and Performance," Interim Technical Report AFWAL-TR-87-2025, DDC No. AD A183881, June 1987.
2. Saba, C.S., Smith, H.A., Keller, M.A., Kauffman, R.E. and Jain, V.J., "Lubricant Evaluation and Performance," Final Technical Report AFWAL-TR-89-2008, DDC No. A208925, April 1989.
3. Saba, C.S. et al., "Lubricant Evaluation and Performance II," Interim Technical Report WL-TR-91-2111, January 1992.
4. Blake, E.S. and Smith, J.O., "Research to Develop a Gas Turbine Lubricant Based on Polyphenyl Ethers," Technical Report ASD-TDR-63-728, March 1964.
5. Schevchenko, R.P., "Lubricant Requirements for High Temperature Bearings," SAE Paper No. 660072, Presented at the Automotive Engineering Congress, Detroit, MI, January 10-14, 1966.
6. Schmidt, L.J., Krimmel, J.A. and Farrell, T.J., "Chain Type Polyphenyl and Poly-nuclear Aromatic Compounds as Base Materials for High Temperature Stable and Radiation Resistant Lubricants and Hydraulic Fluids," WADC Technical Report 56-207, Part III, April 1958.
7. Bolt, R.O. and Carroll, J.G., "Effects of Radiation on Aircraft Lubricants and Fuels," WADC Technical Report 56-646, Part II, April 1958.
8. Blake, E.S., Edwards, J.W., Hammann, W.C. and Reichard, T., "High Temperature Hydraulic Fluids, Part 2-Development of Base Stock," WADC Technical Report 54-532, Part 2, January 1956.
9. Dolle, R.E. "Examination of Basestocks and Fluid Formulations for Use as High Temperature Gas Turbine Lubricants," Technical Report RTD-TDR-63-4065, November 1963.
10. Dolle, R.E. "Basestock Characterization and Formulation Development for High Temperature Gas Turbine Lubricants," Technical Report ASD-TDR-63-177, May 1963.
11. Spar, C., and Damasco, F., "High-Temperature Fluid Lubrication," ASLE Trans., 7, pp. 211-217 (1964).
12. Wills, J.G., Lubrication Fundamentals, Marcel Dekker, Inc., New York and Basel, 1980.

13. Alsaad, M., Bair, S., Sanborn, D.M., and Winer, W.O., "Glass Transitions in Lubricants: Its Relation to Elastohydrodynamic Lubrication (EHD)," ASME Trans., 100, pp. 404-417 (1978).
14. Klaus, E.E., Duda, J.L., and Chao, K.K., "A Study of Wear Chemistry Using a Micro Sample Four-Ball Wear Test," Tribo. Trans., 34(3), pp. 426-432 (1991).
15. Klaus, E.E., Nagarajan, R., Duda, J.L., and Shah, K.M., "The Adsorption of Tribochemical Reaction Products at Solid Surfaces," Proc. Inst. Mech. Eng., International Conference on Tribology--Friction, Lubrication and Wear, Vol. 1, London, 1-3 July 1987.
16. Adam, N.K., The Physics and Chemistry of Surfaces, 3rd Edition, Oxford University Press, 1941.
17. Godfrey, D., "The Lubrication Mechanism of Tricresyl Phosphate on Steel," ASLE Trans., 8, pp. 1-11 (1965).
18. Gauthier, A., Montes, H., and Georges, J.M., "Boundary Lubrication with Tricresyl Phosphate (TCP). Importance of Corrosive Wear," ASLE Trans., 25(4), pp. 445-455 (1981).
19. Klaus, E.E., and Bieber, H.E., "Effects of P<sup>32</sup> Impurities on the Behavior of Tricresyl Phosphate-32 as an Antiwear Additive," ASLE Trans., 8, pp. 12-20 (1965).
20. Bieber, H.E., Klaus, E.E., and Tewksbury, E.J., "A Study of Tricresyl Phosphate as an Additive for Boundary Lubrication," ASLE Trans., 11, pp. 155-161 (1968).
21. Dorinson, A., and Ludema, K.C., Mechanics and Chemistry in Lubrication, Elsevier, New York, 1985.
22. ASTM Method of D4636: "Corrosiveness and Oxidation Stability of Hydraulic Oils, Aircraft Turbine Engine Lubricants, and Other Highly Refined Oils," Published yearly by the American Society for Testing and Materials, 1916 Race Street, Philadelphia, Pennsylvania.
23. Cvitkovic, E., Klaus, E.E., and Lockwood, F., "A Thin-Film Test for Measurement of the Oxidation and Evaporation of Ester-Type Lubricants," ASLE Trans., 22, p. 395 (1979).
24. Klaus, E.E., Cho, L., and Dang, H., "Adaptation of the Penn State Microoxidation Test for the Evaluation of Automotive Lubricants," SAE Paper No. 801362, Sp. Pub. 80-473, pp. 83-92 (1980).
25. ASTM Method of D2272: "Oxidation Stability of Steam Turbine Oils by Rotating Bomb," Published yearly by the American Society for Testing and Materials, 1916 Race Street, Philadelphia, Pennsylvania.

26. ASTM Method of D4742: "Oxidation Stability of Gasoline Automotive Engine Oils by Thin-Film Oxygen Uptake (TFOUT)," Published yearly by the American Society for Testing and Materials, 1916 Race Street, Philadelphia, Pennsylvania.
27. Hsu, S.M., "Review of Laboratory Bench Tests in Assessing the Performance of Automotive Crankcase Oils," *Lubr. Eng.*, 37(12), pp 722-731 (1981).
28. Naidu, S.K., Klaus, E.E., and Duda, J.L., "Kinetic Model for High-Temperature Oxidation of Lubricants," *Ind. Eng. Chem. Prod.*, 25, pp 596-603 (1986).
29. Wang, C.C.J., Duda, J.L., and Klaus, E.E., "A Kinetic Model of Lubricant Deposit Formation Under Thin Film Conditions," STLE Preprint No. 93-AM-7D-1 (1993).
30. Klaus, E.E., Duda, J.L., and Naidu, S.K., "Formation of Lubricating Films at Elevated Temperatures From the Gas Phase," NIST Special Publication 744 (1988).
31. Keller, M.A., and Saba, C.S., "Characterization of Higher Molecular Weight Oxidation Products of Formulated and Unformulated Polyphenyl Ethers," *Tribo. Intern.*, 24(6), pp. 323-328 (1991).
32. McHugh, K.L. and Stark, L.R., "Properties of a New Class of Polyaromatics for Use as High-Temperature Lubricants and Functional Fluids," *ASLE Trans.*, 9, pp. 13-23 (1966).
33. Clark, F.S. and Miller, D.R., "Formulation and Evaluation of C-Ether Fluids as Lubricants Useful to 260°C," NASA-CR-159794, Dec. 1980.
34. Jones, W.R., "The Effect of Oxygen Concentration on the Boundary-Lubricating Characteristics of a C-Ether and Polyphenyl Ether to 300°C," *Wear*, 73, p. 123 (1981).
35. Jones, W.R., "Boundary Lubrication of Formulated C-Ethers in Air to 300°C," *Lub. Eng.*, 32, pp. 530-538 (1976).
36. Sullivan, J.D., "Functional Fluid Compositions Containing Substituted Pyrimidines," US Patent 3939084 (1976)
37. Clark, J.D. and Banniser, L.W., "Compositions Comprising Boron Compounds and Polyphenyl Thioethers," US Patent 3751368 (1973)
38. Jones, W.R. and Morales, W., "Thermal and Oxidative Degradation Studies of Formulated C-Ethers by Gel Permeation Chromatography," NASA-TP-1994, March 1982.
39. Barnard, D., Bateman, L., and Cuneen, J. I., "Oxidation of Organic Sulfides," Chapter 21, *Organic Sulfur Compounds*; Pergamon Press, (1961), Ed. Kharasch, N. pp. 229-247.

40. Clark, F.S. and McHugh, K.L., "Treatment of Poly(Phenyl Thioethers) to Improve Their Color, Odor, and Oxidative Stability and to Decrease Their Corrosiveness to Metals," G.B. Patent 1209500 (1970).
41. Giesecking, C.W., "Improvement of Polyphenyl Thioethers," DE Patent 1903596 (1969).
42. Monsanto Corp., "Treatment of Polyphenyl Thioethers with a Metal," FR Patent 1590674 (1970).
43. Gumprecht, W.H., "PR-143 - A New Class of High-Temperature Fluids," ASLE Trans., 9, pp. 24-30 (1966)
44. Nader, B.S., Kar, K.K., Morgan, T.A., Pawloski, C.E. and Dilling, W.L., "Development and Tribological Properties of New Cyclotriphosphazene High Temperature Lubricants for Aircraft Gas Turbine Engines," Trib. Trans., 35(1), p. 37 (1992).
45. Allcock, H.R., "Heteratom Ring Systems and Polymers," Academic Press, New York 1967.
46. Corbridge, D.E.C., Pearson, M.S., Walling, C., "Topics in Phosphorous Chemistry," Volume 3, Interscience, New York (1966).
47. Stokes, H.N., "On the Chloronitrides of Phosphorous," Am. Chem. J., 19, p. 782 (1897).
48. Allcock, H.R., "Structural Effects in Heteratoms. I. The Influence of Steric Effects on Oligomer-Polymer Interconversions in the Phosphazene (Phosphonitrile) Series. A semiempirical Approach," Inorg. Chem., 5(8), p. 1320 (1966)
49. Fitzsimmons, B.W. and Shaw, R.A., "A Rearrangement of Some Alkoxyphosphazenes," Proc. Chem. Soc., p. 258 (1961).
50. Allcock, H.R. and Best, R.J., "Phosphonitrilic Compounds. Part I. The Mechanism of Phosphonitrilic Chloride Polymerization. Capacitance, Conductance, and Electron-Spin Resonance Studies," Can. J. Chem., 42, p. 447 (1964).
51. Yokoyama, M., Yamada, F., Kawasaki, S. and Susuki, K., "Polymerization of Triphosphonitrile Acid Esters," Kogyo Kagaku Zasshi, 66, p. 613 (1963).
52. Allcock, H.R., Kugel, R.L. and Valan, K.J., "Phosphonitrilic Compounds. VI. High Molecular Weight Poly(alkoxy - and aryloxyphosphazenes)," Inorg. Chem., 5(10), p. 1709 (1966).
53. Ratz, R., et al., "A New Class of Stable Phosphonitrilic Acid Esters. Polyfluoroalkyl Phosphonitrilates," J. Amer. Chem. Soc., 84, p. 551 (1962).

54. Lederle, H., Kober, E. and Ottmann, G., "Fluoroalkyl Phosphonitrilates, a New Class of Potential Fire-Resistant Hydraulic Fluids and Lubricants," J. Chem. Eng. Data, 11(2), p. 221 (1966).
55. Moses, C.A., Guiterraz, P.J., Baber, B.B. and Cuellar, J.P., "High-Temperature Miniaturized Turbine Engine Lubrication System Simulator," Report No. WL-TR-91-2103, February 1992.
56. Smith, H.A., Centers, P.W. and Craig, W.R., "Foaming Characteristics of MIL-L-7808 Turbine Lubricants," Report No. AFAPL-TR-75-91, November 1975.
57. Hsu, S.M., Cummings, A.L. and Clark, D.B., "Evaluation of Automotive Crankcase Lubricants by Differential Scanning Calorimetry," SAE Paper No. 821252 (1982).
58. Walker, J.A. and Tsang, W., "Characterization of Lubricating Oils by Differential Scanning Calorimetry," SAE Paper No. 801383 (1982).
59. Blaine, R.L., "Thermal Analytical Characterization of Oils and Lubricants," Amer. Lab., 50 (January, 1974).
60. Strunks, G.A., Toth, D.K., Saba, C.S., "Geometry of Wear in the Four-Ball Wear Test," Trib. Trans., 35(4), pp. 715-723 (1992).
61. Gong, D., Zhang, P. and Xue, O., "Studies on Relationships Between Structure of Chlorine-containing Compounds and their Wear and Extreme Pressure Behavior," Lubr. Eng., 46(9), pp. 566-572 (1990).
62. Shaw, M.C., "Mechanical Activation -- A Newly Developed Chemical Process," J. Appl. Mechanics, 15, pp. 37-44 (1948).
63. Jones, W.R. Jr., "Ferrographic Analysis of Wear Debris from Boundary Lubrication Experiments with a Five Ring Polyphenyl Ether," ASLE Trans., 18(3), pp. 153-162 (1975).
64. Carre, D.J., "Perfluoropolyalkylether Oil Degradation: Inference of FeF<sub>3</sub> Formation on Steel Surfaces under Boundary Conditions," ASLE Trans., 29(2), pp. 121-125 (1986).
65. Grunberg, L., "A Survey of Exo-Electron Emission Phenomena," Brit. J. Appl. Phys., 9(3), pp. 85-93 (1958).
66. Hermance, H.W., and Egan, T.F., "Organic Deposits on Precious Metal Contacts," Bell System Tech. J., 37, pp. 739-776 (1958).
67. Blau, P.J., "The Units of Wear - Revisited," Lubri. Eng., 45(10), pp. 609-614 (1989).

68. Sakurai, T., Sato, K., Hamaguchi, H. and Matsuo, K., "Effect of Internal Stress on the Wear Behavior of Steel during Boundary Lubrication," ASLE Trans., 17(3), pp. 213-223 (1973).
69. Jones, W.R. Jr., "The Tribological Behavior of Polyphenyl Ether and Polyphenyl Thioether Aromatic Lubricants," NASA Technical Memorandum 100166, July (1987).
70. Klaus, E.E., Wang, J.C., and Duda, J.L., "Thin-Film Deposition Behavior of Lubricants as a Function of Temperature: Lubricant Stability Maps," Lubri. Eng., 48(7), pp. 599-605 (1992).
71. Mahoney, C.L., Barnum, E.R., Kerlin, W.W., and Sax, K.J., "Meta-Linked Polyphenyl Ethers as High-Temperature Radiation-Resistant Lubricants," ASLE Trans., 3, pp. 83-92 (1960).
72. Sayles, R.S., Hamer, J.C. and Ioannides, E., "The Effect of Particulate Contamination in Rolling Bearings--a State of the Art Review," Proc. Instn. Mech. Engrs., Vol. 204, pp. 29-36 (1990).
73. Hamer, J.C., Sayles, R.S. and Ioannides, E., "Deformation Mechanisms and Stresses Created by 3rd Body Debris Contacts and Their Effects on Rolling Bearing Fatigue," Proceedings of the 14th Leeds-Lyon Symposium on Tribology, Paper VIII(ii), pp. 201-208 (1987).
74. Dwyer-Joyce, R.S., Hamer, J.C., Sayles, R.S. and Ioannides, E., "Lubricant Screening for Debris Effects to Improve Fatigue and Wear Life," Proceedings of 18th Leeds-Lyon Symposium on Tribology (Wear Particles--from the Cradle to the Grave), Elsevier, Amsterdam, ed. D. Dowson, C. M. Taylor, M. Godet.
75. Dwyer-Joyce, R.S., Hamer, J.C. and Sayles, R.S., "Surface Damage Effects Caused by Debris in Rolling Bearing Lubricants, with an Emphasis on Friable Materials," Rolling Element Bearings--Towards the 21st Century, Mechanical Engineering Publications for the I. Mech. E., pp. 1-8.
76. Hamer, J.C., Sayles, R.S. and Ioannides, E., "Particle Deformation and Counterface Damage When Relatively Soft Particles are Squashed Between Hard Anvils," Tribo. Trans., 32(3), pp. 281-288 (1989).
77. Sayles, R.S. and Ioannides, E., "Debris Damage in Rolling Bearings and Its Effects on Fatigue Life," ASME Trans., J. of Tribo., Vol. 110, pp. 26-31 (1988).